frontiers | Research Topics

Systems biology and antimicrobial drug resistance

Edited by
Vijay Soni and Saurabh Mishra

Coordinated by
Aditya Kumar Sharma and Neha Dubey

Published in
Frontiers in Microbiology

ISSN 1664-8714
ISBN 978-2-8325-5427-2
DOI 10.3389/978-2-8325-5427-2

About Frontiers

Frontiers is more than just an open access publisher of scholarly articles: it is a pioneering approach to the world of academia, radically improving the way scholarly research is managed. The grand vision of Frontiers is a world where all people have an equal opportunity to seek, share and generate knowledge. Frontiers provides immediate and permanent online open access to all its publications, but this alone is not enough to realize our grand goals.

Frontiers journal series

The Frontiers journal series is a multi-tier and interdisciplinary set of open-access, online journals, promising a paradigm shift from the current review, selection and dissemination processes in academic publishing. All Frontiers journals are driven by researchers for researchers; therefore, they constitute a service to the scholarly community. At the same time, the *Frontiers journal series* operates on a revolutionary invention, the tiered publishing system, initially addressing specific communities of scholars, and gradually climbing up to broader public understanding, thus serving the interests of the lay society, too.

Dedication to quality

Each Frontiers article is a landmark of the highest quality, thanks to genuinely collaborative interactions between authors and review editors, who include some of the world's best academicians. Research must be certified by peers before entering a stream of knowledge that may eventually reach the public - and shape society; therefore, Frontiers only applies the most rigorous and unbiased reviews. Frontiers revolutionizes research publishing by freely delivering the most outstanding research, evaluated with no bias from both the academic and social point of view. By applying the most advanced information technologies, Frontiers is catapulting scholarly publishing into a new generation.

What are Frontiers Research Topics?

Frontiers Research Topics are very popular trademarks of the *Frontiers journals series*: they are collections of at least ten articles, all centered on a particular subject. With their unique mix of varied contributions from Original Research to Review Articles, Frontiers Research Topics unify the most influential researchers, the latest key findings and historical advances in a hot research area.

Find out more on how to host your own Frontiers Research Topic or contribute to one as an author by contacting the Frontiers editorial office: frontiersin.org/about/contact

Systems biology and antimicrobial drug resistance

Topic editors
Vijay Soni — Weill Cornell Medical Center, NewYork-Presbyterian, United States
Saurabh Mishra — Cornell University, United States

Topic coordinators
Aditya Kumar Sharma — University of Illinois Chicago, United States
Neha Dubey — Washington University in St. Louis, United States

Citation
Soni, V., Mishra, S., Sharma, A. K., Dubey, N., eds. (2024). *Systems biology and antimicrobial drug resistance*. Lausanne: Frontiers Media SA.
doi: 10.3389/978-2-8325-5427-2

Table of contents

frontiers | Frontiers in Microbiology

TYPE Editorial
PUBLISHED 02 September 2024
DOI 10.3389/fmicb.2024.1481911

OPEN ACCESS

EDITED AND REVIEWED BY
Miklos Fuzi,
Independent Researcher, Seattle, United States

*CORRESPONDENCE
Vijay Soni
✉ vis2032@med.cornell.edu;
✉ sonivijay07@gmail.com

RECEIVED 16 August 2024
ACCEPTED 21 August 2024
PUBLISHED 02 September 2024

CITATION
Soni V, Sharma AK, Dubey N and Mishra S (2024) Editorial: Systems biology and antimicrobial drug resistance.
Front. Microbiol. 15:1481911.
doi: 10.3389/fmicb.2024.1481911

Editorial: Systems biology and antimicrobial drug resistance

Vijay Soni[1]*, Aditya Kumar Sharma[2,3], Neha Dubey[4] and Saurabh Mishra[5]

[1]Division of Infectious Diseases, Weill Department of Medicine, Weill Cornell Medicine, New York, NY, United States, [2]Department of Pathology, College of Medicine, University of Illinois at Chicago, Chicago, IL, United States, [3]School of Biological and Life Sciences, Galgotias University, Gautam Budh Nagar, Uttar Pradesh, India, [4]Department of Molecular Microbiology, Center for Women's Infectious Disease Research, Washington University School of Medicine, St. Louis, MO, United States, [5]Department of Microbiology and Immunology, Weill Cornell Medicine, New York, NY, United States

KEYWORDS

antimicrobial resistance (AMR), system biology, metabolomics, omics, genomics, proteomics, transcriptomics

Editorial on the Research Topic
Systems biology and antimicrobial drug resistance

For thousands of years, bacterial infections have been the primary cause of mortality. The discovery of antibiotics offered a temporary solution to this crisis, but their effectiveness was short-lived due to the remarkable adaptability and rapid evolutionary strategies employed by bacterial pathogens. As a result, the emergence of antimicrobial resistance (AMR) has become an even more pressing concern, posing a significant threat to global health. With the advent of novel high throughput molecular biology technologies, systems biology has emerged as a powerful tool to study AMR by integrating data from different methods, including genomics, transcriptomics, proteomics, and metabolomics (Figure 1). It is helping to identify novel biomarkers and targets for faster diagnosis and efficient drug development (Figure 1). Considering all these facts we have edited the Research Topic "*Systems Biology and Antimicrobial Drug Resistance*" to cover research articles highlighting the critical issue of bacterial AMR and explore the potential of systems biology in identifying new drug targets and combatting AMR, particularly in *Mycobacterium tuberculosis*, *Acinetobacter* spp., *Staphylococcus aureus*, and *Pseudomonas aeruginosa* infections where only a limited number of antibiotics are available for treatment.

Starting from clinical study from Wu et al. examined the clinical, pathological, and drug-resistant characteristics of patients with spinal and pulmonary tuberculosis. Spinal tuberculosis exhibited a similar pathology of chronic granulomatous inflammation and caseous necrosis. However, the spinal tuberculosis group demonstrated higher amounts of granulation tissue, abscess, acute inflammation, caseous necrosis, and exudation. MRI findings also revealed paravertebral and bilateral psoas muscle abscesses, surrounding soft tissue edema, and infectious vertebral body lesions. In the spinal tuberculosis group, drug resistance analysis revealed higher incidences of resistance to rifampicin (RFP) + isoniazid (INH) + ethambutol (EMB) and RFP + EMB, but lower incidences of resistance to RFP + INH + STR and INH + EMB.

In another clinical work, Hou et al. analyzed Methicillin-resistant *Staphylococcus aureus* (MRSA) strains from a hospital setting in China. Their work is focused on prevalence, antibiotic resistance, and the genomic characteristics of the bacteria. Among

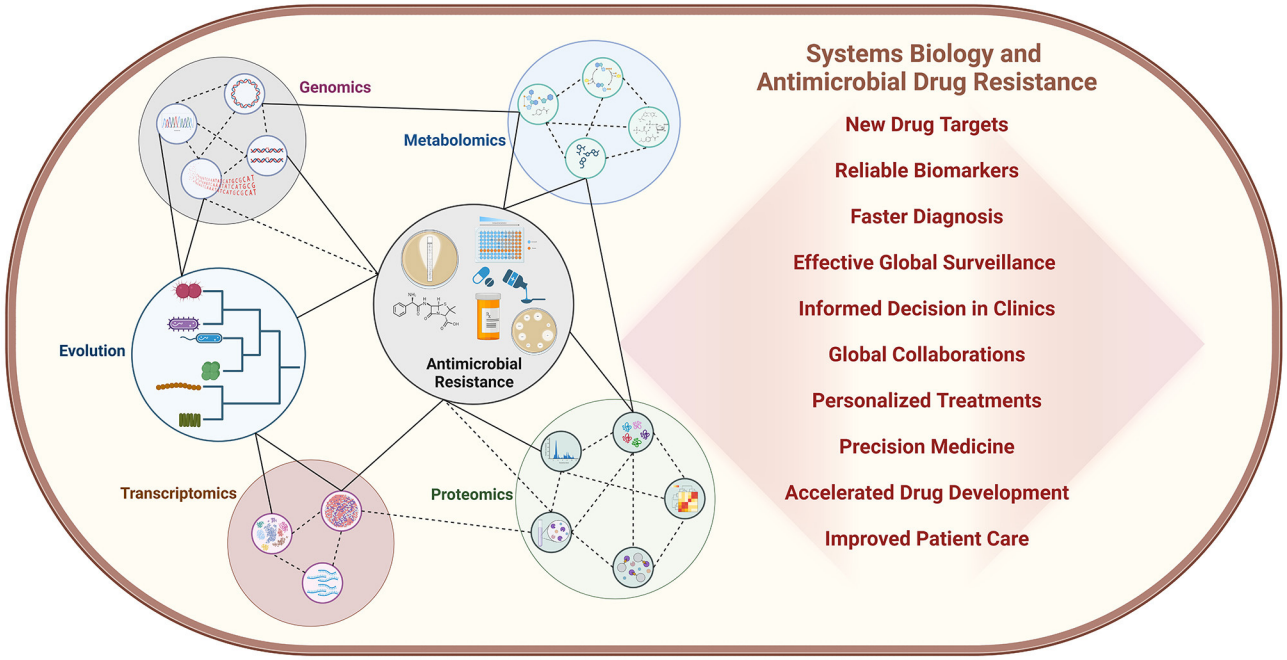

FIGURE 1
Systems biology is playing a crucial role in elucidating bacterial physiology and the development of antimicrobial resistance, revealing complex molecular mechanisms and their interconnected relationships at a systems level. The impact of this field is profound, with far-reaching implications for both clinical practice and research laboratories. Moreover, the integration of artificial intelligence and machine learning technologies is rapidly accelerating progress, unlocking new insights and innovations in the fight against AMR.

212 collected strains, 38 were identified as MRSA and subjected to further analysis. These MRSA strains showed resistance to penicillin, erythromycin, and clindamycin but remained sensitive to vancomycin and linezolid. The study also revealed a high detection rate of biofilm genes within the MRSA strains. Notably, the ST59-SCCmecIV-t437 clone exhibited a higher prevalence of resistance genes and a stronger biofilm-forming capacity. Conversely, the ST59-SCCmecV-t437 clone displayed a higher positive rate for the *pvl* gene, leading to increased pathogenicity and a greater risk of causing systemic infections.

Similarly, Miao et al. investigated the prevalence, genetic makeup, and antibiotic resistance patterns of *Streptococcus pneumoniae* in 263 pneumococcal disease patients at West China Hospital. They revealed 19F as the predominant serotype. Penicillin resistance was notably high, affecting 82.35% of meningitis and 1.22% of non-meningitis cases. The prevalence of *ermB* and *tetM* resistance genes was substantial, correlating with high levels of erythromycin and tetracycline resistance respectively. Interestingly, all isolates remained susceptible to vancomycin and linezolid.

Further, in a related article, Handa et al. investigated the resistance patterns associated with in and outpatients from a tertiary care hospital. This study aimed to identify the resistance patterns of several pathogenic bacteria in a healthcare setting. The investigation encompassed screening nearly ~450 bacterial strains isolated from over ~900 patients through a wide antibiotic susceptibility test screen. Their research has contributed to identifying effective drugs for controlling infections caused by AMR bacteria in the population and for monitoring the prevalence of these drug-resistant bacterial pathogens. Understanding these patterns is crucial for guiding effective treatment strategies toward the challenges associated with the anti-microbial resistance.

Toward understanding the mechanism of AMR, Huangwei et al. investigated mechanisms underlying multi-drug resistance (MDR) in the fungus *Clarireedia jacksonii* by analyzing isolates LT15 and LT586. Their study revealed that LT586 exhibited resistance to three fungicides: iprodione, propiconazole, and boscalid. Using RNA-seq analysis, they found significant differential gene expression between MDR LT586 isolate and the fungicide-sensitive LT15 isolate. LT586 exhibited downregulation of 306 genes involved in metabolic pathways such as butanoate metabolism, terpenoid backbone biosynthesis, tyrosine metabolism, and starch and sucrose metabolism. Conversely, 153 genes were upregulated in LT586, with enrichment of different functional categories including peroxisome function, glycerophospholipid metabolism, protein processing in the endoplasmic reticulum, and ABC transporters. This differential gene expression pattern suggests metabolic reprogramming and enhanced efflux mechanisms as contributing factors to the development of the MDR phenotype in LT586.

Further, Shah et al. performed a proteomics-based analysis to identify novel target proteins in drug-resistant *Prevotella melaninogenica*. The study yielded 1,415 core proteins from 14 complete genome sequences of *P. melaninogenica*. Using subtractive proteomics, reverse vaccinology techniques, and rigorous bioinformatics analysis, 18 candidate proteins were selected. Two of these candidates, ADK95685.1 and ADK97014.1 were chosen for the design of a multi-epitope vaccine against *P. melaninogenica* infection.

In the same direction, Qin et al. have identified the *htpG* gene as a critical factor in antibiotic resistance development in *Vibrio mimicus* SCCF01. Deletion of the *htpG* gene led to increased lipopolysaccharide production, decreased levels of glycerophospholipids, and weakened efflux pump activity. Moreover, the *htpG* deletion strain became less susceptible to β-lactam antibiotics due to impaired peptidoglycan synthesis and disrupted peptidoglycan recycling and regulation.

Additionally, in a related context, research publication from Qiu et al. investigates the antibiotic resistance mechanisms of carbapenem-resistant *Acinetobacter baumannii* (*A. baumannii*) clinical isolates from Guiyang, China. This study enhances the broader understanding of AMR by offering detailed molecular and genetic insights into the mechanisms of carbapenem resistance in *A. baumannii*, a critical nosocomial pathogen. Authors used the combination of multilocus sequence typing (MLST) and transcriptome analysis to identify the genes enriched in the AMR strains of *A. baumannii* isolates. The resistance locus was identified in the genes associated with key bacterial processes including efflux pumps, biofilm formation, and cell wall processes. This provides crucial information for formulating more effective strategies to combat AMR in clinical settings.

Subsequently, the study by Zhu H.-Y. et al. uncovers a key molecular mechanism in the bacteria, *Weissella cibaria* (*W. cibaria*), a bacteria that persists under ciprofloxacin stress. Authors unveiled the molecular mechanism of the PemIK toxin-anti-toxin system, that contributes to the antibiotic resistance behavior of the *W. cibaria* by aiding in the bacterial transition between the actively replicating and persistent state. The endonuclease activity of the toxin PemK of the PemIK system targets the mRNA-encoding enzymes involved in glycolysis, the TCA cycle, and the respiratory chain pathway. This metabolic disruption leads to a decrease in ATP levels in the bacterial cells, and an increase in persister frequency. The authors also identified Arg24 residue of PemK as crucial for its activity. This system allows *W. cibaria* to survive ciprofloxacin treatment not through genetic resistance, but through a phenotypic persistence state. This persistence mechanism can contribute to treatment failures and recalcitrant infections, as a subpopulation of bacteria can survive antibiotic exposure and repopulate once treatment stops.

In continuity, Zhu L. et al. demonstrated the importance of the ISKpn element in conferring *mgrB* gene mutations in ST11 hypervirulent colistin-resistant *Klebsiella pneumonia*. They identified three IS elements inserted themselves into or near *mgrB* gene that confer resistance. These elements are ISKpn26, ISKpn14, and IS903B. Additionally, analyzed isolates exhibited high resistance to multiple antibiotics including TCC (Ticarcillin), TZP (Piperacillin/Tazobactam), CAZ (Ceftazidime), and COL (Colistin), and a significant portion, 85%, displayed resistance to both DOX (Doxycycline) and TOB (Tobramycin). Further analysis identified these isolates as a specific strain (ST11) with six clusters. Notably, all harbored mutations in the *mgrB* gene, potentially acquired through horizontal or clonal transmission.

Moving toward the treatment side, Balkrishna et al. elaborated on the potential of the medicinal plant-derived compounds as a promising adjunct therapy for tuberculosis. The authors investigated the antimycobacterial activity of the medicinal plant *Solanum virginianum* (SVE). SVE extracts were able to inhibit the growth and viability of the *Mycobacterium smegmatis*, a soil-dwelling bacterium of the *Mycobacterium* genus. SVE treatment perturbs the stress tolerance capacity of the *M. smegmatis*, eventually causing an overarching effect on the bacterial cell wall. Importantly, these cell membrane defects lead to enhanced bioavailability or accessibility to the anti-mycobacterial drug, isoniazid. This research study provides a novel plant-based drug molecule that has potential for the adjunct anti-tubercular therapy and can counteract the emerging strains of AMR.

Further, Rodjun et al. conducted a simulation study to optimize dosage regimens for colistin and sitafloxacin, both individually and in combination, against highly resistant *A. baumannii*. The study aimed to identify optimal drug combinations and dosages to effectively treat these infections. By simulating various dosing scenarios and patient conditions, the study determined that a suboptimal colistin dose combined with a supraoptimal sitafloxacin dose could be a promising approach. This combination showed potential for improved treatment outcomes while potentially reducing the risk of adverse effects associated with higher colistin doses. The study highlights the importance of optimizing antibiotic therapy in the face of increasing AMR.

Review article by Shi et al. summarizes the mechanisms responsible for antibiotic resistance in *A. baumannii*, with a particular focus on tigecycline and polymyxin resistance. They highlighted the bacterium's adaptability, showcasing its mechanism of multiple resistance strategies, including antibiotic inactivation, target site modification, altered drug permeability, and other defense mechanisms.

In another review Bhat et al. explored the structure and functions of integrons and their mechanisms. Integrons are natural cloning vectors that facilitate the spread of AMR genes among microbial species. Horizontal gene transfer between different trophic groups is responsible for the dissemination of antibiotic resistance in humans. Additionally, integrons serve as genetic markers for estimating AMR. By estimating antibiotic resistance through integrons, we can better understand their role and develop strategies to counteract the resistance mechanisms evolved by microbes.

In a very unique study, Xiong et al. examined the bacterial composition of extended boar semen and identified *Pseudomonas* species as the predominant bacteria. They isolated a specific strain, designated GXZC, belonging to the *Pseudomonas fluorescens* group. This strain was found to negatively impact sperm quality and exhibit resistance to multiple antibiotics. Also, comparative genomic analysis revealed that the GXZC strain possesses intrinsic and acquired resistance genes. These findings highlight a significant challenge in the long-term storage of extended boar semen due to the presence of the *P. fluorescens* strain.

Another interesting article by Abdelsalam Elshenawy et al. shows a descriptive analysis before and during the COVID-19 pandemic to investigate antibiotic prescribing trends for respiratory tract infections (RTIs). The authors examined antibiotic use in 640 patients with RTIs. Results revealed an increased use of amoxicillin-clavulanic acid and azithromycin. Additionally, there was a rise in antibiotic prescriptions from the "Watch" category during the pandemic, emphasizing the need for

enhanced antibiotic management practices. The insights gained into antibiotic prescribing patterns will aid in addressing antibiotic management challenges.

Lastly, the editorial section is concluded through a comprehensive review by Sharma et al. which compiles the information related to the current state of AMR amongst several pathogenic bacteria and provides important insights into emerging challenges in AMR, highlighting the complexities involved in addressing this global health threat and the need for multifaceted approaches to combat AMR. Addressing AMR demands a multi-faceted approach, including integrating AMR into the Sustainable Development Goals (SDGs) to reinforce global healthcare commitment to tackling this Research Topic.

Overall, we believe that collection of articles in this Research Topic will empower the scientific and clinical communities to make informed decisions, guiding the development of more effective research approaches and treatment strategies. By shedding new light on these critical areas, we hope to accelerate progress and improve outcomes for patients worldwide.

Author contributions

VS: Conceptualization, Investigation, Supervision, Validation, Visualization, Writing – original draft, Writing – review & editing. AS: Formal analysis, Validation, Writing – original draft. ND: Validation, Writing – original draft. SM: Writing – original draft.

Funding

The author(s) declare that no financial support was received for the research, authorship, and/or publication of this article.

Conflict of interest

The authors declare that the research was conducted in the absence of any commercial or financial relationships that could be construed as a potential conflict of interest.

Publisher's note

frontiers | Frontiers in Microbiology

TYPE Original Research
PUBLISHED 14 August 2023
DOI 10.3389/fmicb.2023.1230572

OPEN ACCESS

EDITED BY
Vijay Soni,
NewYork-Presbyterian, United States

REVIEWED BY
Shivangi Rastogi,
University of Maryland, College Park, United States
Arka Banerjee,
NewYork-Presbyterian, United States
Bhagyaraj Ella,
University of Florida, United States

*CORRESPONDENCE
Wen Chen
dr.chen20160224@foxmail.com
Fenghua Wang
13810915901@163.com

†These authors have contributed equally to this work

RECEIVED 29 May 2023
ACCEPTED 28 July 2023
PUBLISHED 14 August 2023

CITATION
Wu R, Li S, Liu Y, Zhang H, Liu D, Liu Y, Chen W and Wang F (2023) A high proportion of caseous necrosis, abscess, and granulation tissue formation in spinal tuberculosis. *Front. Microbiol.* 14:1230572. doi: 10.3389/fmicb.2023.1230572

A high proportion of caseous necrosis, abscess, and granulation tissue formation in spinal tuberculosis

Runrui Wu†, Shanshan Li†, Yadong Liu, Hong Zhang, Dongxu Liu, Yuejiao Liu, Wen Chen* and Fenghua Wang*

Department of Pathology, The 8th Medical Center, Chinese PLA General Hospital, Beijing, China

The special blood circulation, anatomy, and tissue structure of the spine may lead to significant differences in pathological features and drug resistance between spinal tuberculosis and pulmonary tuberculosis. Here, we collected 168 spinal tuberculosis cases and 207 pulmonary tuberculosis cases, and compared their clinical and pathological features as well as drug resistance. From the anatomical location, the highest incidence was of lumbar tuberculosis, followed by thoracic tuberculosis. PET-CT scans showed increased FDG uptake in the diseased vertebrae, discernible peripheral soft tissue shadow, visible internal capsular shadow, and an abnormal increase in FDG uptake. MRI showed infectious lesions in the diseased vertebral body, formation of paravertebral and bilateral psoas muscle abscess, and edema of surrounding soft tissues. As with control tuberculosis, the typical pathological features of spinal tuberculosis were chronic granulomatous inflammation with caseous necrosis. The incidence of granulomas was not statistically different between the groups. However, the proportions of caseous necrosis, acute inflammation, abscess, exudation, and granulation tissue formation in the spinal tuberculosis group were all significantly increased relative to the control tuberculosis group. Compared to the control tuberculosis group, the incidences of resistance to rifampicin (RFP) + isoniazid (INH) + streptomycin (STR) and INH + ethambutol (EMB) were lower in the spinal tuberculosis group, while the incidences of resistance to RFP + INH + EMB and RFP + EMB were higher. Moreover, we also found some differences in drug-resistance gene mutations. In conclusion, there are noticeable differences between spinal *Mycobacterium tuberculosis* and pulmonary tuberculosis in pathological characteristics, drug resistance, and drug resistance gene mutations.

KEYWORDS

spinal tuberculosis, pathological feature, drug resistance, gene, caseous necrosis

1. Introduction

Tuberculosis (TB), a leading cause of mortality worldwide, affects an estimated 10 million individuals annually (Furin et al., 2019). With the emergence of drug-resistant tuberculosis strains and the increase in the HIV infection rate, the number of tuberculosis cases is increasing steadily, and the incidence of osteoarticular tuberculosis is also increasing significantly (Diedrich et al., 2016). As the most severe and prevalent form of bone and joint tuberculosis, spinal tuberculosis, constitutes approximately 50% of these cases (Ali et al., 2019). All segments of the

spine may be affected, with the lumbar spine most commonly affected, followed by the thoracic spine (Liu et al., 2019). Cervical and sacral tuberculosis is relatively rare. The initial symptoms, such as mild pain, stiffness, and loss of muscle strength, are typically nonspecific, often leading to misdiagnoses (Liu et al., 2019). The disease can progress to cause postural abnormalities, spinal deformities, and even paralysis (Jain et al., 2018), severely compromising the patient's quality of life without management (Ali et al., 2019). This suggested a vital role of prompt diagnosis and personalized treatment for improving the prognosis of spinal tuberculosis.

The current diagnosis of tuberculosis involves the evaluation of the patient's medical history, clinical symptoms, physical signs, laboratory tests, and imaging tests. Magnetic Resonance Imaging (MRI) serves as a sensitive modality for the early detection of spinal tuberculosis (Moorthy and Prabhu, 2002) and provide detailed information on early vertebral inflammation and minor swelling of paravertebral soft tissue (Moorthy and Prabhu, 2002; Ali et al., 2019). Moreover, it can aid in the diagnosis of neurological dysfunction and assessing spinal cord compression (Ali et al., 2019). In addition, histopathological examination, encompassing H&E staining, acid-fast staining, and molecular testing, is regarded as the gold standard for the diagnosis of spinal tuberculosis. The typical pathological change of tuberculosis is chronic granulomatous inflammation, with caseous necrosis (Li et al., 2020). However, the spine's relatively limited blood circulation and discharge pathway for necrotic substances may lead to a divergence in the pathology of spinal tuberculosis compared to lung tuberculosis. Li. et al. found that the most common pathologic characteristics of spinal tuberculosis were caseous necrosis, multinuclear giant cells, and granulomatous inflammation (Li et al., 2020). Limited studies revealed the differences.

In the management of spinal tuberculosis, it is crucial that antituberculosis drugs are administered adhering to the principles of early initiation, consistency, complete course treatment, combination therapy, and appropriate dosing. In patients without severe vertebral bone damage and instability, anti-tuberculous drugs alone can promote recovery (Suárez et al., 2019). However, for patients who have severe bone destruction, spinal instability, and spinal nerve compression, surgery is necessary, and antituberculosis drugs are used to keep *Mycobacterium tuberculosis* in a resting state (Kumar et al., 2022). Given these factors, personalized selection of antituberculosis drugs is crucial (Rajasekaran and Khandelwal, 2013; Bhosale et al., 2020). Molecular biology techniques and drug sensitivity tests are currently the main means of detecting antituberculosis drug resistance. However, vertebral puncture can easily damage the spinal cord or important blood vessels and nerves, and the risk is high, especially if tuberculosis has destroyed the vertebral body or surrounding supporting tissue. In this study, the pathological features and drug resistance of spinal tuberculosis were examined, to characterize differences between spinal tuberculosis and pulmonary tuberculosis to inform a more individualized approach to drug regimen selection.

2. Materials and methods

2.1. Participant selection

This study incorporated patients admitted to the 8th Medical Centre of Chinese PLA General Hospital from January 2016 to December 2020. The inclusion criteria were: age over 18 years, spinal surgery or puncture for pathological examination, clinically and pathologically diagnosed *Mycobacterium tuberculosis* infection, and no prior antituberculosis drug treatment before diagnosis. Exclusion criteria encompassed malignancies, severe fungal and bacterial infections, hematologic malignancies, severe trauma, and surgical history. One hundred sixty eight patients with spinal tuberculosis were included and 207 patients with pulmonary tuberculosis were as the control group. This study was approved by the Ethics Committee of the Chinese PLA General Hospital and was performed in accordance with the principles of the Declaration of Helsinki.

2.2. Methods

2.2.1. Imaging examination

In this study, 18F-FDG positron emission tomography (PET/CT) and MRI were used to evaluate spinal tuberculosis, and PET/CT and CT were used to evaluate pulmonary tuberculosis (Vorster et al., 2014). PET/CT can evaluate the spinal morphology and extent of involvement, as well as detect other lesions throughout the body (Gao et al., 2014). In addition, PET/CT can provide glucose metabolism characteristics of spinal tuberculosis and evaluate lesion activity, which is of great significance for early diagnosis, differential diagnosis and curative effect evaluation of spinal tuberculosis (Altini et al., 2020). MRI has a higher imaging resolution for soft tissue than CT and X-ray (Kubihal et al., 2022). MRI can improve the sensitivity and specificity of the diagnosis of spinal tuberculosis and help to evaluate the involvement of the lesion.

2.2.2. H&E staining

All tissue samples underwent fixation in 4% paraformaldehyde, paraffin embedding post gradient dehydration, followed by sectioning (3 μm thickness) and mounting on slides. After baking at 72°C for 30 min, slides underwent dewaxing using xylene for two 10-min intervals, sequentially washed with 100, 90, and 80% gradient anhydrous ethanol for 5 min each time and stained with hematoxylin dye for 30 s. Subsequent steps involved differentiation with 10% hydrochloric acid, blue reversion with ammonia, eosin dye application for 5 s, and dehydration with gradient anhydrous ethanol, transparency with xylene, and sealing with neutral resin. Observations of basic histological features from H&E-stained sections were made under a microscope. Representative tissue sections were chosen for subsequent acid-fast staining and gene detection.

2.2.3. Acid-fast staining

Sections (3 μm thickness) were cut from each sample, adhered to slides, and baked at 72°C for 30 min. The dewaxing process was carried out twice with xylene for 10 min, followed by a 5-min wash with 100, 90, and 80% gradient anhydrous ethanol. The sections were then stained with 2–3 drops of carbolic red dye solution for 2 h and decolorized with 1% hydrochloric alcohol until a light pink hue was achieved. Hematoxylin dye was applied for 30 s, followed by differentiation with 10% hydrochloric acid, and blue reversion with ammonia water. Gradient anhydrous ethanol dehydration, xylene transparency, and neutral resin sealing finalized the process.

2.2.4. Identification of mycobacteria

From each patient tissue specimen, 8–10 sections of 5-10 μm thickness were cut and placed in 1.5 mL centrifuge tubes for dewaxing, lysis, digestion, and DNA extraction. PCR tubes from the genetic test kit (Yaneng Biotechnology Co., Ltd., Shenzhen, China) were utilized to identify Mycobacterial species, and 4 μL of sample DNA was added. Following DNA amplification, the membrane strips and amplification products were placed in tubes with 5–6 mL of solution A and heated in a boiling bath for 10 min. They were then hybridized at 59°C for 1.5 h. Post-hybridization, the membrane strips were washed and incubated for 30 min in solution A containing POD enzyme. The reaction was terminated with purified or deionized water after the membrane strips were placed in the chromogenic solution for 10 min. The detection sites were indicated by blue spots on the membrane strips, and each experiment incorporated both positive and negative controls (Zhang et al., 2021; Li et al., 2022; Figure 1).

2.2.5. Mycobacterial drug resistance mutation gene detection

PCR tubes from the Mycobacterial drug resistance mutation gene detection kit (Yaneng Biotechnology Co., Ltd., Shenzhen, China) were used to add 4 μL of sample DNA. After DNA amplification at specific intervals and temperatures, the membrane strips and amplification products were placed in tubes with 5–6 mL of AT solution, heated in a boiling water bath for 10 min, and then hybridized at 59°C for 1.5 h. After washing and incubation, the strips were placed in a chromogenic solution for 10 min, and the reaction was stopped with purified or deionized water. Blue spots on the membrane strips indicated detected sites, with both positive and negative controls performed in each experiment.

2.3. Drug resistance types definition

Monoresistance refers to resistance to only one antituberculosis drug (Van Rie et al., 2000). Polyresistance refers to resistance to more than one antituberculosis drug but does not include resistance to RFP and INH (Mizukoshi et al., 2021). Multidrug resistance refers to resistance to at least RFP and INH simultaneously (Van Rie et al., 2000). Drug resistance to any drug refers to resistance to any one or more antituberculosis drugs (Van Rie et al., 2000).

2.4. Statistical methods

SPSS25.0 software was used for the statistical analysis. The counting data were described as "case (strain)" and "rate (%)." The chi-square test or Fisher's exact probability test was used to compare drug resistance rates between groups, and $p < 0.05$ was considered statistically significant.

3. Results

3.1. Clinical data

The control group consisted of 207 pulmonary tuberculosis patients, including 117 males and 90 females, with a mean age of 43.86 years. The spinal tuberculosis group included 168 patients, with 92 males and 76 females, and a mean age of 43.48 years. The highest incidence was of lumbar tuberculosis (48.81%), followed by thoracic tuberculosis (38.10%). PET-CT scans showed increased FDG uptake in the diseased vertebrae, discernible peripheral soft tissue shadow, visible internal capsular shadow, and an abnormal increase in FDG uptake (Figure 2A). MRI showed infectious lesions in the diseased vertebrae, paraspinal and bilateral lumbar muscle abscess formation, and peripheral soft tissue edema (Figure 2B). PET-CT and CT results of control tuberculosis group were shown in Supplementary Figure S1.

3.2. Pathological features

The control tuberculosis group had 153 cases (73.91%) of typical granulomatous lesions, 47.34% of which were accompanied by typical caseous necrosis. Some cases were complicated with acute inflammation (23.67%), exudation (26.09%), granulation tissue formation (15.46%), inflammatory necrosis (20.77%), and fibrous hyperplasia (78.74%). No abscesses were identified. Typical granulomatous lesions were seen in 133 cases (79.17%) in the spinal tuberculosis group, of which 89.29% were accompanied by typical caseous necrosis. Some cases were associated with acute inflammation (80.95%), exudation (80.95%), granulation tissue formation (80.95%), inflammatory necrosis (19.05%), fibrous tissue hyperplasia (70.24%), and abscess (21.43%). Statistical analysis showed significant differences in the proportion of caseous necrosis, acute inflammation, abscesses, exudation, and granulation tissue formation between the two groups. Acid-fast staining showed 147 cases in the control tuberculosis group and 122 cases in the spinal tuberculosis group were acid-positive, with no statistically significant differences between the two groups (Tables 1, 2 and Figures 3–5).

3.3. Overall drug resistance

In the control tuberculosis group, susceptibility to all four anti-tuberculosis drugs was observed in 14 samples. Monoresistance was

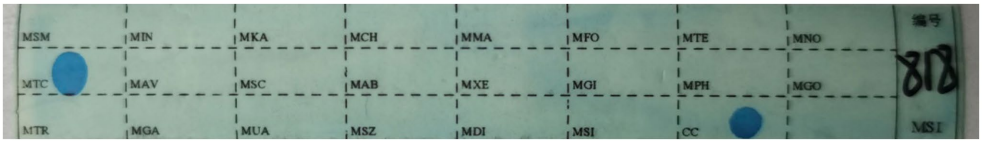

FIGURE 1
The sequence of the detection site on the membrane strip.

10.3389/fmicb.2023.1230572

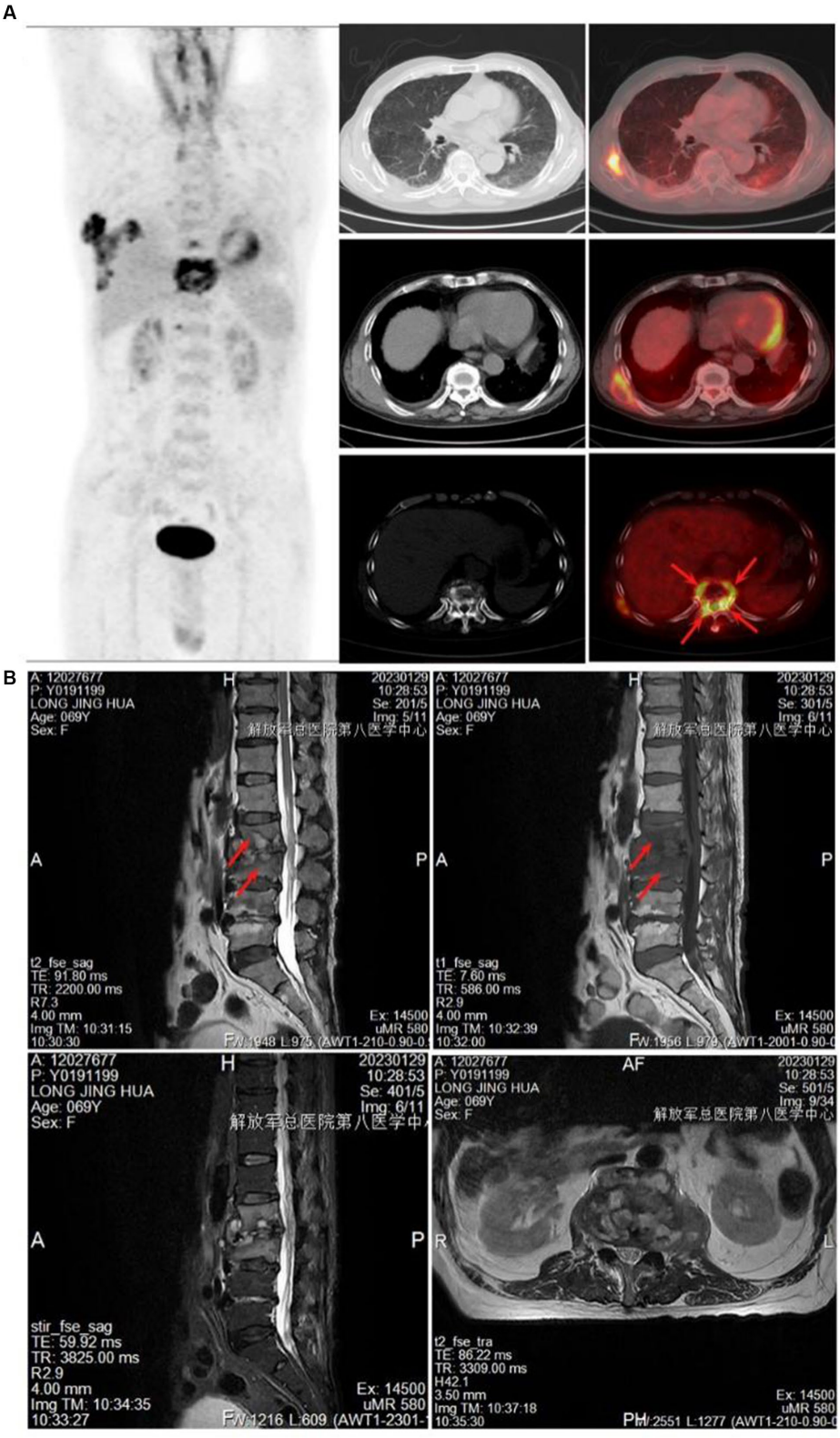

FIGURE 2
Imaging examination. **(A)** PET-CT showed increased FDG uptake in the diseased vertebrae. **(B)** MRI showed infectious lesions in the diseased vertebral body, the formation of paraspinal and bilateral psoas muscle abscesses, and the edema of the surrounding soft tissues.

seen in 42.51% of cases, with INH resistance being the most prevalent at 73.86%. Polyresistance was detected in 42.51% of cases, with the highest rate of resistance being to INH + STR, accounting for 41.70%. Multidrug resistance was found in 20.77% of cases, with the highest resistance rate observed for the RFP + INH + STR combination, at 46.51%.

In the spinal tuberculosis group, 16 samples were found to be sensitive to all four anti-tuberculosis drugs. The rate of monoresistance was 41.07%, with INH resistance being the most common, observed in 73.91% of cases. Polyresistance was detected in 26.19% of cases, with the highest rate of resistance being to the RFP + EMB combination, accounting for 29.55%. The multidrug resistance rate was 22.62%, with the highest resistance rate seen for the RFP + INH + STR + EMB combination, at 42.11%.

Statistical analysis revealed that the rates of resistance to RFP + INH + STR and INH + EMB were lower in the spinal tuberculosis group compared to the control tuberculosis group. Conversely, the rates of resistance to RFP + INH + EMB and RFP + EMB were higher in the spinal tuberculosis group. The detailed data is presented in Table 3.

TABLE 1 Comparison of clinical data and important pathological features.

	Control tuberculosis (n = 207)	Spinal tuberculosis (n = 168)	p value
Gender (Male)	56.52% (n = 117)	54.76% (n = 92)	0.733
Age (year)	43.86 ± 1.21	43.48 ± 1.35	0.833
TB Type (MTB)	100% (n = 207)	100% (n = 168)	/
Methods			
Acid-fast (+)	71.01% (n = 147)	72.62% (n = 122)	0.732
PCR (+)	100% (n = 207)	100% (n = 168)	/
Pathology			
Granulomatous inflammation	73.91% (n = 153)	79.17% (n = 133)	0.194
Caseous necrosis	47.34% (n = 98)	89.29% (n = 150)	<0.001
Abscess	0% (n = 0)	21.43% (n = 36)	<0.001
Inflammatory necrosis	20.77% (n = 43)	19.05% (n = 32)	0.678
Exudation	26.09% (n = 54)	80.95% (n = 136)	<0.001
Acute inflammation	23.67% (n = 49)	80.95% (n = 136)	<0.001
Granulation tissue formation	15.46% (n = 32)	80.95% (n = 136)	<0.001
Fibrous tissue hyperplasia	78.74% (n = 163)	70.24% (n = 118)	0.059

3.4. Drug resistance gene mutation

The control tuberculosis group had 22 mutations in the rpoB gene, of which the 516 codons had the most mutations in D516V (D: aspartic acid →V: valine). Among these mutations, 37 samples showed mutations in one site of a single codon, and 15 samples showed mutations in two sites of a single codon at the same time. katG and inhA mutations were of these types, mainly 315 M mutations, accounting for 57.97%. RpsL mutations were mainly in the form of 88 M mutation, and the EmbB mutations was the 306 M2 mutation.

The spinal tuberculosis group had 22 mutations in the rpoB gene, of which the 516 codons had the most mutations in D516V (D: aspartic acid →V: valine). Among these mutations, 24 samples showed mutations in one site of a single codon, and 14 samples showed in two sites of a single codon at the same time. There were 3 types of katG and inhA mutations, mainly 315 M mutations, accounting for 52.38%. The main form of the RpsL mutations was the 88 M mutation, and the EmbB mutations was the 306 M2 mutation.

In addition, we analyzed their genetic mutations. In the control tuberculosis group, the mutation rate of the D516V + D516G + H526Y + H526D site was 2.90%, but no mutation occurred at this site in the spinal tuberculosis group. The mutation rate of D516V + D516G + H526Y + H526D + S531L + S531W in the spinal tuberculosis group was 3.57%, which was significantly higher than that in the control tuberculosis group. The mutation rate of the EMB306 M2 + 306 M3 site was 2.38% in the spinal tuberculosis group, while no mutation was found at this site in the control tuberculosis group. Specific data was shown in Table 4.

TABLE 2 pathological features of spinal tuberculosis at different sites.

Spinal tuberculosis	Cervical	Thoracic	Lumbar	Thoracolumbar	Lumbosacral	Total
Number of patients	7	64	82	5	10	168
Granulomatous inflammation	5	53	64	3	8	133
Caseous necrosis	7	55	74	5	9	150
Abscess	0	20	14	0	2	36
Inflammatory necrosis	0	18	13	0	1	32
Exudation	5	49	71	4	7	136
Acute inflammation	4	55	67	3	7	136
Granulation tissue formation	4	53	66	5	8	136
Fibrous tissue hyperplasia	5	46	56	3	8	118

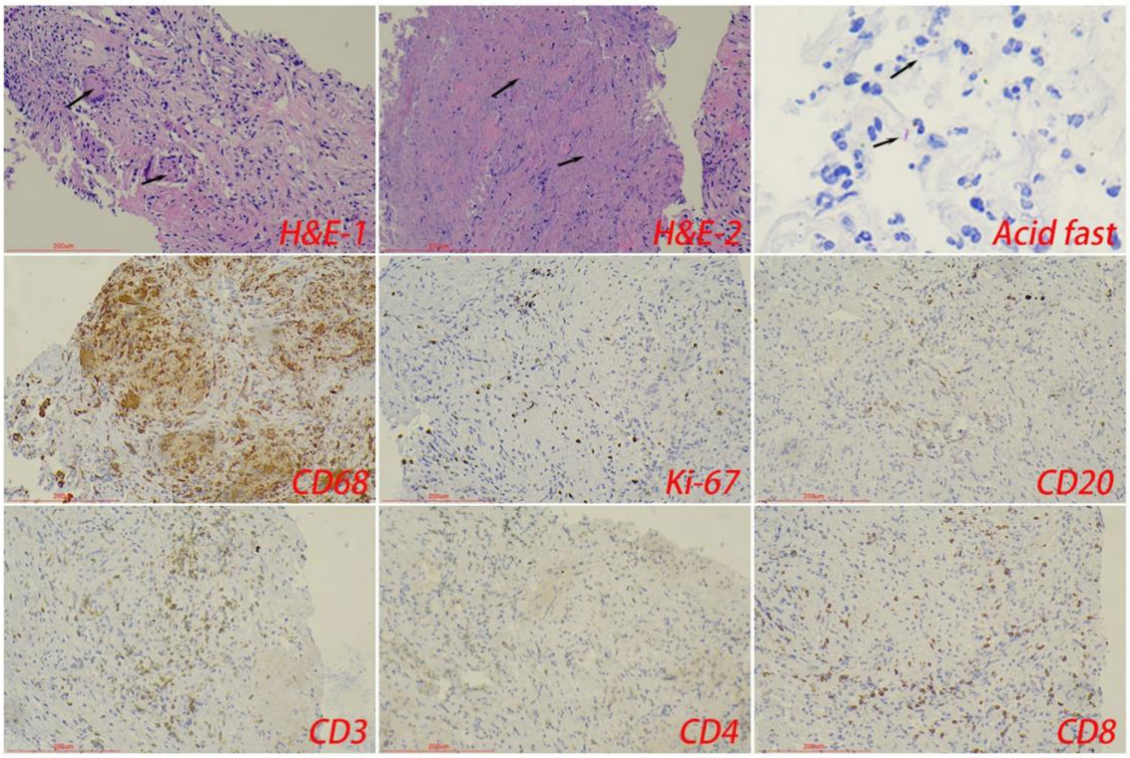

FIGURE 3
The typical pathological manifestations of pulmonary tuberculosis were chronic granulomatous inflammation (H&E-1) with caseous necrosis (H&E-2). Acid-fast staining showed *Mycobacterium tuberculosis*. Immunohistochemical staining was used to label granuloma ($CD68^+$) and inflammatory cell ($CD20^+$B cells, $CD3^+$T cells, $CD4^+$T cells, and $CD8^+$T cells) infiltration. Scale bar: 200 μm; Image magnification: H&E (200×), acid-fast staining (400×), immunohistochemical staining (200×).

4. Discussion

Differences in the epidemiological characteristics, pathogenesis, and pathological features between lung tuberculosis and spinal tuberculosis have been noted (Pandita et al., 2020). Lung tuberculosis is the most common type of tuberculosis and is transmitted mainly by airborne droplets (Torrelles and Schlesinger, 2017). It causes lung infection, leading to symptoms such as cough, sputum, and chest pain, which can be life-threatening in severe cases (Ravimohan et al., 2018). Spinal tuberculosis is a rare but serious form of tuberculosis, usually caused by the spread of *Mycobacterium tuberculosis* to the spine through the bloodstream or lymphatic system (Kumar, 2016). Spinal tuberculosis often presents with symptoms of spinal pain, deformity, and nerve root compression, which may cause spinal cord injury and paralysis in severe cases (Kumar, 2016). Standard anti-tuberculosis therapy remains the mainstay of treatment for lung tuberculosis and spinal tuberculosis, and effective for most of the patients (Singh et al., 2014). For the patients who are not promptly or effectively treated, lung tuberculosis can progress to spinal tuberculosis. Therefore, the timely diagnosis and treatment of lung tuberculosis is important for preventing spinal tuberculosis.

Spinal tuberculosis exhibits unique pathological features. In the early stage, *Mycobacterium tuberculosis* invades the vertebral body and the intervertebral disc, resulting in caseous necrosis (Liu et al., 2019). Caseous necrosis is a special type of coagulated necrosis, which is characterized by unstructured granular red staining substance. As caseous necrosis progresses, the vertebral body gradually collapses, leading to deformity (Mittal et al., 2016); This deformity can cause abnormal spinal curvature and overall spinal deformity. In the late stage of spinal tuberculosis, the caseous material can be reabsorbed, leading to vertebral body hollowing (Izawa, 2015). Simultaneously, infectious inflammation can impact the surrounding bone tissue, potentially leading to dense stomatitis (Izawa, 2015); When the vertebral body becomes deformed, collapses, and hollows out, it may result in nerve root subluxation and compression (Chen et al., 2022); These complications can cause weakness in the lower extremities, paresthesia, urinary dysfunction, and other serious issues. Study showed that the most common pathologic characteristics were caseous necrosis, multinuclear giant cells, and granulomatous inflammation (Li et al., 2020). Our study revealed that 89.19% of patients with spinal tuberculosis developed typical caseous necrosis, a significantly higher rate compared to the control tuberculosis group. This high incidence in the spinal tuberculosis group may be attributed to the unique anatomy and tissue structure around the spine, circulation deprivation, and poor necrotic material drainage. Additionally, the spinal tuberculosis group showed significantly higher occurrences of acute

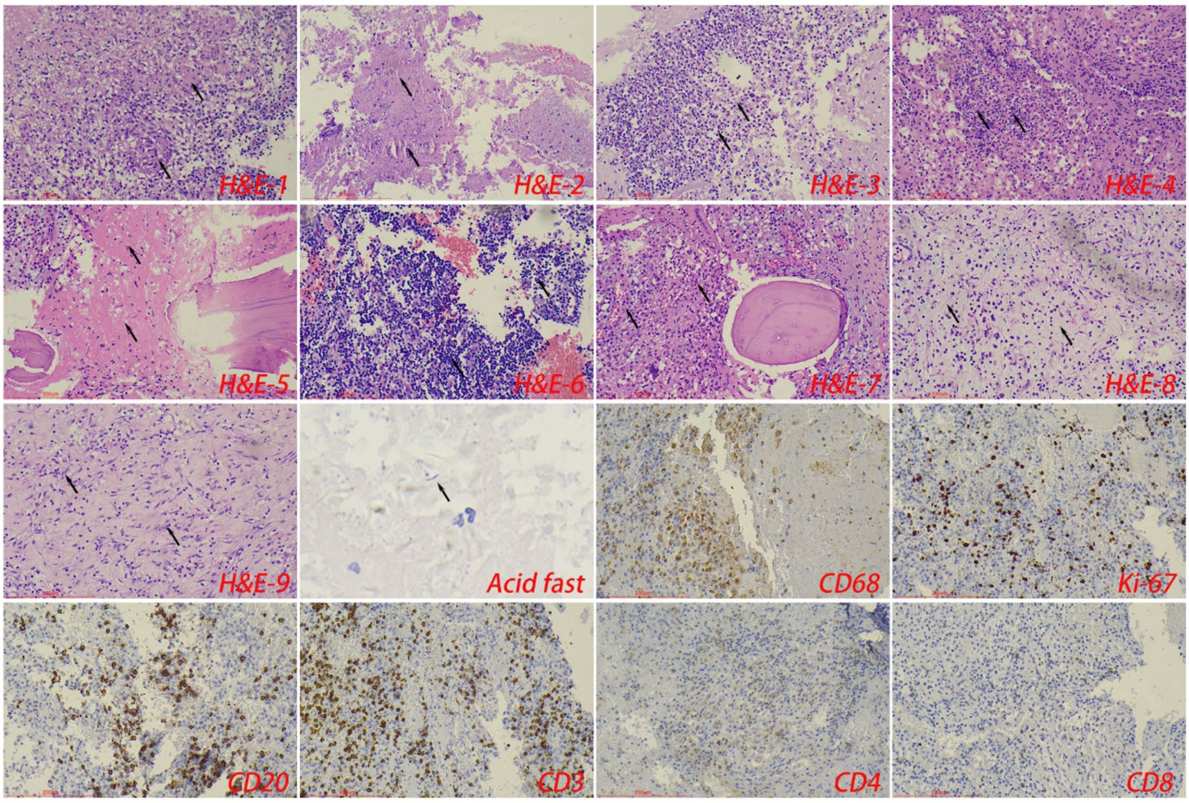

FIGURE 4
The typical pathological manifestations of spinal tuberculosis were chronic granulomatous inflammation (H&E-1) with caseous necrosis (H&E-2). H&E staining showed abscess (H&E-3), inflammatory necrosis (H&E-4), exudation (H&E-5), acute inflammation (H&E-6), and granulation tissue formation (H&E-7), mucous degeneration (H&E-8), and fibrous tissue hyperplasia (H&E-9). Caseous necrosis is a special type of coagulated necrosis, which is characterized by unstructured granular red staining substance. Inflammatory necrosis is tissue necrosis caused by inflammation, and a large number of acute and chronic inflammatory cells can be observed under the microscope. Acid-fast staining showed *Mycobacterium tuberculosis*. Immunohistochemical staining was used to label granuloma ($CD68^+$) and inflammatory cell ($CD20^+$B cells, $CD3^+$T cells, $CD4^+$T cells, and $CD8^+$T cells) infiltration. Scale bar: 200 μm; Image magnification: H&E (200×), acid-fast staining (400×), immunohistochemical staining (200×).

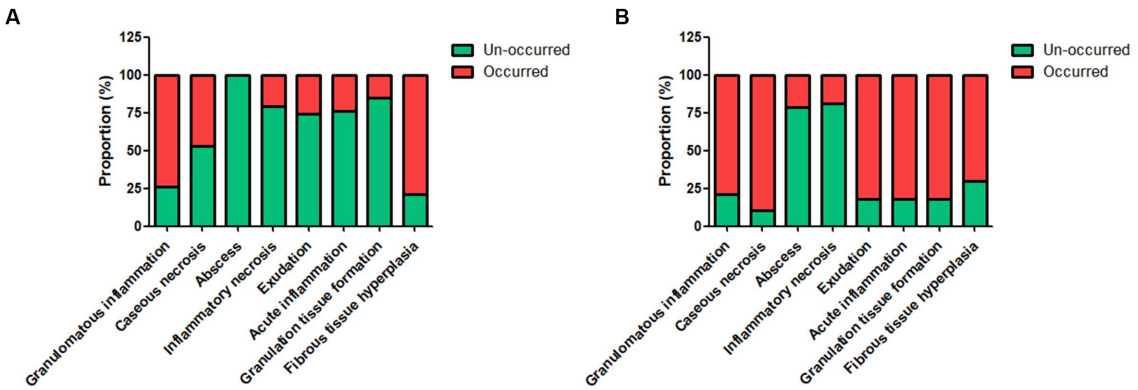

FIGURE 5
The proportion of different pathological features in the control tuberculosis group [n = 207, **(A)**] and spinal tuberculosis group [n = 168, **(B)**]. The proportions of caseous necrosis, acute inflammation, abscess, exudation, and granulation tissue formation in the spinal tuberculosis group were all significantly increased relative to the control tuberculosis group.

TABLE 3 Comparison of overall drug resistance between the spinal tuberculosis group and the control tuberculosis group.

Drug resistance type	Control tuberculosis group (n = 207)	Spinal tuberculosis group (n = 168)	χ^2 values	p value
Monoresistance	88 (42.51)	69 (41.07)	3.704	0.068
RFP resistant	20 (9.66)	13 (7.74)	0.428	0.585
INH resistant	65 (31.40)	51 (30.36)	0.047	0.911
STR resistant	2 (0.97)	3 (1.79)	0.473	0.660
EMB resistant	1 (0.48)	2 (1.19)	0.585	0.585
Multidrug resistance	60 (28.99)	44 (26.19)	0.361	0.564
Resistance to RFP + INH	9 (4.35)	6 (3.57)	0.146	0.795
Resistance to RFP + INH + STR	20 (9.66)	6 (3.57)	5.331	0.024
Resistance to RFP + INH + EMB	0 (0.00)	10 (5.95)	12.659	0.000
Resistance to INH + STR + EMB	14 (6.76)	16 (9.52)	0.960	0.345
Polyresistance	43 (20.77)	38 (22.62)	0.187	0.706
Resistance to RFP + STR	1 (0.48)	5 (2.98)	3.661	0.094
Resistance to RFP + EMB	5 (2.42)	13 (7.74)	5.749	0.026
Resistance to RFP + STR + EMB	6 (2.90)	10 (5.95)	2.117	0.199
Resistance to INH + STR	25 (12.08)	12 (7.14)	2.539	0.120
Resistance to INH + EMB	20 (9.66)	0 (0.00)	17.146	0.00
Resistance to INH + STR + EMB	3 (1.45)	4 (2.38)	0.439	0.705
Resistance to STR + EMB	0 (0.00)	0 (0.00)	0.00	0.00
Fully sensitive	14 (6.76)	16 (9.52)	0.96	0.345
Any drug resistance	197 (95.17)	152 (90.48)	3.165	0.101

RFP, rifampicin; INH, isoniazid; STR, streptomycin; EMB, ethambutol. The value outside the parentheses represents "number of patients," while the value inside the parentheses represents "proportion (%)".

inflammation, abscesses, exudates, and granulation tissue formation than the control tuberculosis group. These unique pathological features significantly increase the difficulty of diagnosis and treatment of spinal tuberculosis.

Classical resistance testing involves the isolation and culture of *mycobacterium tuberculosis* and therefore requires high-level biosafety laboratory and professional operators, which is difficult for pathology departments to achieve. The emergence of drug resistance in *Mycobacterium tuberculosis* is primarily driven by genetic mutations, and identifying these mutations can help inform clinical treatment (Phelan et al., 2016). Resistance to isoniazid typically involves mutations in the katG and inhA promoter regions, particularly at the katG315 site (Seifert et al., 2015). Mutations in the rpoB gene are one of the main mechanisms leading to rifampin resistance, and these mutations occur mainly in the rifampin resistance determining region (RRDR), accounting for more than 95% of all rpoB resistance-associated mutations (Zaw et al., 2018). Mutations in embB and its operon embCAB are closely linked to resistance to ethambutol, and mutations occur most frequently in the ethambutol resistance determining region (ERDR) (Sun et al., 2018). Our results showed that the spinal tuberculosis group differed from the control tuberculosis group in terms of drug resistance and drug resistance gene mutations. Notably, higher proportions of RFP + INH + EMB and RFP + EMB resistance were observed in the spinal tuberculosis group. The reason for this difference may be that the blood circulation in the spinal tuberculosis site is relatively poor, anti-tuberculosis drugs cannot reach effective killing concentrations in caseous necrotic tissue, and residual *mycobacterium tuberculosis* may undergo drug resistance changes. Thus, it is essential to consider these distinct drug resistance profiles when selecting antituberculosis medications. Personalized treatment plans should be developed, considering drug sensitivity test results and individual patient conditions. If treatment efficacy is lacking, immediate measures such as a spinal tap or biopsy should be considered.

Our findings may help in the diagnosis and treatment of spinal tuberculosis. Some spinal tuberculosis showed high metabolic value on PET-CT examination, which was easily misdiagnosed as spinal malignancy or metastatic cancer. It may be related to high glucose metabolism around the focal of tuberculosis. The pathological features of spinal tuberculosis were more complex, and the incidence of caseous necrosis, acute inflammation, abscess, exudation, and granulation tissue formation were significantly higher than those of pulmonary tuberculosis. In the pathological diagnosis, we should rule out the possibility of spinal tuberculosis, even if it only shows acute inflammation, abscision, expulsion, or granulomatous tissue formation. We found some differences in both drug resistance and drug resistance gene mutations, suggesting that there may be some differences in treatment options for spinal tuberculosis and other tuberculosis. Before treating spinal tuberculosis, we should test

10.3389/fmicb.2023.1230572

TABLE 4 Comparison of drug-resistant mutation sites between the control tuberculosis group and the spinal tuberculosis group.

Mutational site	Control tuberculosis group (n = 207)	Spinal tuberculosis group (n = 168)	χ^2 values	p-value
RFP				
D516V	32 (15.46)	20 (11.9)	0.981	0.369
D516G	3 (1.45)	0 (0.00)	2.454	0.256
H526Y	0 (0.00)	1 (0.60)	1.235	0.448
S531L	2 (0.97)	3 (1.97)	0.473	0.660
D516V + D516G	13 (6.28)	13 (7.74)	0.305	0.684
D516V + H526Y	1 (0.48)	2 (1.19)	0.585	0.589
D516V + H526D	6 (2.90)	3 (1.79)	0.49	0.737
D516V + S531L	0 (0.00)	0 (0.00)	0.00	0.000
D516V + D516G + H526D	8 (3.86)	7 (4.17)	0.022	1.000
D516V + D516G + S531L	0 (0.00)	1 (0.60)	1.235	0.448
D516V + D516G + H526Y + H526D	6 (2.90)	0 (0.00)	4.949	0.035
D516V + D516G + H526Y + H526D + S531L	5 (2.42)	3 (1.79)	0.176	0.736
D516V + D516G + H526Y + H526D + S531L + S531W	1 (0.48)	6 (3.57)	4.829	0.048
D516V + D516G + H526D + S531L	1 (0.48)	4 (2.38)	2.539	0.178
D516V + H526Y + H526D	1 (0.48)	1 (0.60)	0.022	1.000
D516V + H526Y + H526D + S531L	0 (0.00)	1 (0.60)	1.235	0.448
D516V + H526D + S531L	2 (0.97)	1 (0.60)	0.161	1.000
D516G + H526Y	0 (0.00)	1 (0.60)	1.235	0.448
D516G + H526D	1 (0.48)	1 (0.60)	0.022	1.000
H526Y + H526D	2 (0.97)	1 (0.60)	0.161	1.000
H526Y + H526D + S531L	0 (0.00)	1 (0.60)	1.235	0.448
H526D + S531L	1 (0.48)	0 (0.00)	0.814	1.000
INH				
315 M	120 (57.97)	88 (52.38)	1.618	0.211
-15 M	6 (2.90)	6 (3.57)	0.136	0.773
-15 M + 315 M	25 (12.08)	24 (14.29)	0.398	0.541
STR				
43 M	15 (7.25)	10 (5.95)	0.617	0.282
88 M	41 (19.81)	29 (17.26)	0.396	0.595
43 M + 88 M	14 (6.76)	16 (9.52)	0.96	0.345
EMB				
306 M1	2 (0.97)	4 (2.38))	1.179	0.414
306 M2	36 (17.39)	36 (21.43)	0.974	0.357
306 M1 + 306 M2	11 (5.31)	12 (7.14)	0.539	0.520
306 M2 + 306 M3	0 (0.00)	4 (2.38)	4.982	0.039
306 M1 + 306 M2 + 306 M3	2 (0.97)	3 (1.79)	0.473	0.660

RFP, rifampicin; INH, isoniazid; STR, streptomycin; EMB, ethambutol; D, Aspartate; V, Valine, G, Glycine; H: Histidine, Y: tyrosine, S: serine, L: leucine, W: tryptophan; The value outside the parentheses represents "number of patients," while the value inside the parentheses represents "proportion (%)".

for drug resistance whenever possible, if conditions permit. However, this study does have some limitations. The relatively small number of cervical tuberculosis cases may not fully represent the disease's pathological characteristics. Additionally, the genetic testing failed to detect resistance to second-line anti-tuberculosis drugs, which detracts from its clinical usefulness. In our subsequent studies, we aim to include more cases and expand the scope of testing for drug resistance genes.

In conclusion, the proportion of caseous necrosis, acute inflammation, abscess, exudation, and granulation tissue formation

increased significantly in the spinal tuberculosis group, and the drug resistance characteristics and drug resistance gene mutations were also different from the control tuberculosis group. This study provides important data to support the diagnosis and treatment of spinal tuberculosis.

Data availability statement

The original contributions presented in the study are included in the article/Supplementary material, further inquiries can be directed to the corresponding authors.

Ethics statement

This study was approved by the Ethics Committee of the Chinese PLA General Hospital and was performed in accordance with the principles of the Declaration of Helsinki.

Author contributions

WC and FW participated in research design. RW, YL, and DL participated in the collection of TB cases. SL and YL performed the experiments. RW performed the data analysis. RW and SL participated in the writing of the manuscript. FW and WC performed visualization. RW, HZ, and SL edited language. All authors contributed to the article and approved the submitted version.

Funding

This work was supported by the National Natural Science Foundation of China (nos: 31800814, 32271411).

Conflict of interest

The authors declare that the research was conducted in the absence of any commercial or financial relationships that could be construed as a potential conflict of interest.

Publisher's note

Supplementary material

The Supplementary material for this article can be found online at: https://www.frontiersin.org/articles/10.3389/fmicb.2023.1230572/full#supplementary-material

References

Ali, A., Musbahi, O., White, V. L. C., and Montgomery, A. S. (2019). Spinal tuberculosis: a literature review. *JBJS Rev.* 7:e9. doi: 10.2106/JBJS.RVW.18.00035

Altini, C., Lavelli, V., Niccoli-Asabella, A., Sardaro, A., Branca, A., et al. (2020). Comparison of the diagnostic value of MRI and whole body (18)F-FDG PET/CT in diagnosis of spondylodiscitis. *J. Clin. Med.* 9:1581. doi: 10.3390/jcm9051581

Bhosale, S., Prabhakar, A., Srivastava, S., Raj, A., Purohit, S., and Marathe, N. (2020). Pattern of drug resistance in primary spinal tuberculosis: a single-center study from India. *Glob. Spine J.* 11, 1070–1075. doi: 10.1177/2192568220941445

Chen, L., Liu, C., Ye, Z., Liang, T., Huang, S., Chen, J., et al. (2022). Multiple spinal tuberculosis with severe kyphosis: a case report. *Front. Surg.* 9:815514. doi: 10.3389/fsurg.2022.815514

Diedrich, C. R., O'Hern, J., and Wilkinson, R. J. (2016). HIV-1 and the *Mycobacterium tuberculosis* granuloma: a systematic review and meta-analysis. *Tuberculosis (Edinb.)* 98, 62–76. doi: 10.1016/j.tube.2016.02.010

Furin, J., Cox, H., and Pai, M. (2019). Tuberculosis. *Lancet* 393, 1642–1656. doi: 10.1016/S0140-6736(19)30308-3

Gao, X., Yang, Z. H., Yuan, Z., and Ye, X. D. (2014). Positron emission tomography/computed tomography images of pulmonary and spinal tuberculosis. *Eur. J. Cardiothorac. Surg.* 46:e34. doi: 10.1093/ejcts/ezu212

Izawa, K. (2015). Histological analysis of bone destruction in spinal tuberculosis. *Kekkaku* 90, 415–420.

Jain, A. K., Jaggi, K. R., Bhayana, H., and Saha, R. (2018). Drug-resistant spinal tuberculosis. *Indian J. Orthop.* 52, 100–107. doi: 10.4103/ortho.IJOrtho_306_17

Kubihal, V., Sharma, R., Krishna Kumar, R. G., Chandrashekhara, S. H., and Garg, R. (2022). Imaging update in spinal tuberculosis. *J. Clin. Orthop. Trauma* 25:101742. doi: 10.1016/j.jcot.2021.101742

Kumar, K. (2016). Spinal tuberculosis, natural history of disease, classifications and principles of management with historical perspective. *Eur. J. Orthop. Surg. Traumatol.* 26, 551–558. doi: 10.1007/s00590-016-1811-x

Kumar, V., Neradi, D., Sherry, B., Gaurav, A., and Dhatt, S. S. (2022). Tuberculosis of the spine and drug resistance: a review article. *Neurosurg. Rev.* 45, 217–229. doi: 10.1007/s10143-021-01595-1

Li, S., Chen, W., Feng, M., Liu, Y., and Wang, F. (2022). Drug resistance and molecular characteristics of *Mycobacterium tuberculosis*: a single center experience. *J. Pers. Med.* 12:2088. doi: 10.3390/jpm12122088

Li, Y., Wang, Y., Ding, H., Zhang, N., Ma, A., Shi, J., et al. (2020). Pathologic characteristics of spinal tuberculosis: analysis of 181 cases. *Int. J. Clin. Exp. Pathol.* 13, 1253–1261.

Liu, Z., et al. (2019). Clinical characteristics of 1378 inpatients with spinal tuberculosis in general hospitals in south-Central China. *Biomed. Res. Int.* 2019:9765253.

Mittal, S., Khalid, M., Sabir, A. B., and Khalid, S. (2016). Comparison of magnetic resonance imaging findings between pathologically proven cases of atypical tubercular spine and tumour metastasis: a retrospective study in 40 patients. *Asian Spine J.* 10, 734–743. doi: 10.4184/asj.2016.10.4.734

Mizukoshi, F., et al. (2021). Molecular epidemiology of drug-resistant *Mycobacterium Tuberculosis* in Japan. *mSphere* 6, e00978–e00920.

Moorthy, S., and Prabhu, N. K. (2002). Spectrum of MR imaging findings in spinal tuberculosis. *Am. J. Roentgenol.* 179, 979–983. doi: 10.2214/ajr.179.4.1790979

Pandita, A., Madhuripan, N., Pandita, S., and Hurtado, R. M. (2020). Challenges and controversies in the treatment of spinal tuberculosis. *J. Clin. Tuberc. Mycob. Dis.* 19:100151. doi: 10.1016/j.jctube.2020.100151

Phelan, J., Coll, F., McNerney, R., Ascher, D. B., Pires, D. E. V., Furnham, N., et al. (2016). *Mycobacterium tuberculosis* whole genome sequencing and protein structure modelling provides insights into anti-tuberculosis drug resistance. *BMC Med.* 14:31. doi: 10.1186/s12916-016-0575-9

Rajasekaran, S., and Khandelwal, G. (2013). Drug therapy in spinal tuberculosis. *Eur. Spine J.* 22, 587–593.

Ravimohan, S., Kornfeld, H., Weissman, D., and Bisson, G. P. (2018). Tuberculosis and lung damage: from epidemiology to pathophysiology. *Eur. Respir. Rev.* 27:170077. doi: 10.1183/16000617.0077-2017

Seifert, M., Catanzaro, D., Catanzaro, A., and Rodwell, T. C. (2015). Genetic mutations associated with isoniazid resistance in *Mycobacterium tuberculosis*: a systematic review. *PLoS One* 10:e0119628. doi: 10.1371/journal.pone.0119628

Singh, A., Budhraj, A., Shrivastava, A., Satyavana, A., Gupta, A., Gupta, M., et al. (2014). Current status of anti-tuberculosis therapy: a patent analysis. *Recent Pat. Antiinfect. Drug Discov.* 9, 25–40. doi: 10.2174/1574891X09666140711111800

Suárez, I., Fünger, S. M., Kröger, S., Rademacher, J., Fätkenheuer, G., and Rybniker, J. (2019). The diagnosis and treatment of tuberculosis. *Dtsch. Arztebl. Int.* 116, 729–735. doi: 10.3238/arztebl.2019.0729

Sun, Q., Xiao, T. Y., Liu, H. C., Zhao, X. Q., Liu, Z. G., Li, Y. N., et al. (2018). Mutations within embCAB are associated with variable level of ethambutol resistance in *Mycobacterium tuberculosis* isolates from China. *Antimicrob. Agents Chemother.* 62:e01279–17. doi: 10.1128/AAC.01279-17

Torrelles, J. B., and Schlesinger, L. S. (2017). Integrating lung physiology, immunology, and tuberculosis. *Trends Microbiol.* 25, 688–697. doi: 10.1016/j.tim.2017.03.007

Van Rie, A., et al. (2000). Classification of drug-resistant tuberculosis in an epidemic area. *Lancet* 356, 22–25. doi: 10.1016/S0140-6736(00)02429-6

Vorster, M., Sathekge, M. M., and Bomanji, J. (2014). Advances in imaging of tuberculosis: the role of ^{18}F-FDG PET and PET/CT. *Curr. Opin. Pulm. Med.* 20, 287–293. doi: 10.1097/MCP.0000000000000043

Zaw, M. T., Emran, N. A., and Lin, Z. (2018). Mutations inside rifampicin-resistance determining region of rpoB gene associated with rifampicin-resistance in *Mycobacterium tuberculosis*. *J. Infect. Public Health* 11, 605–610. doi: 10.1016/j.jiph.2018.04.005

Zhang, Q., Xiao, H., and Yan, L. (2021). PCR-reverse blot hybridization assay in respiratory specimens for rapid detection and differentiation of mycobacteria in HIV-negative population. *BMC Infect. Dis.* 21:264. doi: 10.1186/s12879-021-05934-x

frontiers | Frontiers in Microbiology

TYPE Mini Review
PUBLISHED 31 August 2023
DOI 10.3389/fmicb.2023.1231938

OPEN ACCESS

EDITED BY
Saurabh Mishra,
Cornell University, United States

REVIEWED BY
Deepika Prasad,
Memorial Sloan Kettering Cancer Center, United States
Brendon Lee,
Cornell University, United States

*CORRESPONDENCE
Manzoor Ahmad Mir
✉ drmanzoor@kashmiruniversity.ac.in

RECEIVED 31 May 2023
ACCEPTED 14 August 2023
PUBLISHED 31 August 2023

CITATION
Bhat BA, Mir RA, Qadri H, Dhiman R, Almilaibary A, Alkhanani M and Mir MA (2023) Integrons in the development of antimicrobial resistance: critical review and perspectives. *Front. Microbiol.* 14:1231938. doi: 10.3389/fmicb.2023.1231938

Integrons in the development of antimicrobial resistance: critical review and perspectives

Basharat Ahmad Bhat[1], Rakeeb Ahmad Mir[2], Hafsa Qadri[1], Rohan Dhiman[3], Abdullah Almilaibary[4], Mustfa Alkhanani[5] and Manzoor Ahmad Mir[1]*

[1]Department of Bio-Resources, School of Biological Sciences, University of Kashmir, Srinagar, India, [2]Department of Biotechnology, School of Life Sciences, Central University of Kashmir, Ganderbal, India, [3]Department of Life Sciences, National Institute of Technology (NIT), Rourkela, Odisha, India, [4]Department of Family and Community Medicine, Faculty of Medicine, Al Baha University, Al Bahah, Saudi Arabia, [5]Department of Biology, College of Science, Hafr Al Batin University of Hafr Al-Batin, Hafar Al Batin, Saudi Arabia

Antibiotic resistance development and pathogen cross-dissemination are both considered essential risks to human health on a worldwide scale. Antimicrobial resistance genes (AMRs) are acquired, expressed, disseminated, and traded mainly through integrons, the key players capable of transferring genes from bacterial chromosomes to plasmids and their integration by integrase to the target pathogenic host. Moreover, integrons play a central role in disseminating and assembling genes connected with antibiotic resistance in pathogenic and commensal bacterial species. They exhibit a large and concealed diversity in the natural environment, raising concerns about their potential for comprehensive application in bacterial adaptation. They should be viewed as a dangerous pool of resistance determinants from the "One Health approach." Among the three documented classes of integrons reported viz., class-1, 2, and 3, class 1 has been found frequently associated with AMRs in humans and is a critical genetic element to serve as a target for therapeutics to AMRs through gene silencing or combinatorial therapies. The direct method of screening gene cassettes linked to pathogenesis and resistance harbored by integrons is a novel way to assess human health. In the last decade, they have witnessed surveying the integron-associated gene cassettes associated with increased drug tolerance and rising pathogenicity of human pathogenic microbes. Consequently, we aimed to unravel the structure and functions of integrons and their integration mechanism by understanding horizontal gene transfer from one trophic group to another. Many updates for the gene cassettes harbored by integrons related to resistance and pathogenicity are extensively explored. Additionally, an updated account of the assessment of AMRs and prevailing antibiotic resistance by integrons in humans is grossly detailed—lastly, the estimation of AMR dissemination by employing integrons as potential biomarkers are also highlighted. The current review on integrons will pave the way to clinical understanding for devising a roadmap solution to AMR and pathogenicity.

KEYWORDS

antimicrobial resistance, antibiotic stewardship, horizontal gene transfer, integrons, pathogenicity

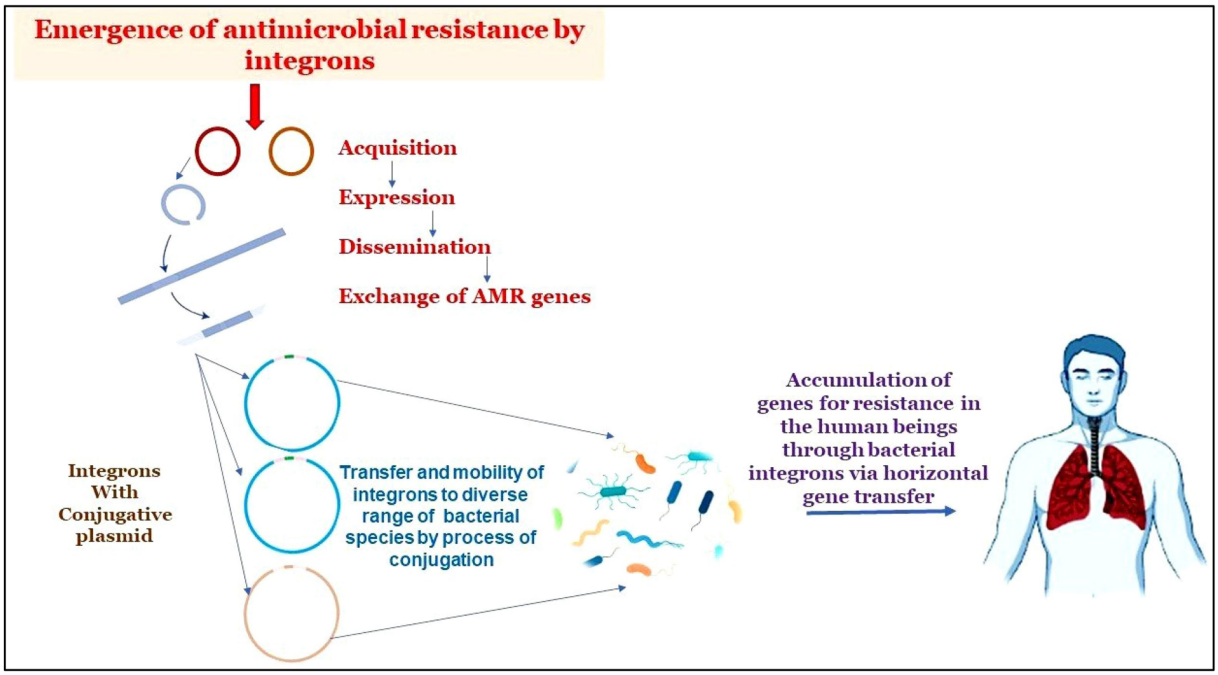

GRAPHICAL ABSTRACT
The graphical abstract displays how integron-aided AMRs to humans: Transposons capture integron gene cassettes to yield high mobility integrons that target res sites of plasmids. These plasmids, in turn, promote the mobility of acquired integrons into diverse bacterial species. The acquisitions of resistant genes are transferred to humans through horizontal gene transfer.

Highlights

- We highlighted the detailed molecular mechanism mediated by integrons to serve as natural cloning and expression vectors to disseminate antimicrobial resistance genes in various microbial species.
- The review emphasizes highlighting integrons as genetic markers for estimating AMR existing in microbial species and their existence in humans.
- The current study underlines the worldwide risk to human health posed by integron-mediated antibiotic-resistance gene cassettes and their transmission to humans.
- The review highlights the spread of AMR through integrons as a global issue. Additionally, we raised concerns about devising strategies to hinder the resistance mechanisms evolved by microbes through the aid of integrons.

Introduction

The mounting threat posed by antimicrobial resistance and engraved pathogenicity on humans forced scientific communities to profoundly investigate the evolution of resistance mechanisms and their responsible agents (Hamdani et al., 2020; Larsson and Flach, 2022; Sheikh et al., 2022). Antibiotic abuse and overuse have resulted in the formation and dissemination of antibiotic-resistance genes (ARGs) and antibiotic-resistant bacteria (ARBs), causing widespread worry around the world in human medicine and livestock breeding (Serwecińska, 2020; Mir et al., 2021; Sheikh et al., 2021b). Since ARGs are commonly found in domestic sewage, mud/dirt, and animal waste in these environments, these ecosystems are considered key reservoirs for ARGs (Wellington et al., 2013; Ding et al., 2019) to many bacterial species, particularly to those causing disease. The ultimate, well-known effects of such accumulated evolutionary events are gradually growing challenges in preventing and treating bacterial diseases. Understanding and recognizing human, animal, and environmental microbiota relationships is crucial because bacteria and genes frequently cross habitats and species boundaries "One Health Concept" (Collignon, 2012; Zinsstag et al., 2012; So et al., 2015; Torren-Edo et al., 2015; World Health Organization, 2015; Collignon and McEwen, 2019) to manage this global health challenge (Wellington et al., 2013; Berendonk et al., 2015; Bengtsson-Palme et al., 2018). Antimicrobial resistance is an ecological issue that affects the wellbeing of people, animals, and the environment. It is characterized by complex interactions involving many microbial populations (Fletcher, 2015; Collignon and McEwen, 2019).

The establishment and prevalence of antimicrobial resistance are caused by various resistance mechanisms, which may be divided into genetic mutation occurring at a low frequency and acquisition of different genes mediated resistance to their host microbes. As a result, it has been determined that acquiring resistance genes is a significant factor in antibiotic resistance's widespread distribution and spread. The resistance is accomplished through vertical or horizontal transfer, with the latter method involving mobile genetic elements like plasmids and transposons (Xu et al., 2011b). Integrons are primarily carried by plasmids or contained within transposons, and their mechanism and function in the movement of microorganisms are well-known and documented (Hall and Collis, 1995; Mazel, 2006), which had also been considered to contribute to the unleashing of "Super Bugs" (Xu et al., 2011b,c).

The exchange of genetic material between bacteria of the same generation is known as horizontal gene transfer (HGT). The heredity of the transferred sequences in the recipient microbe is also crucial for a successful HGT event, in addition to the entry of DNA into the cytoplasm of the recipient cell (Ochman et al., 2000). HGT influences bacterial population's genetic diversity and evolutionary trajectories. For instance, the main factor causing the establishment, recombination, and spread of multidrug resistance among bacterial pathogens is the HGT of mobile genetic elements (MGEs) (Nakamura et al., 2004; Thomas and Nielsen, 2005). MGEs are widespread in bacterial populations due to their ability to physically migrate between host genomes. MGEs include plasmids, bacteriophages, genomic islands (GIs), transposons (Tns), integrons, insertion sequences (ISs), integrative and conjugative elements (ICEs), and tiny inverted-repeat transposable elements, among others (MITEs) (Stokes and Gillings, 2011).

Mobile genetic elements (GEs), such as integrons, may be critical in transferring ARGs across microbial organisms in their surroundings. Integrons may extract ARGs from their surroundings and subsequently incorporate them into their gene cassettes via location-specific recombination (Zhang et al., 2009; Sheikh et al., 2021a). Integrons are thus crucial in developing antibiotic tolerance and the horizontal gene transfer (HGT) of ARGs between bacterial organisms in diverse settings. The discovery of mobile integrons as critical players in the acquisition, mobilization, shuffle, and initiation of expression of gene cassettes, especially those encoding antibiotic resistance (Domingues et al., 2012; Escudero et al., 2015). The genetic elements known as integrons have a location-specific recombination system that enables them to acquire, express, and transfer particular DNA fragments known as gene cassettes (Hall and Collis, 1995).

Integrons are genetic elements that contain a site-specific recombination system able to integrate, express and exchange specific DNA elements, called gene cassettes (Hall and Collis, 1995). The integron is not regarded as a mobile element because it lacks mobility-related functions. In contrast, the gene cassettes contained in integrons are regarded as mobile, even though the spontaneous exchange of gene cassettes is rarely observed experimentally (Guerin et al., 2009; Baharoglu et al., 2010). Nevertheless, sequence-similar integrons appear widespread among bacterial species and genetic backgrounds, suggesting that they are frequently exposed to mechanisms that allow them to disseminate horizontally through bacterial populations (Stokes and Hall, 1989).

The present review article aimed to update the account of gene cassettes harbored by integrons on resistance and pathogenicity and searched to assess existing AMRs and antibiotic resistance by integrons in humans. Lastly, estimating AMR dissemination by employing integrons as potential biomarkers is also highlighted to have an in-depth role in global AMR dissemination. We believe this review will help to understand better how to develop a plan to minimize the global phenomenon of increasing antimicrobial resistance and pathogenicity related to human pathogenic microbes.

Integrons

An integron is generally defined by the presence of an integrase gene (*intI*) and a proximal primary recombination site (attI) (Figure 1; Partridge et al., 2009; Xu et al., 2011a). Structurally, all integrons consist of three main components, including 5′ and 3′ conserved segment and a central variable region between the 5′ and 3′ zone, in which integrons are responsible for the capture and expression of exogenous genes, which are part of the gene cassette. Integrons are accountable for capturing and expressing the exogenous genes that form the gene cassette in this central variable region (Mazel, 2006). The first component of the integron is a gene which produces a tyrosine recombinase (integrase, encoded by the intI gene), required for site-specific recombination inside the integron. The second component is an adjacent recombination site (attI), which the integrase recognizes. The third component is a promoter (Pc), which is situated upstream of the integration and required for the effective process of transcription and expression (Mazel, 2006; Labbate et al., 2009). The promoter aids in the expression of any integrated gene(s). The tyrosine-specific recombinase family, which also comprises the well-known integrase of the λ-phage, includes integrase (IntI) (Grainge and Jayaram, 1999; Carattoli, 2001).

These three components are simple structures with a single open reading frame (ORF) surrounded by a cassette-associated recombination site. They were initially called 59-base elements but are now referred to as *attC* (Gillings, 2014). While the Pc promoter is believed to be present and active in all forms of integrons, this has not been demonstrated for all of them (Ghaly et al., 2021a). Numerous integrase genes found in integrons have LexA binding sites close to their promoter regions allowing them to be regulated by the host LexA protein, which functions as a transcriptional repressor of the SOS response; as demonstrated for a class 1 integrase and in an integrase present in a CI (chromosomal integron) of *Vibrio cholerae* (Guerin et al., 2009; Baharoglu et al., 2010). These findings show that SOS induction can result in increased integrase gene transcription and activity and cassette rearrangements in organisms possessing lexA alleles (Baharoglu et al., 2010) The modulation of integrase transcription is unknown without a LexA ortholog. Integrons might have a single gene cassette or many of them (Hall and Collis, 1995). In most clinical bacterial strains, integrons have no more than 5 cassettes (Bennett, 2008), but integrons containing at least 9 genes for antibiotic tolerance have also been found. (Naas et al., 2001). The INTEGRAL database[1] containing a list of numbered C1 integrons is available (Moura et al., 2009).

Initially, integrons were grouped into a few categories based on their genetic similarity to the integrase intI gene sequence, with classes 1, 2 and 3 receiving major attention (Nield et al., 2001; Domingues et al., 2012). Nevertheless, more DNA sequencing-based research have revealed more of the integrase gene's genetic diversity and discovered over 90 distinct gene variations, questioning the initial classification system in doubt (Gillings et al., 2008; Domingues et al., 2012). Class 4 integron was discovered later in a relationship with chromosomal integrons. *IntI* encodes an integrase (IntI) of the tyrosine recombinase family, which is distinguished by the presence of invariant RHRY (with Y being the catalytic tyrosine) amino-acids in the conserved motifs named box 1 and box 2 (which distinguish intI from other XerC-related integrases) (Xu et al., 2011a). IntI-catalyzed recombination between attI and/or attC sites results in the insertion or excision of cassettes (Figure 1). The class 1 integrase (IntI1) recognizes three types of recombination site: attI1, attC and secondary sites. Binding domains

1 http://integrall.bio.ua.pt/

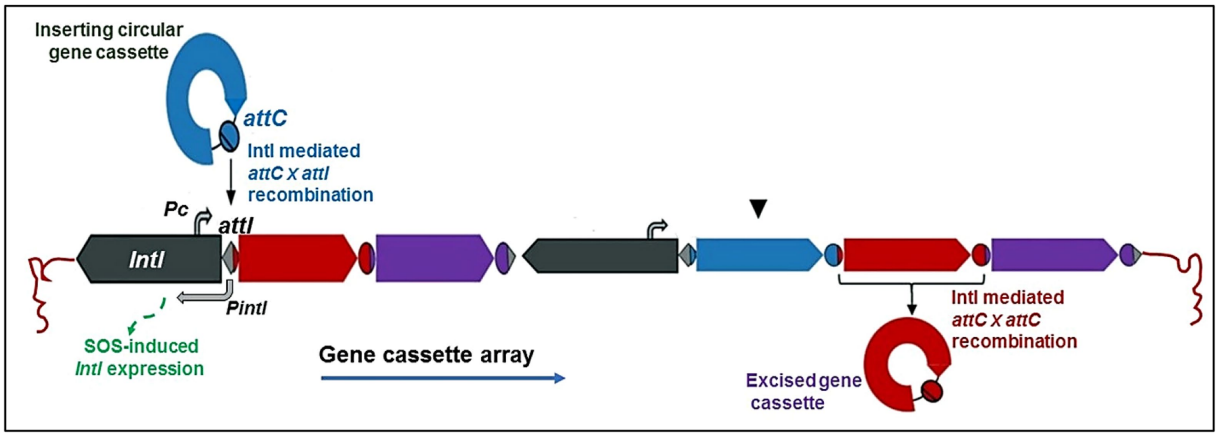

FIGURE 1
Schematic representation of a class 1 integron. The basic integron platform consists of the following: intI, a gene for the integron integrase; Pc, an integron-carried promoter; attI, the integron-associated recombination site; and gene cassettes, sequentially inserted into an array via recombination between attI and the cassette associated-recombination sites, attC (Gillings, 2014; Ghaly et al., 2020a).

and consensus sequences have been determined for these. The attI1 site is a simple site which contains two inverted sequences that bind the integrase and two additional integrase-binding sites known as strong (DR1) and weak (DR2) (Francia et al., 1999; Hall et al., 1999).

Further, Integrons are categorized into 3 primary categories based on their phylogenetic analyzes of sequenced intI genes: the marine γ-proteobacteria group, the soil/freshwater proteobacteria group, and the inverted integrase group (Domingues et al., 2012). C1 integrons are the most common and pervasive, especially in clinical environments, and significantly contribute to the development of antibiotic tolerance (Amin et al., 2021). Although the origin of C1 integron is unknown, it is hypothesized to have existed in different bacterial species before the "antibiotic age (Stokes et al., 2006)." C1 integrons are present in the environment without antibiotic-resistant genes. The initial source of these genomic structures has been speculated to be beta proteobacteria. Tn*402* (also known as Tn*5090*) characteristic features are absent in such types of environmental integrons suggesting that they were integrated into a plasmid-borne Tn*402* transposon carrying a gene cassette imparting host advantage (Gillings et al., 2008). For instance, the *qac* gene, which imparts resistance to quaternary ammonium compounds and thus biocides, has a long history of use in clinical usage; and the su1I gene, confers resistance to sulphonamides. The early association of the Tn*402* transposon's progenitor with a class 1 integrase and an attI1 site is another possible origin of the C1 integrons. Most C1 integrons have the 5'-CS region in the same location (Toleman and Walsh, 2011). The 3'-CS region is thought to be the result of a fusion of the Tn402 transposon's *qacE* gene with the su1I gene, followed by partial deletion of the *qacE* gene; this fusion occurred simultaneously with a deletion event in the Tn*402* transposon's transposition functions, resulting in a structure incapable of self-mobilization (Toleman and Walsh, 2011). Although a few C1 integrons with a complete transposition module have been found, the bulk of C1 integrons are transposons with incomplete transposition modules (Juan et al., 2010; Marchiaro et al., 2010). After the initial generation of C1 integrons, intense selection for antimicrobial tolerance favored the detection of antibiotic tolerance gene cassettes giving rise to the C1 integron components that are familiar to us today (Bennett, 2008; Stokes and Gillings, 2011).

Integrons are further categorized according to their environment, with two distinct types: mobile integrons (MIs) and chromosomal integrons (CIs) (Liebert et al., 1999). CIs are composed of a variable number of gene cassettes between zero and hundreds, the majority of which do not contribute to antimicrobial drug tolerance. Although migration of gene cassettes from CIs has been recorded, CIs are considered sedentary (Liebert et al., 1999; Domingues et al., 2012). In comparison, MIs like C1 integrons carry a restricted number of gene cassettes and are frequently engaged in antimicrobial tolerance propagation (Domingues et al., 2012).

attC SITES

The *attC* domain consists of 2 simple sites, R″ and R′, L′ and L″, respectively, each made up of two conserved "core sites" (7 or 8 bp) (Bouvier et al., 2005). The RH consensus sequence has several connections to the RH simple site and includes the R′ and R″ sites. Similarly, the L′ and L″ parts of the LH consensus sequence are structurally and functionally similar to the LH. The integrase's ability to distinguish among the LH and RH sites in the attC could describe the position of integrated gene cassettes. Additionally, it looks as though L″ is more significant in terms of orientation (Bouvier et al., 2005). In addition to being necessary for orientation, the LH simple site promotes RH activity. (Partridge et al., 2009). A framework known as a gene cassette, typically not detectable during integrations but becomes an essential part of the integron once integrated, connects the *attC* sites to a single ORF in most cases (Deng et al., 2015).

Gene cassettes

Gene cassettes are small movable components carrying a single gene, typically without a promoter or recombination site (*attC*). Gene cassettes are linear when integrated into the C1 integron but circular when left unintegrated or before site-specific insertion (Domingues et al., 2012). They can appear as a separate circular DNA molecule that

cannot be maintained stable throughout cell division or as a linear DNA molecules formed when the free circular element is inserted into the integron in a particular orientation (Mazel, 2006). Prior research has shown that the structural nature of integrons usually lacks cassettes in the variable area (Deng et al., 2015).

Gene cassettes generally lack promoters, although having a coding sequence, which acts as the system's mobile component, and the majority of cassettes encode resistance to a wide variety of antibiotics, with over 130 different antibiotic resistance genes identified to date through distinctive *attC* sites (Hall and Collis, 1995). Most antibiotic families, such as -lactams, rifampicin, etc., and antiseptics from the quaternary ammonium compound family, are resistant to such cassettes (Hall and Collis, 1995).

Site-specific insertion of gene cassettes into the integron

The integration of circular gene cassettes occurs by site-specific recombination between *attI* and *attC*, assisted by the integron integrase. The first resident gene cassette's 5′ end should be the target of insertion. The attI site in the 5'-CS conserved segment of the integron and the *attC* site in the 3'-CS conserved segment of the integron are the two key recombination sites where the integrase interacts with each gene cassette. For four sites inside the attI site, IntI has a high binding affinity (Partridge et al., 2018). It also weakly binds to the cassette's *attC* site (Holmes et al., 2003). This procedure is reversible, and cassettes can be removed as free circular DNA elements (Johansson, 2007). Insertion at the attI site enables the expression of an incoming cassette driven by the neighboring Pc promoter (Razavi et al., 2017). As a tool for genomic innovation, the integron system offers two significant benefits. The bacterial genome initially incorporates additional genetic material through a specialized recombination site (attI) that inhibits the breakdown of existing genes. Secondly, the integron promoter (Pc), via which the freshly integrated gene is expressed, triggers the beginning of natural selection. Any newly generated variants will consequently instantly activate genes resulting in beneficial phenotypes in a population of cells with integrons, each with a unique gene cassette (Michael et al., 2004).An additional site in front of a gene not formerly present on cassettes may result in site-specific recombination between the attI and this secondary site, trapping the gene. The acquisition of the *attC* site, which is most likely achieved by a second stage of recombination from an existing gene cassette, is required to create a full cassette containing the new gene. Almost any gene may become an integron, although secondary-site recombination is uncommon and less effective than primary-site recombination. Integrons are further classified into two classes based on the genomic context of those genes: chromosomal integrons, which are found inside the bacterial chromosome, and mobile integrons, which are associated to transposons (Antelo et al., 2021; Sandoval-Quintana et al., 2022).

Mobility of integron: spreading resistance genes on a global scale

Integrons have been reported to be widespread and found across clinical species, and their movement has been cited as a primary source of concern for clinical antibiotic resistance. Integrons are connected with mobile DNA elements (transposons or plasmids) and antibiotic-tolerance genes, despite their small array dimensions and considerable heterogeneity in the sequence of *attC* sites (Verraes et al., 2013; Partridge et al., 2018). Although self-transposition is defective, existing integrons (mainly class 1 integrons) were thought to represent a potentially mobile genetic element. They're typically seen on plasmids to aid conjugative transfer. They include mobile gene cassettes that can move to other integrons or secondary locations in the bacterial genome (Figure 2). Integrons may carry and propagate antibiotic tolerance genes, making them one of the most significant horizontal transfer pathways for transmitting tolerance/resistance genes across bacteria.

Integrons are a naturally occurring system of capturing and construction enabling microbes to incorporate gene cassettes and then correctly express them to transform them into functional proteins. Gene cassettes can be formed from various ORFs, and it is essential to understand how this process works. To allow for quick adaptability to selection pressure and hence boost the host's overall fitness and advantage, integrons may be able to interchange and stockpile functioning gene cassettes forever (Yu et al., 2013; Deng et al., 2015). Frequent gene cassette arrays in various integron types and their impact on antimicrobial tolerance in various species of bacteria is depicted in Table 1.

Furthermore, several reservoirs and genetic pools for integron, shared between bacteria, may be provided by mobile genetic elements, e.g., transposons, insertion sequences, etc. (Partridge et al., 2018). Integrons are essential for the spread and dispersion of genes associated with resistance. They transfer resistance genes to various drugs between bacteria (Deng et al., 2015). According to numerous findings on integrons from environmental microorganisms, including the high sequence diversity seen and the numerous functional products other than tolerance coded by these cassettes, integrons may have performed significantly in development and expansion for an extended period (Rendueles et al., 2018).

Horizontal gene transfer and integrons

The primary mechanism by which antibiotic resistance spreads is horizontal genetic transfer (Sundström, 1998). Antibiotic resistance genes can also be transmitted via a variety of other mechanisms. One of the most significant forces influencing the development of microorganisms is horizontal gene transfer, or the acquiring of foreign deoxyribonucleic acid by microbes (Il'ina, 2003). It frequently causes the emergence of antibiotic tolerance (Huddleston, 2014; Ma et al., 2017). In clinical practice, most antimicrobial drugs come from or are derived from substances naturally found in the environment, primarily soil. Bacteria in the same domain as these compounds can pick up environmental genes for antibiotic tolerance. There is compelling evidence that this "environmental resistome" can be a rich source for acquiring antibiotic-tolerance genes in bacteria that are relevant to human health (Munita and Arias, 2016). This exchange of genetic material has been particularly linked to the spread of antibiotic tolerance to several widely used antibiotic drugs. The traditional methods by which bacteria acquire external genetic material are (i) transformation (the integration of bare DNA) (Venema, 1979; Johnston et al., 2014), (ii) transduction (mediated by phages) (Ozeki and Ikeda, 1968), and (iii) conjugation (Curtiss Iii, 1969). HGT, which

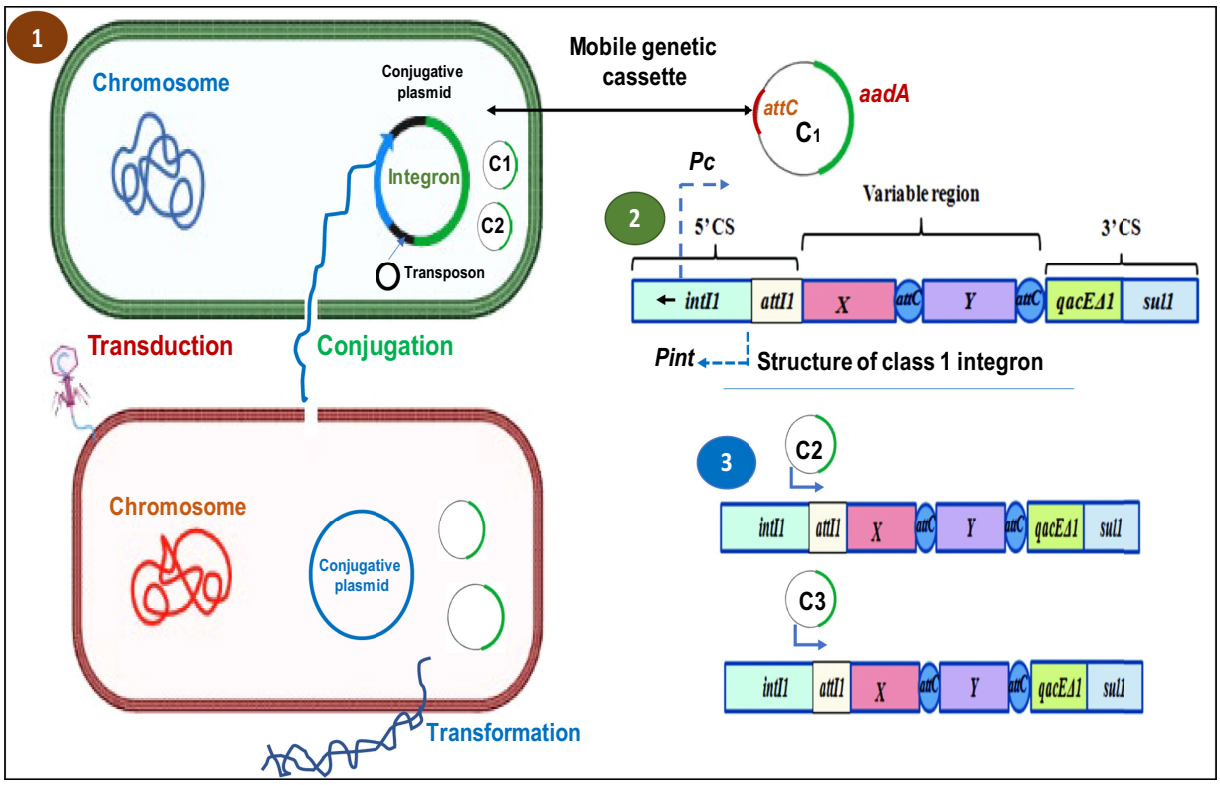

FIGURE 2
Schematic representation of HGT mechanisms in bacteria and the general structure of an integron and gene cassette. (1) HGT mechanism (conjugation, transduction and transformation) in bacteria. (2) The genetic organization of the class 1 integron DNA sequence includes the integrase gene (IntI) and one cassette gene. While the cassette array is expressed from the PC promoter, the integrase is expressed from the Pint promoter. (3) The orientation of insertion of the following genomic cassettes (C2, C3) into the integron structure. It is believed that as a gene is moved further away from the PC promoter, its expression level within the cassettes will decrease (Racewicz et al., 2020).

TABLE 1 Frequent gene cassette arrays in various integron types and their impact on antimicrobial tolerance in distinct species of bacteria (Sabbagh et al., 2021).

Bacteria	Integrons	Gene cassettes	Antibiotics associated with gene cassettes	References
Acinetobacter baumannii	I, II	bla_{CARB-2}, aadA1, aadA2, aadB, dfrA1, dfrA7, dfrA1-gcuF, dfrA1- aadA1, dfr17-aadA5, dfr12-gcuF-aadA2, sat1.	Extended Spectrum Beta–Lactamase, Aminoglycosides, Trimethoprim	Liu et al. (2014), Domingues et al. (2015), and Akrami et al. (2017)
Klebsiella spp.	I, II, III	bla_{CARB-2} bla_{GES-1}, aadA, aadA1, aadB, dfrA1, dfrA7, dfrA1-gcuF, dfrA1- aadA1a, dfr17-aadA5, dfr12-gcuFaadA2.	Extended Spectrum Beta-Lactamase, Trimethoprim, Aminoglycosides,	Wu et al. (2013) and Domingues et al. (2015)
Enterobacter spp	I	aadA1a, aadA2, dfrA7, dfrA1-aadA1a, dfr17-aadA5, dfr12-gcuF-aadA	Aminoglycosides, Trimethoprim	Marathe et al. (2015)
Enterococcus faecalis	I	aadA1a, dfr12-gcuF-aadA2, dfrA1- sat1-aadA1.	Aminoglycosides, Trimethoprim	Sabbagh et al. (2017)
Pseudomonas aeruginosa	I	aadA2, aadB, dfr17-aadA5, dfr12-gcuF- aadA2.	Aminoglycosides, Trimethoprim	Ghaly et al. (2020a)
Staphylococcus aureus	I	aadA1, aadA2, dfr17-aadA5, dfr12- gcuF-aadA2, aacA4-cmlA1	Aminoglycosides, Trimethoprim, Chloramphenicol	Sow et al. (2010)
Escherichia coli	I, II, III	aadA1, aadA2, aadA5 aadB, dfrA1, dfrA5, dfrA7 dfrA12, dfr14, dfrA17, dfrB2, dfrA1-gcuC, dfrA1-aadA1, dfr17-aadA5, dfr12-gcuF-aadA2, dfrA1-sat1-aadA1, dfrA1-sat2-aadA1, estX-sat2-aadA1, blaOXA-101-aac (6′)–Ib, ere2.	Aminoglycosides, Trimethoprim, Extended Spectrum BetaLactamase, Erythromycin.	Kadlec and Schwarz (2008) and Kargar et al. (2014)
Salmonella spp.	I, II	aadA, aadA1a, aadA2, aadA5, aadB, dfrA1, dfrA7, dfrA12, dfrA17, dfrA1- gcuF, dfrA1-aadA1a, dfr17-aadA5, dfr12-gcuF-aadA2, bla_{CARB-2}.	Aminoglycosides, Trimethoprim, Extended Spectrum BetaLactamase.	Antunes et al. (2006) and Domingues et al. (2015)

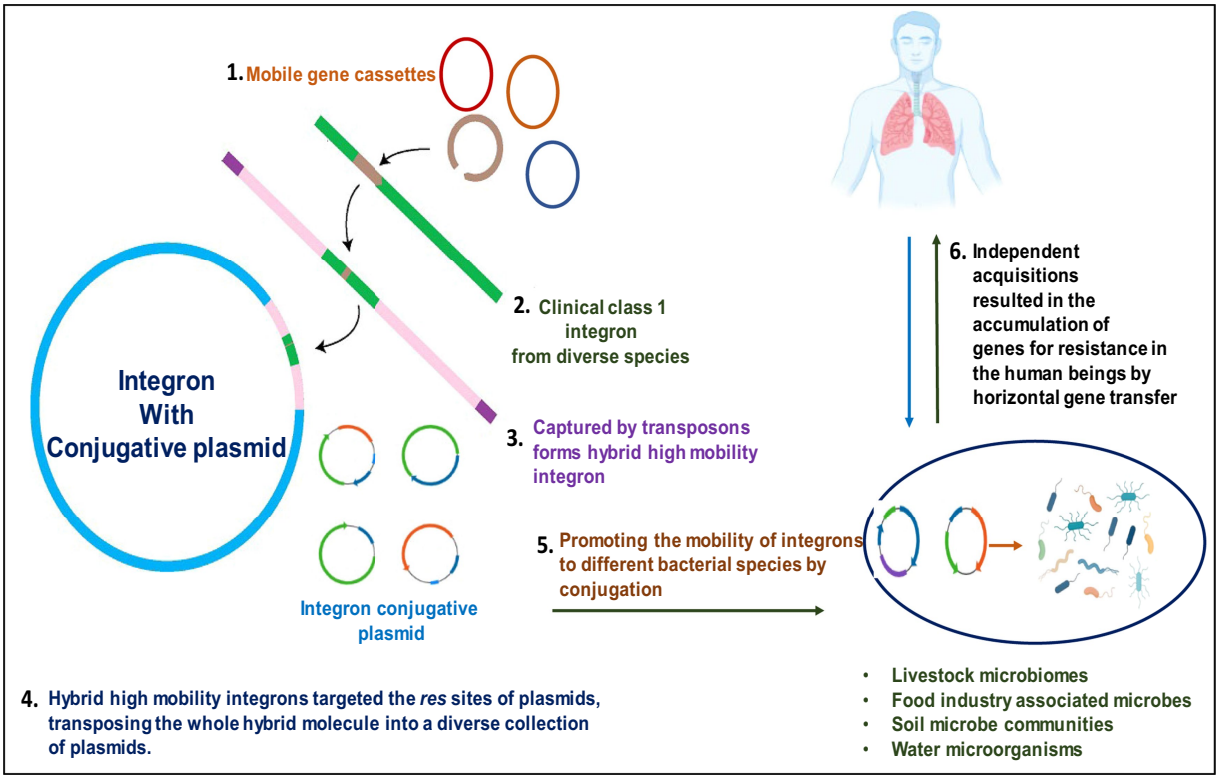

FIGURE 3
Pictorial representation of integron-aided AMRs to humans: (1) transposons capture integron gene cassettes to yield high mobility integrons that target res sites of plasmids. (2). These plasmids, in turn, promote the mobility of acquired integrons into diverse bacterial species. (3). The acquisitions of resistant genes are transferred to humans through horizontal gene transfer.

involves transformation, is by far the most straightforward. However, only a few clinically significant bacterial species can "naturally" incorporate bare DNA to evolve antibiotic tolerance. Conjugation, a reliable method of DNA transfer that includes cell-to-cell contact and is expected to happen often in the human intestinal tract undergoing antibiotic therapy, is a prevalent reason for tolerance in the hospital setting. Although direct chromosome-to-chromosome transfer has been widely characterized, conjugation typically uses Mobile Genetic Components (MGEs) to convey important genetic information (Nwosu, 2001). Plasmids and transposons are the two most important MGEs because they substantially contribute to developing and expanding antibiotic resistance in therapeutically relevant organisms. The most effective methods for assembling antimicrobial tolerance genes are integrons, site-specific recombination systems that can attract open reading frames within mobile gene cassettes. Integrons offer a powerful and relatively straightforward method for adding novel genes to bacterial chromosomes and the tools needed to monitor their expression. They also promote beneficial genetic exchange and are a significant force in the development of bacteria (Munita and Arias, 2016).

Integrons are a type of genetic component which allow exogenous genes to be efficiently captured and expressed and transfer the resistance genes through transposons and plasmids into bacterial species, which can inhabit humans (Figure 3). Their contribution to the antibiotic resistance expansion, particularly among bacteria, is well established. (Boucher et al., 2007). However, it is clear that integrons have a long evolutionary history dating back to their discovery in clinical settings and are a typical component of bacterial genomes. Integrons have been found in many habitats, can transfer between different species and lineages throughout evolutionary history, and can access a sizable number of new genes whose roles are primarily unknown. Integrons are much more significant than just being a characteristic of infections resistant to antibiotics, as evidenced by their function in bacterial adaptability and genome development in natural settings (Boucher et al., 2007).

Human integron-antibiotic resistance gene cassettes: a rising threat

The resistance to antibiotics by microbe's accounts for thousands of human deaths annually on a global scale and is continually increasing as a major threat to humans. Predictably, all the sections of researchers initiate the fight against antibiotic resistance, be it clinical settings, communities, or even agricultural systems, targeted to lower the prevention and transmission of antibiotic tolerance from one interface to another. To overcome this issue, several researchers have suggested initiating a "One-Health approach" to have a holistic viewpoint on antibiotic resistance at the level of animals, including humans, and dissemination patterns or routes in the environment (Collignon, 2013; So et al., 2015; Figure 4). Immense variability in genetic makeup, the higher opportunity for mutations, gene rearrangements, and horizontal gene transfer in microbes result in the higher establishment of microbial tolerance. These resistance genes are

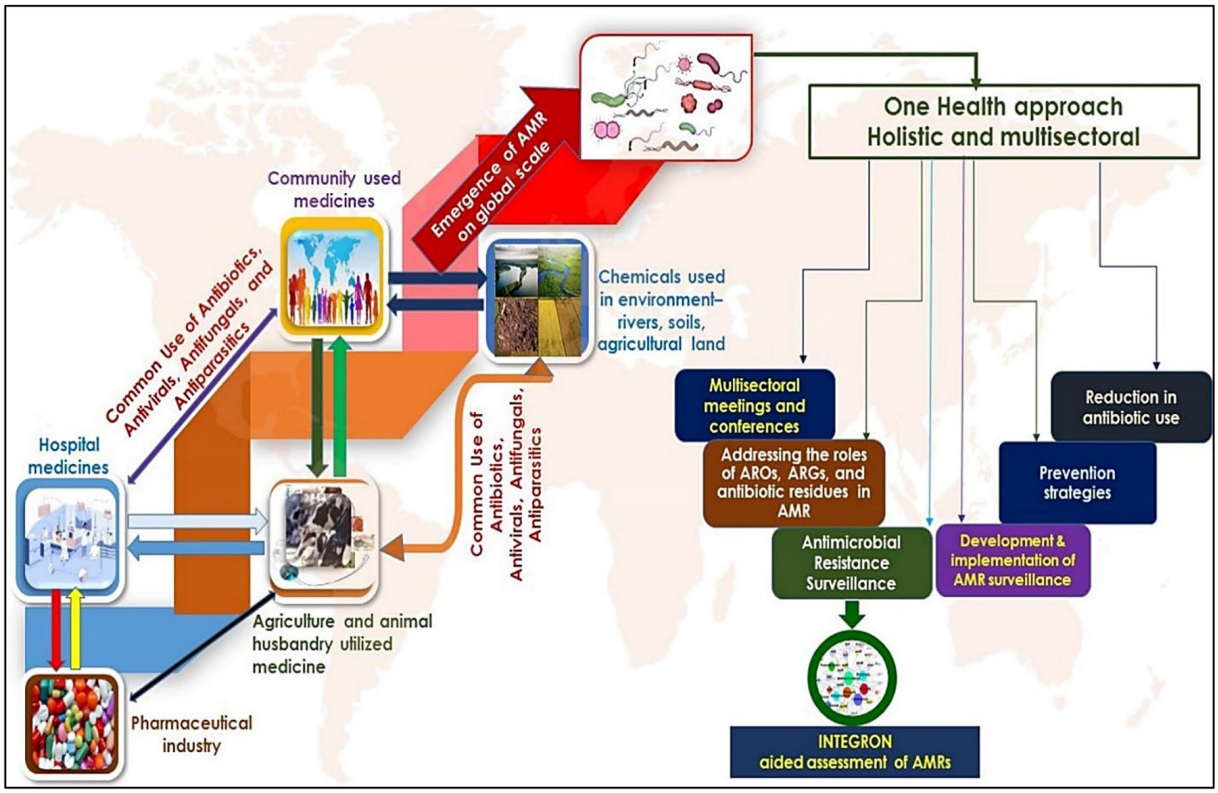

FIGURE 4
Dissemination and evolution of AMRs- the left side of the figure shows the routes through which antimicrobial resistance is developed and transmitted to different levels. Environmental habitats such as rivers, streams, and agricultural settings play a critical role in acquiring additional AMRs mainly disseminated by humans. The right panel of the figure shows the significance of the 'One Health Approach' in addressing the systematic assessment and clinical measures to control the AMRs, most especially by using integrons.

mobilized by mobile genetic factors, e.g., integrons. They are found in diverse habitats carried by various species of bacteria (Cury et al., 2016; Ghaly et al., 2019; Antelo et al., 2021; Dias et al., 2021). For instance, Dias et al. (2021) employed deep sequencing to explore the integron gene cassettes through studies of intI-*attC* amplicons. Integrons harboring antimicrobial resistance are critical in disseminating AMR genes through horizontal transfer via transposons and plasmids to develop multi-resistance (Roe et al., 2003; Gaze et al., 2013). The importance of tracing the resistome in colonizing the human gastrointestinal tract and cattle was investigated by the "One Health" approach, Chainier et al. (2017) by employing integrons as instrumental tools to assess the AMR carriage. The "One-Health approach" approach aims to promote the investigation of AMR dissemination through the integration of human health in conjunction with other animals (Chainier et al., 2017). Human feces samples are submitted to a high-throughput sequencing-based metagenomic analysis to study the prevalence and range of AMRs (Zhang et al., 2011; Ma et al., 2014, 2016).

Moreover, culture-dependent and culture-independent approaches are employed in checking the dissemination and surveillance of AMR (Chainier et al., 2017). Since integrons have remarkably evolved as potential markers to identify the AMRs in human digestive carriages, it is reported that integrons coding antibiotic resistance genes are copiously reported in commensal *E. coli* from human hosts on antibiotics doses (Kheiri and Akhtari, 2016).

Class 1 integrons are found most commonly out of all the different types of integrons. Several studies suggest that integrons are detected in various phyla such as *Actinobacteriota, Acidobacteriota, Cyanobacteria, Bacteroidota, Chloroflexota, Firmicutes, Campylobacterota, Chrysiogenetota, Desulfobacterota, Gemmatimonadota, Proteobacteria, Planctomycetota, Spirochaetota,* and *Verrucomicrobiota* (Cury et al., 2016; Parks et al., 2018; Table 2).

Class 1 integron is the most abundant and clinically significant. Class 1 integrons are crucial in disseminating AMR genes due to their higher mobility, distribution, and abundance than class 2 and 3 (Table 3; Gillings et al., 2008; Ghaly et al., 2021b). The present research on integrons has been on class 1 integrons, with gram-negative bacteria being the primary importance. The earliest multidrug resistance plasmids identified in the 1950s contained class-1 MIs. Latest research has shown that a significant proportion of isolates of *Acinetobacter baumanii*, *Pseudomonas aeruginosa*, *E. coli*, and *Klebsiella pneumoniae* have class 1 integrons (Cambray et al., 2010).

The clinical class 1 integron-integrase gene, intI1, is a good indicator of pollution because: (1) it is connected to genes that confer resistance to antibiotics, disinfectants, and heavy metals; (2) it is found in a wide range of pathogenic and nonpathogenic bacteria; (3) its abundance can change quickly because its host cells can have quick generation times; and (4) a single DNA sequence can measure the relative abundance of multiple bacteria (Gillings et al., 2015).

TABLE 2 Class 1 integron incidence and predominance of Gram-positive and Gram-negative microbial species (Deng et al., 2015).

Gram-negative bacterial strain	Class 1 Integron prevalence and the wide range of gene cassettes	Sampling	References
Vibrio cholera	44/176; *aadB-aadA2-blaP1-dfrA1-dfrA15*	Thailand	Dalsgaard et al. (2000)
Pseudomonas aeruginosa	45.8% (54/118)	Preliminary study in Guangzhou, China	Xu et al. (2009)
Burkholderia	29.4% (5/17); *oxa-aac* (6′-1a)	Ireland	Crowley et al. (2002)
Campylobacter	62/378	Ireland	Shin et al. (2015)
Escherichia coli	59.5% (355/597)	South Thailand	Vinué et al. (2008)
Escherichia coli		Preliminary study in Guangzhou, China	Xu et al. (2011b)
Serratia	1/30; *aacC1-ORFX-ORFY-aadA1*	Canada	Crowley et al. (2008)
Salmonella	36.2% (34/94); *aadA2-bla* (*PSE*-1) (61.76% 21/34); *aadA1-aadA2-bla* (*PSE*-1) (38.23%,13/34)	Animals, Japan	Ahmed et al. (2006)
Stenotrophomonas maltophilia	22% (20/93)	Kaohsiung Medical University	Chang et al. (2004)
Salmonella enteritidis	11.9% (59)	Taiwan	Huang et al. (2013)
Aeromonas	16/41 (39.02%); *dfrA15-cmlA4-aadA2*	Hidalgo, Mexico	Pérez-Valdespino et al. (2009)
Enterobacteriaceae	50/226	Addenbrooke's Hospital	Machado et al. (2008)
Escherichia coli	4/32 (12.5%); *sat-1-aadA*	Meat and meat products, Norway	Sunde (2005)
Klebsiella Pneumoniae	18/26	Bloodstream infections	Xu et al. (2011a)
Shigella	*EstX-aadA1* (3.85%, 1/26)	Hiroshima prefecture, Japan; 2000–2004	Ahmed et al. (2006)
Pseudomonas aeruginosa	High prevalence	Iran	Shahcheraghi et al. (2010)

TABLE 3 Class 2, 3, and 4 integron incidence and predominance in Gram-positive and Gram-negative microbial species (Deng et al., 2015).

Class 2 integrons			
Bacterial strain	Integron prevalence and the wide range of gene cassettes	Sampling	References
Escherichia coli	7.4% (31/417); *dfrA1-sat2-aadA1* (77.4%, 24/31), *estX-sat2-aadA1* (19.4%, 6/31) and *estX-sat2-△aadA1* (3.2%, 1/31)	BfT-GermVet monitoring study, Germany, 2004–2006	Kadlec and Schwarz (2008)
Enterobacteriaceae	34.9% (52/149); II2 (Tn7), III2 (*estX-sat2-aadA1-orfX*, most widely distributed) and IV2 (*aadA1*, first reported)	*E. coli* and *K. pneumoniae* strains from swine and chickens, Portugal	Machado et al. (2008)
Escherichia coli	One out of 322	Irrigation water and associated sediments, El Paso, Presidio and Weslaco	Roe et al. (2003)
Escherichia coli	3.0% (3/100)	Spain	Vinué et al. (2008)
Escherichia coli	3.6% (4/111); *dfrA1-sat1-aadA1*	The preliminary study, Guangzhou, China	Su et al. (2006)
Coliforms	2.7% (5/183)	Rivers in the northern region of Turkey	Ozgumus et al. (2009)
Pseudomonas aeruginosa	19.5% (23/118); *dfrA1-sat1-aadA1*, first report of class 2 integron in this species of bacteria	A preliminary study, Guangzhou, China	Xu et al. (2009)
S. enteritidis	4.3%; *estX-sat2-aadA1*	Poultry samples, Japan	Ahmed et al. (2005)
S. enterica	85 contemporary multidrug resistants D-Tartrate-Positive isolates; *dfrA1-sat1-aadA1*	*S. enterica* Serovar Paratyphi B isolates Germany, 1995–2001	Miko et al. (2003)
S. sonneii	93% (2/43)	Senegal adults diagnosed with diarrhea	Gassama-Sow et al. (2006)
Shigella flexneri	100% (58/58); *dfrA1-sat1-aadA1*	Samples of stool from people suffering from sporadic diarrhea, China, 2005–2006	Zhu et al. (2011)
E. faecalis	Two strains harboring class 1 and 2 integrons; *dfrA1-sat1-aadA1*, first evidence of class 2 integron in G+ bacteria	A preliminary study, Guangzhou, China	Xu et al. (2010)
Class 3 integrons			
Escherichia coli	*ges1/oxa10:aac* (6)	Switzerland	
Serratia marcescens	*imp1/aacA4*	Japan	Collis et al. (2002)
Klebsiella pneumoniae	*ges1/oxa10: aacA4*	Portugal's critical care unit patient's urine	Ploy et al. (2003)
Class 4 integrons			
Vibrio cholerae	Collection de l'Institut Pasteur (CIP)		Shibata et al. (2003) and Poirel et al. (2010)
V. metschnikovii			Shibata et al. (2003)

Integrons gene cassettes evolve antimicrobial resistance in primary clinical settings (Zhu et al., 2017; Ghaly et al., 2020b). These cassettes connected to integrons have been gathered from various genomes from different microbial environments. Despite claims to the contrary, it is believed that not all resistance genes found in microbial systems are represented by the resistance cassettes found in integrons and relatively encode resistance genes coding for nucleotidyl transferases, acetyltransferases, and β-lactamases (Partridge et al., 2018). Systematic screening of integron cassettes, which encode novel virulence, antimicrobial-resistance mechanisms, and pathogenicity, unravels the mechanism of invasion and colonization in human hosts (Bengtsson-Palme et al., 2018). For instance, Oliver et al. (2015) stated that integrons are essential in evolving antibiotic tolerance in *P. aeruginosa,* an opportunistic human pathogenic microbe.

Similarly, Class 4 integron was initially discovered in specific *Vibrio cholerae* chromosomes as a special form of integron. Additionally, it was a part of γ-proteobacterial genomes (Sabbagh et al., 2021). Class 4 integrons have also been a significant source of antibiotic tolerance and bacterial genome development (Poirel et al., 2018). Class 1 integrons were discovered in 1989 and predominate, especially in clinical contexts (Bush and Bradford, 2020; Ghaly et al., 2021a). Complete integrons are not self-moving components in and of themselves.

Furthermore, resistant integrons share many characteristics, including their ability to move, short cassette arrangements, and usually carrying only antibiotic-tolerance genes. On the other hand, these shared characteristics have not inherited traits of integron ancestors but rather the outcome of strong selection pressure during human antibiotic usage. Given the growing issue of antibiotic resistance, understand how bacteria evolve antibiotic resistance. The bulk of gene cassettes containing genes for antibiotic tolerance is acquired, reorganized, and expressed using mobile integrons (MIs), standard components (Qadri et al., 2021; Souque et al., 2021; Sheikh et al., 2021c). These elements, commonly coupled with transposons and conjugative plasmids, have aided pathogenic bacteria to evolve resistance.

Genetic platforms aid the molecular mechanism regarding the integron-mediated shuffling of antibiotic-tolerance genes. For instance, it has been demonstrated that constitutive amplification of the integrase enzyme speeds up the emergence of chloramphenicol tolerance by causing the deletion of cassettes between Pc and the resistance cassette and the development of co-integrates among copies of the integron (Barraud and Ploy, 2015). Molecular studies revealed that carbapenem resistance in *P. aeruginosa* is known to be a significant threat globally by the world health organization (WHO) and is set as an 'extremely significant for scientists to develop novel antibiotic agents (San Millan et al., 2015). Specific reports suggest that integrons such as IntI1 catalysis of cassette insertion depend on specific factors (Vit et al., 2021). For instance, in *Vibrio cholerae*, the endogenous IntI was inactive in other bacterial hosts, proving the role of host factors needed for integron integrases (Vit et al., 2021).

Integrons as genetic markers to provide an estimation of antimicrobial resistance dissemination

AMR is a serious health problem for humans and animals, and it is spread over various environmental environments. It is believed to be a continuing phenomenon that will pose severe threats to all dimensions of life, including animals, humans, and other organisms found environment. It is emerging as the prime focus of an investigation by scientific communities around the globe. The key player in antibiotic tolerance/resistance genes is integrons, which are promoter-less genetic factors carried from one pathogen to another (Cambray et al., 2010). To initiate a broad-spectrum approach, there is an urgent need to evolve methods to detect antibiotic resistance timely. Forefront to tackle these issues, a conjoint approach such as the "One Health approach" relies on integrated surveillance based on analysis of food, veterinary disease, public health, and the environment (Sikkema and Koopmans, 2016).

Regarding recent studies, integrons are potentially employed as molecular markers to deliver an exact, reliable estimation of AMR dissemination across diverse habitats. Integrons are pivotal potential biomarkers currently employed to identify microbes harboring AMR against a range of antibiotics/drugs (Figure 5). For instance, analysis of integron-associated gene cassettes by targeted sequencing validated the role of integrons to identify the diversity of AMRs from complex microbial communities (Ghaly et al., 2020b). Reports suggest that integrons strongly provide a reliable and complete assessment of AMR expansion (Amos et al., 2015; Gillings et al., 2015). As mentioned in the introduction, integrons are of three main classes, viz., grossly involved in AMR spread. In particular, they are strongly linked to gram-negative bacteria (GNB) multidrug tolerance/resistance (Leverstein-van Hall et al., 2003; Barraud et al., 2014).

The class 1 integron is majorly found in humans and animals, whereas class 3 is found in samples collected from diverse environments (Tchuinte et al., 2016). Class 1 integrons mediate lateral transfer of DNA in-between pathogenic and commensal bacteria and thus accumulate antibiotic resistance genes in humans relying on the consumption of antibiotics. For example, in Betaproteobacteria based, class 1 integrons intersect the human food chains and can move between different locations among other bacterial species (Gillings et al., 2008). Moreover, Chainier et al. (2017) assessed the carriage of GNB in human and cattle samples by using the "One Health" approach based on cultivation-independent and cultivation-dependent approaches to check for the existence of integrons. They found class 1 integrons as expected, followed by class 2, with class 3 being more common in cattle than humans (Chainier et al., 2017). The study by Gianluca Corno et al., which examined a freshwater system of a lake–river–lake continuum, showed that class 1 integrons are a good proxy for anthropogenic pollution. They also suggest that this genetic platform is a significant driver of aminoglycoside resistance genes, including high-risk ARGs, a grave concern for human health (Corno et al., 2023).

Similarly, Barraud et al. recently reported the potential of integrons as predictive biomarkers for identifying antibiotic resistance in acute sepsis conditions (Barraud et al., 2022). In conjunction with previous reports, the study suggests integrons as a successful predictive marker for acquired antibiotic resistance through the direction in GNB-positive blood cultures (Barraud et al., 2014). Azizi et al. (2021) evaluated the identification and classification of integrons (class 1, 2, and 3) in strains of *Acinetobacter baumannii,* posing a severe problem for public health in Iran. The finding identified class 1 integrons are predictive biomarkers to validate the existence of MDR phenotypes in the clinical situation. Earlier, PCR-based amplification in Southern

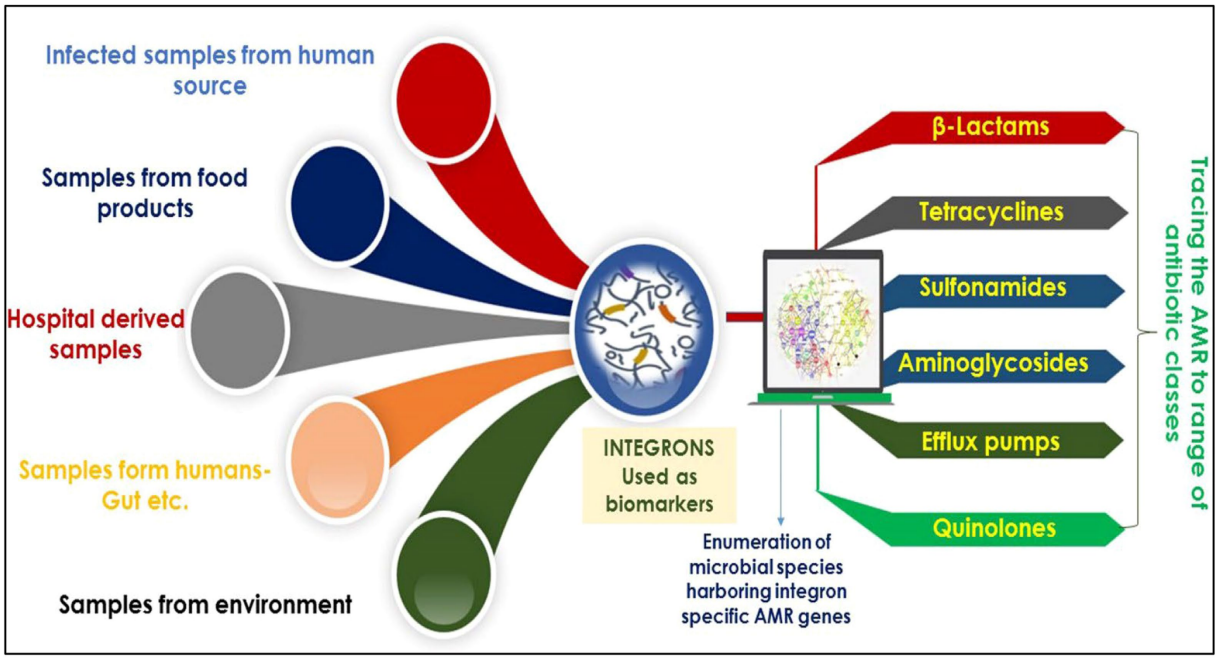

FIGURE 5
An overview showing the pivotal potential of integrons as biomarkers for the identification of AMR against a range of antibiotics/drugs.

Taiwan identified class 1 integrons associated with resistance gene cassettes in *Pseudomonas aeruginosa* (Hsiao et al., 2014). De Paula et al. (2018) identified 40 resistance markers of clinical relevance to humans by subjecting the metagenomic samples to PCR amplification using markers specific to class 1, 2, and 3 integrons. They identified resistance markers against antibiotic agents like, sulfonamide, and quinolones.

Conclusion and future perspectives

The serious global issue of AMR has put immense health-related pressure on humans and forced specialists to devise strategies to cope with resistance mechanisms evolved by microorganisms. Amid the heavy flow of resistance mechanisms from the environment to humans or vice versa, integrons have played a pivotal part in worsening the growth of tolerance through the expression and interchange of tolerance gene cassettes among different species of bacteria. The last decade has revealed the natural face of integrons and their development as the enquiring spectacle of curious clinical distress. These segments of microbial DNA are diverse in their existence and mechanisms and are reported to generate novel microbial genomes that trigger AMR dissemination and complexity. As explained, this immense health importance of integrons prompted us to provide a holistic view of AMRs with special reference to antibiotic resistance, its dissemination, and mobility through integrons. We propose that understanding the structure, functions, mechanism of AMR dissemination, and diversity of microbes identified through integrons will speed up our efforts to overcome AMR globally. As a result, successful mitigation techniques for AMR in humans and the environment are grossly limited due to a poor understanding of integron diversity, its dissemination mechanism, cross-mobility, and complexity. Moreover, we propose the following strategies to combat the microbial resistance mechanism:

- In-depth understanding of molecular structure and functions of integrons by in-silco analysis.
- In-depth investigation of integron evolution mechanism that drives the acquisition of AMR gene cassettes.
- Decrease the routes through which the resistant bacterial species contaminate humans.
- Reduce a load of antibiotics on the microbial pathogens to avoid selection pressure.
- Enumerate the realistic data on antibiotic resistance genes among major environmental habitats such as rivers, agricultural fields, hospitals, communities, etc.

Timely intervention accounting for mobile resistance gene evolution and mobility will prevent the devastating emergence of microbial resistance species threatening humans throughout the globe. We believe rising novel resistance genes in diverse microbial habitats through integrons would further hinder our efforts to devise treatment strategies, such as targeting integrons by antibiotics with adjuvants to inhibit SOS response. Development of new synthetic as well nature-based antimicrobials to combat the AMR (Chakravorty et al., 2020; Terreni et al., 2021; Bhat et al., 2022a,b; Mir et al., 2022a,b; Ashraf et al., 2023). At the end of 2020, there were 43 antibiotics in clinical development, of which, 15 were Phase I, 13 in Phase II, and 13 in Phase III to combat AMR. They include tetracycline derivatives (eravacycline), fourth generation fluoroquinolones (delafloxacin), new combinations between one β-lactam and one β-lactamase inhibitor (meropenem and vaborbactam), siderophore cephalosporins (cefiderocol), new aminoglycosides (plazomicin), and agents in development for treating drug resistant TB (pretomanid) (Terreni

et al., 2021). Our review further bolsters the idea that successful therapeutic plans should focus on integrons, merging antibiotics with additives that restrict integrase function by suppressing the SOS response, favoring resistant bacterial species (Hocquet et al., 2012), limiting the selective pressure on the evolution of integrons. Furthermore, If we successfully manage integron and cassette creation, we may be able to create new biochemical routes for antimicrobial resistance employing integrons as a base to identify new enzymes. To effectively treat patients and employ antibiotics, it is helpful to be aware of the existence of integrons and gene cassettes.

Author contributions

MM and BB designed the work. BB and RM wrote the manuscript and designed the figures. MM, BB, RM, HQ, and RD critically revised and edited the manuscript. All authors have read and approved the manuscript.

Funding

The study was financially supported by Science and Engineering Research Board, Department of Science and Technology (SERB-DST) Govt. of India New Delhi; vide Project Grant No: TAR/001213/2018. We highly appreciate SERB-DST for financial assistance.

Acknowledgments

The authors are thankful to the JK Science Technology and Innovation council DST India, Govt. of India.

Conflict of interest

The authors declare that the research was conducted in the absence of any commercial or financial relationships that could be construed as a potential conflict of interest.

Publisher's note

References

Ahmed, A. M., Furuta, K., Shimomura, K., Kasama, Y., and Shimamoto, T. (2006). Genetic characterization of multidrug resistance in *Shigella* spp. from Japan. *J. Med. Microbiol.* 55, 1685–1691. doi: 10.1099/jmm.0.46725-0

Ahmed, A. M., Nakano, H., and Shimamoto, T. (2005). Molecular characterization of integrons in non-typhoid *Salmonella* serovars isolated in Japan: description of an unusual class 2 integron. *J. Antimicrob. Chemother.* 55, 371–374. doi: 10.1093/jac/dkh534

Akrami, F., Shahandashti, E. F., Yahyapour, Y., Sadeghi, M., Khafri, S., Pournajaf, A., et al. (2017). Integron types, gene cassettes and antimicrobial resistance profile of *Acinetobacter baumannii* isolated from BAL samples in Babol, North of Iran. *Microb. Pathog.* 109, 35–38. doi: 10.1016/j.micpath.2017.05.005

Amin, M. B., Saha, S. R., Islam, M. R., Haider, S. M. A., Hossain, M. I., Chowdhury, A. S. M. H. K., et al. (2021). High prevalence of plasmid-mediated quinolone resistance (PMQR) among *E. coli* from aquatic environments in Bangladesh. *PLoS One* 16:e0261970. doi: 10.1371/journal.pone.0261970

Amos, G. C. A., Gozzard, E., Carter, C. E., Mead, A., Bowes, M. J., Hawkey, P. M., et al. (2015). Validated predictive modelling of the environmental resistome. *ISME J.* 9, 1467–1476. doi: 10.1038/ismej.2014.237

Antelo, V., Giménez, M., Azziz, G., Valdespino-Castillo, P., Falcón, L. I., Ruberto, L. A. M., et al. (2021). Metagenomic strategies identify diverse integron-integrase and antibiotic resistance genes in the Antarctic environment. *MicrobiologyOpen* 10:e1219. doi: 10.1002/mbo3.1219

Antunes, P., Machado, J., and Peixe, L. (2006). Characterization of antimicrobial resistance and class 1 and 2 integrons in *Salmonella enterica* isolates from different sources in Portugal. *J. Antimicrob. Chemother.* 58, 297–304. doi: 10.1093/jac/dkl242

Ashraf, M. V., Pant, S., Khan, M. A. H., Shah, A. A., Siddiqui, S., Jeridi, M., et al. (2023). Phytochemicals as antimicrobials: prospecting Himalayan medicinal plants as source of alternate medicine to combat antimicrobial resistance. *Pharmaceuticals* 16:881. doi: 10.3390/ph16060881

Azizi, O., Fereshteh, S., Nasiri, O., Ghorbani, M., Barzi, S. M., and Badmasti, F. (2021). The occurrence and characterization of class i, ii, and iii integrons among carbapenemase-producing clinical strains of *Acinetobacter baumannii* in Tehran, Iran. *Jundishapur J. Microbiol.* 14, 1–13. doi: 10.5812/jjm.117766

Baharoglu, Z., Bikard, D., and Mazel, D. (2010). Conjugative DNA transfer induces the bacterial SOS response and promotes antibiotic resistance development through integron activation. *PLoS Genet.* 6:e1001165. doi: 10.1371/journal.pgen.1001165

Barraud, O., François, B., Chainier, D., Vignaud, J., and Ploy, M.-C. (2014). Value of integron detection for predicting antibiotic resistance in patients with gram-negative septicaemia. *Int. J. Antimicrob. Agents* 44, 351–353. doi: 10.1016/j.ijantimicag.2014.06.008

Barraud, O., Guichard, E., Chainier, D., Postil, D., Chimot, L., Mercier, E., et al. (2022). Integrons, a predictive biomarker for antibiotic resistance in acute sepsis: the IRIS study. *J. Antimicrob. Chemother.* 77, 213–217. doi: 10.1093/jac/dkab348

Barraud, O., and Ploy, M.-C. (2015). Diversity of class 1 integron gene cassette rearrangements selected under antibiotic pressure. *J. Bacteriol.* 197, 2171–2178. doi: 10.1128/JB.02455-14

Bengtsson-Palme, J., Kristiansson, E., and Larsson, D. G. J. (2018). Environmental factors influencing the development and spread of antibiotic resistance. *FEMS Microbiol. Rev.* 42:fux053. doi: 10.1093/femsre/fux053

Bennett, P. M. (2008). Plasmid encoded antibiotic resistance: acquisition and transfer of antibiotic resistance genes in bacteria. *Br. J. Pharmacol.* 153, S347–S357. doi: 10.1038/sj.bjp.0707607

Berendonk, T. U., Manaia, C. M., Merlin, C., Fatta-Kassinos, D., Cytryn, E., Walsh, F., et al. (2015). Tackling antibiotic resistance: the environmental framework. *Nat. Rev. Microbiol.* 13, 310–317. doi: 10.1038/nrmicro3439

Bhat, B. A., Mir, W. R., Sheikh, B. A., Alkanani, M., and Mir, M. A. (2022a). Metabolite fingerprinting of phytoconstituents from *Fritillaria cirrhosa* D. Don and molecular docking analysis of bioactive peonidin with microbial drug target proteins. *Sci. Rep.* 12:7296. doi: 10.1038/s41598-022-10796-7

Bhat, B. A., Mir, W. R., Sheikh, B. A., Rather, M. A., and Mir, M. A. (2022b). In vitro and in silico evaluation of antimicrobial properties of *Delphinium cashmerianum* L., a medicinal herb growing in Kashmir, India. *J. Ethnopharmacol.* 291:115046. doi: 10.1016/j.jep.2022.115046

Boucher, Y., Labbate, M., Koenig, J. E., and Stokes, H. W. (2007). Integrons: mobilizable platforms that promote genetic diversity in bacteria. *Trends Microbiol.* 15, 301–309. doi: 10.1016/j.tim.2007.05.004

Bouvier, M., Demarre, G., and Mazel, D. (2005). Integron cassette insertion: a recombination process involving a folded single strand substrate. *EMBO J.* 24, 4356–4367. doi: 10.1038/sj.emboj.7600898

Bush, K., and Bradford, P. A. (2020). Epidemiology of β-lactamase-producing pathogens. *Clin. Microbiol. Rev.* 33, e00047–e00019. doi: 10.1128/CMR.00047-19

Cambray, G., Guerout, A.-M., and Mazel, D. (2010). Integrons. *Annu. Rev. Genet.* 44, 141–166. doi: 10.1146/annurev-genet-102209-163504

Carattoli, A. (2001). Importance of integrons in the diffusion of resistance. *Vet. Res.* 32, 243–259. doi: 10.1051/vetres:2001122

Chainier, D., Barraud, O., Masson, G., Couve-Deacon, E., François, B., Couquet, C.-Y., et al. (2017). Integron digestive carriage in human and cattle: a "one Health" cultivation-independent approach. *Front. Microbiol.* 8:1891. doi: 10.3389/fmicb.2017.01891

Chakravorty, A., Rather, G. A., Ali, A., Bhat, B. A., Sana, S. S., Abhishek, N., et al. (2020). "Nano approach: Indian spices as antimicrobial agents" in *Ethnopharmacological investigation of Indian spices* (Pennsylvania, United States: IGI Global), 205–241.

Chang, L.-L., Chen, H.-F., Chang, C.-Y., Lee, T.-M., and Wu, W.-J. (2004). Contribution of integrons, and SmeABC and SmeDEF efflux pumps to multidrug resistance in clinical isolates of *Stenotrophomonas maltophilia*. *J. Antimicrob. Chemother.* 53, 518–521. doi: 10.1093/jac/dkh094

Collignon, P. (2012). The importance of a one Health approach to preventing the development and spread of antibiotic resistance. *Curr. Top. Microbiol. Immunol.* 366, 19–36. doi: 10.1007/82_2012_224

Collignon, P. (2013). Ban routine use of critically important antibiotics in food animals. *BMJ* 347:f4976. doi: 10.1136/bmj.f4976

Collignon, P. J., and Mcewen, S. A. (2019). One health–its importance in helping to better control antimicrobial resistance. *Trop. Med. Infect. Dis.* 4:22. doi: 10.3390/tropicalmed4010022

Collis, C. M., Kim, M.-J., Partridge, S. R., Stokes, H. W., and Hall, R. M. (2002). Characterization of the class 3 integron and the site-specific recombination system it determines. *J. Bacteriol.* 184, 3017–3026. doi: 10.1128/JB.184.11.3017-3026.2002

Corno, G., Ghaly, T., Sabatino, R., Eckert, E. M., Galafassi, S., Gillings, M. R., et al. (2023). Class 1 integron and related antimicrobial resistance gene dynamics along a complex freshwater system affected by different anthropogenic pressures. *Environ. Pollut.* 316:120601. doi: 10.1016/j.envpol.2022.120601

Crowley, D., Cryan, B., and Lucey, B. (2008). First detection of a class 2 integron among clinical isolates of *Serratia marcescens*. *Br. J. Biomed. Sci.* 65, 86–89. doi: 10.1080/09674845.2008.11732803

Crowley, D., Daly, M., Lucey, B., Shine, P., Collins, J. J., Cryan, B., et al. (2002). Molecular epidemiology of cystic fibrosis-linked *Burkholderia cepacia* complex isolates from three national referral centres in Ireland. *J. Appl. Microbiol.* 92, 992–1004. doi: 10.1046/j.1365-2672.2002.01612.x

Curtiss Iii, R. (1969). Bacterial conjugation. *Annu. Rev. Microbiol.* 23, 69–136. doi: 10.1146/annurev.mi.23.100169.000441

Cury, J., Jové, T., Touchon, M., Néron, B., and Rocha, E. P. C. (2016). Identification and analysis of integrons and cassette arrays in bacterial genomes. *Nucleic Acids Res.* 44, 4539–4550. doi: 10.1093/nar/gkw319

Dalsgaard, A., Forslund, A., Serichantalergs, O., and Sandvang, D. (2000). Distribution and content of class 1 integrons in different *Vibrio cholerae* O-serotype strains isolated in Thailand. *Antimicrob. Agents Chemother.* 44, 1315–1321. doi: 10.1128/AAC.44.5.1315-1321.2000

De Paula, A. C. L., Medeiros, J. D., De Azevedo, A. C., De Assis Chagas, J. M., Da Silva, V. L., and Diniz, C. G. (2018). Antibiotic resistance genetic markers and integrons in white soft cheese: aspects of clinical resistome and potentiality of horizontal gene transfer. *Genes* 9:106. doi: 10.3390/genes9020106

Deng, Y., Bao, X., Ji, L., Chen, L., Liu, J., Miao, J., et al. (2015). Resistance integrons: class 1, 2 and 3 integrons. *Ann. Clin. Microbiol. Antimicrob.* 14:45. doi: 10.1186/s12941-015-0100-6

Dias, M. F., De Castro, G. M., De Paiva, M. C., De Paula Reis, M., Facchin, S., Do Carmo, A. O., et al. (2021). Exploring antibiotic resistance in environmental integron-cassettes through intI-attC amplicons deep sequencing. *Braz. J. Microbiol.* 52, 363–372. doi: 10.1007/s42770-020-00409-8

Ding, J., Zhu, D., Hong, B., Wang, H. T., Li, G., Ma, Y. B., et al. (2019). Long-term application of organic fertilization causes the accumulation of antibiotic resistome in earthworm gut microbiota. *Environ. Int.* 124, 145–152. doi: 10.1016/j.envint.2019.01.017

Domingues, S., Da Silva, G. J., and Nielsen, K. M. (2012). Integrons: vehicles and pathways for horizontal dissemination in bacteria. *Mob. Genet. Elem.* 2, 211–223. doi: 10.4161/mge.22967

Domingues, S., Da Silva, G. J., and Nielsen, K. M. (2015). Global dissemination patterns of common gene cassette arrays in class 1 integrons. *Microbiology* 161, 1313–1337. doi: 10.1099/mic.0.000099

Escudero, J. A., Loot, C., Nivina, A., and Mazel, D. (2015). The integron: adaptation on demand. *Microbiol. Spectr.* 3, 3–2. doi: 10.1128/microbiolspec.MDNA3-0019-2014

Fletcher, S. (2015). Understanding the contribution of environmental factors in the spread of antimicrobial resistance. *Environ. Health Prev. Med.* 20, 243–252. doi: 10.1007/s12199-015-0468-0

Francia, M. V., Zabala, J. C., De La Cruz, F., and García Lobo, J. M. (1999). The IntI1 integron integrase preferentially binds single-stranded DNA of the attC site. *J. Bacteriol.* 181, 6844–6849. doi: 10.1128/JB.181.21.6844-6849.1999

Gassama-Sow, A., Diallo, M. H., Boye, C. S., Garin, B., Sire, J. M., Sow, A. I., et al. (2006). Class 2 integron-associated antibiotic resistance in *Shigella sonnei* isolates in Dakar, Senegal. *Int. J. Antimicrob. Agents* 27, 267–270. doi: 10.1016/j.ijantimicag.2005.10.016

Gaze, W. H., Krone, S. M., Larsson, D. G. J., Li, X.-Z., Robinson, J. A., Simonet, P., et al. (2013). Influence of humans on evolution and mobilization of environmental antibiotic resistome. *Emerg. Infect. Dis.* 19:e120871. doi: 10.3201/eid1907.120871

Ghaly, T. M., Geoghegan, J. L., Alroy, J., and Gillings, M. R. (2019). High diversity and rapid spatial turnover of integron gene cassettes in soil. *Environ. Microbiol.* 21, 1567–1574. doi: 10.1111/1462-2920.14551

Ghaly, T. M., Geoghegan, J. L., Tetu, S. G., and Gillings, M. R. (2020a). The peril and promise of integrons: beyond antibiotic resistance. *Trends Microbiol.* 28, 455–464. doi: 10.1016/j.tim.2019.12.002

Ghaly, T. M., Paulsen, I. T., Sajjad, A., Tetu, S. G., and Gillings, M. R. (2020b). A novel family of Acinetobacter mega-plasmids are disseminating multi-drug resistance across the globe while acquiring location-specific accessory genes. *Front. Microbiol.* 11:605952. doi: 10.3389/fmicb.2020.605952

Ghaly, T. M., Penesyan, A., Pritchard, A., Qi, Q., Rajabal, V., Tetu, S. G., et al. (2021a). Methods for the targeted sequencing and analysis of integrons and their gene cassettes from complex microbial communities. *Microb. Genom.* 8:788. doi: 10.1099/mgen.0.000788

Ghaly, T. M., Tetu, S. G., and Gillings, M. R. (2021b). Predicting the taxonomic and environmental sources of integron gene cassettes using structural and sequence homology of attC sites. *Commun. Biol.* 4, 1–8. doi: 10.1038/s42003-021-02489-0

Gillings, M. R. (2014). Integrons: past, present, and future. *Microbiol. Mol. Biol. Rev.* 78, 257–277. doi: 10.1128/MMBR.00056-13

Gillings, M., Boucher, Y., Labbate, M., Holmes, A., Krishnan, S., Holley, M., et al. (2008). The evolution of class 1 integrons and the rise of antibiotic resistance. *J. Bacteriol.* 190, 5095–5100. doi: 10.1128/JB.00152-08

Gillings, M. R., Gaze, W. H., Pruden, A., Smalla, K., Tiedje, J. M., and Zhu, Y.-G. (2015). Using the class 1 integron-integrase gene as a proxy for anthropogenic pollution. *ISME J.* 9, 1269–1279. doi: 10.1038/ismej.2014.226

Grainge, I., and Jayaram, M. (1999). The integrase family of recombinases: organization and function of the active site. *Mol. Microbiol.* 33, 449–456. doi: 10.1046/j.1365-2958.1999.01493.x

Guerin, É., Cambray, G., Sanchez-Alberola, N., Campoy, S., Erill, I., Da Re, S., et al. (2009). The SOS response controls integron recombination. *Science* 324:1034. doi: 10.1126/science.1172914

Hall, R. M., and Collis, C. M. (1995). Mobile gene cassettes and integrons: capture and spread of genes by site-specific recombination. *Mol. Microbiol.* 15, 593–600. doi: 10.1111/j.1365-2958.1995.tb02368.x

Hall, R. M., Collis, C. M., Kim, M. J., Partridge, S. R., Recchia, G. D., and Stokes, H. W. (1999). Mobile gene cassettes and integrons in evolution. *Ann. N. Y. Acad. Sci.* 870, 68–80. doi: 10.1111/j.1749-6632.1999.tb08866.x

Hamdani, S. S., Bhat, B. A., Tariq, L., Yaseen, S. I., Ara, I., Rafi, B., et al. (2020). Antibiotic resistance: the future disaster. *Int. J. Res. Appl. Sci. Biotechnol.* 7:2888 doi: 10.31033/ijrasb.7.4.16

Hocquet, D., Llanes, C., Thouverez, M., Kulasekara, H. D., Bertrand, X., Plésiat, P., et al. (2012). Evidence for induction of integron-based antibiotic resistance by the SOS response in a clinical setting. *PLoS Pathog.* 8:e1002778. doi: 10.1371/journal.ppat.1002778

Holmes, A. J., Holley, M. P., Mahon, A., Nield, B., Gillings, M., and Stokes, H. W. (2003). Recombination activity of a distinctive integron-gene cassette system associated with *Pseudomonas stutzeri* populations in soil. *J. Bacteriol.* 185, 918–928. doi: 10.1128/JB.185.3.918-928.2003

Hsiao, K.-Y., Lee, M.-F., and Peng, C.-F. (2014). Detection and characterization of class 1 integron-associated gene cassettes from *Pseudomonas aeruginosa* isolates in southern Taiwan. *Biomarkers Genom. Med.* 6, 74–78. doi: 10.1016/j.bgm.2014.02.004

Huang, S.-C., Chiu, C.-H., Chiou, C.-S., and Yang, Y.-J. (2013). Multidrug-resistant *Salmonella enterica* serovar Panama carrying class 1 integrons is invasive in Taiwanese children. *J. Formos. Med. Assoc.* 112, 269–275. doi: 10.1016/j.jfma.2012.02.011

Huddleston, J. R. (2014). Horizontal gene transfer in the human gastrointestinal tract: potential spread of antibiotic resistance genes. *Infect. Drug Resist.* 7:167. doi: 10.2147/IDR.S48820

Il'ina, T. S. (2003). The mechanisms of horizontal gene transfer: The role of bacteriophages and integrons in the evolution of pathogenic bacteria. *Mol. Gen. Mikrobiol. Virusol.* 4, 3–10.

Johansson, C. (2007). *Mechanisms and DNA specificity in site-specific recombination of integron cassettes*. Carolina: Uppsala University

Johnston, C., Martin, B., Fichant, G., Polard, P., and Claverys, J.-P. (2014). Bacterial transformation: distribution, shared mechanisms and divergent control. *Nat. Rev. Microbiol.* 12, 181–196. doi: 10.1038/nrmicro3199

Juan, C., Zamorano, L., Mena, A., Albertí, S., Pérez, J. L., and Oliver, A. (2010). Metallo-β-lactamase-producing *Pseudomonas putida* as a reservoir of multidrug resistance elements that can be transferred to successful *Pseudomonas aeruginosa* clones. *J. Antimicrob. Chemother.* 65, 474–478. doi: 10.1093/jac/dkp491

Kadlec, K., and Schwarz, S. (2008). Analysis and distribution of class 1 and class 2 integrons and associated gene cassettes among *Escherichia coli* isolates from swine, horses, cats and dogs collected in the BfT-GermVet monitoring study. *J. Antimicrob. Chemother.* 62, 469–473. doi: 10.1093/jac/dkn233

Kargar, M., Mohammadalipour, Z., Doosti, A., Lorzadeh, S., and Japoni-Nejad, A. (2014). High prevalence of class 1 to 3 integrons among multidrug-resistant diarrheagenic *Escherichia coli* in southwest of Iran. *Osong. Public Health Res. Perspect.* 5, 193–198. doi: 10.1016/j.phrp.2014.06.003

Kheiri, R., and Akhtari, L. (2016). Antimicrobial resistance and integron gene cassette arrays in commensal *Escherichia coli* from human and animal sources in IRI. *Gut Pathog.* 8, 1–10. doi: 10.1186/s13099-016-0123-3

Labbate, M., Case, R. J., and Stokes, H. W. (2009). The integron/gene cassette system: an active player in bacterial adaptation. *Methods Mol. Biol.* 532, 103–125. doi: 10.1007/978-1-60327-853-9_6

Larsson, D. G. J., and Flach, C.-F. (2022). Antibiotic resistance in the environment. *Nat. Rev. Microbiol.* 20, 257–269. doi: 10.1038/s41579-021-00649-x

Leverstein-Van Hall, M. A., Blok, H. E. M., Donders, A. R. T., Paauw, A., Fluit, A. C., and Verhoef, J. (2003). Multidrug resistance among Enterobacteriaceae is strongly associated with the presence of integrons and is independent of species or isolate origin. *J. Infect. Dis.* 187, 251–259. doi: 10.1086/345880

Liebert, C. A., Hall, R. M., and Summers, A. O. (1999). Transposon Tn 21, flagship of the floating genome. *Microbiol. Mol. Biol. Rev.* 63, 507–522. doi: 10.1128/MMBR.63.3.507-522.1999

Liu, C.-C., Tang, C. Y., Chang, K.-C., Kuo, H.-Y., and Liou, M.-L. (2014). A comparative study of class 1 integrons in *Acinetobacter baumannii*. *Gene* 544, 75–82. doi: 10.1016/j.gene.2014.04.047

Ma, L., Li, A.-D., Yin, X.-L., and Zhang, T. (2017). The prevalence of integrons as the carrier of antibiotic resistance genes in natural and man-made environments. *Environ. Sci. Technol.* 51, 5721–5728. doi: 10.1021/acs.est.6b05887

Ma, L., Li, B., and Zhang, T. (2014). Abundant rifampin resistance genes and significant correlations of antibiotic resistance genes and plasmids in various environments revealed by metagenomic analysis. *Appl. Microbiol. Biotechnol.* 98, 5195–5204. doi: 10.1007/s00253-014-5511-3

Ma, L., Xia, Y., Li, B., Yang, Y., Li, L.-G., Tiedje, J. M., et al. (2016). Metagenomic assembly reveals hosts of antibiotic resistance genes and the shared resistome in pig, chicken, and human feces. *Environ. Sci. Technol.* 50, 420–427. doi: 10.1021/acs.est.5b03522

Machado, E., Coque, T. M., Canton, R., Sousa, J. C., and Peixe, L. (2008). Antibiotic resistance integrons and extended-spectrum β-lactamases among Enterobacteriaceae isolates recovered from chickens and swine in Portugal. *J. Antimicrob. Chemother.* 62, 296–302. doi: 10.1093/jac/dkn179

Marathe, N. P., Nagarkar, S. S., Vaishampayan, A. A., Rasane, M. H., Samant, S. A., Dohe, V., et al. (2015). High prevalence of class 1 integrons in clinical isolates of methicillin-resistant *Staphylococcus aureus* from India. *Indian J. Med. Microbiol.* 33, 231–236. doi: 10.4103/0255-0857.154905

Marchiaro, P., Viale, A. M., Ballerini, V., Rossignol, G., Vila, A. J., and Limansky, A. (2010). First report of a Tn402-like class 1 integron carrying blaVIM-2 in *Pseudomonas putida* from Argentina. *J. Infect. Dev. Countr.* 4, 412–416. doi: 10.3855/jidc.1012

Mazel, D. (2006). Integrons: agents of bacterial evolution. *Nat. Rev. Microbiol.* 4, 608–620. doi: 10.1038/nrmicro1462

Michael, C. A., Gillings, M. R., Holmes, A. J., Hughes, L., Andrew, N. R., Holley, M. P., et al. (2004). Mobile gene cassettes: a fundamental resource for bacterial evolution. *Am. Nat.* 164, 1–12. doi: 10.1086/421733

Miko, A., Pries, K., Schroeter, A., and Helmuth, R. (2003). Multiple-drug resistance in D-tartrate-positive *Salmonella enterica* serovar Paratyphi B isolates from poultry is mediated by class 2 integrons inserted into the bacterial chromosome. *Antimicrob. Agents Chemother.* 47, 3640–3643. doi: 10.1128/AAC.47.11.3640-3643.2003

Mir, W. R., Bhat, B. A., Almilaibary, A., Asdaq, S. M. B., and Mir, M. A. (2022a). Evaluation of the in vitro antimicrobial activities of Delphinium roylei: an insight from molecular docking and MD-simulation studies. *Med. Chem.* 18, 1109–1121. doi: 10.2174/1573406418666220429093956

Mir, W. R., Bhat, B. A., Rather, M. A., Muzamil, S., Almilaibary, A., Alkhanani, M., et al. (2022b). Molecular docking analysis and evaluation of the antimicrobial properties of the constituents of *Geranium wallichianum* D. Don ex Sweet from Kashmir Himalaya. *Sci. Rep.* 12:12547. doi: 10.1038/s41598-022-16102-9

Mir, M. A., Bhat, B. A., Sheikh, B. A., Rather, G. A., Mehraj, S., and Mir, W. R. (2021). "Nanomedicine in human Health therapeutics and drug delivery: Nanobiotechnology and Nanobiomedicine" in *Applications of nanomaterials in agriculture, food science, and medicine* (Pennsylvania, United States: IGI Global), 229–251.

Moura, A., Soares, M., Pereira, C., Leitão, N., Henriques, I., and Correia, A. (2009). INTEGRALL: a database and search engine for integrons, integrases and gene cassettes. *Bioinformatics* 25, 1096–1098. doi: 10.1093/bioinformatics/btp105

Munita, J. M., and Arias, C. A. (2016). Mechanisms of antibiotic resistance. *Microbiol. Spectr.* 4:16. doi: 10.1128/microbiolspec.VMBF-0016-2015

Naas, T., Mikami, Y., Imai, T., Poirel, L., and Nordmann, P. (2001). Characterization of In53, a class 1 plasmid-and composite transposon-located integron of *Escherichia coli* which carries an unusual array of gene cassettes. *J. Bacteriol.* 183, 235–249. doi: 10.1128/JB.183.1.235-249.2001

Nakamura, Y., Itoh, T., Matsuda, H., and Gojobori, T. (2004). Biased biological functions of horizontally transferred genes in prokaryotic genomes. *Nat. Genet.* 36, 760–766. doi: 10.1038/ng1381

Nield, B. S., Holmes, A. J., Gillings, M. R., Recchia, G. D., Mabbutt, B. C., Nevalainen, K. M. H., et al. (2001). Recovery of new integron classes from environmental DNA. *FEMS Microbiol. Lett.* 195, 59–65. doi: 10.1111/j.1574-6968.2001.tb10498.x

Nwosu, V. C. (2001). Antibiotic resistance with particular reference to soil microorganisms. *Res. Microbiol.* 152, 421–430. doi: 10.1016/S0923-2508(01)01215-3

Ochman, H., Lawrence, J. G., and Groisman, E. A. (2000). Lateral gene transfer and the nature of bacterial innovation. *Nature* 405, 299–304. doi: 10.1038/35012500

Oliver, A., Mulet, X., López-Causapé, C., and Juan, C. (2015). The increasing threat of *Pseudomonas aeruginosa* high-risk clones. *Drug Resist. Updat.* 21, 41–59. doi: 10.1016/j.drup.2015.08.002

Ozeki, H., and Ikeda, H. (1968). Transduction mechanisms. *Annu. Rev. Genet.* 2, 245–278. doi: 10.1146/annurev.ge.02.120168.001333

Ozgumus, O. B., Sandalli, C., Sevim, A., Celik-Sevim, E., and Sivri, N. (2009). Class 1 and class 2 integrons and plasmid-mediated antibiotic resistance in coliforms isolated from ten rivers in northern Turkey. *J. Microbiol.* 47, 19–27. doi: 10.1007/s12275-008-0206-z

Parks, D. H., Chuvochina, M., Waite, D. W., Rinke, C., Skarshewski, A., Chaumeil, P.-A., et al. (2018). A standardized bacterial taxonomy based on genome phylogeny substantially revises the tree of life. *Nat. Biotechnol.* 36, 996–1004. doi: 10.1038/nbt.4229

Partridge, S. R., Kwong, S. M., Firth, N., and Jensen, S. O. (2018). Mobile genetic elements associated with antimicrobial resistance. *Clin. Microbiol. Rev.* 31, e00088–e00017. doi: 10.1128/CMR.00088-17

Partridge, S. R., Tsafnat, G., Coiera, E., and Iredell, J. R. (2009). Gene cassettes and cassette arrays in mobile resistance integrons. *FEMS Microbiol. Rev.* 33, 757–784. doi: 10.1111/j.1574-6976.2009.00175.x

Pérez-Valdespino, A., Fernández-Rendón, E., and Curiel-Quesada, E. (2009). Detection and characterization of class 1 integrons in Aeromonas spp. isolated from human diarrheic stool in Mexico. *J. Basic Microbiol.* 49, 572–578. doi: 10.1002/jobm.200900095

Ploy, M.-C., Chainier, D., Tran Thi, N. H., Poilane, I., Cruaud, P., Denis, F., et al. (2003). Integron-associated antibiotic resistance in *Salmonella enterica* serovar Typhi from Asia. *Antimicrob. Agents Chemother.* 47, 1427–1429. doi: 10.1128/AAC.47.4.1427-1429.2003

Poirel, L., Carattoli, A., Bernabeu, S., Bruderer, T., Frei, R., and Nordmann, P. (2010). A novel IncQ plasmid type harbouring a class 3 integron from *Escherichia coli*. *J. Antimicrob. Chemother.* 65, 1594–1598. doi: 10.1093/jac/dkq166

Poirel, L., Madec, J.-Y., Lupo, A., Schink, A.-K., Kieffer, N., Nordmann, P., et al. (2018). Antimicrobial resistance in *Escherichia coli*. *Microbiol. Spectr.* 6:26. doi: 10.1128/microbiolspec.ARBA-0026-2017

Qadri, H., Shah, A. H., and Mir, M. (2021). Novel strategies to combat the emerging drug resistance in human pathogenic microbes. *Curr. Drug Targets* 22, 1424–1436. doi: 10.2174/1389450121666201228123212

Racewicz, P., Majewski, M., Madeja, Z. E., Łukomska, A., and Kubiak, M. (2020). Role of integrons in the proliferation of multiple drug resistance in selected bacteria occurring in poultry production. *Br. Poult. Sci.* 61, 122–131. doi: 10.1080/00071668.2019.1697426

Razavi, M., Marathe, N. P., Gillings, M. R., Flach, C.-F., Kristiansson, E., and Joakim Larsson, D. G. (2017). Discovery of the fourth mobile sulfonamide resistance gene. *Microbiome* 5:160. doi: 10.1186/s40168-017-0379-y

Rendueles, O., De Sousa, J. A. M., Bernheim, A., Touchon, M., and Rocha, E. P. C. (2018). Genetic exchanges are more frequent in bacteria encoding capsules. *PLoS Genet.* 14:e1007862. doi: 10.1371/journal.pgen.1007862

Roe, M. T., Vega, E., and Pillai, S. D. (2003). Antimicrobial resistance markers of class 1 and class 2 integron-bearing *Escherichia coli* from irrigation water and sediments. *Emerg. Infect. Dis.* 9:822. doi: 10.3201/eid0907.020529

Sabbagh, P., Ebrahimzadeh-Namvar, A., Ferdosi-Shahandashti, E., Javanian, M., Khafri, S., and Rajabnia, M. (2017). Molecular characterization of *Staphylococcus aureus* strains isolated among hospital staff nasal carriers of Babol, Iran. *Caspian J. Intern. Med.* 8:311. doi: 10.22088/cjim.8.4.311

Sabbagh, P., Rajabnia, M., Maali, A., and Ferdosi-Shahandashti, E. (2021). Integron and its role in antimicrobial resistance: A literature review on some bacterial pathogens. *Iran. J. Basic Med. Sci.* 24:136. doi: 10.22038/ijbms.2020.48905.11208

San Millan, A., Toll-Riera, M., Escudero, J. A., Cantón, R., Coque, T. M., and Maclean, R. C. (2015). Sequencing of plasmids pAMBL1 and pAMBL2 from *Pseudomonas aeruginosa* reveals a Bla VIM-1 amplification causing high-level carbapenem resistance. *J. Antimicrob. Chemother.* 70, 3000–3003. doi: 10.1093/jac/dkv222

Sandoval-Quintana, E., Lauga, B., and Cagnon, C. (2022). Environmental integrons: the dark side of the integron world. *Trends Microbiol.* 31, 432–434. doi: 10.1016/j.tim.2022.01.009

Serwecińska, L. (2020). Antimicrobials and antibiotic-resistant bacteria: a risk to the environment and to public health. *Water* 12:3313. doi: 10.3390/w12123313

Shahcheraghi, F., Badmasti, F., and Feizabadi, M. M. (2010). Molecular characterization of class 1 integrons in MDR *Pseudomonas aeruginosa* isolated from clinical settings in Iran, Tehran. *FEMS Immunol. Med. Microbiol.* 58, 421–425. doi: 10.1111/j.1574-695X.2009.00636.x

Sheikh, B. A., Bhat, B. A., Ahmad, Z., and Mir, M. A. (2021a). Strategies employed to evade the host immune response and the mechanism of drug resistance in *Mycobacterium tuberculosis*: in search of finding new targets. *Curr. Pharm. Biotechnol.* doi: 10.2174/1389201023666211222164938

Sheikh, B. A., Bhat, B. A., Alshehri, B., Mir, R. A., Mir, W. R., Parry, Z. A., et al. (2021b). Nano-drug delivery systems: possible end to the rising threats of tuberculosis. *J. Biomed. Nanotechnol.* 17, 2298–2318. doi: 10.1166/jbn.2021.3201

Sheikh, B. A., Bhat, B. A., Mehraj, U., Mir, W., Hamadani, S., and Mir, M. A. (2021c). Development of new therapeutics to meet the current challenge of drug resistant tuberculosis. *Curr. Pharm. Biotechnol.* 22, 480–500. doi: 10.2174/1389201021666200628021702

Sheikh, B. A., Bhat, B. A., and Mir, M. A. (2022). Antimicrobial resistance: new insights and therapeutic implications. *Appl. Microbiol. Biotechnol.* 106, 6427–6440. doi: 10.1007/s00253-022-12175-8

Shibata, N., Doi, Y., Yamane, K., Yagi, T., Kurokawa, H., Shibayama, K., et al. (2003). PCR typing of genetic determinants for metallo-β-lactamases and integrases carried by gram-negative bacteria isolated in Japan, with focus on the class 3 integron. *J. Clin. Microbiol.* 41, 5407–5413. doi: 10.1128/JCM.41.12.5407-5413.2003

Shin, E., Hong, H., Oh, Y., and Lee, Y. (2015). First report and molecular characterization of a *Campylobacter jejuni* isolate with extensive drug resistance from a travel-associated human case. *Antimicrob. Agents Chemother.* 59, 6670–6672. doi: 10.1128/AAC.01395-15

Sikkema, R., and Koopmans, M. (2016). One Health training and research activities in Western Europe. *Infect. Ecol. Epidemiol.* 6:33703. doi: 10.3402/iee.v6.33703

So, A. D., Shah, T. A., Roach, S., Chee, Y. L., and Nachman, K. E. (2015). An integrated systems approach is needed to ensure the sustainability of antibiotic effectiveness for both humans and animals. *J. Law Med. Ethics* 43, 38–45. doi: 10.1111/jlme.12273

Souque, C., Escudero, J. A., and Maclean, R. C. (2021). Integron activity accelerates the evolution of antibiotic resistance. *elife* 10:e62474. doi: 10.7554/eLife.62474

Sow, A. G., Aïdara-Kane, A., Barraud, O., Gatet, M., Denis, F., and Ploy, M.-C. (2010). High prevalence of trimethoprim-resistance cassettes in class 1 and 2 integrons in Senegalese Shigella spp isolates. *J. Infect. Dev. Ctries.* 4, 207–212. doi: 10.3855/jidc.583

Stokes, H. W., and Gillings, M. R. (2011). Gene flow, mobile genetic elements and the recruitment of antibiotic resistance genes into gram-negative pathogens. *FEMS Microbiol. Rev.* 35, 790–819. doi: 10.1111/j.1574-6976.2011.00273.x

Stokes, H. W. T., and Hall, R. M. (1989). A novel family of potentially mobile DNA elements encoding site-specific gene-integration functions: integrons. *Mol. Microbiol.* 3, 1669–1683. doi: 10.1111/j.1365-2958.1989.tb00153.x

Stokes, H. W., Nesbø, C. L., Holley, M., Bahl, M. I., Gillings, M. R., and Boucher, Y. (2006). Class 1 integrons potentially predating the association with Tn 402-like transposition genes are present in a sediment microbial community. *J. Bacteriol.* 188, 5722–5730. doi: 10.1128/JB.01950-05

Su, J., Shi, L., Yang, L., Xiao, Z., Li, X., and Yamasaki, S. (2006). Analysis of integrons in clinical isolates of *Escherichia coli* in China during the last six years. *FEMS Microbiol. Lett.* 254, 75–80. doi: 10.1111/j.1574-6968.2005.00025.x

Sunde, M. (2005). Prevalence and characterization of class 1 and class 2 integrons in *Escherichia coli* isolated from meat and meat products of Norwegian origin. *J. Antimicrob. Chemother.* 56, 1019–1024. doi: 10.1093/jac/dki377

Sundström, L. (1998). The potential of integrons and connected programmed rearrangements for mediating horizontal gene transfer. *APMIS Suppl.* 84, 37–42. doi: 10.1111/j.1600-0463.1998.tb05646.x

Tchuinte, P. L. S., Stalder, T., Venditti, S., Ngandjio, A., Dagot, C., Ploy, M.-C., et al. (2016). Characterisation of class 3 integrons with oxacillinase gene cassettes in hospital sewage and sludge samples from France and Luxembourg. *Int. J. Antimicrob. Agents* 48, 431–434. doi: 10.1016/j.ijantimicag.2016.06.018

Terreni, M., Taccani, M., and Pregnolato, M. (2021). New antibiotics for multidrug-resistant bacterial strains: latest research developments and future perspectives. *Molecules* 26:2671. doi: 10.3390/molecules26092671

Thomas, C. M., and Nielsen, K. M. (2005). Mechanisms of, and barriers to, horizontal gene transfer between bacteria. *Nat. Rev. Microbiol.* 3, 711–721. doi: 10.1038/nrmicro1234

Toleman, M. A., and Walsh, T. R. (2011). Combinatorial events of insertion sequences and ICE in gram-negative bacteria. *FEMS Microbiol. Rev.* 35, 912–935. doi: 10.1111/j.1574-6976.2011.00294.x

Torren-Edo, J., Grave, K., and Mackay, D. (2015). One Health: the regulation and consumption of antimicrobials for animal use in the EU. *IHAJ* 2, 14–16.

Venema, G. (1979). Bacterial transformation. *Adv. Microb. Physiol.* 19, 245–331. doi: 10.1016/s0065-2911(08)60200-3

Verraes, C., Van Boxstael, S., Van Meervenne, E., Van Coillie, E., Butaye, P., Catry, B., et al. (2013). Antimicrobial resistance in the food chain: a review. *Int. J. Environ. Res. Public Health* 10, 2643–2669. doi: 10.3390/ijerph10072643

Vinué, L., Saenz, Y., Somalo, S., Escudero, E., Moreno, M. A., Ruiz-Larrea, F., et al. (2008). Prevalence and diversity of integrons and associated resistance genes in faecal *Escherichia coli* isolates of healthy humans in Spain. *J. Antimicrob. Chemother.* 62, 934–937. doi: 10.1093/jac/dkn331

Vit, C., Richard, E., Fournes, F., Whiteway, C., Eyer, X., Lapaillerie, D., et al. (2021). Cassette recruitment in the chromosomal Integron of *Vibrio cholerae*. *Nucleic Acids Res.* 49, 5654–5670. doi: 10.1093/nar/gkab412

Wellington, E. M. H., Boxall, A. B. A., Cross, P., Feil, E. J., Gaze, W. H., Hawkey, P. M., et al. (2013). The role of the natural environment in the emergence of antibiotic resistance in gram-negative bacteria. *Lancet Infect. Dis.* 13, 155–165. doi: 10.1016/S1473-3099(12)70317-1

World Health Organization. (2015). *Global action plan on antimicrobial resistance*. Geneva: World Health Organization

Wu, Y.-W., Doak, T. G., and Ye, Y. (2013). The gain and loss of chromosomal integron systems in the Treponemaspecies. *BMC Evol. Biol.* 13:16. doi: 10.1186/1471-2148-13-16

Xu, Z., Li, L., Shi, L., and Shirtliff, M. E. (2011a). Class 1 integron in staphylococci. *Mol. Biol. Rep.* 38, 5261–5279. doi: 10.1007/s11033-011-0676-7

Xu, Z., Li, L., Shirtliff, M. E., Alam, M. J., Yamasaki, S., and Shi, L. (2009). Occurrence and characteristics of class 1 and 2 integrons in *Pseudomonas aeruginosa* isolates from patients in Southern China. *J. Clin. Microbiol.* 47, 230–234. doi: 10.1128/JCM.02027-08

Xu, Z., Li, L., Shirtliff, M. E., Peters, B. M., Li, B., Peng, Y., et al. (2011b). Resistance class 1 integron in clinical methicillin-resistant *Staphylococcus aureus* strains in southern China, 2001–2006. *Clin. Microbiol. Infect.* 17, 714–718. doi: 10.1111/j.1469-0691.2010.03379.x

Xu, Z., Li, L., Shirtliff, M. E., Peters, B. M., Peng, Y., Alam, M. J., et al. (2010). First report of class 2 integron in clinical enterococcus faecalis and class 1 integron in *Enterococcus faecium* in South China. *Diagn. Microbiol. Infect. Dis.* 68, 315–317. doi: 10.1016/j.diagmicrobio.2010.05.014

Xu, Z., Li, L., Zhao, X., Chu, J., Li, B., Shi, L., et al. (2011c). Development and application of a novel multiplex polymerase chain reaction (PCR) assay for rapid detection of various types of staphylococci strains. *Afr. J. Microbiol. Res.* 5, 1869–1873. doi: 10.5897/AJMR11.437

Yu, G., Li, Y., Liu, X., Zhao, X., and Li, Y. (2013). Role of integrons in antimicrobial resistance: A review. *Afr. J. Microbiol. Res.* 7, 1301–1310. doi: 10.22038/ijbms.2020.48905.11208

Zhang, X., Wu, B., Zhang, Y., Zhang, T., Yang, L., Fang, H. H. P., et al. (2009). Class 1 integronase gene and tetracycline resistance genes tetA and tetC in different water environments of Jiangsu Province, China. *Ecotoxicology* 18, 652–660. doi: 10.1007/s10646-009-0332-3

Zhang, T., Zhang, X.-X., and Ye, L. (2011). Plasmid metagenome reveals high levels of antibiotic resistance genes and mobile genetic elements in activated sludge. *PLoS One* 6:e26041. doi: 10.1371/journal.pone.0026041

Zhu, J. Y., Duan, G. C., Yang, H. Y., Fan, Q. T., and Xi, Y. L. (2011). Atypical class 1 integron coexists with class 1 and class 2 integrons in multi-drug resistant *Shigella flexneri* isolates from China. *Curr. Microbiol.* 62, 802–806. doi: 10.1007/s00284-010-9790-3

Zhu, Y.-G., Zhao, Y. I., Li, B., Huang, C.-L., Zhang, S.-Y., Yu, S., et al. (2017). Continental-scale pollution of estuaries with antibiotic resistance genes. *Nat. Microbiol.* 2:16270. doi: 10.1038/nmicrobiol.2016.270

Zinsstag, J., Meisser, A., Schelling, E., Tanner, M., and Bonfoh, B. (2012). From 'two medicines' to 'one health' and beyond: proceeding. *Onderstepoort J. Vet. Res.* 79:492. doi: 10.4102/ojvr.v79i2.492

frontiers | Frontiers in Microbiology

TYPE Original Research
PUBLISHED 22 September 2023
DOI 10.3389/fmicb.2023.1273397

OPEN ACCESS

EDITED BY
Vijay Soni,
Weill Cornell Medical Center, NewYork-Presbyterian, United States

REVIEWED BY
Arka Banerjee,
Weill Cornell Medical Center, NewYork-Presbyterian, United States
Nimi Vashi,
Memorial Sloan Kettering Cancer Center, United States
Karthik Kanagaraj,
Columbia University, United States

*CORRESPONDENCE
Jianhong Wei
✉ wjh5123@163.com
Benjin Xu
✉ bj0726@sxmu.edu.cn

†These authors have contributed equally to this work

RECEIVED 06 August 2023
ACCEPTED 06 September 2023
PUBLISHED 22 September 2023

CITATION
Hou Z, Xu B, Liu L, Yan R, Zhang J, Yin J, Li P and Wei J (2023) Prevalence, drug resistance, molecular typing and comparative genomics analysis of MRSA strains from a tertiary A hospital in Shanxi Province, China. *Front. Microbiol.* 14:1273397. doi: 10.3389/fmicb.2023.1273397

Prevalence, drug resistance, molecular typing and comparative genomics analysis of MRSA strains from a tertiary A hospital in Shanxi Province, China

Zhuru Hou[1,2†], Benjin Xu[2,3,4*†], Ling Liu[2,3,4†], Rongrong Yan[4], Jinjing Zhang[4], Jiaxin Yin[1,2], Peipei Li[1,2] and Jianhong Wei[1*]

[1]Department of Basic Medicine, Fenyang College of Shanxi Medical University, Fenyang, China, [2]Key Laboratory of Lvliang for Clinical Molecular Diagnostics, Fenyang, China, [3]Department of Medical Laboratory Science, Fenyang College of Shanxi Medical University, Fenyang, China, [4]Department of Clinical Laboratory, Fenyang Hospital of Shanxi Province, Fenyang, China

Staphylococcus aureus (*S. aureus*) is an important zoonotic pathogen that causes a high incidence rate and mortality worldwide. This study investigated the prevalence of methicillin-resistant *Staphylococcus aureus* (MRSA) strains in a tertiary A hospital in Shanxi Province, China, in order to determine the major epidemic clones as well as their antibiotic resistance and virulence characteristics. A total of 212 *S. aureus* strains were collected in this hospital, and were subjected to antimicrobial susceptibility testing, detection of virulence genes, resistance genes, and efflux pump genes. Among them, 38 MRSA strains were further subjected to detection of biofilm genes, assessment of biofilm formation ability, MLST, *spa* typing, SCC*mec* typing, and phylogenetic analysis. The majority of *S. aureus* strains came from the neonatology department, with secretions and purulent fluid being the main source of samples. The strains showed high resistance to penicillin (98.11%), erythromycin (64.62%) and clindamycin (59.91%), while being sensitive to vancomycin and linezolid. The detection rates of efflux pump genes and resistance genes were high, and there was a significant correlation between resistance gene types and phenotypes, with *mecA* showing a close correlation with oxacillin. The detection rates of virulence genes and the toxin gene profiles of MSSA and MRSA strains showed significant differences. And the detection rate of biofilm genes in MRSA strains was relatively high, with 13.16% of MRSA strains showing strong biofilm formation ability. The most common epidemic clone of MRSA was ST59-SCC*mec*IV-t437, followed by ST59-SCC*mec*V-t437. The former had a higher detection rate of resistance genes and a stronger biofilm formation ability, while the latter had a higher positive rate for *pvl* gene and stronger pathogenicity, making it more likely to cause systemic infections. Phylogenetic analysis showed that all MRSA strains in this study clustered into three major branches, with distinct differences in antibiotic resistance and virulence characteristics among the branches. ST59-MRSA strains from different species showed consistency and inter-species transmission, but there were differences among ST59-MRSA strains from different geographical locations. In general, most MSSA and MRSA strains exhibited multidrug resistance and carried multiple resistance genes, virulence genes, and biofilm formation genes, warranting further research to elucidate the mechanisms of drug resistance and pathogenesis.

KEYWORDS

MRSA, resistance genes, virulence genes, molecular typing, comparative genomics

1. Introduction

Staphylococcus aureus (*S. aureus*) is a widely distributed Gram-positive pathogenic bacterium that gets its name from the yellow grape-like colonies on culture media (Algammal et al., 2020b). It colonizes various parts of the human body, such as the nasal cavity, skin, throat, and digestive system, and is a major cause of endocarditis, bacteremia, osteomyelitis, and skin and soft tissue infections (Turner et al., 2019). The pathogenicity of *S. aureus* primarily stems from the production of exotoxins, including paton-valentine leukocidin (PVL), hemolysins, staphylococcal enterotoxins (SEs), adhesins, exfoliative toxins, etc., which enter the host's body and cause disease through adhesion and invasion (Oliveira et al., 2018). SEs are the most common exotoxins and include *sea-see*, *seg-sej*, *sel-seq*, *ser-set*, *selk-selq*, *selu-selx*; they can disrupt intestinal functions and lead to food poisoning, often causing clinical symptoms of nausea, vomiting, abdominal pain, and diarrhea. PVL is mainly composed of two proteins encoded by the *lukS-PV* and *lukF-PV* genes, and it targets phagocytes, lymphocytes and natural killer cells, causing skin and soft tissue infections and severe necrotizing pneumonia (Bennett and Thomsen, 2020).

Due to the high pathogenicity of *S. aureus*, antibiotics have been widely used in clinical practice to treat *S. aureus* infections. However, just 2 years after the introduction of methicillin, methicillin-resistant *Staphylococcus aureus* (MRSA) emerged (Barber, 1961). Since then, MRSA strains have spread extensively in countries such as Europe and America, transitioning from hospitals to communities. MRSA has become an important pathogen causing both hospital-acquired and community-acquired infections and has evolved to some strains which develop resistance to virtually all clinically available antibiotics (Mlynarczyk-Bonikowska et al., 2022). MRSA is resistant to almost all β-lactam antibiotics, mainly due to the acquisition of a resistant genomic island called staphylococcal cassette chromosome (SCC) element carrying the *mecA/mecC* gene (SCC*mec*). The SCC*mec* element is a mobile genetic element that inserts into the chromosome of susceptible strains, resulting in the production of penicillin-binding protein (PBP2a/2c) and significantly reducing their affinity for β-lactam antibiotics, thus conferring resistance (Yamaguchi et al., 2020). Additionally, multidrug-resistant MRSA strains have acquired numerous resistance genes, which further enhance their resistance complexity and can be transmitted between different strains and species through mobile elements (Monaco et al., 2017).

As the understanding of the constantly changing epidemiology of MRSA increases, there is a need for rapid and reliable methods to characterize isolates to aid in investigating clone dissemination. The main methods for MRSA genotyping include pulsed field gel electrophoresis (PFGE), multilocus sequence typing (MLST), SCC*mec* typing, and *spa* typing. PFGE typing has high resolution, stable and reproducible results, and can effectively reflect the correlation between bacterial genotype and epidemiology. It is considered the "gold standard" for bacterial genotyping (He and Reed, 2020). MLST is based on the differences in seven housekeeping genes of *S. aureus*. This technique has high accuracy, good reproducibility, and allows typing results to be uploaded to public databases for data sharing and comparison, which is important for understanding strain epidemiological characteristics and genetic evolutionary relationships (Liu and Ji, 2020). SCC*mec* typing is based on the differences in *mec* gene complex and cassette chromosome recombinase (*ccr*) gene complex. It has been certified by the international working group on classification of SCC components and is divided into 14 types, SCC*mec* I - SCC*mec* XIV (Uehara, 2022). *spa* typing is a sequencing typing method based on the polymorphism of the X region sequence of *spa* gene, which encodes staphylococcal protein A. This method is fast, reproducible, and has high resolution, indicating both micro and macro variations, making it suitable for local and global epidemiological studies (Wang, 2020).

MRSA strains exhibit genetic diversity, and the main feature of their molecular epidemiology is the continuous emergence of regionally prevalent strains. The prevalence, drug resistance characteristics, virulence characteristics, and epidemic clones of MRSA vary in different regions and change over time. However, there were few reports on the molecular epidemiological characteristics of MRSA in Shanxi Province, China. Therefore, this study focused on 212 strains of *S. aureus* isolated from a tertiary A hospital in Shanxi Province. We investigated the colonization and departmental distribution of the strains, tested their resistance to commonly used clinical antibiotics, as well as the carriage rate of resistance genes, efflux pump genes and virulence genes. Molecular genetic methods such as SCC*mec* typing, MLST, *spa* typing, and whole-genome sequencing were used to genotype the MRSA isolates from different sources and perform comparative genomic analysis. This study provided initial insights into the prevalence characteristics, drug resistance, and genetic polymorphism of healthcare-associated MRSA in Shanxi Province, revealing the molecular features and evolutionary relationships of MRSA strains. It also provided a theoretical basis for the clinical treatment of MRSA infections and technical support for the tracking of healthcare-associated MRSA infections.

2. Materials and methods

2.1. Sample collection and strain isolation

From May 2021 to October 2022, a total of 212 non-duplicate strains of *S. aureus* were collected and isolated from a tertiary A hospital in Shanxi Province. *S. aureus* isolates were recovered from inpatients and outpatients who had cough, fever, skin abscess, and other clinical symptoms related to infection. These strains included all the isolates of *S. aureus* obtained from patients during this period at this hospital. The identification of the strains was performed using matrix-assisted laser desorption/ionization time-of-flight mass spectrometry (MALDI-TOF/TOF) technology. The resistance to oxacillin was determined through antibiotic susceptibility testing, and the presence of the *mecA* gene was confirmed by PCR, identifying 38 strains as MRSA. This study was approved by the Ethics Committee of Fenyang College, Shanxi Medical University. Being a retrospective study, informed consent was not required.

2.2. Antibiotic susceptibility testing

All strains were subjected to antimicrobial susceptibility testing according to the methods recommended by the Clinical and Laboratory Standards Institute (CLSI, 2015). The VITEK2-compact automated antimicrobial susceptibility analyzer was used to determine the minimum inhibitory concentrations of the strains against 12

antibiotics, including penicllin (10 U), erythromycin (15 μg), clindamycin (2 μg), oxacillin (1 μg), sulfamethoxazole (25 μg), tetracycline (30 μg), gentamicin (10 μg), levofloxacin (5 μg), rifampicin (5 μg), nitrofurantoin (300 μg), vancomycin (30 μg), linezolid (30 μg). ATCC29213 was used as the quality control strain.

2.3. Detection of resistance genes, virulence genes, and biofilm-related genes

PCR was performed to detect the positive rates of various genes, including 8 efflux pump genes (Zhang Hang et al., 2019), 17 resistance genes (Merlino et al., 2002; Chen Cheng et al., 2020), 22 virulence genes (Brakstad et al., 1992; Chen Cheng et al., 2020), and 11 biofilm-related genes (Waryah et al., 2016). The primers and PCR programs for amplification of the relevant genes were performed according to the primer sequences and PCR procedures listed in Supplementary Table S1. After the reaction, 6 × DNA loading buffer was added to the PCR products, and 20 μL of the mixture was loaded onto a 1.5% agarose gel for electrophoresis at 110 V for 40 min. The gel was visualized and images were captured using a UV gel imaging system. The positive rates of each gene were calculated.

2.4. Biofilm formation assay

100 μL of the MRSA strains, stored at −80°C, were added to 10 mL of TSB medium and incubated at 37°C with shaking at 220 rpm for 12 h. Then, 100 μL of the cultured bacterial suspension was added to 10 mL of 0.5% TSBG medium and mixed well. Next, 200 μL of the bacterial suspension was added to each well of a 96-well plate, with each strain occupying 5 wells. The plate was then incubated at 37°C for 24 h. After incubation, the liquid and planktonic bacteria were discarded by adding 200 μL of PBS buffer to each well and washing it three times. The wells were then stained with 100 μL of crystal violet dye and incubated for 30 min. After removing the dye, each well was washed three times with 200 μL of PBS buffer. Finally, 200 μL of 95% ethanol was added to each well, and the optical density at 560 nm was measured within 30 min. TSBG medium served as the negative control, and the critical optical density value was defined as ODc (mean OD of the negative control plus three times its standard deviation). The ability to form biofilms was classified into four categories: OD ≤ ODc, no biofilm formation (−); ODc<OD ≤ 2ODc, weak biofilm formation (+); 2ODc<OD ≤ 4ODc, moderate biofilm formation (++); 4ODc<OD, strong biofilm formation (+++).

2.5. Whole-genome sequencing and comparative genomics analysis

The genomes of a total of 38 MRSA strains were sequenced at the Beijing Genomics Institute (BGI, Shenzhen, China) using a PacBio Sequel II and DNBSEQ platform. The PacBio platform utilized four SMRT cells Zero-Mode Waveguide arrays for sequencing, and the resulting subreads set was generated. Subreads were repaired and the Canu program was employed for self-correction.

The assembled contigs were used for molecular typing, including MLST, *spa*-typing and SCC*mec* typing. These typings were predicted using the Center for Genomic Epidemiology website.[1] For function annotation, the WGS data was annotated some databases, including VFDB (for virulence genes) (Chen et al., 2016), ARDB, CARD (for resistance genes) (Alcock et al., 2020) and COG (Galperin et al., 2015). Analyze the Core/Pan genes of all MRSA strains, as well as the COG functions of these genes. Cluster these strains based on Core/Pan genes, and construct the phylogenetic tree using the TreeBeST with the NJ method. Then 20 strains of ST59 MRSA strains were selected from NCBI, and these strains were compared with ST59 strains in this study to build a phylogenetic tree. The production and processing of images, such as heat maps, box plots, phylogenetic trees and so on, have been utilized on the chiplot online website.[2]

2.6. Statistical analyses

Statistical analyses were performed using Graphpad Pism 9.5 for Windows. Chi-squared test was used for rate analysis, and Pearson correlation test was used for consistency analysis. The $p < 0.05$ was considered to indicate statistical significance. *$p \leq 0.05$; **$p \leq 0.01$; ***$p \leq 0.001$; ****$p \leq 0.0001$.

3. Results

3.1. Sample source and department distribution of *Staphylococcus aureus*

A total of 38 out of the 212 identified *S. aureus* strains were confirmed to be MRSA (Table 1). These strains were sourced from various departments, with both methicillin-susceptible *S. aureus* (MSSA) and MRSA mainly originating from the neonatology department (31/174, 17.82%; 9/38, 23.68%). For MSSA, children (53/174, 30.46%), middle-aged individuals (59/174, 33.91%), and the elderly (54/174, 31.03%) were the predominant affected populations. On the other hand, MRSA primarily affected children (19/38, 50.00%) and the elderly (10/38, 26.32%). The main sources of the strains were secretions and purulent fluid, with 23 and 11 MRSA cases originating from secretions and purulent fluid, respectively. The remaining 4 cases were from sputum, throat swabs, vaginal swabs, and tissue samples. Statistical analysis showed significant differences in age and sample type, in addition to gender and department distribution. Detailed information on the MRSA strains can be found in Supplementary Table S2.

3.2. The drug resistance characteristics of *Staphylococcus aureus* isolates

In this study, *S. aureus* exhibited high resistance rates to penicillin (208/212, 98.11%), erythromycin (137/212, 64.62%), and clindamycin (127/212, 59.91%). It showed sensitivity to vancomycin and linezolid. Oxacillin, sulfamethoxazole, tetracycline, gentamicin, levofloxacin,

1 https://cge.cbs.dtu.dk/services
2 https://www.chiplot.online/

10.3389/fmicb.2023.1273397

TABLE 1 The general information of *S. aureus* isolates.

		Group				χ^2	*p* value
		MSSA	%	MRSA	%		
Sex	Male	102	58.62%	23	60.53%	0.084	0.7721
	Female	72	41.38%	15	39.47%		
Age	≤9 year	53	30.46%	19	50.00%	8.767	0.0326
	9–18 year	8	4.60%	1	2.63%		
	18–50 year	59	33.91%	8	21.05%		
	>50 year	54	31.03%	10	26.32%		
Department	Neonatal pediatrics	31	17.82%	9	23.68%	12.689	0.1776
	Otolaryngology	24	13.79%	7	18.42%		
	Burn department	25	14.37%	3	7.89%		
	Pediatrics	10	5.75%	5	13.16%		
	Orthopedics	10	5.75%	3	7.89%		
	Endocrinology department	11	6.32%	2	5.26%		
	Obstetrics	11	6.32%	1	2.63%		
	General surgery department	7	4.02%	2	5.26%		
	Department of divine surgery	7	4.02%	1	2.63%		
	Other departments	38	21.84%	5	13.16%		
Specimen type	Secretion	116	66.67%	23	60.53%	22.034	0.0002
	Purulent fluid	19	10.92%	11	28.95%		
	Puncture fluid	14	8.05%	0	0		
	Blood	10	5.75%	0	0		
	Others	15	8.62%	4	10.53%		

rifampicin, and nitrofurantoin demonstrated good activity against *S. aureus*, with resistance rates ranging from 0.5 to 17% (Figure 1A). Multiple drug resistance was observed in 57.47% of the MSSA strains and 81.58% of the MRSA strains. One MSSA strain exhibited resistance to all seven antibiotics tested, while 26/38 MRSA strains demonstrated resistance to four or five antibiotics (Figure 1B). Detection of efflux pump genes revealed high detection rates for all genes except *qacA/B* and *smr*, which were not detected in MRSA strains. The detection rates for *norA*, *norB*, *norC*, *mepA*, and *mdeA* genes in MRSA strains were 100%, slightly higher than their detection rates in MSSA strains (Figure 1C). The most common efflux pump gene profile in all strains was *norA-norB-norC-sepA-mepA-mdeA* (120/212, 56.60%). Detection of resistance genes showed that among the 37 oxacillin-resistant strains, 24 were *mecA*-positive, while one strain was sensitive to oxacillin but tested positive for the *mecA* gene. In all strains, quinolone-related genes *gyrA* and *grlA* (174/174, 100%; 32/38, 84.21%), and β-lactam-related gene *blaZ* (142/174, 81.61%; 31/38, 81.58%) exhibited the highest detection rates. But *tet(O)* and *mecC* were not detected in any of the strains (Figure 1D). The most common resistance gene profile in all strains was *blaZ-ermC-gyrA-grlA* (51/212, 24.06%). Consistency analysis of all efflux pump genes, resistance genes, and antibiotic detection results revealed a significant correlation between resistance genotypes and phenotypes, showing a positive correlation. When the Pearson correlation coefficient is greater than 0.4, it indicated a strong correlation. The closely related correlations found in this study were *mecA* and oxacillin ($r = 0.7378$), *aacA-aphD* and gentamicin ($r = 0.6943$), *aacA-aphD* and sulfamethoxazole ($r = 0.598$), *ermB* and gentamicin ($r = 0.4772$), *ermB* and sulfamethoxazole ($r = 0.4127$) (Figure 1E).

3.3. The virulence characteristics of *Staphylococcus aureus* isolates

In this study, all enterotoxin genes were detected, but the detection rates varied significantly among different strains. Among MSSA strains, *seg* had the highest detection rate (132/174, 75.86%), followed by *sei* (116/174, 66.67%), *seln* (110/174, 63.22%), *selo* (108/174, 62.07%), and *selm* (108/174, 62.07%). In MRSA strains, *sea* had the highest detection rate (32/38, 84.21%), followed by *selq* (21/38, 55.26%), *selk* (20/38, 52.63%), and *seb* (19/38, 50.00%). The detection rate of the *pvl* gene was relatively high, and the detection rate in MSSA strains (70/174, 40.23%) was higher than that in MRSA strains (9/38, 23.68%). The detection rates of toxic shock syndrome toxin (*tst*) gene and exfoliative toxin (*eta*) gene were maintained at 2 to 5.5%, while the exfoliative toxin (*etb*) gene was not detected in any strains (Figure 2A). The most common virulence gene profile in all strains was *pvl-seg-sei-selm-seln-selo* (43/212, 20.28%). The distribution of virulence gene numbers in MSSA strains ranged from 0 to 12, with 29.31% of strains

10.3389/fmicb.2023.1273397

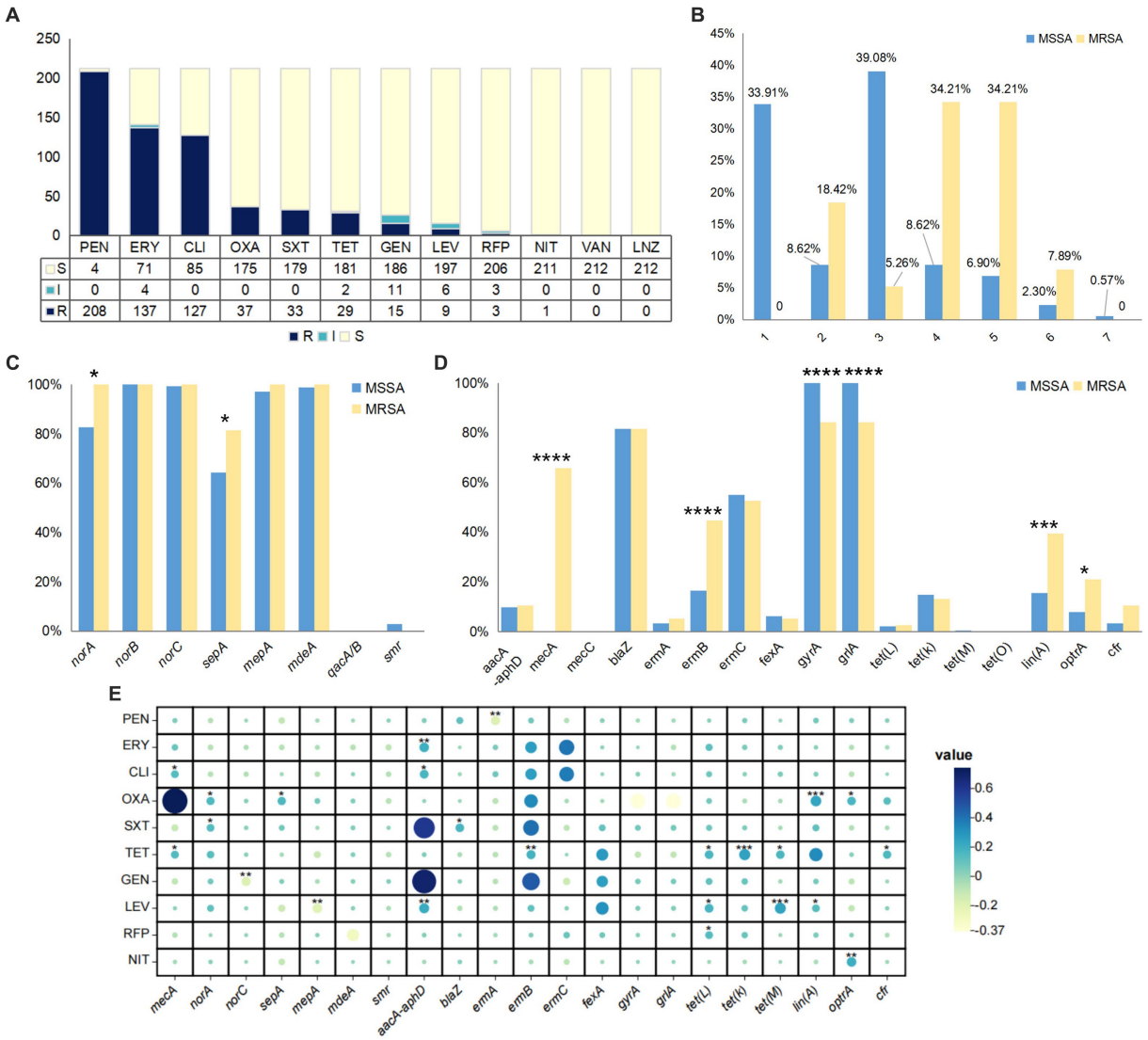

FIGURE 1
The drug resistance characteristics of *S. aureus* isolates. **(A)** The antibiotic susceptibility testing of all strains. PEN, penicillin; ERY, erythromycin; CLI, clindamycin; OXA, oxacillin; SXT, sulfamethoxazole; TET, tetracycline; GEN, gentamicin; LEV, levofloxacin; RFP, rifampicin; NIT, nitrofurantoin; VAN, vancomycin; LNZ, linezolid. **(B)** The number of antibiotic resistance of MSSA and MRSA. **(C)** Detection rate of efflux pump genes. **(D)** The detection rate of resistance genes. **(E)** Consistency between drug resistance genotypes and phenotypes. The size of the circle represents the correlation between the antibiotics and resistance genes, and the closer the correlation, the larger the circle. The $p < 0.05$ was considered to indicate statistical significance. *$p \leq 0.05$; **$p \leq 0.01$; ***$p \leq 0.001$; ****$p \leq 0.0001$.

harboring 6 virulence genes. Low-pathogenicity strains without virulence genes accounted for 6.32% of MSSA strains, while 1.72% of strains had 12 virulence genes and exhibited high pathogenicity. Considering the clinical information, all highly pathogenic strains were derived from the otolaryngology department. MRSA strains mainly had 4 to 6 or 10 virulence genes, generally demonstrating strong pathogenicity (Figure 2B). Figure 2C analyzed the virulence gene profiles of the 38 MRSA strains and showed a complex pattern, with a total of 22 types, among which *sea-seb-selk-selq* were the most common.

3.4. Biofilm detection of MRSA

The positive rates of biofilm-associated genes in the 38 MRSA strains were analyzed in Supplementary Figure S1A, and except for *fib*, which was not detected, the positive rates of the remaining genes were all above 80%. Among them, *clfA*, *clfB*, *fnbA*, *icaA*, *icaB*, *icaC*, and *icaR* were detected in all MRSA strains. The biofilm formation ability test results showed that, except for strains SA17 and SA35, all other strains were capable of biofilm formation (Supplementary Figure S1B). Most strains showed weak (17/38, 44.74%) or moderate (14/38, 36.84%) biofilm formation ability, while only 5 strains showed strong biofilm formation ability (Supplementary Figure S1C).

3.5. Molecular typing of MRSA

A total of 14 MLST types were identified among the 38 MRSA strains, with ST59 being the most prevalent type (19/38, 50.00%), followed by ST22 (3/38, 7.80%) and ST5 (3/38, 7.80%). SCC*mec*

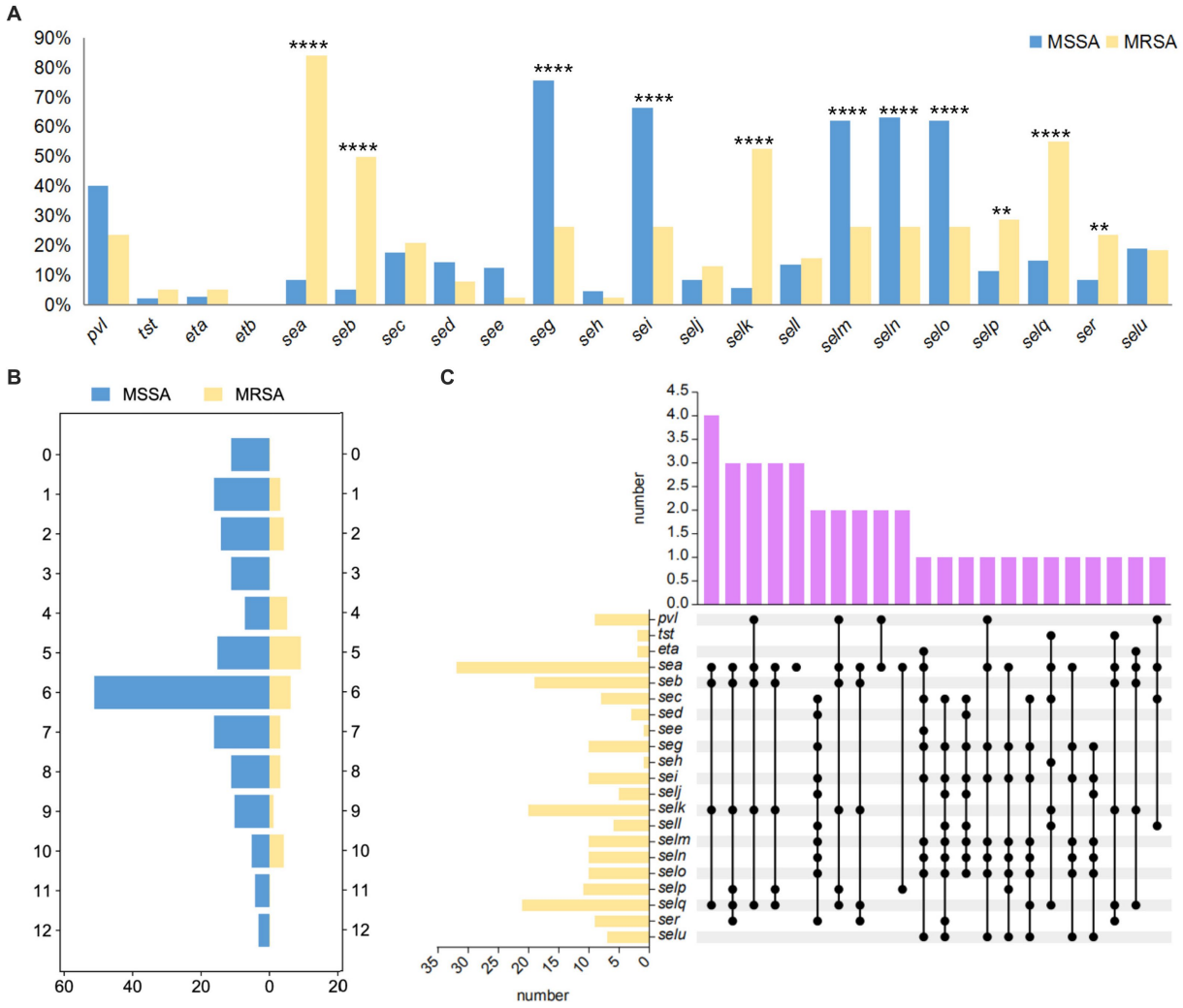

FIGURE 2
The virulence characteristics of *S. aureus* isolates. **(A)** The detection rate of virulence genes of all strains. **(B)** The number of virulence genes of MSSA and MRSA. The horizontal axis represents the number of strains, while the vertical axis represents the number of genes. **(C)** The upset plot of MRSA. The bar chart on the left represents the quantity of various toxic genes. The solid circles represent the intersection between data quantities, meaning that each vertical column of solid circles represents a specific toxic gene profile. The bar chart above represents the quantity of different toxic gene profiles. The $p < 0.05$ was considered to indicate statistical significance. $^{**}p \leq 0.01$; $^{****}p \leq 0.0001$.

typing revealed the presence of three major types and five minor subtypes, including IVa (14/25, 56%), IVc (1/25, 4%), IVg (1/25, 4%), Vb (8/25, 32%), and XII (1/25, 4%). Additionally, 13 MRSA strains were detected to be *mecA*-negative and SCC*mec* element-negative, but still exhibited resistance to oxacillin. In terms of *spa* typing, except for strain SA27, the remaining 37 MRSA strains were classified into 15 types, with t437 being the most prevalent (17/37, 45.95%), followed by t441 (3/37, 8.11%) and t309 (3/37, 8.11%) (Supplementary Table S2). MLST typing, SCC*mec* typing, and *spa* typing showed a close relationship, with all ST22 types corresponding to t309, while ST59 types were predominantly associated with SCC*mec*-IV, V and *spa* t437 and t441. The most common epidemic clone in this study was ST59-SCC*mec* IV-t437 (8/38, 21.05%), followed by ST59-SCC*mec* V-t437 (6/38, 15.79%) and ST59-SCC*mec* IV-t441 (3/38, 7.89%). Analysis of the number of resistance genes and virulence genes in the major types showed that ST59 had a higher number of resistance genes but fewer virulence genes compared to ST5 and ST22. There was no significant difference in the number of resistance genes and virulence genes between SCC*mec* IV and V. The *spa* type t437 exhibited high levels of resistance genes and virulence genes, t441 had more resistance genes but very few virulence genes, and t309 showed the opposite pattern (Figure 3A). Different strains of different molecular types exhibited varying biofilm formation abilities, with ST59-MRSA strains showing higher biofilm formation abilities, and significant differences were observed between ST59-MRSA and ST5-MRSA strains (Figure 3B). Figure 3C analyzed the resistance gene profiles, virulence gene profiles, and biofilm formation abilities of the three major epidemic clones. ST59-SCC*mec* V-t437 had a high positive rate for the *pvl* gene, reaching 66.67%. The *ser* gene rate for the ST59-SCC*mec* IV-t437 type was relatively high at 37.5%, and this type of MRSA strain showed higher biofilm formation abilities.

10.3389/fmicb.2023.1273397

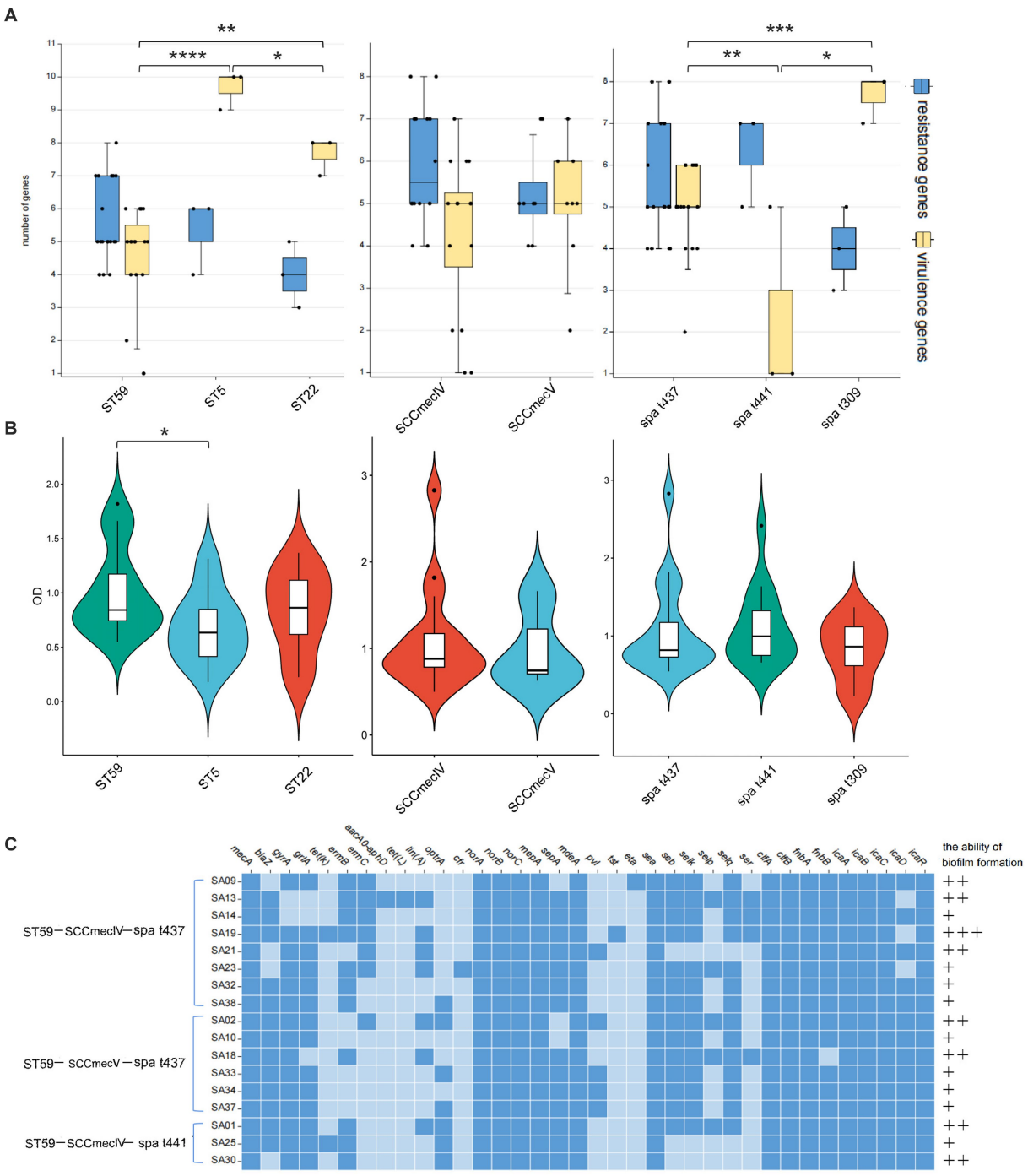

FIGURE 3
The resistance and virulence characteristics of major typings. **(A)** The number of resistant and virulence genes in the main typing strains. The horizontal axis represents different subtypes, while the vertical axis represents the number of genes. The box plot represents the average, upper and lower quartiles of these gene numbers. **(B)** The biofilm formation ability in the main typing strains. The horizontal axis represents different subtypes, while the vertical axis represents OD value. The violin diagram shows the distribution and probability density of biofilm formation ability. **(C)** The gene heatmap of major epidemic typings. Dark blue indicates the presence of this gene, while light blue indicates the absence of this gene. The formation ability of biofilms varies from strong (+++) to weak (+). The $p < 0.05$ was considered to indicate statistical significance. *$p \leq 0.05$; **$p \leq 0.01$; ***$p \leq 0.001$; ****$p \leq 0.0001$.

3.6. Phylogenetic analysis

Core-pan analysis of the 38 MRSA strains revealed a total of 2094 core genes and 0–66 dispensable genes distributed among the strains, with SA03, SA11, and SA26 having the highest number of dispensable genes (Figure 4A). COG functional annotation analysis was performed on the 2094 core genes and 309 dispensable genes, resulting in annotations to 23 and 19 categories, respectively. The core genes were involved in a wide range of functions, primarily in translation, ribosomal structure, and biogenesis (9.98%), followed by amino acid

transport and metabolism (9.60%). The dispensable genes were primarily involved in mobilome: prophages, transposons (16.83%), and replication, recombination, and repair (15.86%) (Figure 4B). A heatmap was created based on the distribution of dispensable genes among different strains, which also showed clustering of the strains. The results revealed that these 38 strains mainly clustered into four major branches, with SA04 and SA07 forming a separate branch that was more distantly related to the other strains (Figure 4C).

According to the analysis of core-pan genes, a phylogenetic tree of the 38 strains was constructed (Figure 5). The results showed that these strains were closely related and mainly clustered into three major branches, clade I, clade II, and clade III. SA04 and SA07 formed a separate branch, clade I. Clade II mainly consisted of strains that were not classified in SCC*mec* typing, and these strains were resistant to oxacillin but did not contain the *mecA* gene. Additionally, the positive rate of the resistance gene *blaZ*, associated with β-lactam antibiotics, was higher than the average level, reaching 85.7% in clade II. Clade III mainly consisted of MRSA strains of ST59 genotype, which exhibited significant differences in resistance and virulence genes compared to clade II. In clade III, the *vanRE* gene had a high detection rate of 100%, while *aph(3′)-IIIa*, *aad(6)*, and *ant6-Ia* had detection rates of 63.6%. In clade II, the detection rates of *vanRE* and *ant6-Ia* were 21.4 and 7.1% respectively, and *aph(3′)-IIIa* and *aad(6)* were not detected. The sulfonamide resistance genes *dfrA* and *dfrG* were not detected in clade III, while they had detection rates of 21.4% in clade II. The *lukD/lukE* gene, associated with leukocidin, had a high detection rate of 71.4% in clade II, while it was 4.5% in clade III. The *lukF-PV/lukS-PV* gene had similar detection rates in clade III and clade II, at 27.2 and 21.4%, respectively. Clade II and clade III had different profiles of common enterotoxin genes, which were *seg-sei-selm-seln-selo-set* and *sea-seb-selk-selq-set*, respectively.

3.7. The evolutionary analysis of ST59-MRSA

In this study, ST59-MRSA was the most common clone type, and a phylogenetic tree of 19 ST59-MRSA strains was constructed based

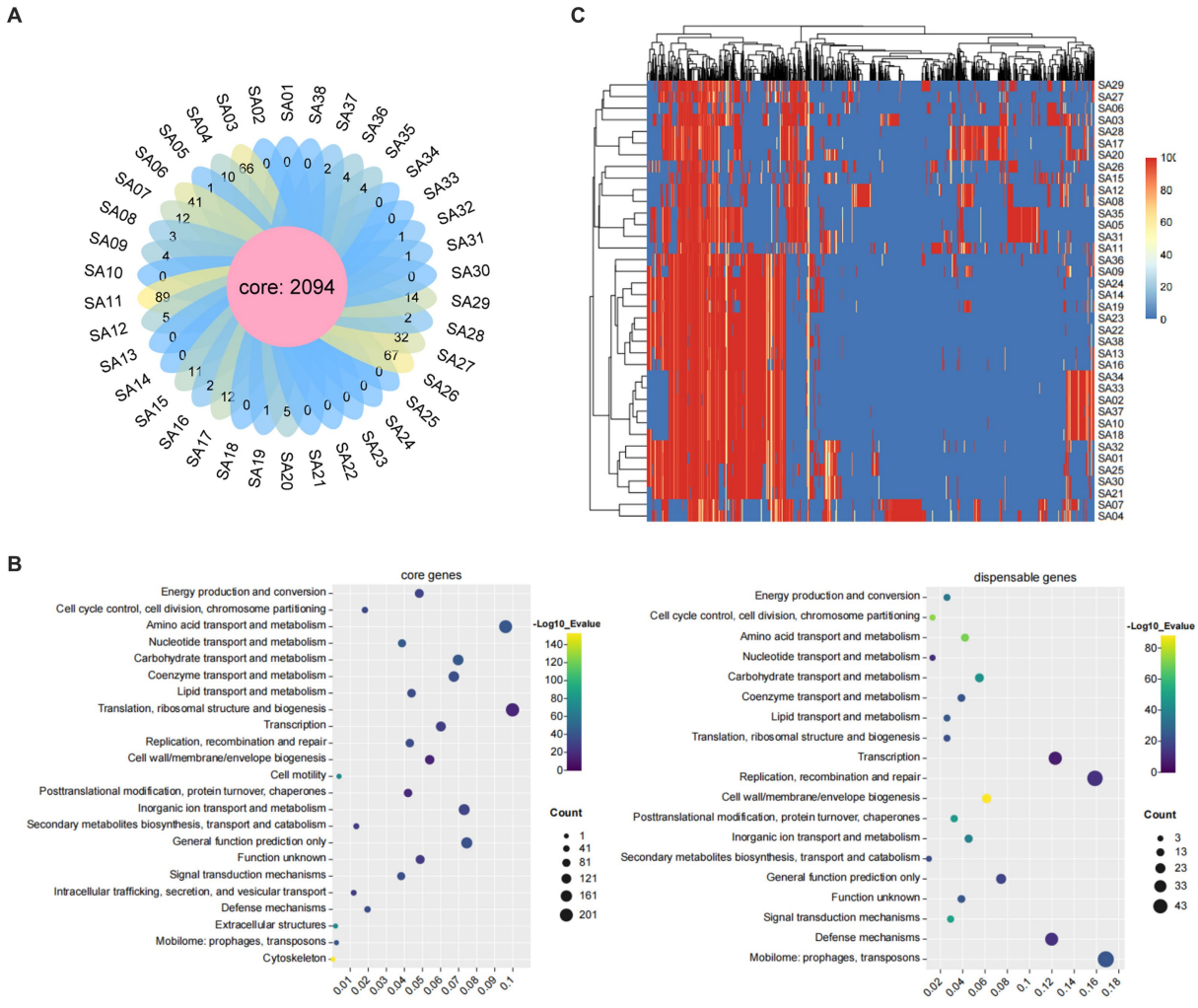

FIGURE 4
The core and pan-genome analyses of 38 MRSA in this study. **(A)** The flower diagram of numbers of core genes and dispensable genes for all the strains. **(B)** The COG functional annotation of core genes and dispensable genes. **(C)** The heat map of dispensable genes. Top are Dispensable gene cluster and left are strain cluster. The similarities of gene are shown in the middle with different color represent different coverage by heat map.

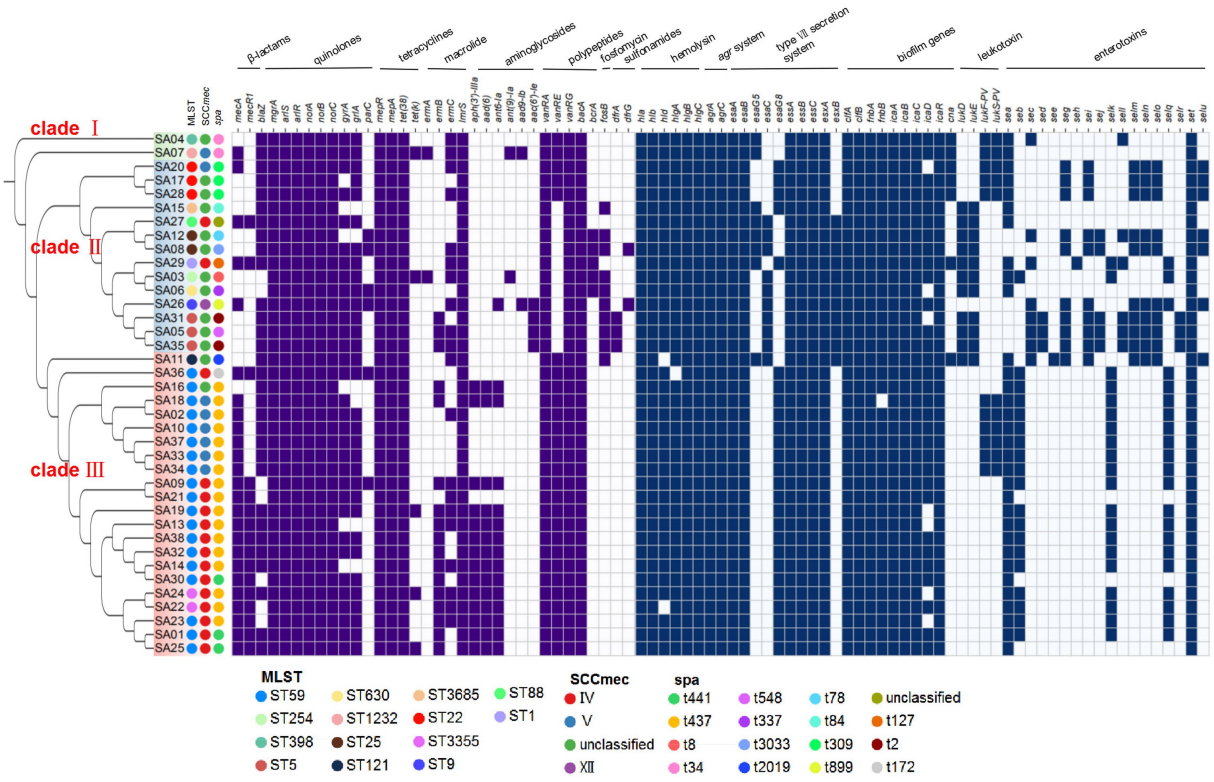

FIGURE 5
The phylogenetic trees of 38 MRSA strains. Perform phylogenetic analysis on 38 MRSA strains and construct a phylogenetic tree. These strains were divided into three branches, namely green (clade I), blue (clade II), and red (clade III). The different colors of the circles represented the different subtypes of the strains. Blocks indicated the presence or absence of these genes, dark blue indicated the presence of these genes, and light blue indicated the absence of these genes.

on core-pan genes (Figures 6A,B). The phylogenetic tree showed that these strains clustered into three branches, indicating diversity. Strains of the ST59-SCC*mec* V-t437 type were closely related and formed a single branch. Figures 6A,B showed that differences in departments and sample types did not have a significant impact on the phylogenetic relationship of strains. Strains from different departments exhibited similarities, while strains from the same department exhibited diversity. COG functional annotation was performed on the 19 ST59-MRSA strains, and they were annotated to 23 entries, showing some variation between the genomes, but primarily annotated to amino acid transport and metabolism and translation, ribosomal structure, and biogenesis (Figure 6C). To study the genetic evolutionary relationship of ST59-MRSA, 22 ST59-MRSA strains were selected from the NCBI database as reference sequences (Supplementary Table S3), and a phylogenetic tree was constructed with them and the 19 ST59-MRSA strains from this study (Figures 6D,E). Except for SA36, the remaining 18 MRSA strains from this study clustered into the same branch. SA36 had the closest relationship with strain SWF.27 from European human sources, both belonging to ST59-t172. Figure 6D showed that ST59-MRSA strains from humans, animals, and food sources were closely related and exhibited consistent relationships. Figure 6E showed that the phylogenetic relationship between strains was related to geographic location, with ST59-MRSA primarily originating from Asia and exhibiting distinct regional characteristics. ST59-MRSA strains from the Americas and Europe tended to be in different evolutionary branches compared to those from Asia.

4. Discussion

MRSA is characterized by its wide spread, fast transmission, and complex resistance mechanisms, making the monitoring and treatment of MRSA an important topic of concern. According to the surveillance by the CHINET surveillance system, *S. aureus* has maintained a high detection rate, while the infection rate of MRSA decreased from 45 to 30% between 2013 and 2021. In some Asian countries, the hospital-acquired MRSA infection rates remain above 20%, with rates reaching as high as 70–80% in countries like South Korea and Vietnam (Chen and Huang, 2014). In our study, the MRSA infection rate was relatively low at 17.9%, below the national average. Children and elderly patients were the most common groups affected by MRSA infection, and there was a significant difference in MRSA infection rates based on age. Previous research has shown a decline in the outpatient visit rate for pyogenic skin and soft tissue infections in pediatrics, but *S. aureus* remains a major cause of invasive bacterial infections in children (Prochaska et al., 2023).

Antibiotic susceptibility testing results showed that most strains exhibited high resistance to penicillin, erythromycin, and clindamycin, while showing good antibacterial activity against vancomycin and linezolid, which is consistent with a multicenter longitudinal study of MRSA strains in China conducted by Wang B. et al. (2022). However, in this study, the resistance rates to tetracycline and gentamicin were 13.68 and 7.08%, respectively, significantly lower than the national average (42.8, 33.5%), which may

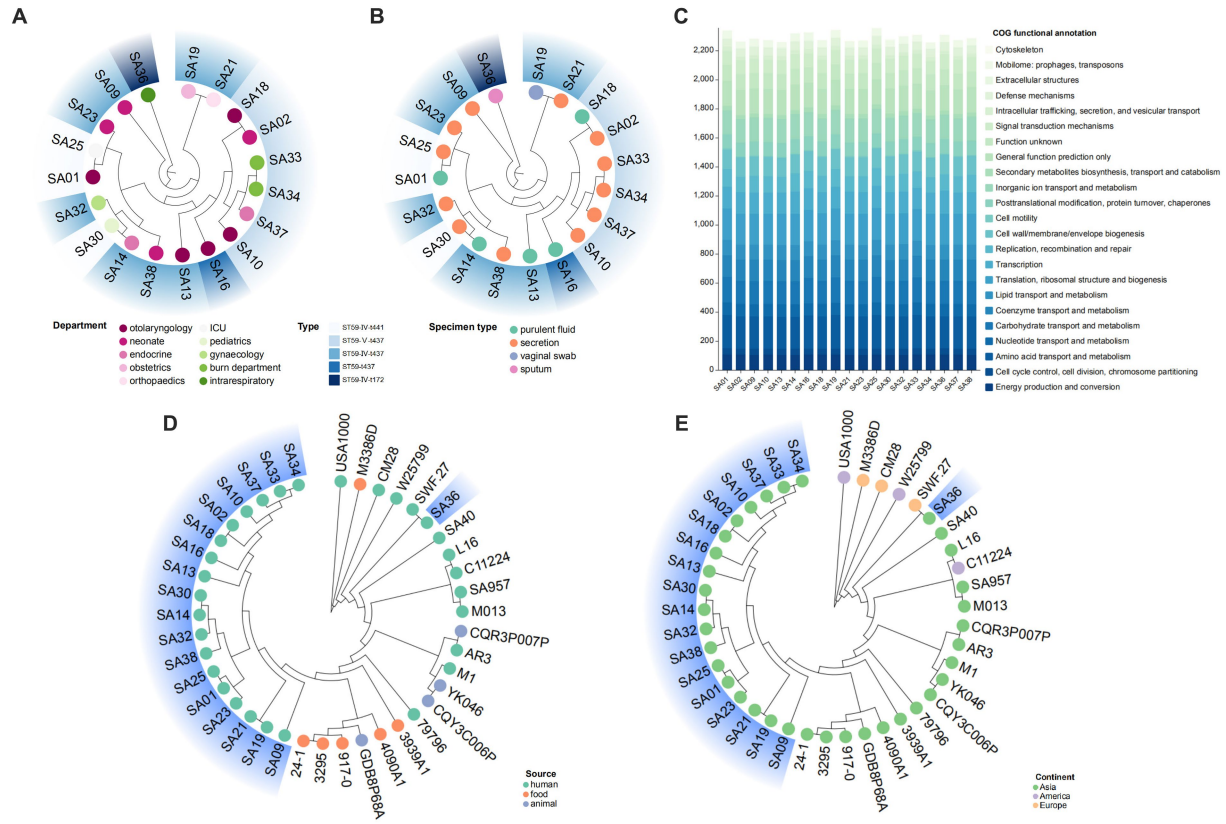

FIGURE 6
The evolutionary analysis of ST59 typing. **(A,B)** The phylogenetic trees of ST59 MRSA strains in this study. Analyze the impact of differences in departments **(A)** and speciman types **(B)** on the genetic relationships of strains. **(C)** The COG functional annotation of ST59 MRSA strains in this study. **(D,E)** The phylogenetic trees of ST59 MRSA strains in this study and 20 reference strains. Analyze the impact of differences in sources **(D)** and continents **(E)** on the genetic evolution of strains.

be due to the lower usage rate of tetracycline and gentamicin in the Shanxi hospital. The multidrug resistance of *S. aureus* is not only present in clinical strains but also in retail water products in China. Monitoring of *S. aureus* in these products found that 90.6% of strains exhibited multidrug resistance, with high resistance against penicillin (88.2%), ampicillin (88.2%), and erythromycin (53.8%) (Rong et al., 2017). In this study, in addition to 81.58% of MRSA strains, 57.47% of MSSA strains also exhibited multidrug resistance, which was associated with the high detection rate of resistance genes and efflux pump genes. The resistance of beta-lactam antibiotics is mainly related to *mecA* and *blaZ*, with a high detection rate of *blaZ* in all strains. It encodes β-lactamase, which mediates the degradation of β-lactam antibiotics (Rocha et al., 2022). We also found 34.21% of MRSA strains showed resistance to oxacillin but were negative for the *mecA* and *mecC* genes. This may be due to the overproduction of β-lactamase or modifications in PBP genes caused by spontaneous amino acid substitutions in the transpeptidase domain (Hou et al., 2023). The detection rate of *pvl* gene in this type of MRSA was only 15.3%, which confirms that this type of MRSA generally does not contain the PVL locus that expresses leukocidin. Resistance to erythromycin is mainly determined by the resistance gene *erm*. Consistent with previous research, the highest positive rates of *ermC* (52.63%) and *ermB* (44.74%) were observed in MRSA strains, with *ermC* playing a dominant role in the mechanism of erythromycin resistance (Li et al., 2019). And also, *erm* can mediate the resistance of *S. aureus* to most macrolides, lincosamides, and streptogramins B (MLS-B), that is the *ermA* or *ermC* genes often determine the inducible resistance to MLS-B in *S. aureus*. The frequency of formation of constitutive variants from inducible *ermA* and *ermC* genes are usually high. The reasons behind constitutive variants include deletions, duplications, insertions, and, to a lesser extent, point mutations found in a region approximately 200 bp upstream of the 5′ end of the *erm* gene (Mlynarczyk-Bonikowska et al., 2022). But in this study, three point mutations (T222C, C224T, G299A) occurred in the *ermB* gene of SA05 and SA09 strains, resulting in ones synonymous mutation (Asn→Asn) and two missense mutations (Thr→Ile, Ser→Asn). However, these mutations do not affect the resistance of both strains to erythromycin and clindamycin. Pearson correlation analysis showed consistency between the resistance genotypes and phenotypes of *S. aureus*, and the use of conserved genes in *S. aureus* was able to successfully predict the resistance phenotype of strains. This suggests that a large hospital can use genomic data features to construct strain prediction models, which can be directly used to determine the drug resistance of strains and guide treatment in the absence of rapid susceptibility results (Wang S. et al., 2022). Therefore, the results of the study on the resistance genotypes and phenotypes of these *S. aureus* strains can serve as a medication guide for the treatment of *S. aureus* infections in this

hospital and assist in the identification and treatment of multidrug-resistant bacteria in clinical practice.

In this study, all isolates contained at least one virulence gene, which plays an important role in colonization, invasion, and infection processes (Patel and Rawat, 2023). Enterotoxin is one of the main causes of foodborne illnesses caused by *S. aureus*. There were significant differences in the enterotoxin gene profiles between MSSA and MRSA strains. The classical enterotoxin genes *sea* (84.21%) and *seb* (50.00%) were more frequently detected in MRSA strains. In a study on subclinical mastitis in cows and water buffaloes, milk samples were collected, and MRSA isolates were tested for toxin genes, with the *sea* gene being the most prevalent (Algammal et al., 2020a). The *sea* gene is heat-stable and can maintain some activity under conditions of 28°C for 121 min. It is commonly detected in foodborne MRSA strains and has a significant association with outbreaks of food poisoning (Lv et al., 2021). The *seb* gene is usually highly expressed in ST59-MRSA, which contributes to widespread systemic infection, which may be the reason for the increased mortality rate of ST59 infection in China (Bae et al., 2021). In MSSA strains, the most common enterotoxin gene profile is *seg-sei-selm-seln-selo*, which belongs to the enterotoxin gene cluster (*egc* cluster). The *egc* cluster functions as a superantigen, activating T lymphocytes and antigen-presenting cells to produce a large amount of cytokines, which can directly cause toxicity to the cardiovascular system (Patel and Rawat, 2023). The *egc* cluster has become a major enterotoxin gene in *S. aureus*, with similar findings in oral *S. aureus* (Kwapisz et al., 2020) and foodborne *S. aureus* (Wu et al., 2019; Igbinosa et al., 2023). We found that the distribution of enterotoxin genes in this hospital is diverse, with different toxin gene distributions in different populations and disease types. Classical enterotoxin genes and *egc* clusters have become the main toxin genes in healthcare-associated and foodborne *S. aureus*. PVL is a two-component toxin composed of LukS and LukF proteins, which bind to C5aR and C5L2, forming channels on the cell membrane of white blood cells, leading to cell lysis and tissue necrosis, causing skin and soft tissue infections (Patel and Rawat, 2023). The detection rate of the *pvl* gene in this study was relatively high at 37.26%, higher than the detection rate of the *pvl* gene isolated from blood samples by Wang et al. (2021). PVL is commonly found in community-acquired methicillin-resistant *Staphylococcus aureus* (CA-MRSA) and has been considered a marker for CA-MRSA (Hou et al., 2023). Therefore, based on the detection rate of *pvl* and preliminary epidemiological investigations indicating that these strains in this study are mostly community-acquired infections, it suggests that CA-MRSA is not only spreading in the community but also increasing in prevalence in hospitals. In addition, the detection rate of *pvl* in MSSA strains (70/174, 40.23%) was higher than that in MRSA strains (9/38, 23.68%), which may be related to the source and number of samples. However, it also indicates that although MRSA has attracted attention due to its multidrug resistance, it is not necessarily more virulent than MSSA.

The clone types of *S. aureus* have geographical advantages, and ST59 is the predominant MRSA clone in China and even Asia (Huh and Chung, 2016). In this study, 50% of the MRSA isolates belonged to the ST59-MRSA. Systematic evolutionary analysis of ST59-MRSA showed consistency among strains isolated from humans, food, and animals, indicating close genetic relatedness. Additionally, the phylogenetic relationship among strains was associated with geographical location, with strains from different continents tending to diverge in evolution. In a study by Wang B. et al. (2022) in 2022, ST59-MRSA accounted for 27.1% of the clinical MRSA isolates in China. Wu et al. (2019) analyzed food-related MRSA in China in 2019 and found that 47.7% of the isolates belonged to ST59-MRSA, and it has been shown that food-related MRSA strains have a high degree of similarity to community-associated MRSA. The distribution of ST59-MRSA is geographically limited and mainly spreads within Asia. However, analysis of isolates from Europe showed that the resistance profiles of European ST59-t437 isolates were similar to those of Asian ST59-t437 isolates, but different from other MRSA isolates in Europe (Glasner et al., 2015).

In this study, the predominant epidemic clones were ST59-SCC*mec*IV-t437 and ST59-SCC*mec*V-t437, both belonging to clade III in the phylogenetic tree but relatively independent, forming two smaller branches. Both clones showed high rates of resistance and virulence gene detection, with resistance genes detected for all antibiotic classes except sulfonamides. The main enterotoxin genes in these clones were the classical enterotoxin genes *sea* and *seb*, and the ST59-SCC*mec*V-t437 clone had a high positive rate for the *pvl* gene, reaching 66.67%. These two clones belong to the Asian-Pacific clone and the Taiwan clone, respectively. Asian-Pacific clone isolates are mostly *pvl*-negative and colonize healthy children, while Taiwan clone carries the *pvl* gene and is generally isolated from critically ill patients. Due to the high expression of *pvl* and *hla* genes in Taiwan clone isolates, it has higher virulence and pathogenic potential compared to the Asian-Pacific clone (Chen et al., 2013). MLST is consistent with *spa* typing, and the ST59 typing is generally associated with t441 and t437. And then we found an ST59-t172 isolate, which is distantly related to other ST59-MRSA strains in this study but closely related to an ST59-t172 isolate from Finland in Europe. It is extremely rare elsewhere and mainly reported in Finland. The ST59-t172 strain mainly spreads among elderly patients and can cause outbreaks of *S. aureus* in environments with low MRSA incidence (Silvola et al., 2022).

5. Conclusion

This study investigated the colonization and distribution of *S. aureus* in a tertiary A hospital in Shanxi, China. It detected the antibiotic resistance, biofilm formation capability, as well as the carriage rates of resistance genes, virulence genes, and biofilm-related genes in the isolates. And then three molecular typing methods and whole-genome sequencing were used to study the molecular characteristics and genetic evolution of MRSA isolates from different sources. It was found that MRSA isolates displayed multidrug resistance, and the carriage of resistance genes and virulence genes exhibited diversity and complexity. The predominant clones were ST59-SCC*mec*IV-t437 and ST59-SCC*mec*V-t437, and ST59-MRSA was closely associated with various hosts, showing diverse patterns of transmission. This study elucidated the molecular characteristics and evolutionary relationship of MRSA isolates, which can contribute to the prevention and control of *S. aureus* infections.

Data availability statement

The datasets presented in this study can be found in online repositories. The names of the repository/repositories and accession

number(s) can be found at: https://www.ncbi.nlm.nih.gov/, PRJNA994481.

Ethics statement

The studies involving humans were approved by Scientific Research Ethics Committee, Fenyang College of Shanxi Medical University. The studies were conducted in accordance with the local legislation and institutional requirements. Written informed consent for participation was not required from the participants or the participants' legal guardians/next of kin in accordance with the national legislation and institutional requirements.

Author contributions

ZH: Conceptualization, Data curation, Investigation, Methodology, Visualization, Writing – original draft, Writing – review & editing. BX: Conceptualization, Data curation, Funding acquisition, Investigation, Methodology, Project administration, Supervision, Visualization, Writing – original draft, Writing – review & editing. LL: Conceptualization, Funding acquisition, Investigation, Project administration, Visualization, Writing – original draft, Writing – review & editing. RY: Writing – review & editing, Investigation, Methodology, Resources, Validation. JZ: Writing – review & editing, Investigation, Methodology, Resources, Validation. JY: Writing – review & editing, Data curation, Investigation, Methodology. PL: Writing – review & editing, Data curation, Investigation, Methodology. JW: Validation, Writing – review & editing, Resources, Software, Supervision.

Funding

The author(s) declare financial support was received for the research, authorship, and/or publication of this article. This study was supported by Fundamental Research Program of Shanxi Province (Grant nos. 20210302123397 and 202203021212351), Key R&D Projects of Introducing High-Level Scientific and Technological Talents in Lvliang City (Grant no. 2021RC-1-4), Project of Lvliang City Science and Technology Program (Grant no. 2020SHFZ29), Science and Technology Innovation Project of Colleges and Universities in Shanxi Province (Grant no. 2020L0749), Special Fund for Key Disciplines of Fenyang College of Shanxi Medical University (Grant no. 2022B14), National College Students' Innovation and Entrepreneurship Training Program (Grant no. 20221569), and Projects of Innovation and Entrepreneurship Training Program for College Students of Fenyang College of Shanxi Medical University (Grant nos. FDC202209, FDC202214, and FDC202215).

Conflict of interest

The authors declare that the research was conducted in the absence of any commercial or financial relationships that could be construed as a potential conflict of interest.

Publisher's note

Supplementary material

The Supplementary material for this article can be found online at: https://www.frontiersin.org/articles/10.3389/fmicb.2023.1273397/full#supplementary-material

References

Alcock, B. P., Raphenya, A. R., Lau, T. T. Y., Tsang, K. K., Bouchard, M., Edalatmand, A., et al. (2020). CARD 2020: antibiotic resistome surveillance with the comprehensive antibiotic resistance database. *Nucleic Acids Res.* 48, D517–D525. doi: 10.1093/nar/gkz935

Algammal, A. M., Enany, M. E., El-Tarabili, R. M., Ghobashy, M. O. I., and Helmy, Y. A. (2020a). Prevalence, antimicrobial resistance profiles, virulence and enterotoxins-determinant genes of MRSA isolated from subclinical bovine mastitis in Egypt. *Pathogens* 9:362. doi: 10.3390/pathogens9050362

Algammal, A. M., Hetta, H. F., Elkelish, A., Alkhalifah, D. H. H., Hozzein, W. N., Batiha, G. E., et al. (2020b). Methicillin-resistant *Staphylococcus aureus* (MRSA): one health perspective approach to the bacterium epidemiology, virulence factors, antibiotic-resistance, and zoonotic impact. *Infect. Drug Resist.* 13, 3255–3265. doi: 10.2147/IDR.S272733

Bae, J. S., Da, F., Liu, R., He, L., Lv, H., Fisher, E. L., et al. (2021). Contribution of staphylococcal enterotoxin B to *Staphylococcus aureus* systemic infection. *J. Infect. Dis.* 223, 1766–1775. doi: 10.1093/infdis/jiaa584

Barber, M. (1961). Methicillin-resistant staphylococci. *J. Clin. Pathol.* 14, 385–393. doi: 10.1136/jcp.14.4.385

Bennett, M. R., and Thomsen, I. P. (2020). Epidemiological and clinical evidence for the role of toxins in *S. aureus* human disease. *Toxins* 12:408. doi: 10.3390/toxins12060408

Brakstad, O. G., Aasbakk, K., and Maeland, J. A. (1992). Detection of *Staphylococcus aureus* by polymerase chain reaction amplification of the nuc gene. *J. Clin. Microbiol.* 30, 1654–1660. doi: 10.1128/jcm.30.7.1654-1660.1992

Chen Cheng, W. J., Tong, W., Jiawei, C., and Guiqin, W. (2020). Analysis of enterotoxin genes, resistance genes and molecular typing of MRSA isolated from dairy cow. *Genomics Appl. Biol.* 39, 1080–1088. doi: 10.13417/j.gab.039.001080

Chen, C. J., and Huang, Y. C. (2014). New epidemiology of *Staphylococcus aureus* infection in Asia. *Clin. Microbiol. Infect.* 20, 605–623. doi: 10.1111/1469-0691.12705

Chen, C. J., Unger, C., Hoffmann, W., Lindsay, J. A., Huang, Y. C., and Gotz, F. (2013). Characterization and comparison of 2 distinct epidemic community-associated methicillin-resistant *Staphylococcus aureus* clones of ST59 lineage. *PLoS One* 8:e63210. doi: 10.1371/journal.pone.0063210

Chen, L., Zheng, D., Liu, B., Yang, J., and Jin, Q. (2016). VFDB 2016: hierarchical and refined dataset for big data analysis--10 years on. *Nucleic Acids Res.* 44, D694–D697. doi: 10.1093/nar/gkv1239

CLSI (2015). *Performance standards for antimicrobial susceptibility testing; twenty-fifth informational supplement*. Wayne, PA: The Clinical and Laboratory Standards Institute.

Galperin, M. Y., Makarova, K. S., Wolf, Y. I., and Koonin, E. V. (2015). Expanded microbial genome coverage and improved protein family annotation in the COG database. *Nucleic Acids Res.* 43, D261–D269. doi: 10.1093/nar/gku1223

Glasner, C., Pluister, G., Westh, H., Arends, J. P., Empel, J., Giles, E., et al. (2015). *Staphylococcus aureus* spa type t437: identification of the most dominant community-associated clone from Asia across Europe. *Clin. Microbiol. Infect.* 21, 163.e1–163.e8. doi: 10.1016/j.cmi.2014.09.010

He, Y., and Reed, S. (2020). Pulsed-field gel electrophoresis typing of *Staphylococcus aureus* strains. *Methods Mol. Biol.* 2069, 79–88. doi: 10.1007/978-1-4939-9849-4_5

Hou, Z., Liu, L., Wei, J., and Xu, B. (2023). Progress in the prevalence, classification and drug resistance mechanisms of methicillin-resistant *Staphylococcus aureus*. *Infect. Drug Resist.* 16, 3271–3292. doi: 10.2147/IDR.S412308

Huh, K., and Chung, D. R. (2016). Changing epidemiology of community-associated methicillin-resistant *Staphylococcus aureus* in the Asia-Pacific region. *Expert Rev. Anti Infect. Ther.* 14, 1007–1022. doi: 10.1080/14787210.2016.1236684

Igbinosa, E. O., Beshiru, A., Igbinosa, I. H., Ogofure, A. G., Ekundayo, T. C., and Okoh, A. I. (2023). Prevalence, multiple antibiotic resistance and virulence profile of methicillin-resistant *Staphylococcus aureus* (MRSA) in retail poultry meat from Edo, Nigeria. *Front. Cell. Infect. Microbiol.* 13:1122059. doi: 10.3389/fcimb.2023.1122059

Kwapisz, E., Garbacz, K., Kosecka-Strojek, M., Schubert, J., Bania, J., and Miedzobrodzki, J. (2020). Presence of egc-positive major clones ST 45, 30 and 22 among methicillin-resistant and methicillin-susceptible oral *Staphylococcus aureus* strains. *Sci. Rep.* 10:18889. doi: 10.1038/s41598-020-76009-1

Li, X., Huang, T., Xu, K., Li, C., and Li, Y. (2019). Molecular characteristics and virulence gene profiles of *Staphylococcus aureus* isolates in Hainan, China. *BMC Infect. Dis.* 19:873. doi: 10.1186/s12879-019-4547-5

Liu, Y., and Ji, Y. (2020). Multilocus sequence typing of *Staphylococcus aureus*. *Methods Mol. Biol.* 2069, 95–102. doi: 10.1007/978-1-4939-9849-4_7

Lv, G., Jiang, R., Zhang, H., Wang, L., Li, L., Gao, W., et al. (2021). Molecular characteristics of *Staphylococcus aureus* from food samples and food poisoning outbreaks in Shijiazhuang, China. *Front. Microbiol.* 12:652276. doi: 10.3389/fmicb.2021.652276

Merlino, J., Watson, J., Rose, B., Beard-Pegler, M., Gottlieb, T., Bradbury, R., et al. (2002). Detection and expression of methicillin/oxacillin resistance in multidrug-resistant and non-multidrug-resistant *Staphylococcus aureus* in Central Sydney, Australia. *J. Antimicrob. Chemother.* 49, 793–801. doi: 10.1093/jac/dkf021

Mlynarczyk-Bonikowska, B., Kowalewski, C., Krolak-Ulinska, A., and Marusza, W. (2022). Molecular mechanisms of drug resistance in *Staphylococcus aureus*. *Int. J. Mol. Sci.* 23:8088. doi: 10.3390/ijms23158088

Monaco, M., Pimentel de Araujo, F., Cruciani, M., Coccia, E. M., and Pantosti, A. (2017). Worldwide epidemiology and antibiotic resistance of *Staphylococcus aureus*. *Curr. Top. Microbiol. Immunol.* 409, 21–56. doi: 10.1007/82_2016_3

Oliveira, D., Borges, A., and Simoes, M. (2018). *Staphylococcus aureus* toxins and their molecular activity in infectious diseases. *Toxins* 10:252. doi: 10.3390/toxins10060252

Patel, H., and Rawat, S. (2023). A genetic regulatory see-saw of biofilm and virulence in MRSA pathogenesis. *Front. Microbiol.* 14:1204428. doi: 10.3389/fmicb.2023.1204428

Prochaska, E. C., Xiao, S., Tamma, P. D., Sick-Samuels, A., Schumacher, C., Gadala, A., et al. (2023). Trends in pediatric community-onset *Staphylococcus aureus* antibiotic susceptibilities over a five-year period in a multihospital health system. *Antimicrob. Steward. Healthc. Epidemiol.* 3:e12. doi: 10.1017/ash.2022.370

Rocha, G. D., Nogueira, J. F., Gomes Dos Santos, M. V., Boaventura, J. A., Nunes Soares, R. A., de Simoni, J., et al. (2022). Impact of polymorphisms in blaZ, blaR1 and blaI genes and their relationship with beta-lactam resistance in *S. aureus* strains isolated from bovine mastitis. *Microb. Pathog.* 165:105453. doi: 10.1016/j.micpath.2022.105453

Rong, D., Wu, Q., Xu, M., Zhang, J., and Yu, S. (2017). Prevalence, virulence genes, antimicrobial susceptibility, and genetic diversity of *Staphylococcus aureus* from retail aquatic products in China. *Front. Microbiol.* 8:714. doi: 10.3389/fmicb.2017.00714

Silvola, J., Grondahl-Yli-Hannuksela, K., Hirvioja, T., Rantakokko-Jalava, K., Rintala, E., Auranen, K., et al. (2022). Whole genome sequencing reveals new links between spa t172/CC59 methicillin-resistant *Staphylococcus aureus* cases in low-endemicity region of Southwest Finland, 2007–2016. *Sci. Rep.* 12:21326. doi: 10.1038/s41598-022-25556-w

Turner, N. A., Sharma-Kuinkel, B. K., Maskarinec, S. A., Eichenberger, E. M., Shah, P. P., Carugati, M., et al. (2019). Methicillin-resistant *Staphylococcus aureus*: an overview of basic and clinical research. *Nat. Rev. Microbiol.* 17, 203–218. doi: 10.1038/s41579-018-0147-4

Uehara, Y. (2022). Current status of staphylococcal cassette chromosome mec (SCCmec). *Antibiotics* 11:86. doi: 10.3390/antibiotics11010086

Wang, X. (2020). Spa typing of *Staphylococcus aureus* isolates. *Methods Mol. Biol.* 2069, 89–94. doi: 10.1007/978-1-4939-9849-4_6

Wang, X., Lin, D., Huang, Z., Zhang, J., Xie, W., Liu, P., et al. (2021). Clonality, virulence genes, and antibiotic resistance of *Staphylococcus aureus* isolated from blood in Shandong, China. *BMC Microbiol.* 21:281. doi: 10.1186/s12866-021-02344-6

Wang, B., Xu, Y., Zhao, H., Wang, X., Rao, L., Guo, Y., et al. (2022). Methicillin-resistant *Staphylococcus aureus* in China: a multicentre longitudinal study and whole-genome sequencing. *Emerg. Microbes Infect.* 11, 532–542. doi: 10.1080/22221751.2022.2032373

Wang, S., Zhao, C., Yin, Y., Chen, F., Chen, H., and Wang, H. (2022). A practical approach for predicting antimicrobial phenotype resistance in *Staphylococcus aureus* through machine learning analysis of genome data. *Front. Microbiol.* 13:841289. doi: 10.3389/fmicb.2022.841289

Waryah, C. B., Gogoi-Tiwari, J., Wells, K., Eto, K. Y., Masoumi, E., Costantino, P., et al. (2016). Diversity of virulence factors associated with west Australian methicillin-sensitive *Staphylococcus aureus* isolates of human origin. *Biomed. Res. Int.* 2016:8651918. doi: 10.1155/2016/8651918

Wu, S., Huang, J., Zhang, F., Wu, Q., Zhang, J., Pang, R., et al. (2019). Prevalence and characterization of food-related methicillin-resistant *Staphylococcus aureus* (MRSA) in China. *Front. Microbiol.* 10:304. doi: 10.3389/fmicb.2019.00304

Yamaguchi, T., Ono, D., and Sato, A. (2020). Staphylococcal cassette chromosome mec (SCCmec) analysis of MRSA. *Methods Mol. Biol.* 2069, 59–78. doi: 10.1007/978-1-4939-9849-4_4

Zhang Hang, Y. F., Xinpu, L., Xurong, W., Jinyin, L., and Hongsheng, L. (2019). Study on relationship between antimicrobial resistance and efflux pump related genes of methicillin-resistant *Staphylococcus aureus* in dairy cow. *Acta Vet. Zootech. Sin.* 50, 2326–2332. doi: 10.11843/j.issn.0366-6964.2019.11.017

frontiers | Frontiers in Microbiology

TYPE Original Research
PUBLISHED 22 September 2023
DOI 10.3389/fmicb.2023.1271798

OPEN ACCESS

EDITED BY
Vijay Soni,
NewYork-Presbyterian, United States

REVIEWED BY
Yaxin Li,
Cornell University, United States
Prabhat Ranjan Singh,
Weill Cornell Medicine, United States
Sujeet Kumar,
The Ohio State University, United States

*CORRESPONDENCE
Mohibullah Shah
✉ mohib@bzu.edu.pk;
✉ mohibusb@gmail.com
Suvash Chandra Ojha
✉ suvash_ojha@swmu.edu.cn

RECEIVED 02 August 2023
ACCEPTED 30 August 2023
PUBLISHED 22 September 2023

CITATION
Shah M, Anwar A, Qasim A, Jaan S, Sarfraz A, Ullah R, Ali EA, Nishan U, Shehroz M, Zaman A and Ojha SC (2023) Proteome level analysis of drug-resistant *Prevotella melaninogenica* for the identification of novel therapeutic candidates. *Front. Microbiol.* 14:1271798. doi: 10.3389/fmicb.2023.1271798

Proteome level analysis of drug-resistant *Prevotella melaninogenica* for the identification of novel therapeutic candidates

Mohibullah Shah[1]*, Amna Anwar[1], Aqsa Qasim[1], Samavia Jaan[1], Asifa Sarfraz[1], Riaz Ullah[2], Essam A. Ali[3], Umar Nishan[4], Muhammad Shehroz[5], Aqal Zaman[6] and Suvash Chandra Ojha[7]*

[1]Department of Biochemistry, Bahauddin Zakariya University, Multan, Pakistan, [2]Medicinal Aromatic and Poisonous Plants Research Center, College of Pharmacy King Saud University, Riyadh, Saudi Arabia, [3]Department of Pharmaceutical Chemistry, College of Pharmacy, King Saud University, Riyadh, Saudi Arabia, [4]Department of Chemistry, Kohat University of Science and Technology, Kohat, Pakistan, [5]Department of Bioinformatics, Kohsar University Murree, Murree, Pakistan, [6]Department of Microbiology and Molecular Genetics, Bahauddin Zakariya University, Multan, Pakistan, [7]Department of Infectious Diseases, The Affiliated Hospital of Southwest Medical University, Luzhou, China

The management of infectious diseases has become more critical due to the development of novel pathogenic strains with enhanced resistance. *Prevotella melaninogenica*, a gram-negative bacterium, was found to be involved in various infections of the respiratory tract, aerodigestive tract, and gastrointestinal tract. The need to explore novel drug and vaccine targets against this pathogen was triggered by the emergence of antimicrobial resistance against reported antibiotics to combat *P. melaninogenica* infections. The study involves core genes acquired from 14 complete *P. melaninogenica* strain genome sequences, where promiscuous drug and vaccine candidates were explored by state-of-the-art subtractive proteomics and reverse vaccinology approaches. A stringent bioinformatics analysis enlisted 18 targets as novel, essential, and non-homologous to humans and having druggability potential. Moreover, the extracellular and outer membrane proteins were subjected to antigenicity, allergenicity, and physicochemical analysis for the identification of the candidate proteins to design multi-epitope vaccines. Two candidate proteins (ADK95685.1 and ADK97014.1) were selected as the best target for the designing of a vaccine construct. Lead B- and T-cell overlapped epitopes were joined to generate potential chimeric vaccine constructs in combination with adjuvants and linkers. Finally, a prioritized vaccine construct was found to have stable interactions with the human immune cell receptors as confirmed by molecular docking and MD simulation studies. The vaccine construct was found to have cloning and expression ability in the bacterial cloning system. Immune simulation ensured the elicitation of significant immune responses against the designed vaccine. In conclusion, our study reported novel drug and vaccine targets and designed a multi-epitope vaccine against the *P. melaninogenica* infection. Further experimental validation will help open new avenues in the treatment of this multi-drug-resistant pathogen.

KEYWORDS

***Prevotella melaninogenica*, drug target, epitope, peptide vaccine, immunoinformatics**

Introduction

Prevotella melaninogenica is a gram-negative, anaerobic, black-pigmented, and short rod-shaped bacterium. It is mainly involved in polymicrobial infections spreading throughout the body and mainly in the respiratory tract. Patients suffering from cystic fibrosis are diagnosed with *Prevotella* species in their respiratory tract (Sherrard et al., 2014). *P. melaninogenica* can be detected in saliva and at the dorsal and lateral sites of the tongue, which contain a high proportion. Mucosal surfaces of the aerodigestive tract, i.e., lungs, are majorly colonized by *Prevotella* species (Könönen and Gursoy, 2022). The oral cavity of humans is also a site of *P. melaninogenica* colonization. This species is involved in diseases of the gastrointestinal tract, acute and chronic ailments of the respiratory tract, and cancers of the digestive tract (Könönen and Gursoy, 2022). An inflammatory disease, oral lichen planus (OLP), is caused by *P. melaninogenica* in the oral mucosa with white striation lesions, repeated erosions, and pain (Zheng et al., 2022).

P. melaninogenica potentially leads to oral lichen planus (OLP) through different mechanisms. It uses T6SS protease to initiate the degradation of the epithelial barrier, which leads to dysfunction and an imbalance in surface flora (Kondo et al., 2018). *P. melaninogenica,* then, infiltrates the basal layer and lamina propria as target antigens, triggering recognition by innate immune cells such as macrophages and keratinocytes. Activation of NF-κB pathways by *P. melaninogenica* leads to the production of various cytokines and chemokines. This, in turn, results in the recruitment and infiltration of CD4+ and CD8+ T lymphocytes that attack epithelial keratinocytes, which causes the degeneration of the basal cell layer and leads to further impairment of the epithelial barrier. This destructive cycle leads to chronic infection and persistent inflammatory responses in OLP (Zheng et al., 2022).

The subgingival plaque represents the existence of *P. melaninogenica* in patients with periodontal diseases. The significance of periodontal abscesses is categorized by periodontal pathogens and black-pigmented microorganisms such as *P. melaninogenica* (He et al., 2013). Pro-inflammatory short-chain fatty acids can be produced due to the enhancement of bacterial pathogenicity in the lungs in the presence of these bacteria. This is one of the mechanisms that cause resistance to antibiotics. Resistance can be caused by resistance genes or the production of an enzyme (beta-lactamase). Resistance can also be developed by repetitive use or administration of high doses of antibiotics, as in patients with cystic fibrosis (Lamoureux et al., 2021).

There is an emerging trend toward developing resistance against tetracycline and penicillin among pigmented species. Beta-lactamase production causes resistance to penicillin (Troil-linde, 1999). A few antibiotics can still be used against *P. melaninogenica* such as metronidazole, clindamycin, imipenem, meropenem, and cefoxitin, but there is a risk of developing resistance against these antimicrobials in the near future (Troil-linde, 1999). Moreover, new therapeutic strategies are required to ensure the prevention of infections caused by *P. melaninogenica*.

The vaccine to combat *P. melaninogenica* infections is still not available. There is no information about the vaccine's development in the literature. This developed a need to design novel drug and vaccine targets that would be helpful in the near future. In this context, this study is aimed at identifying novel drug and vaccine targets against this bacterium to provide alternative potential therapeutic targets for the efficient action of antimicrobials and vaccine candidates (Qasim et al., 2023). The approach employed in this study is significant to minimize labor and focus on the development of vaccine candidates' predictions by utilizing bioinformatics tools.

Materials and methods

The proteins necessary for the survival of *P. melaninogenica* were determined by subtractive proteomics. Different tools and databases were used to find drug and vaccine targets, as shown in Figure 1.

Retrieval of core gene sequences

The complete genome sequences of the 14 strains of *P. melaninogenica* were used to retrieve a core genome from the EDGAR tool version 2 (Blom et al., 2016). Clustering techniques were employed to identify duplicate or paralogous proteins *via* CD-HIT analysis (Li and Godzik, 2006), to remove redundancy. The cutoff value of 60% sequence similarity was kept as a threshold to obtain non-paralogous proteins, which were used for further analysis (Qasim et al., 2023). Alignment coverage was obtained by setting parameters at default.

Determination of human non-homologs

Human host non-homologous proteins were determined by standalone BLASTp analysis, which was used for scanning against species non-paralogous proteins with E-value 1e-20, bitscore ≥100, percent identity ≥35, and query coverage ≥35 (Shah et al., 2021). The human proteome was downloaded from the UniProt database, comprising 1,076,164 proteins.

Further scanning of pathogen proteins was carried out against the human gut microbiome. The NCBI database was used to acquire a human gut microbiome consisting of 75,176 proteins. BLASTp was performed with criteria as follows: E-value 1e-4, bitscore ≥100, percent identity ≥50, and query coverage ≥35, as in our previous studies (Aslam et al., 2020; Shah et al., 2021; Jaan et al., 2022; Qasim et al., 2023). All the homologs were discarded.

Identification of pathogen-essential proteins

After excluding gut microbiome homologs, essential proteins of the pathogen were determined by subjecting proteins to the database of essential genes (DEG) (http://tubic.tju.edu.cn/deg/) (Luo et al., 2021). DEG contains all the genes required for the survival of the pathogen. BLASTp was performed for scanning against DEG with cutoff parameters of E-value 1e-4

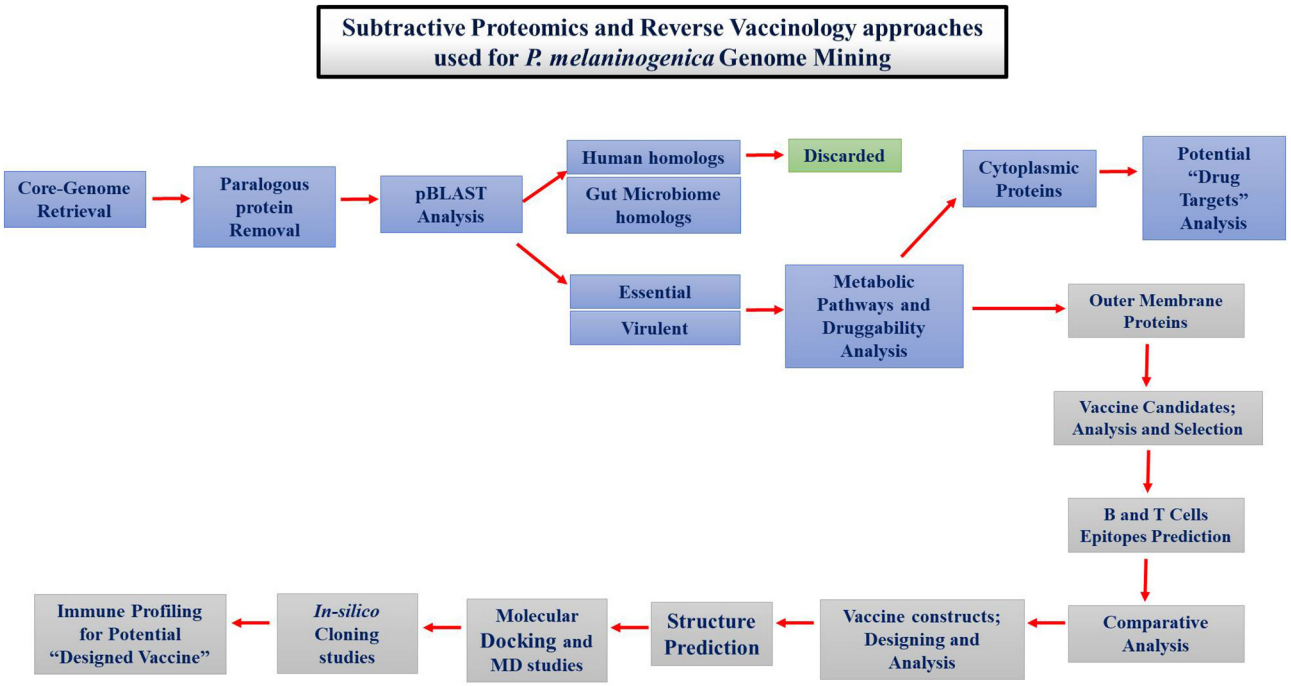

FIGURE 1
Schematic representation of approaches followed for therapeutic studies against *Prevotella melaninogenica* infection.

and bitscore ≥100 for the determination of *P. melaninogenica* essential genes.

Identification of virulence proteins

The host defense mechanism is destroyed by the virulence factors of bacteria, which help to cause the disease through invasion, colonization, and adhesion. Four categories of virulence factors are included in the virulence factor database (VFDB) (Liu et al., 2019), which is used to identify virulence factors in a pathogen. From 25 pathogenic bacteria, offensive, defensive, non-specific, and virulence-related proteins are assembled in this database. Pathogen proteins were subjected to BLASTp analysis against VFDB with parameters, i.e., E-value 1e-4 and bitscore ≥100 (Qasim et al., 2023).

Identification of antibiotic resistance and host–pathogen-interacting proteins

Databases were employed to identify resistant and host–pathogen-interacting proteins with criteria such as E-value 1e-4 and bitscore ≥100. There is an emerging trend toward developing resistance to available antibiotics among bacterial pathogens. Moreover, antibiotic-resistant genes were identified by the ARG-ANNOT database (Gupta et al., 2014), with selected criteria by subjecting pathogen proteins to BLASTp (Aslam et al., 2020). The host–pathogen interaction database (HPIDB v2.0) (Ammari et al., 2016) was used for the curation of host–pathogen protein–protein interactions, which were essential for the survival of a pathogen. Standalone BLASTp was used for the screening of interacting proteins against the HPIDB repository (Aslam et al., 2020).

Metabolic pathway determination

Metabolic pathways of living organisms can be retrieved from the Kyoto Encyclopedia of Genes and Genomes (KEGG) database (Fatoba et al., 2021). Human non-homologous essential proteins were further subjected to KEGG for metabolic pathway determination. Functional annotation of proteins was provided by the KAAS server *via* these metabolic pathways (Nazir et al., 2018). Metabolic pathways of the human host and pathogen were manually compared to find unique and common pathways in the pathogen. KEGG automatic annotation server (KAAS) (Moriya et al., 2007) employs BLASTp analysis for these metabolic pathways. KEGG orthology (KO) identifiers were provided by the KAAS server for proteins (Fatoba et al., 2021). Unique and common pathway proteins were enlisted and categorized into KEGG-dependent and independent proteins. Unique proteins are those involved only in the pathogen-specific pathways but not in humans.

Druggability analysis of proteins

Screening of essential, non-homologous proteins was further performed by subjecting proteins to BLASTp analysis with a cutoff E-value of 1e-4, against the DrugBank database for identification

of druggable proteins (Aslam et al., 2021). All FDA-approved drugs and experimental drugs are contained in the DrugBank database (Law et al., 2014). Druggable targets showed significant matching (80% or more) with FDA-approved drug targets, while proteins not showing any significant matching with already available targets were considered novel targets and used for subsequent analysis.

Subcellular localization prediction and topology analysis

Proteins are located in different positions, including the cytoplasm, inner membrane, periplasmic membrane, and outer membrane, by subcellular localization prediction. Proteins are categorized as drug or vaccine targets according to their location. Cytoplasmic and outer membrane proteins are considered suitable drug and vaccine targets, respectively (Jaan et al., 2022). PSORTb v3.0 (http://www.psort.org/psortb/) was employed for the prediction of the subcellular location of the resulting target proteins. Further validation of proteins was needed to ensure the location, which was carried out by a server named subcellular localization predictor (CELLO v2.5) (http://cello.life.nctu.edu.tw/) (Yu et al., 2014). The STRING database v10.5 (http://string-db.org) (Szklarczyk et al., 2016) was employed for the analysis of protein–protein interactions by setting parameters at default. The number of interactions was presented by hub proteins showing node degree ($K \geq 5$). The transmembrane topology of proteins was predicted by the TMHMM v0.2 server (Krogh et al., 2001). Proteins spanning the lipid membrane are termed transmembrane proteins and are prioritized as potent drug targets (Shah et al., 2021).

Protein structure modeling and validation

Proteins prioritized in the previous step were employed in SWISS-MODEL for the generation of 3D structures. The server uses homology modeling techniques for the prediction of protein structures when experimental structures are not accessible. Reliable protein templates with expected accuracy were generated (Jaan et al., 2022). A protein verification tool called "ERRAT" was used to verify the quality of the 3D structure of proteins. ERRAT signifies the quality of protein by a parameter called an overall quality factor, where a high value (≥50) specifies good quality for non-bonded atomic interactions (Aslam et al., 2020). The molecular weight and theoretical PI of proteins were determined by the ExPasy server.

The estimation of protein pocket ability to bind small molecules with high affinity is a valuable step in the identification of drug targets. PockDrug, an online server (http://pockdrug.rpbs.univ-paris-diderot.fr.), was used to calculate druggable scores for the prioritized targets. Protein structure information and ligand proximity assessment were used to predict the pocket druggability of proteins by using different estimation methods *via* the PockDrug server. By using pocket estimation methods, consistent druggability results were obtained, which differentiated more druggable proteins from less druggable proteins (Shah et al., 2021).

Reverse vaccinology: prediction of antigenic proteins

For the evaluation of the antigenic nature of proteins, VaxiJen server v2.0 was employed for outer membrane and extracellular proteins with criteria, i.e., accuracy rate 70–89% and probability score >0.5 (Doytchinova and VaxiJen, 2007). The allergenicity of the shortlisted proteins was evaluated by the AllergenFP server to distinguish allergens from non-allergens. Allergic proteins that are harmful to the host were discarded in this evaluation (Dimitrov et al., 2014). Different parameters of proteins were assessed by the ExPasy ProtParam tool, calculating molecular weight, theoretical PI, instability index, aliphatic index, half-life, number of amino acids, and GRAVY (Grand Average of Hydropathicity) (Qasim et al., 2023).

Prediction of T-cell epitopes

For a specific pathogen, vaccine targets are identified with the help of T-cell epitopes involved in the elicitation of immune responses. An antigen is processed by an MHC molecule to bind with either cytotoxic or helper T cells (Shah et al., 2021). CD4 or CD8 T cells are stimulated by an epitope defined as the shortest immunogenic peptide having the ability to stimulate immune responses. Two types of major histocompatibility complex (MHC) classes I and II recognized by CD4 and CD8, respectively, are represented by T-cell epitopes (Aslam et al., 2020). MHC prediction was carried out by the Immune Epitope Database (IEDB) server. For the prediction of MHC class-I epitopes, vaccine candidates were subjected to the NetMHCpan 4.1 web server with a percentile rank <0.2, recommended by the IEDB server (Fleri et al., 2017). MHC class-II epitopes were predicted by the IEDB recommendation of 2.22 with an adjusted rank of <0.5. Further evaluation of preferred epitopes was performed.

Prediction of B-cell epitopes

The solvent-exposed regions in the antigen can be identified by the prediction of B-cell epitopes, by which antibodies can be recognized (Nazir et al., 2018). For the prediction of B-cell epitopes, different servers were used. BCPreds, FBCPreds, AAP, and BepiPred online servers were used to predict linear B-cell epitopes. BCPred uses the SVM method, which has 5-fold cross-validation and utilizes five different kernel methods. Linear-length B-cell epitopes were predicted by subsequent kernel followed by FBCPred. Biochemical properties such as amino acid composition, hydrophobicity, hydrophilicity, secondary structure, and surface accessibility of peptides were used to predict linear epitopes by BepiPred (IEDB) (Solanki and Tiwari, 2018).

Antigenicity, allergenicity, toxicity, and conservancy analyses

A designated vaccine candidate must be able to act as an antigen. For this purpose, the VaxiJen v2.0 server was employed with a threshold value of >0.4. The sequence alignment method is used in the VaxiJen server, and the physicochemical properties of peptides are used to confirm their antigenicity (Doytchinova and VaxiJen, 2007). The allergenic properties of vaccine candidates were measured by the AllergenFP server. Another server, ToxinPred, was employed to check the toxic and non-toxic peptides, where non-toxic peptides were selected for further evaluation (Jaan et al., 2022). The conservancy level of epitopes was evaluated by the IEDB server by setting parameters at default, where conserved or variable epitopes could be assessed (Jaan et al., 2022). These properties of epitopes were evaluated for the construction of chimeric vaccines.

Multi-epitope vaccine construction

Multi-epitope vaccine constructs were generated by joining overlapped epitopes of MHC-I, MHC-II, and B cells with the help of amino acid linkers (i.e., EAAAK, GGGS, and KK). To increase the immunogenicity of vaccine constructs, adjuvants were added to the sequence. Four adjuvants, i.e., HBHA protein, L7/L12 ribosomal proteins, beta-defensin, and HBHA conserved sequences, were added to improve the efficacy of vaccine models. PADRE peptide sequences, containing 13 amino acids (i.e., AKFVAAWTLKAAA), were also added, which helped induce CD4+ T cells (Aslam et al., 2020). PADRE sequences help to overcome the problems of polymorphism and elicit better immune responses. Different combinations of vaccine constructs were made and checked for immunogenicity, toxicity, and allergenicity. The SOLPro server was employed to check the solubility of vaccine constructs (Magnan et al., 2009).

Analysis of physicochemical properties

Intrinsic physical and chemical characteristics of a substance are defined as physicochemical properties. For the estimation of physicochemical properties, the ProtParam tool was used, which calculated the number of amino acids, half-life, theoretical PI, instability index, aliphatic index, molecular weight, and GRAVY of vaccine models (Jaan et al., 2022).

Structure analysis

For the prediction of secondary structure, two online servers, i.e., PSIPRED and SOPMA, were used. Properties such as transmembrane helices, bend regions, random coils, and beta sheets can be assessed through these self-optimized prediction methods. A graphic presentation of proteins is obtained as output (Jaan et al., 2022). 3D modeling of chimeric constructs was generated by Phyre2, increasing the accuracy of alignment by using the alignment of the Hidden Markov model (Raza et al., 2021). GalaxyRefine and 3DRefine servers were employed for the refinement of predicted 3D models, in which side chains are rebuilt and repacked. The probable errors of 3D models were checked by the ProSA-web server (Jaan et al., 2022). The Ramachandran plot was obtained by an online server called PROCHECK, which explains the stereochemical properties of the protein (Shah et al., 2021). Phi/Psi angles were assessed by the Ramachandran plot for a comprehensive understanding of the protein backbone.

Disulfide engineering

Vaccine constructs were disulfide-engineered by DbD2, to check the stability and conformational entropy of the protein. Increased stability and decreased conformational entropy of protein can be confirmed by the accessibility of protein, and it can add novel disulfide bonds (Craig and Dombkowski, 2013).

Molecular docking analysis

An energy-minimizing step used to obtain a stable structural configuration of vaccine targets with the ligands is determined by molecular docking analysis. Immune receptor–peptide interactions were inferred by docking vaccine constructs with six various human HLA alleles using the PatchDock server. More refinement and re-scoring of docked complexes were performed by the Fast Interaction Refinement in Molecular Docking (FireDock) server, which gave the 10 best models as a result. Based on the lowest binding energy, the vaccine construct (V5) was prioritized as the best-docked complex (Jaan et al., 2022). Furthermore, TLR4 (toll-like receptor) acquired from PDB (2Z65) was docked with vaccine construct V5 in the same way by the PatchDock server. The top 10 generated models from the FireDock server were redirected to PatchDock for refinement. Assumed refined solutions were recognized by the binding score and global binding energies of docked refined models.

Molecular dynamic simulation

The stability of the docked complex and molecules' behavior was assessed by the molecular dynamic approach. The interaction between the designed vaccine and receptor was estimated by the iMOD server. Four main factors are measured by this tool by estimating the direction and range of basic movements of the docked complex. These factors include Eigenvalue, B-factors, covariance, and deformability. A high Eigenvalue indicates the value of much harder deformation (Jaan et al., 2022).

In silico expression analysis and immune simulation

The possible expression level of vaccine constructs was tested by using the Java Codon Adaptation tool (JCAT), which used back-translated amino acid sequences. *E. coli* (K12 strain) was

selected for the expression of the protein. The high expression level in *E. coli* was verified by the consequential GC content and codon adaptation index (CAI) (Jaan et al., 2022). The rho-independent transcription terminators, cleavage sites of some restriction enzymes, and prokaryotic ribosome binding sites were dodged. SnapGene software was used to introduce codon-adapted sequences into plasmid vector pET30a (+), to construct recombinant plasmid sequences (Solanki and Tiwari, 2018). C-ImmSim server was employed for immune simulation to predict the production of interferons, antibodies, and cytokines in response to a foreign particle. Parameters were set to default (Puzone et al., 2002).

Results

Core protein retrieval and CD-HIT analysis

The core genome method uses conserved sequences of available complete genome strains in accordance with the reference genome. A total of 1,415 core proteins were retrieved from 14 complete genome strains of *P. melaninogenica*. Some proteins are produced in response to duplication events taking place in organisms within one species, known as paralogous proteins. To reduce redundancy in sequences, proteins were subjected to CD-HIT analysis (Li and Godzik, 2006). A total of 1,414 non-paralogous proteins were obtained by subtracting one duplicate protein from the core protein sequences. The threshold was set to 0.6 (60%) sequence similarity.

Human host non-homolog analysis

For the identification of novel targets, bacterial proteins were subjected to homology filters as an essential step for the screening of human host homologs. After removing the proteins homologous to the host proteins, 1,295 candidates were obtained by screening against the human proteome database. Different metabolic reactions such as homeostasis, development, defense system, and physiological functions are performed by the gut flora, which colonizes the human body throughout life (Kho and Lal, 2018). The scanning of core proteins against the human gut microbiota was performed by standalone BLASTp, to prevent the likelihood of serious complications in the host. The resulting 615 proteins were used for downstream analysis.

Identification of essential, virulent, antibiotic-resistant, and interacting proteins

A minimal set of genes required to perform basic cellular functions and important for the survival of an organism are defined as essential genes. A database of essential genes (DEG) based on BLASTp scanning was employed to dig out essential proteins of the pathogen. As a result, 123 proteins were recognized as essential for the maintenance of cellular functions in *P. melaninogenica*. The virulence factor database (VFDB) was used to identify the virulence proteins of the pathogen. The pathogenic capacity of bacteria to infect the host is increased by virulence factors (Aslam et al., 2020). By subjecting proteins to BLASTp scanning, VFDB calculated 19 proteins as virulence factors.

Antibiotic resistance proteins were determined by Antibiotic-Resistant Gene ANNOTation (ARG-ANNOT) (Gupta et al., 2014). This analysis determined three proteins as resistant to antibiotics, which might act as important drug targets in future studies. Host–pathogen protein–protein interactions (HP-PPI) mediate infectious diseases in response to molecular cross-conferences between host and pathogens. For treating infectious diseases, such proteins need to be identified for the discovery of potential drug targets. Proteins were subjected to BLASTp against HPIDB v2.0, which identified only one interacting protein (Ammari et al., 2016). The proteins from this analysis have the potential to be selected as alternative drug targets and deserve further experimental investigation.

Identification of pathogen-specific metabolic pathways

Metabolic pathway analysis is used to find out the preferable drug target as involved in pathogen-specific unique pathways (Dorella et al., 2013). The KEGG database was used to predict the metabolic pathways of *Homo sapiens* (humans) and *P. melaninogenica*, which were 345 and 94, respectively. A manual comparison of human and bacterial metabolic pathways showed that 25 unique pathways were present but absent in the human host, while the remaining 69 pathways were common to both humans and bacteria. The KAAS server was employed for the functional pathway analysis of 114 essential, non-homologous pathogen proteins *via* BLASTp, which assigned them a KO (KEGG orthology) identifier (Fatoba et al., 2021). Out of 114 proteins, only 5 were involved in pathogen-specific unique pathways called KEGG-dependent (Table 1), while the rest of the 109 proteins were categorized as KEGG-independent.

The potential therapeutic targets were represented by the metabolic pathway analysis of non-homologous, essential human proteins. Suitable and least-targeted were identified by applying filters to reduce time, labor, and resources. Druggability screening of the prioritized proteins was performed to find novel druggable targets, which demonstrated that in KEGG-dependent, one protein is a novel target, while in KEGG-independent proteins, 90 proteins are novel and have the potential to be explored as potential drug targets.

Prediction of subcellular localization

Suitable and effective targets can be identified by predicting subcellular location for a comprehensive understanding of the function and mechanisms of proteins. Purification and assay of membrane-localized proteins are critical, so cytoplasmic proteins are favored as potent drug targets (Mondal et al., 2015). For suitable vaccine targets, outer membrane and extracellular proteins were prioritized for elicitation of better immune responses as membrane proteins were exposed to host cells (Nogueira et al., 2021). Subcellular location prediction by CELLO and PSORTb tools

TABLE 1 *P. melaninogenica* unique pathway proteins.

Sr. no.	Protein IDs	KO identifiers	Pathway IDs
1	gi|302149751|gb|ADK96013.1|	K02517	Lipopolysaccharide biosynthesis
2	gi|302150676|gb|ADK96937.1|	K05515	O-Antigen repeat unit biosynthesis
3	gi|302150062|gb|ADK96324.1|	K00865	Biosynthesis of secondary metabolites
4	gi|302149000|gb|ADK95262.1|	K02551	Biosynthesis of secondary metabolites
5	gi|302149929|gb|ADK96191.1|	K03787	Biosynthesis of secondary metabolites
6	gi|302150384|gb|ADK96645.1|	K00919	Biosynthesis of secondary metabolites
7	gi|302150673|gb|ADK96934.1|	K11753	Biosynthesis of secondary metabolites
8	gi|302150062|gb|ADK96324.1|	K00865	Microbial metabolism in diverse environments
9	gi|302149329|gb|ADK95591.1|	K06881	Microbial metabolism in diverse environments
10	gi|302149556|gb|ADK95818.1|	K08678	Biosynthesis of nucleotide sugars
11	gi|302150676|gb|ADK96937.1|	K05515	Beta-Lactam resistance
12	gi|302151208|gb|ADK97469.1|	K01448	Cationic antimicrobial peptide (CAMP) resistance
13	gi|302150566|gb|ADK96827.1|	K07165	Two-component system
14	gi|302150409|gb|ADK96670.1|	K03217	Quorum sensing
15	gi|302150820|gb|ADK97081.1|	K03086	Flagellar assembly
16	gi|302150409|gb|ADK96670.1|	K03217	Bacterial secretion system

showed three proteins to be cytoplasmic and only one protein to be outer membrane in the case of KEGG-dependent proteins. In the case of KEGG-independent proteins, 49 proteins were found to be cytoplasmic and 23 proteins to be outer membrane in location. These proteins were prioritized as drug or vaccine targets for further analysis in accordance with their location.

Drug target prioritization

Further characterization of selected targets was performed by STRING v10.5 databases for the estimation of protein–protein interactions. A significant number of interactions were represented by node degree (K) $\geq$5 as hub proteins (Szklarczyk et al., 2016). This characterization prioritized 20 proteins as suitable targets (Figure 2). The TMHMM server was employed for the prediction of transmembrane helices set to be less than or equal to 1. Due to multiple transmembrane helices, there may be complications in the cloning, expression, and purification of proteins (Solanki and Tiwari, 2018). For this purpose, proteins with more than one helix were excluded, and 18 proteins were selected (Table 2). The molecular weight of selected targets was calculated by the ExPasy tool, which prioritized proteins with <110 KDa molecular weight. Proteins submitted to SWISS-MODEL were checked for model quality estimation by different parameters, i.e., percentage identity, Q-mean, and GMQE scores, which prioritized three drug targets. Protein pocket ability prediction is one of the crucial steps in the development of therapeutic drugs to ensure the affinity of proteins with small drug-like molecules. The PockDrug server was employed for this purpose, which identified significant druggable targets with a drug score of >0.5 (Borrel et al., 2015). Furthermore, the ERRAT server was used to evaluate the quality of models, which was considered significant (85%) for all models.

Antigenic membrane protein selection

Surface-exposed or outer membrane proteins which were exposed to host cells were prioritized for the reverse vaccinology, in the case of gram-negative bacteria. Certain characteristics (i.e., instability index, aliphatic index, PI, GRAVY, and molecular weight) of 24 outer membrane proteins were analyzed by the ProtParam tool. The AlgPred server was employed to check the allergenicity of proteins by using the hybrid method for the best vaccine candidate selection. Antigenicity was estimated by the VaxiJen server based on the threshold of >0.5. Two proteins with IDs ADK95685.1 and ADK97014.1 were selected as the best vaccine targets used for subsequent analysis. By this analysis, it was ensured that induced immune responses were aimed to target the pathogen, not the host cells.

Prediction of lead epitopes

Targeted immune responses are induced by the short peptide fragments of a peptide vaccine; accordingly, allergenic sequences are avoided. A variety of peptides termed epitopes can bind to MHC molecules with high affinity as mutations are possible in MHC-binding epitopes caused by pathogens (Shah et al., 2021). One of the major keystones in the development of vaccines is the B- and T-cell epitope prediction (Li et al., 2014). MHC-I and MHC-II molecules provide both types of T cells, i.e., (i) cytotoxic T cells and (ii) helper T cells, with epitopes. High-binding affinity

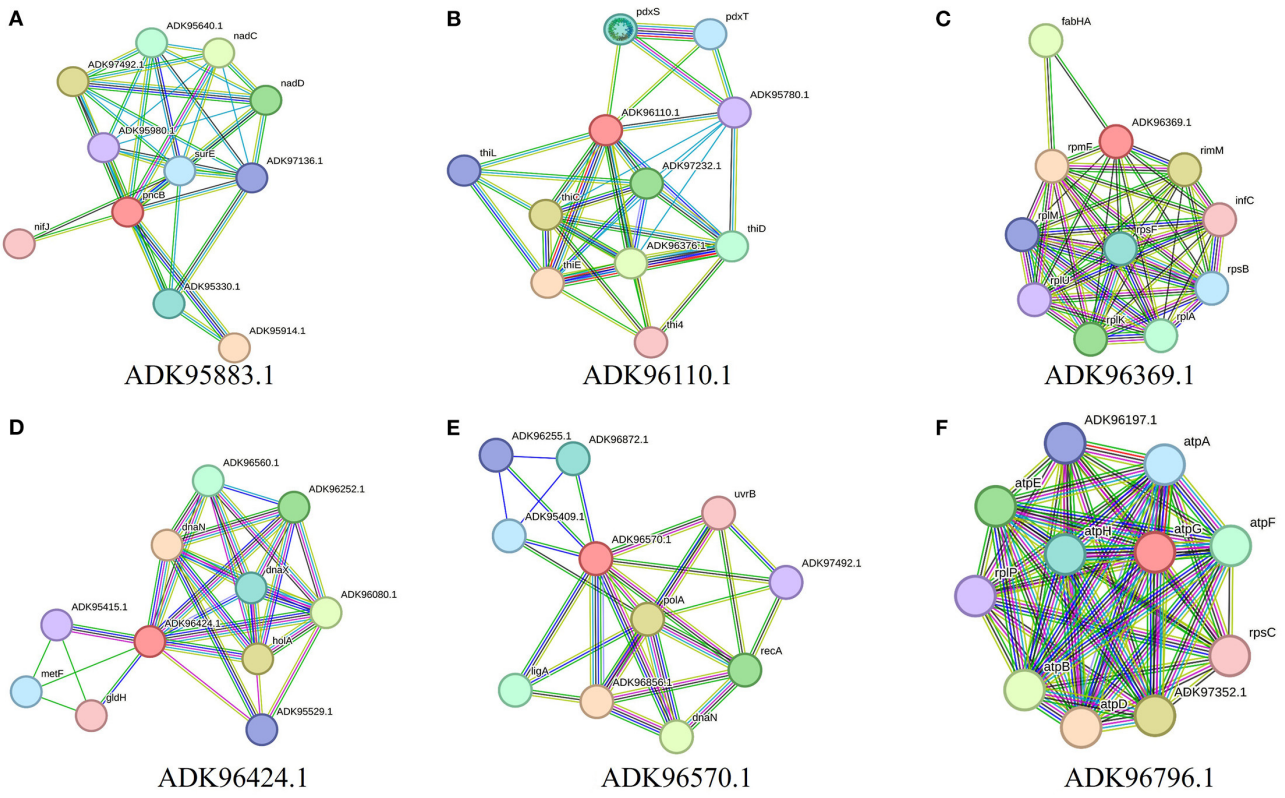

FIGURE 2
Interaction analysis of predicted drug targets with other proteins using STRING database where query proteins are indicated by red color. The proteins with the best predicted three-dimensional structures: **(A)** ADK95883.1, **(B)** ADK96110.1, **(C)** ADK96369.1, **(D)** ADK96424.1, **(E)** ADK96570.1, and **(F)** ADK96796.1, are shown to summarize the drug target's PPI list.

epitopes were predicted by multiple prediction sources to find potent vaccine-candidate epitopes. For the prediction of MHC-binding epitopes in two prioritized vaccine candidates, an IEDB server was employed. For MHC-I binding, the NetMHCpan 4.1 server was used with criteria of <0.2 percentile rank. Hydrogen binding can attach peptides with only 8 to 10 amino acids due to the closed binding site cleft of MHC-I molecules (Nazir et al., 2018). Criteria for binding with human alleles were set to 9-mer length, and predicted 19 and 16 epitopes for both vaccine candidates were used for further analysis. These epitopes were further filtered by toxicity, antigenicity, conservancy, and immunogenicity analyses, which resulted in 5 and 6 final epitopes for chimera vaccine construction.

Due to open and shallow pockets, prediction by MHC-II molecules is less accurate. The IEDB-recommended 2.22 method was employed for the prediction of MHC-II epitopes with a percentile rank <0.5, and the 15-mer length of amino acids was selected due to the higher binding affinity of these molecules as compared with MHC-I (Shah et al., 2021). After screening, the final MHC-II and MHC-I epitopes were selected (Supplementary Tables S1, S2). For the prediction of linear B-cell epitopes, different online servers, i.e., BCPred, BepiPred, FBCPred, and AAP, were employed. The predicted epitopes of T and B cells were compared for the determination of overlapping epitopes (Table 3). These overlapping epitopes may be useful in the development of a vaccine against *P. melaninogenica* in future. Conformational B-cell epitopes have an important role in antigen and antibody association, but unfortunately, these cannot be predicted due to the inaccessibility of the 3D structures of all the proteins.

Vaccine construct modeling

For the construction of chimera vaccine constructs, different combinations of non-toxic, antigenic, and conserved lead epitopes were chosen. On the N-terminal of prioritized epitopes, adjuvants were added to enhance the immunogenic nature of the multi-epitope vaccine. Linkers, i.e., EAAAK, GGGS, and KK, were used to join the adjuvants. Allergenicity and antigenicity of the constructs affected by adjuvants were analyzed by the different combinations of adjuvants (Solanki and Tiwari, 2018). The conformation of designed constructs was not altered by adding linkers. Around the global population, the problems triggered by polymorphisms in HLA-DR molecules can be overcome by adding PADRE sequences (synthetic peptides containing 13 amino acids) to vaccine constructs. Better immune protection and cytotoxic T-lymphocyte (CTL) responses were provided by PADRE sequences (Wu et al., 2010). Different combinations of lead epitopes, adjuvants, and PADRE sequences provided eight vaccine constructs, i.e., V1, V2, V3, V4, V5, V6, V7, and V8 (Table 4).

TABLE 2 Analysis of shortlisted druggable proteins to check transmembrane alpha helices, molecular weight, and node degree (STRING analysis).

Sr. no.	Protein ID	Protein name	TMHMM No.	M. wt (KDa)	Query length	STRING
Metabolic pathway-dependent protein						
1	ADK97401.1	Dihydroneopterin aldolase	0	13	23	6.55
Metabolic pathway-independent proteins						
1	ADK95262.1	2-succinyl-5-enolpyruvyl-6-hydroxy-3-cyclohexene-1-carboxylic-acid synthase	0	61	113	6
2	ADK95358.1	Pyridoxal 5′-phosphate synthase	0	31	77	5.09
3	ADK95511.1	Hypothetical protein	0	23	35	6.36
4	ADK95702.1	NAD-dependent DNA ligase OB-fold domain protein	0	74	155	6.55
5	ADK95883.1	Nicotinate phosphoribosyltransferase	0	49	80	7.82
6	ADK95886.1	Glycosyltransferase	0	33	49	6
7	ADK96013.1	Lipid A biosynthesis (KDO)2-(lauroyl)-lipid IVA acyltransferase	1	39	46	6.55
8	ADK96033.1	YbbR-like protein	0	33	46	6.36
9	ADK96110.1	Putative phosphomethylpyrimidine kinase	0	36	73	7.09
10	ADK96369.1	Putative ACR, COG1399	0	19	34	8.55
11	ADK96424.1	Hypothetical protein	0	43	74	7.45
12	ADK96445.1	Exodeoxyribonuclease VII, large subunit	0	48	89	5.82
13	ADK96570.1	UvrD/REP helicase	0	103	162	6.73
14	ADK96645.1	4-(cytidine 5′-diphospho)-2-C-methyl-D-erythritol kinase	0	31	66	6.18
15	ADK96796.1	ATP synthase F1, gamma subunit	0	36	64	8.73
16	ADK96878.1	Hypothetical protein	1	18	23	6.36
17	ADK96880.1	Hydrolase, tatd family	0	30	56	5.64

Antigenicity, allergenicity, and solubility analysis of vaccine constructs

The antigenic behavior of vaccine constructs was examined by the AntigenPro server with a cutoff value of >0.90. The VaxiJen server was employed to estimate the antigenicity, with a threshold of 0.75 showing good antigenic behavior. The allergic nature of constructs was checked by the AllergenFp, and allergic constructs were excluded as being harmful to the human host. The SOLPro server with a probability score of >0.5 was employed to analyze the solubility of the designed chimeric constructs. GC content (30–70%) and CAI value (0.90–1.0) were considered significant as inferred from the results. The ProtParam tool was used to evaluate properties such as the number of amino acids, aliphatic index, instability index, PI, molecular weight, and GRAVY. Eventually, vaccine constructs V5 and V8 fulfilled the standard criteria and were selected for further investigations (Supplementary Tables S3, S4).

Structure prediction of vaccine constructs

A 2D diagram of the vaccine represents the residues involved in the formation of coils, b-sheets, and a-helices. These particular secondary structures of vaccine are involved in its overall structural stability. The 2D diagram indicates a big picture of the complete structure of the vaccine construct. Therefore, prioritized vaccine constructs (V5 and V8) were subjected to PSIPRED and SOPMA servers for the prediction of secondary structure to evaluate the stability of peptides (Raza et al., 2021). The results revealed by servers calculated the percentage of α-helix (36.90), β-strands (10.69), extended strands (21.80), and random coils (30.61) for V5 (Supplementary Figure S1A). Similarly, percentages for V8 were 29.43, 24.44, 11.22, and 34.91, respectively (Supplementary Figure S1B). The function and stability of proteins are critically analyzed by tertiary structure prediction. The Phyre2 server was employed for the prediction of the tertiary structure of prioritized vaccine constructs (V5 and V8). The vaccine construct V8 was deselected due to limited

TABLE 3 Comparative analysis of predicted epitopes (bold highlights the selected epitopes).

Protein IDs	Sr. no.	Final positions	Final B-cell epitopes
ADK95685.1	1	2, −50	ATRTINGREYTKVDFENKLRHLSDAQELAAMLNELKLPWYYSDFRGKQL
	2	**55–83**	**DTNNVQRRCKTFRLRKKHGGYREITAPKG**
	3	**100–127**	**DEPTPWAFGFVCGRSVVDNARPHVGKRY**
	4	168–199	ATVRTKNNKEVLAQGFATSPTLSNFICREMDK
	5	**208–254**	**QGITFTRYADDLTFSSDTDILRPQGELVQQVKAIVERYGFRLNEEKT**
	6	**268–294**	**LMVTEKVNVSRRYVREIRSLLYIWERY**
	7	303–325	AWKSYRQQHGKTKGHQHCVPLNA
	8	349–375	VSRYTSLQQRSKGDIKEVAYKAYMGKY
	9	377–417	SNSTEDRMTSANVLPNDNTSSRQLGATSSNPYDPRKKSKRI
ADK97014.1	**1**	**15–45**	**VQVSAQSGTNSPYSQYGLGALASQATSFNRG**
	2	52–75	GFHERNQVNYANPASYASVDSLSF
	3	**82–109**	**SLQLTNFEENGNKVNAKNADIEYVVASF**
	4	121–161	LLPYTNVGYNFSNTQNVNAFPSTSSVNATYSNAYNGSGGLH
	5	**165–236**	**LGAGWEPFKGFSFGANIGYLWGTLNRNSTNTYSDSYVNTLSKNYSAQVKSYKVDFGAQYTYAVDKKNELTLG**
	6	253–274	LISTNSQTSISDTTRYVVSNSL
	7	**278–329**	**HTFGVGLMWNHNNRLKFGVDYQLQKWAKLKYPQLTTVNGTTSYNLVDGQFND**
	8	**332–379**	**KFTLGGDYCKGERYRGFFSRMHYRAGFSYASPYLKINGVDGPRELSAS**
	9	**390–427**	**YNNRSMLNISAEWVNQSVTGMIKENMFRINVGFTFNER**

data for three-dimensional structure formation. Hence, V5 was used for tertiary structure, and distortions in protein structure were overcome by refinement of structure. Closeness to the native structure of proteins was acquired by the refinement of models by GalaxyRefine and 3DRefine. Efficient protein structure refinement is obtained by applying knowledge-based force fields and composite physics. Energy minimization steps and repetitive optimization of hydrogen bonding at the atomic level are employed by these online servers for refinement (Raza et al., 2021).

Validation of the refined 3D model was executed by PROCHECK and PROSAweb, which were used to generate the Ramachandran plot. This plot assessment elaborates on the combination and orientation of dihedral angles falling in the disallowed region on the basis of steric hindrance (Maxwell and Popelier, 2017). The Z-score (assessed by PROSA Web) improved from −2.98 to −5.37, which ensured the better quality of models. More than 90% of residues in the most favored regions of the Ramachandran plot indicate the better folding of the protein structure and validate its quality. The results of the Ramachandran plot analysis of our vaccine showed 95.2% of residues in the most favored regions, which indicated the good quality of our vaccine. Visualization of the tertiary structures was made with Pymol v2.5.5 software for better representation (Figure 3).

Disulfide engineering and molecular docking analysis

The designed vaccine construct was stabilized by performing disulfide engineering, where 13 pairs of amino acids were found to be able to make disulfide bonds predicted by the DbD2 server. However, considering the parameters such as energy and chi3, five pairs were considered favorable. The value of energy was calculated to be <4 kcal/mole for 5 pairs, with a chi3 value between −105 and +109.

Favorable interactions between vaccine constructs and HLA alleles were predicted by molecular docking analysis, an energy minimization step. The vaccine construct (V5) was docked with six different HLA alleles, i.e., 1A6A, 1AQD, 2Q6W, 3C5J, 4MD4, and 5NI9, acquired from PDB by using the PatchDock server. For refinement of models, the results were subjected to the FireDock server. Docked complex V5-1AQD fulfilled the criteria by showing the highest docking score (14814) as compared with the docking score of other docked complexes. Vigorous immune-stimulatory and CTL response effects can be elicited by interactions between TLRs (Rana and Akhter, 2016). The vaccine construct (V5) was further docked with TLR4 (toll-like receptor) to enhance immune responses (Table 5). Profound interactions of the docked complex V5-TLR4 were confirmed through binding energy.

10.3389/fmicb.2023.1271798

TABLE 4 Designed multi-epitope vaccine sequences.

Sr. no.	Epitope sequence position	Complete sequence of vaccine construct
1	ADK95685.1 (100–127, 208–254), and ADK97014.1 (52–75, 121–161, 253–274, 332–379, 390–427)	EAAAKMSDLKNLAETLVNLTVKDVNELAAILKDEYGIEPAAAAVVMAGPGAEAAEEKTEFDVILKSAGASKLAVVKLVKD LTGAGLKEAKDMVDGAPAAIKSGISKDEAEALKKQLEEAGAEVELKEAAAKAKFVAAWTLKAAAGGGSDEPTPWAFGFVCGR SVVDNARPHVGKRYGGGSQGITFTRYADDLTFSSDTDILRPQGELVQQVKAIVERYGFRLNEEKTGGGSAKFVAAWTLKAAA GGGSGFHERNQVNYANPASYASVDSLSFHEYGAEALERAGLLPYTNVGYNFSNTQNVNAFPSTSSVNATYSNAYNGSGGLHH EYGAEALERAGLISTNSQTSISDTTRYVVSNSLHEYGAEALERAGKFTLGGDYCKGERYRGFFSRMHYRAGFSYASPYLKIN GVDGPRELSASHEYGAEALERAGYNNRSMLNISAEWVNQSVTGMIKENMFRINVGFTFNERHEYGAEALERAGAKFVAAWTL KAAAGGGS
2	ADK95685.1 (100–127, 208–254), and ADK97014.1 (52–75, 121–161, 253–274, 332–379, 390–427)	EAAAKMAENPNIDDLPAPLLAALGAADLALATVNDLIANLRERAEETRAETRTRVEERRARLTKFQEDLPEQFIELRDK FTTEELRKAAEGYLEAATNRYNELVERGEAALQRLRSQTAFEDASARAEGYVDQAVELTQEALGTVASQTRAVGERAAKL VGIELEAAAKAKFVAAWTLKAAAGGGSDEPTPWAFGFVCGRSVVDNARPHVGKRYGGGSQGITFTRYADDLTFSSDTDIL RPQGELVQQVKAIVERYGFRLNEEKTGGGSAKFVAAWTLKAAAGGGSGFHERNQVNYANPASYASVDSLSFHEYGAEALE RAGLLPYTNVGYNFSNTQNVNAFPSTSSVNATYSNAYNGSGGLHHEYGAEALERAGLISTNSQTSISDTTRYVVSNSLHE YGAEALERAGKFTLGGDYCKGERYRGFFSRMHYRAGFSYASPYLKINGVDGPRELSASHEYGAEALERAGYNNRSMLNIS AEWVNQSVTGMIKENMFRINVGFTFNERHEYGAEALERAGAKFVAAWTLKAAAGGGS
3	ADK95685.1 (100–127, 208–254), and ADK97014.1 (52–75, 121–161, 253–274, 332–379, 390–427)	EAAAKMAENSNIDDIKAPLLAALGAADLALATVNELITNLRERAEETRRSRVEESRARLTKLQEDLPEQLTELREKFTA EELRKAAEGYLEAATSELVERGEAALERLRSQQSFEEVSARAEGYVDQAVELTQEALGTVASQVEGRAAKLVGIELEAAA KAKFVAAWTLKAAAGGGSDEPTPWAFGFVCGRSVVDNARPHVGKRYGGGSQGITFTRYADDLTFSSDTDILRPQGELVQQ VKAIVERYGFRLNEEKTGGGSAKFVAAWTLKAAAGGGSGFHERNQVNYANPASYASVDSLSFHEYGAEALERAGLLPYTN VGYNFSNTQNVNAFPSTSSVNATYSNAYNGSGGLHHEYGAEALERAGLISTNSQTSISDTTRYVVSNSLHEYGAEALERA GKFTLGGDYCKGERYRGFFSRMHYRAGFSYASPYLKINGVDGPRELSASHEYGAEALERAGYNNRSMLNISAEWVNQSVT GMIKENMFRINVGFTFNERHEYGAEALERAGAKFVAAWTLKAAAGGGS
4	ADK95685.1 (100–127, 208–254), and ADK97014.1 (52–75, 121–161, 253–274, 332–379, 390–427)	EAAAKGIINTLQKYYCRVRGGRCAVLSCLPKEEQIGKCSTRGRKCCRRKKEAAAKAKFVAAWTLKAAAGGGSDEPTPWA FGFVCGRSVVDNARPHVGKRYGGGSQGITFTRYADDLTFSSDTDILRPQGELVQQVKAIVERYGFRLNEEKTGGGSAKFVA AWTLKAAAGGGSGFHERNQVNYANPASYASVDSLSFHEYGAEALERAGLLPYTNVGYNFSNTQNVNAFPSTSSVNATYSNA YNGSGGLHHEYGAEALERAGLISTNSQTSISDTTRYVVSNSLHEYGAEALERAGKFTLGGDYCKGERYRGFFSRMHYRAGF SYASPYLKINGVDGPRELSASHEYGAEALERAGYNNRSMLNISAEWVNQSVTGMIKENMFRINVGFTFNERHEYGAEALER AGAKFVAAWTLKAAAGGGS
5	ADK95685.1 (55–83, 268–294), and ADK97014.1 (15–45, 82–109, 165–236, 278–329)	EAAAKMSDLKNLAETLVNLTVKDVNELAAILKDEYGIEPAAAAVVMAGPGAEAAEEKTEFDVILKSAGASKLAVVKLVK DLTGAGLKEAKDMVDGAPAAIKSGISKDEAEALKKQLEEAGAEVELKEAAAKAKFVAAWTLKAAAGGGSDTNNVQRRCKTF RLRKKHGGYREITAPKGGGGSLMVTEKVNVSRRYVREIRSLLYIWERYGGGSAKFVAAWTLKAAAGGGSVQVSAQSGTNSP YSQYGLGALASQATSFNRGHEYGAEALERAGSLQLTNFEENGNKVNAKNADIEYVVASFHEYGAEALERAGLGAGWEPFKG FSFGANIGYLWGTLNRNSTNTYSDSYVNTLSKNYSAQVKSYKVDFGAQYTYAVDKKNELTLGHEYGAEALERAGHTFGVGL MWNHNNRLKFGVDYQLQKWAKLKYPQLTTVNGTTSYNLVDGQFNDHEYGAEALERAGAKFVAAWTLKAAAGGGS
6	ADK95685.1 (55–83, 268–294), and ADK97014.1 (15–45, 82–109, 165–236, 278–329)	EAAAKMAENPNIDDLPAPLLAALGAADLALATVNDLIANLRERAEETRAETRTRVEERRARLTKFQEDLPEQFIELRDK FTTEELRKAAEGYLEAATNRYNELVERGEAALQRLRSQTAFEDASARAEGYVDQAVELTQEALGTVASQTRAVGERAAKLV GIELEAAAKAKFVAAWTLKAAAGGGSDTNNVQRRCKTFRLRKKHGGYREITAPKGGGGSLMVTEKVNVSRRYVREIRSLLY IWERYGGGSAKFVAAWTLKAAAGGGSVQVSAQSGTNSPYSQYGLGALASQATSFNRGHEYGAEALERAGSLQLTNFEENGN KVNAKNADIEYVVASFHEYGAEALERAGLGAGWEPFKGFSFGANIGYLWGTLNRNSTNTYSDSYVNTLSKNYSAQVKSYKV DFGAQYTYAVDKKNELTLGHEYGAEALERAGHTFGVGLMWNHNNRLKFGVDYQLQKWAKLKYPQLTTVNGTTSYNLVDGQF NDHEYGAEALERAGAKFVAAWTLKAAAGGGS
7	ADK95685.1 (55–83, 268–294), and ADK97014.1 (15–45, 82–109, 165–236, 278–329)	EAAAKMAENSNIDDIKAPLLAALGAADLALATVNELITNLRERAEETRRSRVEESRARLTKLQEDLPEQLTELREKFTA EELRKAAEGYLEAATSELVERGEAALERLRSQQSFEEVSARAEGYVDQAVELTQEALGTVASQVEGRAAKLVGIELEAAAK AKFVAAWTLKAAAGGGSDTNNVQRRCKTFRLRKKHGGYREITAPKGGGGSLMVTEKVNVSRRYVREIRSLLYIWERYGGGS AKFVAAWTLKAAAGGGSVQVSAQSGTNSPYSQYGLGALASQATSFNRGHEYGAEALERAGSLQLTNFEENGNKVNAKNADI EYVVASFHEYGAEALERAGLGAGWEPFKGFSFGANIGYLWGTLNRNSTNTYSDSYVNTLSKNYSAQVKSYKVDFGAQYTYA VDKKNELTLGHEYGAEALERAGHTFGVGLMWNHNNRLKFGVDYQLQKWAKLKYPQLTTVNGTTSYNLVDGQFNDHEYGAEA LERAGAKFVAAWTLKAAAGGGS
8	ADK95685.1 (55–83, 268–294), and ADK97014.1 (15–45, 82-109, 165–236, 278–329)	EAAAKGIINTLQKYYCRVRGGRCAVLSCLPKEEQIGKCSTRGRKCCRRKKEAAAKAKFVAAWTLKAAAGGGSDTNNVQR RCKTFRLRKKHGGYREITAPKGGGGSLMVTEKVNVSRRYVREIRSLLYIWERYGGGSAKFVAAWTLKAAAGGGSVQVSAQS GTNSPYSQYGLGALASQATSFNRGHEYGAEALERAGSLQLTNFEENGNKVNAKNADIEYVVASFHEYGAEALERAGLGAGW EPFKGFSFGANIGYLWGTLNRNSTNTYSDSYVNTLSKNYSAQVKSYKVDFGAQYTYAVDKKNELTLGHEYGAEALERAGHT FGVGLMWNHNNRLKFGVDYQLQKWAKLKYPQLTTVNGTTSYNLVDGQFNDHEYGAEALERAGAKFVAAWTLKAAAGGGS

Molecular dynamic simulation

In the cellular environment, the stability of docked complexes was inferred by molecular dynamic simulation studies. The iMOD server was employed to explore the movement of molecules and atoms. The relation of the docked complex between the NMA and the PDB sector was clearly visualized by the B-factor graph (Figure 4A). The coupling between residues was indicated by a covariance matrix, where the motions, i.e., correlated, uncorrelated, and anti-correlated, of different pairs were indicated by red, blue, and white colors, respectively (Figure 4B). The distortion of each residue was counted as the deformability of the complex, as shown in the graphs obtained by the server with higher peaks indicating the greater deformability (Figure 4C). A low Eigenvalue indicates that the complex can be deformed easily. The motion stiffness of the complex was represented by an Eigenvalue (9.549413e-05) (Figure 4D). The Eigenvalue and variance related to each normal mode were found to be in an inverse relation (Figure 4F). The

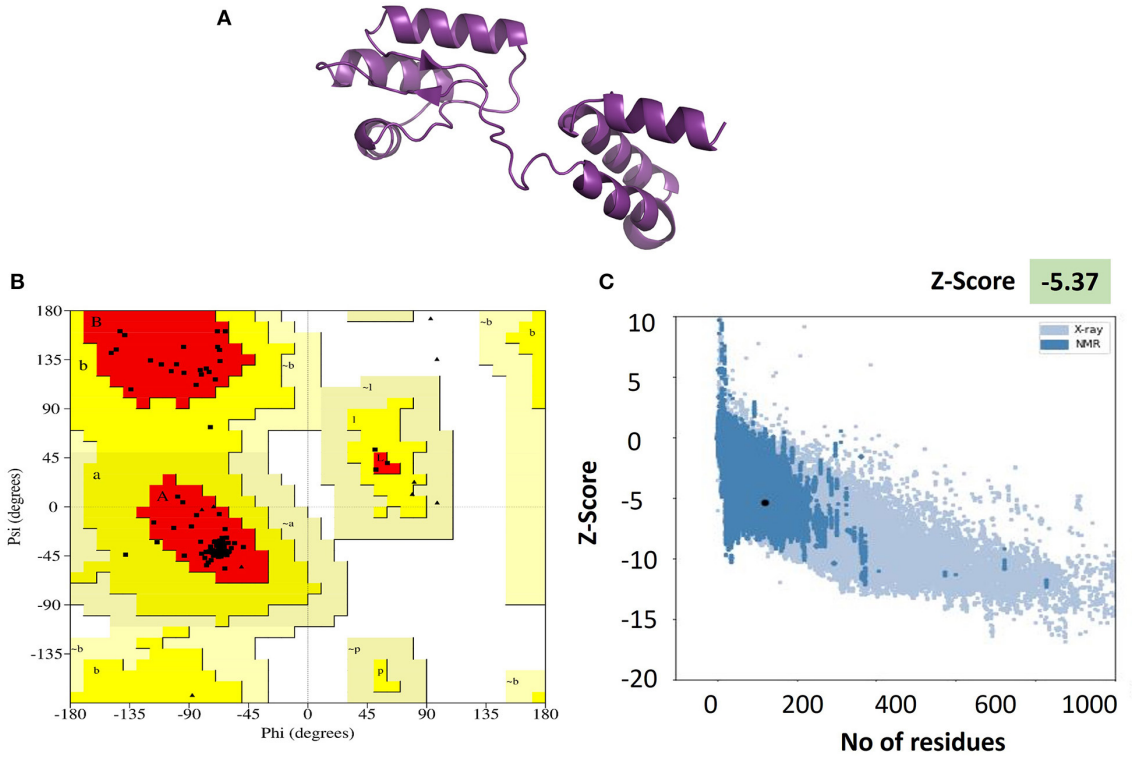

FIGURE 3
(A) Tertiary structure of the vaccine V5 generated and refined by Phyre 2 and GalaxRefine servers, respectively. **(B)** Ramachandran plot exhibiting more than 95% in the Rama-favored regions. **(C)** Vaccine 3D structure validation by ProSA-web. The Z-score of the refined model is −5.37, which is lying inside the score range.

TABLE 5 **Docking analysis for the interaction studies between vaccine construct V5 and major immune receptors.**

Sr. no.	HLA alleles PDB ID	Score	Area	Hydrogen bond energy	Global energy	ACE
1	2Q6W	13,898	1,886.3	−1.25	−15.29	7.27
2	1A6A	14,024	1,894.2	−0.9	−11.84	−2.64
3	5NI9	14,416	1,935.3	−3.07	−16.12	9.23
4	TLR4	14,506	1,932	−2.05	−12.82	13.86
5	4MD4	14,544	1,912.2	−5.03	−21.8	9.32
6	1AQD	14,814	1,867.8	−5.34	−25.38	8.99

elastic network model indicated the stiffness of the residues of the vaccine in the form of springs, with darker grays indicating stiffer springs (Figure 4E). The interpretation obtained from the results confirmed the stability of the docked complex (V5-TLR4) in the cellular environment.

Codon optimization and *in silico* cloning

For the sake of maximal protein expression, the vaccine construct's codon was optimized by JCat (Java Codon Adaptation Tool) in *E. coli* (strain K12). The JCat resource provided the percentage of average GC content up to 70% and CAI value (0.95–1.0) of adapted sequences, which ensured a high expression rate of vaccine constructs in *E. coli*. The adapted codon sequences were introduced in the plasmid vector pET 28a (+) for the construction of recombinant plasmid sequences, which ensured expression and heterologous cloning in *E. coli*. Cloning of the vaccine DNA sequence provided a recombinant vector of 6,804 bp (Supplementary Figure S2).

Immune simulation

Immune simulations play a role in the development of an immune profile of the vaccine construct. The memory of immune cells was observed under C-ImmSim analysis to increase their half-life and successive immune responses by the cell (Bibi et al.,

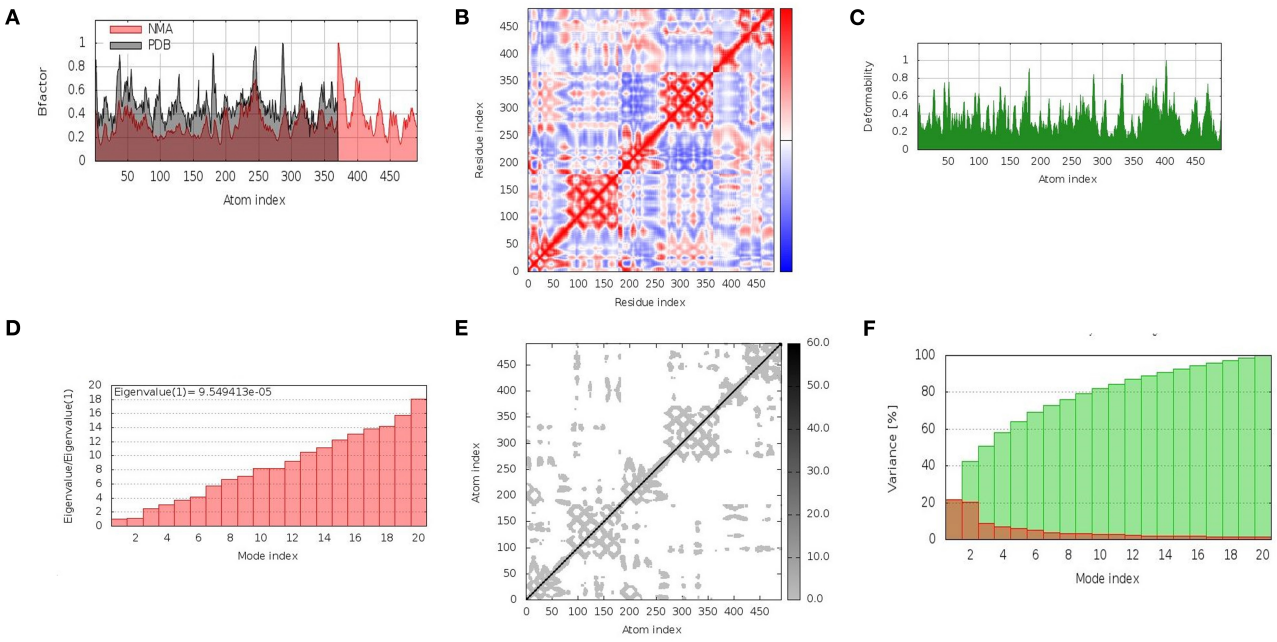

FIGURE 4
Molecular dynamics simulation of vaccine construct (V5)–TLR4 complex. The stability of the protein–protein complex was examined by **(A)** B-factor, **(B)** covariance matrix of residue index, **(C)** deformability, **(D)** Eigenvalue, **(E)** elastic network analysis, and **(F)** variance.

2021). Steadiness and real immune reactions were confirmed by the outcomes of this server. High IgM values indicated a primary immune response. Furthermore, the immunoglobulin expression level (IgG1+IgG2, IgM, and IgG+IgM) was increased, showing a decrease in antigen concentration (Figure 5A), which confirmed an increase in the active B-cell population (Figure 5D). Immunization led to an increase in the concentration of the active cytotoxic and helper T lymphocytes (Figures 5B, C). The cytokinin levels and IFN-gamma-inducing properties were also increased after every dose of the vaccine. Furthermore, the inset plot indicated that the chances of the danger caused by the vaccine are too low (Figure 5E). All the immune responses indicated that our vaccine is capable of causing a potent immune response.

Discussion

P. melaninogenica, due to its irrefutable place within the CF respiratory microbiota in the pathophysiology of oral lichen planus (OLP) and periodontal diseases, has gained the attention of researchers to target this pathogen (Lamoureux et al., 2021). Although discrepancies in antimicrobial rates were observed, a constant increase in resistance is still trending, which provoked the researchers to look for an alternative to the current therapies. Identification of novel therapeutic drugs by targeting the core genes of bacterial species might be favorable. *In silico* approaches have become popular in designing novel drug and vaccine targets against pathogenic organisms with the help of bioinformatics.

While looking for an alternative drug target, subtractive proteomics or genomics were combined with reverse vaccinology to find a suitable vaccine target. In the present study, 14 complete genomes of *P. melaninogenica* were used to extract the core genes of the bacteria, which remain conserved throughout the species. The previous studies involved surveys and other experimental approaches to combat the infections of *P. melaninogenica*, but no *in silico* approaches were applied in the past. A total of 114 proteins were recognized as essential, virulent, antibiotic-resistant, and non-homologous, which could serve as novel drug or vaccine targets determined *by in silico* analysis.

PPI network analysis of these drug candidates filtered the hub proteins after predicting the subcellular location of proteins (Jalili et al., 2016). Druggable screening of the cytoplasmic proteins prioritized the non-homologs as novel discoveries in the identification of therapeutic drug targets against *P. melaninogenica*. A total of 18 proteins were prioritized as potential drug targets, of which 1 is KEGG-dependent and 17 are KEGG-independent (Table 2). Of these proteins, dihydroneopterin aldolase (ADK97401.1) is involved in the conversion of 7,8-dihydroneopterin to 6-hydroxymethyl-7,8-dihydropterin in the folate synthesis pathway of microorganisms. This pathway is very important for the growth and survival of many microorganisms. It was selected as a drug target because its inhibition can cause the death of microorganisms (Wang et al., 2006). Pyridoxal 5′-phosphate (PLP) (ADK95358.1) is an important coenzyme and is involved in a variety of reactions. The pyridoxal 5′-phosphate synthase is responsible for the synthesis of PLP. If PLP-synthase is inhibited in microorganisms, it leads to a decrease in their essential amino acids, leading to growth retardation or death of the microorganisms. Due to this reason, PLP-synthase was prioritized as a potential drug target (Strohmeier et al., 2006). Nicotinate phosphoribosyl transferase (NAPRT) (ADK95883.1) causes the conversion of nicotinic acid into nicotinamide adenine

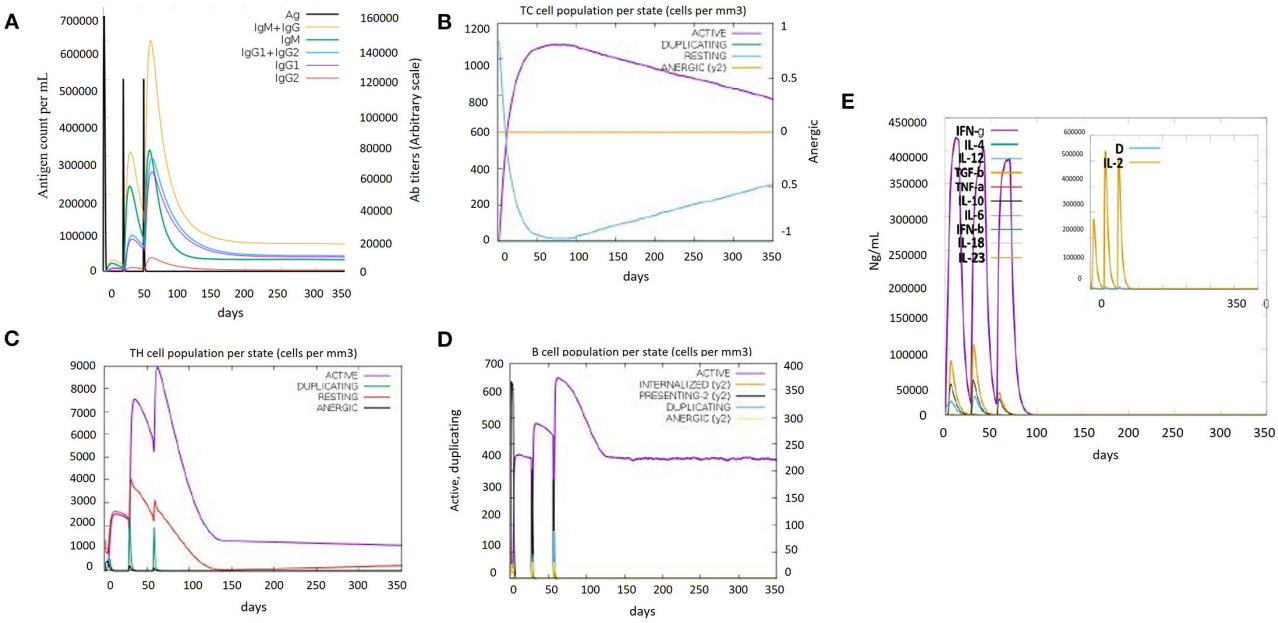

FIGURE 5
Immune simulation results of the designed vaccine construct (V5). **(A)** Immunoglobulin levels with respect to antigen concentration. **(B)** Cytotoxic T-cell population per state. **(C)** Helper T-cell population per state. **(D)** B-cell population per state. **(E)** Cytokine and interleukin levels after vaccine injection. The inset plot indicated high production of IL-2 along with a danger signal.

dinucleotide (NAD) (Audrito et al., 2020). NAD is involved in energy production and the repair of DNA in the event of any damage. If NAPRT is inhibited in bacteria, it can lead to many problems for them. It can also cause sensitivity to certain antibiotics (Ghanem et al., 2022). Glycosyltransferase (ADK95886.1), involved in the interconversion of sugars, was also prioritized as a drug target (Schmid et al., 2016). The putative phosphomethylpyrimidine kinase (ADK96110.1), the homolog of thiD, is involved in the initial stage of the biosynthesis of vitamin B1 (thiamin). Thiamin, in its activated form, thiamin diphosphate (ThDP), is very important for microorganisms. It is essential for many important metabolic processes, such as the breakdown of sugars and amino acids. Therefore, it was considered a drug target (Naz et al., 2019). Lipid A biosynthesis (KDO)2-(lauroyl)-lipid IVA acyltransferase (ADK96013.1) is responsible for the growth of bacterial cells at high temperatures. If this protein is deleted in a bacterium, it cannot survive at temperatures above 33°C (Zhou et al., 2021). Moreover, it is involved in the formation of Lipid A in bacteria, which is very important for the survival of the bacteria. If it is inhibited in bacteria, it can lead to the disruption of its outer membrane, which ultimately results in the death of the bacteria. Thus, it is a potential drug target against bacterial infections (Six et al., 2008). Another potential novel drug target is UvrD (ADK96570.1). It is a versatile protein found in microorganisms. Its role in DNA metabolism is crucial because it plays various functions such as repairing DNA mismatches during replication, participating in nucleotide excision repair and replication, promoting recombination by removing RecA filaments from DNA, and regulating transcription through interactions with RNA polymerase (Ordabayev et al., 2018). Overall, UvrD's involvement in maintaining DNA integrity and genomic stability is essential for the proper functioning of microorganisms (Ordabayev et al., 2018). Its inhibition can cause the death of microorganisms. Due to these reasons, it showed the potential to become a drug target. The gamma subunit of ATP synthase F1 (ADK96796.1) is essential for ATP production through oxidative phosphorylation in microorganisms (Xu et al., 2015). It plays a vital role in controlling ATP synthase activity and maintaining the proton gradient across the membrane. When the gamma subunit is inhibited, ATP synthesis decreases and the proton gradient is disrupted, which can impact various aspects of cellular metabolism, growth, and survival. Prolonged inhibition of ATP synthesis can ultimately result in cell death (Xu et al., 2015). Thus, targeting this important protein may be fatal for the pathogen and is an effective drug target. The novel drug targets, including aldolases, helicases, hydrolases, synthases, and transferases, investigated in this study have not been reported as drug targets in previous studies. According to the centrality–lethality rule, bacterial pathogens can be targeted by the inhibition or knockdown of these proteins.

To treat pathogenic infections, various antibiotics are discovered by using subtractive genomics or proteomics approaches, but there is still a demand to look for chimeric vaccine development due to increased antimicrobial resistance in clinical isolates of *P. melaninogenica*. Outer membrane proteins being involved in host–pathogen interaction were prioritized as potent vaccine targets in the reverse vaccinology approach (Lu et al., 2014). After analyzing different parameters, two vaccine candidates, i.e., reverse transcriptase (ADK95685.1) and hypothetical protein (ADK97014.1), were selected for the chimeric vaccine construction. Host cells are directly exposed to bacterial outer membrane proteins; hence, they are considered to be the most favorable candidate to be used in reverse vaccinology

against invasive pathogens (Rizwan et al., 2017). Bacterial life and pathogenesis depend on these proteins as they play an important role in different functions such as nutrient acquisition, adhesion, and sustaining bacterial membrane integrity (Mishra et al., 2020).

B- and T-cell immunity is stimulated by antigenic regions of proteins in epitope mapping using the immunoinformatic approach, where the non-antigenic portion is excluded. Lead B- and T-cell overlapped epitopes were used to generate chimeric subunit constructs with different combinations of adjuvants and PADRE sequences for better immune responses and to overwhelm the HLA polymorphism throughout the population (Ghaffari-Nazari et al., 2015). Maximal expression of the prioritized vaccine construct (V5) was ensured by *in silico* cloning in pET 28a (+). A stable interaction between ligand and receptor was confirmed by molecular docking of the vaccine construct with human HLAs and TLR4, which showed the highest docking score. Response to antigens directly depends on the human body's defense system, which is fully equipped to respond. Cytokine and chemokine production to mediate cellular immune responses and the recognition of PAMPs (pathogen-associated molecular patterns) are controlled by TLRs, which are present on the surface of immune cells.

Innate and adaptive immunity responses might be possible with the designed vaccine, as inferred by the binding of V5 with TRL4. The stability and dynamic performance of docked complex V5-TLR4 were explored by molecular dynamic simulation, where steady binding of the complex was confirmed by an RMSD plot. Profound immune responses were expected, as predicted by immune simulation. Memory B and T cells were developed, and the production of helper T cells was evident from the results. Efficient Ig production was indicated by a high level of T cells, supporting a humoral response. Moreover, practical implementation of the designed lead vaccine might be advantageous to combat pathogenic diseases of *P. melaninogenica* in the near future, as inferred from *in silico* approaches.

Conclusion

Before doing biological experiments, it is of utmost importance to depend on *in silico* approaches that can give a better idea about the probability and feasibility of discovering novel drug and vaccine targets. In the present study, *in silico* approaches such as subtractive proteomics and reverse vaccinology were applied to prospect proteins to serve them as drug or vaccine candidates from a conserved set of genes obtained from 14 complete genomes of *P. melaninogenica*. Several biological databases, comparative sequence analyses, and druggability analyses were performed to find the most potent drug candidate. Ultimately, 18 proteins were enlisted as prioritized druggable candidates to be addressed as novel targets against the bacterium that had not been reported in previous studies.

Two proteins were selected as vaccine candidates to develop a chimeric subunit vaccine. Maximal expression of the engineered vaccine construct (V5) was ensured by the *in silico* cloning of the chimeric construct in the bacterial system. Furthermore, the vaccine construct (V5) was docked with human immune cell receptors and TRL4 to confirm its stable binding and capability to stimulate cell-mediated immune responses. Steady binding of the docked complex was inferred by the molecular dynamic simulation analysis. Effective immunological memory to control *P. melaninogenica* infections was validated by immune simulation. All the proposed therapeutic targets further need validation in animal models. Various pathogenic strains of *P. melaninogenica* can be targeted by these therapeutic candidates as core genes were the basis of the study. The drug targets and the vaccine construct designed in this study deserve experimental validation to devise the proper treatment for the said pathogen.

Data availability statement

The original contributions presented in the study are included in the article/Supplementary material, further inquiries can be directed to the corresponding authors.

Author contributions

MSha: Conceptualization, Resources, Supervision, Writing—review and editing. AA: Formal analysis, Investigation, Writing—original draft. AQ: Formal analysis, Investigation, Writing—original draft. SJ: Formal analysis, Investigation, Methodology, Writing—original draft. AS: Formal analysis, Investigation, Writing—original draft. RU: Investigation, Methodology, Visualization, Writing—review and editing. EA: Funding acquisition, Visualization, Writing—review and editing. UN: Methodology, Visualization, Writing—review and editing. MShe: Formal analysis, Investigation, Writing—original draft. AZ: Formal analysis, Investigation, Methodology, Writing—original draft. SO: Funding acquisition, Resources, Writing—review and editing.

Funding

The author(s) declare financial support was received for the research, authorship, and/or publication of this article. The authors extend their appreciation to the Deputyship for Research and Innovation, Ministry of Education in Saudi Arabia for funding this research (IFKSUOR3-020-1). This research also supported by the Doctoral Research Fund awarded to SO.

Conflict of interest

The authors declare that the research was conducted in the absence of any commercial or financial relationships that could be construed as a potential conflict of interest.

Publisher's note

All claims expressed in this article are solely those of the authors and do not necessarily represent those of their affiliated

organizations, or those of the publisher, the editors and the reviewers. Any product that may be evaluated in this article, or claim that may be made by its manufacturer, is not guaranteed or endorsed by the publisher.

Supplementary material

The Supplementary Material for this article can be found online at: https://www.frontiersin.org/articles/10.3389/fmicb.2023.1271798/full#supplementary-material

SUPPLEMENTARY TABLE S1
Analysis of MHC-II interacting epitopes (bold highlights the final epitopes).

SUPPLEMENTARY TABLE S2
Analysis of MHC-I interacting epitopes (bold highlights the final epitopes).

SUPPLEMENTARY TABLE S3
Selection of final vaccine constructs.

SUPPLEMENTARY TABLE S4
Physiochemical and general properties analysis of vaccine constructs.

SUPPLEMENTARY FIGURE S1
(A) Vaccine constructs V5 2D structure predicted by PRISIPRED server. **(B)** Vaccine constructs V5 2D structure predicted by PRISIPRED server.

SUPPLEMENTARY FIGURE S2
In silico restriction cloning of final vaccine construct (V5) into the *E. coli* pET28a (+) expression vector where red color shows the cloned vaccine construct.

References

Ammari, M. G., Gresham, C. R., McCarthy, F. M., and Nanduri, B. (2016). HPIDB 2.0: a curated database for host–pathogen interactions. *Database* 16, baw103. doi: 10.1093/database/baw103

Aslam, M., Shehroz, M., Ali, F., Zia, A., Pervaiz, S., Shah, M., et al. (2021). Chlamydia trachomatis core genome data mining for promising novel drug targets and chimeric vaccine candidates identification. *Comp. Biol. Med.* 136, 104701. doi: 10.1016/j.compbiomed.2021.104701

Aslam, M., Shehroz, M., Shah, M., Khan, M. A., Afridi, S. G., Khan, A., et al. (2020). Potential druggable proteins and chimeric vaccine construct prioritization against Brucella melitensis from species core genome data. *Genomics* 112, 1734–1745. doi: 10.1016/j.ygeno.2019.10.009

Audrito, V., Messana, V. G., and Deaglio, S. (2020). NAMPT and NAPRT: two metabolic enzymes with key roles in inflammation. *Front. Oncol.* 10, 358. doi: 10.3389/fonc.2020.00358

Bibi, S., Ullah, I., Zhu, B., Adnan, M., Liaqat, R., Kong, W. B., et al. (2021). *In silico* analysis of epitope-based vaccine candidate against tuberculosis using reverse vaccinology. *Sci. Rep.*11, 1249. doi: 10.1038/s41598-020-80899-6

Blom, J., Kreis, J., Spänig, S., Juhre, T., Bertelli, C., Ernst, C., et al. (2016). EDGAR 2.0: an enhanced software platform for comparative gene content analyses. *Nuc. Acids Res.* 44, W22–W28. doi: 10.1093/nar/gkw255

Borrel, A., Regad, L., Xhaard, H., Petitjean, M., and Camproux, A. C. (2015). PockDrug: a model for predicting pocket druggability that overcomes pocket estimation uncertainties. *J. Chem. Inform. Model.* 55, 882–895. doi: 10.1021/ci5006004

Craig, D. B., and Dombkowski, A. A. (2013). Disulfide by Design 2.0: a web-based tool for disulfide engineering in proteins. *BMC Bioinform.* 14, 1–7. doi: 10.1186/1471-2105-14-S19-S1

Dimitrov, I., Naneva, L., Doytchinova, I., and Bangov, I. (2014). AllergenFP: allergenicity prediction by descriptor fingerprints. *Bioinformatics* 30, 846–851. doi: 10.1093/bioinformatics/btt619

Dorella, F. A., Gala-Garcia, A., Pinto, A. C., Sarrouh, B., Antunes, C. A., Ribeiro, D., et al. (2013). Progression of 'OMICS' methodologies for understanding the pathogenicity of *Corynebacterium pseudotuberculosis*: the Brazilian experience. *Comput. Struct. Biotechnol. J.* 6, e201303013. doi: 10.5936/csbj.201303013

Doytchinova, I. A., and VaxiJen, D. F. (2007). A server for prediction of protective antigens, tumour antigens and subunit vaccines. 8, 4. doi: 10.1186/1471-2105-8-4

Fatoba, A. J., Okpeku, M., and Adeleke, M. A. (2021). Subtractive genomics approach for identification of novel therapeutic drug targets in *Mycoplasma genitalium*. *Pathogens* 10, 921. doi: 10.3390/pathogens10080921

Fleri, W., Paul, S., Dhanda, S. K., Mahajan, S., Xu, X., Peters, B., et al. (2017). The immune epitope database and analysis resource in epitope discovery and synthetic vaccine design. *Front. Immunol.* 8, 278. doi: 10.3389/fimmu.2017.00278

Ghaffari-Nazari, H., Tavakkol-Afshari, J., Jaafari, M. R., Tahaghoghi-Hajghorbani, S., Masoumi, E., Jalali, S. A., et al. (2015). Improving multi-epitope long peptide vaccine potency by using a strategy that enhances CD4+ T help in BALB/c mice. *PLoS ONE* 10, e0142563. doi: 10.1371/journal.pone.0142563

Ghanem, M. S., Caffa, I., Del Rio, A., Franco, J., Parenti, M. D., Monacelli, F., et al. (2022). Identification of NAPRT inhibitors with anti-cancer properties by *in silico* drug discovery. *Pharmaceuticals* 15, 848. doi: 10.3390/ph15070848

Gupta, S. K., Padmanabhan, B. R., Diene, S. M., Lopez-Rojas, R., Kempf, M., Landraud, L., et al. (2014). ARG-ANNOT, a new bioinformatic tool to discover antibiotic resistance genes in bacterial genomes. *Antimicrob. Agents Chemother.* 58, 212–220. doi: 10.1128/AAC.01310-13

He, J., Chang, Q., Hu, F., Feng, X., Zhu, D., Yu, L., et al. (2013). Prevalence and antimicrobial susceptibility of anaerobes from patients with periodontal abscess in China. *J. Antibiot.* 66, 97–98. doi: 10.1038/ja.2012.94

Jaan, S., Shah, M., Ullah, N., Amjad, A., Javed, M. S., Nishan, U., et al. (2022). Multi-epitope chimeric vaccine designing and novel drug targets prioritization against multi-drug resistant Staphylococcus pseudintermedius. *Front. Microbiol.* 13, 971263. doi: 10.3389/fmicb.2022.971263

Jalili, M., Salehzadeh-Yazdi, A., Gupta, S., Wolkenhauer, O., Yaghmaie, M., Resendis-Antonio, O., et al. (2016). Evolution of centrality measurements for the detection of essential proteins in biological networks. *Front. Physiol.* 7, 375. doi: 10.3389/fphys.2016.00375

Kho, Z. Y., and Lal, S. K. (2018). The human gut microbiome—A potential controller of wellness and disease. *Front. Microbiol.* 9, 1–23. doi: 10.3389/fmicb.2018.01835

Kondo, Y., Sato, K., Nagano, K., Nishiguchi, M., Hoshino, T., Fujiwara, T., et al. (2018). Involvement of PorK, a component of the type IX secretion system, in *Prevotella melaninogenica* pathogenicity. *Microbiol. Immunol.* 62, 554–566. doi: 10.1111/1348-0421.12638

Könönen, E., and Gursoy, U. K. (2022). Oral Prevotella species and their connection to events of clinical relevance in gastrointestinal and respiratory tracts. *Front. Microbiol.* 12, 798763. doi: 10.3389/fmicb.2021.798763

Krogh, A., Larsson, B., Von Heijne, G., and Sonnhammer, E. L. (2001). Predicting transmembrane protein topology with a hidden Markov model: application to complete genomes. *J. Mol. Biol.* 305, 567–580. doi: 10.1006/jmbi.2000.4315

Lamoureux, C., Guilloux, C. A., Courteboeuf, E., Gouriou, S., Beauruelle, C., Héry-Arnaud, G., et al. (2021). Prevotella melaninogenica, a sentinel species of antibiotic resistance in cystic fibrosis respiratory niche? *Microorganisms* 9, 1275. doi: 10.3390/microorganisms9061275

Law, V., Knox, C., Djoumbou, Y., Jewison, T., Guo, A. C., Liu, Y., et al. (2014). DrugBank 4.0: shedding new light on drug metabolism. *Nucleic Acids Res.* 42, D1091–D1097. doi: 10.1093/nar/gkt1068

Li, W., and Godzik, A. (2006). Cd-hit: a fast program for clustering and comparing large sets of protein or nucleotide sequences. *Bioinformatics* 22, 1658–1659. doi: 10.1093/bioinformatics/btl158

Li, X., Yang, H. W., Chen, H., Wu, J., Liu, Y., Wei, J. F., et al. (2014). *In silico* prediction of T and B cell epitopes of der f 25 in *Dermatophagoides farinae*. *Int. J. Genomics*. 2014, 3905. doi: 10.1155/2014/483905

Liu, B., Zheng, D., Jin, Q., Chen, L., and Yang, J. (2019). VFDB 2019: a comparative pathogenomic platform with an interactive web interface. *Nuc. Acids Res.* 47, D687–D692. doi: 10.1093/nar/gky1080

Lu, J., Yu, Y., Zhu, I., Cheng, Y., and Sun, P. D. (2014). Structural mechanism of serum amyloid A-mediated inflammatory amyloidosis. *Proc. Nat. Acad. Sci.* 111, 5189–5194. doi: 10.1073/pnas.1322357111

Luo, H., Lin, Y., Liu, T., Lai, F. L., Zhang, C. T., Gao, F., et al. (2021). DEG 15, an update of the Database of Essential Genes that includes built-in analysis tools. *Nucleic Acids Res.* 49, D677–D686. doi: 10.1093/nar/gkaa917

Magnan, C. N., Randall, A., and Baldi, P. (2009). SOLpro: accurate sequence-based prediction of protein solubility. *Bioinformatics* 25, 2200–2207. doi: 10.1093/bioinformatics/btp386

Maxwell, P. I., and Popelier, P. L. (2017). Unfavorable regions in the ramachandran plot: is it really steric hindrance? The interacting quantum atoms perspective. *J. Comput. Chem.* 38, 2459–2474. doi: 10.1002/jcc.24904

Mishra, M., Panda, S., Barik, S., Sarkar, A., Singh, D. V., Mohapatra, H., et al. (2020). Antibiotic resistance profile, outer membrane proteins, virulence factors and genome sequence analysis reveal clinical isolates of Enterobacter are potential pathogens compared to environmental isolates. *Front. Cell. Infect. Microbiol.* 10, 54. doi: 10.3389/fcimb.2020.00054

Mondal, S. I., Ferdous, S., Jewel, N. A., Akter, A., Mahmud, Z., Islam, M. M., et al. (2015). Identification of potential drug targets by subtractive genome analysis of *Escherichia coli* O157:H7: an *in silico* approach. *Adv. Appl. Bioinform. Chem.* 49-63. doi: 10.2147/AABC.S88522

Moriya, Y., Itoh, M., Okuda, S., Yoshizawa, A. C., and Kanehisa, M. (2007). KAAS: an automatic genome annotation and pathway reconstruction server. *Nuc. Acids Res.* 35(suppl_2), W182-W185. doi: 10.1093/nar/gkm321

Naz, K., Naz, A., Ashraf, S. T., Rizwan, M., Ahmad, J., Baumbach, J., et al. (2019). PanRV: pangenome-reverse vaccinology approach for identifications of potential vaccine candidates in microbial pangenome. *BMC Bioinform.* 20, 1–10. doi: 10.1186/s12859-019-2713-9

Nazir, Z., Afridi, S. G., Shah, M., Shams, S., and Khan, A. (2018). Reverse vaccinology and subtractive genomics-based putative vaccine targets identification for Burkholderia pseudomallei Bp1651. *Microb. Pathog.* 125, 219–229. doi: 10.1016/j.micpath.2018.09.033

Nogueira, W. G., Jaiswal, A. K., Tiwari, S., Ramos, R. T., Ghosh, P., Barh, D., et al. (2021). Computational identification of putative common genomic drug and vaccine targets in *Mycoplasma genitalium*. *Genomics* 113, 2730–2743. doi: 10.1016/j.ygeno.2021.06.011

Ordabayev, Y., Nguyen, B., Niedziela-Majka, A., and Lohman, T. (2018). Regulation of UvrD helicase activity by MutL. *Biophys. J.* 114, 444a. doi: 10.1016/j.bpj.2017.11.2455

Puzone, R., Kohler, B., Seiden, P., and Celada, F. (2002). IMMSIM, a flexible model for in machina experiments on immune system responses. *Future Gen. Comput. Syst.* 18, 961972. doi: 10.1016/S0167-739X(02)00075-4

Qasim, A., Jaan, S., Wara, T. U., Shehroz, M., Nishan, U., Shams, S., et al. (2023). Computer-aided genomic data analysis of drug-resistant *Neisseria gonorrhoeae* for the Identification of alternative therapeutic targets. *Front. Cell. Infect. Microbiol.* 13, 1017315. doi: 10.3389/fcimb.2023.1017315

Rana, A., and Akhter, Y. (2016). A multi-subunit based, thermodynamically stable model vaccine using combined immunoinformatics and protein structure based approach. *Immunobiology* 221, 544–557. doi: 10.1016/j.imbio.2015.12.004

Raza, M. T., Mizan, S., Yasmin, F., Akash, A. S., and Shahik, S. M. (2021). Epitope-based universal vaccine for Human T-lymphotropic virus-1 (HTLV-1). *PLoS ONE* 16, e0248001. doi: 10.1371/journal.pone.0248001

Rizwan, M., Naz, A., Ahmad, J., Naz, K., Obaid, A., Parveen, T., et al. (2017). VacSol: a high throughput *in silico* pipeline to predict potential therapeutic targets in prokaryotic pathogens using subtractive reverse vaccinology. *BMC Bioinform.* 18, 1–7. doi: 10.1186/s12859-017-1540-0

Schmid, J., Heider, D., Wendel, N. J., Sperl, N., and Sieber, V. (2016). Bacterial glycosyltransferases: challenges and opportunities of a highly diverse enzyme class toward tailoring natural products. *Front. Microbiol.* 7, 182. doi: 10.3389/fmicb.2016.00182

Shah, M., Jaan, S., Fatima, B., Javed, M. S., Amjad, A., Khan, A., et al. (2021). Delineating novel therapeutic drug and vaccine targets for *Staphylococcus cornubiensis* NW1T through computational analysis. *Int. J. Pept. Res. Ther.* 27, 181–195. doi: 10.1007/s10989-020-10076-w

Sherrard, L. J., Schaible, B., Graham, K. A., McGrath, S. J., McIlreavey, L., Hatch, J., et al. (2014). Mechanisms of reduced susceptibility and genotypic prediction of antibiotic resistance in Prevotella isolated from cystic fibrosis (CF) and non-CF patients. *J. Antimicrob. Chemoth.* 69, 2690–2698. doi: 10.1093/jac/dku192

Six, D. A., Carty, S. M., Guan, Z., and Raetz, C. R. (2008). Purification and mutagenesis of LpxL, the lauroyltransferase of *Escherichia coli* lipid A biosynthesis. *Biochemistry* 47, 8623–8637. doi: 10.1021/bi800873n

Solanki, V., and Tiwari, V. (2018). Subtractive proteomics to identify novel drug targets and reverse vaccinology for the development of chimeric vaccine against *Acinetobacter baumannii*. *Sci. Rep.* 8, 9044. doi: 10.1038/s41598-018-26689-7

Strohmeier, M., Raschle, T., Mazurkiewicz, J., Rippe, K., Sinning, I., Fitzpatrick, T. B., et al. (2006). Structure of a bacterial pyridoxal 5′-phosphate synthase complex. *Proc. Nat. Acad. Sci.* 103, 19284–19289. doi: 10.1073/pnas.0604950103

Szklarczyk, D., Morris, J. H., Cook, H., Kuhn, M., Wyder, S., Simonovic, M., et al. (2016). The STRING database in 2017: quality-controlled protein–protein association networks, made broadly accessible. *Nuc. Acids Res. 14,* gkw937. doi: 10.1093/nar/gkw937

Troil-linde, B. O. (1999). *Prevotella pallens* genotypes and *in vitro* susceptibilities to selected antimicrobial. *Agents* 43 2383–2388.

Wang, Y., Li, Y., and Yan, H. (2006). Mechanism of dihydroneopterin aldolase: functional roles of the conserved active site glutamate and lysine residues. *Biochemistry* 45, 15232–15239.

Wu, C. Y., Monie, A., Pang, X., Hung, C. F., and Wu, T. C. (2010). Improving therapeutic HPV peptide-based vaccine potency by enhancing CD4+ T help and dendritic cell activation. *J. Biomed. Sci.* 17, 1–10. doi: 10.1186/1423-0127-17-S1-S1

Xu, T., Pagadala, V., and Mueller, D. M. (2015). Understanding structure, function, and mutations in the mitochondrial ATP synthase. *Microb. Cell* 2, 105. doi: 10.15698/mic2015.04.197

Yu, C. S., Cheng, C. W., Su, W. C., Chang, K. C., Huang, S. W., Hwang, J. K., et al. (2014). CELLO2GO: a web server for protein subCELlular LOcalization prediction with functional gene ontology annotation. *PLoS ONE* 9, e99368. doi: 10.1371/journal.pone.0099368

Zheng, S. W., Xu, P., Cai, L. T., Tan, Z. W., Guo, Y. T., Zhu, R. X., et al. (2022). The presence of Prevotella melaninogenica within tissue and preliminary study on its role in the pathogenesis of oral lichen planus. *Oral Dis.* 28, 1580–1590. doi: 10.1111/odi.13862

Zhou, Q., Tan, X., Meng, X., Wang, J., Ji, F., Wang, X., et al. (2021). Identification of four secondary acyltransferases for lipid A biosynthesis in *Vibrio parahaemolyticus*. *Biotechnol. Appl. Biochem.* 68, 1486–1500. doi: 10.1002/bab.2070

frontiers | Frontiers in Microbiology

TYPE Original Research
PUBLISHED 28 September 2023
DOI 10.3389/fmicb.2023.1277320

OPEN ACCESS

EDITED BY
Vijay Soni,
NewYork-Presbyterian, United States

REVIEWED BY
Maruti Nandan Rai,
University of Illinois at Urbana-Champaign, United States
Pratima Saini,
Wistar Institute, United States
Yaxin Li,
Cornell University, United States

*CORRESPONDENCE
Wei Zhang
✉ zhangweiliuxin@163.com
Yang Liu
✉ ly13767160474@sina.com

†These authors have contributed equally to this work and share first authorship

RECEIVED 14 August 2023
ACCEPTED 11 September 2023
PUBLISHED 28 September 2023

CITATION
Zhu L, Li P, Zhang G, He Z, Tao X, Ji Y, Yang W, Zhu X, Luo W, Liao W, Chen C, Liu Y and Zhang W (2023) Role of the ISKpn element in mediating mgrB gene mutations in ST11 hypervirulent colistin-resistant *Klebsiella pneumoniae*. *Front. Microbiol.* 14:1277320. doi: 10.3389/fmicb.2023.1277320

Role of the ISKpn element in mediating mgrB gene mutations in ST11 hypervirulent colistin-resistant *Klebsiella pneumoniae*

Lanlan Zhu[1†], Ping Li[1,2,3†], Guangyi Zhang[1], Zhiyong He[4], Xingyu Tao[1,2], Yicheng Ji[5], Wenjing Yang[5], Xiaofang Zhu[5], Wanying Luo[1,2], Wenjian Liao[1], Chuanhui Chen[1], Yang Liu[6,7]* and Wei Zhang[1,2]*

[1]Department of Pulmonary and Critical Care Medicine, The First Affiliated Hospital of Nanchang University, Nanchang University, Nanchang, China, [2]Jiangxi Institute of Respiratory Disease, The First Affiliated Hospital of Nanchang University, Nanchang, China, [3]Yichun People's Hospital, Yichun, China, [4]First Clinical Medical College of Nanchang University, Nanchang University, Nanchang, China, [5]Department of Hospital Infection Control, First Affiliated Hospital of Nanchang University, Nanchang University, Nanchang, China, [6]National Regional Center for Respiratory Medicine, Jiang Xi Hospital of China-Japan Friendship Hospital, Nanchang, China, [7]Department of Clinical Microbiology, The First Affiliated Hospital of Nanchang University, Nanchang University, Nanchang, China

Background: Colistin has emerged as a last-resort therapeutic against antibiotic-resistant bacterial infections, particularly those attributed to carbapenem-resistant Enterobacteriaceae (CRE) like CRKP. Yet, alarmingly, approximately 45% of multidrug-resistant *Klebsiella pneumoniae* strains now manifest resistance to colistin. Through our study, we discerned that the synergy between carbapenemase and IS elements amplifies resistance in *Klebsiella pneumoniae*, thereby narrowing the existing therapeutic avenues. This underscores the instrumental role of IS elements in enhancing colistin resistance through mgrB disruption.

Methods: From 2021 to 2023, 127 colistin-resistant *Klebsiella pneumoniae* isolates underwent meticulous examination. We embarked on an exhaustive genetic probe, targeting genes associated with both plasmid-mediated mobile resistance-encompassing *bla*KPC, *bla*NDM, *bla*IMP, *bla*VIM, *bla*OXA-48-like, and *mcr-1* to *mcr-8*-and chromosome-mediated resistance systems, including *PhoP/Q*, *PmrA/B*, and *mgrB*. PCR amplification revealed the presence of virulence-associated genes from the *pLVPK* plasmid, such as *rmpA*, *rmpA2*, *iucA*, *iroB*, and *peg344*. *mgrB* sequencing was delegated to Sangon Biotech, Shanghai, and the sequences procured were validated using BLAST. Our search for IS elements was navigated through the IS finder portal. Phenotypically, we harnessed broth microdilution (BMD) to ascertain the MICs of colistin. To sketch the clonal lineage of mgrB-mutated CoR-Kp isolates, sophisticated methodologies like MLST and PFGE were deployed. S1-PFGE unraveled the intrinsic plasmids in these isolates. Our battery of virulence assessment techniques ranged from the string test and capsular serotyping to the serum killing assay and the *Galleria mellonella* larval infection model.

Results: Among the 127 analyzed isolates, 20 showed an enlarged *mgrB* PCR amplicon compared to wild-type strains. These emerged over a three-year period: three in 2021, thirteen in 2022, and four in 2023. Antimicrobial susceptibility tests revealed that these isolates consistently resisted several drugs, notably TCC,

TZP, CAZ, and COL. Additionally, 85% resisted both DOX and TOB. The MICs for colistin across these strains ranged between 16 to 64 mg/L, with a median of 40 mg/L. From a genetic perspective, MLST unanimously categorized these *mgrB*-mutated CoR-hvKp isolates as ST11. PFGE further delineated them into six distinct clusters, with clusters A and D being predominant. This distribution suggests potential horizontal and clonal genetic transmission. Intriguingly, every mgrB-mutated CoR-hvKP isolate possessed at least two virulence genes akin to the *pLVPK-like* virulence plasmid, with *iroB* and *rmpA2* standing out. Their virulence was empirically validated both *in vitro* and *in vivo*. A pivotal discovery was the identification of three distinct insertion sequence (IS) elements within or near the mgrB gene. These were:ISKpn26 in eleven isolates, mainly in cluster A, with various insertion sites including +74, +125, and an upstream −35.ISKpn14 in four isolates with insertions at +93, −35, and two upstream at −60.IS903B present in five isolates, marking positions like +74, +125, +116, and −35 in the promoter region. These diverse insertions, spanning six unique locations in or near the mgrB gene, underscore its remarkable adaptability.

Conclusion: Our exploration spotlights the ISKpn element's paramount role in fostering *mgrB* gene mutations in ST11 hypervirulent colistin-resistant *Klebsiella pneumoniae*. Employing MLST and PFGE, we unearthed two primary genetic conduits: clonal and horizontal. A striking observation was the ubiquitous presence of the *KPC* carbapenemase gene in all the evaluated ST11 hypervirulent colistin-resistant *Klebsiella pneumoniae* strains, with a majority also harboring the *NDM* gene. The myriad mgrB gene insertion locales accentuate its flexibility and the overarching influence of IS elements, notably the pervasive IS5-like variants ISKpn26 and IS903B. Our revelations illuminate the escalating role of IS elements in antibiotic resistance within ST11 hypervirulent colistin-resistant *Klebsiella pneumoniae*, advocating for innovative interventions to counteract these burgeoning resistance paradigms given their profound ramifications for prevailing treatment modalities.

KEYWORDS

colistin-resistant *Klebsiella pneumoniae*, ISKpn, mgrB, ST11, hypervirulent

1. Introduction

The dramatic rise in antibiotic resistance among Gram-negative bacteria since the 1970s has emerged as a significant global challenge (Nordmann and Poirel, 2019). Global resistance levels are alarmingly elevated, driven in part by the overuse and misuse of antibiotics and compounded by insufficient infection prevention and control strategies (Imai et al., 2019; Jean et al., 2022). Notably, strains of *Escherichia coli*, *Klebsiella pneumoniae* (KP), *Acinetobacter baumannii*, and *Pseudomonas aeruginosa*, presenting as multidrug-resistant (MDR), extensively drug-resistant (XDR), and pan-drug-resistant (PDR), are increasingly exhibiting diverse resistance mechanisms (Imai et al., 2019). As per data from the China Antimicrobial Surveillance Network, *Klebsiella pneumoniae* is distinguished as the second most epidemiologically pertinent pathogen within Chinese tertiary hospitals (Qiao et al., 2018). It is of particular concern that the incidence of carbapenem-resistant *Klebsiella pneumoniae* (CRKP) surged dramatically, from 3.0% in 2005 to 24.2% in 2022.[1]

Klebsiella pneumoniae (cKP) is a frequent cause of infections in healthcare settings, often harboring plasmids that code for antimicrobial resistance (Pu et al., 2023). In China, the sequence type (ST) 11 carbapenem-resistant *Klebsiella pneumoniae* (CRKP) stands as the predominant strain (Liao et al., 2020). The ST11 *Klebsiella pneumoniae*, renowned as the most widespread MDR lineage in Asia (Xu et al., 2017), was initially identified as a hypervirulent strain in China (Yang et al., 2022). While hypervirulent *Klebsiella pneumoniae* (hvKp) is acknowledged as a life-threatening pathogen, it has historically exhibited fewer associations with resistance compared to classical *Klebsiella pneumoniae* strains (Choby et al., 2020). HvKP is characteristically linked with invasive community-acquired infections and often carries virulence plasmids, like the *pLVPK* plasmid, which encodes key mucoid regulators such as rmpA, aerobactin, and salmochelin (Chen et al., 2004). Notably, the recent emergence of strains that are both carbapenem-resistant and hypervirulent (CR-HvKP) has led to exceedingly high mortality infections in various nations (Xie et al., 2021). Recent observations indicate that in Chinese intensive care units (ICUs), the ST11 hypervirulent CRKp strain (hv-CRKp) has been on the rise post-colonization by carbapenem-susceptible *Klebsiella pneumoniae* (CSKp) (Yang et al., 2022). This strain demonstrates heightened transmissibility, robust resistance, and

1 https://www.chinets.com/

significant virulence, posing a grave risk to public health (Jin et al., 2021; Xie et al., 2021).

In light of the multidrug resistance displayed by CRKP isolates, colistin, or polymyxin E, has been the mainstay therapeutic intervention for the most formidable antibiotic-resistant bacterial infections, especially those attributed to carbapenem-resistant *Enterobacteriaceae* (Falagas and Kasiakou, 2005). This antimicrobial agent exhibits efficacy against an array of Gram-negative bacilli (Zhang et al., 2018). By January 2017, China had approved polymyxin for intravenous therapeutic use in bacterial infection cases (Pan et al., 2018). Disturbingly, contemporary data indicate an approximate 45% colistin resistance rate among MDR *Klebsiella pneumoniae* (Falagas and Kasiakou, 2005). Capitalizing on the breakthroughs in whole-genome sequencing, Liu pinpointed the rise of colistin-resistant and hypervirulent MDR *Klebsiella pneumoniae* (CoR-HvKp) during 2017–2018 (Liu et al., 2022). In a parallel vein, Chen's research highlighted the *in vivo* resistance emergence to colistin and tigecycline in carbapenem-resistant hypervirulent *Klebsiella pneumoniae* within China (Chen et al., 2021). Concerningly, strains resistant to polymyxin have made their presence felt on a global scale (Gharaibeh and Shatnawi, 2019).

Resistance to colistin in *Klebsiella pneumoniae* is primarily ascribed to mutations that cause dysregulation of the two-component systems (TCSs) *PmrAB*, *PhoPQ*, or *CrrAB* (Bhagirath et al., 2019). Additionally, the acquisition of a plasmid bearing the mobilized colistin resistance gene (mcr1) also confers resistance (Liu et al., 2016). Notably, while multiple TCSs contribute to lipid A modifications, mutations that nullify the functionality of the small regulatory protein *mgrB* account for colistin resistance in nearly 70% of *Klebsiella pneumoniae* strains (Jin et al., 2021; Bray et al., 2022). *mgrB* is a compact regulatory transmembrane protein, composed of 47 amino acids, that holds a pivotal function in antibiotic resistance (Bray et al., 2022). When inactivated, *mgrB* triggers an augmentation in lipid A modifications, subsequently conferring resistance to colistin (Groisman, 2001; Cheng et al., 2010). In the research spearheaded by Taher Uz Zaman et al., 23 non-replicating, colistin-resistant *Klebsiella pneumoniae* isolates were meticulously scrutinized. These isolates encompassed eight unique sequence types (STs) and predominantly manifested mutations in the *mgrB* or *PhoP* genes (Uz Zaman et al., 2018). Notably, ten isolates bore the ISKpn14 insertion sequence, while ISKpn28 and IS903 were identified in four and three isolates, respectively. It's compelling to note the distinct strain distribution in their findings compared to our own, underscoring the innovative facet of our investigation. Parallelly, a study by Stephen Mark Edward Fordham et al. revealed that specific plasmids encode mobilizable IS elements. When integrated into the *mgrB* gene of *Klebsiella pneumoniae*, these elements lead to its inactivation, paving the way for colistin resistance (Fordham et al., 2022). The team's exploration delved deep into evaluating the prevalence of *mgrB*-disruptive insertion sequences like ISL3 (ISKpn25), IS5 (ISKpn26), ISKpn14, and IS903B present on these plasmids. An intriguing find was the presence of antimicrobial resistance genes on these IS-rich plasmids, particularly those imparting resistance to carbapenems. Of these insertion sequences, ISKpn25 has garnered attention in multiple nations. In contrast, the prevalence of ISKpn26, ISKpn14, and IS903B appears to be acutely heightened in China. Under antibiotic stress, bacteria demand significant genomic modifications to introduce beneficial variations, which are beyond the scope of simple point mutations. Insertion sequences (ISs) play a pivotal role in enabling such changes. Many mutations in mgrB are mediated by these IS elements. In tandem with the presence of carbapenemase, these IS elements might amplify the drug resistance in *K. pneumoniae*, thereby constricting already limited treatment avenues. Expanding upon Bray et al.'s findings on the chromosome-mediated mechanism in CoR-HvKp isolates (Bray et al., 2022), our research accentuates the pronounced role of IS elements in facilitating colistin resistance through mgrB disruption.

2. Materials and methods

2.1. Bacterial isolates and clinical data collection

From May 2021 to April 2023, 127 distinct clinical colistin-resistant *Klebsiella pneumoniae* isolates were obtained from the First Affiliated Hospital of Nanchang University in China. Each isolate was identified using both the VITEK 2 automated system (bioMérieux, France) and the MALDI-TOF MS system (Bruker Daltonics, Billerica, MA, United States). All isolates were stored at −80°C until needed for further analysis. Antimicrobial susceptibility testing was conducted and interpreted according to the Clinical and Laboratory Standards Institute (CLSI) breakpoints (document M100-S32).

Clinical data for this study were sourced from the Electronic Medical Records of inpatients at the First Affiliated Hospital of Nanchang University. These data encompassed patient demographics, isolation dates, clinical diagnoses, specimen types, ward admissions, antimicrobial treatments, and hospitalization outcomes (Supplementary Table S2). The study's methodologies and consent procedures received approval from the Ethical Committee of the First Affiliated Hospital of Nanchang University.

2.2. Identification of antibiotic-resistance and virulence-plasmid pLVPK-borne genes

All isolates were evaluated for the presence of genes coding for plasmid-mediated mobile-resistance genes (*bla*KPC, *bla*NDM, *bla*IMP, *bla*VIM, *bla*OXA-48-like, and mcr-1 to mcr-8), chromosome-mediated two-component systems (*PhoP/Q* and *PmrA/B*), *mgrB*, and virulence plasmid *pLVPK*-borne genes (*rmpA*, *rmpA2*, *iucA*, *iroN*, and *peg344*). This assessment was executed using polymerase chain reaction (PCR) amplification, in line with previously described methodologies (Chen et al., 2021). PCR products were then visualized through agarose gel electrophoresis.

For sequence analysis of *mgrB*, the services of Sangon Biotech (Shanghai, China) were utilized. Both nucleotide and the consequent protein sequences were subsequently analyzed using the Basic Local Alignment Search Tool (blaST) program available at the National Center for Biotechnology Information website.[2] Insertion sequences (ISs) were evaluated via the IS finder website.[3]

2 www.ncbi.nlm.nih.gov

3 www-is.biotoul.fr

Of note, 20 isolates yielded an *mgrB* PCR amplicon product noticeably larger than that observed in wild-type strains (Supplementary Figure S1). To elucidate the cause of this amplified gene size, these 20 mutated *mgrB* CoR-Kp isolates were selected for further analysis (Poirel et al., 2015).

2.3. Colistin antimicrobial susceptibility testing

The minimum inhibitory concentrations (MICs) of colistin were ascertained using the broth microdilution (BMD) method, recognized as the gold-standard reference in line with the Clinical and Laboratory Standards Institute (CLSI) M100-S32 criteria. With the standard transitioning from resistance breakpoints to an intermediate categorization, susceptibility evaluations for colistin were conducted following the guidelines established by the European Committee on Antimicrobial Susceptibility Testing (EUCAST). For *Klebsiella pneumoniae*, colistin MICs were interpreted as follows: susceptibility is denoted by MIC values ≤2 mg/L, while resistance is indicated by values >2 mg/L.

2.4. Molecular analyses

2.4.1. Multilocus sequence typing and pulsed-field gel electrophoresis

MLST and PFGE were used for assessing the clonal relationship of the selected *mgrB*-mutated CoR-Kp isolates.

MLST employs seven conserved housekeeping genes: *gapA*, *infB*, *mdh*, *pgi*, *phoE*, *rpoB*, and *tonB*, as per the guidelines provided on the Pasteur Institute MLST website. The resulting amplicons were purified and dispatched to Sangon Biotech (Shanghai, China) for sequencing. The resultant sequences were then matched with those catalogued in the MLST database to establish the sequence type (ST) (Li et al., 2023).

PFGE was executed following the standardized protocol recommended by the CDC (CDC, 2013). The enzyme XbaI from TaKaRa was employed for the procedure. The generated DNA fragments were segregated using the CHEF DR III system (Bio-Rad, Richmond, CA, United States). To serve as a molecular weight standard, the *Salmonella serotype Braenderup* strain H9812 was incorporated. Following the electrophoretic separation, the generated DNA patterns were then analysed using the BioNumerics software (version 7.6). The software facilitated the construction of a dendrogram based on the unweighted Pair-Group Method with Arithmetic means (UPGMA) and employed the Dice similarity coefficient (SD). The setting allowed for a 1.5% position tolerance. For the isolates to be deemed genetically similar, it was essential for their Dice coefficient correlation to surpass 80%. This threshold was set based on the "possibly related (4–6 bands difference)" criteria as posited by Tenover et al. (1995).

2.4.2. S1-pulsed field gel electrophoresis

S1-PFGE, utilizing S1 nuclease from TaKaRa, was employed to evaluate the plasmid content of *mgrB*-mutated CoR-Kp. The separation of plasmid fragments was accomplished using the CHEF DR III system (Bio-Rad, Richmond, CA, United States), with the *Salmonella serotype Braenderup* isolate H9812 as a molecular reference.

2.5. Virulence assessment of *mgrB*-mutated CoR-Kp

2.5.1. Hyperviscous phenotype detection (string test)

The hypermucoviscous phenotype was assessed using the string test. A positive result was defined by the formation of strings ≥5 mm upon stretching with a sterile inoculation loop. For this test, *Klebsiella pneumoniae* strains NTUH-K2044 and ATCC700603 served as positive and negative controls, respectively.

2.5.2. Serum killing assay

A serum killing assay was conducted to evaluate *in vitro* virulence, adapted from the method previously described (Li et al., 2023). Serum was procured from healthy donors and preserved at −80°C. Bacterial inocula, at a concentration of 106 CFU during the mid-log phase, were exposed to 75% pooled human serum. The enumeration of viable bacteria was conducted at intervals of 0, 1, 2, and 3 h post-exposure, under conditions of 37°C and 200 rpm agitation. Each bacterial strain underwent a minimum of three independent assays. The serum susceptibility was delineated into six gradations, which were further categorized as: highly sensitive (grades 1–2), intermediately sensitive (grades 3–4), resistant (grades 5–6). Grade 1 designation implied that the viable count was <10% of the original inoculum post 1 and 2 h, and diminished to <0.1% at the 3 h mark. In contrast, grade 2 was characterized by a viable count between 10 and 100% post the 1 h interval but was less than 10% after 3 h. Grade 3 counts surpassed the initial inoculum after 1 h but remained below 100% at the subsequent 2 h and 3 h intervals. Grade 4 counts consistently exceeded the original inoculum after 1 and 2 h, but fell short of 100% after 3 h. Grade 5 counts continuously surpassed the inoculum across all time intervals, but evidenced a decrement in the third hour. Lastly, a grade 6 classification was characterized by consistently increasing viable counts across all time points. *Klebsiella pneumoniae* ATCC 700603 and hvKP strain NTUH-K2044 were utilized as benchmark controls, with serum sensitivities graded at 2 (sensitive) and 5 (resistant), respectively.

2.5.3. *Galleria mellonella* infection model

In vivo virulence was assessed using the *Galleria mellonella* infection model, a technique previously established (Tsai et al., 2016). Specifically, 10 pathogen-free *Galleria mellonella* larvae, each weighing between 250 and 350 mg (sourced from Tianjin Huiyude Biotech Company, Tianjin, China), were selected for each bacterial strain. Mid-log-phase cultures were prepared, washed, and resuspended in PBS. Each larva was then inoculated with 1 × 10^6 CFU in a 10 uLvolume, delivered to the hemocoel through the rear left proleg. Larval survival was monitored at 24 h intervals over a span of 4 days, maintaining the larvae in a dark environment at 37°C within petri dishes. These tests were replicated thrice. The LD50 value, derived from the Galleria model, serves as a marker for determining hypervirulence in *Klebsiella pneumoniae* isolates. For reference controls, the HvKP strain NTUH-K2044 represented high virulence, while PBS denoted low virulence.

3. Results

3.1. Overall prevalence of colistin-resistant *Klebsiella pneumoniae* strains in a Chinese tertiary hospital

Between May 2021 and April 2023, our hospital collected 1,921 clinical isolates of *Klebsiella pneumoniae*. Out of these, 127 (6.6%) were identified as colistin-resistant strains. Further screening via PCR amplification and sequencing identified 20 of these colistin-resistant strains as having mutations in the *mgrB* gene (Figure 1; Supplementary Figure S1).

3.2. Antimicrobial susceptibility testing for *mgrB* mutation colistin-resistant *Klebsiella pneumoniae* isolates

Antimicrobial susceptibility testing of the 20 *Klebsiella pneumoniae* isolates with *mgrB* mutations revealed universal resistance to TCC, TZP, CAZ, FEP, CSl, ATM, CIP, LVX, MNO, SXT, IPM, MEM, and COL. Additionally, 85% of the strains exhibited resistance to DOX and TOB (Figure 2). The colistin MIC values for these strains spanned a range of 16–64 μg/mL, with a median value of 40 μg/mL (Figure 2).

3.3. Demographic characteristics and molecular typing of *mgrB* mutation hypervirulent colistin-resistant *Klebsiella pneumoniae* isolates

As detailed in Supplementary Table S1, the temporal distribution of isolates was as follows: 3 in 2021, 13 in 2022, and 4 in 2023. The patients from whom these isolates were collected had a median age of 58.8 ± 14.7 years, spanning from 23 to 83 years. Males represented 55% (11/20) of the patients. The isolates originated from diverse clinical sources, such as sputum, blood, bronchoalveolar lavage fluid (BALF), pus and others. These patients were admitted across various hospital wards, including the intensive care unit (ICU), respiratory department, neurosurgery department, hematology department, gastroenterology department, rehabilitation department, and other specialized wards. Notably, half of the patients (10/20) were in the ICU. The observed mortality rate amongst this cohort was 60% (12/20), as depicted in Supplementary Table S1.

As highlighted in Figure 3, MLST analysis revealed that all *mgrB*-mutated CoR-hvKp isolates were categorized as ST11 (100%, 20/20). PFGE analysis discerned six distinct clusters among the 20 isolates, with the majority clustering within groups A and D. This clustering suggests dual genetic transmission modes for these strains: both horizontal and clonal transmission.

As depicted in Figure 4, the primary carbapenemase determinants were *bla*KPC (100%, 20/20) and *bla*NDM (60%, 12/20). None of the isolates tested positive for the OXA-48, VIM, or IMP genes. Supplementary Table S1 provides a comprehensive breakdown of the distribution of resistance genes, virulence factors, and sequence types (STs) among the isolates.

All isolates carried the pLVPK virulence plasmid, with distributions as follows: *rmpA* (45%, 9/20), *rmpA2* (95%, 19/20), *iroN* (95%, 19/20), *iucA* (85%, 17/20), and *peg344* (40%, 8/20). Notably, none of the isolates tested positive for the *PhoQ/PhoP* and *pmrA/B* genes. Furthermore, five isolates harbored both the mutated *mgrB* gene and a mcr positive gene, specifically *mcr-1* (2/20), *mcr-7* (1/20), and *mcr-8* (4/20).

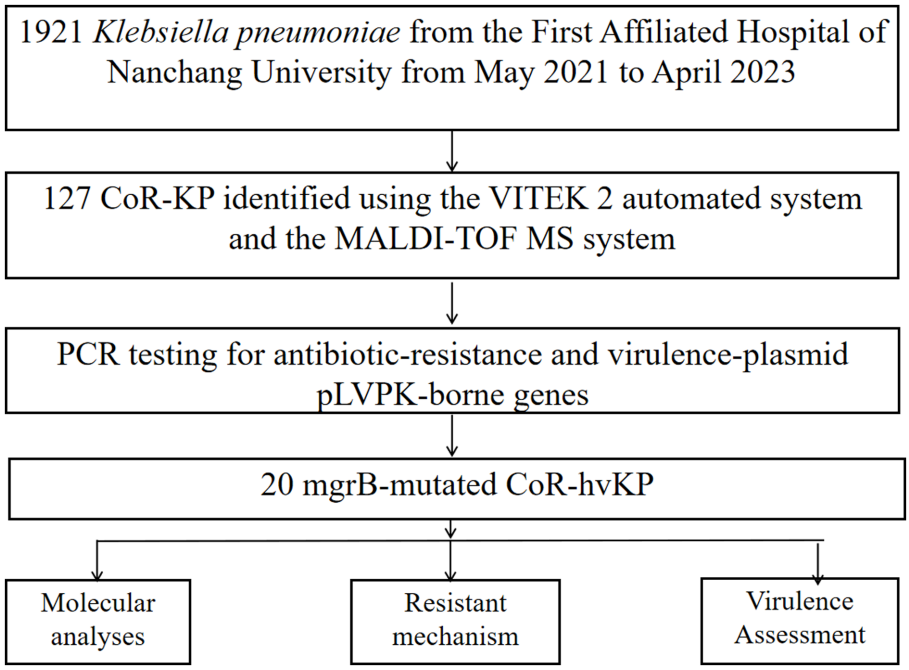

FIGURE 1
Flowchart illustrating the step-by-step methodology employed in the study.

Antimicrobial susceptibility results for selected strains																
	Antimicrobial susceptibility result(MICs,mg/L)															
Isolates No.	Isolates date	VITEK-2 system														Broth dilution
		TCC	TZP	CAZ	FEP	CSL	ATM	IPM	MEM	CIP	LVX	DOX	MNO	TOB	SXT	COL
CoR-KP21	2021/8/27	≥128	≥128	≥64	≥32	≥64	≥64	≥16	≥16	≥4	≥8	≥16	≥16	≥16	≥320	16
CoR-KP24	2021/9/14	≥128	≥128	≥64	≥32	≥64	≥64	≥16	≥16	≥4	≥8	≥16	≥16	≥16	≥320	32
CoR-KP31	2021/12/5	≥128	≥128	≥64	≥32	≥64	≥64	≥16	≥16	≥4	≥8	≥16	≥16	≥16	≥320	32
CoR-KP35	2022/1/31	≥128	≥128	≥64	≥32	≥64	≥64	≥16	≥16	≥4	≥8	≥16	≥16	≥16	≥320	32
CoR-KP36	2022/2/7	≥128	≥128	≥64	≥32	≥64	≥64	≥16	≥16	≥4	≥8	≥16	≥16	≥16	≥320	32
CoR-KP37	2022/2/9	≥128	≥128	≥64	≥32	≥64	≥64	≥16	≥16	≥4	≥8	≥16	≥16	≥16	≥320	16
CoR-KP49	2022/3/20	≥128	≥128	≥64	≥32	≥64	≥64	≥16	≥16	≥4	≥8	≥16	≥16	≥16	≥320	64
CoR-KP50	2022/3/21	≥128	≥128	≥64	≥32	≥64	≥64	≥16	≥16	≥4	≥8	≥16	≥16	≤1	≥320	16
CoR-KP57	2022/4/1	≥128	≥128	≥64	≥32	≥64	≥64	≥16	≥16	≥4	≥8	≤8	≥16	≤1	160	32
CoR-KP59	2022/4/2	≥128	≥128	≥64	≥32	≥64	≥64	≥16	≥16	≥4	≥8	≥16	≥16	≥16	≥320	64
CoR-KP61	2022/4/13	≥128	≥128	≥64	≥32	≥64	≥64	≥16	≥16	≥4	≥8	≥16	≥16	≥16	≥320	16
CoR-KP62	2022/4/15	≥128	≥128	≥64	≥32	≥64	≥64	≥16	≥16	≥4	≥8	≥16	≥16	≥16	≥320	32
CoR-KP64	2022/4/20	≥128	≥128	≥64	≥32	≥64	≥64	≥16	≥16	≥4	≥8	≥16	≥16	≥16	≥320	32
CoR-KP66	2022/4/26	≥128	≥128	≥64	≥32	≥64	≥64	≥16	≥16	≥4	≥8	≤8	≥16	≤1	<=20	64
CoR-KP83	2022/8/8	≥128	≥128	≥64	≥32	≥64	≥64	≥16	≥16	≥4	≥8	≥16	≥16	≥16	≥320	64
CoR-KP90	2022/10/7	≥128	≥128	≥64	≥32	≥64	≥64	≥16	≥16	≥4	≥8	≥16	≥16	≥16	≥320	64
CoR-KP97	2023/1/4	≥128	≥128	≥64	≥32	≥64	≥64	≥16	≥16	≥4	≥8	≥16	≥16	≥16	≥320	32
CoR-KP119	2023/3/10	≥128	≥128	≥64	≥32	≥64	≥64	≥16	≥16	≥4	≥8	≤8	≥16	≤1	<=20	64
CoR-KP122	2023/3/18	≥128	≥128	≥64	≥32	≥64	≥64	≥16	≥16	≥4	≥8	≥16	≥16	≥16	≥320	64
CoR-KP125	2023/3/28	≥128	≥128	≥64	≥32	≥64	≥64	≥16	≥16	≥4	≥8	≥16	≥16	≥16	≥320	32

FIGURE 2
Antibiotic susceptibility profiles for the 20 *mgrB*-mutated CoR-Kp isolates. TCC, Ticarcillin; TZP, Piperacillin/Tazobactam; CAZ, Ceftazidime; FEP, Cefepime; CSL, Cefoperazone/Sulbactam; ATM, Aztreonam; IPM, imipenem; MEM, meropenem; CIP, Ciprofloxacin; LVX, Levofloxacin; DOX, Doxycycline; MNO, Minocycline; TOB, Tobramycin; SXT, Trimethoprim/Sulfamethoxazole; COL, colistin; Red, resistant; Green, susceptible.

3.4. Virulence analysis of *mgrB* mutation hypervirulent colistin-resistant *Klebsiella pneumoniae* isolates

As illustrated in Figure 4, all the *mgrB* mutative CoR-hvKP isolates were found to harbor at least two virulence genes situated on a *pLVPK*-like virulence plasmid, including the *iroN*, *iucA*, *peg-344*, *rmpA*, and *rmpA2* genes. Both the string test and biofilm formation assays yielded positive results for these isolates, signifying their virulence potential. Capsular serotyping identified 16 isolates as K64 and 4 as K20, with no detection of K1 and K2 types (Figure 3). Interestingly, the K64 serotype is noted as the most prevalent among *KPC*-2-producing *Klebsiella pneumoniae* in China.

These results underline the isolates' hypervirulent nature, evidenced by the presence of hypermucoviscosity and plasmid-borne genes akin to *pLVPK*. *In vitro* assessments corroborated this observation, with the strains displaying marked serum resistance; the survival rate was approximately 95% following a 60 min incubation with serum (Figure 4).

Further validation of the hypervirulent phenotype in all these CoR-hvKP was obtained through the *Galleria mellonella* infection model. As depicted in Figure 4, when a 10^6 CFU suspension of the isolates was used to infect *Galleria mellonella* larvae, all isolates exhibited a survival rate of fewer than 48 h. This pattern was akin to the virulent strain NTUH-K2044, emphasizing the notable virulence attributes of these CoR-hvKP isolates.

3.5. Iskpn element as a key target for inactivation/mutation of the *mgrB* in CoR-HvKp

The *mgrB* gene was PCR-amplified in 127 CoR-Kp isolates. Subsequent sequence analysis revealed that 20 isolates produced a larger amplicon relative to a wild-type isolate (Supplementary Figure S1). Three distinct elements from two IS families were identified, either within the open reading frame (ORF) or the promoter of the *mgrB* gene. Of the 127 isolates, 11 carried ISKpn26, four harbored ISKpn14, and five contained IS903B within their *mgrB* gene. The orientation and insertion site varied, as illustrated in Figure 5.

In the eleven isolates with ISKpn26, nine had insertions at position +74, one at +125, and one at −35 (promoter region, upstream of the start codon) (Figures 5A–C). Among the four isolates with ISKpn14, one showed insertion at +93, one at −35, and two at −60 (promoter region, upstream of the start codon) (Figures 5D–F). Of the five isolates with IS903B, two had insertions at +74, one each at +125, +116, and −35 (promoter region, upstream of the start codon) (Figures 5G–I). The left and right inverted repeats (IRs) were delineated, with the sequences as follows: ISKpn26 IRL: GGAAGGTGCGAACAAGTTCCTGATATGAGATCATCATATTCA TCCGGAGC, IRR: GGAAAGTGCGAATAAGCAGGTCATTTC TTCCCAAGCTGACTCGTTGATTA; ISKpn14 IRL: GGTGATGCTA CCAACTTGCTGATTTAGTGTATAATGGTGTTTTTGAGGTG, IRR: GGTAATGACTCCAATTTACTGATAGTGTTTTATGTTCAG ATAGTGCCCGA; IS903B IRL: GGCTTTGTTGAATAAA

10.3389/fmicb.2023.1277320

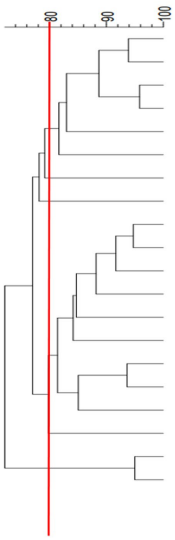

Isolation	MLST	Serotype	PFGE cluster	Transposon	Family	Identity (%)	alignment length(bp)	orientation of insertion	The site of insertion	mgrB gene
CoR-KP125	11	K64	A	ISKpn26	IS5	99	1196	opposite	+74	mutation
CoR-KP50	11	K64	A	ISKpn26	IS5	100	1196	opposite	+74	mutation
CoR-KP24	11	K64	A	ISKpn26	IS5	99	1196	opposite	+74	mutation
CoR-KP62	11	K64	A	ISKpn26	IS5	99	1196	opposite	-35	inactivation
CoR-KP36	11	K64	A	ISKpn26	IS5	99	1196	opposite	+74	mutation
CoR-KP37	11	K64	A	ISKpn26	IS5	99	1196	opposite	+74	mutation
CoR-KP119	11	K64	B	ISKpn14	IS1	100	768	opposite	144	inactivation
CoR-KP21	11	K64	C	ISKpn26	IS5	99	1196	opposite	+74	mutation
CoR-KP97	11	K64	D	ISKpn26	IS5	100	1196	opposite	+125	mutation
CoR-KP61	11	K64	D	ISKpn26	IS5	99	1196	opposite	+74	mutation
CoR-KP122	11	K64	D	ISKpn26	IS5	99	1196	opposite	+74	mutation
CoR-KP35	11	K20	D	IS903B	IS5	97.15	1054	same	+116	mutation
CoR-KP83	11	K64	D	IS903B	IS5	97.15	1054	same	-35	inactivation
CoR-KP57	11	K64	D	IS903B	IS5	97.15	1054	opposite	+74	mutation
CoR-KP90	11	K64	D	ISKpn14	IS1	100	768	opposite	+93	mutation
CoR-KP125	11	K20	D	IS903B	IS5	97.15	1054	opposite	+126	mutation
CoR-KP49	11	K20	D	IS903B	IS5	97.15	1054	opposite	+74	mutation
CoR-KP31	11	K64	E	ISKpn26	IS5	99	1196	opposite	+74	mutation
CoR-KP66	11	K20	F	ISKpn14	IS1	100	768	opposite	-60	inactivation
CoR-KP59	11	K64	F	ISKpn14	IS1	100	768	opposite	-60	inactivation

FIGURE 3
PFGE typing of the 20 *mgrB*-mutated CoR-Kp isolates. Genomic DNA from each research strain was digested with Xba I. The digests were then subjected to PFGE, producing diagnostic genomic DNA fragmentation fingerprints. The dendrogram representing the PFGE profiles was clustered using UPGAMA based on Dice similarity, analyzed with the bionumerics software. The red line marks the 80% similarity boundary.

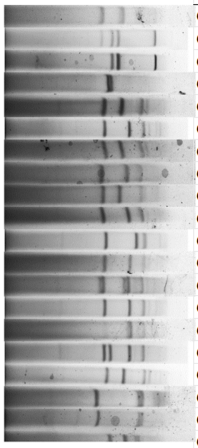

Isolation	Carbapenemase gene	mcr gene	Virulence gene	Biofilm formation (OD590nm)	Serum resistance test	Galleria mellonella
CoR-KP90	KPC,NDM	NA	mpA2,iroN,iucA	positive	6 level	High toxic
CoR-KP66	KPC,NDM	mcr-1,mcr-7,mcr-8	mpA2,iroN,iucA	positive	2 level	High toxic
CoR-KP59	KPC	mcr-1	mpA2,iroN	positive	4 level	High toxic
CoR-KP83	KPC,NDM	mcr-8	mpA2,iroN,iucA	positive	2 level	High toxic
CoR-KP35	KPC	NA	mpA2,iroN,iucA	positive	1 level	High toxic
CoR-KP62	KPC,NDM	NA	mpA,rmpA2,iroN,iucA,peg-344	positive	1 level	High toxic
CoR-KP31	KPC,NDM	NA	mpA2,iroN,iucA	positive	2 level	High toxic
CoR-KP125	KPC,NDM	NA	mpA2,iroN,iucA	positive	2 level	High toxic
CoR-KP97	KPC	NA	mpA2,iroN,iucA	positive	2 level	High toxic
CoR-KP21	KPC,NDM	NA	mpA,rmpA2,iroN,iucA,peg-344	positive	5 level	High toxic
CoR-KP122	KPC,NDM	NA	mpA2,iroN,iucA	positive	1 level	High toxic
CoR-KP24	KPC,NDM	NA	mpA,rmpA2,iroN,iucA,peg-344	positive	1 level	High toxic
CoR-KP49	KPC	mcr-8	mpA,rmpA2,iucA	positive	5 level	High toxic
CoR-KP36	KPC,NDM	mcr-8	mpA,rmpA2,iroN,iucA,peg-344	positive	4 level	High toxic
CoR-KP119	KPC,NDM	NA	mpA,rmpA2,iroN,iucA,peg-344	positive	2 level	High toxic
CoR-KP125	KPC,NDM	NA	mpA2,iroN,iucA	positive	5 level	High toxic
CoR-KP37	KPC	NA	mpA,rmpA2,iroN,iucA,peg-344	positive	1 level	High toxic
CoR-KP50	KPC	NA	mpA,rmpA2,iroN,iucA,peg-344	positive	4 level	High toxic
CoR-KP57	KPC	NA	mpA2,iroN	positive	1 level	High toxic
CoR-KP61	KPC	NA	mpA,iroN,peg-344	positive	5 level	High toxic

FIGURE 4
S1-PFGE typing of the 20 *mgrB*-mutated CoR-Kp isolates. Genomic DNA from each research strain was digested with S1, and the resultant DNA fragments were separated using a CHEF DR III apparatus.

TCGAACTTTTGCTGAGTTGAAGGATCAGATCACG, IRR: GGCTTTGTTGAATAAATCAGATTTCGGGTAAGTCTCCCCCG TAGCGGGTT (Figures 5A,D,G). The direct repeat (DR) sequences were: ISKpn26 DR: TTAA; ISKpn14 DR: GGCTGCCTG; IS903B DR: CTCAGATGC (Figures 5A,D,G). Further details on transposons identified in the 20 mgrB-mutated CoR-HvKp isolates using ISfinder are provided in Supplementary Table S3. No mutations were detected in other components of the signaling system, such as the *PhoP/Q* and *PmrA/B* compartments.

4. Discussion

Colistin and tigecycline represent some of the limited therapeutic options available for infections caused by carbapenem-resistant Enterobacteriaceae (CRE) (Gharaibeh and Shatnawi, 2019). Alarmingly, the prevalence of carbapenem-resistant hypervirulent *Klebsiella pneumoniae* (CR-hvKP) in China is higher than previously anticipated (Yang et al., 2022). This increased prevalence raises concerns about the potential acquisition of resistance to colistin,

10.3389/fmicb.2023.1277320

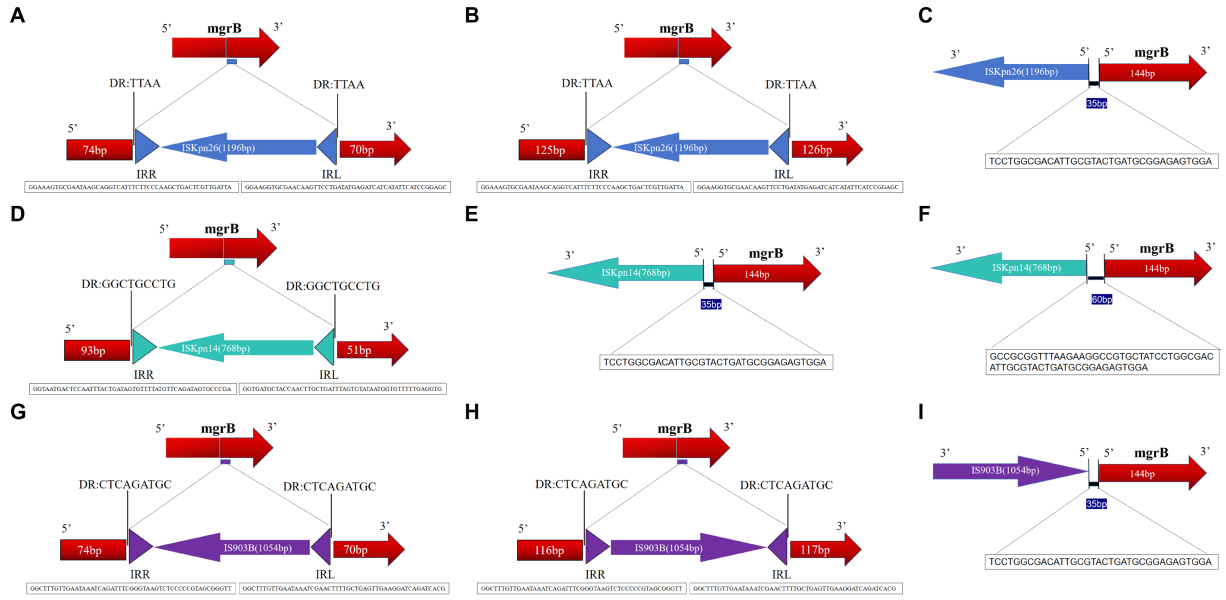

FIGURE 5
Schematic depiction of distinct insertion events observed within the *mgrB* gene. The left and right inverted repeats corresponding to each IS are denoted as IRR and IRL, respectively. (1) For the 11 isolates featuring the ISKpn26 insertion: nine exhibited insertions at position +74 **(A)**; one had an insertion at +125 **(B)**; one displayed an insertion at −35, located in the promoter region upstream of the start codon **(C)**. (2) Among the four isolates with the ISKpn14 insertion: one demonstrated an insertion at +93 **(D)**; one had its insertion at −35 **(E)**; two revealed insertions at −60, situated in the promoter region upstream of the start codon **(F)**. (3) For the five isolates bearing the IS903B insertion: two presented insertions at +74 **(G)**; one showed insertions each at positions +125 **(H)**, +116 **(I)**, and −35 (located in the promoter region upstream of the start codon).

tigecycline, and ceftazidime/avibactam in CR-hvKP, potentially leading to severe clinical consequences (Liao et al., 2020). To counteract this emerging trend, it is imperative to manage and judiciously apply antibiotics.

In this study, we provide insights into the molecular mechanisms governing colistin resistance in ST11 hypervirulent *Klebsiella pneumoniae*. Utilizing MLST and PFGE analyses, we discerned two predominant genetic transmission modes among these strains: clonal and horizontal. Intriguingly, among the *mgrB*-mutated CoR-HvKp isolates, five tested positive for the plasmid-borne mcr gene. This finding underscores the convergence of both chromosomal and plasmid-mediated resistance strategies. Our observations are consistent with the recent work of Zhang et al. (2018). A salient point from our findings is that, in comparison to *mgrB* mutations (75%, 15/20), the inactivation of *mgrB* (25%, 5/20) manifested a pronounced increase in colistin resistance, in tandem with augmented virulence.

Previous literature has established that the *mgrB* gene alterations are prevalent mechanisms attributing to colistin resistance in *Klebsiella pneumoniae* (Zhang et al., 2018; Bray et al., 2022). In a comprehensive study by Stephen and colleagues, it was elucidated that certain plasmids encode for mobilizable IS elements. These elements, when integrated into the *mgrB* gene of *Klebsiella pneumoniae*, result in the gene's inactivation, thereby leading to colistin resistance. The research delved into assessing the prevalence of specific *mgrB*-gene disruptive insertion elements, namely ISL3 (ISKpn25), IS5 (ISKpn26), ISKpn14, and IS903B, present on these plasmids. Additionally, these plasmids containing IS elements underwent an extensive analysis to identify antimicrobial resistance genes, with a keen focus on those that confer resistance to carbapenems. Notably, while ISKpn25 is widespread and found in numerous countries, the occurrences of ISKpn26, ISKpn14, and IS903B are particularly pronounced in China (Fordham et al., 2022). The IS5-like insertion element is predominantly implicated in *mgrB* disruption in this bacterium (Poirel et al., 2015). In our cohort, we discerned that 80% of the IS elements (namely ISKpn26 and IS903B) are members of the IS5 family, while the remaining 20% (ISKpn14) affiliate with the IS1 family (Supplementary Table S2). It's worth noting that ISKpn26 displays 99% amino acid similarity to IS5, but this similarity diminishes to 91% at the DNA level. IS903B, another member of the IS5 family, diverges from both IS903 and IS102 by 34 and 61 nucleotides, respectively. Historically, IS903, an IS5 family member, has been implicated in antibiotic resistance, functioning either as a resistance gene carrier or as an agent modifying antibiotic targets.

Among the isolates, eleven with ISKpn26 insertion were grouped into four distinct PFGE clusters (A, C, D, E). Notably, all isolates in the PFGE cluster A exhibited ISKpn26 insertion. Meanwhile, the four isolates with ISKpn14 insertion were categorized into three PFGE clusters (B, D, F). These findings suggest that ISKpn26 and ISKpn14 potentially employ dual genetic transmission modes: horizontal and clonal. Contrarily, IS903B may represent a single clonal expansion, as all five isolates with this insertion aligned with the single PFGE cluster D.

The mutations in mgrB were mostly mediated by insertion elements (IS). Interestingly, isolates carrying either of the two insertion elements (IS903B and ISKpn14) were found to harbor more mcr genes. This finding indicates that the colistin resistance mechanism in these strains (IS903B and ISKpn14) involves both chromosomal and plasmid-mediated factors. In a parallel study conducted by Taher Uz

Zaman and his team, 23 non-replicating colistin-resistant *Klebsiella pneumoniae* isolates from Europe were investigated. These isolates spanned eight distinct sequence types (STs) and exhibited mutations primarily in either the *mgrB* or *PhoP* genes. Notably, ISKpn14 was detected in 10 of the isolates, ISKpn28 in four, and IS903 in three. A striking observation was the different strain distribution when compared to our findings, highlighting the innovative aspect of our research (Taher Uz Zaman et al., 2018). The orientation and insertion sites exhibited variability, as demonstrated in Figure 5. Despite the IS element being inserted across seven distinct locations within the *mgrB* gene, the +74 site emerges as a preferential insertion hotspot. Furthermore, 11 isolates from the IS-5 family (ISKpn26 and IS903B) shared the same integration site (+74) within the *mgrB* gene but fell into disparate PFGE clusters. This pattern insinuates a probable recombination event at this chromosomal location. Further investigations are warranted to explore the spacers potentially triggering the translocation of these elements from plasmids to the chromosome, a shift that could metamorphose the multi-drug-resistant pathogen into a pan-drug-resistant entity.

The key discovery of this study is the prevalent role of the ISKpn element in the inactivation or mutation of the *mgrB* gene in ST11 hypervirulent colistin-resistant *Klebsiella pneumoniae*. Remarkably, all the isolates in this study exhibited hypervirulent characteristics. Our data reveals that ST11 Hypervirulent *Klebsiella pneumoniae* is the most common strain circulating in our hospital, yet the isolates carrying the IS element in this study date from 2021, pinpointing the insertion as a recent phenomenon. Hypervirulent colistin-resistant *Klebsiella pneumoniae* with *mgrB* mutations have recently been reported in various regions globally, signaling the emergence of an endemic ColR clone (Dong et al., 2018; Bolourchi et al., 2021; Chen et al., 2021; Liu et al., 2022).

Another pivotal observation from our study is the pronounced prevalence of carbapenemase genes, notably *bla*KPC (present in 100%, 20/20 of the samples) and *bla*NDM (in 55%, 11/20), within the ST11 hypervirulent colistin-resistant *Klebsiella pneumoniae*. This suggests the IS element might have a contributory role in mediating resistance, extending beyond colistin to encompass carbapenems. This aligns with prior research on tigecycline resistance in *Klebsiella pneumoniae*, where the IS5 element is integrated into the promoter region of the putative efflux pump operon, kpgABC (Schnetz and Rak, 1992; Zhang and Saier, 2009). There's a pressing need for further studies to elucidate the mechanisms-specifically the spacers-prompting these elements' transfer from plasmids to the chromosome. Such a shift has the potential to escalate a multi-drug-resistant pathogen to a pan-drug-resistant phenotype (Lv et al., 2020; Sun et al., 2020).

Single nucleotide deletions leading to frame shifts and subsequent premature stop codons have been extensively documented in colistin resistance among *Klebsiella pneumoniae* and other bacterial species (Dong et al., 2018; Lv et al., 2020). In our study, we observed disruptions in the *mgrB* gene by IS elements. Such disruptions shortened the CDS region of the *mgrB* gene to less than 144 bases, causing a frame shift. Despite the limited number of isolates examined, our findings resonate with the hypothesis that, under stressors like antibiotic exposure, bacteria may necessitate significant genomic structural modifications to introduce vital adaptive variations. Such modifications could be beyond the reach of mere point mutations, making IS elements a more effective mechanism for these changes (Schnetz and Rak, 1992; Poirel et al., 2015; Dong et al., 2018).

5. Conclusion

Our research highlights the critical role of the ISKpn element in the mutation of the *mgrB* gene in ST11 hypervirulent colistin-resistant *Klebsiella pneumoniae*. Through MLST and PFGE analyses, we delineated two principal genetic transmission methods, clonal and horizontal. Notably, all the studied isolates harbored the *bla*KPC carbapenemase gene, while 55% also presented the *bla*NDM gene. The extensive insertion points observed within the *mgrB* gene exemplify its inherent adaptability. Particularly dominant were the IS5-like elements, ISKpn26 and IS903B. These findings illuminate the increasing significance of IS elements in antibiotic resistance, especially via *mgrB* disruption. The adaptability of the *mgrB* gene underscores bacterial evolutionary dynamics, emphasizing the pressing need for advanced strategies to address these evolving resistance mechanisms, given the challenges they introduce to existing therapeutic approaches.

Data availability statement

The original contributions presented in the study are included in the article/Supplementary material, further inquiries can be directed to the corresponding authors.

Author contributions

LZ: Investigation, Methodology, Writing – original draft. PL: Investigation, Methodology, Writing – original draft. GZ: Formal analysis, Writing – original draft. ZH: Formal analysis, Writing – original draft. XT: Formal analysis, Writing – original draft. YJ: Writing – original draft. WY: Writing – original draft. XZ: Writing – original draft. LW: Formal analysis, Writing – original draft. WL: Writing – original draft. CC: Writing – original draft. YL: Conceptualization, Writing – review & editing. WZ: Conceptualization, Writing – review & editing.

Funding

The author(s) declare financial support was received for the research, authorship, and/or publication of this article. This study received financial support from the National Natural Science Foundation of China (Grants: 82260403 and 82102411). Support was also provided by the Natural Science Foundation of Jiangxi Province (Grants: 20224BAB216084, 20232BAB206003, and 2018BBG78021), the Jiangxi Province Double Thousand Plan Scientific and Technological Innovation High-end Talent Project (Grant: jsxq2019201102), the Natural Science Foundation of Jiangxi Province (Grant: 20202BAB206002), and Jiangxi Provincial Administration of Traditional Chinese Medicine Science and Technology Plan (Grant: 2020A0382). Additional funding was secured from the first affiliated hospital of Nanchang University Young Talents Scientific Research Breeding Fund (Grant: YFYPY202114).

Conflict of interest

The authors declare that the research was conducted in the absence of any commercial or financial relationships that could be construed as a potential conflict of interest.

Publisher's note

All claims expressed in this article are solely those of the authors and do not necessarily represent those of their affiliated organizations, or those of the publisher, the editors and the reviewers. Any product that may be evaluated in this article, or claim that may be made by its manufacturer, is not guaranteed or endorsed by the publisher.

Supplementary material

The Supplementary material for this article can be found online at: https://www.frontiersin.org/articles/10.3389/fmicb.2023.1277320/full#supplementary-material

References

Bhagirath, A. Y., Li, Y., Patidar, R., Yerex, K., Ma, X., Kumar, A., et al. (2019). Two component regulatory systems and antibiotic resistance in gram-negative pathogens. *Int. J. Mol. Sci.* 20:71781. doi: 10.3390/ijms20071781

Bolourchi, N., Shahcheraghi, F., Giske, C. G., Nematzadeh, S., Noori Goodarzi, N., Solgi, H., et al. (2021). Comparative genome analysis of colistin-resistant OXA-48-producing Klebsiella pneumoniae clinical strains isolated from two Iranian hospitals. *Ann. Clin. Microbiol. Antimicrob.* 20:74. doi: 10.1186/s12941-021-00479-y

Bray, A. S., Smith, R. D., Hudson, A. W., Hernandez, G. E., Young, T. M., George, H. E., et al. (2022). Mgr B-dependent Colistin resistance in Klebsiella pneumoniae is associated with an increase in host-to-host transmission. *mBio* 13:e0359521. doi: 10.1128/mbio.03595-21

CDC. (2013). *Standard Operating Procedure for PulseNet PFGE of Vibrio cholera and Vibrio parahaemolyticus*. Available at: https://www.cdc.gov/pulsenet/PDF/vibrio_pfge_protocol-508c.pdf

Chen, Y. T., Chang, H. Y., Lai, Y. C., Pan, C. C., Tsai, S. F., and Peng, H. L. (2004). Sequencing and analysis of the large virulence plasmid pLVPK of Klebsiella pneumoniae CG43. *Gene* 337, 189–198. doi: 10.1016/j.gene.2004.05.008

Chen, J., Zeng, Y., Zhang, R., and Cai, J. (2021). In vivo emergence of colistin and tigecycline resistance in carbapenem-resistant hypervirulent Klebsiella pneumoniae during antibiotics treatment. *Front. Microbiol.* 12:702956. doi: 10.3389/fmicb.2021.702956

Cheng, H. Y., Chen, Y. F., and Peng, H. L. (2010). Molecular characterization of the pho PQ-PmrD-PmrAB mediated pathway regulating polymyxin B resistance in Klebsiella pneumoniae CG43. *J. Biomed. Sci.* 17:60. doi: 10.1186/1423-0127-17-60

Choby, J. E., Howard-Anderson, J., and Weiss, D. S. (2020). Hypervirulent Klebsiella pneumoniae – clinical and molecular perspectives. *J. Intern. Med.* 287, 283–300. doi: 10.1111/joim.13007

Dong, N., Yang, X., Zhang, R., Chan, E. W., and Chen, S. (2018). Tracking microevolution events among ST11 carbapenemase-producing hypervirulent Klebsiella pneumoniae outbreak strains. *Emerg Microbes Infect.* 7:146. doi: 10.1038/s41426-018-0146-6

Falagas, M. E., and Kasiakou, S. K. (2005). Colistin: the revival of polymyxins for the management of multidrug-resistant gram-negative bacterial infections. *Clin. Infect. Dis.* 40, 1333–1341. doi: 10.1086/429323

Fordham, SME, Mantzouratou, A, and Sheridan, E. (2022). Prevalence of insertion sequence elements in plasmids relating to mgrB gene disruption causing colistin resistance in Klebsiella pneumoniae. *Microbiologyopen.* 11:e1262. doi: 10.1002/mbo3.1262

Gharaibeh, M. H., and Shatnawi, S. Q. (2019). An overview of colistin resistance, mobilized colistin resistance genes dissemination, global responses, and the alternatives to colistin: a review. *Vet World.* 12, 1735–1746. doi: 10.14202/vetworld.2019.1735-1746

Groisman, E. A. (2001). The pleiotropic two-component regulatory system pho P-PhoQ. *J. Bacteriol.* 183, 1835–1842. doi: 10.1128/jb.183.6.1835-1842.2001

Imai, Y., Meyer, K. J., Iinishi, A., Favre-Godal, Q., Green, R., Manuse, S., et al. (2019). A new antibiotic selectively kills gram-negative pathogens. *Nature* 576, 459–464. doi: 10.1038/s41586-019-1791-1

Jean, S. S., Harnod, D., and Hsueh, P. R. (2022). Global threat of carbapenem-resistant gram-negative bacteria. *Front. Cell. Infect. Microbiol.* 12:823684. doi: 10.3389/fcimb.2022.823684

Jin, X., Chen, Q., Shen, F., Jiang, Y., Wu, X., Hua, X., et al. (2021). Resistance evolution of hypervirulent carbapenem-resistant Klebsiella pneumoniae ST11 during treatment with tigecycline and polymyxin. *Emerg Microbes Infect.* 10, 1129–1136. doi: 10.1080/22221751.2021.1937327

Li, P., Luo, W. Y., Xiang, T. X., Peng, T. X., Luo, S., He, Z. Y., et al. (2023). Isolation of Hv-CRKP with co-production of three carbapenemases (Bla (KPC), Bla (OXA-181) or (OXA-232), and Bla (NDM-1)) and a virulence plasmid: a study from a Chinese tertiary hospital. *Front. Microbiol.* 14:1182870. doi: 10.3389/fmicb.2023.1182870

Liao, W., Liu, Y., and Zhang, W. (2020). Virulence evolution, molecular mechanisms of resistance and prevalence of ST11 carbapenem-resistant Klebsiella pneumoniae in China: a review over the last 10 years. *J. Glob. Antimicrob. Resist.* 23, 174–180. doi: 10.1016/j.jgar.2020.09.004

Liu, Y. Y., Wang, Y., Walsh, T. R., Yi, L. X., Zhang, R., Spencer, J., et al. (2016). Emergence of plasmid-mediated colistin resistance mechanism MCR-1 in animals and human beings in China: a microbiological and molecular biological study. *Lancet Infect. Dis.* 16, 161–168. doi: 10.1016/s1473-3099(15)00424-7

Liu, X., Wu, Y., Zhu, Y., Jia, P., Li, X., Jia, X., et al. (2022). Emergence of colistin-resistant hypervirulent Klebsiella pneumoniae (CoR-HvKp) in China. *Emerg. Microbes Infect.* 11, 648–661. doi: 10.1080/22221751.2022.2036078

Lv, L., Wan, M., Wang, C., Gao, X., Yang, Q., Partridge, S. R., et al. (2020). Emergence of a plasmid-encoded resistance-nodulation-division efflux pump conferring resistance to multiple drugs, including Tigecycline, in Klebsiella pneumoniae. *MBio* 11:19. doi: 10.1128/mBio.02930-19

Nordmann, P., and Poirel, L. (2019). Epidemiology and diagnostics of carbapenem resistance in gram-negative bacteria. *Clin. Infect. Dis.* 69, S521–S528. doi: 10.1093/cid/ciz824

Pan, S., Huang, X., Wang, Y., Li, L., Zhao, C., Yao, Z., et al. (2018). Efficacy of intravenous plus intrathecal/intracerebral ventricle injection of polymyxin B for post-neurosurgical intracranial infections due to MDR/XDR acinectobacter baumannii: a retrospective cohort study. *Antimicrob. Resist. Infect. Control* 7:8. doi: 10.1186/s13756-018-0305-5

Poirel, L., Jayol, A., Bontron, S., Villegas, M. V., Ozdamar, M., Turkoglu, S., et al. (2015). The mgr B gene as a key target for acquired resistance to colistin in Klebsiella pneumoniae. *J. Antimicrob. Chemother.* 70, 75–80. doi: 10.1093/jac/dku323

Pu, D., Zhao, J., Lu, B., Zhang, Y., Wu, Y., Li, Z., et al. (2023). Within-host resistance evolution of a fatal ST11 hypervirulent carbapenem-resistant Klebsiella pneumoniae. *Int. J. Antimicrob. Agents* 61:106747. doi: 10.1016/j.ijantimicag.2023.106747

Qiao, M., Ying, G. G., Singer, A. C., and Zhu, Y. G. (2018). Review of antibiotic resistance in China and its environment. *Environ. Int.* 110, 160–172. doi: 10.1016/j.envint.2017.10.016

Schnetz, K., and Rak, B. (1992). IS5: a mobile enhancer of transcription in Escherichia coli. *Proc. Natl Acad. Sci. U. S. A* 89, 1244–1248. doi: 10.1073/pnas.89.4.1244

Sun, S., Gao, H., Liu, Y., Jin, L., Wang, R., Wang, X., et al. (2020). Co-existence of a novel plasmid-mediated efflux pump with colistin resistance gene MCR in one plasmid confers transferable multidrug resistance in Klebsiella pneumoniae. *Emerg. Microbes Infect.* 9, 1102–1113. doi: 10.1080/22221751.2020.1768805

Tenover, F. C., Arbeit, R. D., Goering, R. V., Mickelsen, P. A., Murray, B. E., Persing, D. H., et al. (1995). Interpreting chromosomal DNA restriction patterns produced by pulsed-field gel electrophoresis: criteria for bacterial strain typing. *J. Clin. Microbiol.* 33, 2233–2239. doi: 10.1128/jcm.33.9.2233-2239.1995

Tsai, C. J., Loh, J. M., and Proft, T. (2016). Galleria mellonella infection models for the study of bacterial diseases and for antimicrobial drug testing. *Virulence* 7, 214–229. doi: 10.1080/21505594.2015.1135289

Uz Zaman, T, Albladi, M, Siddique, MI, Aljohani, SM, and Balkhy, HH. (2018). Insertion element mediated mgrB disruption and presence of ISKpn28 in colistin-resistant Klebsiella pneumoniae isolates from Saudi Arabia. *Infect Drug Resist.* 11, 1183–1187. doi: 10.2147/IDR.S161146

Xie, M., Yang, X., Xu, Q., Ye, L., Chen, K., Zheng, Z., et al. (2021). Clinical evolution of ST11 carbapenem resistant and hypervirulent Klebsiella pneumoniae. *Commun. Biol.* 4:650. doi: 10.1038/s42003-021-02148-4

Xu, L., Sun, X., and Ma, X. (2017). Systematic review and meta-analysis of mortality of patients infected with carbapenem-resistant Klebsiella pneumoniae. *Ann. Clin. Microbiol. Antimicrob.* 16:18. doi: 10.1186/s12941-017-0191-3

Yang, X., Sun, Q., Li, J., Jiang, Y., Li, Y., Lin, J., et al. (2022). Molecular epidemiology of carbapenem-resistant hypervirulent Klebsiella pneumoniae in China. *Emerg Microbes Infect.* 11, 841–849. doi: 10.1080/22221751.2022.2049458

Zhang, R., Dong, N., Huang, Y., Zhou, H., Xie, M., Chan, E. W., et al. (2018). Evolution of tigecycline-and colistin-resistant CRKP (carbapenem-resistant Klebsiella pneumoniae) in vivo and its persistence in the GI tract. *Emerg. Microbes Infect.* 7:127. doi: 10.1038/s41426-018-0129-7

Zhang, Z., and Saier, M. H. (2009). A novel mechanism of transposon-mediated gene activation. *PLoS Genet.* 5:e1000689. doi: 10.1371/journal.pgen.1000689

frontiers | Frontiers in Microbiology

TYPE Original Research
PUBLISHED 29 September 2023
DOI 10.3389/fmicb.2023.1266045

OPEN ACCESS

EDITED BY
Vijay Soni,
NewYork-Presbyterian, United States

REVIEWED BY
Yaxin Li,
Cornell University, United States
Prabhat Ranjan Singh,
Weill Cornell Medicine, United States
Biplab Singha,
University of Massachusetts Medical School, United States

*CORRESPONDENCE
Hu Jian
✉ jaffyhu@njau.edu.cn
Zhou Yuxin
✉ rita1720@126.com

RECEIVED 25 July 2023
ACCEPTED 30 August 2023
PUBLISHED 29 September 2023

CITATION
Huangwei Z, Peiyuan J, Yixuan K, Zhimin Y, Yuxin Z, Geunhwa J and Jian H (2023) Genome-wide transcriptional analyses of *Clarireedia jacksonii* isolates associated with multi-drug resistance.
Front. Microbiol. 14:1266045.
doi: 10.3389/fmicb.2023.1266045

Genome-wide transcriptional analyses of *Clarireedia jacksonii* isolates associated with multi-drug resistance

Zhang Huangwei[1], Jin Peiyuan[1], Kong Yixuan[1], Yang Zhimin[1], Zhou Yuxin[2]*, Jung Geunhwa[3] and Hu Jian[1]*

[1]College of Agro-Grassland Science, Nanjing Agricultural University, Nanjing, China, [2]Institute of Botany, Jiangsu Province and Chinese Academy of Sciences, Nanjing, China, [3]Stockbridge School of Agriculture, University of Massachusetts, Amherst, MA, United States

Emerging multidrug resistance (MDR) in *Clarireedia* spp. is a huge challenge to the management of dollar spot (DS) disease on turfgrass. Insight into the molecular basis of resistance mechanisms may help identify key molecular targets for developing novel effective chemicals. Previously, a MDR isolate (LT586) of *C. jacksonii* with significantly reduced sensitivities to propiconazole, boscalid, and iprodione, and a fungicide-sensitive isolate (LT15) of the same species were isolated from creeping bentgrass (*Agrostis stolonifera* L.). The present study aimed to further explore the molecular mechanisms of resistance by using genome-wide transcriptional analyses of the two isolates. A total of 619 and 475 differentially expressed genes (DEGs) were significantly down and upregulated in the MDR isolate LT586, compared with the sensitive isolate LT15 without fungicide treatment. Three hundreds and six and 153 DEGs showed significantly lower and higher expression in the MDR isolate LT586 than those in the sensitive isolate LT15, which were commonly induced by the three fungicides. Most of the 153 upregulated DEGs were xenobiotic detoxification-related genes and genes with transcriptional functions. Fifty and 17 upregulated DEGs were also commonly observed in HRI11 (a MDR isolate of the *C. jacksonii*) compared with the HRS10 (a fungicide-sensitive isolate of same species) from a previous study without and with the treatment of propiconazole, respectively. The reliability of RNA-seq data was further verified by qRT-PCR method using a few select potentially MDR-related genes. Results of this study indicated that there were multiple uncharacterized genes, possibly responsible for MDR phenotypes in *Clarireedia* spp., which may have important implications in understanding the molecular mechanisms underlying MDR resistance.

KEYWORDS

RNA-seq, dollar spot, multidrug resistance, *Clarireedia* spp., fungicide resistance

1. Introduction

Dollar spot (DS) is one of the most economically important diseases of turfgrass worldwide (Salgado-Salazar et al., 2018). Multiple species in the genus *Clarireedia* (formerly *Sclerotinia homoeocarpa*) have been reported to cause DS, including *C. homoeocarpa*, *C. bennettii*, *C. jacksonii*, *C. monteithian*, *C. paspali*, and *C. hainanense* (Salgado-Salazar et al., 2018; Hu et al., 2019a,b; Zhang et al., 2022). Management of DS requires repeated inputs of fungicides with

different chemical groups. Benzimidazole carbamates (MBCs), dicarboximides (DCFs), 14α-demethylase inhibitors (DMIs), and succinate dehydrogenase inhibitors (SDHIs) are among the most frequently used fungicide classes for DS control in the last few decades (Popko et al., 2012; Stephens and Kaminski, 2019). Due to widespread, repeated uses of fungicidal compounds as well as many other factors such as management location, environmental conditions, genetic regulation, and turfgrass species (Koch et al., 2009; Latin, 2011; Stephens and Kaminski, 2019), resistance to these chemical groups in *Clarireedia* spp. have been reported in many regions around the world (Miller et al., 2002; Jo et al., 2006; Koch et al., 2009; Lee et al., 2017). Moreover, multiple fungicide resistant (MFR) or multi-drug resistant (MDR) populations have emerged in the United States of America, Japan, as well as China, recently (Sang et al., 2015, 2018; Zhang et al., 2021), which makes DS disease increasingly difficult to control.

In the genus *Clarireedia*, resistance mechanisms to different chemical groups of fungicides have been systemically revealed in *C. jacksonii*. Hulvey et al. (2012) found that overexpression of two genes, *ShCYP51B* and *ShatrD* in the DS pathogen *C. jacksonii*, was responsible for reduced DMI fungicide sensitivity. Sang et al. (2016) found that nonsynonymous polymorphisms in codon 366 (isoleucine to asparagine) in histidine kinase gene (*Shos1*) and overexpression of *ShPDR1* led to DCFs resistance in *C. jacksonii* isolates. Hu et al. (2018) found that nonsynonymous polymorphisms at codon 198 and 200 in *β-tubulin* were responsible for high and medium resistance to MBC fungicide thiophanate-methyl, respectively. The H267Y mutation in *SdhB* was determined to be responsible for resistance to boscalid and penthiopyrad in *C. jacksonii* isolates from Japan, and the G91R mutation in *SdhC* was confirmed to be a direct factor conferring resistance to boscalid, fluxapyroxad, isofetamid, and penthiopyrad in *C. jacksonii* isolates from the United States (Popko et al., 2018).

There are two different types of resistance to multiple fungicides: MFR and MDR. Generally, MFR is often caused by accumulation of different mutations at the corresponding fungicide target genes (e.g., *CYP51B*, *β-tubulin*, *os1* and *Sdh* genes in *Clarireedia* spp.), while the mechanisms of MDR in plant pathogenic fungi were often associated with overexpression of single or multiple drug efflux transporters, including ATP-binding cassette (ABC) and major facilitator superfamily (MFS) transporters (Nakaune et al., 2002; Omrane et al., 2015; Sang et al., 2015). In *C. jacksonii*, Sang et al. (2015) demonstrate that MDR is partially attributable to the pleiotropic drug resistance (PDR) transporter gene, *ShPDR1*. Furthermore, they found that a gain-of-function mutation (ATG to ACG at codon 853, M853T) in the fungus-specific transcription factor *ShXDR1* led to constitutive and induced overexpression of cytochrome P450s (CYP450s) and ABC transporters, which are responsible for MDR (Sang et al., 2018). In the previous study, we found that multiple isolates of *C. jacksonii* showed decreased sensitivities to fungicides with different mode of actions (Zhang et al., 2021). Preliminary studies revealed that no consistent mutations were found on the fungicide target genes in the resistant isolates, which suggested that they were MDR rather than MFR isolates. To further characterize if similar mechanisms of MDR responsible for the above-mentioned resistant isolates of *C. jacksonii* found in China, we sequenced *ShXDR1* gene in the sensitive and resistant isolates, but no M853T mutation on *ShXDR1* was found. The mechanisms of MDR in *C. jacksonii* or other species in *Clarireedia* may be complex and need to be thoroughly investigated.

Comparative transcriptomics is a powerful tool to elucidate the molecular mechanisms of fungicide resistance. RNA-seq analyses have been used to uncover the molecular mechanisms of resistance to DMI, SDHI, or MDR in many pathogenic fungi, including *Clarireedia* spp., *Aspergillus fumigates* (Fan et al., 2021), *Fusarium virguliforme* (Sang et al., 2021), and *Cercospora beticola* (Bolton et al., 2016). In this study, the goal is to identify the genes that are differentially expressed between fungicide-sensitive and presumably MDR isolates of *C. jacksonii* under exposures to three different fungicides, propiconazole, boscalid, and iprodione. Comparative transcriptomics was applied to glean insight into the potential variations at transcriptomic level. The results provide additional molecular clues that will aid in elucidating the mechanisms and metabolic pathways related to MDR in *Clarireedia* spp.

2. Materials and methods

2.1. Fungal isolates

Fungal isolates LT15 and LT586 were recovered from symptomatic leaf blades of creeping bentgrass (*Agrostis stolonifera* L.). Sensitivities of the two isolates to iprodione, propiconazole and boscalid were determined *in vitro* using the respective discriminatory concentrations described in the previous study (Zhang et al., 2021). Agar plugs (5 mm in diameter) were inoculated on PDA plates amended with iprodione (1.0 μg/mL), propiconazole (0.1 μg/mL), and boscalid (10 μg/mL). The non-amended PDA plates served as controls. After 3 days' incubation, the diameter of colonies was perpendicularly measured twice. The percentage (%) of relative mycelia growth was calculated as the average diameter on fungicide-amended medium divided by the average diameter on non-amended medium and multiplied by 100.

There are several species in the genus of *Clarireedia*. The two isolates tested here were identified to the species level, *C. jacksonii* by sequencing the nuclear ribosomal internal transcribed spacer (ITS) with the universal primer of ITS4 and ITS5 (Supplementary Table S1). ITS has proved useful to differentiate different species in the genus *Clarireedia* in previous studies, and the phylogenetic tree constructed from ITS produced a topology like the combined multi-locus dataset (Salgado-Salazar et al., 2018; Aynardi et al., 2019). Maximum likelihood method was used for constructing phylogenetic tree of select known and published isolates using the Tamura 3-parameter model in MEGA7 and tested with 1,000 bootstrap replicates (Kumar et al., 2016; Hu et al., 2019a,b).

2.2. Mycelial preparation and total RNA extraction

The mycelia of the two isolates were prepared for RNA extraction with the method described previously with some modifications (Hulvey et al., 2012). In brief, isolates were inoculated into 25 mL of potato dextrose broth (PDB) with eight agar plugs (5 mm in diameter) and grown for 3 days at 25°C and 150 rpm. Propiconazole (EC, Banner Maxx, Syngenta Crop Protection), iprodione (EC, Rovral, FMC), and boscalid (WG, Cantus, BASF) were added to the tubes with the final concentrations at 0.1, 1, and 10 μg/mL, respectively (Sang et al., 2018; Zhang et al., 2021). The untreated samples were added with same

volume of sterile water (Zhang et al., 2021). Tubes were lightly shaken on a benchtop shaker for 1 h. Approximately 100 mg of mycelia for each sample was harvested by vacuum filtration, transferred into a 2-mL screw cap tube, and immediately dropped into liquid nitrogen. Frozen samples were stored at −80°C freezer until further processing. Three biological replicates of each treatment were generated. Total RNA was extracted from each sample (a total of 24 samples) using RNAsimple Total RNA Kit (TIANGEN Biotech, Beijing).

2.3. Transcriptome sequencing, assembly, and annotation

Total RNA of each sample was sent to Biomarker Technologies (Beijing, China) for cDNA library preparation and sequencing. RNA concentration and purity were measured using NanoDrop 2000 (Thermo Fisher Scientific, Wilmington, DE, United States). RNA integrity was assessed using the RNA Nano 6000 Assay Kit of the Agilent Bioanalyzer 2100 system (Agilent Technologies, CA, United States). 1 μg RNA per sample was used for constructing cDNA library. Sequencing libraries were generated using NEBNext UltraTM RNA Library Prep Kit for Illumina (New England Biolabs, United States) following manufacturer's instructions. RNA-seq was performed on an Illumina HiSeq4000 platform (Illumina, CA, United States). After sequencing, reads containing adapter, poly-N or low quality reads were removed through in-house perl scripts[1] to produce clean data sets. Q20, Q30, GC-content, and sequence duplication level of the clean data were calculated. High quality clean data sets were mapped to the *C. jacksonii* reference genome (Zhang et al., 2023) with Hisat2 software (Kim et al., 2015). Only reads with a perfect match or one mismatch were further analyzed and annotated.

Gene functions were annotated through the following databases: NCBI non-redundant protein sequences (Nr), NCBI non-redundant nucleotide sequences (Nt), Protein family (Pfam), Clusters of Orthologous Groups of proteins (KOG/COG), Swiss-Prot, KEGG Ortholog database (KO), and Gene Ontology (GO).

2.4. Functional analysis of differentially expressed genes

Gene expression levels were estimated by fragments per kilobase of transcript per million fragments mapped (FPKM). The formula for FPKM calculation was: FPKM = (cDNA fragments)/mapped fragments (millions) × transcript length (kb). Differential expressed genes (DEGs) were analyzed by using the R package DESeq2 (Love et al., 2014). The value of $p < 0.05$, $|\log_2\text{Fold Change}| \geq 1.5$ and FPKM > 0.05 were set as the threshold for the identifications of DEGs. Principal component analysis (PCA) and heat map analysis were performed using BMKCloud.[2] Enrichment analysis of the DEGs was implemented by the R package GOseq based on Wallenius non-central hypergeometric distribution (https://cran.r-project.org/; Young et al., 2021). We used KOBAS software to test the statistical enrichment of the DEGs in KEGG pathways (Bu et al., 2021).

2.5. Quantitative real time RT-PCR validation of RNA-seq data

The relative expressions of selected DEGs were assayed with quantitative real-time PCR (qRT-PCR) before and after treatments with propiconazole, iprodione, and boscalid as described above. Total RNA was extracted with RNAsimple Total RNA Kit (TIANGEN Biotech, Beijing), cDNA synthesis from total RNA was conducted with the one-step gDNA removal and cDNA synthesis super mix kit (TransGen Biotech, Beijing). cDNA was diluted to 10-fold, and 1 μL (100 ng) of cDNA which was used for qRT-PCR with HiScript II Q RT SuperMix (Vazyme Biotech, Nanjing). qRT-PCR was conducted on LightCycler 480 II (Roche Life Sciences, Swiss). The actin (*Shact*) gene of *C. jacksonii* was selected as the housekeeping gene, primers for quantifying *Shact* and *ShPDR1* gene were used as reported by Hulvey et al. (2012), and primers for *ShCYP68* gene quantification were used according to Sang et al. (2018). Other primers were designed with Primer5 (https://www.researchgate.net/journal/Biotech-Software-Internet-Report-1527-9162; Supplementary Table S1). The comparative threshold cycle (C_T) method was used for the calculation of relative gene expression. Linear regression analysis of the selected DEGs was performed with FPKM values from RNA-Seq and relative expression values from RT-qPCR.

3. Results

3.1. Genetic background and fungicide sensitivities of the isolates for RNA-seq

Phylogenetic analysis based on ITS sequences revealed that the two isolates LT15 and LT586 belonged to the same species: *C. jacksonii* (Supplementary Figure S1). *In vitro* sensitivity assays confirmed that the isolate LT586 showed significantly reduced sensitivities to iprodione, propiconazole, and boscalid (Figure 1A) compared with the isolate LT15 ($p < 0.001$) (Figure 1B). No point mutations were found on the fungicide target genes (*ShCYP51B*, *Shβ-tubulin*, *Shos1*, and *ShSdh* genes) in LT586, suggesting that LT586 is a MDR isolate of *C. jacksonii* (Figure 1).

3.2. Transcriptomic assembly data

In this study, comparative transcriptomic analyses were conducted to identify the DEGs between the two isolates (LT15 and LT586) without or with the treatments of propiconazole, boscalid, and iprodione (Supplementary Table S2). A total of 39,386,718-59,568,566 clean reads were obtained from 24 libraries. GC content was ranging from 48.75 to 49.23% and the percentage of Q30 base was 93.27% or above (Supplementary Table S2). By iterative alignment, 93.56–95.79% of the clean reads were successfully mapped to *C. jacksonii* reference genome (Zhang et al., 2023). Of the mapped reads, 92.49–94.59% of them was mapped to unique loci, while 0.80–1.26% of the reads was mapped to multiple loci in the reference genome (Supplementary Table S2). The raw

1 https://www.perl.org/

2 www.biocloud.net

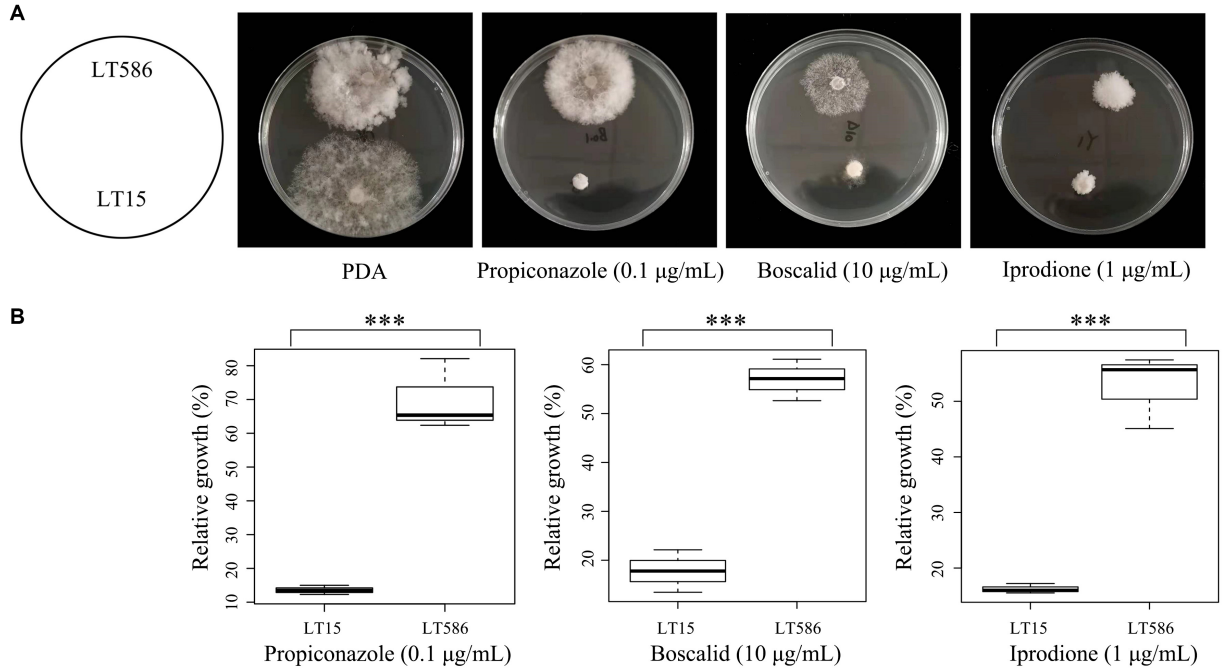

FIGURE 1
Mycelial growth of the MDR isolate (LT586) and fungicide-sensitive isolate (LT15) of *Clarireedia jacksonii* on non-amended PDA and propiconazole, boscalid, and iprodione amended PDA at 0.1, 10, and 1 μg/mL, respectively. *** means significant difference between the two strains under the fungicide treatment with p value < 0.001.

RNA sequences were deposited in NCBI SRA Database under BioProject accession number PRJNA1007393.

3.3. Differential expression between the two isolates without fungicide treatments

Principal component analysis revealed that different compartments were clustered apparently, PC1 and PC2 explained 24.87 and 16.88% variation between the two isolates without and with fungicide treatment, respectively (Figure 2A). The DEGs were identified, a total of 619 and 475 DEGs were significantly down- and upregulated in the MDR isolate LT586, compared with the sensitive isolate LT15 without fungicide treatment (Figure 2B).

Clusters of Orthologous Groups of proteins function analysis revealed that all these DEGs were mainly involved in general function prediction (23.29–99%), secondary metabolites biosynthesis, transport, catabolism (12–51%), and energy production and conversion (9.88–42%; Supplementary Figure S2). KEGG pathway of all the DEGs were classified into four groups, which included cellular process, environmental information processing, genetic information processing, and metabolism (Supplementary Figure S3). KEGG pathway analysis revealed that these DEGs were mainly involved in protein processing in endoplasmic reticulum ($n = 22$), terpenoid backbone biosynthesis ($n = 10$), tyrosine metabolism ($n = 13$), diterpenoid biosynthesis ($n = 3$), and steroid biosynthesis ($n = 10$; Figure 2C). GO function analysis showed that the molecular functions of all these DEGs were mainly involved in dioxygenase activity ($n = 10$), monooxygenase activity ($n = 19$), iron ion binding ($n = 26$), oxidoreductase activity ($n = 24$), and heme binding ($n = 29$); the biological processes were mainly involved in steroid biosynthetic process ($n = 4$), DNA integration ($n = 9$), L-arabinose metabolic process ($n = 4$), tryptophan catabolic process to kynurenine ($n = 5$), and mycotoxin biosynthetic process ($n = 11$); the cellular components were mainly involved in integral component of membrane ($n = 257$; Figure 2D).

3.4. Differential expression between the two isolates induced by the treatment of three fungicides

RNA-seq analyses revealed that 398, 351, and 530 genes were significantly upregulated, while 736, 529, and 668 genes were significantly downregulated in MDR isolate LT586, compared with the sensitive isolate LT15 under the treatment of propiconazole, boscalid, and iprodione, respectively (Figure 3A). A total of 306 and 153 genes showed significantly lower and higher expressions in the MDR isolate LT586 than those in the sensitive isolate LT15, which were commonly induced by the three fungicides (Figure 3B). KEGG pathway enrichment analysis revealed that the 306 downregulated genes were mainly enriched in butanoate metabolism ($n = 6$), terpenoid backbone biosynthesis ($n = 6$), tyrosine metabolism ($n = 6$), and starch and sucrose metabolism ($n = 7$; Figure 3C); the 153 upregulated genes were mainly enriched in peroxisome ($n = 4$), glycerophospholipid metabolism ($n = 4$), protein processing in endoplasmic reticulum ($n = 5$), and ABC transporters ($n = 4$; Figure 3D).

Heatmap analysis showed that the 153 DEGs were clustered apparently in LT15 and LT586, and were significantly higher expressed in the MDR isolate LT586 under the treatments by the three fungicides (Figure 3E). The function of 153 upregulated DEGs further

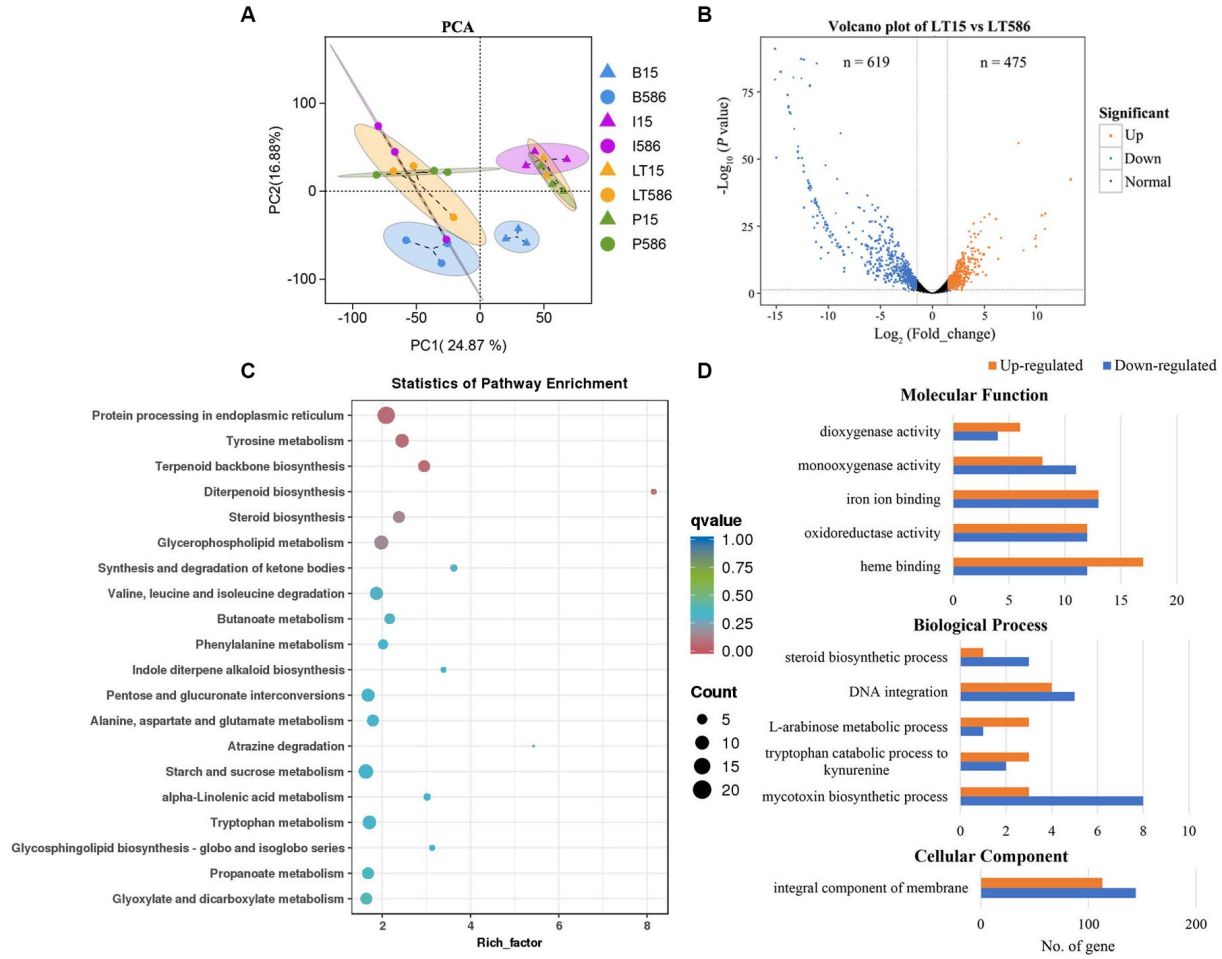

FIGURE 2
Differential expression analysis between the MDR isolate LT586 and the sensitive isolate LT15 without fungicide treatments. **(A)** Principal component analysis (PCA) of the two isolates with and without the treatments of propiconazole (P15, P586), boscalid (B15, B586), and iprodione (I15, I586), each treatment had three replicates. **(B)** Volcano plot of the DEGs. **(C)** KEGG pathway enrichment analysis of all the DEGs. Rich_factor represents the proportion of genes annotated to a certain pathway in the DEGs compared to all genes annotated, the larger the rich_factor, and the more significance in the enrichment level of the DEGs in this pathway. **(D)** GO functions enrichment analysis of the upregulated and downregulated DEGs.

characterized, which were mainly classified into seven molecular function terms, five biological processes, and three cellular components (Figure 3F). The molecular functions of the 153 DEGs were mainly involved in FAD binding, monooxygenase activity, transmembrane transporter activity, heme binding, zinc ion binding, ATP binding, and oxidoreductase activity. The five biological processes were intracellular signal transduction, response to stimulus, cellular protein metabolic process, L-arabinose metabolic process, and carbohydrate metabolic process. The cellular components included extracellular region, cytoplasm, and integral component of membrane (Figure 3F). The specific information of the genes with Pfam function annotations were shown in Supplementary Table S3. Most of them were involved in the functions of xenobiotic detoxification-related genes, which mainly included oxidoreductase activity, transferase activity, ATPase activity, and transmembrane movement of substance.

There were 10 genes involved in oxidoreductase activity (GE10720_g, GE15552_g, GE05437_g, GE03831_g, GE03356_g, GE02832_g, GE09522_g, GE05251_g, GE10755_g, and GE01921_g), which mainly included the functions of alcohol dehydrogenase, zinc-binding dehydrogenase, and NADH: flavin oxidoreductase. Nine genes were involved in ATP binding, including three ABC transporter genes (GE04562_g, GE10243_g, and GE13106_g), one Cdc48 subfamily gene (GE15443_g), one asparagine synthase gene (GE01321_g), one E1-E2 ATPase gene (GE06702_g), two fungal protein kinase genes (GE09508_g, GE16043_g), and one Hsp70 protein encoding gene (GE08240_g). Of the three ABC transporter genes involved in ATP binding (Schoonbeek et al., 2001; Sang et al., 2015), two (GE04562_g = *ShPDR1*, and GE10243_g = *ShatrD*) had been shown to be associated with MDR in *C. jacksonii* (Sang et al., 2018). There were seven genes involved in heme binding, including six CYP450s genes (GE00961_g, GE07314_g, GE05983_g, GE10739_g, GE14553_g, and GE06676_g) and one glycosyl hydrolase family 20 gene (GE05305_g). Three of the six CYP450s genes (GE10739_g = *CYP561*, GE14553_g = *CYP65*, GE00961_g = *CYP68*) were also involved in monooxygenase activity and had been shown to be associated with MDR in *C. jacksonii* (Sang et al., 2018). Seven genes were involved in transmembrane transporter activity, with five genes encoding MFS proteins

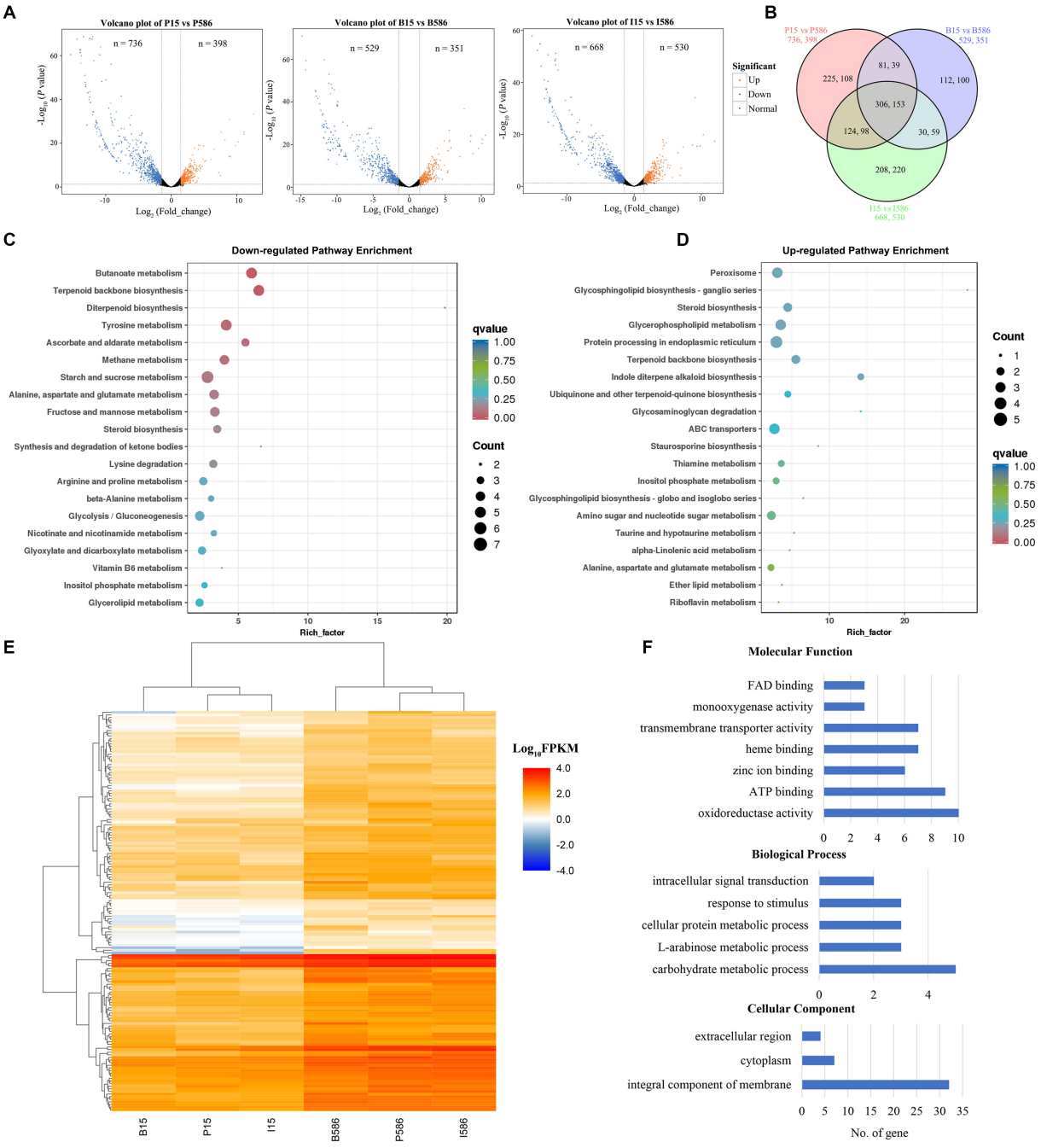

FIGURE 3
Differentially expressed genes (DEGs) in the MDR isolate LT586 compared with the sensitive isolate LT15 under the treatments of propiconazole (P), boscalid (B), and iprodione (I). **(A)** Volcano plot of the DEGs. **(B)** Venn plot analysis. **(C)** KEGG pathway enrichment analysis of 306 downregulated DEGs commonly induced by the three fungicides. Rich_factor represents the proportion of genes annotated to a certain pathway in the DEGs compared to all genes annotated. The larger the rich_factor, the more significance in the enrichment level of the DEGs in this pathway. **(D)** KEGG pathway enrichment analysis of 153 upregulated DEGs commonly induced by the three fungicides. **(E)** Heat map analysis of the 153 upregulated DEGs commonly induced by the three fungicides. **(F)** GO functions enrichment analysis of the 153 upregulated DEGs commonly induced by the three fungicides.

(GE09014_g, GE09100_g, GE09161_g, GE00853_g, and GE09173_g), one encoding sugar and other transporter protein (GE02436_g), and one encoding POT family protein (GE10772_g). Three of the MFS genes (GE09014_g, GE09100_g, and GE09173_g) were highly homologous with YLL028W (*Tpo1*), YLL028W (*Tpo1*), and YNL065W (*Aqr1*) in yeast (Supplementary Table S3), which had been shown to be associated with fungicide resistance by active efflux of xenobiotics (Kretschmer et al., 2009; Omrane et al., 2015). Three genes were involved in FAD binding (GE05437_g, GE13986_g, and GE13409_g). Eight genes were involved in zinc ion binding (GE05988_g, GE06509_g, GE09053_g, GE09312_g, GE09402_g, GE10720_g, GE12966_g, and GE15454_g), which mainly included

the functions of zinc finger domain and fungal specific transcription factor domain.

3.5. Comparison with the published data

The transcriptome data from a previously published paper (Sang et al., 2018) were re-analyzed and mapped to the reference genome used in this study (Supplementary Table S2). Three hundred and sixty-nine genes were significantly upregulated in the MDR isolate HRI11, as compared with the sensitive isolate HRS10 under no fungicide-treatment (Supplementary Figure S4A). Fifty of these genes also showed significantly higher expression in LT586 than LT15 from this study (Supplementary Figure S4B). Most of the differentially expressed genes between the two studies were both from the same gene families, such as major facilitator superfamily, CYP450s, and fungal specific transcription factors (Supplementary Figure S4C).

In the previously published paper (Sang et al., 2018), *C. jacksonii* isolates were only treated by propiconazole, therefore the transcriptional expression analyses between the two studies were based on the data of propiconazole treatments. A total of 203 (PHRS10 vs. PHRI11) and 398 (PLT15 vs. PLT586) genes were significantly upregulated in the MDR isolates HRI11 and LT586 after treatment of propiconazole (Figure 4A). Seventeen genes showed commonly upregulated overexpression in the two MDR isolates, which included the following five genes (*CYP561*, *CYP65*, *CYP68*, *ShPDR1*, and *ShatrD*), confirmed to be related with MDR function in the MBio paper (Sang et al., 2018; Figure 4B). These genes showed a generally constitutive overexpression and fungicide-induced expression trend in the two MDR isolates, except for *CYP65*, which was only induced expressed under the treatment of boscalid in this study (Figure 4C).

3.6. qRT-PCR analysis of key DEGs involved in fungicide resistance

To validate the expression pattern of some key DEGs involved in fungicide resistance from RNA-Seq analysis, three zinc finger transcript factor genes (GE07854_g, GE09003_g, and GE09664_g), four MFS transporter genes (GE06394_g, GE09014_g, GE09100_g, and GE09173_g), one CYP450 gene (GE00961_g), and two ABC transporter genes (GE13106_g and GE04562_g) were further quantified with qRT-PCR (Figure 5A). The $\log_2$-transformed relative expression values determined by qRT-PCR and RNA-seq were positively correlated ($R^2 = 0.7776$, $p < 0.001$; Figure 5B). The result of qRT-PCR analysis was consistent with the RNA-seq data.

4. Discussion

Clarireedia jacksonii is the most widely distributed DS pathogen species across the world (Viji et al., 2004; Hu et al., 2019a,b). Due to widespread, repeated uses of multiple fungicide classes for DS control, MFR and MDR have become an increasing issue in *C. jacksonii*

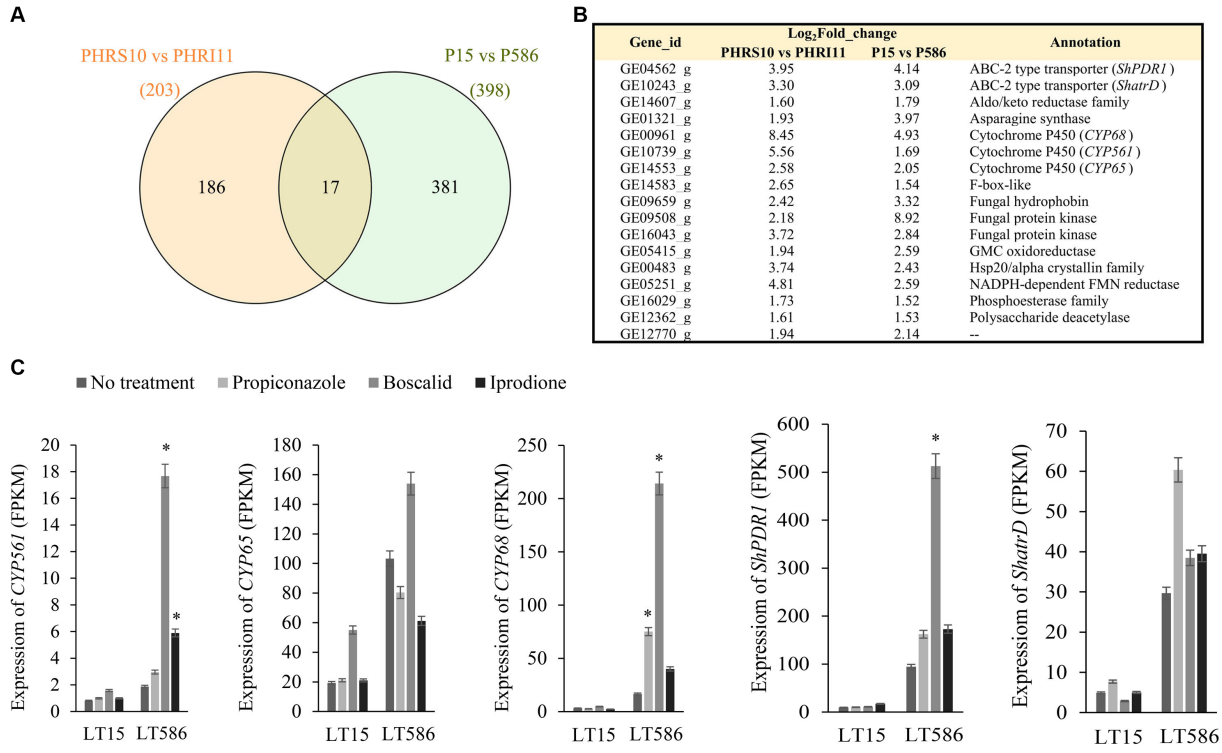

Gene_id	Log2Fold_change		Annotation
	PHRS10 vs PHRI11	P15 vs P586	
GE04562_g	3.95	4.14	ABC-2 type transporter (*ShPDR1*)
GE10243_g	3.30	3.09	ABC-2 type transporter (*ShatrD*)
GE14607_g	1.60	1.79	Aldo/keto reductase family
GE01321_g	1.93	3.97	Asparagine synthase
GE00961_g	8.45	4.93	Cytochrome P450 (*CYP68*)
GE10739_g	5.56	1.69	Cytochrome P450 (*CYP561*)
GE14553_g	2.58	2.05	Cytochrome P450 (*CYP65*)
GE14583_g	2.65	1.54	F-box-like
GE09659_g	2.42	3.32	Fungal hydrophobin
GE09508_g	2.18	8.92	Fungal protein kinase
GE16043_g	3.72	2.84	Fungal protein kinase
GE05415_g	1.94	2.59	GMC oxidoreductase
GE00483_g	3.74	2.43	Hsp20/alpha crystallin family
GE05251_g	4.81	2.59	NADPH-dependent FMN reductase
GE16029_g	1.73	1.52	Phosphoesterase family
GE12362_g	1.61	1.53	Polysaccharide deacetylase
GE12770_g	1.94	2.14	--

FIGURE 4
Significantly upregulated genes in HRS10 plus propiconazole vs. HRI11 plus propiconazole and LT15 plus propiconazole vs. LT586 plus propiconazole. **(A)** Venn plot analysis. **(B)** The specific information of 17 commonly upregulated genes through Venn plot analysis. **(C)** Gene expressions of *CYP561*, *CYP65*, *CYP68*, *ShPDR1*, and *ShatrD* in the MDR isolate LT586 and the sensitive isolate LT15 according to RNA-seq data. *means significant difference between the fungicide treatment group and the PDA treatment group in the LT586 isolate value of $p < 0.05$.

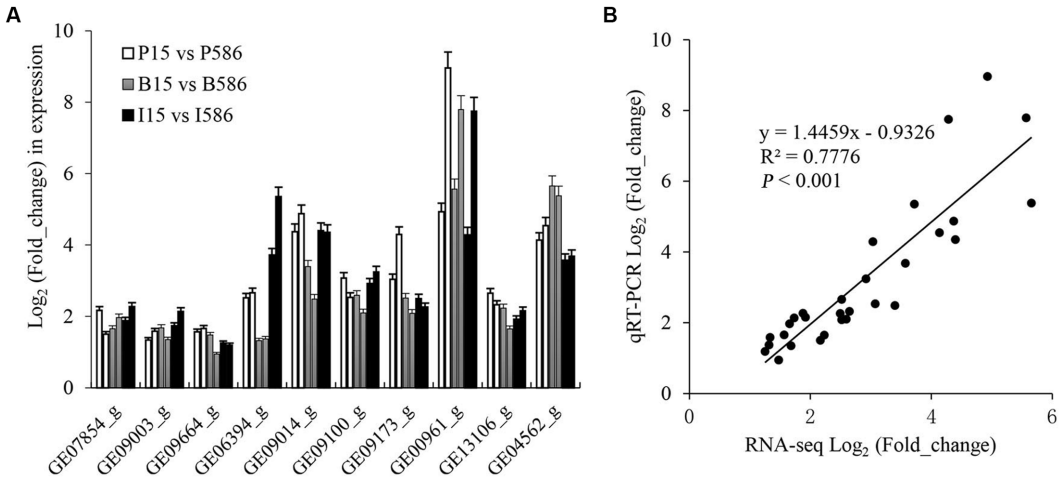

FIGURE 5
Expression analysis of 10 potentially MDR related genes by qRT-PCR and RNA-seq method. **(A)** Comparison analysis between the two methods, the left and right column with same color refer to RNA-seq and qRT-PCR method, respectively. **(B)** Correlation of the log_2-transformed relative expression values obtained by qRT-PCR and RNA-seq method.

populations from different regions or countries in recent years (Sang et al., 2016; Stephens and Kaminski, 2019; Zhang et al., 2021). In this study, fungicide sensitivity tests and comparative analyses of fungicide target genes clearly indicated that the *C. jacksonii* isolate LT586 resistant to multiple fungicides was a MDR isolate. At present, MDR in fungal pathogens has become great concerns both in clinical and agricultural fields (Leroux et al., 2012; Sang et al., 2015). Several mechanisms have been reported to cause MDR in pathogenic fungi (Nakaune et al., 2002; Thakur et al., 2008; Kretschmer et al., 2009; Sang et al., 2018). Therefore, we profiled the response of two *C. jacksonii* isolates contrasting in sensitivity to different active ingredients of three fungicide classes: iprodione, propiconazole, and boscalid, to identify the genes involved in MDR. Moreover, we compared the results between this study and a previous study (Sang et al., 2018) to get a better understanding of MDR mechanisms.

This study identified common MDR-related genes, which have also been described in study of Sang et al. (2018), as well as new genes potentially related to MDR. We observed that many genes were constitutively or induced over-expressed by the three fungicides in the MDR isolate LT586 (Figures 2, 3). In general, both constitutive and induced expressions of MDR-related genes can lead to MDR (Sang et al., 2018). Therefore, there were still a substantial number of DEG changes between LT15 and LT586 even in the absence of fungicide treatment. Moreover, the genetic differences also might contribute to the constitutive changes of the DEGs between the two isolates. In this study, both constitutive and induced DEGs were identified between the two isolates, which provided us a better reference to locate the potential MDR genes for further analyses. Among these DEGs identified, some have been previously characterized to be associated with MDR in *C. jacksonii* (Sang et al., 2018), some homologous genes were identified to be responsible for fungicide resistance in other fungi, which have not been studied in *C. jacksonii*. It is proposed that the MDR mechanisms in *C. jacksonii* are complicated and need to be further investigated.

When compared with the data from a similar study conducted by Sang et al. (2018), we found same and novel DEGs between the two studies, which suggested that the MDR mechanisms in *C. jacksonii* might have common as well as contrasting regulatory pathways, depending on the origins of the isolates. There are two main reasons that may contribute to the differences between the two studies. Firstly, the *C. jacksonii* isolates used in the two studies were different in genetic background and fungicide sensitivities. The key genes regulating MDR in these isolates might be selected differently by different ways of fungicide uses or different environment conditions (Koch et al., 2009; Latin, 2011). Secondly, the isolates in the current study were treated by three fungicides, while only propiconazole was used to treat *C. jacksonii* isolates in the study by Sang et al. (2018).

Modifications, over-expression of target genes, and over-expression of efflux transporters in plasma membranes are well known mechanisms of fungicide resistance in filamentous fungi (Sang et al., 2018). Transcriptome analysis in this study revealed that the target gene of DMI, propiconazole (*CYP51*) was significantly upregulated in LT586, while the target genes of SDHI, boscalid (*SdhB*, *SdhC*, and *SdhD*) and dicarboximide, iprodione (*Shos1*) did not show differential expressions between the two isolates (Supplementary Figure S5). Combined with no mutations found on these target genes, indicated that the observed MDR in LT586 was probably caused by the over-expressions of *CYP51* and other genes involved in xenobiotics detoxification systems. A significantly higher level of resistance to propiconazole observed in LT586 further supported partial contribution of *CYP51* to MDR. Further investigations should be oriented to characterize if there exist commonly regulatory factors responsible for over-expressions of *CYP51* as well as the genes in xenobiotics detoxification systems simultaneously.

General xenobiotics detoxification systems work through pathways that can be divided into three phases. Phase I includes metabolizing enzymes such as CYPs, that catalyze xenobiotics, phase II involves conjugating enzymes (e.g., glutathione S-transferase) by adding polar molecules onto compounds (Xu et al., 2005), and in phase III secretion system, ABC transporters or other transmembrane transporters export parent and/or metabolized compounds (Ihunnah et al., 2011). Previous study revealed that the constitutive and induced over-expressions of three phase I metabolizing enzyme genes *CYP561*, *CYP65*, and *CYP68*,

two phase III transporter genes *ShPDR1* and *ShatrD* were associated with MDR in *C. jacksonii* (Sang et al., 2018). However, in this study, *CYP65* in the MDR isolate LT586 was only upregulated in response to the treatment of boscalid, but not propiconazole or iprodione. Overexpression of different CYPs displayed various sensitivities to different chemical groups of fungicides, which might be due to the different substrate specificity of CYPs (Moktali et al., 2012). Beside the three above CYPs, three other CYPs were significantly upregulated in the MDR isolate LT586. Further studies are needed to characterize the full functional roles of these differentially expressed CYPs found in this study, which may gain a better understanding of the associations between these different CYPs and MDR. In this study, one phase II glutathione S-transferase (GE09048_g) showed constitutive and induced overexpression in the MDR isolate LT586, this gene was only constitutively overexpressed in the MDR isolate HRS11 in the previous study (Sang et al., 2018). The different expression patterns in different MDR isolates are expected and suggest the role of the gene in fungicide resistance needs to be further investigated.

Notably, the family members including ABC transporters, MFS transporters, zinc-cluster transcription factors, and CYP450s were significantly enriched in these potential multidrug resistant DEGs (Supplementary Table S3). Regarding MFS transporters, they are generally less understood compared with ABC transporters. MFS transporter genes such as GE09014_g, GE09100_g, and GE09173_g in this study (Supplementary Table S3) were highly homologous with YLL028W (*Tpo1*), YLL028W (*Tpo1*), and YNL065W (*Aqr1*) in yeast. *Tpo1* was demonstrated to confer resistance to benzoic acid in *Saccharomyces cerevisiae*, and under the controls of the Gcn4 and Stp1 transcription factors involved in the response to amino acid availability (Godinho et al., 2017). However, the sequences of these three genes are consistent in MDR isolate LT586 and fungicide sensitive isolate LT15 without point mutations. Therefore, the roles of these MFS genes in fungicide resistance and the interactive mechanisms between MFS genes and other transcription factors need to be further studied.

In addition, it has been not well characterized how fungi transcriptionally regulate and coordinate MDR related genes. Transcription factors have been confirmed to play important roles in drug resistance in multiple pathogenic fungi and they generally interacted with downstream target genes or other transcription factors (Nakaune and Nakano, 2007; Thakur et al., 2008; Wang et al., 2018). To date, only the transcription factor ShXDR1 has been demonstrated to regulate downstream MDR related genes in *C. jacksonii* (Sang et al., 2018). Our results indicated that essential and specific roles for other fungal transcription factors in regulating MDR of *Clarireedia* spp. should be investigated (Supplementary Table S3). Further genetic transformation and protein interactive analyses will help better understand if other transcription factors are involved in MDR, and how they regulate MDR in *Clarireedia* spp.

5. Conclusion

In this study, we utilized comparative transcriptomics to glean insight into the potential MDR-related genes associated with the reduced sensitivities to multiple fungicides (propiconazole, boscalid, and iprodione) in *C. jacksonii* isolates, comparative analyses were also conducted with the datasets from the current and a previous study (Sang et al., 2018). Common as well as novel DEGs were found to be associated with MDR in this study. The molecular functions of these DEGs were mainly involved in xenobiotic detoxification-related systems and transcriptional regulations. The results obtained from this study will provide valuable information for further identifying the molecular mechanisms of MDR. The study also strongly indicated that the MDR mechanisms in *C. jacksonii* are complicated, which need to be thoroughly characterized through functional studies in the future.

Data availability statement

The datasets presented in this study can be found in online repositories. The raw RNA sequences were deposited in NCBI SRA Database under BioProject accession number PRJNA1007393.

Author contributions

ZH: Conceptualization, Data curation, Formal Analysis, Visualization, Writing – original draft. JP: Data curation, Software, Validation, Writing – review & editing. KY: Data curation, Writing – review & editing. YZ: Conceptualization, Supervision, Writing – review & editing. ZY: Conceptualization, Supervision, Writing – review & editing. JG: Supervision, Writing – review & editing. HJ: Writing – review & editing, Conceptualization, Funding acquisition.

Funding

The author(s) declare financial support was received for the research, authorship, and/or publication of this article. We thank National Natural Science Foundation of China (grant number: 32272597), the Postgraduate Research & Practice Innovation Program of Jiangsu Province (KYCX23_0830), and Jiangsu Institute of Botany Talent Fund (JIBTF202212) for financial supports of this research.

Conflict of interest

The authors declare that the research was conducted in the absence of any commercial or financial relationships that could be construed as a potential conflict of interest.

Publisher's note

Supplementary material

The Supplementary material for this article can be found online at: https://www.frontiersin.org/articles/10.3389/fmicb.2023.1266045/full#supplementary-material

References

Aynardi, B. A., Jiménez-Gasco, M. M., and Uddin, W. (2019). Effects of isolates of Clarireedia jacksonii and Clarireedia monteithiana on severity of dollar spot in turfgrasses by host typ e. *Eur. J. Plant Pathol.* 155, 817–829. doi: 10.1007/s10658-019-01813-z

Bolton, M. D., Ebert, M. K., Faino, L., Varas, V. R., Jonge, R., Peer, Y. V., et al. (2016). RNA-sequencing of Cercospora beticola DMI-sensitive and-resistant isolates after treatment with tetraconazole identifies common and contrasting pathway induction. *Fungal Genet. Biol.* 92, 1–13. doi: 10.1016/j.fgb.2016.04.003

Bu, D., Luo, H., Huo, P., Wang, Z., Zhang, S., He, Z., et al. (2021). KOBAS-i: intelligent prioritization and exploratory visualization of biological functions for gene enrichment analysis. *Nucleic Acids Res.* 49, 317–325.

Fan, Y., Wang, Y., Korfanty, G. A., Archer, M., and Xu, J. (2021). Genome-wide association analysis for triazole resistance in Aspergillus fumigatus. *Pathogens* 10:701. doi: 10.3390/pathogens10060701

Godinho, C. P., Mira, N. P., Cabrito, T. R., Teixeira, M. C., Alasoo, K., Guerreiro, J., et al. (2017). Yeast response and tolerance to benzoic acid involves the Gcn 4-and Stp1-regulated multidrug/multixenobiotic resistance transporter Tpo1. *Appl. Microbiol. Biotechnol.* 101, 5005–5018. doi: 10.1007/s00253-017-8277-6

Hu, J., Deng, S., Gao, T., Lamour, K., Liu, X., and Ren, H. (2018). Thiophanate-methyl resistance in Sclerotinia homoeocarpa from golf courses in China. *Pestic. Biochem. Physiol.* 152, 84–89. doi: 10.1016/j.pestbp.2018.09.004

Hu, J., Zhou, Y. X., Gao, T., Geng, J. M., Dai, Y., Ren, H. Y., et al. (2019a). Resistance risk assessment for fludioxonil in Sclerotinia homoeocarpa in China. *Pestic. Biochem. Physiol.* 156, 123–128. doi: 10.1016/j.pestbp.2019.02.011

Hu, J., Zhou, Y. X., Geng, J. M., Dai, Y., Ren, H. Y., and Lamour, K. (2019b). A new dollar spot disease of turfgrass caused by Clarireedia paspali. *Mycol. Prog.* 18, 1423–1435. doi: 10.1007/s11557-019-01526-x

Hulvey, J., Popko, J. T. Jr., Sang, H., Berg, A., and Jung, G. (2012). Overexpression of ShCYP51B and ShatrD in Sclerotinia homoeocarpa isolates exhibiting practical field resistance to a demethylation inhibitor fungicide. *Appl. Environ. Microbiol.* 78, 6674–6682. doi: 10.1128/AEM.00417-12

Ihunnah, C. A., Jiang, M., and Xie, W. (2011). Nuclear receptor PXR, transcriptional circuits and metabolic relevance. *Biochim. Biophys. Acta* 1812, 956–963.

Jo, Y. K., Niver, A. L., Rimelspach, J. W., and Boehm, M. J. (2006). Fungicide sensitivity of Sclerotinia homoeocarpa from golf courses in Ohio. *Plant Dis.* 90, 807–813. doi: 10.1094/PD-90-0807

Kim, D., Langmead, B., and Salzberg, S. L. (2015). HISAT: a fast spliced aligner with low memory requirements. *Nat. Methods* 12, 357–360. doi: 10.1038/nmeth.3317

Koch, P. L., Grau, C. R., Jo, Y. K., and Jung, G. (2009). Thiophanate-methyl and propiconazole sensitivity in Sclerotinia homoeocarpa populations from golf courses in Wisconsin and Massachusetts. *Plant Dis.* 93, 100–105. doi: 10.1094/PDIS-93-1-0100

Kretschmer, M., Leroch, M., Mosbach, A., Walker, A. S., Fillinger, S., Mernke, D., et al. (2009). Fungicide-driven evolution and molecular basis of multidrug resistance in field populations of the grey mould fungus Botrytis cinerea. *PLoS Pathog.* 5:e1000696. doi: 10.1371/journal.ppat.1000696

Kumar, S., Stecher, G., and Tamura, K. (2016). MEGA7: molecular evolutionary genetics analysis version 7.0 for bigger datasets. *Mol. Biol. Evol.* 33, 1870–1874. doi: 10.1093/molbev/msw054

Latin, R. (2011). *A Practical Guide to Turfgrass Fungicides*. St. Paul, MN: American Phytopathological Society

Lee, J. W., Choi, J., and Kim, J. W. (2017). Triazole fungicides sensitivity of Sclerotinia homoeocarpa in Korean golf courses. *Plant Pathol. J.* 33, 589–596. doi: 10.5423/PPJ.OA.06.2017.0114

Leroux, P., Gredt, M., Remuson, F., Micoud, A., and Walker, A. S. (2012). Fungicide resistance status in French populations of the wheat eyespot fungi Oculimacula acuformis and Oculimacula yallundae. *Pest Manag. Sci.* 69, 15–26.

Love, M., Huber, W., and Anders, S. (2014). Moderated estimation of fold change and dispersion for RNA-seq data with DESeq2. *Genome Biol.* 15:550.

Miller, G. L., Stevenson, K. L., and Burpee, L. L. (2002). Sensitivity of Sclerotinia homoeocarpa isolates to propiconazole and impact on control of dollar spot. *Plant Dis.* 86, 1240–1246. doi: 10.1094/PDIS.2002.86.11.1240

Moktali, V., Park, J., Fedorova-Abrams, N. D., Park, B., Choi, J., Lee, Y. H., et al. (2012). Systematic and searchable classification of cytochrome P450 proteins encoded by fungal and oomycete genomes. *BMC Genomics* 13:525.

Nakaune, R., Hamamoto, H., Imada, J., Akutsu, K., and Hibi, T. (2002). Genomics: a novel ABC transporter gene, PMR5, is involved in multidrug resistance in the phytopathogenic fungus Penicillium digitatum. *Mol. Gen. Genomics.* 267, 179–185. doi: 10.1007/s00438-002-0649-6

Nakaune, R., and Nakano, M. (2007). Benomyl resistance of Colletotrichum acutatum is caused by enhanced expression of β-tubulin 1 gene regulated by putative leucine zipper protein CaBEN1. *Fungal Genet. Biol.* 44, 1324–1335. doi: 10.1016/j.fgb.2007.03.007

Omrane, S., Sghyer, H., Audéon, C., Lanen, C., Duplaix, C., Walker, A., et al. (2015). Fungicide efflux and the MgMFS1 transporter contribute to the multidrug resistance phenotype in Zymoseptoria tritici field isolates. *Environ. Microbiol.* 17, 2805–2823. doi: 10.1111/1462-2920.12781

Popko, J. T. Jr., Ok, C. H., Campbell-Nelson, K., and Jung, G. (2012). The association between in vitro propiconazole sensitivity and field efficacy of five new England Sclerotinia homoeocarpa populations. *Plant Dis.* 96, 552–561. doi: 10.1094/PDIS-06-11-0524

Popko, J. T. Jr., Sang, H., Lee, J., Yamada, T., Hoshino, Y., and Jung, G. (2018). Resistance of Sclerotinia homoeocarpa field isolates to succinate dehydrogenase inhibitor fungicides. *Plant Dis.* 102, 2625–2631. doi: 10.1094/PDIS-12-17-2025-RE

Salgado-Salazar, C., Beirn, L. A., Ismaiel, A., Boehm, M. J., Carbone, I., Putman, A., et al. (2018). Clarireedia: A new fungal genus comprising four pathogenic species responsible for dollar spot disease of turfgrass. *Fungal Biol.* 122, 761–773. doi: 10.1016/j.funbio.2018.04.004

Sang, H., Chang, H. X., Choi, S., Son, D., Lee, G., and Chilvers, M. I. (2021). Genome-wide transcriptional response of the causal soybean sudden death syndrome pathogen Fusarium virguliforme to a succinate dehydrogenase inhibitor fluopyram. *Pest Manag. Sci.* 78, 530–540.

Sang, H., Hulvey, J. P., Green, R., Xu, H., Im, J., Chang, T., et al. (2018). A xenobiotic detoxification pathway through transcriptional regulation in filamentous fungi. *MBio* 9, e00457–e00418.

Sang, H., Hulvey, J. P., Popko, J. T. Jr., Lopes, J., Swaminathan, A., Chang, T., et al. (2015). A pleiotropic drug resistance transporter is involved in reduced sensitivity to multiple fungicide classes in Sclerotinia homoeocarpa (F.T. Bennett). *PMol. Plant Pathol.* 16, 251–261. doi: 10.1111/mpp.12174

Sang, H., Popko, J. T. Jr., Chang, T., and Jung, G. (2016). Molecular mechanisms involved in qualitative and quantitative resistance to the dicarboximide fungicide iprodione in Sclerotinia homoeocarpa field isolates. *Phytopathology* 107, 198–207.

Schoonbeek, H., Sorbo, G. D., and Waard, M. (2001). The ABC transporter BcatrB affects the sensitivity of Botrytis cinerea to the phytoalexin resveratrol and the fungicide fenpiclonil. *Mol. Plant-Microbe Interact.* 14, 562–571. doi: 10.1094/MPMI.2001.14.4.562

Stephens, C. M., and Kaminski, J. (2019). In vitro fungicide-insensitive profiles of Sclerotinia homoeocarpa populations from Pennsylvania and the surrounding region. *Plant Dis.* 103, 214–222. doi: 10.1094/PDIS-07-18-1149-RE

Thakur, J. K., Arthanari, H., Yang, F., Pan, S. J., Fan, X., Breger, J., et al. (2008). A nuclear receptor-like pathway regulating multidrug resistance in fungi. *Nature* 452, 604–609. doi: 10.1038/nature06836

Viji, G., Uddin, W., O'Neill, N. R., Mischke, S., and Saunders, J. A. (2004). Genetic diversity of Sclerotinia homoeocarpa isolates from turfgrasses from various regions in North America. *Plant Dis.* 88, 1269–1276. doi: 10.1094/PDIS.2004.88.11.1269

Wang, Z. Q., Meng, F. Z., Zhang, M. M., Yin, L. F., Yin, W. X., Lin, Y., et al. (2018). A putative Zn_2Cy_6 transcription factor is associated with isoprothiolane resistance in magnaporthe oryzae. *Front. Microbiol.* 9:2608.

Xu, C., Li, Y. T., and Kong, A. J. (2005). Induction of phase I, II and III drug metabolism/transport by xenobiotics. *Arch. Pharm. Res.* 28, 249–268. doi: 10.1007/BF02977789

Young, M., Wakefield, M. J., Smyth, G. K., and Oshlack, A. (2021). Gene ontology analysis for RNA-seq: accounting for selection bias. *Genome Biol.* 11:R14.

Zhang, H. W., Dong, Y. L., Jin, P. Y., Hu, J., Lamour, K., and Yang, Z. M. (2023). Genome resources for four Clarireedia species causing dollar spot on diverse turfgrasses. *Plant Dis.* 107, 929–934. doi: 10.1094/PDIS-08-22-1921-A

Zhang, H. W., Dong, Y. L., Zhou, Y. X., Hu, J., Lamour, K., and Yang, Z. M. (2022). Clarireedia hainanense: a new species is associated with dollar spot of turfgrass in Hainan, China. *Plant Dis.* 106, 996–1002. doi: 10.1094/PDIS-08-21-1853-RE

Zhang, H. W., Jiang, S., Zhao, Z., Guan, J., and Yang, Z. M. (2021). Fungicide sensitivity of Clarireedia spp. isolates from golf courses in China. *Crop Prot.* 149:105785. doi: 10.1016/j.cropro.2021.105785

frontiers | Frontiers in Microbiology

TYPE Original Research
PUBLISHED 06 October 2023
DOI 10.3389/fmicb.2023.1279630

OPEN ACCESS

EDITED BY
Vijay Soni,
NewYork-Presbyterian, United States

REVIEWED BY
Tushar Dhanani,
Florida Agricultural and Mechanical University, United States
Biplab Singha,
University of Massachusetts Medical School, United States

*CORRESPONDENCE
Ping Qian
qianp@mail.hzau.edu.cn

RECEIVED 18 August 2023
ACCEPTED 18 September 2023
PUBLISHED 06 October 2023

CITATION
Xiong Z, Hong Z, Li X, Gao D, Wang L, Liu S, Zhao J, Li X and Qian P (2023) The multidrug-resistant *Pseudomonas fluorescens* strain: a hidden threat in boar semen preservation. *Front. Microbiol.* 14:1279630. doi: 10.3389/fmicb.2023.1279630

The multidrug-resistant *Pseudomonas fluorescens* strain: a hidden threat in boar semen preservation

Zhixuan Xiong[1,2,3], Ziqiang Hong[1,2,3], Xinxin Li[1,2,3], Dongyang Gao[1,2,3], Linkang Wang[1,2,3], Shudan Liu[1,2,3], Junna Zhao[1,2,3], Xiangmin Li[1,2,3] and Ping Qian[1,2,3]*

[1]National Key Laboratory of Agricultural Microbiology, Hubei Hongshan Laboratory, Huazhong Agricultural University, Wuhan, Hubei, China, [2]College of Veterinary Medicine, Huazhong Agricultural University, Wuhan, Hubei, China, [3]Key Laboratory of Preventive Veterinary Medicine in Hubei Province, The Cooperative Innovation Center for Sustainable Pig Production, Wuhan, Hubei, China

Although the bacterial composition of boar ejaculate has been extensively studied, the bacterial composition of extended boar semen is often overlooked, despite the potential risks these microorganisms may pose to the long-term preservation of extended boar semen at 15–17°C. In this study, we characterized the bacterial community composition of extended semen and discovered that *Pseudomonas* spp. was the dominant flora. The dominant strains were further isolated and identified as a potential new species in the *Pseudomonas fluorescens* group and named *GXZC* strain, which had adverse effects on sperm quality and was better adapted to growth at 17°C. Antimicrobial susceptibility testing showed that the *GXZC* strain was resistant to all commonly used veterinary antibiotics. Whole-genome sequencing (WGS) and genome annotation revealed the large genetic structure and function [7,253,751 base pairs and 6,790 coding sequences (CDSs)]. Comparative genomic analysis with the closest type strains showed that the *GXZC* strain predicted more diversity of intrinsic and acquired resistance genes to multi-antimicrobial agents. Taken together, our study highlights a problem associated with the long-term storage of extended boar semen caused by a *P. fluorescens* group strain with unique biological characteristics. It is essential to develop a new antibacterial solution for the long-term preservation of boar semen.

KEYWORDS

boar semen preservation, *Pseudomonas fluorescens*, microbial resistance, whole-genome sequencing, antibiotic resistance island

Introduction

Artificial insemination (AI) is widely used in global pig production to facilitate improvements in fertility, genetics, labor, and herd health (Knox, 2016). In pig AI, more than 99% of boar semen is stored in a nutrient-rich liquid state at 15–20°C (Johnson et al., 2000; Pezo et al., 2019). Long-term extenders are now widely used in commercial extended semen to meet the rapid development of AI and increase the flexibility of semen use, based on their ability to preserve sperm for 7–12 days after collection (Karageorgiou et al., 2016). However, the boar semen collection process is not aseptic, and freshly collected boar ejaculate often contains bacterial contamination which sources animal (e.g., feces, hair, and human) and non-animal (e.g., water, feed, and air) (Althouse et al., 2000). The bacterial composition

of boar ejaculate is complex (Althouse et al., 2000, 2008; Althouse and Lu, 2005; Godia et al., 2020; Zhang et al., 2020). Some bacterial strains isolated from boar semen have been shown to reduce sperm quality (motility, plasma membrane integrity, acrosome, etc.), such as Enterobacteriaceae family (Luis Ubeda et al., 2013), *Clostridium perfringens* (Sepulveda et al., 2013), *Pseudomonas aeruginosa* (Sepulveda et al., 2016), *Enterobacter cloacae* (Prieto-Martinez et al., 2014), *Staphylococcus aureus* (Li et al., 2017), *Proteus mirabilis* (Gao et al., 2018), and *Proteus vulgaris* (Delgado-Bermudez et al., 2020). Previous studies have reported bacterial thresholds between $\times 10^3$ and $\times 10^7$ CFU/ml before adverse effects on sperm quality or fertility become apparent (Auroux et al., 1991; Diemer et al., 1996; Bussalleu et al., 2011; Sepulveda et al., 2013, 2014; Prieto-Martinez et al., 2014; Pinart et al., 2017; Delgado-Bermudez et al., 2020).

Antibiotics are commonly added to commercial extenders as the primary approach to control bacteria (Althouse et al., 2000). According to national regulatory requirements (Union, 1992; CSAMR, 2019), antibacterial substances, as essential components of commercial extenders, are strictly regulated by the requirements of local laws or regulations. Antibiotics commonly used in semen diluents include the β-lactams (penicillins, cephalosporins), aminoglycosides (gentamicin, streptomycin, and amikacin), macrolides (tylosin, spectinomycin), and lincosamides (lincomycin) (Santos and Silva, 2020). Aminoglycosides are the most commonly used antibiotics in boar semen (Mazurova and Vinter, 1991; Bryla and Trzcinska, 2015; Waberski et al., 2019).

Recently, the demand for long-term semen preservation has increased in the efficient and competitive pig industry in China. However, long-term storage in nutrient-rich container with antimicrobial agents facilitates the development of drug resistance in bacteria. The potential risks associated with bacterial contamination in long-term storage of extended boar semen cannot be ignored. Therefore, this study aimed to characterize the composition of the extended boar semen microbiome, isolate the predominant microorganisms, and explore their potential risks.

Materials and methods

Sampling processing

Three healthy and sexually mature (1–2 years of age) boars were randomly selected from the artificial insemination (AI) station of Yangxiang Farming Co., Ltd., which is a floor building with air filtration, temperature, humidity, and wind speed-controlled automatically. Boars were farmed in the same condition. The brief procedures are presented in Figure 1.

The collection and processing of ejaculates were conducted according to the minimum bacterial contamination protocol (Althouse et al., 2000). Each ejaculate was filtered through gauze to remove the gel. In total, 10 ml of ejaculate is diluted in sterile Beltsville thawing solution (BTS) to the concentration of 2.5×10^7 spermatozoa/ml (Pursel and Johnson, 1975) and seems as antibiotic-free group (detailed descriptions in the Supplementary material). Each of the remaining ejaculates was processed with the commercial manufacturing requirements of the AI station. In brief, the ejaculates diluted in Zenolong® (Beikang, Taizhou, China; with gentamicin added), to the same sperm concentration, and cooled to 17°C. Then, they were packaged in 60 ml plastic bags (IMV, Shanghai, China). Three of packaged extended semen doses of each boar were stored at 17°C for 12 days. After 0, 3, 6, 9, and 12 days of fluid storage at 17°C, the extended semen total sperm motility (TSM, including progressive motility and non-progressive motility) was measured using a computer-assisted semen analysis (CASA) system (HTR-IVOS II, Hamilton Thorne Research, Beverly, MA, United States; software settings are presented in Supplementary Table S1), and composition of bacterial community was characterized by 16S rRNA high-throughput sequencing. Considering the low bacterial concentrations which were not 16S rRNA sequenced for analysis at the early stages of stored extended semen, samples collected each time were shaken (37°C, 180 rpm) for 24 h to get the high-concentration bacterial communities and seem as group II. Previously unprocessed samples were seemed as group I.

DNA extraction and 16s rRNA high-throughput sequencing

The MagBeads Fast DNA™ Kit for Soil (MP Biomedicals, Santa Ana, CA, United States) was used to extract total genomic DNA from groups I and II. The concentration was determined using a fluorometer (Qubit Fluorometer, Invitrogen), and <0.3 ng/μl did not meet the detection requirements. The samples were discarded.

PCR amplification of the bacterial 16S rRNA gene V3-V4 region was performed using the forward primer 338F and reverse primer 806R (Chen et al., 2017; Hu et al., 2018). The PCR products were purified using the QIAquick PCR Purification Kit (Qiagen, China), followed by end-repair mix and incubation at 20°C for 30 min. The end-repaired DNA was, then, purified, followed by A-tail mix and incubation at 37°C for 30 min. The purified adenylated 3′-end DNA was combined with adapter and ligation mix, and the ligation reaction was incubated at 16°C for 12–16 h. Adapter-ligated DNA was selected by running a 2.5% agarose gel for approximately 2.5 to 3 h to recover the target fragments. The gel is purified using QIAquick Gel Extraction Kit (Qiagen, China). The final library was quantified using two methods: determining the average molecular length using the Agilent 2100 Bioanalyzer instrument and quantifying the library by real-time quantitative PCR (qPCR) (TaqMan Probe). The raw reads were filtered to remove adaptors and low-quality and ambiguous bases. The paired-end reads were, then, merged to the tags using the Fast Length Adjustment of SHort reads (FLASH) (version 1.2.11, http://ccb.jhu.edu/software/FLASH/) (Magoc and Salzberg, 2011). These tags were clustered into operational taxonomic units (OTUs) at a 97% cutoff value using UPARSE software (version 7.0.1090, http://drive5.com/uparse/) (Edgar, 2013). Chimera sequences were detected by comparing the Gold database using UCHIME (version 4.2.40, http://drive5.com/uchime/uchime) (Edgar et al., 2011). The OTU representative sequences were, then, taxonomically classified with a minimum confidence threshold of 0.6 using the Ribosomal Database Project (RDP) Classifier (version 2.2, http://rdp.cme.msu.edu/) and trained on the Greengenes database (version 201305)

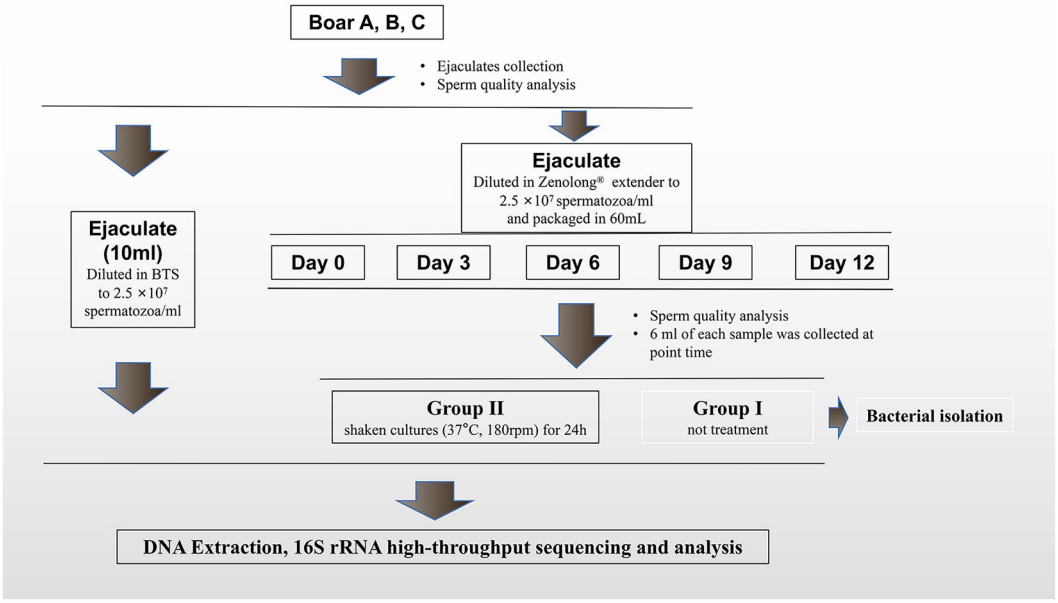

FIGURE 1
Sampling processing.

using QIIME (version 1.8, http://qiime.sourceforge.net/) (Caporaso et al., 2010). The OTU abundance statistics table of each sample was obtained by comparing all tags with the OTUs using the USEARCH global method (version 7.0.1090, http://www.drive5.com/usearch) (Edgar, 2010). Bar graphs of different classification levels were plotted using the R package (version 3.4.1).

Bacterial isolation and characterization

The samples stored for the last day of group I were inoculated on TSA and stored at 17°C and 37°C, respectively, for 36 h. Five colonies with visually distinguishable colony morphologies were picked from the 17°C and 37°C samples. These colonies were designated as GXZC-number. The single primary colony was continuously purified for three passages. The resulting colonies were subjected to 16S DNA sequencing (Tsingke, Wuhan, China), and the sequences were identified using the BLAST (blastn) tool on the National Center for Biotechnology Information (NCBI) website (https://www.ncbi.nlm.nih.gov/).

The growth of the isolated strains was analyzed in flat-bottomed 100-well microtiter plates by measuring the optical density at 600 nm (OD600) every 30 min using the Bioscreen C system (Labsystems Oy, Helsinki, Finland) with shaking (180 rpm) at 17°C, 27°C, and 37°C.

Antimicrobial susceptibility testing was performed according to the Clinical Laboratory Standards Institute (CLSI) guidelines using the Kirby–Bauer agar diffusion or microdilution method (CLSI, 2022). Standard strains of *Escherichia coli* ATCC 25922 and *Pseudomonas aeruginosa* ATCC 27853 were used for quality control. Susceptibility testing was conducted against ampicillin, ceftiofur, cefquinome, gentamicin, neomycin, kanamycin, spectinomycin, sulfisoxazole, trimethoprim–sulfamethoxazole, doxycycline, enrofloxacin, chloramphenicol, florfenicol, tilmicosin, tiamulin, and colistin (according to the CLSI guidelines, the microdilution method is acceptable, and disk diffusion methods should not be performed for colistin). These antibiotics are commonly used as veterinary drugs (CSAMR, 2019). CLSI (2018, 2022) and European Committee on Antimicrobial Susceptibility Testing EUCAST (2022) criteria only provide minimum inhibitory concentration (MIC) for gentamicin, sulfisoxazole, doxycycline, and chloramphenicol. For the remaining 12 antibiotics, zone diameter and MIC breakpoints were not provided, and thus, the results are presented as zone diameter or MIC (colistin) values.

Assessment of the effect of isolated strains on boar semen

The isolated strains were cultured in tryptic soy broth (TSB) (BD, Spark MD, USA) at 27°C or 37°C for 16 h in a shaking bath to assess the pathogenicity of the isolated bacteria on boar sperm. Then, strains were inoculated into the extended semen. The commercial extended semen doses (Yangxiang, Guigang, China), with a concentration of 2.5 $\times 10^7$ spermatozoa/ml, were collected from the healthy boar and divided into seven aliquots of 8 ml each. One aliquot was used as a control (non-infected samples), while the others were infected with isolated strain at the following initial bacterial concentrations (day 0): 2×10^2, 2×10^4, and 2×10^6 CFU/ml. Non-infected and infected samples were stored in sealed tubes at 17°C for 12 days. TSM was measured using the CASA

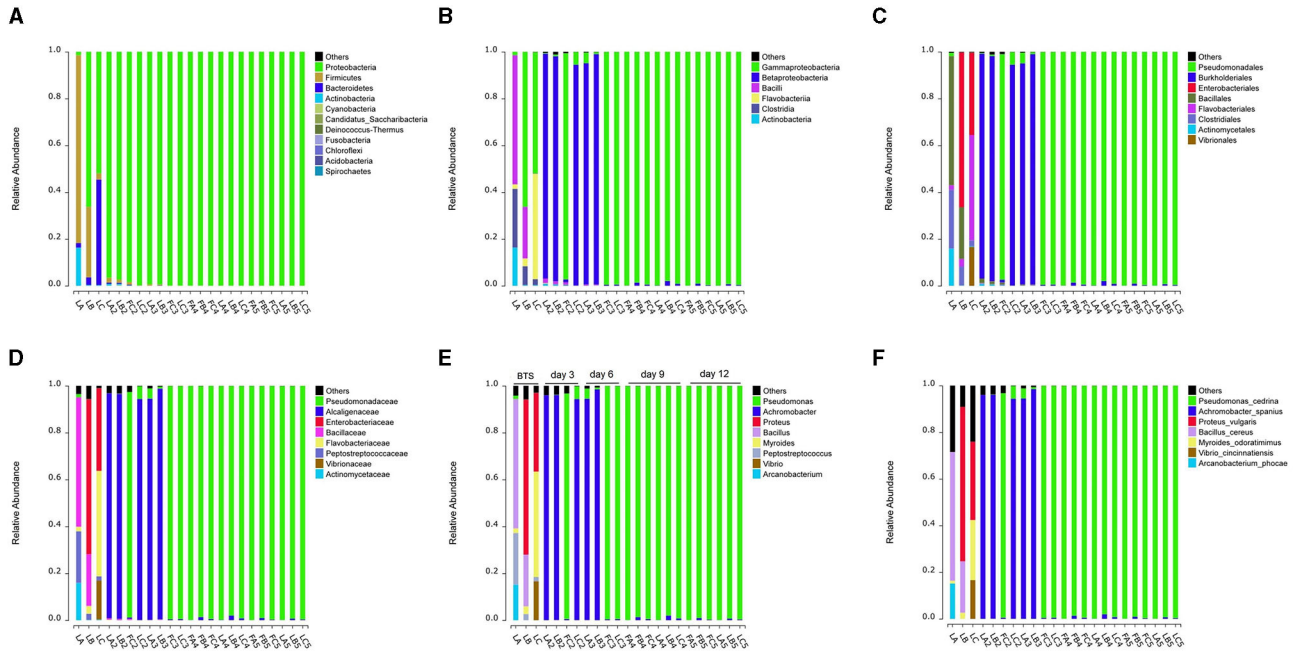

FIGURE 2
Variations in bacterial community composition of extended semen stored for days. **(A–E)** Shifts in bacterial taxonomic compositions at several taxonomic levels, including phylum **(A)**, class **(B)**, order **(C)**, family **(D)**, genus **(E)**, and species **(F)**. "LA, LB, and LC" are samples that the ejaculate was diluted in sterile BTS. All remaining are samples that the ejaculate was diluted in Zenolong®. "FC2, FC3, FA4, FB4, FC4, FA5, FB5, and FC5" are Group I in which the samples were stored at 17°C for the right time (3, 6, 9, or 12 days). Moreover, "LA, LB, LC, LA2, LB2, LC2, LA3, LB3, LC3, LA4, LB4, LC4, LA5, LB5, and LC5" are Group II in which the samples were stored in an incubator under shaking condition with 180 rpm at 37°C for 24 h after having 17°C storages. A, B, and C represent three boars, respectively; numbers 2, 3, 4, and 5 represent 3, 6, 9, and 12 days, where the extended semen was stored. "F" and "L" represent groups I and II, respectively.

system (HTR-IVOS II, Hamilton Thorne Research, Beverly, MA, United States) at 0, 2, 4, 6, 8,10, and 12 days. Simultaneously, bacterial growth was evaluated at each infectious dose and time point using plate culture with tryptic soy agar (TSA) (BD, Spark MD, United States).

Whole-genome sequencing, annotation, and gene prediction

The genome was sequenced using a combination of Illumina NovaSeq6000 (Illumina, San Diego, CA, USA) and Nanopore PromethION sequencing platforms (Oxford Nanopore Technologies, Oxford, UK). The original image data were converted into sequence data by base calling, resulting in raw reads that were saved as a FASTQ file with read sequences and quality information. After removing low-quality data using quality information statistics, the reads were assembled into a contig to generate a complete genome with seamless chromosomes and plasmids using CAUN (version 1.6) and the Hierarchical Genome Assembly Process (HGAP) (Chin et al., 2013; Koren et al., 2017). Finally, the PacBio assembly results were corrected using Illumine reads.

Glimmer (version 3.02, http://ccb.jhu.edu/software/glimmer/index.shtml) and GeneMarkS (version 4.3, http://topaz.gatech.edu/GeneMark) were used for CDS prediction (Besemer et al., 2001; Delcher et al., 2007). tRNA-scan-SE (version 2.0, http://trna.ucsc.edu/software/) was used for tRNA prediction (Chan and Lowe, 2019). Barrnap (https://github.com/tseemann/barrnap) was used for rRNA prediction.

The predicted CDSs were annotated from NCBI non-redundant (NR) (ftp://ftp.ncbi.nlm.nih.gov/blast/db/), Swiss-Prot (https://web.expasy.org/docs/swiss-prot_guideline.html), Protein families (Pfam) (http://pfam.xfam.org/), Gene Ontology (GO) (http://geneontology.org/), Clusters of Orthologous Groups (COG) (https://www.ncbi.nlm.nih.gov/research/cog/), and Kyoto Encyclopedia of Genes and Genomes (KEGG) (https://www.genome.jp/kegg/) databases using Blast2go (version 2.5, https://www.blast2go.com/), Diamond (version 0.8.35, https://github.com/bbuchfink/diamond), and HMMER (version 3.1, http://www.hmmer.org/) sequence alignment tools. Each set of query proteins was aligned with the databases, and the annotations of best-matched subjects (e-value $< 10^{-5}$) were obtained for gene annotation.

Genome-based species identification

To carry out subsequent comparative genomic analyses, we performed species identification based on whole-genome sequence using the online Type (Strain) Genome Server (TYGS) (https://tygs.dsmz.de/) (Meier-Kolthoff and Goeker, 2019) and JSpeciesWS (version3.9.8, https://jspecies.ribohost.com/jspeciesws/#analyse) (Richter et al., 2016).

10.3389/fmicb.2023.1279630

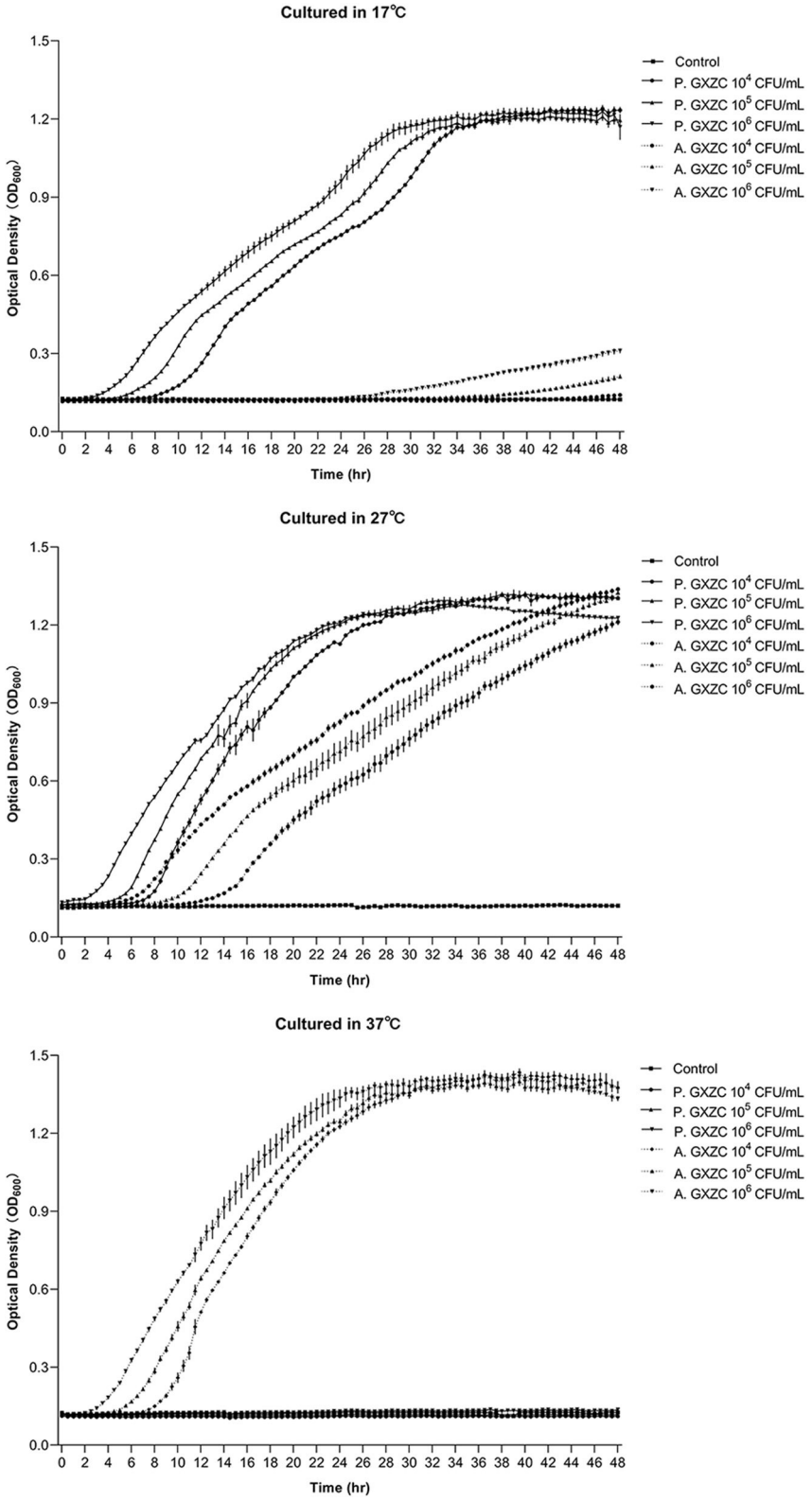

FIGURE 3
Bacterial proliferation curve at different temperature. The proliferation curve of *P. GXZC* and *A. GXZC* with inoculation of three 10-fold ratio gradient concentrations at 17°C, 27°C, and 37°C, respectively. Data are shown as mean ± SD. n = 3.

TABLE 1 Antimicrobial susceptibility testing.

Antimicrobial agent	*P. GXYX*	*A. GXYX*
Microdilution method	*MIC (μg/mL)*	
Gentamicin	R	R
Sulfisoxazole	R	R
Doxycycline	R	S
Chloramphenicol	R	S
Colistin	2048	32
Kirby–Bauer agar diffusion method	*Inhibition zone diameter (mm)*	
Ampicillin (10 μg)	0	26
Ceftiofur (30 μg)	0	0
Cefquinome (30 μg)	0	0
Gentamicin (10 μg)	0	0
Neomycin (30 μg)	10	14
Kanamycin (30 μg)	0	0
Spectinomycin (100 μg)	4	5
Sulfisoxazole (300 μg)	0	0
Trimethoprim–Sulfamethoxazole (1.25/23.75 μg)	0	0
Doxycycline (30 μg)	0	17
Enrofloxacin (10 μg)	0	14
Chloramphenicol (30 μg)	0	25
Florfenicol (30 μg)	0	27
Tilmicosin (15 μg)	0	0
Tiamulin (30 μg)	0	0

[a]R, Resistant was designated using suggested MIC breakpoints (gentamicin, ≥ 16 μg/ml; sulfisoxazole, ≥ 512 μg/ml; doxycycline, ≥ 16 μg/ml; chloramphenicol, ≥32 μg/ml) from CLSI reference for non-Enterobacteriaceae.
[b]S, Susceptible was designated using suggested MIC breakpoints (doxycycline, ≤4 μg/ml; chloramphenicol, ≤8 μg/ml) from CLSI reference for non-Enterobacteriaceae.

Antibiotic resistance genes and comparative genomics analysis

Antibiotic resistance genes were annotated and identified using the online Resistance Gene Identifier (RGI) (version 6.0.1, https://card.mcmaster.ca/analyze/rgi) (select criteria: "Perfect, Strict and Loose hits," Exclude nudge, High quality/coverage) (Alcock et al., 2022). The ResFinder software (version 4.1, https://cge.food.dtu.dk/services/ResFinder-4.1/) program (identity ≥ 80%, coverage ≥ 60%) within ResFinder data was used to identify the acquired antimicrobial resistance genes. Based on the average nucleotide identity (ANI) data and the phylogenetic tree, the closest homologs to the isolated strain were selected for resistance gene prediction and comparative analysis.

Data analysis

The data were analyzed using GraphPad Prism 8.0 (San Diego, CA, USA). The data from three independent experiments were presented as means and standard deviations (SD). TSM was compared by Duncan's multiple range tests using one-way analysis of variance (ANOVA) when the F-value was significant ($p < 0.05$). The correlation among the above-mentioned methods was evaluated by linear regression analysis.

Data availability

Whole-genome sequencing data of the *P. GXZC* strain were submitted to the NCBI (Pseudomonas sp. GXZC, assembly accession: GCF_026967615.1). The BioProject number for the complete genome sequence was PRJNA909457.

Result

Pseudomonas spp. was the dominant genus in the later stages of semen storage

After 6 months of investigation in a group with approximately 10,000 boars from three clusters of AI stations distributed throughout China, we observed a high percentage of *Pseudomonas* isolates and flora composition during the late storage stage (storage time > 9 days) of extended boar semen (data not shown). The three randomly selected boars were consistent with the previous background investigation. The extended semen of three boars also showed similar results, with a rapid decrease in total sperm motility (TSM) (Supplementary Figure S1) and an increased proportion of *Pseudomonas* spp. with increasing storage time (Figure 2).

Due to the initially low bacterial levels present in semen during the early stage of semen storage, 12 samples contained <0.3 ng/μl of genomic DNA and were discarded (Supplementary Table S2). To better comprehend the diversity of bacterial composition, the collected semen was incubated at a temperature of 37°C to facilitate rapid bacterial growth. By utilizing 16S rRNA high-throughput sequencing, we were able to partially elucidate the bacterial population, particularly in the extenders without antibiotics (BTS extender), which can be notably more complex. In conclusion, the community diversity decreased after the addition of antibiotics and after 12-day storage at 17°C (Supplementary Figure S2). In the later stages of storage (9 and 12 days), all samples were dominated by *Pseudomonas* spp. (relative abundance: 99.05%—99.86%), followed by *Achromobacter* spp. (relative abundance: 0.06%—1.95%) (Figure 2E, Supplementary Table S3).

P. GXZC strain identified as a strain of *Pseudomonas fluorescens* group with adaptation to 17°C temperature and multidrug resistance

All colony morphologies of samples inoculated on TSA were visually consistent at the same temperature. However, colony morphologies were different between 17°C and 37°C. Sequence alignment exhibited that the isolates stored at 17°C were all *Pseudomonas* spp. The sequences shared 100% identity, designated

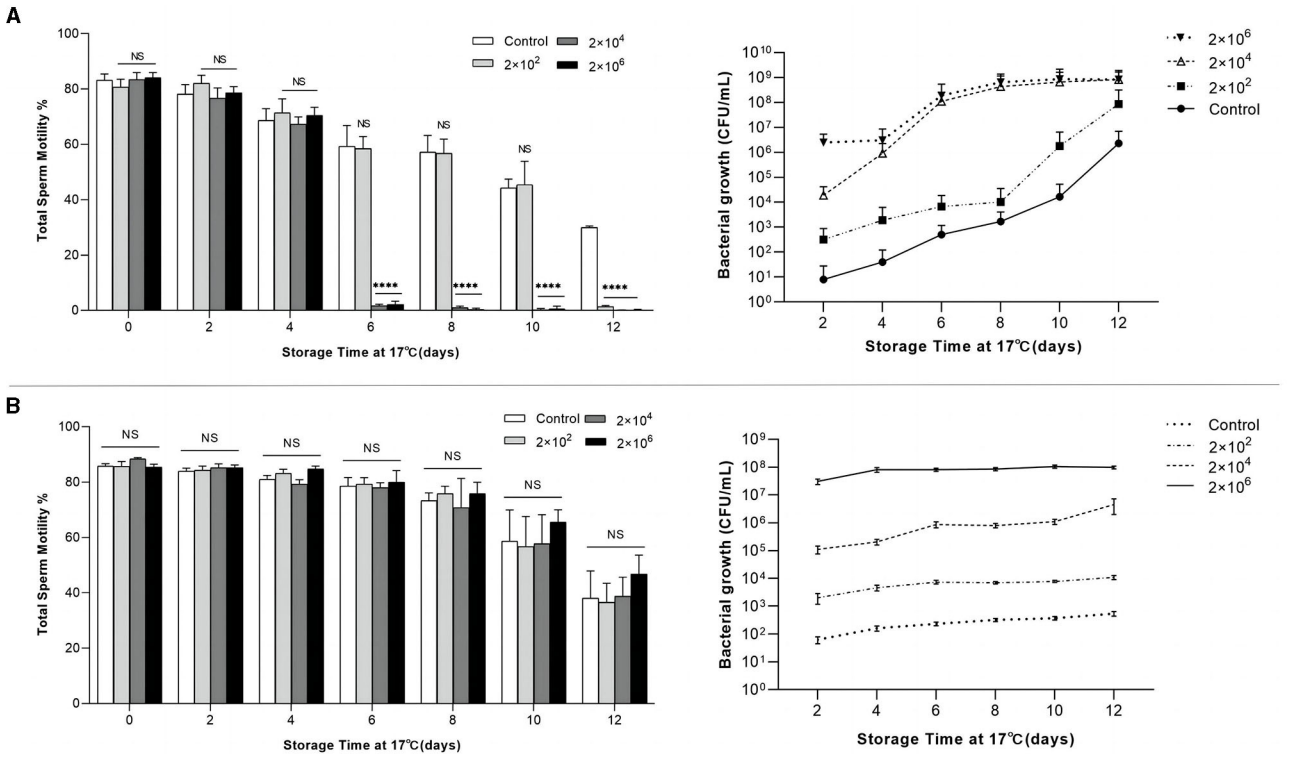

FIGURE 4
Relation of total sperm motility and bacterial growth in extended semen. Total sperm motility of extended semen incubated with different infectious concentrations (2×10^2, 2×10^4, and 2×10^6 CFU/ml) over 12 days of storage at 17°C, and bacterial growth plotted by colonies counted directly after incubating the TSA plates at 28°C for 24 h. **(A)** Incubated with P. GXYX strain. **(B)** Incubated with A. GXYX strain. Data are shown as mean ± SD. $n = 3$. "NS": no significant; $^{****}p < 0.0001$.

as *P. GXZC* strain. Similarly, the isolates stored at 37°C were all *Achromobacter* spp., and the sequences shared 100% identity, designated as *A. GXZC* strain. No other bacteria were isolated. However, it could not identify the groups or species using only 16S rRNA sequence comparisons. Multilocus sequence typing (MLST) was performed to identify the groups and species of *Pseudomonas* spp. using combined 16S rRNA, *gyrB, rpoD,* and *rpoB* sequences (Ait Tayeb et al., 2005; Mulet et al., 2009; Edgar, 2010), and *Achromobacter* spp. were identified based on 16S rRNA and *recA* sequences (Gomila et al., 2014). The sequencing primers are shown in Supplementary Table S4. *P. GXYX* was identified as *P. azotoformans* (with a threshold of 97% similarity for the species) within *P. fluorescens* group (Mulet et al., 2010), and *A. GXYX* was identified as *A. xylosoxidans* (with a threshold of 98% similarity for the species) (Gomila et al., 2014).

P. GXZC and *A. GXZC* had significantly different proliferation curves at 17°C, 27°C, and 37°C, respectively (Figure 3). At 17°C, *P. GXZC* proliferated more actively than *A. GXZC*. The strain entered the log phase from 2 to 8 h and then the stationary phase from 28 to 34 h, inoculating three 10-fold ratio gradient concentrations. Conversely, *A. GXZC* proliferation entered the log phase at the later stages of the experiment and did not enter the stationary phase until the end time. However, at 37°C, *P. GXZC* could not proliferate, while *A. GXZC* proliferation entered the log phase from 2 to 8 h and the stationary phase from 24 to 30 h. Although both isolated strains proliferated actively at 27°C, *P. GXZC* exhibited faster proliferation than *A. GXZC*, with an earlier point of entering the log and stationary phases.

Antimicrobial susceptibility testing showed that *P. GXZC* strain exhibited resistance to gentamicin, sulfisoxazole, doxycycline, and chloramphenicol (Table 1). For the 12 antibiotics lacking zone diameter or MIC breakpoints, only zone diameter or MIC values are provided (referring to the criteria of *P. aeruginosa*, *P. GXZC* strain could identify resistance to colistin).

The *P. GXZC* strain harmed sperm vitality in extended semen storage

A study has confirmed a positive correlation between pregnancy rate and semen motility (Lucca et al., 2021). Herein, the effect of *P. GXZC* strain on the vitality of sperm was determined. The growth dynamics of the *P. GXZC* and *A. GXZC* strains are shown in Figure 4 and are notably different during the 12-day storage period at 17°C. Consistent with the assessment results above, *P. GXZC* proliferates actively in extended semen at 17°C (Figure 4A). All groups inoculated with different concentration of *P. GXZC* strain reach the stationary phase at approximately 10^8 CFU/ml in liquid extended semen. The proliferation of the *P. GXZC* strain adversely affected sperm vitality in the later stages of extended semen storage. On day 6, the tube containing 2×10^6

TABLE 2 Genomic properties of P. GXZC strain.

Characteristics	Value
Genome size (bp)	7,253,751
GC content (%)	60.23
Topology	Circular
Chromosome size (bp)	7,059,625
Plasmid size (bp)	194,126
Chromosome GC content (%)	60.39
Plasmid GC content (%)	54.28
Chromosome	1
Plasmid	1
tRNA	73
rRNA (5S,16S,23S)	20
CDS (chromosome, plasmid)	6,790
Genes assigned to NR	6,765
Genes assigned to Swiss-Prot	4,902
Genes assigned to COG	5,409
Genes assigned to KEGG	2,217
Genes assigned to GO	4,756
Genes assigned to Pfam	5,691

CFU/ml or 2 × 10^4 CFU/ml of *P. GXZC* differed significantly from the negative control. On day 12, all treatments differed from the control. It seems that only when the bacteria proliferate to a certain concentration (> 10^6 CFU/ml), they show significant negative effects on sperm vitality. In contrast, *A. GXZC* proliferation was extremely slow in liquid extended semen at 17°C. Moreover, there were no differences (Figure 4B) in the TSM between the treatments and the negative control over the entire time.

Genomic characteristics of *P. GXZC* strain

The general characteristics of the P. GXZC strain genome are shown in Table 2, which consisted of 7,253,751 base pairs with an average G + C content of 60.23%. The genome contained approximately 6,790 predicted CDSs and 73 tRNA and 20 rRNA genes (8, 5S; 6, 16S; and 6, 23S) (Figure 5). The CDS numbers allocated to the different databases are presented in Table 2.

Species determination of *P. GXZC* based on whole-genome sequencing

P. GXZC strain does not belong to any species in the Type (Strain) Genome Server (TYGS) database and is potentially a new species in *P. fluorescens* group. The closest type strain genomes are *Pseudomonas canadensis* Feb-92 strain (assembly accession: GCF_026967615.1) and *Pseudomonas simiae* CCUG 50988 (assembly accession: GCF_900111895.1) (Figure 6).

The best-matching type strain is *P. canadensis* Feb-92 (assembly accession: GCF_026967615.1, type strain), with an average nucleotide identity based on BLAST+ (ANIb) data of 92.4% using the JSpeciesWS (Supplementary Table S5). We selected the four best-matching type strains with ANIb > 90%, namely, *P. canadensis* Feb-92 (assembly accession: GCF_000503215.1), *P. canadensis* PA-6-2A (assembly accession: GCF_021605905.1), *P. simiae* CCUG 50988 (assembly accession: GCF_900111895.1), and *P. simiae* PCL1751 (assembly accession: GCF_000934565.1), to conduct a comparative analysis with *P. GXZC*.

Comparative analysis of antibiotic resistance genes (ARGs)

Based on the phylogenetic tree and ANIb, the four *Pseudomonas* strains conducted a comparative analysis with *P. GXZC*. ARGs of all strains were predicted and categorized by drug classes using online RGI 6.0.1. All strains were predicted diverse and large drug-resistant genes (Table 3). However, the *GXZC* strain has more ARG hits than other comparison strains with the following drug classes: aminoglycoside antibiotic (with perfect or strict criteria only), tetracycline antibiotic, fluoroquinolone antibiotic, macrolide antibiotic, penam, cephalosporin, disinfecting agents and antiseptics, sulfonamide antibiotic, nitroimidazole antibiotic, and lincosamide antibiotic. Except for penam, all drug classes are widely used in pig farms.

Antimicrobial resistance island of *P. GXZC*

The study identified nine acquired AMR genes conferring resistance to three drug classes of antibiotics in the chromosome of the *GXZC* strain using ResFinder 4.1 (Table 4). Four other close-type strains were unidentified. *P. GXZC* strain accepted nine acquired AMR genes conferring resistance to aminoglycoside antibiotics. Aminoglycosides are the most commonly used antibacterial additives in extended boar semen.

Using IslandViewer 4 with the IslandPath-DIMOB method (Bertelli et al., 2017), we identified 15 gene islands (GI) in the chromosome. One acquired AMR is located in one GI. The other eight acquired AMR genes were clustered in another 81.6-kb GI. This GI contains three types of mobile genetic elements, two integrons, three IS elements, and two transposons (Figure 7). This antimicrobial resistance island structure represents the potential for rapidly acquiring resistance markers under antimicrobial pressure. Alignment with MAUVE (version 1.1.3) revealed that similar GI structures are absent at the homologous location of the other two best-matching type strains (Figure 7).

Discussion

Our study reviewed previous experiments on the assessment of semen quality during long-term preservation (Huo et al., 2002; Dube et al., 2004; Bussalleu et al., 2017; Shaoyong et al., 2019; Li et al., 2022), and we found that sperm motility analysis is the most widely used and effective method. In commercial extended

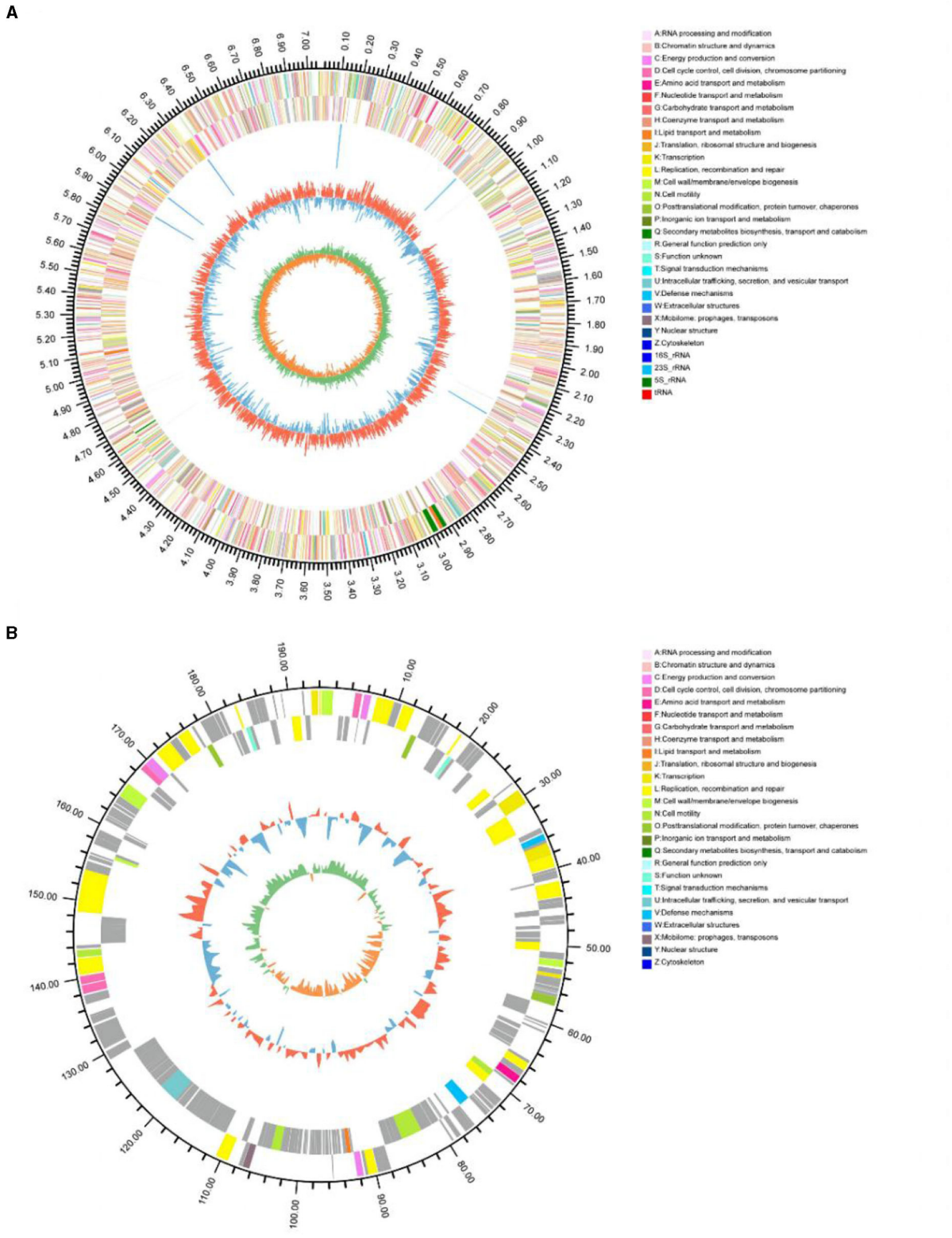

FIGURE 5
Circular representation of the *P. GXZC* genome structure. **(A)** Circular representation of chromosome; **(B)** Circular representation of plasmid. The outermost circle of the diagram is the genome size identification; the second and third circles are CDS on positive and negative strands, and different colors indicate the functional classification of different COGs of CDS; the fourth circle is rRNA, tRNA; the fifth circle is GC content, the outer red part indicates that the GC content of the region is higher than the (average GC content of the whole genome, and the higher the peak indicates the larger the difference with the average GC content The innermost circle is the GC-Skew value, the specific algorithm is G-C/G+C.

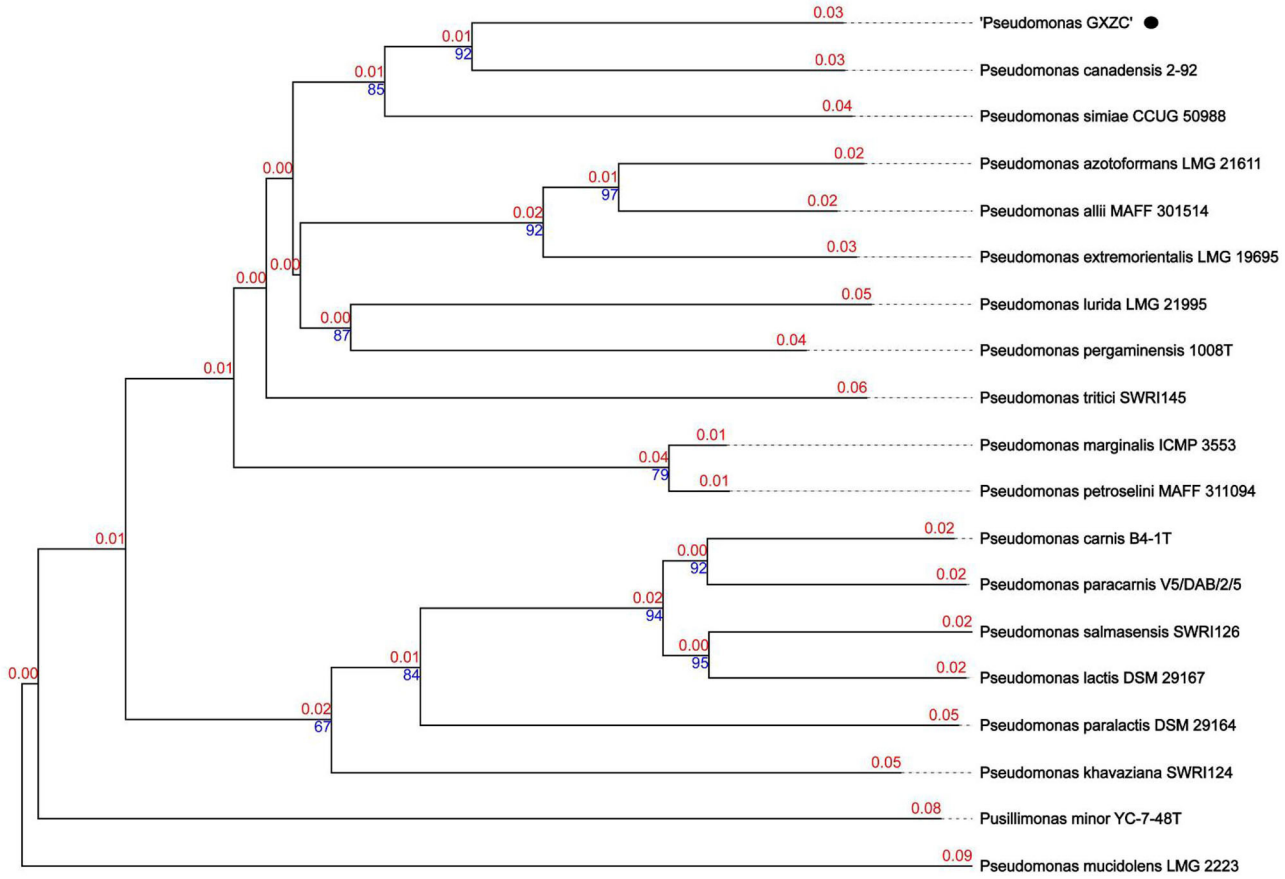

FIGURE 6
Phylogenetic relationships of *P. GXZC* whole genome was conducted in Type (Strain) Genome Server (TYGS) (date: 02 March 2023).

semen production, TSM analysis performed by CASA is essential for quality control (Amann and Waberski, 2014). To simplify the evaluation of our experiments and facilitate statistical analysis, TSM analysis was exclusively used in our research.

Although various factors contribute to semen deterioration in a commercial extender containing antibiotics during extended storage, microbial contamination is a significant risk factor. High-throughput sequencing revealed dynamic bacterial proliferation during extended semen storage. *Pseudomonas* spp. was observed to gradually become the dominant flora in 12-day long-term semen storage. The result appears to be relative to an environment of 17°C and antibiotic supplements.

Pseudomonas is one of the most complex bacterial genus and comprises the largest number of gram-negative bacteria species (Gomila et al., 2015). Many isolations initially identified as "*P. fluorescens* species" are now reclassified as "*P. fluorescens* species complex" (Scales et al., 2014) or *P. fluorescens* intrageneric groups based on MLST (Mulet et al., 2010). MLST is a rapid genotyping method, but it has low resolution and is insufficient for species typing for *P. fluorescens* group to perform comparative genomic analysis. With the phylogenetic tree and ANIb database on WGS (Richter et al., 2016), *P. GXZC* strain was identified as a potential new species in *Pseudomonas fluorescens* group eventually. WGS is a gold standard method to identify *Pseudomonas* species (Tohya et al., 2022).

Most members of the *P. fluorescens* species complex (from the environment) optimum growth temperature are <30 °C, and their growth decreases as temperature rises above 30°C (Buchon et al., 2000; Zhang et al., 2019). This species complex is the most frequently reported "psychrotrophic bacteria" in cold-stored raw fluid milk and deteriorates stored milk (Craven and Macauley, 1993; Shah, 1994; Wiedmann et al., 2000; Dogan and Boor, 2003; Gunasekera et al., 2003; Du et al., 2022). It was the primary isolated strain among all contaminants in some studies (Dogan and Boor, 2003; de Oliveira et al., 2015; Du et al., 2022). The storage environment of the extended boar semen appears to be similar to that of raw fluid milk. In our study, *P. GXZC* actively proliferated at 17°C and 27°C but did not proliferate at 37°C and entered a viable-but-not-culturable (VBNC) state (Bunker et al., 2004). This may be one of the main reasons for *P. GXZC* to be the dominant flora in the 12-day storage of extended semen experiment.

We first confirmed that the isolated strain of *P. fluorescens* had a negative effect on sperm vitality when the bacteria proliferated to a certain concentration (> 10^6 CFU/ml). The negative effect of *P. fluorescens* on sperm motility is concentration-dependent. The characteristic may be related to sperm damage caused by bacterial outer membrane vesicles (OMVs) or lipopolysaccharide

10.3389/fmicb.2023.1279630

TABLE 3 Summary of predicted ARGs categorized by drug classes using Resistance Gene Identifier (RGI).

RGI criteria[a]	Drug class	*P. GXZC*[b]	*P. canadensis* PA-6-2A	*P. canadensis* Feb-92	*P. simiae* CCUG 50988	*P. simiae* PCL1751
Perfect	**Aminoglycoside antibiotic**	3	0	0	0	0
Strict	**Aminoglycoside antibiotic**	1	0	0	0	0
	Cephalosporin	1	1	1	1	1
	Disinfecting agents and antiseptics	1	1	1	1	1
	Fluoroquinolone antibiotic	5	6	5	5	5
	Glycopeptide antibiotic	1	1	1	1	1
	Glycylcycline	1	1	1	1	1
	Penam	1	1	1	1	1
	Phenicol antibiotic	1	1	1	1	1
	Phosphonic acid antibiotic	1	1	1	0	0
	Rifamycin antibiotic	1	1	1	1	1
	Tetracycline antibiotic	5	5	4	1	4
Loose	**Tetracycline antibiotic**	187	181	178	171	169
	Fluoroquinolone antibiotic	185	180	170	163	160
	Macrolide antibiotic	142	139	137	133	129
	Penam	113	111	108	106	102
	Aminoglycoside antibiotic	94	98	98	81	83
	Peptide antibiotic	78	74	73	69	69
	Phenicol antibiotic	77	77	68	69	68
	Cephalosporin	68	67	64	61	61
	Disinfecting agents and antiseptics	67	62	57	58	58
	Cephamycin	55	56	54	50	50
	Carbapenem	48	50	49	43	43
	Aminocoumarin antibiotic	38	43	46	41	40
	Diaminopyrimidine antibiotic	35	37	32	33	33
	Monobactam	34	36	35	33	33
	Penem	28	30	29	28	28
	Glycopeptide antibiotic	27	28	28	27	27
	Sulfonamide antibiotic	13	10	12	12	12
	Rifamycin antibiotic	12	15	13	14	14
	Glycylcycline	10	10	8	10	10
	Nitroimidazole antibiotic	8	7	7	7	7
	Lincosamide antibiotic	7	6	6	6	6
	Nucleoside antibiotic	7	6	6	5	5
	Bicyclomycin-like antibiotic	5	6	6	5	6
	Antibacterial free fatty acids	4	3	3	4	4
	Oxazolidinone antibiotic	4	4	4	4	4
	Pleuromutilin antibiotic	4	4	4	4	3
	Elfamycin antibiotic	3	4	4	4	4
	Fusidane antibiotic	3	3	3	3	3
	Mupirocin-like antibiotic	3	3	3	3	3

(Continued)

TABLE 3 (Continued)

RGI criteria[a]	Drug class	*P. GXZC*[b]	*P. canadensis* PA-6-2A	*P. canadensis* Feb-92	*P. simiae* CCUG 50988	*P. simiae* PCL1751
	Phosphonic acid antibiotic	3	15	16	13	13
	Streptogramin antibiotic	3	3	4	3	4
	Isoniazid-like antibiotic	2	4	5	2	2
	Polyamine antibiotic	1	1	1	1	1
	Salicylic acid antibiotic	1	1	1	1	1
	Streptogramin A antibiotic	1	1	2	2	2
	Streptogramin B antibiotic	1	1	1	1	1

[a]RGI Criteria: "Perfect, Strict, Loose" have been mentioned in the published articles. A more technical definition of these terms refers to this website (https://github.com/arpcard/rgi/issues/140).
[b]Plasmid sequences of the P. GXZC strain were not predicted ARG hits using the same criteria in CARD.

TABLE 4 Acquired antibiotic resistance genes predicted using ResFinder 4.1.

Class	Resistance gene	Phenotype	Location	Gene position	Identity (%)	GI position
Aminoglycoside	aph(3")-Ib	Streptomycin	Chromosome	398950–399753		(364961–446597)
	aph(6)-Id	Streptomycin		405693–406436	100.00	
	aph(3")-Ib	Streptomycin		406529–407332	100.00	
	aph(3')-Ia	Neomycin, Kanamycin, Lividomycin, Paromomycin, Ribostamycin		404542–405357	99.88	
	aph(6)-Id	Streptomycin		398114–398857	99.87	
Folate pathway antagonist	sul1	Sulfamethoxazole		415230–415844	100.00	
	sul1	Sulfamethoxazole		423055–423581	100.00	
Tetracycline	tet(G)	Doxycycline, Tetracycline		419498–420673	100.00	
Aminoglycoside	aac(3)-IId	Apramycin, Gentamicin, Tobramycin, Dibekacin, Netilmicin, Sisomicin	Chromosome	7023795–7024655	99.88	(70181560–7044848)

(LPS) (He et al., 2017; Gao et al., 2018) and the reduction in sperm protein phosphorylation levels (Sepulveda et al., 2016).

Pasteurization (70–80°C) can treat refrigerated raw milk, but for extended semen, antibiotics are one of the few options to inhibit bacterial proliferation in extended semen. However, antimicrobial susceptibility testing demonstrated that *P. GXZC* developed a high level of resistance to almost all commonly used veterinary antibiotics, including colistin, a the last resort for combating multidrug-resistant Gram-negative bacteria (MDR-GNB) (Singhal et al., 2022).

As a member of the species complex, *P. GXZC* strain has 6,790 predicted CDSs and diverse mechanisms of drug resistance. Numerous resistant phenotypes in this complex were related to intrinsic, adaptive, and acquired antimicrobial resistance mechanisms (Silverio et al., 2022). Whole-genome sequencing has revealed that the *P. GXZC* strain has more drug-resistant genes than closely related strains (identified based on WGS), which may be related to antibiotic use in extended boar semen or treating boars. Although previous studies have reported that transferable resistance mechanisms are rare in this complex, we confirmed horizontal gene transfer (HGT) of antimicrobial resistance in *P. GXZC* (Silverio et al., 2022). The mechanism of antibiotic resistance includes reduced permeability to antibiotic, antibiotic efflux, antibiotic inactivation, and antibiotic target alteration (Chopra and Roberts, 2001; Zeng and Jin, 2003; Xiao and Hu, 2012; Ashenafi et al., 2014; Chung et al., 2015; Kapoor et al., 2017). The resistance island with eight clustered resistance genes and various mobile genetic elements may indicate that these strains acquire resistance genes more rapidly than previously assumed. Our results suggest that adding antibiotics seems difficult to resolve the multidrug-resistant *P. fluorescens* strains and is an unsustainable approach to microbial control in extended semen.

P. fluorescens species complex are ubiquitous microorganisms in the environment (Scales et al., 2014). Although several previous studies have identified the presence of *P. fluorescens* in boar semen, the risks it poses in boar semen storage have not been taken seriously. This may be attributed to the past practice of storing extended semen for a short period, during which bacteria did not have sufficient time to proliferate and cause significant damage to sperm. However, with the growing adoption of commercial long-term extended semen which semen storage time shift from shorter storage durations to longer periods, the adverse effects of bacterial proliferation on extended semen storage should be given more attention. The biological characteristics exhibited by *P. GXZC*, as explored in this study, may pose a challenge for long-term semen storage. Several studies have attempted boar semen storage at 5°C

10.3389/fmicb.2023.1279630

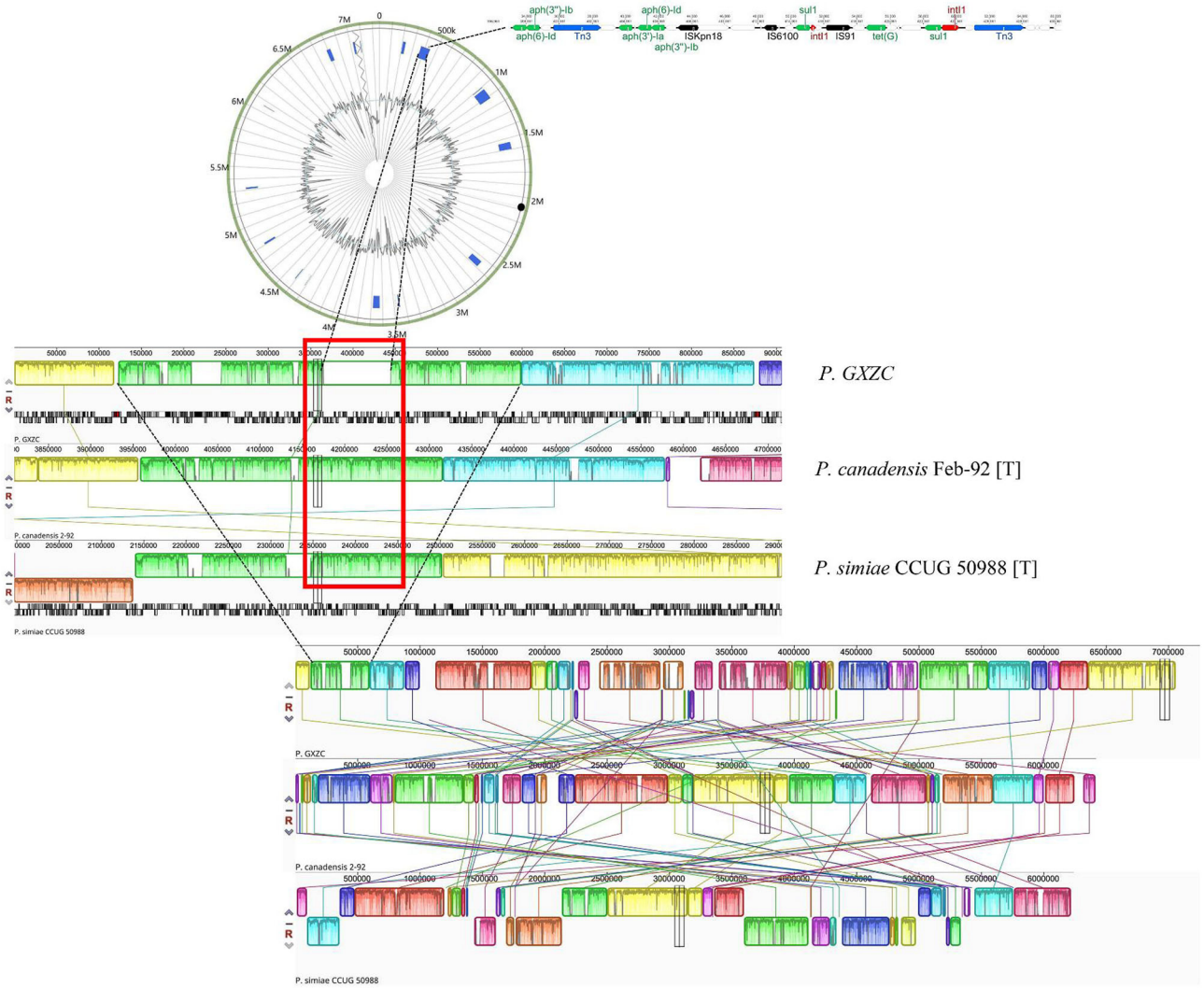

FIGURE 7
Antimicrobial resistance island of *P. GXZC* strain. Whole-genome alignment of *P. GXZC*, with two types of strains, *P. canadensis* Feb-92 and *P. simiae* CCUG 50988, is conducted using MAUVE. At the homologous site (in the red box), *P. GXZC* strain has an approximately 81kb insertion which is identified as an antimicrobial resistance island.

in the absence of antibiotics (Paschoal et al., 2020; Jakel et al., 2021), which seem to similarly consider the impact of these cold-adapted proliferating or psychrotrophic bacteria.

Conclusion

Our study identified a potential new species *GXZC* strain in *P. fluorescens* group as the dominant flora in extended boar semen. This strain exhibited adverse effects on sperm quality. The strain can better adapt to growth at a moderately low temperature (17°C) and has multidrug resistance. Whole-genome sequencing and comparative genomic analysis revealed that the strain developed devise intrinsic resistance and horizontal resistance gene transfer. The unregulated proliferation of multidrug-resistant *P. fluorescens* within commercial extenders presents potential risks to the long-term preservation of extended boar semen at 17°C and can impact the success of artificial insemination (AI) procedures. In AI facilities, heightened attention should be given to the prevalence of this type of bacterial contamination, and more effective antimicrobial and hygienic management strategies should be developed to control it.

Data availability statement

The datasets presented in this study can be found in online repositories. The names of the repository/repositories and accession number(s) can be found in the article/Supplementary material.

Ethics statement

The animal study was approved by Laboratory Animal Monitoring Committee of Huazhong Agricultural University. The study was conducted in accordance with the local legislation and institutional requirements.

Author contributions

ZX: Conceptualization, Data curation, Investigation, Methodology, Writing—original draft, Writing—review and editing. ZH: Writing—review and editing, Data curation. XinL: Writing—review and editing. DG: Writing—review and editing. LW: Writing—review and editing. SL: Data curation, Investigation, Writing—review and editing. JZ: Data curation, Investigation, Writing—review and editing. XiaL: Funding acquisition, Supervision, Writing—review and editing. PQ: Conceptualization, Writing—review and editing.

Funding

This study was supported by grants from the Yingzi Tech and Huazhong Agricultural University Intelligent Research Institute of Food Health [Nos. IRIFH202302 and IRIFH202209] and the Fundamental Research Funds for the Central Universities [2662016PY004].

Conflict of interest

The authors declare that the research was caonducted in the absence of any commercial or financial relationships that could be construed as a potential conflict of interest.

Publisher's note

All claims expressed in this article are solely those of the authors and do not necessarily represent those of their affiliated organizations, or those of the publisher, the editors and the reviewers. Any product that may be evaluated in this article, or claim that may be made by its manufacturer, is not guaranteed or endorsed by the publisher.

Supplementary material

The Supplementary Material for this article can be found online at: https://www.frontiersin.org/articles/10.3389/fmicb.2023.1279630/full#supplementary-material

References

Ait Tayeb, L., Ageron, E., Grimont, F., and Grimont, P. A. D. (2005). Molecular phylogeny of the genus pseudomonas based on rpob sequences and application for the identification of isolates. *Res. Microbiol.* 156, 763–773 doi: 10.1016/j.resmic.2005.02.009

Alcock, B. P., Huynh, W., Chalil, R., Smith, K. W., Raphenya, A. R., and Wlodarski, M. A., et al. (2022). Card 2023: expanded curation, support for machine learning, and resistome prediction at the comprehensive antibiotic resistance database. *Nucleic. Acids. Res.* 51, D690–D699. doi: 10.1093/nar/gkac920

Althouse, G., and Lu, K. (2005). Bacteriospermia in extended porcine semen. *Theriogenology* 63, 573–584. doi: 10.1016/j.theriogenology.2004.09.031

Althouse, G. C., Kuster, C. E., Clark, S. G., and Weisiger, R. M. (2000). Field investigations of bacterial contaminants and their effects on extended porcine semen. *Theriogenology* 53, 1167–1176. doi: 10.1016/S0093-691X(00)00261-2

Althouse, G. C., Pierdon, M. S., and Lu, K. G. (2008). Thermotemporal dynamics of contaminant bacteria and antimicrobials in extended porcine semen. *Theriogenology* 70, 1317–1323. doi: 10.1016/j.theriogenology.2008.07.010

Amann, R. P., and Waberski, D. (2014). Computer-assisted sperm analysis (casa): capabilities and potential developments. *Theriogenology* 81, 5–17. doi: 10.1016/j.theriogenology.2013.09.004

Ashenafi, M., Ammosova, T., Nekhai, S., and Byrnes, W. M. (2014). Purification and characterization of aminoglycoside phosphotransferase aph(6)-id, a streptomycin-inactivating enzyme. *Mol. Cell. Biochem.* 387, 207–216. doi: 10.1007/s11010-013-1886-1

Auroux, M., Jacques, L., Mathieu, D., and Auer, J. (1991). Is the sperm bacterial ratio a determining factor in impairment of sperm motility—an *in vitro* study in man with escherichia-coli. *Int. J. Androl.* 14, 264–270. doi: 10.1111/j.1365-2605.1991.tb01091.x

Bertelli, C., Laird, M. R., Williams, K. P., Lau, B. Y., Hoad, G., and Winsor, G. L., et al. (2017). Islandviewer 4: expanded prediction of genomic islands for larger-scale datasets. *Nucleic Acids Res.* 45, W30–W35. doi: 10.1093/nar/gkx343

Besemer, J., Lomsadze, A., and Borodovsky, M. (2001). Genemarks: a self-training method for prediction of gene starts in microbial genomes. Implications for finding sequence motifs in regulatory regions. *Nucleic. Acids. Res.* 29, 2607–2618. doi: 10.1093/nar/29.12.2607

Bryla, M., and Trzcinska, M. (2015). Quality and fertilizing capacity of boar spermatozoa during liquid storage in extender supplemented with different antibiotics. *Anim. Reprod. Sci.* 163, 157–163. doi: 10.1016/j.anireprosci.2015.11.005

Buchon, L., Laurent, P., Gounot, A., and Guespin-Michel, J. (2000). Temperature dependence of extracellular enzymes production by psychrotrophic and psychrophilic bacteria. *Biotechnol. Lett.* 22, 1577–1581. doi: 10.1023/A:1005641119076

Bunker, S. T., Bates, T. C., and Oliver, J. D. (2004). Effects of temperature on detection of plasmid or chromosomally encoded gfp- and lux-labeled pseudomonas fluorescens in soil. *Environ. Biosafety Res.* 3, 83–90. doi: 10.1051/ebr:2004008

Bussalleu, E., Sancho, S., Briz, M. D., Yeste, M., and Bonet, S. (2017). Do antimicrobial peptides pr-39, pmap-36 and pmap-37 have any effect on bacterial growth and quality of liquid-stored boar semen? *Theriogenology* 89, 235–243. doi: 10.1016/j.theriogenology.2016.11.017

Bussalleu, E., Yeste, M., Sepúlveda, L., Torner, E., Pinart, E., and Bonet, S. (2011). Effects of different concentrations of enterotoxigenic and verotoxigenic e. Coli on boar sperm quality. *Anim. Reprod. Sci.* 127, 176–182. doi: 10.1016/j.anireprosci.2011.07.018

Caporaso, J. G., Kuczynski, J., Stombaugh, J., Bittinger, K., Bushman, F. D., and Costello, E. K., et al. (2010). Qiime allows analysis of high-throughput community sequencing data. *Nat. Methods.* 7, 335–336. doi: 10.1038/nmeth.f.303

Chan, P. P., and Lowe, T. M. (2019). Trnascan-se: searching for trna genes in genomic sequences. *Meth. Mol. Biol. (Clifton, N.J.).* 1962, 1–14. doi: 10.1007/978-1-4939-9173-0_1

Chen, C., Song, X., Wei, W., Zhong, H., Dai, J., and Lan, Z., et al. (2017). The microbiota continuum along the female reproductive tract and its relation to uterine-related diseases. *Nat. Commun.* 8, 875. doi: 10.1038/s41467-017-00901-0

Chin, C., Alexander, D. H., Marks, P., Klammer, A. A., Drake, J., and Heiner, C., et al. (2013). Nonhybrid, finished microbial genome assemblies from long-read smrt sequencing data. *Nat. Methods.* 10, 563. doi: 10.1038/nmeth.2474

Chopra, I., and Roberts, M. (2001). Tetracycline antibiotics: mode of action, applications, molecular biology, and epidemiology of bacterial resistance. *Microbiol. Mol. Biol. Rev. Mmbr.* 65, 232–260. doi: 10.1128/MMBR.65.2.232-260.2001

Chung, H., Kim, K., Hong, S. S., Hong, S. G., Lee, K., and Chong, Y. (2015). The sul1 gene in stenotrophomonas maltophilia with high-level

resistance to trimethoprim/sulfamethoxazole. *Ann. Lab. Med.* 35, 246–249. doi: 10.3343/alm.2015.35.2.246

CLSI (2018). *Performance Standards for Antimicrobial Disk and Dilution Susceptibility Tests for Bacteria Isolated from Animals [(5th ed.), CLSI VET01ed., Vol.]* Wayne, PA: Clinical and Laboratory Standards Institute.

CLSI (2022). *Performance Standards for antimicrobial susceptibility testing ((30th ed.), CLSI supplement M100ed., Vol.)*. Wayne, PA, USA: Clinical and Laboratory Standards Institute. (Reprinted.

Craven, H. M., and Macauley, B. J. (1993). Microorganisms in pasteurised milk after refrigerated storage. I. Identification of types. *Aust. J. Dairy Technol.* 47, 38–45

CSAMR (2019). National food safety standard maximum residue limits of veterinary drugs in foods (GB 31650-2019 ed., Vol.). Beijing, China: China State Administration For Marketregulation.

de Oliveira, G. B., Favarin, L., Luchese, R. H., and McIntosh, D. (2015). Psychrotrophic bacteria in milk: how much do we really know? *Braz. J. Microbiol.* 46, 313–321. doi: 10.1590/S1517-838246220130963

Delcher, A. L., Bratke, K. A., Powers, E. C., and Salzberg, S. L. (2007). Identifying bacterial genes and endosymbiont dna with glimmer. *Bioinformatics* 23, 673–679. doi: 10.1093/bioinformatics/btm009

Delgado-Bermudez, A., Bonet, S., Yeste, M., and Pinart, E. (2020). Long-term storage of boar seminal doses contaminated with proteus vulgaris: a dose-dependent effect on sperm motility and sperm-bacteria interaction. *Anim. Reprod. Sci.* 216, 6349. doi: 10.1016/j.anireprosci.2020.106349

Diemer, T., Weidner, W., Michelmann, H., Schiefer, H., Rovan, E., and Mayer, F. (1996). Influence of escherichia coli on motility parameters of human spermatozoa *in vitro*. *Int. J. Androl.* 19, 271–277. doi: 10.1111/j.1365-2605.1996.tb00475.x

Dogan, B., and Boor, K. (2003). Genetic diversity and spoilage potentials among pseudomonas spp. Isolated from fluid milk products and dairy processing plants. *Appl. Environ. Microbiol.* 69, 130–138. doi: 10.1128/AEM.69.1.130-138.2003

Du, B., Meng, L., Liu, H., Zheng, N., Zhang, Y., and Zhao, S., et al. (2022). Diversity and proteolytic activity of pseudomonas species isolated from raw cow milk samples across china. *Sci. Total Environ.* 838. doi: 10.1016/j.scitotenv.2022.156382

Dube, C., Beaulieu, M., Reyes-Moreno, C., Guillemette, C., and Bailey, J. (2004). Boar sperm storage capacity of bts and androhep plus: viability, motility, capacitation, and tyrosine phosphorylation. *Theriogenology* 62, 874–886. doi: 10.1016/j.theriogenology.2003.12.006

Edgar, R. C. (2010). Search and clustering orders of magnitude faster than blast. *Bioinformatics* 26, 2460–2461. doi: 10.1093/bioinformatics/btq461

Edgar, R. C. (2013). Uparse: highly accurate otu sequences from microbial amplicon reads. *Nat. Methods*. 10, 996. doi: 10.1038/nmeth.2604

Edgar, R. C., Haas, B. J., Clemente, J. C., Quince, C., and Knight, R. (2011). Uchime improves sensitivity and speed of chimera detection. *Bioinformatics* 27, 2194–2200. doi: 10.1093/bioinformatics/btr381

EUCAST (2022). *Breakpoints tables for interpretation of mics and zone diameter (Version 12.0ed., Vol.).* Sweden: European Committee on Antimicrobial Susceptibility Testing.

Gao, H., Gao, Y., Yang, C., Dong, D., Yang, J., and Peng, G., et al. (2018). Influence of outer membrane vesicles of proteus mirabilis isolated from boar semen on sperm function. *Vet. Microbiol.* 224, 34–42. doi: 10.1016/j.vetmic.2018.08.017

Godia, M., Ramayo-Caldas, Y., Zingaretti, L. M., Darwich, L., Lopez, S., and Rodriguez-Gil, J. E., et al. (2020). A pilot rna-seq study in 40 pietrain ejaculates to characterize the porcine sperm microbiome. *Theriogenology* 157, 525–533. doi: 10.1016/j.theriogenology.2020.08.001

Gomila, M., Pena, A., Mulet, M., Lalucat, J., and Garcia-Valdes, E. (2015). Phylogenomics and systematics in pseudomonas. *Front. Microbiol.* 6, 214. doi: 10.3389/fmicb.2015.00214

Gomila, M., Prince-Manzano, C., Svensson-Stadler, L., Busquets, A., Erhard, M., and Martinez, D. L., et al. (2014). Genotypic and phenotypic applications for the differentiation and species-level identification of achromobacter for clinical diagnoses. *PLoS ONE*. 9, doi: 10.1371/journal.pone.0114356

Gunasekera, T., Dorsch, M., Slade, M., and Veal, D. (2003). Specific detection of pseudomonas spp. In milk by fluorescence in situ hybridization using ribosomal rna directed probes. *J. Appl. Microbiol.* 94, 936–945. doi: 10.1046/j.1365-2672.2003.01930.x

He, B., Guo, H., Gong, Y., and Zhao, R. (2017). Lipopolysaccharide-induced mitochondrial dysfunction in boar sperm is mediated by activation of oxidative phosphorylation. *Theriogenology* 87, 1–8. doi: 10.1016/j.theriogenology.2016.07.030

Hu, J., Ma, L., Nie, Y., Chen, J., Zheng, W., and Wang, X., et al. (2018). A microbiota-derived bacteriocin targets the host to confer diarrhea resistance in early-weaned piglets. *Cell Host Microbe*. 24, 817–832. doi: 10.1016/j.chom.2018.11.006

Huo, L., Ma, X., and Yang, Z. (2002). Assessment of sperm viability, mitochondrial activity, capacitation and acrosome intactness in extended boar semen during long-term storage. *Theriogenology* 58, 1349–1360. doi: 10.1016/S0093-691X(02)00953-6

Jakel, H., Scheinpflug, K., Muhldorfer, K., Gianluppi, R., Lucca, M. S., and Mellagi, A., et al. (2021). *In vitro* performance and *in vivo* fertility of antibiotic-free preserved boar semen stored at 5 degrees c. *J. Anim. Sci. Biotechnol.* 12, 9. doi: 10.1186/s40104-020-00530-6

Johnson, L., Weitze, K., Fiser, P., and Maxwell, W. (2000). Storage of boar semen. *Anim. Reprod. Sci.* 64, 133–134. doi: 10.1016/S0378-4320(00)00200-1

Kapoor, G., Saigal, S., and Elongavan, A. (2017). Action and resistance mechanisms of antibiotics: a guide for clinicians. *J. Anaesthesiol. Clin. Pharmacol*. 33, 300–305. doi: 10.4103/joacp.JOACP_349_15

Karageorgiou, M. A., Tsousis, G., Boscos, C. M., Tzika, E. D., Tassis, P. D., and Tsakmakidis, I. A. (2016). A comparative study of boar semen extenders with different proposed preservation times and their effect on semen quality and fertility. *Acta Vet. Brno*. 85, 23–31. doi: 10.2754/avb201685010023

Knox, R. V. (2016). Artificial insemination in pigs today. *Theriogenology* 85, 83–93. doi: 10.1016/j.theriogenology.2015.07.009

Koren, S., Walenz, B. P., Berlin, K., Miller, J. R., Bergman, N. H., and Phillippy, A. M. (2017). Canu: scalable and accurate long-read assembly via adaptive k-mer weighting and repeat separation. *Genome Res.* 27, 722–736. doi: 10.1101/gr.215087.116

Li, D., Zhang, W., Tian, X., He, Y., Xiao, Z., and Zhao, X., et al. (2022). Hydroxytyrosol effectively improves the quality of pig sperm at 17 degrees c. *Theriogenology* 177, 172–182. doi: 10.1016/j.theriogenology.2021.10.018

Li, Y., Fu, J., Li, P., Yang, Q., Wang, L., and Xie, W., et al. (2017). Effects of staphylococcus aureus on motility and protein phosphorylation modification of boar sperm during storage *in vitro*. *Acta Veterinaria Et Zootechnica Sinica*. 48, 1665–1673

Lucca, M. S., Gianluppi, R. D. F., Goncalves Mellagi, A. P., Bortolozzo, F. P., Wentz, I., and Ulguim, R. D. R. (2021). Effects of the classification of boars according to progressive sperm motility and the extender type on the reproductive performance of a single fixed-time insemination. *Theriogenology* 161, 120–125. doi: 10.1016/j.theriogenology.2020.11.018

Luis Ubeda, J., Ausejo, R., Dahmani, Y., Falceto, M. V., Usan, A., and Malo, C., et al. (2013). Adverse effects of members of the enterobacteriaceae family on boar sperm quality. *Theriogenology* 80, 565–570. doi: 10.1016/j.theriogenology.2013.05.022

Magoc, T., and Salzberg, S. L. (2011). Flash: fast length adjustment of short reads to improve genome assemblies. *Bioinformatics* 27, 2957–2963. doi: 10.1093/bioinformatics/btr507

Mazurova, J., and Vinter, P. (1991). The effects of some antibiotics on microorganisms contaminating boar ejaculates. *Vet. Med.* 36, 213–223

Meier-Kolthoff, J. P., and Goeker, M. (2019). Tygs is an automated high-throughput platform for state-of-the-art genome-based taxonomy. *Nat. Commun.* 10, 3. doi: 10.1038/s41467-019-10210-3

Mulet, M., Bennasar, A., Lalucat, J., and García-Valdés, E. (2009). An rpod-based pcr procedure for the identification of pseudomonas species and for their detection in environmental samples. *Mol. Cell. Probes.* 23, 140–147. doi: 10.1016/j.mcp.2009.02.001

Mulet, M., Lalucat, J., and García-Valdés, E. (2010). Dna sequence-based analysis of the pseudomonas species. *Environ. Microbiol.* 12, 1513–1530. doi: 10.1111/j.1462-2920.2010.02181.x

Paschoal, A. F. L., Luther, A., Jaekel, H., Scheinpflug, K., Muehldorfer, K., and Bortolozzo, F. P., et al. (2020). Determination of a cooling-rate frame for antibiotic-free preservation of boar semen at 5 degrees c. *PLoS ONE*. 15, e0234339. doi: 10.1371/journal.pone.0234339

Pezo, F., Romero, F., Zambrano, F., and Segundo Sanchez, R. (2019). Preservation of boar semen: an update. *Reprod. Domest. Anim.* 54, 423–434. doi: 10.1111/rda.13389

Pinart, E., Domenech, E., Bussalleu, E., Yeste, M., and Bonet, S. (2017). A comparative study of the effects of escherichia coli and clostridium perfringens upon boar semen preserved in liquid storage. *Anim. Reprod. Sci.* 177, 65–78. doi: 10.1016/j.anireprosci.2016.12.007

Prieto-Martinez, N., Bussalleu, E., Garcia-Bonavila, E., Bonet, S., and Yeste, M. (2014). Effects of enterobacter cloacae on boar sperm quality during liquid storage at 17 degrees c. *Anim. Reprod. Sci.* 148, 72–82. doi: 10.1016/j.anireprosci.2014.05.008

Pursel, V., and Johnson, L. (1975). Freezing of boar spermatozoa - fertilizing-capacity with concentrated semen and a new thawing procedure. *J. Anim. Sci.* 40, 99–102. doi: 10.2527/jas1975.40199x

Richter, M., Rossello-Mora, R., Gloeckner, F. O., and Peplies, J. (2016). Jspeciesws: a web server for prokaryotic species circumscription based on pairwise genome comparison. *Bioinformatics* 32, 929–931. doi: 10.1093/bioinformatics/btv681

Santos, C. S., and Silva, A. R. (2020). Current and alternative trends in antibacterial agents used in mammalian semen technology. *Anim. Reprod.* 17, 111. doi: 10.21451/1984-3143-AR2019-0111

Scales, B. S., Dickson, R. P., LiPuma, J. J., and Huffnagle, G. B. (2014). Microbiology, genomics, and clinical significance of the pseudomonas fluorescens species complex, an unappreciated colonizer of humans. *Clin. Microbiol. Rev.* 27, 927–948. doi: 10.1128/CMR.00044-14

Sepulveda, L., Bussalleu, E., Yeste, M., and Bonet, S. (2014). Effects of different concentrations of pseudomonas aeruginosa on boar sperm quality. *Anim. Reprod. Sci.* 150, 96–106. doi: 10.1016/j.anireprosci.2014.09.001

Sepulveda, L., Bussalleu, E., Yeste, M., and Bonet, S. (2016). Effect of pseudomonas aeruginosa on sperm capacitation and protein phosphorylation of boar spermatozoa. *Theriogenology* 85, 1421–1431. doi: 10.1016/j.theriogenology.2015.12.025

Sepulveda, L., Bussalleu, E., Yeste, M., Torner, E., and Bonet, S. (2013). How do different concentrations of clostridium perfringens affect the quality of extended boar spermatozoa? *Anim. Reprod. Sci.* 140, 83–91. doi: 10.1016/j.anireprosci.2013.04.013

Shah, N. (1994). Psychrotrophs in milk - a review. *Milchwissenschaft-Milk Sci. Int.* 49, 432–437

Shaoyong, W., Li, Q., Ren, Z., Xiao, J., Diao, Z., and Yang, G., et al. (2019). Effects of kojic acid on boar sperm quality and anti-bacterial activity during liquid preservation at 17 c. *Theriogenology* 140, 124–135. doi: 10.1016/j.theriogenology.2019.08.020

Silverio, M. P., Kraychete, G. B., Rosado, A. S., and Bonelli, R. R. (2022). Pseudomonas fluorescens complex and its intrinsic, adaptive, and acquired antimicrobial resistance mechanisms in pristine and human-impacted sites. *Antibiotics-Basel.* 11, 985. doi: 10.3390/antibiotics11080985

Singhal, L., Singh, C., and Gautam, V. (2022). "7.06 – colistin," in ed. T. Kenakin. Cambridge, MA: Elsevier. 123–135.

Tohya, M., Teramoto, K., Watanabe, S., Hishinuma, T., Shimojima, M., and Ogawa, M., et al. (2022). Whole-genome sequencing-based re-identification of pseudomonas putida/fluorescens clinical isolates identified by biochemical bacterial identification systems. *Microbiol. Spectr.* 10, 21. doi: 10.1128/spectrum.02491-21

Union, E. (1992). *Council directive 92/65/eec laying down animal health requirements governing trade in and imports into the community of animals, semen, ova and embryos not subject to animal health requirements laid down in specific community rules referred to in annex a (i) to directive 90/425/eec.* Bruxels: Official Journal of the European Communities, L254–L268.

Waberski, D., Luther, A., Gruenther, B., Jaekel, H., Henning, H., and Vogel, C., et al. (2019). Sperm function in vitro and fertility after antibiotic-free, hypothermic storage of liquid preserved boar semen. *Sci. Rep.* 9. doi: 10.1038/s41598-019-51319-1

Wiedmann, M., Weilmeier, D., Dineen, S., Ralyea, R., and Boor, K. (2000). Molecular and phenotypic characterization of pseudomonas spp. isolated from milk. *Appl. Environ. Microbiol.* 66, 2085–2095. doi: 10.1128/AEM.66.5.2085-2095.2000

Xiao, Y., and Hu, Y. (2012). The major aminoglycoside-modifying enzyme aac(3)-ii found in escherichia coli determines a significant disparity in its resistance to gentamicin and amikacin in china. *Microbial. Drug Res. (Larchmont, N.Y.).* 18, 42–46. doi: 10.1089/mdr.2010.0190

Zeng, L., and Jin, S. (2003). Aph(3′)-iib, a gene encoding an aminoglycoside-modifying enzyme, is under the positive control of surrogate regulator hpaa. *Antimicrob. Agents Chemother.* 47, 3867–3876 doi: 10.1128/AAC.47.12.3867-3876.2003

Zhang, C., Bijl, E., Svensson, B., and Hettinga, K. (2019). The extracellular protease aprx from pseudomonas and its spoilage potential for uht milk: a review. *Compr. Rev. Food. Sci. Food Saf.* 18, 834–852. doi: 10.1111/1541-4337.12452

Zhang, J., Liu, H., Yang, Q., Li, P., Wen, Y., and Han, X., et al. (2020). Genomic sequencing reveals the diversity of seminal bacteria and relationships to reproductive potential in boar sperm. *Front. Microbiol.* 11, 1873. doi: 10.3389/fmicb.2020.01873

frontiers | Frontiers in Microbiology

TYPE Original Research
PUBLISHED 30 November 2023
DOI 10.3389/fmicb.2023.1275909

OPEN ACCESS

EDITED BY
Vijay Soni,
NewYork-Presbyterian, United States

REVIEWED BY
Tushar Dhanani,
Florida Agricultural and Mechanical University, United States
Madhavi Annamanedi,
West Virginia University, United States
Arka Banerjee,
NewYork-Presbyterian, United States

*CORRESPONDENCE
Preecha Montakantikul
preecha.mon@mahidol.ac.th

RECEIVED 16 August 2023
ACCEPTED 15 September 2023
PUBLISHED 30 November 2023

CITATION
Rodjun V, Montakantikul P, Houngsaitong J, Jitaree K and Nosoongnoen W (2023) Pharmacokinetic/pharmacodynamic (PK/PD) simulation for dosage optimization of colistin and sitafloxacin, alone and in combination, against carbapenem-, multidrug-, and colistin-resistant *Acinetobacter baumannii*. *Front. Microbiol.* 14:1275909. doi: 10.3389/fmicb.2023.1275909

Pharmacokinetic/pharmacodynamic (PK/PD) simulation for dosage optimization of colistin and sitafloxacin, alone and in combination, against carbapenem-, multidrug-, and colistin-resistant *Acinetobacter baumannii*

Vipavee Rodjun[1], Preecha Montakantikul[2]*, Jantana Houngsaitong[2], Kamonchanok Jitaree[3] and Wichit Nosoongnoen[2]

[1]Faculty of Pharmacy, Siam University, Bangkok, Thailand, [2]Division of Clinical Pharmacy, Department of Pharmacy, Faculty of Pharmacy, Mahidol University, Bangkok, Thailand, [3]Division of Pharmacy Practice, Faculty of Pharmaceutical Sciences, Ubon Ratchathani University, Ubon Ratchathani, Thailand

To the best of our knowledge, to date, no study has investigated the optimal dosage regimens of either colistin or sitafloxacin against drug-resistant *Acinetobacter baumannii* (*A. baumannii*) infections by using specific parameters. In the current study, we aimed to explore the optimal dosage regimens of colistin and sitafloxacin, either in monotherapy or in combination therapy, for the treatment of carbapenem-, multidrug-, and colistin-resistant *A. baumannii* infections. A Monte Carlo simulation was applied to determine the dosage regimen that could achieve the optimal probability of target attainment (PTA) and cumulative fraction of response (CFR) (≥90%) based on the specific parameters of each agent and the minimal inhibitory concentration (MIC) of the clinical isolates. This study explored the dosage regimen of 90, 50, 30, and 10 mL/min for patients with creatinine clearance (CrCL). We also explored the dosage regimen for each patient with CrCL using combination therapy because there is a higher possibility of reaching the desired PTA or CFR. Focusing on the MIC90 of each agent in combination therapy, the dosage regimen for colistin was a loading dose of 300 mg followed by a maintenance dose ranging from 50 mg every 48 h to 225 mg every 12 h and the dosage regimen for sitafloxacin was 325 mg every 48 h to 750 mg every 12 h. We concluded that a lower-than-usual dose of colistin based on specific pharmacokinetic data in combination with a higher-than-usual dose of sitafloxacin could be an option for the treatment of carbapenem-, multidrug-, and colistin-resistant. *A. baumannii.* The lower dose of colistin might show a low probability of adverse reaction, while the high dose of sitafloxacin should be considered. In the current study, we attempted to find if there is a strong possibility of drug selection against crucial drug-resistant pathogen infections in a situation where there is a lack of new antibiotics. However, further study is needed to confirm the results of this simulation study.

KEYWORDS

colistin, sitafloxacin, *Acinetobacter baumannii*, Monte Carlo simulation, multidrug-resistant *Acinetobacter baumannii*, carbapenem-resistant *Acinetobacter baumannii*, combination

Introduction

Acinetobacter baumannii (*A. baumannii*) is one of the most important gram-negative pathogens that cause various nosocomial infections (García-Garmendia et al., 2001; Cisneros and Rodríguez-Baño, 2002; Werarak et al., 2012; Sieniawski et al., 2013; Almasaudi, 2018; Centers for Disease Control and Prevention, n.d.). Drug-resistant *A. baumannii* infections, including multidrug-resistant *A. baumannii* (MDR-AB), carbapenem-resistant *A. baumannii* (CRAB), and colistin-resistant *A. baumannii* (CoR-AB) infections, are a crucial problem because they cause prolonged hospitalization and a high mortality rate (Sunenshine et al., 2007; Kaye and Pogue, 2015). The study by Appaneal et al. showed that the inpatient mortality rate was higher in those with MDR-AB than those with non-MDR-AB infection (aOR 1.61) and in those with CRAB than non-CRAB infection (aOR 1.68). A hospitalization duration of more than 10 days was higher in those with MDR-AB compared to those with non-MDR-AB infection and in those with CRAB compared to those with non-CRAB infection (Appaneal et al., 2022). Moreover, the clinical outcomes were worse among patients with MDR-AB and/or CRAB infections (Appaneal et al., 2022). Similarly, the meta-analysis showed that the CRAB could increase the risk of high mortality rate in patients (Lemos et al., 2014). Compared to colistin-susceptible AB infection, patients with CoR-AB bloodstream infection had higher mortality (100% vs. 50%, respectively ($p = 0.001$)) and died sooner ($p = 0.006$) (Papathanakos et al., 2020).

Colistin has gained attention for its use in the treatment of drug-resistant *A. baumannii* infections (Falagas et al., 2010; Lim et al., 2011; Batirel et al., 2014; Kalin et al., 2014; López-Cortés et al., 2014; Yilmaz et al., 2015; Amat et al., 2018; Liang et al., 2018; Dickstein et al., 2019). The optimal dosage regimens for colistin have been investigated from the past to the present based on the population pharmacokinetic model and pharmacokinetic/pharmacodynamic (PK/PD) index of colistin (Garonzik et al., 2011; Nation et al., 2017). The usual PK/PD index of colistin is the average steady-state plasma colistin concentration ($C_{ss,avg}$). However, recent studies found that the most predictive PK/PD index of colistin against *A. baumannii* was the ratio of the area under the unbound concentration-time curve to the minimum inhibitory concentration (*f*AUC/MIC) (Dudhani et al., 2010; Cheah et al., 2015). A common adverse drug reaction from colistin is nephrotoxicity, which occurs in a dose- and time-dependent manner (Spapen et al., 2011; Dai et al., 2014). Therefore, the challenge of exploring a colistin dosage regimen is focused on both increasing efficacy and lowering toxicity.

Sitafloxacin is a fluoroquinolone that has shown excellent *in vitro* activity against drug-resistant *A. baumannii* (Dong et al., 2015; Huang et al., 2015; Rodjun et al., 2020). Its population pharmacokinetic model and PK/PD index have also been studied (Tanigawara et al., 2013). A key feature of sitafloxacin is its excellent penetration into the epithelial lining fluid (ELF) of critically ill patients with pneumonia; according to the data of Paiboonvong et al., the AUC0–8 h of ELF/unbound plasma ratio was 0.85 (Paiboonvong et al., 2019). Moreover, sitafloxacin in combination with colistin can decrease the MIC values of either colistin or sitafloxacin. This *in vitro* activity was observed when using this combination against extensively drug-resistant *A. baumannii* (XDR-AB) (Dong et al., 2015), MDR-AB, CRAB, and CoR-AB (Rodjun et al., 2020).

The World Health Organization (WHO) announced that there are declining private investments and a lack of innovation in the development of new antibiotics. Over 30 antibiotics are still in the clinical development pipeline (Kmietowicz, 2017; Butler et al., 2022). Because of the lack of novel antibiotics to treat drug-resistant bacterial infections, the standard guideline for treating drug-resistant pathogen infections still recommends using familiar antibiotics or some regimens that use the combination therapy (Tamma et al., 2023). The combination regimens of colistin with other antibiotics such as sulbactam, tigecycline, and carbapenems have been options for the management of drug-resistant *A. baumannii* infections (Garonzik et al., 2011; Lim et al., 2011; Batirel et al., 2014; Kalin et al., 2014; López-Cortés et al., 2014; Amat et al., 2018; Dickstein et al., 2019). From a previous *in vitro* study with sitafloxacin, the combination of colistin and sitafloxacin is one interesting possibility. This study aimed to explore the optimal dosage regimens of colistin and sitafloxacin, either in monotherapy or in combination therapy, for the treatment of MDR-AB, CRAB, and CoR-AB infections using a Monte Carlo simulation that was based on the specific population pharmacokinetics and PK/PD index of each agent.

Materials and methods

Microbiology

Data on *A. baumannii* were obtained from a prior study by Rodjun et al. (2020). Three hundred *A. baumannii* clinical isolates were comprised of MDR-AB–263 isolates (87.7%), CRAB–258 isolates (86%), and CoR-AB–43 isolates (14.3%). The MIC50/90 of colistin in MDR-AB and CRAB was 2/4 mg/L and that of CoR-AB was 8/8 mg/L. The MIC50/90 of sitafloxacin in MDR-AB and CRAB was 1/2 mg/L and that of CoR-AB was 0.5/1 mg/L. The MIC50/90 of colistin in combination regimens in MDR-AB and CRAB was 0.5/1 mg/L and that of CoR-AB was 1/2 mg/L. The MIC50/90 of sitafloxacin in combination regimens in MDR-AB and CRAB was 0.5/1 mg/L and that of CoR-AB was 0.25/1 mg/L.

Pharmacokinetic model

Colistin

The population pharmacokinetic models for colistimethate sodium (CMS) and colistin were two-compartment and one-compartment models, respectively. We used pharmacokinetic data from Nation et al. (2017), who studied the dosing guidance for colistin in critically ill

TABLE 1 Population pharmacokinetic parameters of colistin (Nation et al., 2017).

Agent	Parameter	Unit	Estimate	%SE	%IIV
CMS	V1	L	12.9	-	40.4
	V2	L	16.1	-	70.9
	CLD1	L	9.57	10.5	80.1
	CLR	L/h/CrCL	0.0340	6.85	75.2
	$CLNR_{CMS}$	L/h	2.52	3.71	39.8
Colistin	V3	L	57.2	5.13	43.5
	CLT_C	L/h	3.59	-	37.9
	CLR_C	L/h/CrCL	0.00834	27.7	-
	$CLNR_C$	L/h	3.11	4.38	-

V1, Central volume for CMS, V2, Peripheral volume for CMS, CLD1, Distributional clearance between the central and peripheral compartments for CMS, CLR, Renal clearance of CMS, CLNRCMS, Non-renal clearance of CMS, V3, volume of distribution of formed colistin, CLTC, Total clearance of colistin, CLRC, Renal clearance of colistin, CLNRC, Non-renal clearance of colistin, %SE, standard error or the precision of the estimates, %IIV, inter-individual variability in the population (standard deviation, SD, were calculated from %IVV x mean), CrCL, creatinine clearance, CMSC, mass of CMS in the central compartment, CMSp, mass of CMS in the peripheral compartment, colistin, mass of colistin in the single compartment, R1, infusion rate of CMS, CLTCMS, total intrinsic clearance for CMS.

patients with a CrCL of 0–236 mL/min. The parameters were randomly generated for each estimated mean, and the %IIV of the parameters are shown in Table 1. The equations below were modified according to the study of Garonzik et al. (2011) and represent the differential equations for the disposal of CMS and colistin. The unbound fraction of 0.49 +/− 0.11, determined by ultracentrifugation in samples collected from the patients in the prior study, was used (Nation et al., 2017).

$$\frac{dCMSc}{dt} = R1 - CLD1 \times \left(\frac{CMSc}{V1} - \frac{CMSp}{V2}\right) - \left(CLT_{CMS} \times \frac{CMSc}{V1}\right) \quad (1)$$

$$\frac{\mathrm{dCMSp}}{\mathrm{dt}} = CLD1 \times \left(\frac{CMSc}{V1} - \frac{CMSp}{V2}\right) \quad (2)$$

$$\frac{dColistin}{dt} = CLNR_{CMS} \times \frac{CMSc}{V1} - \left(CLT_C \times \frac{Colistin}{V3}\right) \quad (3)$$

Sitafloxacin

The population pharmacokinetic model for oral sitafloxacin was assumed to follow the one-compartment model with first-order absorption (Tanigawara et al., 2013). We used pharmacokinetic data from Tanigawara et al. (2013), who used clinical data from clinical pharmacology studies, including a study on healthy, elderly but renally impaired patients (Nakashima et al., 1995; Nakashima, 2008; Nakashima and Kawada, 2008; Sekino, 2008), and the clinical PK/PD study on patients with respiratory tract infections (Saito et al., 2008). The parameters are shown in Table 2. The equation below was used to calculate the plasma sitafloxacin concentration (Jambhekar and Breen, 2012). An unbound fraction of sitafloxacin of 0.388 was used (Tanigawara et al., 2013).

$$\frac{dX}{dt} = K_a X_a - KX, \quad (4)$$

where dX/dt = the rate of change of the amount of drug in the plasma, X = the mass of drug in the plasma at time t, X_a = the mass of absorbable drug at time t, K_a and K = the first-order of absorption and elimination rate constants, respectively, K_aX_a = the first-order rate of absorption, and KX = the first-order rate of elimination.

TABLE 2 Population pharmacokinetic parameters of sitafloxacin (Tanigawara et al., 2013).

Agent	Parameter	Unit	Estimate	ω^2
Sitafloxacin	CL_t/F	L	2.58 x CrCL	0.0757
	V/F	L/Kg	1.72	0.087
	k_a	h^{-1}	1.67	4.57

CLt, total clearance, V, volume of distribution (age < 65 years), ka, absorption constant in a fasted state, ω 2, the variance of the estimated value (SD were calculated from the square root of ω 2 × 100% × estimate).

Pharmacokinetic or pharmacodynamic index

Colistin

The pharmacokinetic/pharmacodynamic index (PK/PD) index of colistin is characterized by fAUC/MIC ≥7.4, which showed a 2-$\log_{10}$ reduction of MDR *A. baumannii* clinical isolate strain 248-01-C.248 (MIC of colistin is 1 mg/L) in a mouse model with a thigh infection. This value resulted in bacterial burdens in mouse thighs determined at 2 h after inoculation (untreated controls) and 24 h later (untreated controls and colistin-treated subjects) (Cheah et al., 2015). The model with the thigh infection has been used in most *in vivo* studies (Craig, 1998) and is considered to be the gold standard for evaluating the efficacy of antimicrobials since its high degree of translation to human patients (Yedle et al., 2023). Moreover, the thigh infection model is considered to be an adequate simulator because the model allows for the dissemination of the offending pathogen in blood and viscera to occur as in the clinical status of bacteremia (Pantopoulou et al., 2007).

Sitafloxacin

The PK/PD index of sitafloxain is characterized by fAUC/MIC >30, which showed an eradication effect of 96.4% on respiratory tract infection (RTIs) isolates. This value was determined for individual PK

parameters with MIC in 91 RTI isolates, and the attainment rates of the *f*AUC/MIC were calculated (Tanigawara et al., 2013).

Simulated dosage regimens

Colistin

The dosage regimens were chosen according to the study of Nation et al. (2017), the guidelines of the European Medicine Agency (EMA) (Nation et al., 2016) and the United States Food and Drug Administration (FDA) (Nation et al., 2016), and the recommended dosage regimens by Siriraj Hospital, Thailand, and our study's dosage regimens. The creatinine clearance (CrCL) values used for the simulation were 90, 50, 30, and 10 mL/min. Each dose was infused for 30 min, and each dosage regimen starts with the loading dose (LD) of 450 mg or 300 mg. The maintenance doses vary from 50 mg every 48 h to 450 mg every 12 h according to the CrCL value.

Sitafloxacin

The dosage regimens were chosen according to the manufacturer's recommendations (Pharmaceuticals and Medical Devices Agency, n.d.) and our study's dosage regimens. The regimens were administered orally to an inpatient in a fasted state who weighed 60 kg and was under 65 years of age. The CrCL values used in this study were 90, 50, 30, and 10 mL/min. The doses vary from 50 mg every 48 h to 1,500 mg every 12 h according to the CrCL value.

Monte Carlo simulation

A Monte Carlo Simulation (Crystal Ball version 2017; Decisioneering Inc., Denver, CO United States) was applied to generate 10,000 subjects for each regimen. Log-normal distributions were studied for between-patient variability of each parameter except the unbound fraction of colistin, which was studied by the uniform distribution. The probability of target attainment (PTA) was determined as the percentage of all 10,000 estimates that achieved or exceeded the pharmacodynamic surrogate indices of each agent. Both colistin and sitafloxacin use *f*AUC/MIC. The AUC was determined using the linear trapezoidal rule, while *f* was the unbound fraction of each agent. The MIC values were calculated from a prior study (Rodjun et al., 2020). The cumulative fraction of response (CFR) was calculated as the proportion of %PTA of each MIC according to the MIC distribution. The PTA and CFR (Asuphon et al., 2016; Jitaree et al., 2019; Leelawattanachai et al., 2020), which we calculated at the steady state, were considered optimal at ≥90%. This study was approved by the Ethics Committee of the Faculty of Dentistry/Faculty of Pharmacy, Mahidol University, Phutthamonthon District, Nakhon Pathom, Thailand (COE.No.MU-DT/PY-IRB 2020/001.1501).

Result

Colistin monotherapy

The dosage regimens of colistin that achieved a PTA of ≥90% for the MIC50 of MDR-AB and CRAB (2 mg/L) were the maintenance doses of 225 mg every 12 h, 150 mg every 24 h, 75 mg every 24 h, and 50 mg every 24 h for CrCL values of 90, 50, 30, and 10 mL/min, respectively. The dosage regimens that achieved a PTA of ≥90% for the MIC90 of MDR-AB and CRAB (4 mg/L) were maintenance doses of 300 mg every 12 h, 150 mg every 24 h, and 75 mg every 24 h for CrCL values of 50, 30, 10 mL/min, respectively. The dosage regimens that achieved a PTA of ≥90% for the MIC50/90 of CoR-AB (8 mg/L) were maintenance doses of 450 mg every 12 h, 300 mg every 12 h, and 150 mg every 24 h for CrCL values 50, 30, and 10 mL/min, respectively. No dosage regimen was recommended for patients with CrCL 90 mL/min at MIC of 2 and 4 mg/L.

The dosage regimens of colistin that achieved a CFR of ≥90% for MDR-AB and CRAB were maintenance doses of 300 mg every 12 h, 150 mg every 12 h, 150 mg every 24 h, and 50 mg every 24 h for CrCL values of 90, 50, 30, and 10 mL/min, respectively. The maintenance doses of 450 mg every 12 h, 300 mg every 12 h, and 150 mg every 24 h were recommended for patients with CrCL values 50, 30, and 10 mL/min, respectively. No dosage regimen was recommended for patients with CrCL values of 90 mL/min.

As can be observed from the results, a lower CrCL value (50, 30, and 10 mL/min) can achieve the target by the usual dosage regimen including the USFDA recommended. Meanwhile, a CrCL value of 90 mL/min should be used in our regimen, which is higher than the usual dose. The results table of colistin monotherapy is shown in the Supplementary Table S1.

Sitafloxacin monotherapy

The dosage regimens that achieved a PTA of ≥90% for the MIC50 of CoR-AB (0.5 mg/L) were doses of 375 mg every 12 h, 225 mg every 12 h, 250 mg every 24 h, and 175 mg every 48 h for CrCL values of 90, 50, 30, and 10 mL/min, respectively. The dosage regimen that achieved a PTA of ≥90% for the MIC50 of MDR-AB and CRAB, and the MIC90 of CoR-AB (1 mg/L) were doses of 750 mg every 12 h, 425 mg every 12 h, 500 mg every 24 h, and 325 mg every 48 h for CrCL values of 90, 50, 30, and 10 mL/min, respectively. The dosage regimens that achieved a PTA of ≥90% for the MIC90 of MDR-AB and CRAB (2 mg/L) were doses of 1,500 mg every 12 h, 750 mg every 12 h, 1,000 mg every 24 h, and 675 mg every 48 h for CrCL values of 90, 50, 30, and 10 mL/min, respectively.

The dosage regimens of sitafloxacin that achieved a CFR of ≥90% of MDR-AB and CRAB were doses of 1,500 mg every 12 h, 750 mg every 12 h, and 500 mg every 48 h for CrCL 90, 50, and 10 mL/min, respectively. For CrCL 30 mL/min, these doses were 800 mg every 24 h and 750 mg every 24 h of MDR-AB and CRAB, respectively. The dosage regimens for CoR-AB were 1,000 mg every 12 h, 500 mg every 12 h, 750 mg every 24 h, and 500 mg every 48 h for CrCL values of 90, 50, 30, and 10 mL/min, respectively.

As can be observed from the results, the manufacturer's regimen cannot reach the target in any CrCL values. All the recommended dosage regimens were generated in this study. The lowest dose to achieve the target was 500 mg every 48 h. The results table of sitafloxacin monotherapy is shown in the Supplementary Table S2.

Colistin in combinations

The dosage regimens of colistin in combinations that achieved a PTA of ≥90% for the MIC50 of MDR-AB and CRAB (0.5 mg/L) were

maintenance doses of 100 mg every 24 h for CrCL values of 90 mL/min and 50 mg every 48 h for 50, 30, and 10 mL/min. The dosage regimens that achieved a PTA of ≥90% for the MIC90 of MDR-AB, CRAB, and the MIC50 of CoR-AB (1 mg/L) were maintenance doses of 150 mg every 12 h for CrCL 90 mL/min, 75 mg every 24 h for CrCL 50 mL/min, and 50 mg every 48 h for CrCL 30 and 10 mL/min. The dosage regimens for the MIC90 of CoR-AB were the same as those for the MIC50 of MDR-AB and CRAB in monotherapy.

The dosage regimens that achieved a CFR of ≥90% for MDR-AB and CRAB were maintenance doses of 100 mg every 12 h for CrCL 90 mL/min and 50 mg every 48 h for CrCL values of 50, 30, and 10 mL/min. The maintenance doses for CoR-AB were 180 mg every 12 h, 150 mg every 24 h, 75 mg every 24 h, and 50 mg every 48 h for CrCL values of 50, 30, and 10 mL/min, respectively.

Overall, the doses of colistin in combination were lower than in monotherapy. The lower CrCL values (50, 30, and 10 mL/min) can achieve the target by the usual regimen while the CrCL values of 90 mL/min should use a higher dose, especially at MIC 2 mg/L.

Sitafloxacin in combinations

The dosage regimens of sitafloxacin in combinations that achieved a PTA of ≥90% for the MIC50 of CoR-AB (0.25 mg/L) were doses of 200 mg every 12 h, 125 mg every 12 h, 125 mg every 24 h, and 50 mg every 24 h for CrCL values of 90, 50, 30, and 10 mL/min, respectively. The dosage regimens that achieved a PTA of ≥90% for the MIC50 of MDR-AB and CRAB (0.5 mg/L) were the same as those for the MIC50 of CoR-AB in monotherapy. The dosage regimens that achieved a PTA of ≥90% for the MIC90 of MDR-AB and CRAB (1 mg/L) were the same as those for the MIC50 of MDR-AB and CRAB (1 mg/L) in monotherapy.

The optimal doses of sitafloxacin in combinations that achieved a CFR of ≥90% for MDR-AB and CRAB were doses of 750 mg every 12 h, 400 mg every 12 h, 500 mg every 24 h, and 300 mg every 48 h for CrCL values of 90, 50, 30, and 10 mL/min, respectively. The dosage regimens that achieved a CFR of ≥90% for CoR-AB were doses of 750 mg every 12 h, 400 mg every 12 h, 300 mg every 24 h, and 200 mg every 48 h for CrCL values of 90, 50, 30, and 10 mL/min, respectively.

The dosage regimens in combinations were lower than those in monotherapy. However, the manufacturer's regimen cannot reach the target in any CrCL values.

The PTA analyses of various colistin and sitafloxacin regimens and CrCL are shown in Figures 1, 2, respectively. The PTA and CFR of each dosage regimen are shown in Tables 3–5 and in Supplementary material.

Discussion

The infection caused by drug-resistant *A. baumannii* is a serious problem, especially MDR-AB and CRAB. Because of the various types of antibiotics that the pathogen resists, the choice of drug is limited. This study focuses on the use of colistin, which is known as the last resort for gram-negative bacteria, especially the drug-resistant pathogen. Moreover, sitafloxacin was chosen based on the good activity from the previous study (Rodjun et al., 2020). This is the first study to explore colistin dosage regimens based on the new pharmacokinetic/pharmacodynamic (PK/PD) index of *A. baumannii*. To date, the recommended colistin dosage regimen aims to achieve the desired $C_{ss,avg}$, especially at 2 mg/L (Garonzik et al., 2011; Nation et al., 2017), formerly the susceptibility breakpoint of gram-negative isolates, including *Acinetobacter* spp. This study used *f*AUC/MIC ≥7.4 as the desired index (Cheah et al., 2015). We ran simulations starting with a loading dose of 300 mg (the same as in the reference dosage regimens) and 450 mg, expecting them to rapidly reach the steady state of colistin. The reference dosage regimens recommended by FDA, EMA, Siriraj, and Nation et al. for the simulation in patients with a CrCL value of ≥90 mL/min cannot achieve the specific index at a PTA of ≥90%; however, our study's dosage regimens can achieve it with the maintenance dose of 225 mg every 12 h at breakpoint MIC. The results of Jitaree et al., who studied the optimal dosage of colistin against carbapenem-resistant *Klebsiella pneumonia* and carbapenem-resistant *Escherichia coli* (Jitaree et al., 2019), were consistent with ours. In a patient who has a normal renal function (≥80 mL/min), one cannot use the reference dosage regimen to achieve the specific index (*f*AUC/MIC ≥25) when using the breakpoint as a desired MIC. Therefore, the usual colistin dosage regimens cannot achieve the specific index of each important gram-negative isolate in a patient who has normal renal function. However, the reference dosage regimen can achieve the specific index in a patient who has renal impairment (≤50 mL/min). Interestingly, our new dosage regimens (150 mg, 75 mg, and 50 mg every 24 h for CrCL value of 50, 30, and 10 mL/min, respectively), which are lower than the lowest reference dose (114 mg every 12 h, 150 mg every 24 h, and 60 mg every 24 h for CrCL value of 50, 30, and 10 mL/min, respectively), can achieve the target. To the best of our knowledge, the most common adverse event observed with colistin is dose-dependent nephrotoxicity (Nation et al., 2014; Eljaaly et al., 2021). A lower dose should be considered to reduce the risk of nephrotoxicity in a patient who has renal function impairment. However, patients with good renal function seem to be using the higher than usual. The other adverse reaction is neurotoxicity (Spapen et al., 2011). Though colistin is the last resort for the treatment of infection by a drug-resistant organism, the rate of colistin resistance is currently a problem (Cai et al., 2012). The reference dosage regimen for colistin cannot be used against the colistin-resistant *A. baumannii* in this study (MIC ≥2 mg/L), especially in a patient who has CrCL ≥50 mL/min. Therefore, combination regimens should be considered. However, the international consensus guidelines (Tsuji et al., 2019) for the optimal use of polymyxins recommended the use of a $C_{ss,avg}$ of 2 mg/L instead of the new index because of the differences in the protein binding of mice and humans. However, our study used a protein binding profile from Nation et al. (2017), who ran simulations in a critically ill patient. The PK/PD index at a $C_{ss,avg}$ of 2 mg/L did not depend on the variation in MIC values, which might complicate the choice of optimal doses. The new PK/PD index used in this study can be applied to any MIC value. Moreover, our PK/PD index is specific for *A. baumannii* (Cheah et al., 2015).

Sitafloxacin, the fluoroquinolone antibiotic, demonstrates the concentration-dependent killing effect. The lower concentration showed less bacteriological efficacy (Tanigawara et al., 2013). The reference regimen for sitafloxacin monotherapy (50–100 mg every 12–48 h) cannot achieve the specific index in each CrCL at a PTA of ≥90%, while our study's regimens can (≥175 mg every 48 h). We used the same PK/PD index as Tanigawara et al., who were the only authors

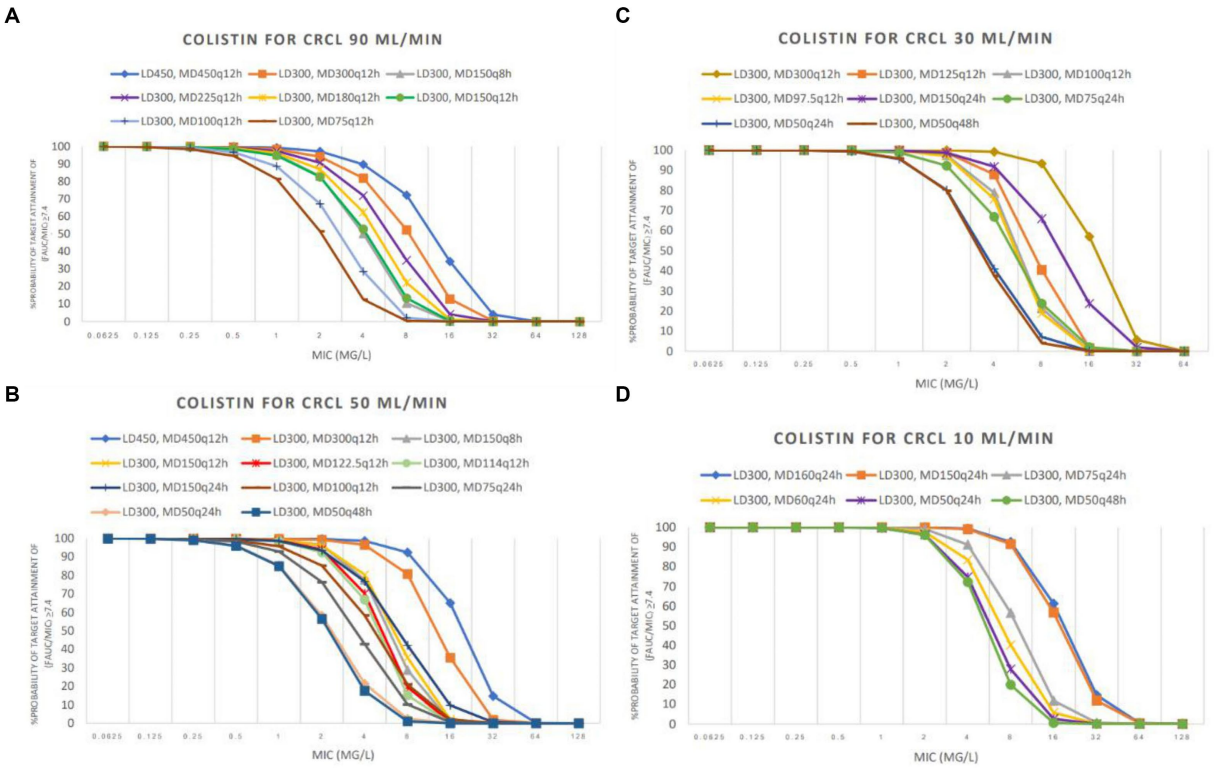

FIGURE 1
Probability of target attainment (PTA) achieved with colistin used in groups CrCL 90 mL/min **(A)**, CrCL 50 mL/min **(B)**, CrCL 30 mL/min **(C)**, and CrCL 10 mL/min **(D)**. LD: loading dose (in mg colistin base activity), MD: maintenance doses (in mg colistin base activity).

to study the PK/PD index of sitafloxacin, *f*AUC/MIC ≥30 (Huang et al., 2015), but there were differences between their MIC values and ours. The lowest MIC from the study by Tanigawara et al. was ≤0.025 mg/L, which was less than the focus MIC value of this study, ≥0.5 mg/L, which led them to a lower recommended dose than the one in this study. In fact, the approved indications of sitafloxacin are likely to be a mild infection or community-acquired infection (Pharmaceuticals and Medical Devices Agency, n.d.), which is why the manufacturer-recommended dose seems to be low.

The colistin-sitafloxacin combination led to a greater opportunity to explore the optimal dosage regimen to achieve a PTA of 90% based on the specific PK/PD index. Because the MIC50/90 of CoR-AB (2 mg/L) was reduced to at least the intermediate breakpoint (Clinical and Laboratory Standards Institute, 2022) (≤2 mg/L), this study could determine the dosage regimen for all CrCL values. Although the MIC of sitafloxacin was also reduced, the dosage regimens that achieve a PTA of 90% are still higher than the reference dosage regimens. For example, 50 mg of sitafloxacin every 24 h was obtained for a patient with a CrCL value of 10 mL/min, while the recommended dose is 50 mg every 48 h. To our knowledge, fluoroquinolones are concentration-dependent antibiotics (Lode et al., 1998) and sitafloxacin is a fluoroquinolone antibiotic agent (Sun et al., 2021). Therefore, higher doses can have greater efficacy in isolate eradication. Saito et al. (2008) showed greater efficacy of sitafloxacin in a higher dose, which is consistent with our result that a higher dose achieved a higher PTA percentage. The point of concern is the possibility of a dose-dependent adverse drug reaction. Feldman et al. used sitafloxacin at a high dose (400 mg intravenously once daily) for the treatment of hospitalized patients with pneumonia and showed a 5% rate of drug-related adverse events but no severe reactions (Feldman et al., 2001). In a previous report, the dose-dependent prolongation of QTcF occurred after the administration of supratherapeutic dosages of sitafloxacin of 400, 600, or 800 mg twice daily to healthy volunteers (mean change in the QTcF interval of 0, 6, and 10 ms, respectively) (Keating, 2011). The highest recommended dose of sitafloxacin from this study for combination therapy in a patient with a CrCL value of 90 mL/min was 200–750 mg every 12 h, which might increase the QTcF. However, no reports of serious adverse reactions or adverse events based on recent data on sitafloxacin were observed.

This study explored all dosage regimens in a patient with various CrCL values, focusing on the one that achieved a PTA of 90% for the MIC90 of each agent in combination therapy. A colistin dose lower than the usual one seems to have led to less nephrotoxicity, while a dose of sitafloxacin appears to be higher than the usual regimen. A patient who is administered a high dose requires close monitoring.

An optimal CFR of ≥90% was used in this study. Some dosage regimens were different from the dosage regimen for a PTA of ≥90% because of the MIC distribution. The dose of sitafloxacin that achieved a CFR of ≥90% was lower than that which achieved a PTA of 90% in each CrCL value. The major MIC distribution of sitafloxacin in our study was lower than 0.5 mg/L (Rodjun et al., 2020), which increases the probability of achieving the desired CFR. The doses of colistin required to achieve a CFR of ≥90% in MDR-AB and CRAB for each CrCL were the same because most of the isolates in these two groups overlapped. Thus, the opportunity to achieve the desired CFR was dependent on the MIC distribution.

Our study has several limitations. First, this study used the PK/PD index from the thigh infection in the mouse model. For the treatment

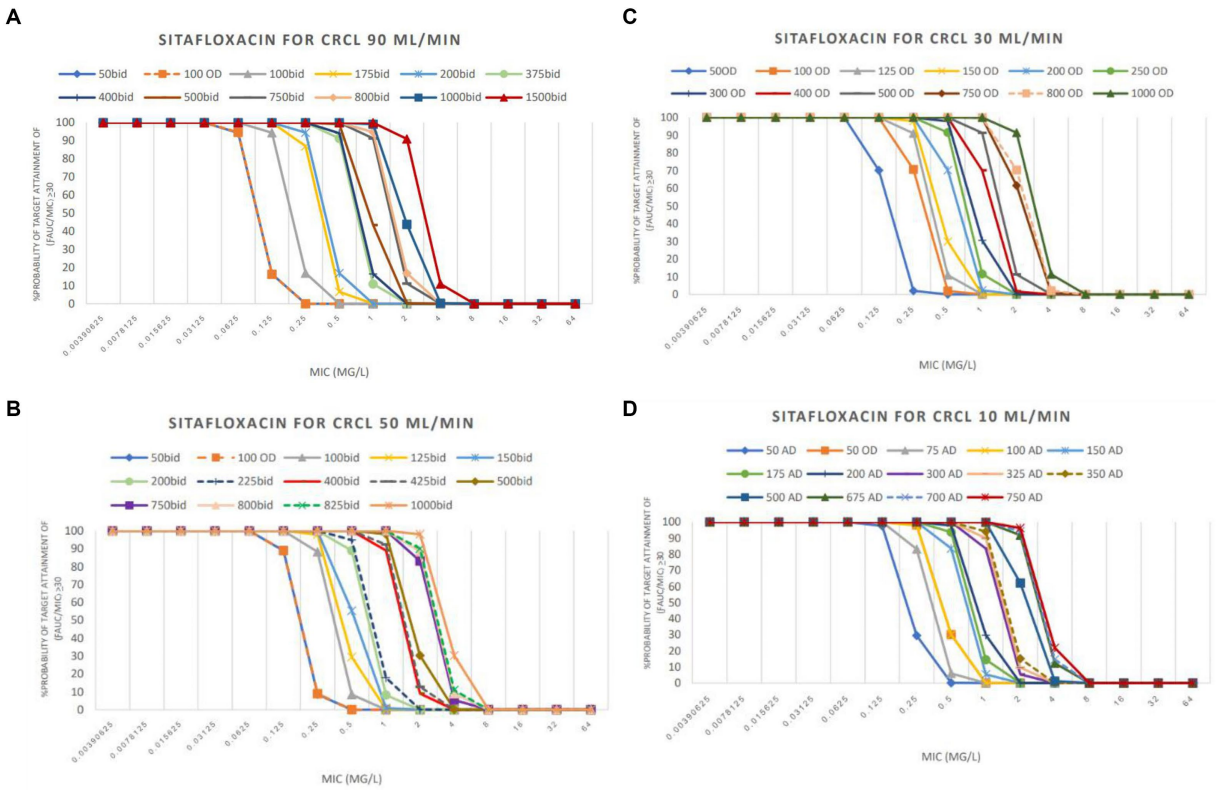

FIGURE 2
PTA achieved with sitafloxacin used in groups CrCL 90 mL/min **(A)**, CrCL 50 mL/min **(B)**, CrCL 30 mL/min **(C)**, and CrCL 10 mL/min **(D)**.

TABLE 3 The lowest recommended dose of colistin-sitafloxacin: focus on the MIC_{90} of each agent in combination.

CrCL (mL/min)	MIC_{90} (mg/L)	
	Colistin: 1 (MDR-AB, CRAB) Sitafloxacin: 1	Colistin: 2 (CoR-AB) Sitafloxacin: 1
90 mL/min	Colistin: LD 300 mg, MD 150 mg q 12 h Sitafloxacin: 750 mg q 12 h	Colistin: LD 300 mg, MD 225 mg q 12 h Sitafloxacin: 750 mg q 12 h
50 mL/min	Colistin: LD 300 mg, MD 75 mg q 24 h Sitafloxacin: 425 mg q 12 h	Colistin: LD 300 mg, MD 150 mg q 24 h Sitafloxacin: 425 mg q 12 h
30 mL/min	Colistin: LD 300 mg, MD 50 mg q 48 h Sitafloxacin: 500 mg q 24 h	Colistin: LD 300 mg, MD 75 mg q 24 h Sitafloxacin: 500 mg q 24 h
10 mL/min	Colistin: LD 300 mg, MD 50 mg q 48 h Sitafloxacin: 325 mg q 48 h	Colistin: LD 300 mg, MD 50 mg q 24 h Sitafloxacin: 325 mg q 48 h

of other types of infections, another specific index should be considered. Drug-resistant *A. baumannii*, including MDR-AB, CRAB, and CoR-AB, could be treated by combination therapy because it increases the probability of achieving the specific target. Second, most of the recommended doses from this study were different from the reference dosage regimens. Therefore, close monitoring of clinical efficacy and toxicity is necessary. Third, our dosing recommendation used two population pharmacokinetics of two agents (colistin and sitafloxacin) to simulate. Therefore, our dosing recommendation for colistin and sitafloxacin could be used only in patients with similar characteristics to this study. According to the population pharmacokinetic model, for instance, there is a difference in the APACHE II score, the comorbid condition, the CrCL, the volume of distribution, and the drug clearance in critically ill patients compared to the healthy population. These parameters affect the plasma colistin level, which is important to reach the desired target in critically ill patients. Although the population pharmacokinetic analysis of sitafloxacin was based on the study on non-critically ill patients, the oral form of this drug should be considered for absorption in critically ill patients. However, we believe that sitafloxacin might have poor absorption as critically ill patients are hemodynamically unstable. The low plasma concentration might have occurred and cannot reach the target. Fourth, drug interaction should be considered because sitafloxacin (fluoroquinolone group) could reduce absorption when concomitant with antacids, ferrous sulfate, and other metallic cation-containing compounds (Deppermann and Lode, 1993) (this study simulates based on the fasted state of patient). Finally, this study used the PD index of efficacy. Thus, we cannot predict the resistant situation. However, the high dose of sitafloxacin should not develop pathogen resistance. The low dose of colistin in the combination therapy was against the lower MIC than usual. They should not develop pathogen resistance either. Currently, the problem with using colistin and sitafloxacin in combination is that there are no data that relate to the clinical outcome in terms of resistant genes. Although this

TABLE 4 %Probability of target attainment (PTA) and %Cumulative fraction of response (CFR) of the studied colistin regimens for each type of isolate in combinations.

Dosage regimen	Daily MD	%PTA of MDR-AB and CRAB		%CFR MDR-AB	%CFR CRAB	%PTA of CoR-AB		%CFR CoR-AB
		MIC_{50} (0.5 mg/L)	MIC_{90} (1 mg/L)			MIC_{50} (1 mg/L)	MIC_{90} (2 mg/L)	
CrCL 90 mL/min								
LD 300 mg, MD 150 mg q 8 h (Siriraj)	450 mg	98.88	95.54	96.99	97.03	95.54	83.31	88.45
LD 300 mg, MD 225 mg q12h (Our study)	450 mg	99.27	97.23	98.12	98.12	97.23	**90.62**	92.66
LD 300 mg, MD 180 mg q 12 h (Nation et al.)	360 mg	98.89	96.05	97.38	97.41	96.05	87.20	**90.37**
LD 300 mg, MD150 mg q 12 h (Siriraj, EMA, and FDA)	300 mg	98.39	**94.29**	96.37	96.41	**94.29**	82.22	87.48
LD 300 mg, MD 100 mg q 12 h (Our study)	200 mg	96.72	89.24	**93.40**	**93.47**	89.24	68.14	80.04
LD 300 mg, MD 100 mg q 24 h (Our study)	100 mg	**93.26**	82.11	89.26	89.37	82.11	58.91	73.35
LD 300 mg, MD 75 mg q 24 h (Our study)	75 mg	88.72	73.27	83.85	84.00	73.27	45.32	64.03
CrCL 50 mL/min								
LD 300 mg, MD 150 mg q 12 h (Siriraj, EMA, and FDA)	300 mg	99.82	99.2	99.25	99.25	99.2	96.17	95.42
LD 300 mg, MD 122.5 mg q 12 h (Nation et al.)	245 mg	99.8	98.89	98.97	98.98	98.89	94.08	93.90
LD 300 mg, MD 114 mg q 12 h (FDA)	228 mg	99.76	98.62	98.77	98.79	98.62	92.49	93.07
LD 300 mg, MD 150 mg q 24 h (Our study)	150 mg	99.72	98.63	98.91	98.92	98.63	**93.48**	94.63
LD 300 mg, MD 100 mg q 24 h (Our study)	100 mg	99.00	95.71	97.24	97.27	95.71	85.22	89.60
LD 300 mg, MD 75 mg q 24 h (Our study)	75 mg	98.33	**92.91**	95.61	95.67	**92.91**	76.38	84.95
LD 300 mg, MD 50 mg q 24 h (Our study)	50 mg	96.14	85.50	91.55	91.65	85.50	58.13	75.10
LD 300 mg, MD 50 mg q 48 h (Our study)	25 mg	**95.97**	85.00	**91.23**	**91.33**	85.00	56.42	74.24
CrCL 30 mL/min								
LD 300 mg, MD 125 mg q 12 h (EMA)	250 mg	99.98	99.89	99.66	99.66	99.89	98.63	96.76
LD 300 mg, MD 100 mg q 12 h (Siriraj)	200 mg	99.96	99.68	99.45	99.45	99.68	97.36	95.38
LD 300 mg, MD 97.5 mg q 12 h (Nation et al.)	195 mg	99.98	99.71	99.44	99.42	99.71	97.08	95.20
LD 300 mg, MD 150 mg q 24 h (FDA)	150 mg	99.96	99.78	99.72	99.72	99.78	98.61	97.88
LD 300 mg, MD 75 mg q 24 h (Our study)	75 mg	99.83	98.82	98.88	98.90	98.82	**92.20**	**93.49**
LD 300 mg, MD 50 mg q 24 h (Our study)	50 mg	99.42	96.17	97.23	97.28	96.17	80.11	87.71
LD 300 mg, MD 50 mg q 48 h (Our study)	25 mg	**99.40**	**95.80**	**97.08**	**97.13**	**95.80**	79.82	87.29
CrCL 10 mL/min								
LD 300 mg, MD 160 mg q 24 h (Nation)	160 mg	100	100	99.97	99.97	100	99.99	99.65
LD 300 mg, MD 150 mg q 24 h (Siriraj and EMA)	150 mg	100	99.99	99.96	99.96	100	99.91	99.57
LD 300 mg, MD 60 mg q 24 h (FDA)	60 mg	99.99	99.85	99.60	99.60	99.85	97.61	96.42
LD 300 mg, 50 mg q 24 h (Our study)	50 mg	99.99	99.68	99.43	99.43	99.68	96.25	95.35
LD 300 mg, MD 50 mg q 48 h (Our study)	25 mg	**100**	**99.73**	**99.41**	**99.41**	**99.73**	**96.04**	**94.95**

LD, loading dose (in mg colistin base activity), MD, maintenance dose (in mg colistin base activity), EMA, European Medicines Agency, FDA, Food and Drug Administration of United States, Nation et al.: The research from Nation et al. our study: the proposed regimens in our study. The bold font shows the PTA achieved for ≥ 90% at the lowest dose.

10.3389/fmicb.2023.1275909

TABLE 5 %PTA and %CFR of the studied sitafloxacin regimens for each type of isolate in combinations.

Dosage regimen	Daily dose (mg)	%PTA of MDR-AB and CRAB		%CFR MDR-AB	%CFR CRAB	%PTA of CoR-AB		%CFR CoR-AB
		MIC_{50} (0.5 mg/L)	MIC_{90} (1 mg/L)			MIC_{50} (0.25 mg/L)	MIC_{90} (1 mg/L)	
CrCL 90 mL/min								
750 mg q 12 h (Our study)	1,500 mg	100	**91.25**	93.82	93.04	100	**91.25**	**97.12**
500 mg q 12 h (Our study)	1,000 mg	99.15	43.48	47.60	47.03	100	43.48	78.84
400 mg q 12 h (Our study)	800 mg	**94.14**	16.4	73.79	73.20	100	16.46	88.95
375 mg q 12 h (Our study)	750 mg	91.29	10.95	71.28	70.70	99.99	10.95	87.97
200 mg q 12 h (Our study)	400 mg	16.79	0.01	34.85	34.28	94.47	0.01	72.51
175 mg q 12 h (Our study)	350 mg	6.61	0	28.91	28.36	86.99	0	67.72
100 mg q 12 h (Manufacturer)	200 mg	0.02	0	12.27	11.99	16.94	0	36.54
100 mg q 24 h (Manufacturer)	100 mg	0	0	6.66	6.44	0.0	0	18.06
50 mg q 12 h (Manufacturer)	100 mg	0	0	6.64	6.43	0.03	0	18.04
CrCL 50 mL/min								
500 mg q 12 h (Our study)	1,000 mg	100	98.2	96.06	95.34	100	98.2	98.21
425 mg q 12 h (Our study)	850 mg	100	**92.32**	94.12	93.34	100	**92.32**	97.26
400 mg q12 h (Our study)	800 mg	99.99	88.93	93.22	92.43	100	88.93	**96.85**
225 mg q12 h (Our study)	450 mg	**94.83**	17.78	74.40	73.81	100	17.78	89.19
200 mg q 12 h (Our study)	400 mg	88.82	8.11	69.54	68.98	100	8.11	87.31
150 mg q12 h (Our study)	300 mg	55.24	0.87	53.00	52.43	99.6	0.87	81.00
125 mg q 12 h (Our study)	250 mg	29.35	0.09	41.08	40.50	**97.92**	0.09	76.01
100 mg q 12 h (Manufacturer)	200 mg	8.47	0.02	29.97	29.42	88.22	0.02	68.54
100 mg q 24 h (Manufacturer)	100 mg	0	0	10.56	10.31	8.94	0	32.42
50 mg q 12 h (Manufacturer)	100 mg	0	0	10.49	10.24	8.54	0	32.25
CrCL 30 mL/min								
500 mg q 24 h (Our study)	500 mg	100	**91.31**	93.84	93.06	100	**91.31**	97.13
400 mg q 24 h (Our study)	400 mg	99.88	70.16	88.63	87.88	100	70.16	94.92
300 mg q 24 h (Our study)	300 mg	97.82	30.58	78.64	78.01	100	30.58	**90.86**
250 mg q 24 h (Our study)	250 mg	**91.50**	11.53	71.50	70.93	100	11.53	88.06
200 mg q 24 h (Our study)	200 mg	70.23	2.27	59.99	59.43	99.88	2.27	83.69
150 mg q 24 h (Our study)	150 mg	29.79	0.06	41.27	40.69	97.94	0.06	76.09
125 mg q 24 h (Our study)	125 mg	10.87	0.01	31.58	31.02	**91.07**	0.01	70.13
100 mg q 24 h (Our study)	100 mg	1.96	0	23.70	23.20	70.7	0	60.13
50 mg q 24 h (Manufacturer)	50 mg	0	0	8.72	8.49	2.03	0	26.91
CrCL 10 mL/min								
500 mg q 48 h (Our study)	250 mg	100	99.78	97.52	96.94	100	99.78	99.10
350 mg q 48 h (Our study)	175 mg	99.99	94.11	94.61	93.84	100	94.11	97.48
325 mg q 48 h (Our study)	162.5 mg	100	**90.01**	93.49	92.70	100	**90.01**	96.97
300 mg q 48 h (Our study)	150 mg	99.99	83.5	91.85	91.07	100	83.5	96.26
200 mg q 48 h (Our study)	100 mg	97.79	29.77	78.44	77.81	100	29.77	**90.78**
175 mg q 48 h (Our study)	87.5 mg	**93.68**	14.52	73.15	72.57	100	14.52	88.69
150 mg q 48 h (Our study)	75 mg	83.58	5.44	66.62	66.06	99.98	5.44	86.20
100 mg q 48 h (Our Study)	50 mg	30.01	0.11	41.37	40.79	97.88	0.11	76.10
50 mg q 24 h (Our study)	50 mg	30.09	0.07	41.45	40.87	**98.17**	0.07	76.23
75 mg q 48 h (Our study)	37.5 mg	6.04	0	27.93	27.39	83.22	0	66.05
50 mg q 48 h (Manufacturer)	25 mg	0.13	0	14.84	14.51	29.51	0	42.27

Our study: the proposed regimens in our study, manufacturer: the recommended dosage regimens from the manufacturer of sitafloxacin. The bold font shows the PTA achieved for ≥ 90% at the lowest dose.

10.3389/fmicb.2023.1275909

study uses data from the most recent publications, further study is needed to confirm the results of this simulation study.

Data availability statement

The original contributions presented in the study are included in the article/Supplementary material, further inquiries can be directed to the corresponding author.

Ethics statement

This study was approved by the Ethics Committee of the Faculty of Dentistry/Faculty of Pharmacy, Mahidol University (COE. No.MU-DT/PY-IRB2020/001.1501).

Author contributions

VR: Conceptualization, Data curation, Formal analysis, Investigation, Methodology, Project administration, Writing – original draft, Writing – review & editing. PM: Conceptualization, Project administration, Supervision, Validation, Writing – review & editing. JH: Methodology, Resources, Writing – review & editing. KJ: Methodology, Writing – review & editing. WN: Methodology, Writing – review & editing.

Funding

The author(s) declare that no financial support was received for the research, authorship, and/or publication of this article.

Acknowledgments

We thank Orarik Asuphon from Department of Pharmacy Practice, Faculty of Pharmaceutical Sciences, Naresuan University, Thailand, Pannee Leelawattanachai from Department of Pharmacy, Faculty of Medicine Vajira Hospital, Navamindradhiraj University, Thailand, and Taniya Paiboonvong from Department of Pharmacy Practice, College of Pharmacy, Rangsit University, Thailand for the valuable advice of this manuscript.

Conflict of interest

The authors declare that the research was conducted in the absence of any commercial or financial relationships that could be construed as a potential conflict of interest.

Publisher's note

All claims expressed in this article are solely those of the authors and do not necessarily represent those of their affiliated organizations, or those of the publisher, the editors and the reviewers. Any product that may be evaluated in this article, or claim that may be made by its manufacturer, is not guaranteed or endorsed by the publisher.

Supplementary material

The Supplementary material for this article can be found online at: https://www.frontiersin.org/articles/10.3389/fmicb.2023.1275909/full#supplementary-material

References

Almasaudi, S. B. (2018). Acinetobacter spp. as nosocomial pathogens: epidemiology and resistance features. *Saudi J. Biol. Sci.* 25, 586–596. doi: 10.1016/j.sjbs.2016.02.009

Amat, T., Gutiérrez-Pizarraya, A., Machuca, I., Gracia-Ahufinger, I., Pérez-Nadales, E., Torre-Giménez, Á., et al. (2018). The combined use of tigecycline with high-dose colistin might not be associated with higher survival in critically ill patients with bacteraemia due to carbapenem-resistant *Acinetobacter baumannii*. *Clin. Microbiol. Infect.* 24, 630–634. doi: 10.1016/j.cmi.2017.09.016

Appaneal, H. J., Lopes, V. V., LaPlante, K. L., and Caffrey, A. R. (2022). Treatment, clinical outcomes, and predictors of mortality among a national cohort of admitted patients with *Acinetobacter baumannii* infection. *Antimicrob. Agents Chemother.* 66, e01975–e01921. doi: 10.1128/aac.01975-21

Asuphon, O., Montakantikul, P., Houngsaitong, J., Kiratisin, P., and Sonthisombat, P. (2016). Optimizing intravenous fosfomycin dosing in combination with carbapenems for treatment of *Pseudomonas aeruginosa* infections in critically ill patients based on pharmacokinetic/pharmacodynamic (PK/PD) simulation. *Int. J. Infect. Dis.* 50, 23–29. doi: 10.1016/j.ijid.2016.06.017

Batirel, A., Balkan, I. I., Karabay, O., Agalar, C., Akalin, S., Alici, O., et al. (2014). Comparison of colistin-carbapenem, colistin-sulbactam, and colistin plus other antibacterial agents for the treatment of extremely drug-resistant *Acinetobacter baumannii* bloodstream infections. *Eur. J. Clin. Microbiol. Infect. Dis.* 33, 1311–1322. doi: 10.1007/s10096-014-2070-6

Butler, M. S., Henderson, I. R., Capon, R. J., and Blaskovich, M. A. (2022). Antibiotics in the clinical pipeline as of. *J. Antibiot.* 76, 431–473. doi: 10.1038/s41429-023-00629-8

Cai, Y., Chai, D., Wang, R., Liang, B., and Bai, N. (2012). Colistin resistance of *Acinetobacter baumannii*: clinical reports, mechanisms and antimicrobial strategies. *J. Antimicrob. Chemother.* 67, 1607–1615. doi: 10.1093/jac/dks084

Centers for Disease Control and Prevention. (n.d.) Available at: https://www.cdc.gov/hai/organisms/acinetobacter.html (Accessed March 21, 2022).

Cheah, S. E., Wang, J., Nguyen, V. T., Turnidge, J. D., Li, J., and Nation, R. L. (2015). New pharmacokinetic/pharmacodynamic studies of systemically administered colistin against *Pseudomonas aeruginosa* and *Acinetobacter baumannii* in mouse thigh and lung infection models: smaller response in lung infection. *J. Antimicrob. Chemother.* 70, 3291–3297. doi: 10.1093/jac/dkv267

Cisneros, J. M., and Rodríguez-Baño, J. (2002). Nosocomial bacteremia due to *Acinetobacter baumannii*: epidemiology, clinical features and treatment. *Clin. Microbiol. Infect.* 8, 687–693. doi: 10.1046/j.1469-0691.2002.00487.x

Clinical and Laboratory Standards Institute. *Performance standards for antimicrobial susceptibility Testing*. Thirty-two informational supplement. CLSI document M100-Swayne; CLSI: Wayne, PA, USA, (2022).

Craig, W. A. (1998). Pharmacokinetic/pharmacodynamic parameters: rationale for antibacterial dosing of mice and men. *Clin. Infect. Dis.* 26, 1–10. doi: 10.1086/516284

Dai, C., Li, J., Tang, S., Li, J., and Xiao, X. (2014). Colistin-induced nephrotoxicity in mice involves the mitochondrial, death receptor, and endoplasmic reticulum pathways. *Antimicrob. Agents Chemother.* 58, 4075–4085. doi: 10.1128/AAC.00070-14

Deppermann, K. M., and Lode, H. (1993). Fluoroquinolones: interaction profile during enteral absorption. *Drugs* 45, 65–72. doi: 10.2165/00003495-199300453-00013

Dickstein, Y., Lellouche, J., Ben Dalak Amar, M., Schwartz, D., Nutman, A., Daitch, V., et al. (2019). Ben Dalak Amar M, Schwartz D, Nutman a, Daitch V, Yahav D, Leibovici L, Skiada a, Antoniadou a, Daikos GL, Andini R, Zampino R, Durante-Mangoni E, Mouton JW, Friberg LE, Dishon Benattar Y, Bitterman R, Neuberger a, Carmeli Y, Paul M; AIDA study group. Treatment outcomes of colistin- and carbapenem-resistant *Acinetobacter baumannii* infections: an exploratory subgroup analysis of a randomized clinical trial. *Clin. Infect. Dis.* 69, 769–776. doi: 10.1093/cid/ciy988

Dong, X., Chen, F., Zhang, Y., Liu, H., Liu, Y., and Ma, L. (2015). In vitro activities of sitafloxacin tested alone and in combination with rifampin, colistin, sulbactam, and tigecycline against extensively drug-resistant *Acinetobacter baumannii*. *Int. J. Clin. Exp. Med.* 8, 8135–8140.

Dudhani, R. V., Turnidge, J. D., Nation, R. L., and Li, J. (2010). fAUC/MIC is the most predictive pharmacokinetic/pharmacodynamic index of colistin against *Acinetobacter baumannii* in murine thigh and lung infection models. *J. Antimicrob. Chemother.* 65, 1984–1990. doi: 10.1093/jac/dkq226

Eljaaly, K., Bidell, M. R., Gandhi, R. G., Alshehri, S., Enani, M. A., Al-Jedai, A., et al. (2021). Colistin nephrotoxicity: meta-analysis of randomized controlled trials. *Open Forum Infect. Dis.* 8:ofab026. doi: 10.1093/ofid/ofab026

Falagas, M. E., Rafailidis, P. I., Ioannidou, E., Alexiou, V. G., Matthaiou, D. K., Karageorgopoulos, D. E., et al. (2010). Colistin therapy for microbiologically documented multidrug-resistant gram-negative bacterial infections: a retrospective cohort study of 258 patients. *Int. J. Antimicrob. Agents* 35, 194–199. doi: 10.1016/j.ijantimicag.2009.10.005

Feldman, C., White, H., O'Grady, J., Flitcroft, A., Briggs, A., and Richards, G. (2001). An open, randomised, multi-Centre study comparing the safety and efficacy of sitafloxacin and imipenem/cilastatin in the intravenous treatment of hospitalised patients with pneumonia. *Int. J. Antimicrob. Agents* 17, 177–188. doi: 10.1016/S0924-8579(00)00344-7

García-Garmendia, J. L., Ortiz-Leyba, C., Garnacho-Montero, J., Jiménez-Jiménez, F. J., Pérez-Paredes, C., Barrero-Almodóvar, A. E., et al. (2001). Risk factors for *Acinetobacter baumannii* nosocomial bacteremia in critically ill patients: a cohort study. *Clin. Infect. Dis.* 33, 939–946. doi: 10.1086/322584

Garonzik, S. M., Li, J., Thamlikitkul, V., Paterson, D. L., Shoham, S., Jacob, J., et al. (2011). Population pharmacokinetics of colistin methanesulfonate and formed colistin in critically ill patients from a multicenter study provide dosing suggestions for various categories of patients. *Antimicrob. Agents Chemother.* 55, 3284–3294. doi: 10.1128/AAC.01733-10

Huang, Y. S., Wang, J. T., Sheng, W. H., Chuang, Y. C., and Chang, S. C. (2015). Comparative in vitro activity of sitafloxacin against bacteremic isolates of carbapenem resistant *Acinetobacter baumannii* complex. *J. Microbiol. Immunol. Infect.* 48, 545–551. doi: 10.1016/j.jmii.2014.02.002

Jambhekar, S. S., and Breen, P. J. (Eds.) (2012). Basic Pharmacokinetics. *Extravascular routes of drug administration.*

Jitaree, K., Sathirakul, K., Houngsaitong, J., Asuphon, O., Saelim, W., Thamlikitkul, V., et al. (2019). Pharmacokinetic/pharmacodynamic (PK/PD) simulation for dosage optimization of colistin against carbapenem-resistant *Klebsiella pneumoniae* and carbapenem-resistant *Escherichia coli*. *Antibiotics (Basel)* 8:125. doi: 10.3390/antibiotics8030125

Kalin, G., Alp, E., Akin, A., Coskun, R., and Doganay, M. (2014). Comparison of colistin and colistin/sulbactam for the treatment of multidrug resistant *Acinetobacter baumannii* ventilator-associated pneumonia. *Infection* 42, 37–42. doi: 10.1007/s15010-013-0495-y

Kaye, K. S., and Pogue, J. M. (2015). Infections caused by resistant gram-negative bacteria: epidemiology and management. *Pharmacotherapy* 35, 949–962. doi: 10.1002/phar.1636

Keating, G. M. (2011). Sitafloxacin. *Drugs* 71, 731–744. doi: 10.2165/11207380-000000000-00000

Kmietowicz, Z. (2017). Few novel antibiotics in the pipeline. *WHO* 358:j4339. doi: 10.1136/bmj.j4339

Leelawattanachai, P., Wattanavijitkul, T., Paiboonvong, T., Plongla, R., Chatsuwan, T., Usayaporn, S., et al. (2020). Evaluation of intravenous Fosfomycin disodium dosing regimens in critically ill patients for treatment of carbapenem-resistant Enterobacterales infections using Monte Carlo simulation. *Antibiotics (Basel)* 9:615. doi: 10.3390/antibiotics9090615

Lemos, E. V., de La Hoz, F. P., Einarson, T. R., McGhan, W. F., Quevedo, E., Castañeda, C., et al. (2014). Carbapenem resistance and mortality in patients with *Acinetobacter baumannii* infection: systematic review and meta-analysis. *Clin. Microbiol. Infect.* 20, 416–423. doi: 10.1111/1469-0691.12363

Liang, C. A., Lin, Y. C., Lu, P. L., Chen, H. C., Chang, H. L., and Sheu, C. C. (2018). Antibiotic strategies and clinical outcomes in critically ill patients with pneumonia caused by carbapenem-resistant *Acinetobacter baumannii*. *Clin. Microbiol. Infect.* 24, 908.e1–908.e7. doi: 10.1016/j.cmi.2017.10.033

Lim, S. K., Lee, S. O., Choi, S. H., Choi, J. P., Kim, S. H., Jeong, J. Y., et al. (2011). The outcomes of using colistin for treating multidrug resistant Acinetobacter species bloodstream infections. *J. Korean Med. Sci.* 26, 325–331. doi: 10.3346/jkms.2011.26.3.325

Lode, H., Borner, K., and Koeppe, P. (1998). Pharmacodynamics of fluoroquinolones. *Clin. Infect. Dis.* 27, 33–39. doi: 10.1086/514623

López-Cortés, L. E., Cisneros, J. M., Fernández-Cuenca, F., Bou, G., Tomás, M., Garnacho-Montero, J., et al. (2014). Fernández-Cuenca F, Bou G, Tomás M, Garnacho-Montero J, Pascual a, Martínez-Martínez L, Vila J, Pachón J, Rodríguez Baño J; GEIH/REIPI-Ab2010 group. Monotherapy versus combination therapy for sepsis due to multidrug-resistant *Acinetobacter baumannii*: analysis of a multicentre prospective cohort. *J. Antimicrob. Chemother.* 69, 3119–3126. doi: 10.1093/jac/dku233

Nakashima, M. (2008). Pharmacokinetics of sitafloxacin (DU-6859a) in healthy volunteers (in Japanese). *Jpn. J. Chemother.* 56, 154–155.

Nakashima, M., and Kawada, Y. (2008). Pharmacokinetic profiles of sitafloxacin in patients with renal dysfunction (in Japanese). *Jpn. J. Chemother.* 56, 21–24.

Nakashima, M., Uematsu, T., Kosuge, K., Umemura, K., Hakusui, H., and Tanaka, M. (1995). Pharmacokinetics and tolerance of DU-6859a, a new fluoroquinolone, after single and multiple oral doses in healthy volunteers. *Antimicrob. Agents Chemother.* 39, 170–174. doi: 10.1128/AAC.39.1.170

Nation, R. L., Garonzik, S. M., Li, J., Thamlikitkul, V., Giamarellos-Bourboulis, E. J., Paterson, D. L., et al. (2016). Updated US and European dose recommendations for intravenous colistin: how do they perform? *Clin. Infect. Dis.* 62, 552–558. doi: 10.1093/cid/civ964

Nation, R. L., Garonzik, S. M., Thamlikitkul, V., Giamarellos-Bourboulis, E. J., Forrest, A., Paterson, D. L., et al. (2017). Dosing guidance for intravenous colistin in critically-ill patients. *Clin. Infect. Dis.* 64, 565–571. doi: 10.1093/cid/ciw839

Nation, R. L., Velkov, T., and Li, J. (2014). Colistin and polymyxin B: peas in a pod, or chalk and cheese? *Clin. Infect. Dis.* 59, 88–94. doi: 10.1093/cid/ciu213

Paiboonvong, T., Nosoongnoen, W., Sathirakul, K., Tangsujaritvijit, V., Kaemapairoj, J., Tragulpiankit, P., et al. (2019). Pharmacokinetics and penetration of sitafloxacin into alveolar epithelial lining fluid in critically ill Thai patients with pneumonia. *Antimicrob. Agents Chemother.* 63, e00800–e00819. doi: 10.1128/AAC.00800-19

Pantopoulou, A., Giamarellos-Bourboulis, E. J., Raftogannis, M., Tsaganos, T., Dontas, I., Koutoukas, P., et al. (2007). Colistin offers prolonged survival in experimental infection by multidrug-resistant *Acinetobacter baumannii*: the significance of co-administration of rifampicin. *Int. J. Antimicrob. Agents* 29, 51–55. doi: 10.1016/j.ijantimicag.2006.09.009

Papathanakos, G., Andrianopoulos, I., Papathanasiou, A., Priavali, E., Koulenti, D., and Koulouras, V. (2020). Colistin-resistant *Acinetobacter baumannii* bacteremia: a serious threat for critically ill patients. *Microorganisms* 8:287. doi: 10.3390/microorganisms8020287

Pharmaceuticals and Medical Devices Agency (n.d.). "Gracevit tablets, fine granules (sitafloxacin hydrate)" in *Approval review information on ethical drugs [internet]* (Tokyo: Daiichi Sankyo Co., Ltd) Japanesehttp://www.info.pmda.go.jp/shinyaku/P200800006/index.html

Rodjun, V., Houngsaitong, J., Montakantikul, P., Paiboonvong, T., Khuntayaporn, P., Yanyongchaikit, P., et al. (2020). In vitro activities of colistin and Sitafloxacin combinations against multidrug-, carbapenem-, and colistin-resistant *Acinetobacter baumannii* using the broth microdilution checkerboard and time-kill methods. *Antibiotics (Basel)* 9:516. doi: 10.3390/antibiotics9080516

Saito, A., Tanigawara, Y., Watanabe, A., Aoki, N., Niki, Y., Kohno, S., et al. (2008). Open study of sitafloxacin in patients with respiratory tract infections: PK-PD study (in Japanese). *Jpn. J. Chemother* 56, 63–80.

Sekino, H. (2008). Pharmacokinetic profiles of sitafloxacin in elderly volunteer (in Japanese). *Jpn. J. Chemother.* 56, 18–20.

Sieniawski, K., Kaczka, K., Rucińska, M., Gagis, L., and Pomorski, L. (2013). *Acinetobacter baumannii* nosocomial infections. *Pol. Przegl. Chir.* 85, 483–490. doi: 10.2478/pjs-2013-0075

Spapen, H., Jacobs, R., Van Gorp, V., Troubleyn, J., and Honoré, P. M. (2011). Renal and neurological side effects of colistin in critically ill patients. *Ann. Intensive Care* 1:14. doi: 10.1186/2110-5820-1-14

Sun, L. N., Sun, G. X., Yang, Y. Q., Shen, Y., Huang, F. R., Xie, L. J., et al. (2021). Effects of ABCB1, UGT1A1, and UGT1A9 genetic polymorphisms on the pharmacokinetics of Sitafloxacin granules in healthy subjects. *Clin. Pharmacol. Drug Dev.* 10, 57–67. doi: 10.1002/cpdd.848

Sunenshine, R. H., Wright, M. O., Maragakis, L. L., Harris, A. D., Song, X., Hebden, J., et al. (2007). Multidrug-resistant Acinetobacter infection mortality rate and length of hospitalization. *Emerg. Infect. Dis.* 13, 97–103. doi: 10.3201/eid1301.060716

Tamma, P. D., Aitken, S. L., Bonomo, R. A., Mathers, A. J., van Duin, D., and Clancy, C. J. (2023). Infectious Diseases Society of America 2023 guidance on the treatment of antimicrobial resistant gram-negative infections. *Clin. Infect. Dis.*:ciad428. doi: 10.1093/cid/ciad428

Tanigawara, Y., Kaku, M., Totsuka, K., Tsuge, H., and Saito, A. (2013). Population pharmacokinetics and pharmacodynamics of sitafloxacin in patients with community-acquired respiratory tract infections. *J. Infect. Chemother.* 19, 858–866. doi: 10.1007/s10156-013-0580-2

Tsuji, B. T., Pogue, J. M., Zavascki, A. P., Paul, M., Daikos, G. L., Forrest, A., et al. (2019). International consensus guidelines for the optimal use of the polymyxins: endorsed by the American college of clinical pharmacy (ACCP), European society of clinical microbiology and infectious diseases (ESCMID), infectious diseases society of America (IDSA), international society for anti-infective pharmacology (ISAP), society of critical care medicine (SCCM), and society of infectious diseases pharmacists (SIDP). *Pharmacotherapy* 39, 10–39. doi: 10.1002/phar.2209

Werarak, P., Waiwarawut, J., Tharavichitkul, P., Pothirat, C., Rungruanghiranya, S., Geater, S. L., et al. (2012). *Acinetobacter baumannii* nosocomial pneumonia in tertiary care hospitals in Thailand. *J. Med. Assoc. Thail.* 95 Suppl 2, S23–S33.

Yedle, R., Reniguntla, M. K., Puttaswamy, R., Puttarangappa, P., Hiremath, S., Nanjundappa, M., et al. (2023). Neutropenic rat thigh infection model for evaluation of the pharmacokinetics/pharmacodynamics of anti-infectives. *Microbiol. Spectr.* 11, e00133–e00123. doi: 10.1128/spectrum.00133-23

Yilmaz, G. R., Guven, T., Guner, R., Kocak Tufan, Z., Izdes, S., Tasyaran, M. A., et al. (2015). Colistin alone or combined with sulbactam or carbapenem against *A. baumannii* in ventilator-associated pneumonia. *J. Infect. Dev. Ctries.* 9, 476–485. doi: 10.3855/jidc.6195

frontiers | Frontiers in Microbiology

TYPE Original Research
PUBLISHED 11 December 2023
DOI 10.3389/fmicb.2023.1298858

OPEN ACCESS

EDITED BY
Saurabh Mishra,
Cornell University, United States

REVIEWED BY
Feng Zhou,
Henan Institute of Science and Technology, China
Biplab Singha,
University of Massachusetts Medical School, United States

*CORRESPONDENCE
Rasha Abdelsalam Elshenawy
✉ r.a.elshenawy@herts.ac.uk

RECEIVED 22 September 2023
ACCEPTED 20 November 2023
PUBLISHED 11 December 2023

CITATION
Abdelsalam Elshenawy R, Umaru N and Aslanpour Z (2023) WHO AWaRe classification for antibiotic stewardship: tackling antimicrobial resistance – a descriptive study from an English NHS Foundation Trust prior to and during the COVID-19 pandemic. *Front. Microbiol.* 14:1298858. doi: 10.3389/fmicb.2023.1298858

WHO AWaRe classification for antibiotic stewardship: tackling antimicrobial resistance – a descriptive study from an English NHS Foundation Trust prior to and during the COVID-19 pandemic

Rasha Abdelsalam Elshenawy*, Nkiruka Umaru and Zoe Aslanpour

Department of Pharmacy, School of Life and Medical Sciences, University of Hertfordshire, Hatfield, United Kingdom

Antimicrobial resistance (AMR) is a silent and rapidly escalating pandemic, presenting a critical challenge to global health security. During the pandemic, this study was undertaken at a NHS Foundation Trust in the United Kingdom to explore antibiotic prescribing trends for respiratory tract infections (RTIs), including pneumonia, and the COVID-19 pandemic across the years 2019 and 2020. This study, guided by the WHO's AWaRe classification, sought to understand the impact of the pandemic on antibiotic prescribing and antimicrobial stewardship (AMS). The research methodology involved a retrospective review of medical records from adults aged 25 and older admitted with RTIs, including pneumonia, in 2019 and 2020. The application of the AWaRe classification enabled a structured description of antibiotic use. The study evaluated antibiotic use in 640 patients with RTIs. Notably, it observed a slight increase in the use of amoxicillin/clavulanic acid and a substantial rise in azithromycin prescriptions, highlighting shifts in prescribing trends. Despite these changes, some antibiotics displayed steady consumption rates. These findings highlight the importance of understanding antibiotic use patterns during the AMR threat. The increase in the usage of "Watch" category antibiotics during the pandemic emphasises the urgency of robust AMS measures. The research confirms that incorporating the AWaRe classification in prescribing decisions is crucial for patient safety and combating antibiotic misuse. This study provides essential insights into the changing landscape of antibiotic prescribing during a global health crisis, reinforcing the necessity for ongoing AMS vigilance to effectively address AMR challenges.

KEYWORDS

AWaRe, antibiotic stewardship, COVID-19, NHS, hospitals, antimicrobial resistance

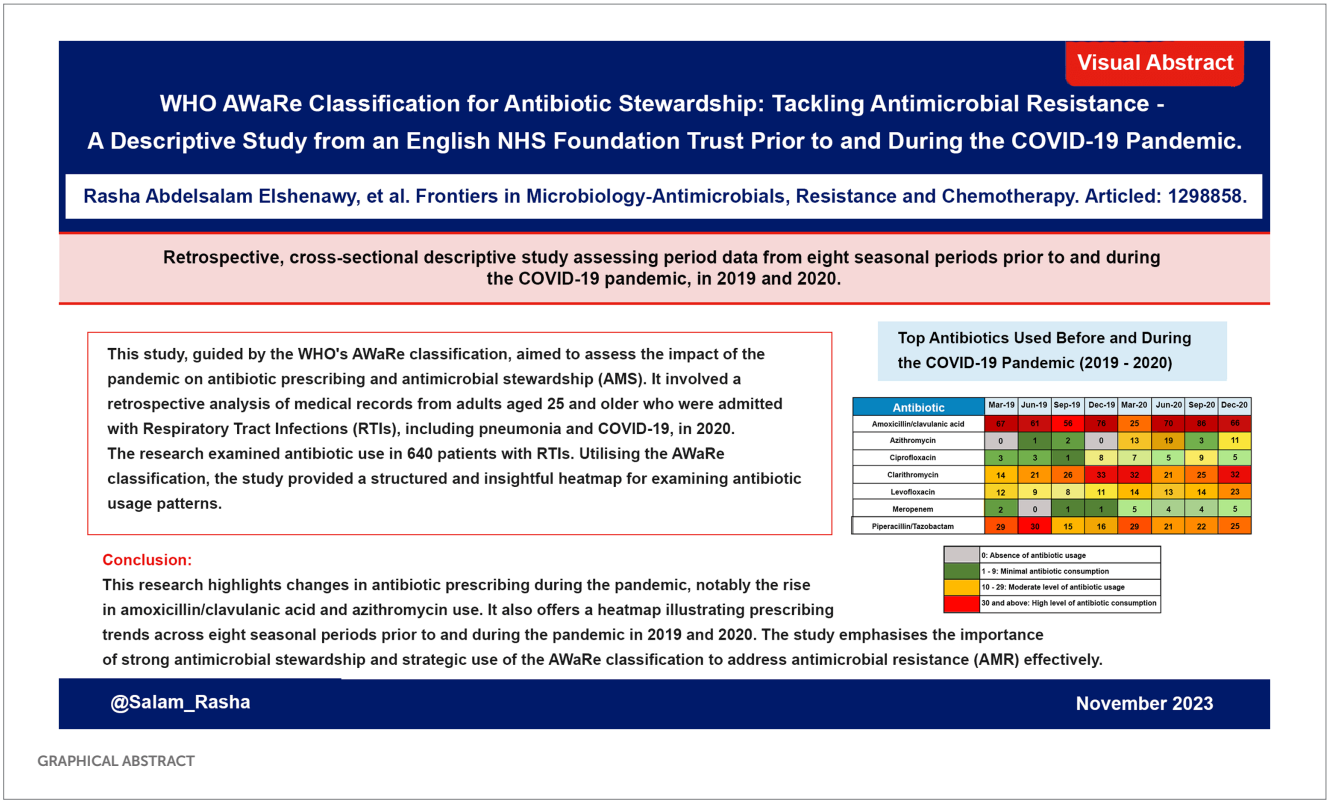

GRAPHICAL ABSTRACT

Introduction

Antimicrobial resistance (AMR) constitutes a silent and rapidly escalating pandemic, presenting a critical challenge to global health security (Salam et al., 2023). The introduction of penicillin in the 1920s was a transformative era in the field of infection management, significantly diminishing mortality rates associated with infections (Elshenawy et al., 2023). Despite these advances, the emergence and escalation of AMR, primarily attributed to the inappropriate prescription of antibiotics, casts a long shadow over these achievements. It was projected that AMR infection rates could escalate to 10 million cases by the year 2050 (O'Neill, 2014). Notably, in 2019, AMR was implicated in the deaths of over 1.2 million individuals globally. In response to this growing crisis, the implementation of antimicrobial stewardship (AMS) has become increasingly imperative (Murray, 2022). AMS advocates for the judicious use of antibiotics, thereby optimising treatment outcomes and minimising the development of resistance (National Institute for Health and Care Excellence, 2015). The World Health Organization (WHO) has actively contributed to this endeavour by developing the AWaRe classification system (www.who.int, 2023). This framework is instrumental in guiding the global implementation of AMS and promoting responsible antibiotic usage, aligning with the strategic objectives outlined in the UK's Five-Year AMR Strategic Plan (Department of Health and Social Care, 2019). This alignment emphasised an integrated international commitment to addressing and mitigating the challenges posed by AMR (Tejpar et al., 2022).

In the AWaRe tool, antibiotics are divided into three categories: access, watch, and reserve. Each category is based on its respective effect on AMR. The "Access" antibiotics are characterised by their narrow spectrum of activity, typically resulting in fewer side effects, a reduced likelihood of antimicrobial resistance selection, and lower costs. They are strongly recommended for empiric treatment of common infections and should be readily available. Conversely, "Watch" antibiotics carry a higher risk of promoting antimicrobial resistance and are primarily prescribed for patients with more severe conditions, predominantly within hospital settings. Vigilant monitoring of these antibiotics is vital to prevent their overuse. "Reserve" antibiotics, however, are considered the last resort and should be employed only when dealing with severe infections caused by multidrug-resistant pathogens. Their use should be reserved for critical situations. The AWaRe classification underscores the importance of restricting the use of "Watch" and "Reserve" category antibiotics. By 2023, the WHO aims for at least 60% of all antibiotic consumption to come from the Access group (www.who.int, 2023).

The COVID-19 pandemic has profoundly impacted global healthcare systems and various aspects of people's lives worldwide (World Health Organization, 2021). An inevitable consequence of the pandemic has been the increase in inappropriate antibiotic use, contributing to rising AMR rates (Subramanya et al., 2021). This is despite WHO guidelines advising against antibiotics unless there is strong evidence of a secondary bacterial infection (World Health Organization, 2020). Surprisingly, it was found that 70% of COVID-19 patients were administered antimicrobials (Pérez de la Lastra et al., 2022). Consequently, the inappropriate use of antibiotics during the COVID-19 pandemic may exacerbate the global challenge of AMR (Nandi et al., 2023). This research aimed to examine the use of antibiotics in the initial and subsequent treatment stages of RTIs, including pneumonia, both prior to pandemic (PP) and during the pandemic (DP) at one English National Health Service (NHS) Foundation Trust. In order to provide an in-depth

understanding of the impact of the pandemic on antibiotic prescribing, we analysed data from eight seasonal time points in 2019 and 2020.

Method

Study design

A retrospective cross-sectional patient records review study was conducted to investigate AMS and the AWaRe classification of antibiotics in adult patients aged 25 and older. These patients were admitted to an English NHS Foundation Trust in the United Kingdom during 2019 and 2020. The study comprehensively describes antibiotic prescribing patterns utilising a methodological approach based on retrospective cross-sectional analysis. For sampling, the systematic method was employed to consistently select patient medical record data from a larger dataset at the Trust. Initially, data from 4,830 records (2,755 from 2019 and 2,075 from 2020) were extracted. After applying inclusion and exclusion criteria and eliminating duplicate records, the numbers were narrowed down to 1,188 for 2019 and 939 for 2020. Subsequently, a random selection of 80 records for each of the four-time points in 2019, as well as 80 records from 2020, was conducted using Excel's Random function. This resulted in a total of 640 patient records (as shown in Figure 1). The systematic sampling method ensured equal representation across the patient population and was consistently applied across all eight seasonal time points, spanning from Spring 2019 to Winter 2020. This approach streamlined the sampling process whilst ensuring a comprehensive representation of the patient population.

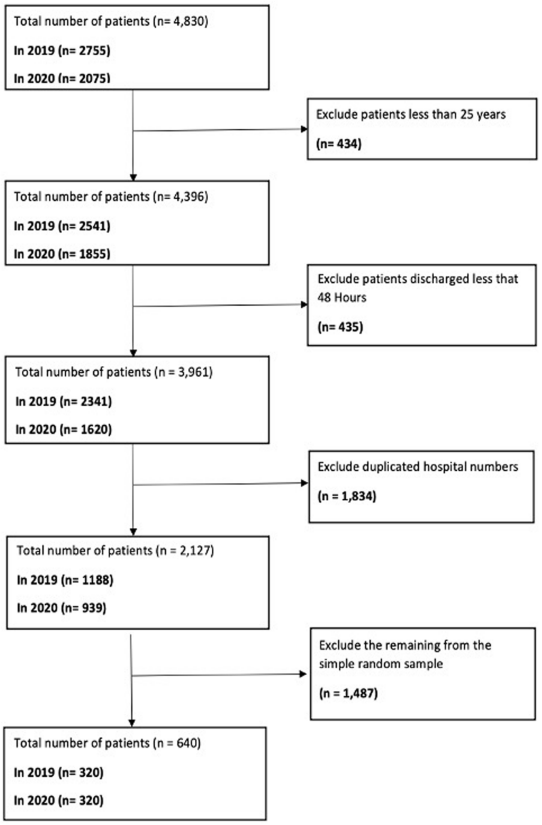

FIGURE 1
Data filtering algorithm for extracting a representative sample of 640 patient medical records from 2019 and 2020.

Sample size

According to estimations by Public Health England, approximately 20% of antibiotic prescriptions in the UK are potentially inappropriate. For this study, the sample size was determined using Minitab statistical software, taking into account the total population size, a margin of error set at 10%, and a confidence interval of 95%. The data collection involved patient records across eight different seasonal time points spanning 2019 and 2020. The analysis encompassed a total of 640 medical records, divided evenly between 2019 (pre-pandemic period) and 2020 (during the pandemic period), with each year comprising four seasonal time points. To ensure a robust and representative sample, a systematic sampling method was employed to select 80 patients for each of these intervals.

Study population (inclusion/exclusion criteria)

A stratified sampling strategy was employed to ensure maximum diversity amongst the included medical records. The inclusion criteria comprise the following: (i) adult patients aged 25 years and older; (ii) patients admitted to the Trust; (iii) patients admitted in 2019 and 2020; (iv) patients prescribed antibiotics for RTIs, including pneumonia; and (v) pregnant women and immunocompromised patients. However, patients who spent less than 48–72 h in the Accident and Emergency (A&E) department, patients who were not prescribed antibiotics, and children were excluded from this study.

Data source

The primary author (RAE) was responsible for gathering data from the patient's electronic patient records within the Trust, strictly following the inclusion and exclusion criteria established for the study.

Data collection

Data were collected from the medical records of 640 patients within the Foundation Trust in accordance with the specified inclusion and exclusion guidelines. Data were collected from eight-time points, with four-time points PP: (i) March (Spring 2019); (ii) June (Summer 2019); (iii) September (Autumn 2019); and (iv) December (Winter 2019). Additionally, four-time points occurred DP: (i) March (Spring 2020) – the first wave of COVID-19; (ii) June (Summer 2020) – the first lockdown; (iii) September (Autumn 2020) – the second wave of the pandemic; and (iv) December (Winter 2020) – the vaccination rollout.

Data extraction

A data extraction tool was utilised to retrieve essential information from 320 medical records of patients diagnosed with RTIs, such as pneumonia, in the pre-pandemic year of 2019. Additionally, the same tool was used to extract data from another set of 320 records of patients diagnosed with RTIs, including pneumonia and COVID-19, during the pandemic in 2020. The data extraction tool was set up in line with the guidelines of the WHO AWaRe Tool1 (www.who.int, 2023). This study focussed exclusively on antibiotics utilised for treating RTIs. Following the categorisation by the WHO AWaRe Tool, 10 antibiotics were classified under the "Access" group, 11 were identified as "Watch" antibiotics, and 3 were allocated to the "Reserve" category, as shown in Figure 2. The data extraction tool encompassed comprehensive details, including patient demographics, initial diagnosis, and the usage of first- and second-course antibiotics. Adhering to the guidelines of the WHO AWaRe Tool, the primary author dedicated approximately 45 min to each patient's medical record for the successful extraction of the required data.

Pilot study

The primary author conducted a pilot study in which data were derived from 10 patient medical records at each time point,

WHO Access, Watch, Reserve (AWaRe) classification for antibiotics evaluation and monitoring before and during the COVID-19 pandemic

	Mar-19	Jun-19	Sep-19	Dec-19	Mar-20	Jun-20	Sep-20	Dec-20
Access								
Amoxicillin	2	1	2	3	6	6	0	1
Amoxicillin/clavulanic acid	67	61	56	76	25	70	86	66
Benzylpenicillin	1	0	2	0	3	0	0	0
Doxycycline	1	1	3	2	1	2	0	1
Flucloxacillin	2	2	3	2	0	5	2	1
Gentamicin	0	0	0	0	0	2	0	0
Metronidazole	3	7	2	0	4	4	2	4
Sulfamethoxazole/Trimethoprim	0	1	1	0	4	2	0	0
Clindamycin	1	0	0	0	0	0	0	0
Cephalexin	0	0	2	1	1	0	0	0
Watch								
Azithromycin	0	1	2	0	13	19	3	11
Ceftazidime	2	2	0	0	0	1	0	0
Ceftriaxone	0	0	0	1	1	0	1	0
Cefuroxime	0	0	1	0	0	0	0	0
Ciprofloxacin	3	3	1	8	7	5	9	5
Clarithromycin	14	21	26	33	32	21	25	32
Levofloxacin	12	9	8	11	14	13	14	23
Meropenem	2	0	1	1	5	4	4	5
Piperacillin/Tazobactam	29	30	15	16	29	21	22	25
Teicoplanin	0	0	1	0	3	0	0	0
Vancomycin	1	4	0	1	0	1	0	0
Reserve								
Aztreonam	0	0	0	0	0	1	0	0
Cefazidime/Azobactam	0	0	2	0	0	0	0	0
Linezolid	3	2	1	1	0	0	1	1

	0: Absence of antibiotic usage
	1 - 9: Minimal antibiotic consumption
	10 - 29: Moderate level of antibiotic usage
	30 and above: High level of antibiotic consumption

FIGURE 2
Heatmap for antibiotic use in 2019 and 2020 according to AWaRe criteria.

accumulating 80 patient medical records in 2019 and 2020. The primary objectives of this pilot study were to provide an initial characterisation of the data and to evaluate the viability of the data extraction instrument in addressing the research queries. Descriptive statistical analysis was employed to interpret this initial data. The findings from this pilot study indicated that the data extraction tool was effective in meeting all the objectives of the study. The data generated and extracted during the pilot phase were not included in the study's final analysis.

Validity and reliability of the data extraction tool

The lead author (RAE) developed the data extraction tool using literature sources, the AMS toolkit from Public Health England (PHE), and the World Health Organization's (WHO) AWaRe Tool. The tool's components were finalised through collaborative discussions amongst the authors. To validate the tool, RAE and an AMS pharmacist at the research NHS Foundation Trust independently extracted data from 10 medical records at each sample time point. A minimum agreement rate of 80% was set as the standard for tool validation. Additionally, to assess the tool's reliability, RAE and the AMS pharmacist separately conducted data extractions from the same set of samples. The inter-rater reliability was measured by the percentage of agreement in their independently extracted data, with any variances resolved through joint discussions.

Patient characteristics

Data were extracted from patient medical records for those admitted in 2019 and 2020, specifically focussing on patients diagnosed primarily with RTIs, including pneumonia, and COVID-19 positive cases, as COVID-19 has the potential to cause secondary bacterial infections that necessitate antibiotic treatment. For patients admitted in 2020, during the pandemic, cases of COVID-19 were also included in the data extraction. The selection of primary RTI diagnoses was guided by the pertinent categories in the International Classification of Diseases, 10th Revision (ICD-10). The extracted data focussed on antibiotics given at admission, empirical antibiotic treatments, and antibiotics prescribed within 48–72 h or 5–7 days following admission.

Patient and public involvement

The study protocol was submitted to the Citizens Senate, an organization focussed on patient care with a considerable representation of elderly individuals. They provided useful suggestions and comments.

Registration

This study has been officially registered with the ISRCTN registry. The ISRCTN registry is a primary registry acknowledged by the WHO and the International Committee of Medical Journal Editors (ICMJE), accepting all clinical research studies (www.isrctn.com, 2022). Moreover, it was registered in Octopus, the global primary research record (Octopus, 2019).

Data analysis

This study identified the initial antibiotic prescribed for each patient according to the main diagnosis of RTIs, PP, and DP. Additionally, AMS was evaluated using the AWaRe classification, descriptive statistics, and data analysis software, Excel 2019 for Windows (www.microsoft.com, 2019).

Results

WHO AWaRe tool: antibiotic usage in RTIs

This research examined the antibiotics prescribed for RTIs in 640 patients admitted between 2019 and 2020. In the Figure 1 heatmap, each row represents a different antibiotic, whilst each column corresponds to a specific seasonal month from 2019 to 2020. The colour intensity of each cell in the heatmap represents the frequency of prescriptions for each antibiotic used in treating RTIs, including pneumonia and COVID-19-positive cases, across the 640 patients admitted during those years. This visualization is particularly informative given that COVID-19 can lead to secondary bacterial infections requiring antibiotic intervention. Darker colours indicate higher prescription rates, providing a visual representation of prescribing trends over time. The heatmap uses a colour-coded system to reflect the levels of antibiotic consumption over several months, from March 2019 to December 2020. Antibiotics are categorised into three groups based on the World Health Organization's Access, Watch, and Reserve (AWaRe) classification, which is designed to promote the proper use of antibiotics to combat resistance. In this heatmap figure, antibiotic consumption was categorised into four levels based on values, with the highest value being 86 and the lowest value being 0. These categories were as follows: 0 represented the absence of antibiotic usage, 1–9 represented minimal antibiotic consumption, 10–29 represented a moderate level of antibiotic usage, and 30 and above represented the highest level of antibiotic consumption (Figure 2). The categorisation of data in Figure 2 is derived from a literature review and the clinical relevance of antibiotic prescribing trends.

The "Access" category includes essential antibiotics that should be widely available. In this category, amoxicillin/clavulanic acid showed a substantial increase, starting at 67 in March 2019 and peaking at 86 in September 2020, indicating high usage. Flucloxacillin also demonstrated an increase from 2 in March 2019 to 5 in June 2020, suggesting moderate use. The "Watch" group comprises antibiotics that have the higher potential for resistance and should be used more cautiously. In this study, azithromycin usage escalated from zero in March 2019 to 19 in June 2020, showing a high level of use. Clarithromycin started at 21 in June 2019 and increased to 32 by December 2020. Ciprofloxacin and levofloxacin also saw increases in their

consumption levels over the study period. Piperacillin/tazobactam maintained a consistently high consumption level of 29 in March 2019 and March 2020. Meropenem showed a modest increase from 2 in March 2019 to 5 in December 2020. In the "Reserve" category, which includes antibiotics that should be reserved for treating infections caused by multidrug-resistant organisms, linezolid maintained a high consumption level of 3 in March 2019 without any substantial increase through 2020. Aztreonam and ceftazidime/avibactam show minimal increases in usage.

Notably, there was an increase in the total usage of antibiotics in the "Access" category, reaching 305 in 2019 and slightly decreasing to 298 in 2020. In contrast, the "Reserve" category saw a reduction in use, declining from 9 to 3. Meanwhile, the "Watch" category experienced a significant increase in 2020, with usage escalating to 386, up from 259 in the previous year.

The top seven prescribed antibiotics before and during the COVID-19 pandemic

Figure 3 shows the use of the seven most commonly prescribed antibiotics in both PP and DP, further detailed in Supplement 1. In 2019, amoxicillin/clavulanic acid was the most frequently prescribed antibiotic, accounting for 247 instances. This trend persisted in 2020 with 260 instances, maintaining its top position. In 2020, compared to 2019, there was an increase in prescriptions for most of the other antibiotics. For instance, clarithromycin saw an increase from 94 prescriptions in 2019 to 100 in 2020. Piperacillin/tazobactam also witnessed a slight increase, from 90 instances in 2019 to 97 in 2020. Additionally, 2020 showed increased prescriptions of levofloxacin, azithromycin, and ciprofloxacin compared to 2019. Levofloxacin prescriptions increased from 40 in 2019 to 64 in 2020. Azithromycin had a surge, increasing from 12 in 2019 to 46 in 2020. Ciprofloxacin also displayed a increasing trend, going from 15 in 2019 to 26 in 2020, whilst meropenem's usage modestly increased in 2020, from 10 to 18 instances.

Discussion

This study examined the prescribing patterns of antibiotics at an English NHS Foundation Trust, employing the AWaRe classification system for antibiotics used in treating RTIs, including pneumonia, and taking into account cases positive for COVID-19 in the year 2020. This AWaRe classification serves as an effective means for tracking antibiotic usage, establishing goals, and observing the impact of stewardship initiatives aimed at enhancing antibiotic utilisation and combating antimicrobial resistance. The WHO's 13th General Programme of Work for the years 2019–2023 sets a target for countries to achieve at least 60% of their total antibiotic consumption from antibiotics categorised in the access group (www.who.int, 2021). COVID-19 highlighted the effectiveness of antimicrobial stewardship (AMS) in combating AMR by guiding strategic choices during the pandemic and encouraging judicious antibiotic use. Findings from this study showed that amoxicillin/clavulanic acid, classified in the "Access group," emerged as the most frequently prescribed antibiotic (Elshenawy et al., 2023).

This study observed a significant increase in the use of azithromycin, an antibiotic categorised in the "Watch" group. This categorisation indicates a need for more cautious use due to a higher potential for resistance development. This upward trend in azithromycin usage aligns with findings from a variety of international research efforts. In India, studies by Mugada et al. (2021) and Sharma et al. (2021) reported similar patterns, reflecting a broader shift in antibiotic prescription practices. In Malaysia, Mohamad et al. (2022) also observed an increase. In Zambia, findings by Mudenda et al. (2022, 2023) further corroborate these findings, suggesting both a regional and a global increase in reliance on azithromycin. Additionally, research conducted in several Eastern Mediterranean countries, including studies by Kalungia et al. (2022) and Jirjees et al. (2022), and in other regions such as Ghana, as noted by Amponsah et al. (2022), has also observed this trend, highlighting a consistent global shift towards increased usage of this particular antibiotic. These studies collectively emphasise the growing preference for azithromycin

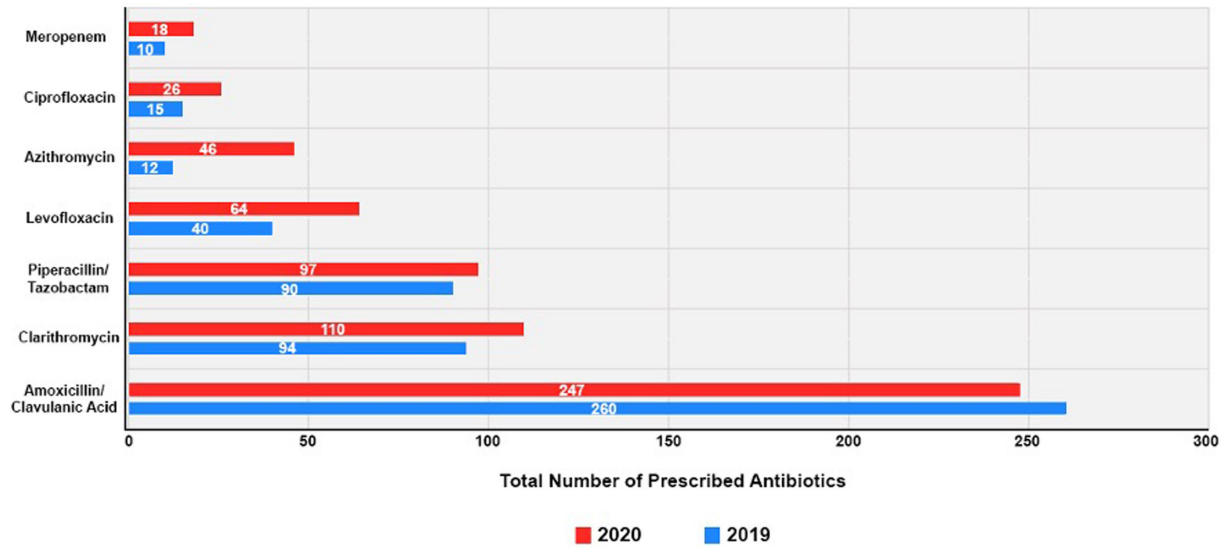

FIGURE 3
Seven commonly prescribed antibiotics prior to and during the COVID-19 pandemic.

across diverse geographical and clinical settings (Mugada et al., 2021; Sharma et al., 2021; Amponsah et al., 2022; Jirjees et al., 2022; Kalungia et al., 2022; Mohamad et al., 2022; Mudenda et al., 2022; Mudenda et al., 2023).

Possible reasons for this increase could be the rise in respiratory tract infections, including pneumonia, suspected to be COVID-19 during the pandemic, as well as the early inclusion of antibiotics, such as azithromycin, in COVID-19 treatment protocols (Mugada et al., 2021). A study conducted in Zambia in 2022 analysed antibiotic prescriptions (443 instances) and found that ceftriaxone and metronidazole were the most commonly prescribed antibiotics. A total of 42.1% of antibiotics in the "Watch" category exceeded recommended limits, emphasising the urgent need for improved antimicrobial stewardship and adherence to guidelines (Mudenda et al., 2023). An increasing trend in the use of antibiotics categorised in the "Watch group" has been observed in this study. This trend may stem from concerns regarding the effectiveness of "Access group" antibiotics, their availability, and patient demands. It highlights the necessity for enhanced availability of "Access group" antibiotics and a reduction in the utilisation of "Watch group" antibiotics, which are more prone to resistance.

In the "Watch" category, antibiotic use significantly increased during the COVID-19 pandemic in 2020, totalling 386 compared to 259 in the pre-pandemic year of 2019. This trend illuminates evolving prescribing practices and highlights the necessity of enhanced antibiotic stewardship. The study also revealed that antibiotics in the "Watch" group were the most used, accounting for 45.8% of the total, with the "Access" group following at 42.7% and the "Reserve" group comprising 12.5% of the usage. In Ghana, a study conducted in 2022 revealed that there was a notable inclination towards prescribing antibiotics from the "Access" group. This trend reflects specific regional prescribing patterns and underscores the dominant role of "Access" group antibiotics in these countries' healthcare practices. In India, antibiotic use was compared over 2 years using the AWaRe index tool. The study, retrospective in nature, analysed data from January 2017 to December 2018. Results showed a shift in antibiotic consumption: in 2017, 53.31% of antibiotics used were from the "Access" category, 40.09% from "Watch", and 3.40% from "Reserve". In 2018, these figures changed to 41.21, 46.94, and 8.15%, respectively, indicating a 17% increase in "Watch" and 140% in "Reserve" category usage, suggesting evolving resistance (Sharma et al., 2021). The study revealed that in 2020, during the COVID-19 pandemic, there was a substantial increase in the usage of levofloxacin, azithromycin, and ciprofloxacin compared to their consumption levels in 2019, highlighting a shift in antibiotic prescribing patterns during the health crisis.

Analysing the impact of the COVID-19 pandemic on antibiotic prescribing patterns within the UK NHS Trust during 2019 and 2020 presents a multifaceted challenge. The study indicates an increased use of specific antibiotics such as levofloxacin, azithromycin, and ciprofloxacin in 2020, which might be linked to the treatment approaches and uncertainties prevalent in the early stages of the pandemic. Additionally, the pandemic led to notable shifts in healthcare practices, potentially influencing these prescribing behaviours. However, the study's retrospective and cross-sectional nature may not fully capture all the confounding factors, such as the severity of infections or varied patient health conditions. The data, whilst indicative, might not comprehensively represent all cases or the complete spectrum of clinical decision-making, making it difficult to precisely quantify the direct impact of the pandemic on antibiotic prescribing patterns. This study is descriptive, providing a visual tool to observe antibiotic prescriptions in 2019 and 2020, as well as to visualise how the COVID-19 pandemic impacted antibiotic prescribing. It also identifies areas requiring AMS implementation. Additionally, identify the areas required for AMS implementation. Although estimating patient days was vital, it presented challenges in this study, necessitating further research on this aspect.

Limitations

The study has several limitations. It excludes children under 12 years old and faces challenges in accurately calculating patient days, potentially affecting the evaluation of antibiotic use compared to patient volume. The study's focus on a limited number of prescriptions may not encompass the entire range of prescribing behaviours. As a retrospective and cross-sectional analysis, it has limitations in considering the varied health statuses and treatment reactions of patients and may not effectively measure compliance with clinical prescribing guidelines. These factors indicate that the study might not provide a comprehensive assessment of the impact of antibiotic prescribing on patient outcomes.

Conclusion

This study provides valuable insights into the dynamics of antibiotic prescribing within a UK NHS Foundation Trust during the COVID-19 era. Analysing data from 640 patients, it reveals shifts in antibiotic use for respiratory infections, including pneumonia and COVID-19, across four seasonal phases. Key findings reveal a progressive increase in the use of amoxicillin/clavulanic acid in the Access category from March 2019 to September 2020. In the Watch category, there was a notable increase in the consumption of antibiotics such as azithromycin, clarithromycin, ciprofloxacin, and levofloxacin within the same timeframe. Piperacillin/tazobactam usage remained consistently high, whilst meropenem saw a slight uptick. This pivotal study not only traces the evolution of prescribing practices during the pandemic but also highlights the critical need for vigilant antimicrobial stewardship to combat resistance and safeguard patient health.

Data availability statement

The datasets presented in this article are not readily available because this data is restricted and confidential with the institution policy. Requests to access the datasets should be directed to r.a.elshenawy@herts.ac.uk.

Ethics statement

The studies involving humans were approved by Ethical approval for this study was granted by the Health Research Authority (HRA), with the Research Ethics Committee (REC) assigning reference number 22/EM/0161. In compliance with this approval, the study protocol underwent review and received approval from the University

of Hertfordshire (UH) ethics committee under the reference LMS/PGR/NHS/02975. The authors have no conflicts of interest to disclose. The studies were conducted in accordance with the local legislation and institutional requirements. Written informed consent for participation was not required from the participants or the participants' legal guardians/next of kin in accordance with the national legislation and institutional requirements.

Author contributions

RE: Formal analysis, Investigation, Methodology, Validation, Visualization, Writing – original draft. NU: Supervision, Visualization, Writing – review & editing. ZA: Supervision, Visualization, Writing – review & editing.

Funding

The author(s) declare that no financial support was received for the research, authorship, and/or publication of this article.

Conflict of interest

The authors declare that the research was conducted in the absence of any commercial or financial relationships that could be construed as a potential conflict of interest.

Publisher's note

Supplementary material

The Supplementary material for this article can be found online at: https://www.frontiersin.org/articles/10.3389/fmicb.2023.1298858/full#supplementary-material

References

Amponsah, O. K. O., Nagaraja, S. B., Ayisi-Boateng, N. K., Nair, D., Muradyan, K., Asense, P. S., et al. (2022). High levels of outpatient antibiotic prescription at a district hospital in Ghana: results of a cross-sectional study. *Int. J. Environ. Res. Public Health* 19:10286. doi: 10.3390/ijerph191610286

Department of Health and Social Care (2019). UK 5-year action plan for antimicrobial resistance 2019 to 2024. GOV.UK. Available at: https://www.gov.uk/government/publications/uk-5-year-action-plan-for-antimicrobial-resistance-2019-to-2024.

Elshenawy, R. A., Umaru, N., Alharbi, A. B., and Aslanpour, Z. (2023). Antimicrobial stewardship implementation before and during the COVID-19 pandemic in the acute care settings: a systematic review. *BMC Public Health* 23:309. doi: 10.1186/s12889-023-15072-5

Jirjees, F., Ahmed, M., Sayyar, S., Amini, M., Al-Obaidi, H., and Aldeyab, M. A. (2022). Self-medication with antibiotics during COVID-19 in the Eastern Mediterranean region countries: a review. *Antibiotics* 11:733. doi: 10.3390/antibiotics11060733

Kalungia, A. C., Mukosha, M., Mwila, C., Banda, D., Mwale, M., Kagulura, S., et al. (2022). Antibiotic use and stewardship indicators in the first- and 2 second-level hospitals in Zambia: findings and implications 3 for the future. *Antibiotics* 11:1626. doi: 10.3390/antibiotics11111626

Mohamad, I.-N., Wong, C. K.-W., Chew, C.-C., Leong, E. L., Lee, B. H., Moh, C. K., et al. (2022). The landscape of antibiotic usage among COVID-19 patients in the early phase of pandemic: a Malaysian national perspective. *J. Pharm. Policy Pract.* 15:4. doi: 10.1186/s40545-022-00404-4

Mudenda, S., Chomba, M., Chabalenge, B., Hikaambo, C. N., Banda, M., and Daka, V. (2022). Antibiotic prescribing patterns in adult patients according to the WHO AWaRe classification: a multi-facility cross-sectional study in primary healthcare hospitals in Lusaka, Zambia. *Pharmacol. Pharm.* 13, 379–392. doi: 10.4236/pp.2022.1310029

Mudenda, S., Nsofu, E., Chisha, P., Daka, V., Chabalenge, B., Mufwambi, W., et al. (2023). Prescribing patterns of antibiotics according to the WHO AWaRe classification during the COVID-19 pandemic at a teaching hospital in Lusaka, Zambia: implications for strengthening of antimicrobial stewardship programmes. *Pharmacoepidemiology* 2, 42–53. doi: 10.3390/pharma2010005

Mugada, V., Mahato, V., Andhavaram, D., and Vajhala, S. M. (2021). Evaluation of prescribing patterns of antibiotics using selected indicators for antimicrobial use in hospitals and the access, watch, reserve (AWaRe) classification by the World Health Organization. *Turk. J. Pharm. Sci.* 18, 282–288. doi: 10.4274/tjps.galenos.2020.11456

Murray, C. J. (2022). Global burden of bacterial antimicrobial resistance in 2019: a systematic analysis. *Lancet* 399, 629–655. doi: 10.1016/S0140-6736(21)02724-0

Nandi, A., Pecetta, S., and Bloom, D. E. (2023). Global antibiotic use during the COVID-19 pandemic: analysis of pharmaceutical sales data from 71 countries, 2020–2022. *EClinicalMedicine* 57:101848. doi: 10.1016/j.eclinm.2023.101848

National Institute for Health and Care Excellence (2015). Overview | Antimicrobial stewardship: systems and processes for effective antimicrobial medicine use | Guidance | NICE. Nice.org.uk. Available at: https://www.nice.org.uk/guidance/ng15.

O'Neill, J. (2014). Antimicrobial resistance: tackling a crisis for the health and wealth of nations. Available at: https://amr-review.org/sites/default/files/AMR%20Review%20Paper%20-%20Tackling%20a%20crisis%20for%20the%20health%20and%20wealth%20of%20nations_1.pdf.

Octopus. (2019). Octopus.ac. Available at: https://doi.org/10.57874/372b-6747.

Pérez de la Lastra, J. M., Anand, U., González-Acosta, S., López, M. R., Dey, A., Bontempi, E., et al. (2022). Antimicrobial Resistance in the COVID-19 Landscape: Is There an Opportunity for Anti-Infective Antibodies and Antimicrobial Peptides?. *Frontiers in Immunology* 13. doi: 10.3389/fimmu.2022.921483

Salam, M. A., Al-Amin, M. Y., Salam, M. T., Pawar, J. S., Akhter, N., Rabaan, A. A., et al. (2023). Antimicrobial resistance: a growing serious threat for global public health. *Healthcare* 11:1946. doi: 10.3390/healthcare11131946

Sharma, R., Bansal, A., and Prakash, R. (2021). Adoption of the World Health Organization access, watch reserve index to evaluate and monitor the use of antibiotics at a tertiary care hospital in India. *Perspect. Clin. Res.* 13, 90–93. doi: 10.4103/picr.picr_202_19

Subramanya, S. H., Czyż, D. M., Acharya, K. P., and Humphreys, H. (2021). The potential impact of the COVID-19 pandemic on antimicrobial resistance and antibiotic stewardship. *Virusdisease* 32, 330–337. doi: 10.1007/s13337-021-00695-2

Tejpar, S., Rogers Van Katwyk, S., Wilson, L., and Hoffman, S. J. (2022). Taking stock of global commitments on antimicrobial resistance. *BMJ Glob. Health* 7:e008159. doi: 10.1136/bmjgh-2021-008159

World Health Organization (2020). Antibiotic resistance. World Health Organization. Available at: https://www.who.int/news-room/fact-sheets/detail/antibiotic-resistance.

World Health Organization (2021). The impact of COVID-19 on global health goals. www.who.int. Available at: https://www.who.int/news-room/spotlight/the-impact-of-covid-19-on-global-health-goals.

www.isrctn.com. (2022). ISRCTN. Available at: https://www.isrctn.com/ISRCTN14825813.

www.microsoft.com. (2019). Microsoft Excel Spreadsheet Software | Microsoft 365. Available at: https://www.microsoft.com/en-gb/microsoft-365/excel?ef_id=_k_2d81b39af5e21516b9f9d6c8cb8c7dc2_k_&OCID=AIDcmmp20rgnjr_SEM__k_2d81b39af5e21516b9f9d6c8cb8c7dc2_k_&msclkid=2d81b39af5e21516b9f9d6c8cb8c7dc2 (Accessed Nov 13, 2023).

www.who.int. (2021). 2021 AWaRe classification. Available at: https://www.who.int/publications/i/item/2021-aware-classification.

www.who.int. (2023). AWaRe classification of antibiotics for evaluation and monitoring of use, 2023. Available at: https://www.who.int/southeastasia/publications/i/item/WHO-MHP-HPS-EML-2023.04#:~:text=The%20AWaRe%20classification%20of%20antibiotics (Accessed Nov 13, 2023).

frontiers | Frontiers in Microbiology

TYPE Original Research
PUBLISHED 04 January 2024
DOI 10.3389/fmicb.2023.1295065

OPEN ACCESS

EDITED BY
Vijay Soni,
NewYork-Presbyterian, United States

REVIEWED BY
Prabhat Ranjan Singh,
Weill Cornell Medicine, United States
Vishma Pratap Sur,
Institute of Biotechnology (ASCR), Czechia
Yaxin Li,
Cornell University, United States

*CORRESPONDENCE
Yi Geng
✉ gengyisicau@126.com

†These authors have contributed equally to this work and share first authorship

RECEIVED 20 September 2023
ACCEPTED 04 December 2023
PUBLISHED 04 January 2024

CITATION
Qin Z, Peng K, Feng Y, Wang Y, Huang B, Tian Z, Ouyang P, Huang X, Chen D, Lai W and Geng Y (2024) Transcriptome reveals the role of the *htpG* gene in mediating antibiotic resistance through cell envelope modulation in *Vibrio mimicus* SCCF01. *Front. Microbiol.* 14:1295065. doi: 10.3389/fmicb.2023.1295065

Transcriptome reveals the role of the *htpG* gene in mediating antibiotic resistance through cell envelope modulation in *Vibrio mimicus* SCCF01

Zhenyang Qin[1†], Kun Peng[1†], Yang Feng[1], Yilin Wang[1], Bowen Huang[1], Ziqi Tian[1], Ping Ouyang[1], Xiaoli Huang[2], Defang Chen[2], Weimin Lai[1] and Yi Geng[1]*

[1]College of Veterinary Medicine, Sichuan Agricultural University, Chengdu, Sichuan, China, [2]Department of Aquaculture, Sichuan Agricultural University, Chengdu, Sichuan, China

HtpG, a bacterial homolog of the eukaryotic 90 kDa heat-shock protein (Hsp90), represents the simplest member of the heat shock protein family. While the significance of Hsp90 in fungal and cancer drug resistance has been confirmed, the role of HtpG in bacterial antibiotic resistance remains largely unexplored. This research aims to investigate the impact of the *htpG* gene on antibiotic resistance in *Vibrio mimicus*. Through the creation of *htpG* gene deletion and complementation strains, we have uncovered the essential role of *htpG* in regulating the structural integrity of the bacterial cell envelope. Our transcriptomics analysis demonstrates that the deletion of *htpG* increases the sensitivity of *V. mimicus* to antimicrobial peptides, primarily due to upregulated lipopolysaccharide synthesis, reduced glycerophospholipid content, and weakened efflux pumps activity. Conversely, reduced sensitivity to β-lactam antibiotics in the Δ*htpG* strain results from decreased peptidoglycan synthesis and dysregulated peptidoglycan recycling and regulation. Further exploration of specific pathway components is essential for a comprehensive understanding of *htpG*-mediated resistance mechanisms, aiding in the development of antimicrobial agents. To our knowledge, this is the first effort to explore the relationship between *htpG* and drug resistance in bacteria.

KEYWORDS

HtpG, *Vibrio mimicus*, transcriptome, drug resistance, cell wall, cell membrane

1 Introduction

The highly conserved Heat shock proteins (HSP) family, found in both prokaryotic and eukaryotic organisms, rapidly adjusts expression under stress conditions, playing essential roles in protein processes (folding, structural maintenance, and disaggregation) and critical cellular pathways (Backe et al., 2020). They are categorized into six families based on molecular weight, one of which is the 90 kDa heat-shock protein (Hsp90). The high-temperature protein G (HtpG) is a bacterial homolog of the eukaryotic Hsp90 and constitutes a significant proportion of the total protein content (0.36% at 37°C; Mason et al., 1999). Furthermore, HtpG has been identified as a virulence factor across multiple bacterial pathogens (Grudniak et al., 2018; Dong et al., 2021), it plays a crucial role in bacterial resistance to various environmental stresses (Garcia-Descalzo et al., 2011; Honoré et al., 2017),

host defense responses, and adaptation to the host environment. Thus, the function of HtpG is critical for survival and dispersal in host and environment habitats of bacterial pathogens. Over the past decades, eukaryotic Hsp90 has emerged as a crucial target for cancer therapy (Lacey and Lacey, 2021) and the treatment of fungal infections (Li et al., 2022; Yin et al., 2022), resulting in numerous ongoing clinical trials evaluating Hsp90 inhibitors (Graner, 2021; Marcyk et al., 2021; Li and Luo, 2022). Cancer research has demonstrated that Hsp90 promotes malignant behaviors of cancer cells (Lacey and Lacey, 2021), such as uncontrolled proliferation, immune evasion, therapy resistance, and so on. Disruption of the chaperone mechanism of Hsp90 represents a potential method to inhibit tumor, as it can enhance the drug sensitivity of cancer cells (Li et al., 2019; Mathieu et al., 2019). Studies in fungi have demonstrated that elevated Hsp90 levels expedite the emergence of resistance to fungicides (Iyer et al., 2022), while reducing Hsp90 activity significantly increases the efficacy of fungicides (Fu et al., 2022; Li et al., 2022). However, it is surprising that there is little literature addressing the contribution of Hsp90 (HtpG) to bacterial drug resistance, particularly in the context of bacterial resistance emerging a global health challenge.

V. mimicus is an emerging zoonotic gram-negative bacterial pathogen that can infect a wide range of fish species (Guardiola-Avila et al., 2021), including Siluriformes, Cypriniformes, and Perciformes (Elgendy et al., 2022), as well as crustaceans (Jiang et al., 2022), resulting in severe vibriosis. The disease has rapid onset, rapid progression, and high mortality that can reach 80–100% (Geng et al., 2014). Additionally, *V. mimicus* can endanger human health by contamination food, water, and wounds (Yang et al., 2021), leading to life-threatening cholera-like diarrhea and septicemia. *V. mimicus* shares a remarkably similar genome and ecological niche with *Vibrio cholerae*, displaying adaptability to the human host (Hernandez-Robles et al., 2021), thereby positioning itself as a potential pandemic pathogen (Halder et al., 2022). Antibiotics are currently the most critical method of combating bacterial diseases. However, it has been observed that *V. mimicus* has started exhibiting resistance under the pressure of prolonged clinical antibiotic usage. A wealth of global evidence suggests its continuous evolution or acquisition of resistance to various drugs, notably β-lactam antibiotics such as ampicillin, amoxicillin, penicillin G, and carbenicillin (Beshiru et al., 2020; Karen Alvarez-Contreras et al., 2021; Elgendy et al., 2022), alongside polymyxin B, azithromycin (Gxalo et al., 2021), sulfamethoxazole, trimethoprim (Adesiyan et al., 2021), and doxycycline (Adesiyan et al., 2021). Given the potential risk of significant outbreaks, the challenges associated with treating infections, and the emerging trend of drug resistance, it becomes imperative to initiate research into the mechanisms of drug resistance in *V. mimicus* at an early stage.

In this study, we assessed changes in drug resistance resulting from *htpG* gene deletion in *V. mimicus* and characterized the global transcriptome changes pre- and post-gene deletion. By integrating phenotypic assessments with variations gene expression variations, we aimed to uncover the underlying mechanisms through which bacterial *htpG* contributes to drug resistance.

2 Materials and methods

2.1 Bacterial strains and culture conditions

The bacterial strains and plasmids used in this study are listed in Table 1. The strains were cultured in the Luria-Bertani (LB) medium at 28, 37, or 42°C. In Δ*htpG*/p*htpG* Strain, synthesis of HtpG was induced by addition of final concentrations 100 μg/mL L-arabinose (Solarbio, L8060, Beijing, China) at time of culture.

2.2 Construction of the *htpG* deletion strain and complemented strain

Natural transformation of *V. mimicus* (Yu et al., 2019) was employed to create the *htpG* deletion mutant strain. Briefly, the process involved connecting the upstream and downstream homologous arms of the target gene with the chloramphenicol-resistant gene from the plasmid pKD3 by fusion PCR (specific primers are in Table 2). The fused PCR fragment was introduced into the WT strain by natural transformation. Colonies containing the correct gene deletions were subsequently transformed with the FLP recombinase plasmid pCP20 to remove the chloromycetin resistance marker, and the pCP20 was then cured from the resulting strain by continuous passage at 42°C. Finally, the mutant strain was selected for PCR and sequencing to verify the accurate deletion and genomic location of the target gene (specific primers are in Table 2). Colony with no *htpG* gene and pCP20 detected were used as the *htpG* deletion strain Δ*htpG*. The wild-type *htpG* gene was cloned in a pBAD24 expression vector with the arabinose promoter, then electro-transformed into Δ*htpG* competent cells as

TABLE 1 Bacterial strains and plasmids used in this study.

Strain or plasmid	Description	Reference or source
V. mimicus		
SCCF01	Pathogenic wild-type (WT)	Yu et al., 2020
Δ*htpG*	WT with a deletion in *htpG* gene	This study
Δ*htpG*/p*htpG*	Δ*htpG* with complement plasmid contain *htpG* gene	This study
Escherichia coli		
DH5α	Competent cells for plasmid cloning	Tsingke Biotech Co., Ltd
Plasmid		
pKD3	Plasmid with FRT-flanked chloramphenicol-resistance gene	Miaolingbio Co., Ltd
pCP20	Temperature-sensitive plasmids, introduce FLP recombinase, Amp^r	Miaolingbio Co., Ltd
pBAD24	Inducible expression plasmid, Amp^r	Biofeng Biotech Co., Ltd

the complemented strain Δ*htpG*/*phtpG*. Furthermore, expression levels of *htpG* gene were analyzed by RT-qPCR (primers see VM_10215 gene in Supplementary Table 1).

2.3 Growth curves and biochemical characterization

Bacterial strains were cultured for 18 h before the start of the experiments and were then diluted to an optical density (OD_{600}) of one. Subsequently, the cultures were diluted 1:100 into LB medium and maintained at 28°C with shaking at 180 r/min. We recorded OD_{600} readings at 60-min intervals over a 24-h period. Biochemical analyses were conducted using the automated identification system Vitek® 2 GN ID cards (bioMerieux, France). Each experiment included three parallel samples, and statistical analysis was performed using GraphPad Prism 9.0 (GraphPad Software, San Diego, CA).

2.4 Antibiotic susceptibility testing

We performed antimicrobial susceptibility testing for 30 antibiotics using the disk diffusion method recommended by aquatic animal clinical and CLSI guidelines. The antibiotic disks were obtained from Hangzhou Microbial Reagent Co., Ltd (Hangzhou, China). The various drugs and their targets used in this study are summarized in Supplementary Table 2, covers 12 different classes of antibiotics and related compounds, namely: penicillins, carbapenems, cephalosporins, aminoglycosides, macrolides, polypeptides, sulfonamides, quinolones, rifamycins, chloramphenicol, tetracyclines, and nitrofuran. Each strain underwent triplicate testing with a single drug, and the mean value was used to determine its diameter of the bacteriostasis circle. Data analysis and visualization were performed using R software packages, including ggplot2 (Version 3.4.0), aplot (Version 0.1.9), and ggtree (Version 3.6.2). Subsequently, the normalized diameter of the bacteriostasis circle was used to generate the heatmap.

2.5 Measurement of cell envelope permeability

Cell membrane and cell wall permeability were assessed using propidium iodide (PI) and alkaline phosphatase (ALP) assay kits. The bacteria were cultured for 8 h to reach the mid-logarithmic phase. Subsequently, they were washed in 100 mM PBS (pH 7.3), and the cell density of the bacterial suspensions was adjusted to an OD_{600} of 0.4–0.5, ensuring uniform cell counts for each bacterial strain. Then, PI (Solarbio, C0080) was added to a final concentration of 10 mM and incubated at 28°C for 30 min. The fluorescence value was measured using a fluorescence plate reader (Thermo, Varioskan Flash) with excitation wavelength at 535 nm and an emission wavelength at 615 nm. The bacterial culture supernatants were collected and centrifuged at 12,000 r/min for 10 min. The ALP activity detection assay was performed using the AKP/ALP detection kit (Solarbio, BC2140) following the manufacturer's instructions. The measurements were performed in triplicate, and the data were presented as mean ± SE. Significance ($p < 0.05$) was determined using one-way ANOVA.

2.6 Transmission electron microscopy (TEM) analysis of the cell envelope

After being grown on LB agar at 28°C for 18 h, the colony was fixed overnight in 0.1 M sodium phosphate buffer (pH 7.4) containing 3% glutaraldehyde at 4°C. Samples were fixed in 0.1 M sodium phosphate buffer (pH 7.4) containing 1% OsO_4 for 2 h. Subsequently, they were sequentially dehydrated in 50, 70, 80, 90, 95, and 100% ethanol, and finally in 100% acetone, with each dehydration step lasting for 15 min. The samples were embedded in 812 epoxy resin monomer (SPI) and then sliced into ultrathin sections measuring 60–80 nm using a Leica UC7 ultrathin microtome. These sections were subsequently stained with uranyl acetate and lead citrate before being imaged at 80 kV using a JEOL JEM-1400FLASH transmission electron microscope. The assessment of cell wall structure integrity involved calculating the percentage of cells with abnormal structures from images taken at a 12,000× magnification. Cells with intact and well-defined cell wall structures were considered normal, while those displaying cell wall undulating folds or rupture, or expanded periplasmic space were categorized as having abnormal structures.

2.7 RNA extraction and sequencing

The 18-h cultures of *V. mimicus* SCCF01 and Δ*htpG* strains were diluted to an OD_{600} of 1 before initiating the experiments. Subsequently, cultures were diluted 1:100 into 5 mL LB medium and incubated at 28°C with shaking for 12 h. Bacterial cultures were centrifuged at 12,000 r/min for 5 min. Total RNA was extracted from the bacterial precipitate using RNAprep Pure Cell/Bacteria Kit (TIANGEN, Beijing, China) following the manufacturer's instructions and genomic DNA was removed using DNase I (TaKaRa). Then RNA quality was determined by 2100 Bioanalyser (Agilent) and was checked by RNase-free agarose gel electrophoresis, and quantified using the ND-2000 (NanoDrop Technologies). Only high-quality RNA sample ($OD_{260/280} = 1.8$–2.2, $OD_{260/230} \geq 2.0$, RIN ≥ 6.5, 28S:18S ≥ 1.0, >10 μg) was used to construct sequencing library.

The transcriptome library was prepared using the TruSeq™ Stranded Total RNA Library Prep Kit (Illumina, San Diego, CA). Ribosomal RNA (rRNA) depletion was performed using the Ribo-Zero Magnetic kit from Epicenter, and then fragmented using a fragmentation buffer. Subsequently, double-stranded cDNA was synthesized using the SuperScript double-stranded cDNA synthesis kit (Invitrogen, CA) with random hexamer primers (Illumina, San Diego, CA). The synthesized cDNA underwent end-repair, phosphorylation, and "A" base addition following Illumina's library construction protocol. Subsequently, the second-strand cDNA was digested using UNG (Uracil-N-Glycosylase). The cDNA fragments were then size-selected through agarose gel electrophoresis, PCR amplified, and sequenced using the Illumina HiSeq™ X Ten

TABLE 2 Primers used in gene deletion and PCR identification.

Primers name	Primers sequence 5′ to 3′	Product length (bp)	Primers' role
UP	(F) TCTGGTGGTTGCTGGCCTCT	2,974	Targeting fragments preparation
	R: cgaagcagctccagcctacaACTTTTGTCGATTCTACTAA		
DN	(F) ggaccatggctaattcccatAATCGCTCCGTTTACTTCTG	3,311	
	R: AAACGGCAGGTGGATGGGCG		
CM	(F) TTAGTAGAATCGACAAAAGTtgtaggctggagctgcttcg	1,072	
	R: CAGAAGTAAACGGAGCGATTatgggaattagccatggtcc		
UD-TC	(F) GATTAAACGTTGTGCTTGAGGT	2,116(Wild-type *htpG*), 1,180(*htpG* replaced by a chloramphenicol resistance cassette), 250 (*htpG* deletion)	Strains genetype detection
	R: TCCATATCTCACTTGCACATCA		
HTPG	(F) ACCACCAATAAAGAAACTCG	1,864	The *htpG* gene near-full-length sequences detection
	R: CCGCACTCAAGAATTGTGAC		

platform with a read length of 2×150 bp. This study included three biological replicates.

2.8 Transcriptomic analysis

The fastp software[1] (Version 0.20.1) was used to clean and evaluate the qualities of the raw reads from sequencing. The reads containing the adapter, poly-N, and more than 40% low-quality bases (Q < 20) were cleaned. The cleaned reads were mapped onto the genome of the *V. mimicus* SCCF01 strain (GenBank accession no. GCA_001767355) as the reference genome using bowtie2 (Version 2.2.9). Gene Ontology (GO) and Kyoto Encyclopedia of Genes and Genomes (KEGG) pathway annotation and enrichment analyses were based on the GO Database[2] and KEGG pathway database.[3] Gene expression levels were calculated and normalized as TPM approach using by RSEM[4] (Version 1.3.1). The differential gene expression was analyzed using the DESeq2 package[5] (Version 1.24.0), in which the p was adjusted by the Benjamini-Hochberg (BH) method, belonging to the False Discovery Rate (FDR) for correction. The genes with the adjusted $p < 0.05$ and the absolute value of $\log_2$ (FC) > 1 were deemed as the DEGs. The GO enrichment and KEGG enrichment were conducted using the clusterProfiler package (Guangchuang et al., 2012) to identify the biological functions and pathways mainly affected by the DEGs. Analyses not mentioned above were conducted using the online platform of Majorbio Cloud Platform[6] (Ren et al., 2022).

1 https://github.com/OpenGene/fastp
2 http://www.geneontology.org/
3 http://www.genome.jp/kegg/
4 http://deweylab.github.io/RSEM/
5 http://bioconductor.org/packages/stats/bioc/DESeq2/
6 https://www.majorbio.com

2.9 Validation of RNA sequencing

To validate the results obtained from the transcriptome, we selected 10 upregulated genes and 11 downregulated genes of interest for two-step RT-qPCR verification with the same RNA-seq samples. Reverse transcription was performed using the *Evo M-MLV* RT Master Mix for qPCR kit (AG11706, Accurate Biology, China), and real-time qPCR was carried out using the SYBR® Green *Pro Taq* HS Premix kit (AG11701, Accurate Biology, China). The Bio-Rad CFX96 qPCR System was used for RT-qPCR, and using the reaction as follows: initial denaturation at 95°C for 30 s, followed by 40 cycles of reaction at 95°C for 5 s and 60°C for 30 s. The melting curve was generated at the end of the cycle to confirm the specificity of the amplification product. Each PCR reaction was repeated three times. Gene expression was calculated and compared using the $2^{-\Delta\Delta Ct}$ method, with *16s rRNA* serving as an endogenous reference. The primers used for the experiment are listed in Supplementary Table 1.

3 Results

3.1 Deletion and complementation of *htpG* exhibit no effect on bacterial growth and principal biochemical phenotype

PCR and RT-qPCR were employed to verify the successful construction of the *htpG* deletion and complementation strain. Agarose gel eletrophoresis of PCR products revealed that the fragments were shorter when using the primer pair UD-TC-F/R in Δ*htpG* and Δ*htpG*/*phtpG*, indicating the deletion of *htpG* in the bacterial genome. With the primer pair HTPG-F/R, fragments of the *htpG* gene size (1,864 bp) were present in Δ*htpG*/p*htpG* and the WT strain (Figure 1A). All strains were verified by sequencing, confirming the successful construction of *htpG* gene deletion and complementation strains. Expression of *htpG* was significantly higher in complemented strains than

in parent strains (Figure 1B). Furthermore, these three strains exhibited similar growth curves (Figure 1C), indicating that the deletion and overexpression complementation of *htpG* do not impact the growth of *V. mimicus* under experimental conditions. In the biochemical characterization test of these strains, only six out of 47 indicators showed inconsistencies, namely Tyrosine arylaminases (TyrA), succinate alkalinization (SUCT), phosphatase (PHOS), ornithine decarboxylase (ODC), coumarate (CMT), and Glu-Gly-Arg-arylamidase (GGAA). However, these differences did not impact the high confidence of the identification results, as shown in Supplementary Table 3. This suggests that *htpG* gene deletion and complementation do not significantly affect the principal biochemical phenotype of *V. mimicus*.

3.2 The deletion of *htpG* affects *V. mimicus* antibiotic resistance targeting the cell envelope

By utilizing a normalized heatmap (Figure 2A), we observed a generally consistent trend in the resistance changes of *htpG* gene deletion and complemented strains to a wide range of antibiotics targeting the same mechanism. The sensitivity of the Δ*htpG* to cefixime (CFX), spectinomycin (SPEC), cotrimoxazole (CTRXZ), azithromycin (AZM), rifampicin (RIF), sulfafurazole (SIX), Polymyxin B (PMB), and carbenicillin (CARB) was significantly increased (difference value $>$ 2 mm; Figure 2B-a), while the sensitivity to cefradine (CEF), imipenem (IPM), piperacillin (PIP), and penicillin (PEN) was significantly decreased (difference value $>$ 2 mm; Figure 2B-b). Besides, the resistance of the Δ*htpG*/p*htpG* to PMB, CEF, and IPM could be restored to WT strain level (Figure 2B). The Δ*htpG*/*phtpG* strain maintained resistance level to norfloxacin (NRF), levofloxacin (LVFX), ciprofloxacin (CPFX), enrofloxacin (ENR), RIF, AZM, CTRXZ, SPEC, and CFX, indicating that the complementation of the *htpG* gene could not restore resistance changes to these antibiotics. In addition, resistance to doxycycline (DOX), neomycin (NEO), amikacin (AMK), and kanamycin (KAN) in *V. mimicus* was not affected by either *htpG* deletion or complementation, indicating that *htpG* does not mediate the regulation of resistance to these four antibiotics. Due to the presence of the AMP resistance gene on the pBAD24 plasmid, the diameter of the bacteriostasis zone for the Δ*htpG*/*phtpG* strain against certain penicillin drugs, namely CARB, PEN, amoxicillin (AMX), and ampicillin (AMP) was 0 mm, and there was an increased resistance to augmentine (AUG) and piperacillin (PIP). Among the 12 drugs with significantly altered sensitivity, seven of them target the cell wall or cell membrane.

3.3 The *htpG* maintains the permeability and structural integrity of the cell envelope

To confirm the impact of *htpG* deletion and complementation on cell envelope, we assessed the permeability and integrity of the cell membrane and cell wall. Deletion of *htpG* resulted in a significant reduction in both alkaline phosphatase (ALP) levels and propyl iodide (PI; $p < 0.01$). Meanwhile, the complemented strain restored this phenotype (Figures 3A, B), indicating a positive correlation between *htpG* and cell wall and cell membrane permeability. On the other hand, TEM images showed intact and well-defined cell wall and membrane in the majority of the WT strain cells (Figure 3D). Compared with the WT strain, the Δ*htpG* strain cell wall structure was disordered, the distance between the cell membrane and the cell wall widened, and the cell shrank slightly; clearer, rounded, and well-demarcated structures were observed in the cytoplasm (Figure 3E). Complemented strain cells' morphology became closer to WT cells (Figure 3F). The statistics revealed that the proportion of cells with abnormal cell wall structures significantly increased from 26.68 ± 3.73% to 61.27 ± 9.67% ($p < 0.0001$) following *htpG* gene deletion. However, this proportion decreased to 29.60 ± 5.98% after gene product complementation (Figure 3C). Therefore, *htpG* plays a role in maintaining the structural integrity of the cell envelope in *V. mimicus*.

3.4 Transcriptome analysis reveals the global regulatory functions of *htpG* in *V. mimicus*

To further investigate the impact of *htpG* deletion on the overall gene expression in *V. mimicus* and elucidate the mechanisms governing its effects on cell membrane permeability and integrity, we conducted transcriptomic analysis. The transcriptome analysis of the WT strain SCCF01 and the deletion strain Δ*htpG* detected a total of 4,167 genes, out of which 1,337 were identified as differentially expressed genes (DEGs, fold changes$\geq$2 or $\leq$0.5, $p \leq 0.05$, detailed information see in Supplementary Table 4), including 1,221 mRNAs (636 upregulated and 585 downregulated; Figures 4A, C, Supplementary Figure 1A). Venn analysis revealed that out of 4,068 genes with TPM $>$ 1, 17 were unique to the WT group, while 16 were unique to the Δ*htpG* group (Figure 4B). Correlation analysis of samples demonstrated higher correlations within groups compared to those between groups, indicating robust repeatability within each group (Figure 4D, Supplementary Figure 1B). GO enrichment analysis (Supplementary Table 5) revealed up-regulated mRNAs were associated with cellular energy metabolism, process regulation, and bacterial locomotion (Figure 4E), while down-regulated mRNAs were linked to metabolic regulation, stress adaptation, and substance transport (Figure 4F). Furthermore, all DEGs were mapped to 166 KEGG pathways (Supplementary Table 6). The enriched KEGG pathways included pivotal processes such as the two-component system, bacterial chemotaxis, flagellar assembly, and pyruvate metabolism (Figure 4G). A significant number of DEGs were implicated in energy source and amino acid biosynthesis and metabolism, exemplified by pathways such as the citrate cycle (TCA cycle), fatty acid degradation, butanoate metabolism, tryptophan metabolism, and valine, leucine, and isoleucine degradation.

10.3389/fmicb.2023.1295065

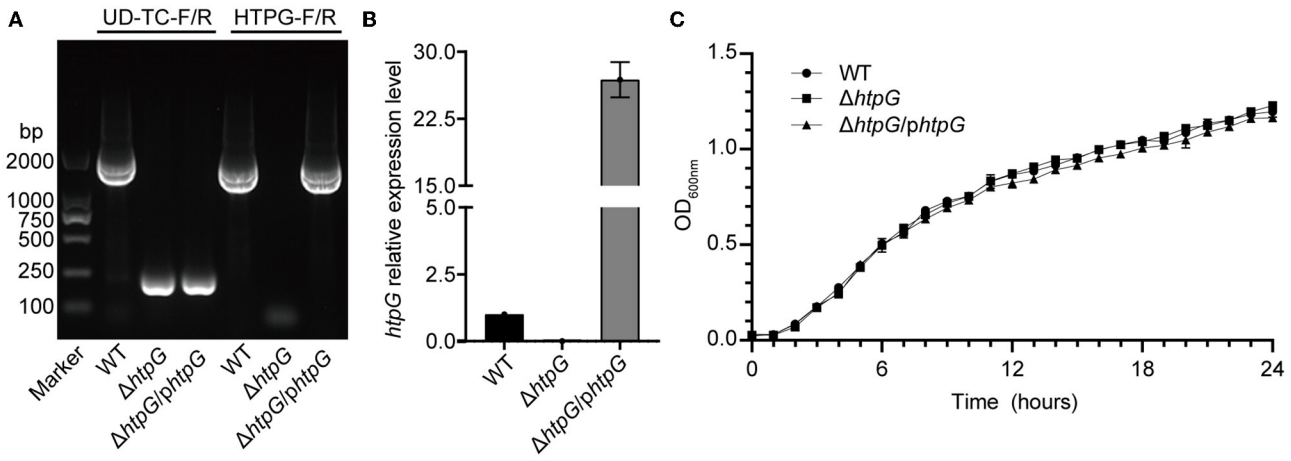

FIGURE 1
Identification of *htpG* gene deletion and complementation strains. **(A)** Electrophoretogram displaying the results of strains validation by PCR (the UD-TC-F/R primers were used to confirm gene knockout from the specified genomic position, while the HTPG-F/R primers were used to identify the presence of the target gene within the bacterial strain). **(B)** Relative expression level of the *htpG* gene among the test strains determined by RT-qPCR. **(C)** Growth curves of the tested strains under 28°C with shaking.

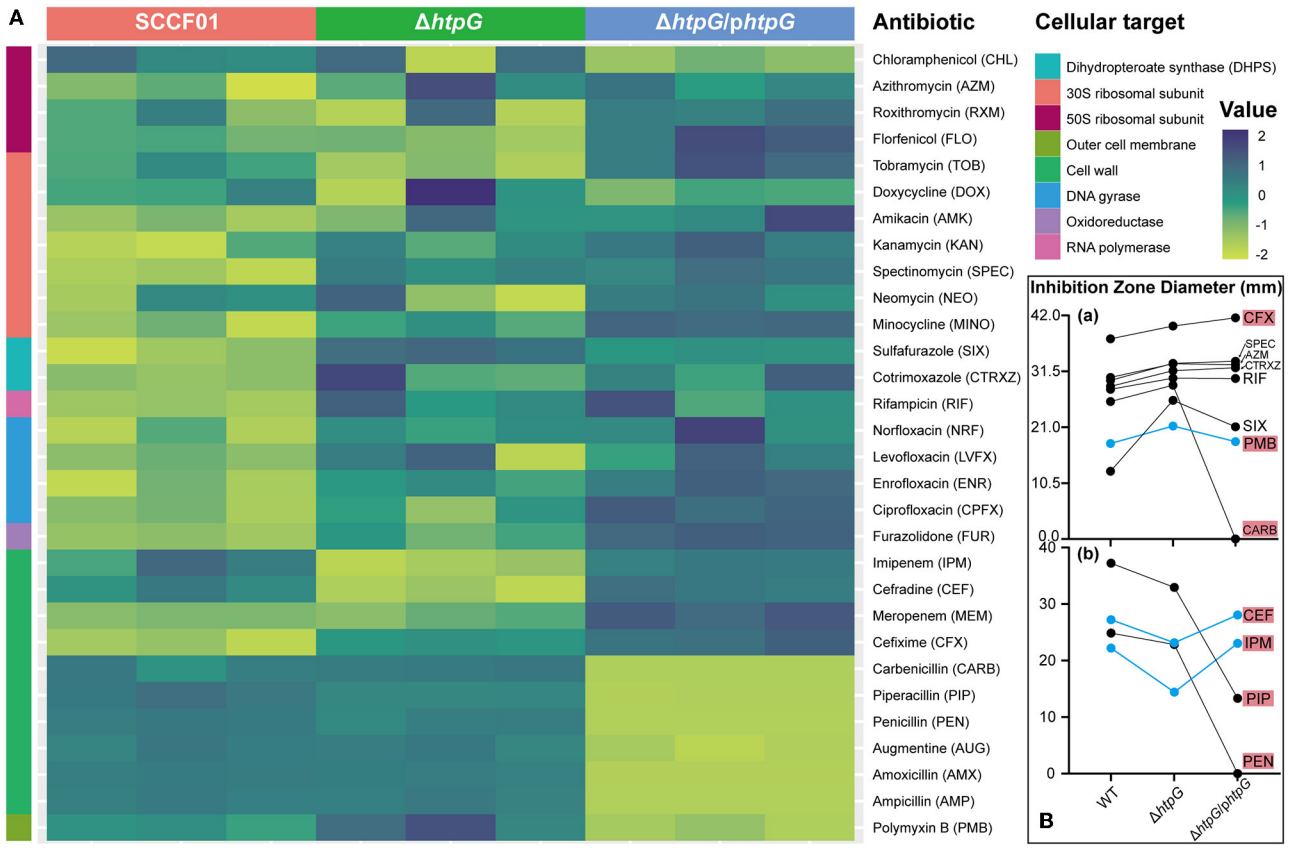

FIGURE 2
Impact of *V. mimicus htpG* gene deletion and complementation on sensitivity to thirty antibiotics. **(A)** Heatmap of antibiotic resistance of the tested bacterial strains based on normalized inhibition zone diameters (susceptibility results are categorized by cellular targets. Dark blue represents the maximum diameter of the inhibition zone, while light green represents the minimum diameter. The transition from light green to dark blue indicates a gradual increase in the inhibition zone diameter). **(B)** Changes in the inhibition zone diameters for twelve antibiotics exhibiting significant sensitivity alterations. (a) Eight antibiotics with upregulated drug sensitivity. (b) Four antibiotics with downregulated drug sensitivity (blue lines represent restored resistance phenotypes in the complemented strains. Abbreviations on the right side indicate the corresponding antibiotics, with a red background denoting antibiotics targeting the cell membrane or cell wall).

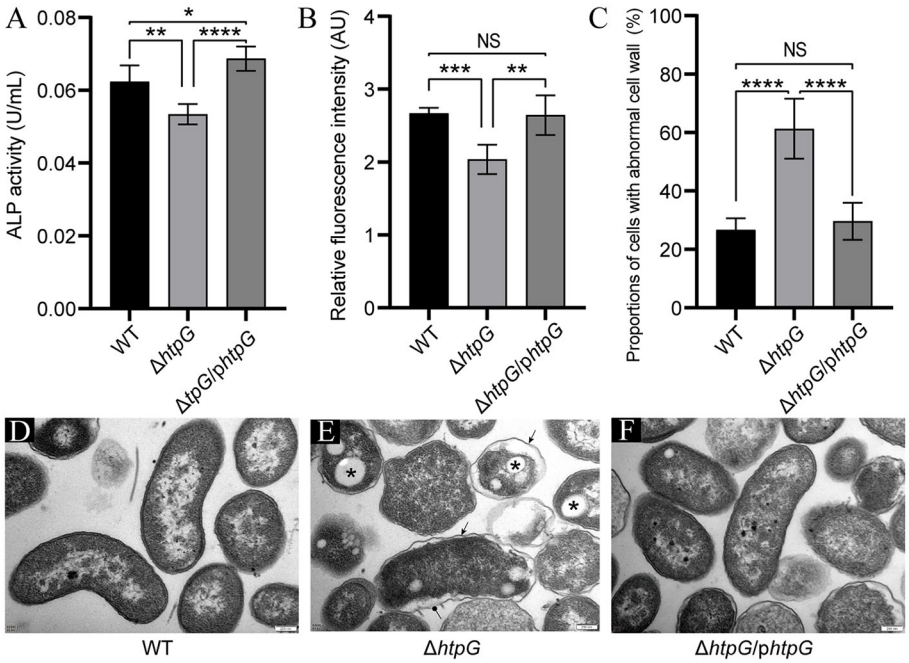

FIGURE 3
Impact of *htpG* deletion and complementation on cell wall and cell membrane permeability and integrity. **(A)** Alkaline phosphatase (ALP) activity in culture supernatant. **(B)** Relative propyl iodide (PI) fluorescence intensity in collected bacterial cells. **(C)** Quantification of the proportion of cells exhibiting abnormal cell wall structures based on transmission electron microscopy (TEM) images captured at a magnification of 12,000×. **(D–F)** TEM images of *V. mimicus* WT **(D)**, Δ*htpG* **(E)**, and Δ*htpG*/p*htpG* **(F)** strains [scale bar = 200 μm; sharp arrows in **(E)** point to cell wall undulating folds, circular solid arrows point to ruptured cell walls, and asterisks denote presumed accumulation of Poly-3-d-hydroxybutyrate (PHB)].

3.5 The deletion of *htpG* alters cell membrane components expression, including lipopolysaccharides, glycerophospholipids, and membrane proteins

Further, we conducted a detailed analysis of the significant gene expression changes affecting various key components of the cell envelope to elucidate the specific impact of *htpG*. Initially, we examined genes related to cellular membrane components, which are also associated with antimicrobial peptide resistance. In the intricate biosynthesis and assembly pathway of Lipopolysaccharide (LPS), notable upregulation was observed in VM_14500 (lpxL), VM_05370 (*lapB*), VM_05365 (*lapA*), and VM_05420 (*ictB*) (Figure 5A). These genes are critical for processes such as lipid A biosynthesis, O-antigen linkage, and LPS assembly. However, no significant impact was detected on other genes within this pathway. Including VM_16900 (*dgkA*), VM_18070 (*glpQ*), VM_18900 (*pgpB*), VM_17045 (*glpC*), VM_17040 (*glpB*), and VM_17035 (*glpA*), the key enzymes in the synthesis pathways of the major intracellular membrane constituents, Phosphatidylethanolamine (PE) and phosphatidylglycerol (PG), exhibited significant downregulation, with only VM_03635 (*cdsA*) showing a significant upregulation (Figure 5A). These findings suggest that the deletion of *htpG* promotes the synthesis of LPS while inhibiting glycerophospholipid biosynthesis. Regarding drug resistance-associated porins, VM_05465 (*ompA*), VM_20310 (*ompW*), and VM_18400 (*lamB*) were upregulated, while VM_06845 (*ompA*) and VM_12035 (*ompU*) were downregulated (Figure 5B). Notably, the porin genes associated with drug resistance exhibited an overall upregulation in terms of fold change in expression.

As for the ATP-binding cassette transporter (ABC) family proteins involved in nutrient uptake, toxin secretion, and antibiotic efflux for bacterial resistance, 12 DEGs exhibited significant variation. These DEGs can be classified into three operons associated with drug resistance (Figure 5D). The complete *MacAB-TolC* operon, including VM_07115 (*yvrO*), VM_07120 (*macB*), VM_07125 (*macB*), VM_07130 (*tolC*), and VM_07135 (*macA*), was significantly downregulated (Figure 5B). The VM_05500 (*yejA*), VM_05490 (*yejB*), VM_05495 (*yejE*), and VM_05505 (*yejF*) which belong to the *YejABEF* operon, were significantly down-regulated (Figure 5C). Conversely, within the *SapABCDF* operon, VM_06550 (*sapB*), VM_06545 (*sapC*), and VM_06535 (*sapF*) exhibited significant upregulation, whereas VM_06540 (*sapD*) and VM_06555 (*sapA*), also part of this operon, showed elevated expression (though not significant; Figure 5C).

3.6 The deletion of *htpG* causes profound peptidoglycan metabolism disruption

Subsequently, our analysis focused on genes related to the major component of the cell wall, peptidoglycan, including biosynthesis, recycling, and regulation. These components are

10.3389/fmicb.2023.1295065

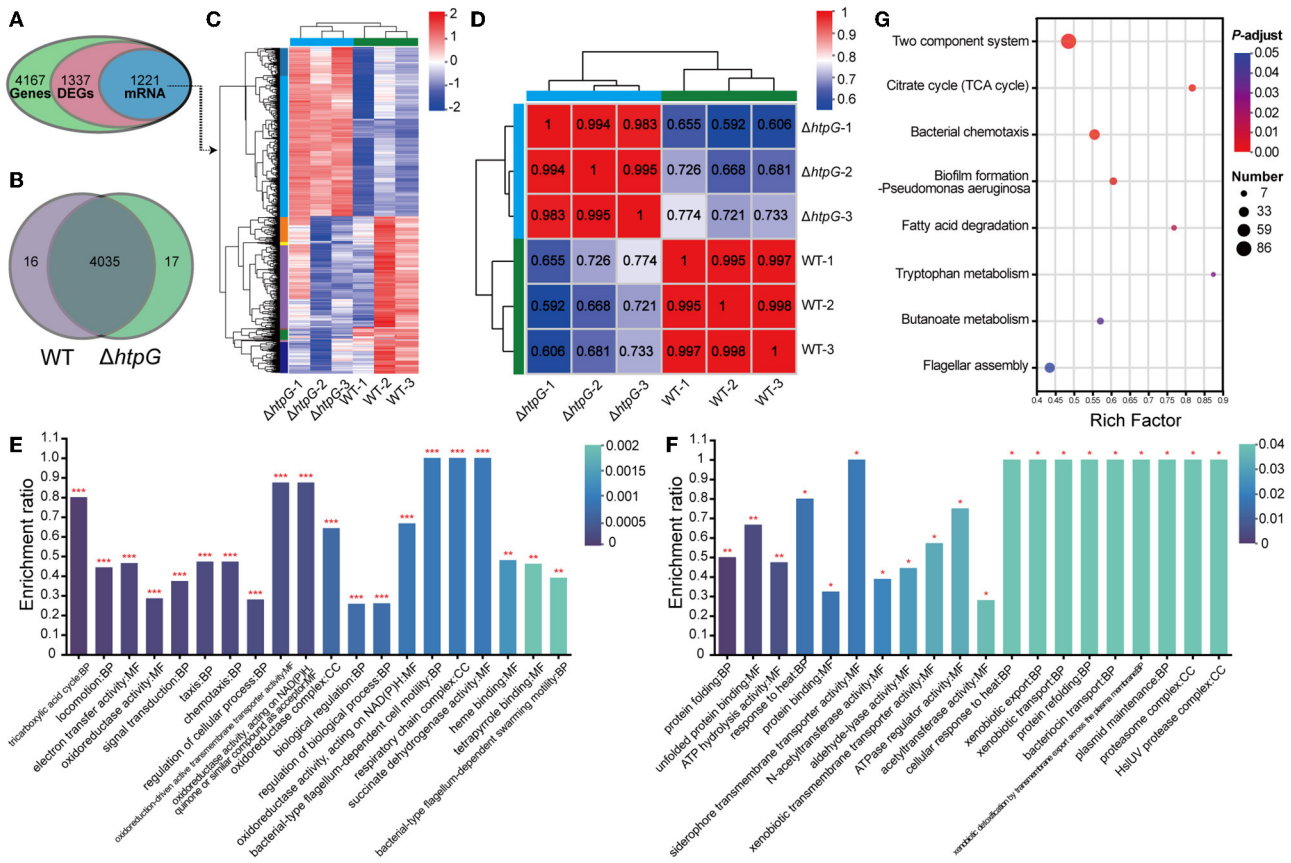

FIGURE 4
Overview of the transcriptome profiles of *V. mimicus* WT and Δ*htpG* strains. **(A)** The number of genes obtained for analysis after transcriptome data quality control, quantification, and filtering. **(B)** The number of genes with expression levels TPM > 1 that are unique or shared between the two bacterial strains. **(C)** Heat map overview of the expression levels of 1,221 differentially expressed mRNA in the two bacterial strains. Higher expression is represented in red, while lower expression is represented in blue. **(D)** Heat map depicting the expression correlation among samples from the two groups. The numbers indicate the correlation coefficients between corresponding samples; closer values to 1 are shown in red, and lower values are displayed in blue. **(E, F)** GO enrichment analysis results of 636 up-regulated mRNAs **(E)** and 585 down-regulated mRNAs **(F)**. The top 20 enriched terms are presented. The vertical axis represents the enrichment ratio, where higher values indicate greater enrichment. The color signifies the significance of enrichment, with *** denoting FDR < 0.001, ** for FDR < 0.01, and * for FDR < 0.05. **(G)** KEGG pathway enrichment analysis of the 1,221 differentially expressed mRNA. The x-axis represents the Rich Factor, with larger values indicating higher enrichment levels. The size of the points reflects the number of genes in the pathway, and the color of the points represents the *p*-adjust value.

pivotal in peptidoglycan metabolism and serve as essential and well-established targets for β-lactam antibiotics (Kang and Boll, 2022). In the Peptidoglycan biosynthesis pathway, two DEGs located at its initiation, VM_12770 (D-alanyl-D-alanine ligase, DDL), and VM_08260 (alanine racemase, ALR), exhibited significant upregulation. Conversely, at terminal end of the pathway, two DEGs belonging to the penicillin-binding proteins (PBPs), VM_01760 (mrcA/PBP1a) and VM_20665 (dacC/PBP5), responsible for regulating peptidoglycan layer synthesis and assembly, displayed significant downregulation (Figure 6B). This downregulation markedly impacts cell wall peptidoglycan production and structure.

The bacterial oligopeptide permeases (opp) operon belongs to the ABC superfamilies and is involved in cell wall metabolism by recycling peptidoglycan and peptide into the cytoplasm (Singh et al., 2020). In the *V. mimicus* SCCF01 strain, the entire *oppABCDF* operon was annotated (Figure 6D), and following *htpG* deletion, the substrate-binding protein OppA (VM_09400) exhibited significantly upregulation, whereas the ATP-binding protein OppF (VM_19555) showed significant downregulation (Figure 6C). This indicates an enhanced *oppABCDF* complex affinity for cell wall peptides and peptidoglycan, but the systemic energy supply is insufficient.Bacteria sense and ensure the stability of the cell envelope by utilizing the two-component CpxA/CpxR system and phage shock protein (psp) system. Within the *V. mimicus* SCCF01 strain, a complete *cpxARP* operon has been annotated. Upon *htpG* deletion, VM_01505 (*cpxA*, pressure receptor) and VM_01510 (*cpxR*, response regulator) are significantly upregulated, while VM_01515 (*cpxP*, stress adaptor protein) shows significant downregulation (Figure 6A). This indicates the activation of the cpx system. However, the key activator NlpE (VM_05160) of this complex, and downstream effector protein DegP (VM_12340) were downregulated, although not significantly (Figure 6A). This implies that the optimal activation of the cpx system might not have been achieved or that other unexplored response pathways could be involved. In

10.3389/fmicb.2023.1295065

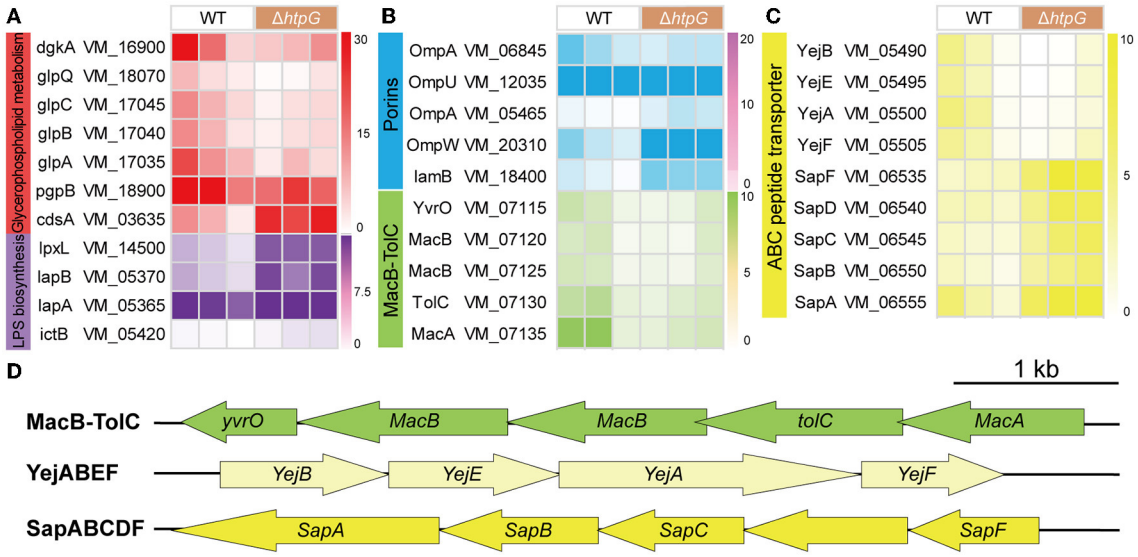

FIGURE 5
The impact of *htpG* deletion on the gene expression of cell membrane components. **(A–C)** Heat map of gene expression related to cellular membrane components. **(A)** Lipopolysaccharide (LPS) biosynthesis and glycerophospholipid metabolism, **(B)** Porin and Mac-TolC efflux pumps, **(C)** ABC peptide transporter. **(D)** The operon structure of Mac-TolC efflux pump and ABC peptide transporter gene cluster of *V. mimicus*. Scale bar = 1,000 bp.

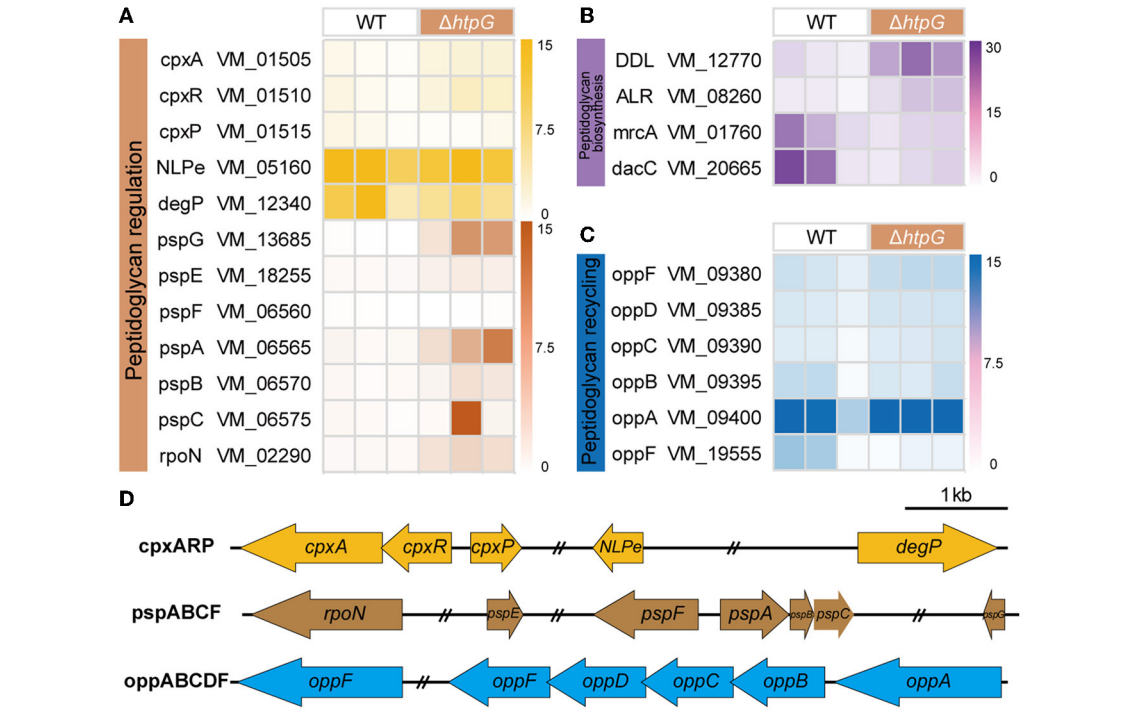

FIGURE 6
The effect of *htpG* deletion on the expression of peptidoglycan metabolism-related genes. **(A–C)** Heat map of gene expression related to peptidoglycan metabolism. **(A)** Peptidoglycan regulation, **(B)** peptidoglycan biosynthesis, and **(C)** peptidoglycan recycling. **(D)** The operon structure of the peptidoglycan regulation and recycling gene cluster of *V. mimicus*. Scale bar = 1,000 bp, double slash marks indicate the presence of sequence gaps.

addition, a classical psp system was annotated, consisting of a *pspFABC* gene cluster and the more distantly located *pspG* (VM_13685) and *pspE* (VM_18255) genes (Figure 6D). Among them, only VM_06565 (*pspA*) and VM_13685 (*pspG*) exhibit significant upregulation. Simultaneously, VM_02290 (*rpoN*), which transcribes the operon along with pspF, also shows

significant upregulation (Figure 6A). This highlights the activation of the psp system, which contributes to the stabilization of both the cell membrane and the peptidoglycan layer.

3.7 Verification by RT-qPCR

The differential log-transformed expression fold change of selected DEGs obtained by RT-qPCR and RNA-seq is depicted in the Figure 7A. The gene expression trends observed in RT-qPCR are similar to those in RNA-seq, with a correlation coefficient of $R^2 = 0.9256$, indicating a strong correlation between the two transcriptions (Figure 7B). The inconsistency may result from variations in sensitivity and procedures between transcriptome sequencing and RT-qPCR.

4 Discussion

This study demonstrated that the most significant alterations in antibiotic resistance, primarily targeting the cell envelope, result from the deletion of *htpG*, which compromises the permeability and integrity of the cell envelope. Subsequent transcriptomic analysis of specific genes revealed that *htpG* promotes resistance to antimicrobial peptides by regulating LPS and glycerophospholipid synthesis on the cell membrane, as well as the functionality of MacAB-TolC and YejABEF pumps. Furthermore, it was confirmed that *htpG* mediates the synthesis, recycling, and regulation of peptidoglycans on the cell wall, thereby contributing to increased sensitivity of the strain to β-lactam antibiotics. This highlights the intricate and widespread engagement of *htpG* in bacterial physiological processes, motivating us to further explore a nuanced comprehension of how *htpG* precisely facilitates or hinders resistance to specific categories of drugs. The necessity for further specific experimental research on the regulation of the *htpG* gene in bacterial drug resistance pathways arises from several factors. Firstly, given the potential pandemic risk associated with *V. mimicus* and the escalating trend of antibiotic resistance, it is paramount to initiate investigations into its resistance mechanisms promptly. This research not only facilitates early interventions, including drug guidance, but also contributes to the identification of crucial biomarkers for monitoring. Additionally, the drug resistance mechanisms unveiled in this study have a nearly universal presence in Gram-negative bacteria, and a detailed exploration of their interplay offers new targets for combating drug-resistant pathogens. Furthermore, our study highlights the pivotal role played by the *htpG* gene in regulating sensitivity to critical antibiotics, such as polymyxin B, and imipenem, which are of substantial clinical significance. Imipenem, in particular, serves as a highly recommended frontline defense against severe infections caused by multidrug-resistant bacteria, while polymyxin B remains a global last-resort option. Furthermore, the existence of inhibitors designed for eukaryotic Hsp90 proteins highlights the potential for repurposing these agents to develop safe and effective tools for suppressing bacterial drug resistance. Lastly, previous studies have highlighted that these inhibitors also possess the potential to suppress bacterial virulence (Wickner et al., 2021). Thus, an in-depth exploration of the regulatory networks governing these specific genes promises for identifying future therapeutic targets and improve susceptibility to antimicrobial peptides and β-lactam antibiotics, critical steps in advancing antimicrobial therapy.

Gram-negative bacteria have a multi-layered envelope consisting of an outer membrane (OM), inner membrane (IM), and peptidoglycan (PGN) layer. Both the outer and inner membranes feature a phospholipid bilayer structure rich in proteins, while the OM is additionally adorned with lipopolysaccharides (LPS). LPS constitute a pivotal component of the OM in the majority of Gram-negative bacteria, playing a crucial role in safeguarding bacteria from environmental stressors and contributing to antibiotic resistance and pathogenesis (Di Lorenzo et al., 2022). Polymyxin B disrupts the stability of the OM by targeting phospholipids and, with higher affinity, the lipid A domain of LPS (Ledger et al., 2022). In *V. mimicus*, the deletion of *htpG* resulted in a significant upregulation of four genes involved in LPS biosynthesis and assembly pathways. In particular, LapA and LapB serve as checkpoints for the proper assembly of LPS, ensuring that only fully synthesized LPS are delivered to the Lpt complex, a process crucial for bacterial growth. This may result in an increased accumulation of LPS on the bacterial surface, thereby enhancing the binding and lethality of polymyxin B, which aligns with the observed changes in antibiotic resistance phenotypes. In the biosynthesis pathway of glycerophospholipids (Figure 8A), the enzyme complex GlpA/B/C is responsible for converting dihydroxyacetone phosphate into glycerol-3-phosphate, which serves as a precursor for phospholipid synthesis. On the other hand, GlpQ, which functions as a periplasmic glycerophosphoryl diester phosphodiesterase, has the ability to hydrolyze deacylated phospholipids into glycerol-3-phosphate and alcohol. This strategy involves bacteria modifying the surface properties of phospholipids as a means to evade antimicrobial peptides. In the final step, PgpB synthesizes phosphatidylglycerol (PG) from its precursor, phosphatidylglycerol phosphate (PGP). Additionally, because of its extensive substrate connectivity, PgpB plays a crucial role in linking the biosynthesis of membrane glycerophospholipids and cell wall polysaccharides. The significant downregulation of these five genes may inhibit glycerophospholipid synthesis, disrupt the balance of its production, and consequently affect membrane fluidity, permeability, and stability. In *Staphylococcus aureus*, reduced phosphatidylglycerol content results in a more a more negative net charge, thereby enhancing the binding of cationic antimicrobial peptides and increasing sensitivity (Nishi et al., 2004), which is consistent with the phenotypic changes observed in this study.

In the drug-resistant membrane proteins, porins exhibited an overall upregulation (Figure 8B-a). The contribution of *ompU*, *ompA*, *ompW*, and *lamB* genes to the susceptibility of several β-lactams has been confirmed in pathogenic bacteria such as *V. cholerae*, *Acinetobacter baumannii*, *Salmonella enterica*, and *Klebsiella pneumoniae*, respectively (Nguyen et al., 2009; Garcia-Sureda et al., 2011; Smani et al., 2014; Ko and Choi, 2022). Surprisingly, despite the upregulation of porin expression due to *htpG* deletion in *V. mimicus*, its sensitivity to β-lactams decreased, suggesting that porins may not be the primary targets for β-lactams resistance. Besides drug resistance, porins also serve as essential nutrient uptake channels in bacteria, regulated by responsive regulatory elements coordinating with stress pathways

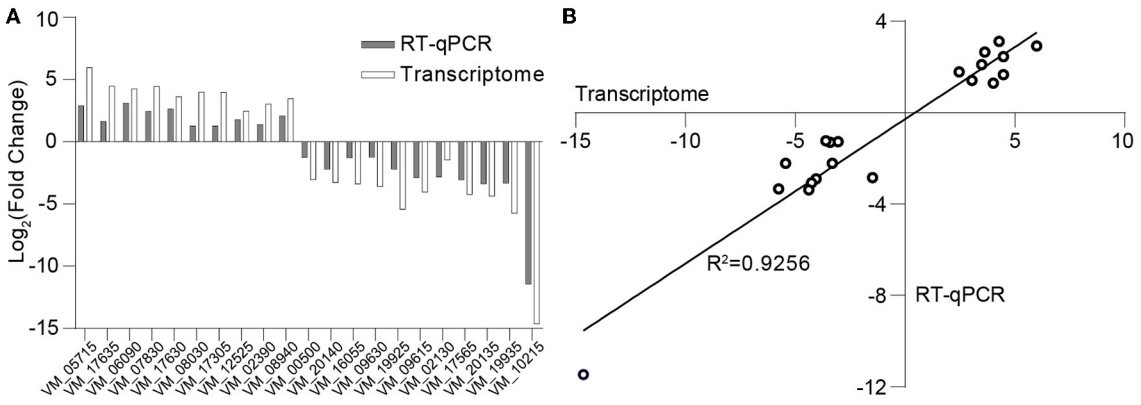

FIGURE 7
Validation of transcriptome data through RT-qPCR. **(A)** Log-transformed expression fold change achieved via RT-qPCR and RNA-seq for the selected genes. **(B)** Correlation between the differential expression ratio (log_2) determined by RT-qPCR and RNA-seq for the selected differentially expressed genes.

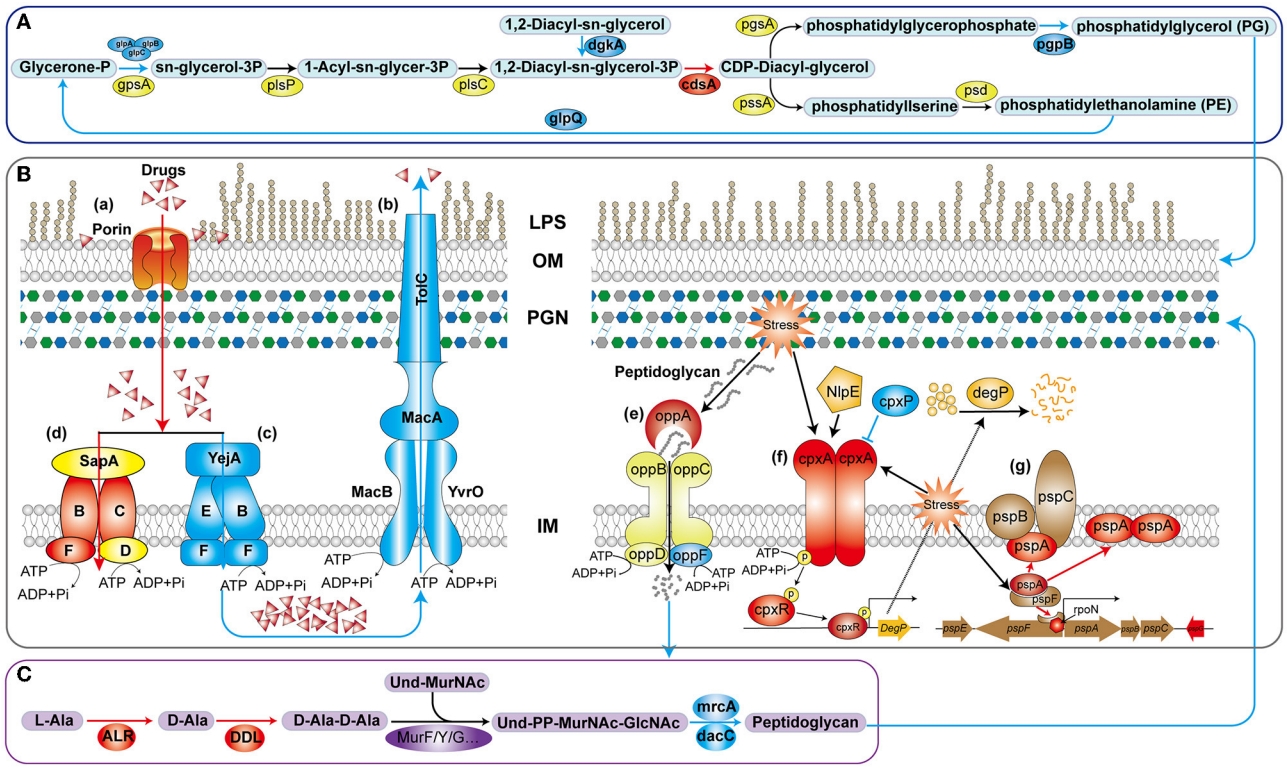

FIGURE 8
Schematic diagram of the mechanism of *htpG*-mediated antimicrobial peptide and β-lactam antibiotics resistance in *V. mimicus*. The blue lines and color patches represent down-regulated processes or genes corresponding to proteins, while the red ones represent up-regulated ones. **(A)** Key pathways in glycerophospholipid biosynthesis. **(B)** Drug-resistant membrane proteins (a–d) and metabolic mechanism peptidoglycan (e–g). LPS, lipopolysaccharide; OM, outer membrane; PGN, peptidoglycan; IM, inner membrane. **(C)** Key reactions in peptidoglycan synthesis for bacterial cell wall.

(Fernández and Hancock, 2013). Therefore, the increased porin expression might represent an adaptive response to unfavorable conditions caused by the absence of the vital molecular chaperone protein HtpG. All five genes within the MacAB-TolC efflux pump displayed significant downregulation. MacAB, in conjunction with the OM protein TolC, creates a tripartite channel that facilitates the efflux of a diverse range of antimicrobial compounds, as well as endogenous molecules and toxins (Figure 8B-b). Studies conducted on *E. coli* and clinical isolates of several other bacteria have substantiated that overexpression of MacA and MacB proteins imparts resistance to macrolide antibiotics and antimicrobial peptides like polymyxin B (Greene et al., 2018). This study also

observed a significant decrease in resistance to azithromycin (AZM) and polymyxin B (PMB) in the Δ*htpG* strain (Figure 2B-a), which is consistent with the findings of these two studies, indicating the significant role of the MacAB-TolC efflux pump in the *htpG*-mediated regulation of antimicrobial resistance in *V. mimicus*. Two high-affinity peptide ABC transport systems, YejABEF and SapABCDF, have been confirmed to confer resistance to antimicrobial peptides in bacteria. The potential mechanism involves transferring antimicrobial peptides into the cytoplasm, thereby keeping them away from their targets and exposing them to intracellular degradation (Figure 8B-c, d; Garai et al., 2017). Studies in *Salmonella enterica* and *S. typhimurium* have also shown that enhancing the function of YejABEF and SapABCDF systems increases resistance to antimicrobial peptides (Groisman et al., 1992; Eswarappa et al., 2008). However, upon deleting the *htpG*, these two functionally similar systems exhibit completely opposite gene expression patterns. Considering the decreased resistance of the Δ*htpG* strain to polymyxin B, we speculate that the overall downregulation of the YejABEF pump plays a predominant role, while the compensatory upregulation of the SapABCDF pump counterbalances its physiological impact. Further investigation into the regulatory interactions and the order of significance of these systems will contribute to a clearer understanding of specific targets for the development of strategies to reduce polymyxin resistance.

In addition to the cell membrane, the cell wall, mainly composed of peptidoglycan, is also an crucial component of the bacterial envelope. Alanine racemase (Alr) and d-Alanine-d-alanine ligase (Ddl) are the key enzymes in the D-Ala-D-Ala branch of peptidoglycan biosynthesis (Qin et al., 2021; Figure 8C) and are an important drug discovery target. Alr is responsible for supplying d-alanine, while Ddl facilitates the condensation of two alanine molecules utilizing ATP, which serves as the terminal peptide in peptidoglycan monomer formation. On the other hand, PBPs regulates the assembly of bacterial cell wall peptidoglycan layers, and are targets of β-lactams. The MrcA (PBP1A) and dacC (PBP5) are major peptidoglycan synthases (Kang and Boll, 2022) and D-alanyl-D-alanine carboxypeptidases, respectively, located at the end of the peptidoglycan biosynthetic pathway. In the Δ*htpG* strain, enzymes responsible for synthesizing peptidoglycan precursors were upregulated, while those involved in synthesizing the final product were downregulated. Consequently, it can be inferred that the reduction in the final product, peptidoglycan, severely impacts cell wall synthesis and structure. Simultaneously, the decrease in PBPs would lead to a reduction in β-lactam targets, thereby enhancing resistance correspondingly. This is consistent with the observed phenotypic changes in this study. The upregulation of *ddl* and *alr* may be attributed to the presence of negative feedback regulation within the peptidoglycan synthesis pathway. Furthermore, peptidoglycan is a sugar-amino acid polymer, possesses high immunogenicity. To conserve energy and evade host detection, bacteria recycle peptidoglycan by transporting it into the cytoplasm for new synthesis (Singh et al., 2020). The bacterial oligopeptide permeases (opp) system, a membrane-associated complex comprising five proteins of the ABC transport family (Figure 8B-e), plays a crucial role in peptidoglycan and cell wall peptide recycling in Gram-negative bacteria. Upon deleting the *htpG*, the substrate-binding protein VM_09400 (*oppA*) exhibited significant upregulation, indicating that the bacterium reinforces the recycling of cell wall peptides and peptidoglycan by increasing *oppA* production. However, the ATP-binding protein VM_19555 (*oppF*), responsible for energy supply, showed significant downregulation, indicating insufficient energy for the system and a potential failure in the recycling of cell wall peptides and peptidoglycan.

Owing to the vital role of the cell envelope, prokaryotes have developed diverse mechanisms to meticulously oversee and preserve the integrity of their cell envelope. Two such systems are the CpxA/CpxR two-component system and the phage shock protein (psp) system. The Cpx system can regulate the function of some peptidoglycan amidases or AcrAB-TolC efflux pumps, thereby modifying bacterial resistance to some β-lactam and cationic antimicrobial peptide antibiotics. This system includes the pressure-sensing kinase CpxA located in the IM, the response regulator CpxR in the cytoplasm, and the auxiliary periplasmic protein CpxP, which inhibits CpxA through a direct dynamic interaction (Figure 8B-f). Normal activation of The Cpx system boosts chaperone and protease expression, along with enhancing peptidoglycan modifications by proteins, all contributing to the response of cell to envelope stress (Mitchell and Silhavy, 2019). In the process of activation and response, two of the famous proteins are NlpE, an OM lipoprotein that acts as a signaling module activator (Cho et al., 2023), and DegP, a periplasmic protease triggered to break down misfolded proteins upon CpxA/CpxR system activation. However, this study observed that the gene expression levels of *nlpE* (VM_05160) and *degP* (VM_12340) were downregulated, although not significantly. It suggests that response of the Cpx system to envelope stress may be attenuated. Further investigation could be needed to understand the specific factors or mechanisms responsible for this observation and its implications for bacterial stress responses and antibiotic resistance. In another psp system (Figure 8B-g), under non-stress conditions, pspA inhibits the activity of the transcription factor pspF. However, in response to envelope stress, pspA dissociates from pspF, allowing pspF to activate RNA polymerase factor sigma-54 (RpoN) dependent transcription of the psp operon. Furthermore, pspA not only associates with the membrane-bound pspBC to maintain membrane stability but also directly interfaces with the cell membrane, ensuring its stability. Consequently, pspA serves as a regulatory element, sensor module, and effector protein, highlighting its central role within the psp network (Popp et al., 2022). In Δ*htpG* strain, only the core genes *pspA*, functionally uncharacterized *pspG*, and the transcriptional regulator *rpoN* were significantly upregulated, while other gene changes were not significant. This suggests that the bacteria are responding to the envelope stress triggered by *htpG* deletion to adapt to external pressures, but downstream genes are not transcriptionally regulated in response, indicating the presence of other regulatory mechanisms or unobserved responses.

5 Conclusions

In conclusion, the increased sensitivity of Δ*htpG* strain to antimicrobial peptides can be attributed to multiple factors: (1)

upregulation of LPS synthesis, providing more binding targets; (2) reduction in glycerophospholipid content, promoting charge interactions between drugs and bacterial cells; (3) reduced efflux activity of the MacAB-TolC pump, leading to increased drug retention within cells; (4) weakened inward transport and digestion of the YejABEF pump, allowing more drugs to remain in their active forms. Meanwhile, the decreased sensitivity of the Δ*htpG* strain to β-lactam antibiotics can be attributed to: (1) reduced peptidoglycan synthesis, resulting in fewer PBPs and targets; (2) dysregulation of peptidoglycan recycling and envelope stress response. Further exploration of specific pathway components is essential for a comprehensive understanding of *htpG*-mediated resistance mechanisms, aiding in antimicrobial agent development.

Data availability statement

The datasets presented in this study can be found in online repositories. The names of the repository/repositories and accession number(s) can be found at: https://bigd.big.ac.cn/gsa/browse/CRA009391.

Author contributions

ZQ: Conceptualization, Data curation, Formal analysis, Investigation, Methodology, Project administration, Visualization, Writing—original draft, Writing—review & editing. KP: Data curation, Investigation, Methodology, Visualization, Writing—review & editing. YF: Writing—review & editing. YW: Software, Visualization, Writing—review & editing. BH: Data curation, Formal analysis, Methodology, Writing—review & editing. ZT: Methodology, Validation, Writing—review & editing. PO: Project administration, Resources, Writing—review & editing. XH: Funding acquisition, Project administration, Resources, Writing—review & editing. DC: Project administration, Resources, Writing—review & editing. WL: Project administration, Resources, Writing—review & editing. YG: Data curation, Funding acquisition, Resources, Supervision, Writing—review & editing.

Funding

The author(s) declare financial support was received for the research, authorship, and/or publication of this article. This research was supported by National Natural Science Foundation of China (32373174), Sichuan Natural Science Foundation (24NSFSC0858), and Sichuan Innovation Team Project of Agricultural Industry Technology System (SCCXTD-15).

Conflict of interest

The authors declare that the research was conducted in the absence of any commercial or financial relationships that could be construed as a potential conflict of interest.

Publisher's note

Supplementary material

The Supplementary Material for this article can be found online at: https://www.frontiersin.org/articles/10.3389/fmicb.2023.1295065/full#supplementary-material

SUPPLEMENTARY FIGURE 1
DEGs volcano plot and PCA analysis of transcriptional profiles of *V. mimicus* WT and Δ*htpG* strains. **(A)** The volcano plot of DEGs between *V. mimicus* WT and Δ*htpG* strains, including mRNA and sRNA. Red dots represent up-regulated DEGs, blue dots represent down-regulated DEGs, and gray dots represent no differentially expressed genes. **(B)** Principal Component Analysis (PCA) based on sample expression levels is performed (the x and y-axis represent the calculated values of the principal components, with each point representing a different sample. The distance between samples indicates their similarity, and the ellipses denote the 95% confidence interval).

SUPPLEMENTARY TABLE 1
Primers used for RT-qPCR analysis.

SUPPLEMENTARY TABLE 2
List of antibacterial agents and their targets.

SUPPLEMENTARY TABLE 3
Biochemical phenotype of test strains.

SUPPLEMENTARY TABLE 4
Partial annotation and expression level of all DEGs.

SUPPLEMENTARY TABLE 5
Go enrichment analysis of up-regulated mRNA.

SUPPLEMENTARY TABLE 6
KEGG enrichment analysis of all DEGs.

References

Adesiyan, I. M., Bisi-Johnson, M. A., Ogunfowokan, A. O., and Okoh, A. I. (2021). Occurrence and antibiogram signatures of some Vibrio species recovered from selected rivers in South West Nigeria. *Environ. Sci. Pollut. Res.* 28, 42458–42476. doi: 10.1007/s11356-021-13603-4

Backe, S. J., Sager, R. A., Woodford, M. R., Makedon, A. M., and Mollapour, M. (2020). Post-translational modifications of hsp90 and translating the chaperone code. *J. Biol. Chem.* 295, 11099–11117. doi: 10.1074/jbc.REV120.011833

Beshiru, A., Okareh, O. T., Okoh, A. I., and Igbinosa, E. O. (2020). Detection of antibiotic resistance and virulence genes of Vibrio strains isolated from ready-to-eat shrimps in delta and Edo states, Nigeria. *J. Appl. Microbiol.* 129, 17–36. doi: 10.1111/jam.14590

Cho, S., Dekoninck, K., and Collet, J. (2023). Envelope-stress sensing mechanism of RCS and CPX signaling pathways in gram-negative bacteria. *J. Microbiol.* 61, 317–329. doi: 10.1007/s12275-023-00030-y

Di Lorenzo, F., Duda, K. A., Lanzetta, R., Silipo, A., De Castro, C., and Molinaro, A. (2022). A journey from structure to function of bacterial lipopolysaccharides. *Chem. Rev.* 122, 15767–15821. doi: 10.1021/acs.chemrev.0c01321

Dong, T., Wang, W., Xia, M., Liang, S., Hu, G., Ye, H., et al. (2021). Involvement of the heat shock protein htpg of *Salmonella typhimurium* in infection and proliferation in hosts. *Front. Cell. Infect. Microbiol.* 11, 758898. doi: 10.3389/fcimb.2021.758898

Elgendy, M. Y., Abdelsalam, M., Kenawy, A. M., and Ali, S. E. (2022). Vibriosis outbreaks in farmed nile tilapia (*Oreochromis niloticus*) caused by *Vibrio mimicus* and *V. cholerae*. *Aquac. Int.* 30, 2661–2677. doi: 10.1007/s10499-022-00921-8

Eswarappa, S. M., Panguluri, K. K., Hensel, M., and Chakravortty, D. (2008). The yejabef operon of *Salmonella* confers resistance to antimicrobial peptides and contributes to its virulence. *Microbiology* 154, 666–678. doi: 10.1099/mic.0.2007/011114-0

Fernández, L., and Hancock, R. E. W. (2013). Adaptive and mutational resistance: role of porins and efflux pumps in drug resistance. *Clin. Microbiol. Rev.* 26, 163. doi: 10.1128/CMR.00094-12

Fu, C., Beattie, S. R., Jezewski, A. J., Robbins, N., Whitesell, L., Krysan, D. J., et al. (2022). Genetic analysis of hsp90 function in *Cryptococcus neoformans* highlights key roles in stress tolerance and virulence. *Genetics* 220, iyab164. doi: 10.1093/genetics/iyab164

Garai, P., Chandra, K., and Chakravortty, D. (2017). Bacterial peptide transporters: messengers of nutrition to virulence. *Virulence* 8, 297–309. doi: 10.1080/21505594.2016.1221025

Garcia-Descalzo, L., Alcazar, A., Baquero, F., and Cid, C. (2011). Identification of *in vivo* hsp90-interacting proteins reveals modularity of hsp90 complexes is dependent on the environment in psychrophilic bacteria. *Cell Stress Chaperones*. 16, 203–218. doi: 10.1007/s12192-010-0233-7

Garcia-Sureda, L., Juan, C., Domenech-Sanchez, A., and Alberti, S. (2011). Role of *Klebsiella pneumoniae* lamb porin in antimicrobial resistance. *Antimicrob. Agents. Chemother.* 55, 1803–1805. doi: 10.1128/AAC.01441-10

Geng, Y., Liu, D., Han, S., Zhou, Y., Wang, K., Huang, X., et al. (2014). Outbreaks of vibriosis associated with *Vibrio mimicus* in freshwater catfish in china. *Aquaculture*. 433, 82–84. doi: 10.1016/j.aquaculture.2014.05.053

Graner, M. W. (2021). Making hsp90 inhibitors great again? Unite for better cancer immunotherapy. *Cell Chem. Biol.* 28, 118–120. doi: 10.1016/j.chembiol.2021.02.002

Greene, N. P., Kaplan, E., Crow, A., and Koronakis, V. (2018). Antibiotic resistance mediated by the macb abc transporter family: a structural and functional perspective. *Front. Microbiol.* 9, 950. doi: 10.3389/fmicb.2018.00950

Groisman, E. A., Parra-Lopez, C., Salcedo, M., Lipps, C. J., and Heffron, F. (1992). Resistance to host antimicrobial peptides is necessary for *Salmonella* virulence. *Proc. Natl. Acad. Sci. U. S. A.* 89, 11939–11943.

Grudniak, A. M., Klecha, B., and Wolska, K. I. (2018). Effects of null mutation of the heat-shock gene htpg on the production of virulence factors by *Pseudomonas aeruginosa*. *Future Microbiol.* 13, 69–80. doi: 10.2217/fmb-2017-0111

Guangchuang, Y., Li-Gen, W., Yanyan, H., and Qing-Yu, H. (2012). Cluster profiler: an R package for comparing biological themes among gene clusters. *Omics* 118, 284–287. doi: 10.1089/omi.2011.0118

Guardiola-Avila, I., Sanchez-Buso, L., Acedo-Felix, E., Gomez-Gil, B., Zuniga-Cabrera, M., Gonzalez-Candelas, F., et al. (2021). Core and accessory genome analysis of *Vibrio mimicus*. *Microorganisms* 9, 10191. doi: 10.3390/microorganisms9010191

Gxalo, O., Digban, T. O., Igere, B. E., Olapade, O. A., Okoh, A. I., and Nwodo, U. U. (2021). Virulence and antibiotic resistance characteristics of Vibrio isolates from rustic environmental freshwaters. *Front. Cell. Infect. Microbiol.* 11, 732001. doi: 10.3389/fcimb.2021.732001

Halder, M., Saha, S., Mookerjee, S., and Palit, A. (2022). Exploring the dynamics of toxigenic environmental *Vibrio mimicus* and its comparative analysis with *Vibrio cholerae* of the southern gangetic delta. *Arch. Microbiol.* 204, 420. doi: 10.1007/s00203-022-03028-z

Hernandez-Robles, M. F., Natividad-Bonifacio, I., Alvarez-Contreras, A. K., Tercero-Alburo, J. J., Quinones-Ramirez, E. I., and Vazquez-Salinas, C. (2021). Characterization of potential virulence factors of *Vibrio mimicus* isolated from fishery products and water. *Int. J. Microbiol.* 2021, 8397930. doi: 10.1155/2021/8397930

Honoré, F. A., Méjean, V., and Genest, O. (2017). Hsp90 is essential under heat stress in the bacterium *Shewanella oneidensis*. *Cell Rep.* 19, 680–687. doi: 10.1016/j.celrep.2017.03.082

Iyer, K. R., Robbins, N., and Cowen, L. E. (2022). The role of *Candida albicans* stress response pathways in antifungal tolerance and resistance. *Iscience* 25, 103953. doi: 10.1016/j.isci.2022.103953

Jiang, Z., Gao, X., Jiang, Q., Zhu, X., Zhou, Y., Zhang, Z., et al. (2022). Genomic characterization and pathogenicity analysis of the *Vibrio mimicus* y4 causing red body disease in *Macrobrachium nipponense*. *Aquaculture* 548, 737701. doi: 10.1016/j.aquaculture.2021.737701

Kang, K. N., and Boll, J. M. (2022). Pbp1a directly interacts with the divisome complex to promote septal peptidoglycan synthesis in *Acinetobacter baumannii*. *J. Bacteriol.* 204, 22. doi: 10.1128/jb.00239-22

Karen Alvarez-Contreras, A., Irma Quinones-Ramirez, E., and Vazquez-Salinas, C. (2021). Prevalence, detection of virulence genes and antimicrobial susceptibility of pathogen Vibrio species isolated from different types of seafood samples at "la nueva viga" market in mexico city. *Antonie. Van. Leeuwenhoek*. 114, 1417–1429. doi: 10.1007/s10482-021-01591-x

Ko, D., and Choi, S. H. (2022). Mechanistic understanding of antibiotic resistance mediated by envz/ompr two-component system in *Salmonella enterica* serovar enteritidis. *J. Antimicrob. Chemother.* 77, 2419–2428. doi: 10.1093/jac/dkac223

Lacey, T., and Lacey, H. (2021). Linking hsp90's role as an evolutionary capacitator to the development of cancer. *Cancer Treat. Res. Commun.* 28, 100400. doi: 10.1016/j.ctarc.2021.100400

Ledger, E. V. K., Sabnis, A., and Edwards, A. M. (2022). Polymyxin and lipopeptide antibiotics: membrane-targeting drugs of last resort. *Microbiology* 168, 1136. doi: 10.1099/mic.0.001136

Li, C., Tu, J., Han, G., Liu, N., and Sheng, C. (2022). Heat shock protein 90 (hsp90)/histone deacetylase (hdac) dual inhibitors for the treatment of azoles-resistant *Candida albicans*. *Eur. J. Med. Chem.* 227, 113961. doi: 10.1016/j.ejmech.2021.113961

Li, Y., Chen, Y., Qiu, C., Ma, X., Lei, K., Cai, G., et al. (2019). 17-allylamino-17-demethoxygeldanamycin impeded chemotherapy through antioxidant activation via reducing reactive oxygen species-induced cell death. *J. Cell. Biochem.* 120, 1560–1576. doi: 10.1002/jcb.27397

Li, Z., and Luo, Y. (2022). Hsp90 inhibitors and cancer: prospects for use in targeted therapies (review). *Oncol. Rep.* 49, 1. doi: 10.3892/or.2022.8443

Marcyk, P. T., LeBlanc, E. V., Kuntz, D. A., Xue, A., Ortiz, F., Trilles, R., et al. (2021). Fungal-selective resorcylate aminopyrazole hsp90 inhibitors: optimization of whole-cell anticryptococcal activity and insights into the structural origins of cryptococcal selectivity. *J. Med. Chem.* 64, 1139–1169. doi: 10.1021/acs.jmedchem.0c01777

Mason, C., Dunner, J., Indra, P., and Colangelo, T. (1999). Heat-induced expression and chemically induced expression of the *Escherichia coli* stress protein htpg are affected by the growth environment. *Appl. Environ. Microbiol.* 65, 3433–3440.

Mathieu, C., Messaoudi, S., Fattal, E., and Vergnaud-Gauduchon, J. (2019). Cancer drug resistance: rationale for drug delivery systems and targeted inhibition of hsp90 family proteins. *Cancer Drug Resist.* 2, 381–398. doi: 10.20517/cdr.2019.26

Mitchell, A. M., and Silhavy, T. J. (2019). Envelope stress responses: balancing damage repair and toxicity. *Nat. Rev. Microbiol.* 17, 417–428. doi: 10.1038/s41579-019-0199-0

Nguyen, D. T., Ngo, T. C., Tran, H. H., Nguyen, T. P. L., Nguyen, B. M., Morita, K., et al. (2009). Two different mechanisms of ampicillin resistance operating in strains of *Vibrio cholerae* o1 independent of resistance genes. *Fems Microbiol. Lett.* 298, 37–43. doi: 10.1111/j.1574-6968.2009.01693.x

Nishi, H., Komatsuzawa, H., Fujiwara, T., McCallum, N., and Sugai, M. (2004). Reduced content of lysyl-phosphatidylglycerol in the cytoplasmic membrane affects susceptibility to moenomycin, as well as vancomycin, gentamicin, and antimicrobial peptides, in *Staphylococcus aureus*. *Antimicrob. Agents. Chemother.* 48, 4800–4807. doi: 10.1128/AAC.48.12.4800-4807.2004

Popp, P. F., Gumerov, V. M., Andrianova, E. P., Bewersdorf, L., Mascher, T., Zhulin, I. B., et al. (2022). Phyletic distribution and diversification of the phage shock protein stress response system in bacteria and archaea. *Msystems* 7, e134821. doi: 10.1128/msystems.01348-21

Qin, Y., Xu, L., Teng, Y., Wang, Y., and Ma, P. (2021). Discovery of novel antibacterial agents: recent developments in d-alanyl-d-alanine ligase inhibitors. *Chem. Biol. Drug Des.* 98, 305–322. doi: 10.1111/cbdd.13899

Ren, Y., Yu, G., Shi, C., Liu, L., Guo, Q., Han, C., et al. (2022). Majorbio cloud: a one-stop, comprehensive bioinformatic platform for multiomics analyses. *Imeta* 1, e12. doi: 10.1002/imt2.12

Singh, R., Liechti, G., Slade, J. A., and Maurelli, A. T. (2020). *Chlamydia trachomatis* oligopeptide transporter performs dual functions of oligopeptide transport and peptidoglycan recycling. *Infect. Immun.* 88, 20. doi: 10.1128/IAI.00086-20

Smani, Y., Fabrega, A., Roca, I., Sanchez-Encinales, V., Vila, J., and Pachon, J. (2014). Role of ompa in the multidrug resistance phenotype of *Acinetobacter baumannii*. *Antimicrob. Agents. Chemother.* 58, 1806–1808. doi: 10.1128/AAC.02101-13

Wickner, S., Nguyen, T. L., and Genest, O. (2021). The bacterial hsp90 chaperone: cellular functions and mechanism of action. *Annu. Rev. Microbiol.* 75, 719–739. doi: 10.1146/annurev-micro-032421-035644

Yang, A., Yassin, M., and Phan, T. (2021). *Vibrio mimicus* wound infection in a burn patient. *Radiol. Case Rep*. 16, 1348–1351. doi: 10.1016/j.radcr.2021.03.021

Yin, W., Wu, T., Liu, L., Jiang, H., Zhang, Y., Cui, H., et al. (2022). Species-selective targeting of fungal hsp90: design, synthesis, and evaluation of novel 4,5-diarylisoxazole derivatives for the combination treatment of azole-resistant candidiasis. *J. Med. Chem.* 65, 5539–5564. doi: 10.1021/acs.jmedchem.1c01991

Yu, Z., Wang, E., Geng, Y., Wang, K., Chen, D., Huang, X., et al. (2019). Multiplex genome editing by natural transformation in *vibrio mimicus* with potential application in attenuated vaccine development. *Fish Shellfish Immunol.* 92, 377–383. doi: 10.1016/j.fsi.2019.06.025

Yu, Z., Wang, E., Geng, Y., Wang, K., Chen, D., Huang, X., et al. (2020). Complete genome analysis of *vibrio mimicus* strain sccf01, a highly virulent isolate from the freshwater catfish. *Virulence* 11, 23–31. doi: 10.1080/21505594.2019.1702797

frontiers | Frontiers in Microbiology

TYPE Correction
PUBLISHED 13 March 2024
DOI 10.3389/fmicb.2024.1381070

OPEN ACCESS

APPROVED BY
Frontiers Editorial Office,
Frontiers Media SA, Switzerland

*CORRESPONDENCE
Yi Geng
gengyisicau@126.com

†These authors have contributed equally to this work and share first authorship

RECEIVED 02 February 2024
ACCEPTED 05 February 2024
PUBLISHED 13 March 2024

CITATION
Qin Z, Peng K, Feng Y, Wang Y, Huang B, Tian Z, Ouyang P, Huang X, Chen D, Lai W and Geng Y (2024) Corrigendum: Transcriptome reveals the role of the *htpG* gene in mediating antibiotic resistance through cell envelope modulation in *Vibrio mimicus* SCCF01. *Front. Microbiol.* 15:1381070. doi: 10.3389/fmicb.2024.1381070

Corrigendum: Transcriptome reveals the role of the *htpG* gene in mediating antibiotic resistance through cell envelope modulation in *Vibrio mimicus* SCCF01

Zhenyang Qin[1†], Kun Peng[1†], Yang Feng[1], Yilin Wang[1], Bowen Huang[1], Ziqi Tian[1], Ping Ouyang[1], Xiaoli Huang[2], Defang Chen[2], Weimin Lai[1] and Yi Geng[1*]

[1]College of Veterinary Medicine, Sichuan Agricultural University, Chengdu, Sichuan, China, [2]Department of Aquaculture, Sichuan Agricultural University, Chengdu, Sichuan, China

KEYWORDS

HtpG, *Vibrio mimicus*, transcriptome, drug resistance, cell wall, cell membrane

A corrigendum on

Transcriptome reveals the role of the *htpG* gene in mediating antibiotic resistance through cell envelope modulation in *Vibrio mimicus* SCCF01

by Qin, Z., Peng, K., Feng, Y., Wang, Y., Huang, B., Tian, Z., Ouyang, P., Huang, X., Chen, D., Lai, W., and Geng, Y. (2024). *Front. Microbiol.* 14:1295065. doi: 10.3389/fmicb.2023.1295065

In the published article, there was an error in the **Funding** statement, page 13.

The previous Funding statement:

"The author(s) declare financial support was received for the research, authorship, and/or publication of this article. This research was supported by National Natural Science Foundation of China (32373174), Sichuan Natural Science Foundation (2024YJ2011), and Sichuan Innovation Team Project of Agricultural Industry Technology System (SCCXTD-15).

The correct Funding statement appears below:

The author(s) declare financial support was received for the research, authorship, and/or publication of this article. This research was supported by National Natural Science Foundation of China (32373174), Sichuan Natural Science Foundation (24NSFSC0858), and Sichuan Innovation Team Project of Agricultural Industry Technology System (SCCXTD-15).

The authors apologize for this error and state that this does not change the scientific conclusions of the article in any way. The original article has been updated.

Publisher's note

frontiers | Frontiers in Microbiology

TYPE Review
PUBLISHED 22 January 2024
DOI 10.3389/fmicb.2024.1332108

OPEN ACCESS

EDITED BY
Vijay Soni,
Weill Cornell Medical Center, United States

REVIEWED BY
Bhagyaraj Ella,
University of Florida, United States
Tushar Dhanani,
Florida Agricultural and Mechanical University, United States

*CORRESPONDENCE
Mingli Zhu
✉ mlzhhz@163.com

RECEIVED 02 November 2023
ACCEPTED 08 January 2024
PUBLISHED 22 January 2024

CITATION
Shi J, Cheng J, Liu S, Zhu Y and Zhu M (2024) *Acinetobacter baumannii*: an evolving and cunning opponent.
Front. Microbiol. 15:1332108.
doi: 10.3389/fmicb.2024.1332108

Acinetobacter baumannii: an evolving and cunning opponent

Jingchao Shi[1,2,3], Jianghao Cheng[1], Shourong Liu[4], Yufeng Zhu[1] and Mingli Zhu[1]*

[1]Open Laboratory Medicine, Hangzhou Xixi Hospital Affiliated to Zhejiang Chinese Medical University, Hangzhou, China, [2]Department of Clinical Laboratory, Affiliated Jinhua Hospital, Zhejiang University School of Medicine, Jinhua, China, [3]Graduate School, Zhejiang Chinese Medical University, Hangzhou, China, [4]Department of Infectious Disease, Hangzhou Xixi Hospital Affiliated to Zhejiang Chinese Medical University, Hangzhou, China

Acinetobacter baumannii is one of the most common multidrug-resistant pathogens causing nosocomial infections. The prevalence of multidrug-resistant *A. baumannii* infections is increasing because of several factors, including unregulated antibiotic use. *A. baumannii* drug resistance rate is high; in particular, its resistance rates for tigecycline and polymyxin—the drugs of last resort for extensively drug-resistant *A. baumannii*—has been increasing annually. Patients with a severe infection of extensively antibiotic-resistant *A. baumannii* demonstrate a high mortality rate along with a poor prognosis, which makes treating them challenging. Through carbapenem enzyme production and other relevant mechanisms, *A. baumannii* has rapidly acquired a strong resistance to carbapenem antibiotics—once considered a class of strong antibacterials for *A. baumannii* infection treatment. Therefore, understanding the resistance mechanism of *A. baumannii* is particularly crucial. This review summarizes mechanisms underlying common antimicrobial resistance in *A. baumannii*, particularly those underlying tigecycline and polymyxin resistance. This review will serve as a reference for reasonable antibiotic use at clinics, as well as new antibiotic development.

KEYWORDS

***Acinetobacter baumannii*, resistance mechanisms, tigecycline, polymyxin, antimicrobial resistance**

1 Introduction

Acinetobacter baumannii, an aerobic, nonfermenting, gram-negative, rod-shaped bacterium, is commonly found in water, soil, air, and other natural environments; it can also colonize the skin, conjunctiva, oral cavity, respiratory tract, gastrointestinal tract, and genitourinary tract of healthy individuals (Dexter et al., 2015; Carvalheira et al., 2021). *A. baumannii* demonstrates strong adhesion and ability to colonize various surfaces; moreover, it is resistant to not only dry and moist conditions but also general disinfectants and ultraviolet radiation. These characteristics render *A. baumannii* a major pathogen, frequently causing opportunistic nosocomial infections, including wound infections, central nervous system infections, abdomen infections, urinary tract infections, and bacteremia, in immunocompromised patients (Munoz-Price and Weinstein, 2008). According to the CHINET's bacterial drug resistance surveillance data, *A. baumannii* was one of the top five predominantly distributed surveilled strains, as well as the second leading nonfermenting, gram-negative bacterium in China. Moreover, 71.5 and 72.3% of the *A. baumannii* strains were resistant to imipenem and meropenem, respectively, and ≥50% of the *A. baumannii* strains

were resistant to other antimicrobials. In other words, *A. baumannii* has strong drug resistance and the ability to transmit clonally (Hu et al., 2022). Uncontrolled antibiotic use has led to global epidemics caused by multidrug-resistant, extensively drug-resistant, and pandrug-resistant *A. baumannii* (Bassetti et al., 2018; Assimakopoulos et al., 2023). Because it can elude the effects of antimicrobials, the World Health Organization has designated *A. baumannii* as one of the most dangerous ESKAPE pathogens; other ESKAPE pathogens include *Enterococcus faecalis*, *Staphylococcus aureus*, *Klebsiella pneumoniae*, *Pseudomonas aeruginosa*, and *Enterobacter* spp. (Denissen et al., 2022). Plasmid splicing, integrons, transposons, and other mechanisms are involved in the clonal transfer of drug resistance genes between different strains (Chen et al., 2017; Ambrose et al., 2023). The increase in antimicrobial resistance has resulted in a global public health emergency (Amann et al., 2019). In particular, the increase in *A. baumannii* antibiotic resistance has led to major obstacles in clinical treatment. Moreover, bacterial drug resistance has become a focus of clinical medicine and public health security. *A. baumannii* demonstrates considerable resistance to many antibiotics, which makes combination therapy the mainstay of current clinical treatment. However, no combination therapy has been noted to significantly lower mortality or enhance clinical response in patients with *A. baumannii* infections. To develop novel antibiotics and manage the spread of illness effectively, thoroughly comprehending the mechanisms underlying *A. baumannii* antibiotic resistance is crucial.

2 *Acinetobacter baumannii* drug resistance mechanisms

Compared with other bacteria, *A. baumannii* has a highly sophisticated resistance mechanism. For instance, it includes various antimicrobial-inactivating enzymes (particularly β-lactamases) and efflux pump overexpression, as well as alterations in antibiotic target location and outer membrane protein permeability (Table 1, Figure 1).

2.1 Mechanisms underlying β-lactamase production

β-Lactamases destroy the β-lactam rings of penicillins, cephalosporins, monocyclics, and carbapenems, rendering them inactive and without their antibacterial properties. Most *A. baumannii* strains produce β-lactamases as their primary method of defense against β-lactam antibiotics. β-Lactamases can be divided into classes A, B, C, and D according to Ambler's molecular structure categorization (i.e., sequence characterization of β-lactamase's amino-terminal end) (Lee et al., 2017).

Serine proteases such as penicillinase, cephalosporinase, carbenicillin hydrolase, and extended-spectrum β-lactamases (ESBLs) are class A β-lactamases. Most ESBLs are class A enzymes, whereas a few of them are class D enzymes. The several types of class A ESBLs include TEM, SHV, CTX-M, and others (e.g., PER, KPC, VEB, GES, BES, and SFO). Černiauskienė et al. (2023) detected TEM, SHV, PER, VEB, KPC, and other ESBLs in *A. baumannii*. TEM-type ESBLs, detected most frequently in *A. baumannii*, are the main mechanisms underlying β-lactam antibiotic resistance in *A. baumannii*. *A. baumannii* may hydrolyze carbapenems, first discovered in the United States and now found in many other countries (Robledo et al., 2010). Furthermore, GES-22 ESBL-producing *A. baumannii* has developed resistance to even typical ESBL inhibitors, such as sulbactam, clavulanate, and tazobactam; in particular, it exhibits high potassium clavulanate and sulbactam hydrolysis efficiency (Saral et al., 2016). Chromosomes and plasmids are the primary carriers of class A β-lactamase genes; moreover, these genes may be acquired through conjugation, transformation, or transduction.

Class B β-lactamases are also called metallo-β-lactamases (MBLs) because they have catalytically active centers that require the involvement of metal ions such as Zn^{2+}. MBLs extensively hydrolyze most anti-β-lactamase medications, which also decreases their bactericidal activity. Imipenem has a particularly large hydrolysis capacity. Monocyclic antibiotics, including aztreonam (ATM), are an exception to this. MBLs are also resistant to conventional enzyme inhibitors such as sulbactam, tazobactam, and clavulanate; they can be inhibited by metal chelating compounds, which bind to metal ions and ethylene diamine tetraacetic acid (López et al., 2019). *A. baumannii* MBLs can be mainly divided into IMP, VIM, SIM, and NDM types. New Delhi MBL (NDM-1) is a highly effective enzyme, recently discovered to have a large capacity to hydrolyze carbapenem medicines, and bacteria bearing the NDM-1 gene exhibit pandrug resistance. Therefore, NDM-1-carrying bacteria are also called superbugs. The NDM-1 gene is mainly located on the bacterial plasmid, with a small portion located on their chromosome (Ayibieke et al., 2018). Chen et al. (2017) demonstrated that the NDM-1 gene can be transmitted from one strain to another through plasmids and that plasmids play a key role in the outbreak of pandrug-resistant *A. baumannii*. Therefore, particular attention must be toward the spread of NDM-1-carrying *A. baumannii*.

The occurrence of newer MBLs has been reported in recent years. Currently, cefiderocol or the combination of CZA and ATM (CZA/ATM) is the preferred first-line treatment for infections of bacteria with MBL-mediated resistance. However, bacteria have developed resistance to cefiderocol, CZA/ATM, or both; the currently available data indicate that the effectiveness of cefiderocol and CZA/ATM against MBL-producing bacteria is inadequate, and treatment is linked to a high (albeit decreasing) mortality rate. Consequently, the therapeutic requirement for MBL inhibitors, particularly related to primary clinically significant MBLs, remains unfulfilled. Nevertheless, researchers are currently focused on creating clinically effective MBL inhibitors, such as those with metal-binding pharmacophores, which serve as coordination or a bridge between Zn_1 and Zn_2 (Yang W. et al., 2023; Yang Y. et al., 2023).

Class C β-lactamases, also known as AmpC enzymes or cephalosporinases, target cephalosporins and are not inhibited by clavulanate. AmpC enzymes are the primary reason that *A. baumannii* develop resistance to third-generation cephalosporins; they are encoded by the *A. baumannii* chromosome at a high carrier rate. AmpC enzymes are expressed more abundantly when the insertion sequence ISAba1 is present upstream of their genes. AmpC enzymes are divided into chromotype (ADC) and plasmid-type (DHA). *Acinetobacter*'s chromosomal *ampC* may have descended from a common β-lactamase gene progenitor, and it shares a closer relationship with *Acinetobacter* than other bacteria (Liu and Liu, 2015). Infections of *A. baumannii* that produces AmpC enzymes are currently treated using carbapenems and fourth-generation

TABLE 1 Mechanism of drug resistance in *Acinetobacter baumannii*.

Resistant mechanism	Class or subgroup	Gene	References
β-Lactamases	Ambler class A	TEM, SHV, PER, VEB, KPC	Černiauskienė et al. (2023)
	Ambler class B	IMP, VIM, SIM, NDM	Chen et al. (2017), López et al. (2019), Ayibieke et al. (2018)
	Ambler class C	AmpC	Liu and Liu (2015)
	Ambler class D	OXA23 family OXA24 family OXA51 family OXA58 family OXA143 family OXA235 family	Lin and Lan (2014), June et al. (2016), Huang et al. (2015), Donald et al. (2000), Avci et al. (2023), Zhao et al. (2019), Oliveira et al. (2019), Liao et al. (2015)
Aminoglycoside modifying enzymes	Aminoglycoside acetyltransferases (AACs)	AAC(3)-I AAC(3)-II AAC(6′)-I ANT(2″)-I ANT(2″)-II APH(3′)-I APH(3″)-II	Lin and Lan (2014), Lin et al. (2015), Sheikhalizadeh et al. (2017)
	Aminoglycoside nucleotidyltranferases (ANTs)		
	Aminoglycoside phosphotransferases (APHs)		
	16S rRNA methylase	armA	Gholami et al. (2017)
Changing the target locations	DNA gyrase and topoisomerase	gyrA, parC	Gu et al. (2015)
	Penicillin-binding protein (PBPs)	PBP2, PBP1	Cochrane and Lohans (2020), Toth et al. (2022)
Formation of biofilms	Biofilms	BfmRS, abaI, epsA, pglC, ompA	Geisinger et al. (2018), Yang et al. (2019), Romero et al. (2008)
Overexpression of the external discharge pumping system	RND superfamily	AdeABC AdeIJK AdeDE AdeFGH	Yoon et al. (2013), Modarresi et al. (2015), Chang et al. (2016), Lin et al. (2014), Meyer et al. (2022), Darby et al. (2023), AlQumaizi et al. (2022), Hou et al. (2012)
	MFS superfamily	TetA, TetB	Lomovskaya et al. (2018), Sumyk et al. (2021)
		CraA	Foong et al. (2019)
		AmvA	Rostami et al. (2021)
	MATE family	AbeM	Srinivasan et al. (2015)
	SMR family	AbeS	Lytvynenko et al. (2016)
	ABC superfamily	MsbA	Hammerstrom et al. (2015)
Changes in outer membrane pore proteins	Omp	CarO, HMP, OprD	Wu et al. (2016), Smani et al. (2014), Fonseca et al. (2013)
Mechanisms of resistance to tigecycline			
Efflux pump	RND superfamily	AdeABC AdeIJK AdeFGH	Jo and Ko (2021), Salehi et al. (2021), Hornsey et al. (2010), Lin et al. (2014), Gerson et al. (2018), Deng et al. (2014), Li et al. (2017)
	ABC superfamily	MsbA	Chen et al. (2014)
		MacAB-TolC	Lin et al. (2017b)
	MFS superfamily	tetA, tet(Y)	Wang et al. (2021) Liu et al. (2023)
	AcrAB-TolC	hns	
Modified enzyme mediated	Tet(X)	Tet(X), Tet(X3), Tet(X5), Tet (X6)	Cui et al. (2021), He et al. (2019), Chen et al. (2021)

(Continued)

TABLE 1 (Continued)

Resistant mechanism	Class or subgroup	Gene	References
Change in outer membrane permeability		plsC abrP gnaA	Li et al. (2015), Li et al. (2016), Xu et al. (2019)
Changes in drug targets		rpsJ trm rrf	Hammerstrom et al. (2015), Beabout et al. (2015), Chen et al. (2014), Ghalavand et al. (2022), Zheng et al. (2023), Hua et al. (2021)
DNA damage-induced reactions		recA, recBCD	Ajiboye et al. (2018)
Mechanisms of resistance to colistin			
Modification of LPS structures	PEtN	PmrA, PmeB, PmrC EptA	Olaitan et al. (2014), Potron et al. (2019), Sun et al. (2020), Kabic et al. (2023), Nurtop et al. (2019), Gerson et al. (2020) Trebosc et al. (2019), Ye et al. (2023)
		mcr-4.3, mcr-1, mcr-2, mcr-3	Martins-Sorenson et al. (2020), Snyman et al. (2021), Ma et al. (2019), Al-Kadmy et al. (2020)
	Galactosamine	NaxD	Chin et al. (2015)
Loss of LPS		lpxA, lpxC, lpxD	Moffatt et al. (2011), Nurtop et al. (2019), Jovcic et al. (2021), Thi Khanh Nhu et al. (2016), Carretero-Ledesma et al. (2018), Wand et al. (2015)
Overexpression of efflux pumps	EmrAB effector pump system	emrB	Lin et al. (2017a), Ni et al. (2016)
Mutations in outer membrane constituent proteins	Non-LPX proteins lipoprotein	lpsB LptD VacJ, PldA	Hood et al. (2013), Dafopoulou et al. (2015), Lean et al. (2014), Yang W. et al. (2023); Yang Y. et al. (2023) Bojkovic et al. (2015) Thi Khanh Nhu et al. (2016)

cephalosporins; nevertheless, attention should be made to the prevalence of AmpC enzyme–producing *A. baumannii*.

Class D β-lactamases are also called oxacillin (OXA) enzymes because of their ability to hydrolyze semisynthetic penicillins, such as oxacillin. They also have hydrolytic activity against cephalosporins and carbapenems. These β-lactamases feature has carboxylated lysine at its center, which leads to its distinct catalytic mechanism. The presence of MBLs and OXA enzymes is a main mechanism underlying carbapenem resistance in *A. baumannii* (Lin and Lan, 2014).

OXA enzymes prevalent in *A. baumannii* mainly include OXA23 and OXA24 family enzymes, as well as OXA51, OXA58, OXA143, and OXA235. Of them, OXA51 occurs naturally in *A. baumannii* but with weak carbapenem-hydrolyzing ability (June et al., 2016). In a UK study, the OXA51 gene was found in all *A. baumannii* isolates, and the presence of an ISAba1 insertion sequence in the OXA51 gene enhanced carbapenem hydrolysis (Huang et al., 2015). OXA23, the first class D β-lactamase that can hydrolyze carbapenems through plasmid delivery, was originally known as *Acinetobacter* resistant to imipenem (ARI) 1 (Paton et al., 1993; Scaife et al., 1995; Donald et al., 2000). In reality, OXA23 can be put into chromosomes or plasmids by using various genetic elements as vectors, including transposons and insertion sequences (Avci et al., 2023). The rate of drug-resistant organisms increases with the number of mobile elements found simultaneously in OXA23-positive *A. baumannii*, which is enhanced by the presence of ISAba1 (Oliveira et al., 2019; Zhao et al., 2019). The presence of OXA23 is the main reason that *A. baumannii* develops carbapenem resistance. *A. baumannii* may transfer the OXA24 gene to other strains by secreting vesicles from its outer membrane (Rumbo et al., 2011). In addition, *A. baumannii* outer membrane vesicles facilitate OXA58 gene transfer and OXA58 release. The presence of carbapenems enhances OXA58 vesicle release, and the vesicles can protect carbapenem-sensitive *A. baumannii* (Liao et al., 2014, 2015).

2.2 Aminoglycoside-modifying enzymes and 16S rRNA methylase

The major mechanism underlying *A. baumannii*'s resistance to aminoglycosides is aminoglycoside-modifying enzyme (AME) and 16s rRNA methylase production. AMEs can be divided into three categories: aminoglycoside acetyltransferases (AACs), aminoglycoside nucleotidyltranferases (ANTs), and aminoglycoside phosphotransferases (APHs), encoded by *aac*, *ant*, and *aph*, respectively. These enzymes are typically found in transposons, integrons, and plasmids and are responsible for the spread of drug-resistant genes (Lin and Lan, 2014). APHs phosphorylate the free hydroxyl groups, whereas both AACs and ANTs acetylate them. AMEs detected in *A. baumannii* include AAC(3)-I, AAC(3)-II,

AAC(6′)-I, ANT(2″)-I, ANT(2″)-II, APH(3′)-I, and APH(3″)-II. Drug resistance results from AMEs' ability to modify particular aminoglycoside groups, change covalent bonding, block medications from attaching to the target ribosome, and prevent bacterial protein production.

Many multidrug-resistant *A. baumannii* isolates have demonstrated various combinations of AMEs. Lin et al. (2015) reported that five aminoglycoside resistance genes coexisted in 37.5% of aminoglycoside-resistant *A. baumannii*. Drugs and resistance genes are correlated in varied ways: AAC(3′)-Ia is associated with tobramycin and amikacin resistance; AAC(3′)-IIa is associated with kanamycin resistance; ANT(2′)-Ia is associated with tobramycin, gentamicin, kanamycin, and amikacin resistance; and APH(3′)-Via is associated with amikacin and kanamycin resistance (Sheikhalizadeh et al., 2017).

Another major aminoglycoside resistance mechanism in *A. baumannii* is 16S rRNA methylation; it reduces the affinity of medications for aminoglycosides (Gholami et al., 2017). Examples of common 16S rRNA methylase genes include *armA*, *rmtA*, *rmtB*, *rmC*, *rmtD*, *rmtE*, *rmtF*, *rmtG*, *rmtH*, and *npmA*. *A. baumannii* possesses many armA genes, possibly contributing to the organism's resistance to aminoglycosides.

2.3 DNA gyrase and topoisomerase gene mutations and plasmid quinolone resistance genes

Quinolones are synthetic antimicrobial drugs with the basic structure of 4-quinolones. They demonstrate antimicrobial effects by inhibiting bacterial DNA replication, specifically targeting topoisomerase IV and DNA gyrase. The tetramer DNA gyrase is composed of two A subunits (GraA) and two B subunits (GraB), encoded by *gyrA* and *gyrB*, respectively. DNA breaks and rejoins when a DNA gyrase subunit is present; in particular, ATP hydrolysis is catalyzed by a B subunit. Topoisomerase IV has two C subunits, encoded by *parC*, and two E subunits, encoded by *parE*. In *A. baumannii*, quinolone resistance is primarily caused by mutations in *gyrA* and *parC*. Quinolones cannot bind to DNA gyrase and topoisomerase IV with structural changes in complexes, preventing DNA replication and leading to drug resistance (Gu et al., 2015). Mutations in *gyrA* single genes lead to moderate resistance, whereas those in *gyrA* and *parC* result in high resistance.

A novel mechanism underlying drug resistance, revealed in recent years, includes the presence of plasmid quinolone resistance (PMQR) genes. The PMQR genes can be divided into three classes: the quinolone-specific effectors (QepA and OqxAB), the aminoglycoside acetyltransferase [AAC(6′)-Ib-cr], and the Pnr family. In *A. baumannii*, DNA gyrase and topoisomerase IV are shielded from ciprofloxacin inhibition by Qnr, which is encoded by *qnr*. Point mutations in the target location render bacteria with *qnr* prone to drug resistance (Higuchi et al., 2014). AAC(6′)-Ib-cr is a mutant of AAC(6′)-Ib, which acetylates free amino-containing quinolones.

2.4 Changes in outer membrane pore proteins

When their envelope's permeability is altered, bacteria can become resistant to antibiotics, hampering their effectiveness frequently. Outer membrane protein (Omp) is a specialized channel protein located in the lipid bilayer structure either embedded in the cell membrane or on the cell membrane surface of gram-negative bacteria. Cell membrane permeability becomes altered when Omp is damaged,

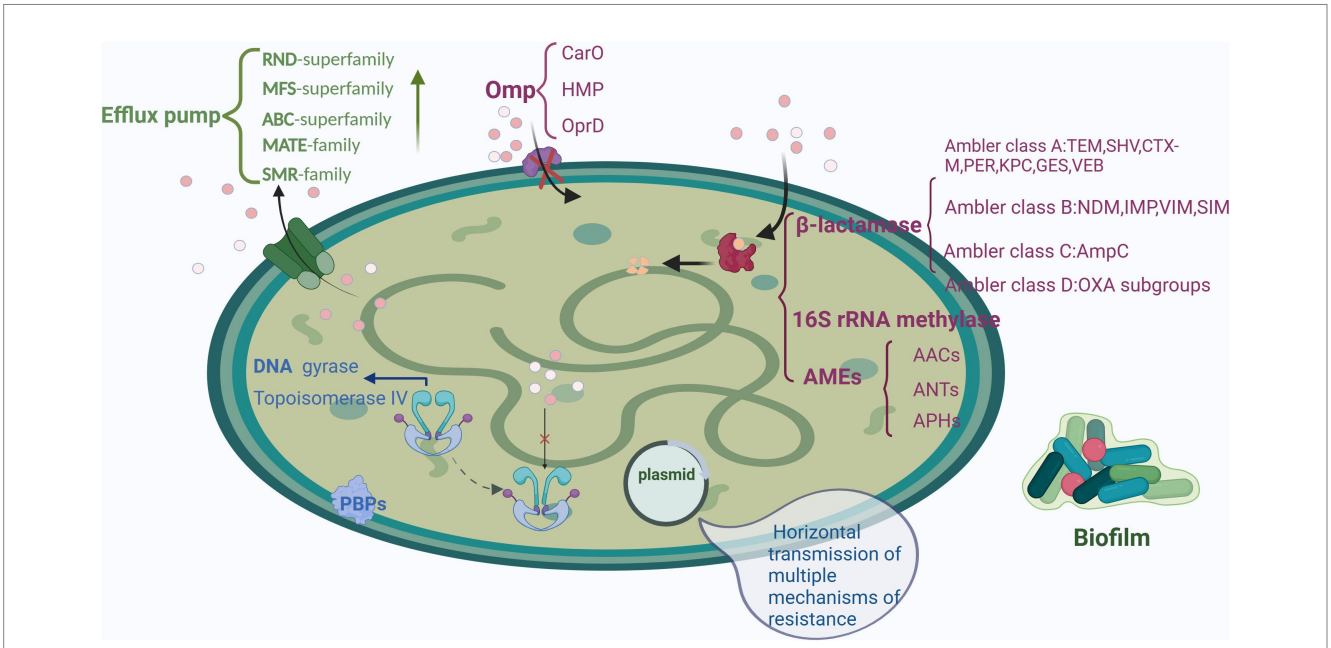

FIGURE 1
Mechanisms underlying drug resistance in *A. baumannii*: β-lactamase production, AMEs, and 16S rRNA methylase, efflux pump overexpression, antibiotic target location alterations, Omp permeability alterations, and biofilm formation. Created with BioRender.com.

absent, or expressed at low levels. Consequently, drugs cannot bind to PBPs on the bacterial membrane, preventing them from inhibiting bacterial cell wall synthesis; this ultimately leads to drug resistance development.

Membrane pore proteins associated with *A. baumannii* drug resistance mainly include carbapenem-resistant associated out membrane protein (CarO), heat-modifiable protein (HMP), and OprD. In *A. baumannii*, resistance to β-lactamases is caused by high similarity among *A. baumannii* HMP, *P. aeruginosa* OmpF, and *Escherichia coli* OmpA. OXA23 carbapenemase interacts with OmpA and CarO, and this interaction may contribute to drug resistance (Wu et al., 2016). Resistance to amtronam, chloramphenicol, and nalidixic acid is also associated with OmpA (Smani et al., 2014). When *A. baumannii* generating OXA23 or OXA51 carbapenenase loses Omp29, its resistance to imipenem increases (Fonseca et al., 2013).

2.5 Alterations in PBPs

Bacterial cell walls are composed of PBPs. Carbapenems and other β-lactamases target D,D-transpeptidase (TP) in PBPs; this leads to the prevention of bacterial cell wall formation, followed by bacterial death (Cochrane and Lohans, 2020). In target bacteria, alterations in PBP structure or expression can lead to the loss of or reduction in β-lactam antibiotics' binding affinity to PBPs; this makes the target bacteria resistant to β-lactam antibiotics. A decline in PBP2 expression is associated with bacterial carbapenem resistance. Toth et al. (2022) reported that PBP3 is necessary for *A. baumannii* survival, PBP1a inactivation results in partial cell lysis and bacterial growth retardation, and PBP2 inactivation amplifies these effects. The authors noted that the triple PBP1a/PBP1b/PBP2 mutant *A. baumannii* displayed a fourfold to eightfold increase in sensitivity to β-lactam antibiotics, whereas all other mutants demonstrated an increase in twofold to fourfold increase in sensitivity to β-lactam antibiotics. The simultaneous inhibition of PBP1a and PBP2 or the use of PBPs in combination with LdtJ, in addition to the critical PBP3, may be possible approaches for the development of novel therapeutics against *A. baumannii*.

2.6 Biofilm formation

A biofilm is a collection of bacteria and extracellular matrix, which adheres to the surfaces of biological tissues or nonbiological objects. It is a type of bacterial growth, similar to planktonic bacteria; it forms when bacteria secrete extracellular lipoproteins, polysaccharide matrix, fibrous proteins, and other substances wrapped around the bacteria themselves to create a microcolony structure. *A. baumannii* is a bacterium that often forms biofilms. The biofilm formation process is rapid, requiring approximately 24 h of cultivation *in vitro*, and involves five stages: reversible adhesion, irreversible attachment, microcolony formation, colonization or maturation, and dispersal (Pakharukova et al., 2018; Biswas and Mettlach, 2019). Biofilm resistance mechanisms include changes in permeability, inactivation of drugs via antimicrobial-inactivating enzymes immobilized on biofilm surface, nutrient and oxygen limitations, biofilm phenotype uniqueness, and immune evasion. The biofilm gene *bfmRS* has a hyperactive allele, which promotes resistance to serum complement killing, as well as tolerance to various antimicrobial medications via mechanisms including defense against attack by anti-β-amidase medicines (Geisinger et al., 2018). In extensively drug-resistant *A. baumannii*, drug resistance is strongly associated with its biofilm-associated genes *abaI*, *epsA*, *pglC*, *ompA*, and the class I integron gene. Moreover, biofilms may have the capacity to horizontally transfer genes, facilitating quick expression and migration of drug-resistant genes (Romero et al., 2008; Yang et al., 2019).

2.7 External discharge pump system overexpression

Efflux pumps constitute a unique efflux system found on bacterial outer membranes. The development of multidrug and extensive drug resistance development is facilitated by the presence of efflux pumps, which can remove pharmaceuticals from bacterial cells, lower antibiotic concentrations in bacterial cells, and diminish the medications' bactericidal effects (Pagdepanichkit et al., 2016). Currently, five main types of efflux pump families are known to be associated with bacterial resistance: the ATP-binding cassette (ABC) superfamily, the small multidrug-resistant protein (SMR) family, the resistance nodulation division (RND) superfamily, the multidrug and toxic compound extrusion (MATE) superfamily, and the major facilitator (MFS) superfamily (Opazo et al., 2009; Coyne et al., 2011). Of these, the RND superfamily is the earliest discovered and most well-studied efflux pump family in *A. baumannii*. The RND superfamily, primarily consisting of AdeABC, AdeIJK, AdeDE, AdeXYZ, and AdeFGH efferent pump systems, can supply energy via the proton transmembrane concentration gradient (Nowak et al., 2015).

The AdeABC efflux pump system is the most crucial efflux system in *A. baumannii*. Some researchers have also suggested that *adeABC* is a marker for *A. baumannii* resistance. *adeABC*, encoding AdeA (membrane fusion protein), AdeB (intima efflux protein), and AdeC (outer membrane channel protein), is found in the chromosomal genome of *A. baumannii*. The AdeRS two-component regulatory system controls the AdeABC efflux pump system (Yoon et al., 2013). The upstream region of *adeABC* comprises *adeRS*, encoding the response regulator protein (AdeR) and the receptor protein (AdeS). AdeA, AdeB, and AdeC all demonstrate different expression levels. Although some studies have reported that AdeA has the highest detection rate among clinical isolates, PCR amplification data have revealed that AdeB has the highest detection rate (Modarresi et al., 2015). In general, AdeB is considered the most significant component of the AdeABC effusion pump system. Compared with *adeA*, *adeB* has a larger impact on carbapenem antibiotic resistance (Lee et al., 2010). The expression of the efflux pump gene *adeABC* is significantly higher in multidrug-resistant strains of *A. baumannii* than in drug-sensitive strains; moreover, *adeR* mutation alters the corresponding amino acids, indicating that the importance of *adeR* in multidrug resistance development (Chang et al., 2016). Lin et al. (2014) reported that *adeS* is the primary gene controlling the AdeABC system and that some point mutations in *adeS* can result in increased efflux pump production. In Germany, Meyer et al. (2022) reported that *A. baumannii* can resist the effects of disinfectants such as benzalkonium chloride, ethanol, and chlorhexidine *in vivo* by overexpressing the AdeABC efflux pump system.

Baumann–Acinetobacter RND superfamily proteins have been identified in two efflux pump systems, one of which is AdeIJK. The AdeIJK efflux pump system, a key mechanism underlying RND action in *Acinetobacter*, exhibits traits unique to each species. The AdeIJK efflux pump system can pump numerous antibiotics, including carbapenems, fluoroquinolones, tetracycline, lincomycin, neomycin, and tigecycline. All *Acinetobacter* spp. depend on AdeIJK to survive and maintain homeostasis; this is because AdeIJK plays essential roles in cells, such as regulating the lipid composition of cell membranes. AdeABC and AdeFGH have only been discovered in the Acinetobacter subgroup linked to infection (Darby et al., 2023). AdeJ becomes strongly expressed when *adeN*, the regulator gene upstream of *adeIJK*, becomes inactivated; this prevents antibacterials from entering bacteria.

AdeFGH, which can mediate the efflux of quinolones, macrolides, and tetracycline medicines but not aminoglycosides and β-lactamases, was initially described by French researchers in 2010. AlQumaizi et al. (2022) reported that AdeG may influence the sensitivity of *A. baumannii* to carbapenem. AdeFGH shares only 40% homology with AdeABC and AdeIJK. The 337 amino-acid–long region upstream of *adeFGH* is transcribed in a direction opposite to the direction in which AdeL, the transcription regulator of AdeFGH, is transcribed. Overexpression of the efflux pump gene *adeFGH* may be a result of changes in the *adeL* mutation locus (Coyne et al., 2010).

When AdeDE is overexpressed, the AdeDE efflux pump system—including the membrane fusion protein AdeD and the inner membrane efflux protein AdeE—can reduce the concentration of medications such as ceftazidime and rifampicin and thus increase drug resistance. Hou et al. (2012) reported the coexistence of AdeE and AdeB in a few *A. baumannii* isolates.

The MFS superfamily includes AmvA, CraA, TetA, and TetB. In *A. baumannii*, TetA mediates tetracycline resistance, whereas TetB mediates resistance to both tetracyclines and minocyclines (Lomovskaya et al., 2018). However, whether TetA and TetB induce drug resistance to tigecycline remains unknown. However, TetA and TetB do not cooccur in the same strain of *A. baumannii*. The TetA regulatory gene *tetR* encodes TetA repressor (Sumyk et al., 2021). In *A. baumannii*, a homolog of *E. coli* effector MdfA is linked to chloramphenicol resistance development in relation to CraA (Foong et al., 2019). Finally, in *A. baumannii*, disinfectant efflux is associated with the AmvA efflux pump (Rostami et al., 2021).

AbeM, a MATE family member, is an H^+-linked multidrug efflux pump present in *A. baumannii*. The minimum inhibitory concentration (MIC) of drugs such as aminoglycosides, fluoroquinolones, sulfonamides, and chloramphenicol can be increased through the overexpression of the efflux pump gene *abeD* (Srinivasan et al., 2015). The SMR family member AbeS is clonally highly expressed in *E. coli*, and it is identical to EmrE in *E. coli*. AbeS can reduce cellular concentrations of neomycin, macrolides, mycotoxins, and fluoroquinolones in *E. coli* (Lytvynenko et al., 2016).

3 Mechanisms underlying tigecycline resistance

Tigecycline, a third-generation tetracycline derivative, was the first glycylcycline antibiotic authorized for clinical use. Tigecycline—by attaching to the A position of 16S rRNA of the 30S subunit of the bacterial ribosome—mainly inhibits aminoacyl tRNA entry, peptide chain extension, bacterial protein synthesis, and bacterial growth. Tigecycline's affinity for bacterial ribosomes is four times that of minocycline and more than 100 times that of tetracyclines. Therefore, tigecycline demonstrated a greater antibacterial activity and a wider antibacterial range—aiding it in overcoming TetM-mediated tetracycline resistance (Jenner et al., 2013). Although tigecycline demonstrates considerable antibacterial effects against *A. baumannii* despite the bacterium's strong resistance potential and high viability, cases of tigecycline-resistant *A. baumannii* infections have been reported as early as 2007 (Peleg et al., 2007). Furthermore, the prevalence of *A. baumannii* resistance to tigecycline is increasing clinically. The emergence of the strains with direct or indirect resistance to tigecycline may have been due to the long-term selection pressure of various antibacterial drugs. The main mechanisms underlying tigecycline resistance in *A. baumannii* are classified into five categories: efflux pump overexpression, outer membrane permeability alterations, drug target alterations, modified enzyme–mediated resistance, and DNA damage induction (Table 1, Figure 2).

3.1 Influence of efflux pumps

The AdeABC efflux pump system was the first reported tigecycline resistance mechanism in *A. baumannii*. AdeABC overexpression results in reduced tigecycline susceptibility in *A. baumannii*. Currently, most studies agree that in *A. baumannii*, AdeB is crucial for the efflux of tigecycline via the AdeABC efflux pump. AdeB expression and the lowest inhibitory concentration of tigecycline are linearly associated in *A. baumannii* (Yuhan et al., 2016). Efflux pump inhibitors such as reserpine, PH-arg-β-naphthylamide dihydrochloride, and carbonyl cyanide 3-chlorophenylhydrazone (CCCP) have inhibitory effects and a tendency to increase tigecycline sensitivity by two to eight times in *A. baumannii* (Coyne et al., 2011).

During AdeABC exocycling, the two-component regulatory system AdeRS upstream of AdeABC plays a major role. In a South Korean study, the overexpression of AdeABC efflux pumps due to the ISAba1 insertion in *adeS* may have caused tigecycline resistance. However, the tigecycline-resistant subpopulation was unstable with continuous passage in antibiotic-free conditions. The addition of ISAba10 to AdeR and nucleotide modification of AdeS in some mutants may be responsible for the reversal of tigecycline sensitivity via an antibiotic-free passage (Jo and Ko, 2021). Some AdeS mutations, such as G186V and A1a94val, are associated with AdeABC overexpression (Hornsey et al., 2010; Salehi et al., 2021). The strong expression of AdeABC is regulated by another two-component regulatory system called BaeSR (Lin et al., 2014). However, additional relevant research determining the relationship between BaeSR and AdeRS is needed.

All strains of *A. baumannii* possess the AdeIJK efflux pump system, which may be involved in the bacterium's endogenous resistance process. In *A. baumannii*, when AdeIJK is inhibited, the MIC of tigecycline decreases by three to eight times. Similarly, when AdeABC is inhibited, tigecycline's MIC decreases by 85 times. These observations indicate that AdeABC and AdeIJK function concurrently to reduce tigecycline resistance. Notably, growth inhibition increases with an increase in the amount of inducer in *A. baumannii* when the *adeIJK* operon is cloned and overexpressed.

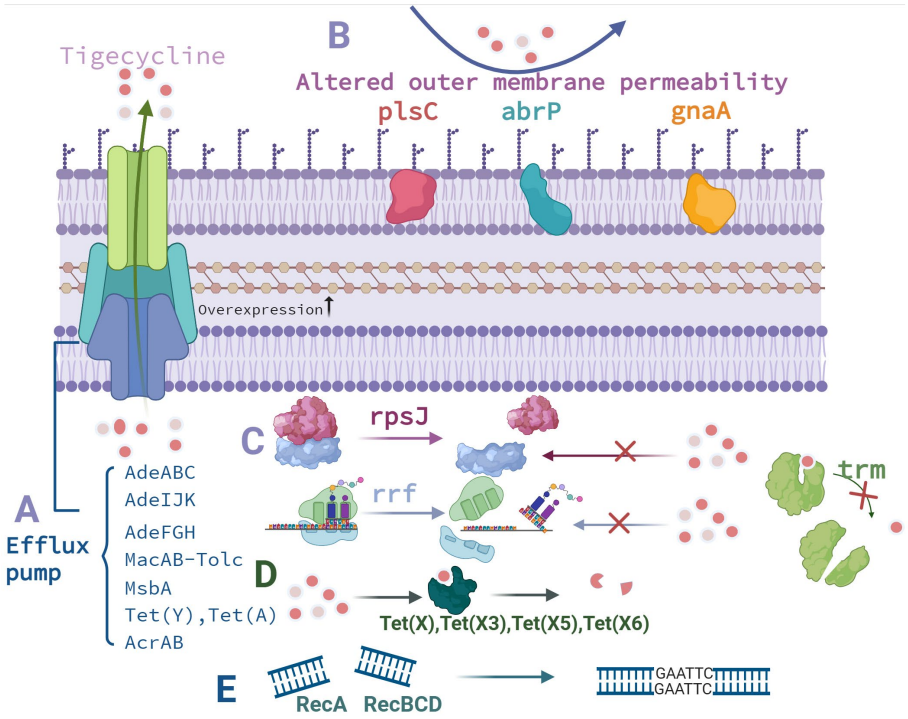

FIGURE 2
Mechanisms underlying tigecycline resistance in *A. baumannii*. **(A)** Influence of efflux pumps. **(B)** Outer membrane permeability alterations. **(C)** Drug target alterations. **(D)** Enzyme-mediated drug resistance modifications. **(E)** DNA damage–induced reactions. Created with BioRender.com.

In particular, *adeIJK* overexpression leads to growth suppression and deleterious reactions in *A. baumannii* (Damier-Piolle et al., 2008). The AdeIJK regulator gene, *adeN*, has been noted to have three amino acid mutations in a whole genome sequence of tigecycline-resistant *A. baumannii*; moreover, one-third of *A. baumannii* isolates have been noted to demonstrate an ISAba1 insertion, resulting in the aforementioned *adeN* mutations. Furthermore, *adeJ* expression is upregulated by two to six times (Gerson et al., 2018). In general, AdeN may inhibit the *adeIJK* operon in tigecycline-sensitive *A. baumannii*.

AdeL is the transcription factor regulating the AdeFGH efflux pump upstream, and point mutations in *adeL* can increase *adeG* expression up to 100-fold (Coyne et al., 2010). However, Deng et al. (2014) noted that drug-resistant and -sensitive *A. baumannii* demonstrate similar levels of *adeG* expression. Certain strains exhibiting elevated *adeFGH* expression do not exhibit an *adeL* mutation. Therefore, transcription factors other than AdeL may regulate *adeFGH* expression in *A. baumannii*. Moreover, *adeFGH* expression is negatively regulated by SoxR in *A. baumannii*; therefore, *soxR* overexpression may lead to increased tigecycline sensitivity in the bacterium (Li et al., 2017).

In contrast to other efflux pump systems, ABC uses energy through ATP-bound hydrolysis to perform pumping tasks. Hammerstrom et al. (2015) noted that MsbA in a tigecycline-resistant *A. baumannii* group was substantially different from that in other groups; the authors concluded that the differences were due to functional changes that facilitated tigecycline efflux. However, Chen et al. (2014) did not observe any discernible variations in the effects of MsbA on tigecycline resistance. Studies confirming MsbA's effects on tigecycline are therefore required. Tigecycline-resistant *A. baumannii* has been noted to have considerably elevated expression of MacB, which is part of the MacAB-TolC efflux pump system (Lin et al., 2017a). Further research determining the effects of the MacAB-TolC efflux pump system on tigecycline resistance, as well as the underlying mechanisms, in *A. baumannii* is warranted. Wang et al. (2021) discovered *tet(Y)*, the first tigecycline resistance-related gene associated with plasmids, in China. The introduction of plasmid p2016GDAB1 containing *tet(Y)* through electroporation resulted in a 16-fold increase in the MIC of tigecycline, whereas *tet(Y)* overexpression on a 72,156-base pair (bp) plasmid increased it by twofold to fourfold. Furthermore, the authors noted that p2016GDAB1 contained the regulatory gene *tetR*, which increased the MIC of tigecycline by 128 times after regulating *tet(Y)* and *tetA(39)* transcription. Strong tigecycline resistance may be a result of combined mediation by Tet(Y) and TetA(39). Liu et al. (2023) indicated that their screened tigecycline-resistant *A. baumannii* 17978R became resistant to tigecycline, possibly after the loss of plasmids containing *hns* or after the insertion of *hns* through an insertion sequence. This possibly increased TonB expression, which then increased the efflux pump expression. Furthermore, insertion sequence insertion may have resulted in the deletion of *acrR*, encoding AcrR, which inhibits the efflux pump AcrAB and thus increases efflux pump expression.

3.2 Modification of enzyme-mediated drug resistance

Tet(X) is a riboflavin-dependent monooxygenase, initially identified in *Bacteroides tenuis* transposons Tn4351 and Tn4400. NADPH and Mg^{2+} cause tigecycline hydroxylation and inactivation. The Tet(X) family, encoded by eight genes, is associated with considerable levels of tigecycline resistance. Tet(X), Tet(X3), Tet (X5), and Tet(X6) can increase tigecycline resistance in *A. baumannii* (Cui et al., 2021). Tet(X3) renders all tetracyclines—including tigecycline, as well as the recently FDA-approved elacycline and omacycline—are inactive; this increases the MIC of tigecycline by 64–128 times. Through hydroxylation of Tet(X5) and Tet(X6), resistance to many antimicrobials, including tigecycline, can be induced in *A. baumannii*. Finally, translocation and recombination mediated by IScr2, a recently discovered insertion sequence, IScr2, accelerate the spread of Tet(X5) (He et al., 2019; Chen et al., 2021).

3.3 Outer membrane permeability alterations

1-Acyl3-glycerol phosphate acyltransferase, encoded by *plsC*, is involved in bacterial outer membrane formation. Li et al. (2015) induced drug resistance in clinical isolates of tigecycline-sensitive *A. baumannii*, yielding a drug-resistant strain called 19,606-M24, and noted that *omp38*, *hp*, and *plsC* are the possible resistance genes based on their whole genome sequencing results. In their follow-up studies, the authors concluded that only frameshift mutation in *plsC* is linked to tigecycline resistance and, through flow cytometry, that the *plsC* mutation leads to changes in the strain's cell membrane. Li et al. (2016) also discovered *abrP*, a gene linked to resistance to drug, including tigecycline. The mutant's phenotype could be recovered by introducing wildtype *abrP*. The authors also discovered that the *abrP*-deficient mutant had enhanced cell membrane permeability, which reduced its cell growth rate. Taken together, these results confirmed that *abrP* is crucial for *A. baumannii* resistance and adaptation.

Tigecycline resistance is also associated with *gnaA*. In particular, Xu et al. (2019) discovered *gnaA* inserted by ISAba16 transposons in MDR-ZJ06M, a multidrug-resistant and virulent *A. baumannii* strain. The isolates had significantly increased tigecycline resistance. However, the supplementary experiment revealed no change in MICs of tigecycline. Therefore, further experimental evidence demonstrating the role of *gnaA* in tigecycline resistance development is required.

3.4 Drug target alterations

rpsJ encodes the ribosome S10 protein. Mutation in *rpsJ* causes the S10 protein ring to shift structurally, in turn altering the shape of 16S rRNA and reducing the affinity between tigecycline and ribosome (Beabout et al., 2015). *trm* encodes S-adenosyl-L-methionine-dependent methyltransferase (AdoMet). Through whole genome sequencing, Chen et al. (2014) identified mutant *trm* in the *A. baumannii* strain 19606-T8 (MIC = 8 mg/L), experimentally engineered to develop tigecycline resistance. Although AdoMet has been hypothesized to be crucial for moderate tigecycline resistance induction, how it mediates the loss of sensitivity to tigecycline remains unknown. In *A. baumannii*, tigecycline resistance is strongly influenced by mutations in *trm*, and tigecycline-resistant strains with *trm* mutations exhibit various amino acid alterations, including M378K, K291R, H312P, and S94A (Ghalavand et al., 2022). However, in both tigecycline-resistant and -sensitive *A. baumannii*, Zheng et al. (2023) noted mutations in *trm* and *plsC* but not in *rpsJ*. As such, additional studies confirming the influence of mutations in *trm*, *plsC*, and *rpsJ* on the emergence of tigecycline resistance in *A. baumannii* are warranted.

rrf encodes ribosome recycling factor (RRF). Hammerstrom et al. (2015) discovered a mutation in *rrf* in tigecycline-resistant *A. baumannii*; the authors hypothesized that this mutation reduces mRNA translation, affects tigecycline and ribosome binding, and eventually, results in tigecycline resistance. Hua et al. (2021) confirmed this hypothesis through Western blotting and multiribosome spectrum analysis: mutations in *rrf* reduced RRF expression, affecting the ribosome cycle process. Through an *in situ* complementarity experiment, the authors also demonstrated that mutations in *rrf* were associated with tigecycline resistance in *A. baumannii*.

3.5 DNA damage–induced reactions

Antimicrobials can cause bacterial death via DNA damage. However, RecA and RecBCD together can repair this damage. RecBCD is crucial for DNA double-stranded break repair, whereas RecA is the primary enzyme involved in homologous recombination and recombination repair. RecA also contributes to stress and virulence responses in *A. baumannii*. Ajiboye et al. (2018) performed deletion experiments with recA and recBCD in *A. baumannii* and noted considerable reductions in the bacterium's tigecycline, gentamicin, and polymyxin MICs. These results indicated that the recA- and recBCD-mediated repair pathways may protect *A. baumannii* from the effects of antimicrobials, eventually resulting in the development of drug resistance.

4 Mechanisms underlying polymyxin resistance

Bacillus polymyxa produces polymyxins, which are polypeptides with antibacterial properties and can be divided into classes A, B, C, D, and E. Polymyxin B and colistin are the most frequently prescribed medications in clinical practice (Cassir et al., 2014). In the 1950s, polymyxins were used for the first time in clinical settings. Because their low toxicity and comparable bactericidal and antibacterial spectra, polymyxins B and E are frequently used. Some multidrug-resistant gram-negative organisms, such as *K. pneumoniae* and *P. aeruginosa*, can cause pulmonary infections (Lenhard et al., 2019). However, the use of polymyxins has been since restricted because they may cause neurotoxicity and nephrotoxicity.

The recent rise of multidrug-resistant, extensively drug-resistant, and pandrug-resistant bacteria has led to a renaissance of antimicrobials for the discovery of drugs of last resort. Moreover, additional clinical studies have focused their attention on polymyxin use (Carrasco et al., 2021). Polymyxins primarily function as a

bactericide by disrupting the lipopolysaccharide (LPS) structure in the outer membranes of gram-negative bacteria. Negatively charged lipid A in LPS interacts with positively charged polymyxin residues such as 4-amino-L-arabinose (l-Ara4N) and phosphoethanolamine (PEtN). Colistin can bind with these negatively charged phosphate groups in place of Ca^{2+} and Mg^{2+}. Because LPS has a higher affinity than bivalent cations, its stability is compromised. This leads to the destruction of the bacterial outer membrane, a decrease in the serous membrane's surface tension, an increase in its permeability, the loss of the serous membrane's barrier function, and the leakage of bacterial contents, eventually resulting in bacterial death (Jeannot et al., 2017).

For multidrug-resistant *A. baumannii*, polymyxin use is one of the few remaining treatments; in particular, it is used as a drug of last resort for life-threatening infections. Polymyxin-resistant *A. baumannii* has emerged with the increase in the clinical use of polymyxins. A recent meta-analysis revealed that the polymyxin resistance rate of *A. baumannii* was higher in Southeast Asian and eastern Mediterranean countries than in other countries (totaling 11.2%); it was the highest in Lebanon (17.5%) and China (11.8%) but the lowest in Germany (0.2%) (Pormohammad et al., 2020). The prevalence of polymyxin-resistant strains has increased due to increased polymyxin use as a rescue treatment for multidrug-resistant *A. baumannii* infections. However, a comprehensive set of standardized practices or conventional treatment recommendations for polymyxin use is unavailable in different countries or regions. In an epidemiological investigation of polymyxin-resistant *A. baumannii*, the multilocus sequence typing subtypes ST92 and ST208 were noted to be identical. Therefore, polymyxin-resistant *A. baumannii* strains may have spread significantly throughout Europe, Asia, and North America (Novović and Jovčić, 2023).

The mechanisms underlying polymyxin resistance in *A. baumannii* are categorized as follows: LPS and lipid A loss, LPS structure modification, plasmid-mediated polymyxin resistance, efflux pump resistance mechanism, and outer membrane component protein mutations (Table 1, Figure 3).

4.1 LPS loss

Gram-negative bacteria have long been thought to require LPS production to survive (Zhang et al., 2013). Only a few bacteria, including *A. baumannii*, *Moraxella kataxa*, and *Neisseria meningitida* (Steeghs et al., 1998; Peng et al., 2005; Moffatt et al., 2010), have been found to thrive without LPS thus far. Mutation in *lpxA*, *lpxC*, or *lpxD*—involved in lipid A production—leads to the complete disappearance of LPS in *A. baumannii*. Through the addition of an insertion sequence element from the IS4 family (which is comparable to the ISX03 element), Moffatt et al. (2011) discovered that *lpxD* is deleted in resistant strains of *A. baumannii*, which resulted in LPS loss and resistance development. Moreover, the authors discovered that ISAba11 inactivated *lpxA* and *lpxC* of *in vitro* polymyxin resistance variants in *A. baumannii* ATCC19606. Lipid A biosynthesis is caused by the deletion, substitution, and insertion of different *lpxA*, *lpxC*, and *lpxD* nucleotides, and the combination of mutations in *lpxC*, *lpxD*, and the *pmrAB* operon may result in a synergistic effect of polymyxin resistance. However, some drug-resistant bacteria demonstrated *lpxA*, *lpxC*, and *lpxD* downregulation, reducing LPS production (Thi Khanh Nhu et al., 2016; Nurtop et al., 2019; Jovcic et al., 2021). *In vitro*, the LPS-deficient mutant strain developed slower and was less pathogenic than the wildtype strain (Wand et al., 2015; Carretero-Ledesma et al., 2018).

lpx mutant strains are more vulnerable to lysozyme released by neutrophils and are more susceptible to neutrophil cell-mediated killing. LPS loss may expand the pathways through which lysozyme can enter periplasmic peptidoglycans, facilitating lysozyme targeting and increasing antimicrobial activity against LPS-deficient collisin-resistant bacterial strains (Kamoshida et al., 2020). LPS-deficient *A. baumannii* demonstrates greater vulnerability to other antimicrobials such as carbapenems, quinolones, tigecycline, and rifampicin despite appearing to have strong polymyxin resistance. It also demonstrated greater susceptibility to certain disinfectants, including ethanol, chlorhexidine, and phenol-based cleaners.

Moderate fitness loss is linked to the absence of LPS. LPS loss reduces *A. baumannii*'s pathogenicity and fitness and leads to variations in biofilm development and viability under iron restriction. LPS-deficient *A. baumannii* demonstrates alterations in signaling through toll-like receptors and enhances susceptibility to host antimicrobial peptides, suggesting that host factors contribute to decreased fitness (Moffatt et al., 2013). Reduced biofilm development after LPS deletion increases the possibility of the affected strains lacking the necessary biofilm-forming mechanism component. The biochemical mechanism underlying the considerable abnormalities resulting from LPS deficiency under iron restriction. A mechanism underlying this outcome may involve LPS deficiency leading to changes in the membrane composition of *A. baumannii*, limiting its ability to import extracellular iron (Carretero-Ledesma et al., 2018; Kamoshida et al., 2020, 2022).

4.2 LPS structure modifications

The addition of PEtN to lipid A in *A. baumannii* is crucial for polymyxin resistance development. Phosphate groups added to PEtN at both the 4′ and 1′ locations cause the LPS component to have a negative charge and reduce PEtN's propensity for binding polymyxin (Olaitan et al., 2014). Alterations in the two-component regulatory system PmrAB causes overexpression of the PEtN transferase PmrC, resulting in polymyxin resistance (Potron et al., 2019). Polymyxin-sensitive strains can alter into polymyxin-resistant phenotypes as a result of partial deletion mutations in PmrB. PmrCAB expression may be increased as a result of a mutation in PmrB through PmrA activation (Adams et al., 2009). Mutations in PmrA alone also increase *A. baumannii*'s resistance to polymyxin (Sun et al., 2020). However, in some instances, little to no link has been noted between PmrAB and high PmrC expression (Kabic et al., 2023). Therefore, PmrC may be regulated by regulatory mechanisms other than those of PmrAB. Few studies have examined the connection between mutations in PmrC and polymyxin resistance thus far. I42V and L150F, two prevalent *pmrC* variants, may be linked to polymyxin resistance (Nurtop et al., 2019). *A. baumannii* is more resistant to polymyxin when PmrC R125P mutations and PmrB alterations are combined (Gerson et al., 2020). Gerson et al. (2019) revealed that three polymyxin resistance-related mutations in PmrB cause PmrC expression to increase or decrease, demonstrating that PmrB is not the only protein regulating *pmrC* expression in *A. baumannii*.

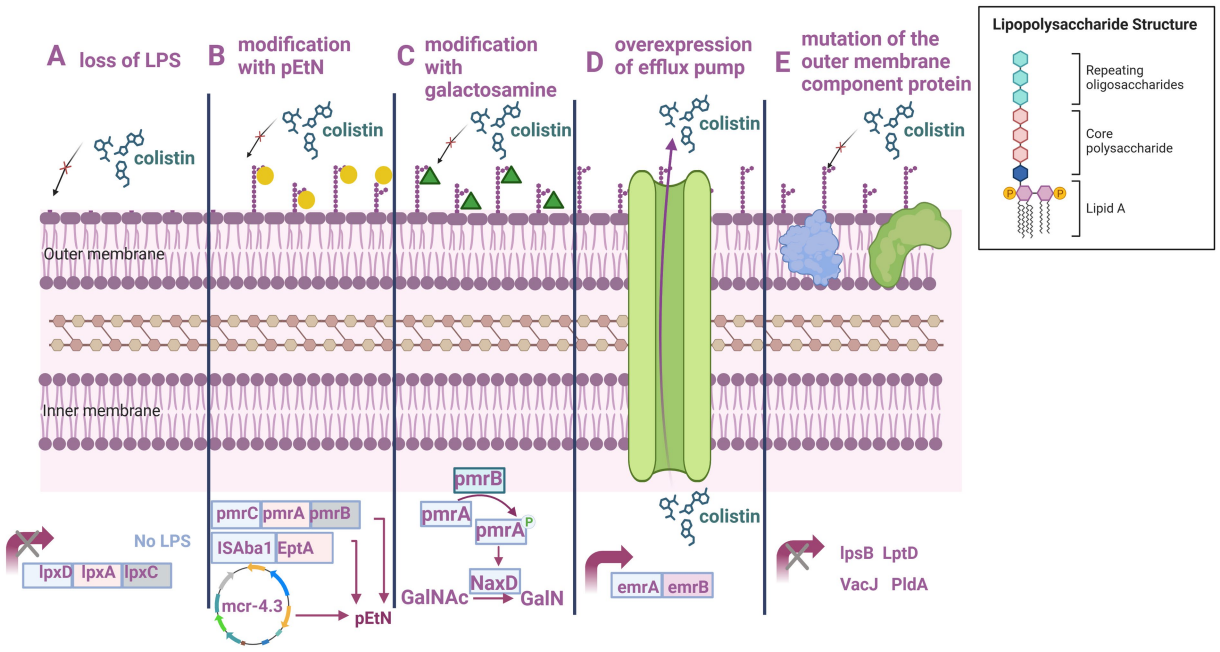

FIGURE 3
Mechanism underlying polymyxin resistance in *A. baumannii*. **(A)** LPS loss. **(B)** PEtN modification. **(C)** Galactosamine modification. **(D)** Efflux pump overexpression. **(E)** Outer membrane component protein mutations. Created with BioRender.com.

Clinical *A. baumannii* strains exhibit significant levels of polymyxin resistance as a result of ISAba125 insertion into the gene encoding the global regulator H-NS. The expression of the distal gene is triggered by the insertion of the insertion sequence element in this gene, which is another PmrC homolog called phosphoethanolamine transferase (EptA), the product of which shares 93% homology with PmrC. Although *eptA* alone in the bacterial genome cannot impart resistance to polymyxin, the integration of ISAba1 upstream of *eptA* might result in an increase in the enzyme's production (Trebosc et al., 2019).

In a Chinese study, ISAba1 insertion was noted to occur between 13 and 18 bp upstream of *eptA*. The authors hypothesized that *eptA* expression is not dependent on the distance between ISAba1 and *eptA* transcription initiation. In *A. baumannii*, EptA is activated more directly when ISAba1 is inserted upstream of *eptA*, leading to polymyxin resistance. Moreover, under the strain of continuous polymyxin therapy, random insertion events may lead to an increase in the frequency of polymyxin resistance in the future (Ye et al., 2023). Despite the absence of L-Ara4N, the sensor kinase PmrB regulates NaxD deacetylase, a major mediator of lipid A alteration resulting in polymyxin resistance, in *A. baumannii* (Chin et al., 2015).

4.3 Plasmid-mediated polymyxin resistance

The plasmid-mediated gene *mcr*, encoding a PEtN transferase, was first discovered in a Chinese strain of polymyxin-resistant *E. coli* SHP45, isolated from a pig with *Mcr1*. In *E. coli*, Mcr added phosphoethanolamine to lipid A, producing mutagenic polymyxin resistance (Liu et al., 2016). Thus far, 10 *mcr* genes, ranging from *mcr-1* to *mcr-10*, have been reported in the environment, animals, food, and humans (Hussein et al., 2021). In Brazil, a meningitis patient's cerebrospinal fluid was noted to include *A. baumannii* contained with *mcr-4.3* in 2008. This gene can maintain polymyxin-resistant resistance through LPS modification. The pET-26b-*mcr-4.3*-transformed *E. coli* was noted to develop polymyxin resistance (Martins-Sorenson et al., 2020). However, in South Africa, recombinant expression of *mcr-4.3* in *A. baumannii* did not confer polymyxin resistance in *E. coli* (Snyman et al., 2021). pAB18PR065, harboring *mcr-4.3*, could not be transferred in the splicing, transformation, and electroporation assays (Ma et al., 2019). An *mcr-4.3*-carrying *A. baumannii* strain has also been isolated from pig feces; however, further related research is required. *A. baumannii* harboring *mcr-1*, *mcr-2*, and *mcr-3* was also discovered in Iraq (Al-Kadmy et al., 2020).

4.4 Drug resistance due to efflux pumps

Laboratory-induced polymyxin-resistant *A. baumannii* demonstrated a 1.6 times increase in expression of EmrB from the EmrAB efflux pump system. *A. baumannii* becomes more sensitive to polymyxin after *emrB* deletion. These results indicate that the EmrAB efflux pump system reduces *A. baumannii*'s susceptibility to polymyxin. EmrAB efflux pump system has been postulated to be a crucial mechanism underlying polymyxin resistance through pumping and cytoplasmic acidification; this result requires further confirmation. The aforementioned mechanisms are similar to those of the efflux pump/potassium antiporter system, which mediates polymyxin resistance in *Yersinia* when induced at higher temperatures (≥37°C) (Lin et al., 2017a). Wiradiputra et al. (2023) reported that *A. baumannii* with low polymyxin resistance demonstrates at least two

times increase in *emrB* and *ompW* expression. Ni et al. (2016) noted that using the efflux pump inhibitor CCCP considerably reduces the MIC of polymyxin in *A. baumannii*. These results further confirm that efflux pump systems contribute to polymyxin resistance.

4.5 Outer membrane component protein mutations

Mutations in some non-LPX proteins that make up the outer membrane of *A. baumannii* also contribute to increased polymyxin resistance. *lpsB* encodes a glycosyltransferase, involved in LPS synthesis. Mutations in *lpsB* lead to a reduction in polymyxin permeability (Hood et al., 2013). Mutations in *lpsB* identified thus far include H181Y, 241 K, D146G, G218H, E219S, and T331I (Lean et al., 2014; Dafopoulou et al., 2015; Yang W. et al., 2023; Yang Y. et al., 2023). Mutations in *lptD* also interfere with LPS translocation to the outer membrane, resulting in moderate polymyxin resistance in *A. baumannii* (Bojkovic et al., 2015). A Vietnamese study concluded that mutations in the lipoprotein VacJ and the phospholipase PldA—believed to maintain the lipid asymmetry of the outer membrane—lead to polymyxin resistance in *A. baumannii* (Thi Khanh Nhu et al., 2016). Lipid metabolism is a major pathway. Polymyxin acts by disrupting the membrane, and *lpsB* mutant strains are defective in the production of main outer membrane components; therefore, the effects of polymyxin and *lpsB* mutation on lipid metabolism overlap significantly (Hood et al., 2013).

5 Conclusions and future prospects

Nonstandardized use of antibiotics has led to the development of antibiotic resistance among pathogenic microorganisms. By 2050, diseases due to antibiotic-resistant bacteria may lead to 10 million deaths annually (Carr et al., 2019). In most hospitals worldwide, *A. baumannii* causes nosocomial infections, including bloodstream infections, wound infections, urinary tract infections, meningitis, and pneumonia associated with ventilator use. *A. baumannii* bloodstream infections are associated with a high mortality rate. Drug-resistant *A. baumannii* can possess nearly all bacterial resistance pathways along with a considerably unlimited capacity for antibiotic resistance development. *A. baumannii* can produce all forms of β-lactamases. Moreover, carbapenem-resistant *A. baumannii* (CRAB) detection rate remains high. Almost all *A. baumannii* strains discovered thus far express aminoglycoside-altering enzymes. Numerous clinical isolates have exhibited a high level of different efflux pumps. The related resistance genes have been noted to inhibit the bactericidal activity of aminoglycosides, carbapenems, quinolones, and broad-spectrum cephalosporins. Because of their comparatively low rates of resistance, tigecycline and polymyxin are considered drugs of last resort for *A. baumannii* infection treatment. However, with the annual increase in tigecycline and polymyxin use, the number of cases of infection due to *A. baumannii* resistant to these antibiotics is increasing globally. Furthermore, polymyxins have some nephrotoxicity and neurotoxicity, and tigecycline can result in notably low plasma concentrations when following the tigecycline instructions recommended dosing regimen. In general, given the availability of additional efficient treatment options, tigecycline and polymyxin should not be administered alone.

Because of the dearth of solid clinical evidence justifying the use of any one medication therapy, antibiotics are frequently used in combination for the treatment of illnesses with high mortality rates. Medicines with antibacterial activity at first may cause resistance, and patients with a CRAB infection are typically extremely sick with more consequences. Therefore, two or more active medications should be used in all applicable situations (Tamma et al., 2022). Combination regimens based on polymyxin, tigecycline, and sulbactam have often been reported. For instance, sulbactam-based combinations (polymyxin + sulbactam or tigecycline + sulbactam) had better synergistic effects than polymyxin + tigecycline (Qu et al., 2020). However, no combination regimen can reduce mortality significantly or improve clinical response considerably. Therefore, more clinical and *in vivo* study data are needed to explore effective combination regimens.

Few novel medications specifically targeting CRAB are currently available. For instance, cefiderocol, a novel ferriferous cephalosporin that penetrates the cell membrane of gram-negative bacteria via a unique route, is highly effective at eliminating all gram-negative bacteria. To reach the cytoplasm at a large concentration, cefiderocol forms complexes with trivalent iron ions and, via the bacterial ferritransporter, becomes transported through the outer cell membrane into the inner wall of the cell. There, by binding to the receptor, cefiderocol prevents cell wall synthesis (Domingues et al., 2023). Eravacycline, a synthetic tetracycline that, similar to other tetracyclines, binds to the 30S ribosome subunit of bacteria and suppresses protein synthesis. Similar to that of tigecycline, eravacycline's activity is not influenced by ribosome-protective proteins (Hetzler et al., 2022). Durlobactam, a novel diazadicycloctanone β-lactamase inhibitor, effectively inhibits class A, C, and D β-lactamases (Papp-Wallace et al., 2023). Dulobactam + sulbactam have been noted to effectively restore the sulbactam sensitivity of CRAB clinical isolates (August et al., 2023). New-generation polymyxin-type antibacterial adjuvants, including SPR206, MRX-8, and QPX9003, are also being assessed in the clinical trial stage (Aslan et al., 2022). However, certain drug-resistant *A. baumannii* have been discovered during the development of new drugs, including cefiderocol. In other words, cautious prescription and consistently monitored use of these novel antibiotics, along with regular assessment of bacterial drug resistance, are highly warranted.

Since the beginning of the postantibiotic era, the focus of contemporary research on novel therapeutics for *A. baumannii* infections has moved from antibiotic production to that of nonantibiotic compounds. Medications targeting virulence factors can reduce pathogenicity or improve sensitivity by inhibiting *A. baumannii* or its virulence factors. Medications that do not produce an excessive load on bacterial metabolism are less likely to induce resistance in the target bacteria (Saipriya et al., 2020). Therapies for *A. baumannii* infections currently under development include immunotherapeutics (Buchhorn de Freitas and Hartwig, 2022), photodynamic therapy (Bustamante and Palavecino, 2023), subunit vaccine therapy (Yang et al., 2022), phage therapy (Tan et al., 2022), and antimicrobial

peptide therapy (Rangel et al., 2023). Research in other fields may also indirectly influence future *A. baumannii* treatments.

Author contributions

JS: Visualization, Writing – original draft, Writing – review & editing. JC: Visualization, Writing – review & editing. SL: Writing – review & editing. YZ: Writing – review & editing. MZ: Writing – review & editing.

Funding

The author(s) declare financial support was received for the research, authorship, and/or publication of this article. This work was supported by the Science and Technology Project from Health Commission of Zhejiang Province of the People's Republic of China (grant number 2023KY974) and the Hangzhou Health Science and Technology Key project (grant number ZD20220040). The funders had no role in the study design, data collection and analysis, decision to publish, or preparation of the manuscript.

Conflict of interest

The authors declare that the research was conducted in the absence of any commercial or financial relationships that could be construed as a potential conflict of interest.

Publisher's note

References

Adams, M. D., Nickel, G. C., Bajaksouzian, S., Lavender, H., Murthy, A. R., Jacobs, M. R., et al. (2009). Resistance to colistin in *Acinetobacter baumannii* associated with mutations in the PmrAB two-component system. *Antimicrob. Agents Chemother.* 53, 3628–3634. doi: 10.1128/aac.00284-09

Ajiboye, T. O., Skiebe, E., and Wilharm, G. (2018). Contributions of RecA and RecBCD DNA repair pathways to the oxidative stress response and sensitivity of *Acinetobacter baumannii* to antibiotics. *Int. J. Antimicrob. Agents* 52, 629–636. doi: 10.1016/j.ijantimicag.2018.07.022

Al-Kadmy, I. M. S., Ibrahim, S. A., Al-Saryi, N., Aziz, S. N., Besinis, A., and Hetta, H. F. (2020). Prevalence of genes involved in Colistin resistance in *Acinetobacter baumannii*: first report from Iraq. *Microb. Drug Resist.* 26, 616–622. doi: 10.1089/mdr.2019.0243

AlQumaizi, K. I., Kumar, S., Anwer, R., and Mustafa, S. (2022). Differential gene expression of efflux pumps and Porins in clinical isolates of MDR *Acinetobacter baumannii*. *Life (Basel)* 12:419. doi: 10.3390/life12030419

Amann, S., Neef, K., and Kohl, S. (2019). Antimicrobial resistance (AMR). *Eur. J. Hosp. Pharm.* 26, 175–177. doi: 10.1136/ejhpharm-2018-001820

Ambrose, S. J., Hamidian, M., and Hall, R. M. (2023). The extensively antibiotic resistant ST111 *Acinetobacter baumannii* isolate RBH2 carries an extensive mobile element complement of plasmids, transposons and insertion sequences. *Plasmid* 128:102707. doi: 10.1016/j.plasmid.2023.102707

Aslan, A. T., Akova, M., and Paterson, D. L. (2022). Next-generation Polymyxin class of antibiotics: a ray of Hope illuminating a dark road. *Antibiotics (Basel)* 11:1711. doi: 10.3390/antibiotics11121711

Assimakopoulos, S. F., Karamouzos, V., Eleftheriotis, G., Lagadinou, M., Bartzavali, C., Kolonitsiou, F., et al. (2023). Efficacy of Fosfomycin-containing regimens for treatment of bacteremia due to Pan-drug resistant *Acinetobacter baumannii* in critically ill patients: a case series study. *Pathogens* 12:286. doi: 10.3390/pathogens12020286

August, B., Matlob, A., and Kale-Pradhan, P. B. (2023). Sulbactam-Durlobactam in the treatment of Carbapenem-resistant *Acinetobacter baumannii* infections. *Ann. Pharmacother.* doi: 10.1177/10600280231204566 [Epub ahead of print].

Avci, F. G., Tastekil, I., Jaisi, A., Ozbek Sarica, P., and Sariyar Akbulut, B. (2023). A review on the mechanistic details of OXA enzymes of ESKAPE pathogens. *Pathog. Glob. Health* 117, 219–234. doi: 10.1080/20477724.2022.2088496

Ayibieke, A., Sato, W., Mahazu, S., Prah, I., Addow-Thompson, J., Ohashi, M., et al. (2018). Molecular characterisation of the NDM-1-encoding plasmid p2189-NDM in an *Escherichia coli* ST410 clinical isolate from Ghana. *PLoS One* 13:e0209623. doi: 10.1371/journal.pone.0209623

Bassetti, M., Righi, E., Vena, A., Graziano, E., Russo, A., and Peghin, M. (2018). Risk stratification and treatment of ICU-acquired pneumonia caused by multidrug- resistant/extensively drug-resistant/pandrug-resistant bacteria. *Curr. Opin. Crit. Care* 24, 385–393. doi: 10.1097/mcc.0000000000000534

Beabout, K., Hammerstrom, T. G., Perez, A. M., Magalhães, B. F., Prater, A. G., Clements, T. P., et al. (2015). The ribosomal S10 protein is a general target for decreased tigecycline susceptibility. *Antimicrob. Agents Chemother.* 59, 5561–5566. doi: 10.1128/aac.00547-15

Biswas, I., and Mettlach, J. (2019). A simple static biofilm assay for *Acinetobacter baumannii*. *Methods Mol. Biol.* 1946, 159–165. doi: 10.1007/978-1-4939-9118-1_15

Bojkovic, J., Richie, D. L., Six, D. A., Rath, C. M., Sawyer, W. S., Hu, Q., et al. (2015). Characterization of an *Acinetobacter baumannii* lptD deletion strain: permeability defects and response to inhibition of lipopolysaccharide and fatty acid biosynthesis. *J. Bacteriol.* 198, 731–741. doi: 10.1128/jb.00639-15

Buchhorn de Freitas, S., and Hartwig, D. D. (2022). Promising targets for immunotherapeutic approaches against *Acinetobacter baumannii*. *Microb. Pathog.* 173:105855. doi: 10.1016/j.micpath.2022.105855

Bustamante, V., and Palavecino, C. E. (2023). Effect of photodynamic therapy on multidrug-resistant *Acinetobacter baumannii*: a scoping review. *Photodiagn. Photodyn. Ther.* 43:103709. doi: 10.1016/j.pdpdt.2023.103709

Carr, C., Smith, A., Marturano, M., Hakki, L., Friedman, J., Guidry, C., et al. (2019). Ventilator-associated pneumonia: how do the different criteria for diagnosis match up? *Am. Surg.* 85, 992–997. doi: 10.1177/000313481908500941

Carrasco, L. D. M., Dabul, A. N. G., Boralli, C. M., Righetto, G. M., Carvalho, I. S. E., Dornelas, J. V., et al. (2021). Polymyxin resistance among XDR ST1 Carbapenem-resistant *Acinetobacter baumannii* clone expanding in a teaching hospital. *Front. Microbiol.* 12:622704. doi: 10.3389/fmicb.2021.622704

Carretero-Ledesma, M., García-Quintanilla, M., Martín-Peña, R., Pulido, M. R., Pachón, J., and McConnell, M. J. (2018). Phenotypic changes associated with Colistin resistance due to lipopolysaccharide loss in *Acinetobacter baumannii*. *Virulence* 9, 930–942. doi: 10.1080/21505594.2018.1460187

Carvalheira, A., Silva, J., and Teixeira, P. (2021). Acinetobacter spp. in food and drinking water - a review. *Food Microbiol.* 95:103675. doi: 10.1016/j.fm.2020.103675

Cassir, N., Rolain, J. M., and Brouqui, P. (2014). A new strategy to fight antimicrobial resistance: the revival of old antibiotics. *Front. Microbiol.* 5:551. doi: 10.3389/fmicb.2014.00551

Černiauskienė, K., Dambrauskienė, A., and Vitkauskienė, A. (2023). Associations between β-lactamase types of Acinetobacter baumannii and antimicrobial resistance. *Medicina (Kaunas)* 59:1386. doi: 10.3390/medicina59081386

Chang, T. Y., Huang, B. J., Sun, J. R., Perng, C. L., Chan, M. C., Yu, C. P., et al. (2016). AdeR protein regulates adeABC expression by binding to a direct-repeat motif in the intercistronic spacer. *Microbiol. Res.* 183, 60–67. doi: 10.1016/j.micres.2015.11.010

Chen, C., Cui, C. Y., Wu, X. T., Fang, L. X., He, Q., He, B., et al. (2021). Spread of tet(X5) and tet(X6) genes in multidrug-resistant *Acinetobacter baumannii* strains of animal origin. *Vet. Microbiol.* 253:108954. doi: 10.1016/j.vetmic.2020.108954

Chen, Q., Li, X., Zhou, H., Jiang, Y., Chen, Y., Hua, X., et al. (2014). Decreased susceptibility to tigecycline in *Acinetobacter baumannii* mediated by a mutation in trm encoding SAM-dependent methyltransferase. *J. Antimicrob. Chemother.* 69, 72–76. doi: 10.1093/jac/dkt319

Chen, J., Xiuzhen, W. U., Liu, K., Xuefei, H. U., Chen, K., Zhang, L., et al. (2017). NDM-1 gene and other carbapenemase genes in *Acinetobacter baumannii* in Jiangxi area. *Chinese J. Infect. Control* 16, 109–114. doi: 10.3969/j.issn.1671-9638.2017.02.003

Chin, C. Y., Gregg, K. A., Napier, B. A., Ernst, R. K., and Weiss, D. S. (2015). A PmrB-regulated deacetylase required for lipid a modification and Polymyxin resistance in *Acinetobacter baumannii*. *Antimicrob. Agents Chemother.* 59, 7911–7914. doi: 10.1128/aac.00515-15

Cochrane, S. A., and Lohans, C. T. (2020). Breaking down the cell wall: strategies for antibiotic discovery targeting bacterial transpeptidases. *Eur. J. Med. Chem.* 194:112262. doi: 10.1016/j.ejmech.2020.112262

Coyne, S., Courvalin, P., and Périchon, B. (2011). Efflux-mediated antibiotic resistance in Acinetobacter spp. *Antimicrob. Agents Chemother.* 55, 947–953. doi: 10.1128/aac.01388-10

Coyne, S., Rosenfeld, N., Lambert, T., Courvalin, P., and Périchon, B. (2010). Overexpression of resistance-nodulation-cell division pump AdeFGH confers multidrug resistance in *Acinetobacter baumannii*. *Antimicrob. Agents Chemother.* 54, 4389–4393. doi: 10.1128/aac.00155-10

Cui, C. Y., He, Q., Jia, Q. L., Li, C., Chen, C., Wu, X. T., et al. (2021). Evolutionary trajectory of the Tet(X) family: critical residue changes towards high-level Tigecycline resistance. *mSystems* 6:e00050-21. doi: 10.1128/mSystems.00050-21

Dafopoulou, K., Xavier, B. B., Hotterbeekx, A., Janssens, L., Lammens, C., Dé, E., et al. (2015). Colistin-resistant *Acinetobacter baumannii* clinical strains with deficient biofilm formation. *Antimicrob. Agents Chemother.* 60, 1892–1895. doi: 10.1128/aac.02518-15

Damier-Piolle, L., Magnet, S., Brémont, S., Lambert, T., and Courvalin, P. (2008). AdeIJK, a resistance-nodulation-cell division pump effluxing multiple antibiotics in *Acinetobacter baumannii*. *Antimicrob. Agents Chemother.* 52, 557–562. doi: 10.1128/aac.00732-07

Darby, E. M., Bavro, V. N., Dunn, S., McNally, A., and Blair, J. M. A. (2023). RND pumps across the genus Acinetobacter: AdeIJK is the universal efflux pump. *Microb. Genom.* 9:mgen000964. doi: 10.1099/mgen.0.000964

Deng, M., Zhu, M. H., Li, J. J., Bi, S., Sheng, Z. K., Hu, F. S., et al. (2014). Molecular epidemiology and mechanisms of tigecycline resistance in clinical isolates of *Acinetobacter baumannii* from a Chinese university hospital. *Antimicrob. Agents Chemother.* 58, 297–303. doi: 10.1128/aac.01727-13

Denissen, J., Reyneke, B., Waso-Reyneke, M., Havenga, B., Barnard, T., Khan, S., et al. (2022). Prevalence of ESKAPE pathogens in the environment: antibiotic resistance status, community-acquired infection and risk to human health. *Int. J. Hyg. Environ. Health* 244:114006. doi: 10.1016/j.ijheh.2022.114006

Dexter, C., Murray, G. L., Paulsen, I. T., and Peleg, A. Y. (2015). Community-acquired *Acinetobacter baumannii*: clinical characteristics, epidemiology and pathogenesis. *Expert Rev. Anti-Infect. Ther.* 13, 567–573. doi: 10.1586/14787210.2015.1025055

Domingues, S., Lima, T., Saavedra, M. J., and Da Silva, G. J. (2023). An overview of Cefiderocol's therapeutic potential and underlying resistance mechanisms. *Life (Basel)* 13:1427. doi: 10.3390/life13071427

Donald, H. M., Scaife, W., Amyes, S. G., and Young, H. K. (2000). Sequence analysis of ARI-1, a novel OXA beta-lactamase, responsible for imipenem resistance in *Acinetobacter baumannii* 6B92. *Antimicrob. Agents Chemother.* 44, 196–199. doi: 10.1128/aac.44.1.196-199.2000

Fonseca, E. L., Scheidegger, E., Freitas, F. S., Cipriano, R., and Vicente, A. C. (2013). Carbapenem-resistant *Acinetobacter baumannii* from Brazil: role of carO alleles expression and blaOXA-23 gene. *BMC Microbiol.* 13:245. doi: 10.1186/1471-2180-13-245

Foong, W. E., Tam, H. K., Crames, J. J., Averhoff, B., and Pos, K. M. (2019). The chloramphenicol/H+ antiporter CraA of *Acinetobacter baumannii* AYE reveals a broad substrate specificity. *J. Antimicrob. Chemother.* 74, 1192–1201. doi: 10.1093/jac/dkz024

Geisinger, E., Mortman, N. J., Vargas-Cuebas, G., Tai, A. K., and Isberg, R. R. (2018). A global regulatory system links virulence and antibiotic resistance to envelope homeostasis in *Acinetobacter baumannii*. *PLoS Pathog.* 14:e1007030. doi: 10.1371/journal.ppat.1007030

Gerson, S., Betts, J. W., Lucaßen, K., Nodari, C. S., Wille, J., Josten, M., et al. (2019). Investigation of novel pmrB and eptA mutations in isogenic *Acinetobacter baumannii* isolates associated with Colistin resistance and increased virulence *in vivo*. *Antimicrob. Agents Chemother.* 63:e01586-18. doi: 10.1128/aac.01586-18

Gerson, S., Lucaßen, K., Wille, J., Nodari, C. S., Stefanik, D., Nowak, J., et al. (2020). Diversity of amino acid substitutions in PmrCAB associated with colistin resistance in clinical isolates of *Acinetobacter baumannii*. *Int. J. Antimicrob. Agents* 55:105862. doi: 10.1016/j.ijantimicag.2019.105862

Gerson, S., Nowak, J., Zander, E., Ertel, J., Wen, Y., Krut, O., et al. (2018). Diversity of mutations in regulatory genes of resistance-nodulation-cell division efflux pumps in association with tigecycline resistance in *Acinetobacter baumannii*. *J. Antimicrob. Chemother.* 73, 1501–1508. doi: 10.1093/jac/dky083

Ghalavand, Z., Eslami, G., Hashemi, A., Sadredinamin, M., Yousefi, N., and Dehbanipour, R. (2022). Characterization of sequence types and mechanisms of resistance to Tigecycline among *Acinetobacter baumannii* isolated from children. *Curr. Microbiol.* 79:285. doi: 10.1007/s00284-022-02976-5

Gholami, M., Haghshenas, M., Moshiri, M., Razavi, S., Pournajaf, A., Irajian, G., et al. (2017). Frequency of 16S rRNA Methylase and aminoglycoside-modifying enzyme genes among clinical isolates of *Acinetobacter baumannii* in Iran. *Iran. J. Pathol.* 12, 329–338. doi: 10.30699/ijp.2017.27989

Gu, D. X., Hu, Y. J., Zhou, H. W., Zhang, R., and Chen, G. X. (2015). Substitutions of Ser83Leu in GyrA and Ser80Leu in ParC associated with quinolone resistance in *Acinetobacter pittii*. *Microb. Drug Resist.* 21, 345–351. doi: 10.1089/mdr.2014.0057

Hammerstrom, T. G., Beabout, K., Clements, T. P., Saxer, G., and Shamoo, Y. (2015). *Acinetobacter baumannii* repeatedly evolves a Hypermutator phenotype in response to Tigecycline that effectively surveys evolutionary trajectories to resistance. *PLoS One* 10:e0140489. doi: 10.1371/journal.pone.0140489

He, T., Wang, R., Liu, D., Walsh, T. R., Zhang, R., Lv, Y., et al. (2019). Emergence of plasmid-mediated high-level tigecycline resistance genes in animals and humans. *Nat. Microbiol.* 4, 1450–1456. doi: 10.1038/s41564-019-0445-2

Hetzler, L., Kollef, M. H., Yuenger, V., Micek, S. T., and Betthauser, K. D. (2022). New antimicrobial treatment options for severe gram-negative infections. *Curr. Opin. Crit. Care* 28, 522–533. doi: 10.1097/mcc.0000000000000968

Higuchi, S., Shikata, M., Chiba, M., Hoshino, K., and Gotoh, N. (2014). Characteristics of antibiotic resistance and sequence type of *Acinetobacter baumannii* clinical isolates in Japan and the antibacterial activity of DS-8587. *J. Infect. Chemother.* 20, 256–261. doi: 10.1016/j.jiac.2013.12.001

Hood, M. I., Becker, K. W., Roux, C. M., Dunman, P. M., and Skaar, E. P. (2013). Genetic determinants of intrinsic colistin tolerance in *Acinetobacter baumannii*. *Infect. Immun.* 81, 542–551. doi: 10.1128/iai.00704-12

Hornsey, M., Ellington, M. J., Doumith, M., Thomas, C. P., Gordon, N. C., Wareham, D. W., et al. (2010). AdeABC-mediated efflux and tigecycline MICs for epidemic clones of *Acinetobacter baumannii*. *J. Antimicrob. Chemother.* 65, 1589–1593. doi: 10.1093/jac/dkq218

Hou, P. F., Chen, X. Y., Yan, G. F., Wang, Y. P., and Ying, C. M. (2012). Study of the correlation of imipenem resistance with efflux pumps AdeABC, AdeIJK, AdeDE and AbeM in clinical isolates of *Acinetobacter baumannii*. *Chemotherapy* 58, 152–158. doi: 10.1159/000335599

Hu, F., Guo, Y., Zhu, D., Wang, F., Jiang, X., and Xu, Y. (2022). CHINET surveillance of antimicrobial resistance among the bacterial isolates in 2021. *Chin. J. Infect. Chemother.* 22, 521–530. doi: 10.16718/j.1009-7708.2022.05.001

Hua, X., He, J., Wang, J., Zhang, L., Zhang, L., Xu, Q., et al. (2021). Novel tigecycline resistance mechanisms in *Acinetobacter baumannii* mediated by mutations in adeS, rpoB and rrf. *Emerg. Microbes Infect.* 10, 1404–1417. doi: 10.1080/22221751.2021.1948804

Huang, C., Long, Q., Qian, K., Fu, T., Zhang, Z., Liao, P., et al. (2015). Resistance and integron characterization of *Acinetobacter baumannii* in a teaching hospital in Chongqing, China. *New Microbes New Infect.* 8, 103–108. doi: 10.1016/j.nmni.2015.09.015

Hussein, N. H., Al-Kadmy, I. M. S., Taha, B. M., and Hussein, J. D. (2021). Mobilized colistin resistance (mcr) genes from 1 to 10: a comprehensive review. *Mol. Biol. Rep.* 48, 2897–2907. doi: 10.1007/s11033-021-06307-y

Jeannot, K., Bolard, A., and Plésiat, P. (2017). Resistance to polymyxins in gram-negative organisms. *Int. J. Antimicrob. Agents* 49, 526–535. doi: 10.1016/j.ijantimicag.2016.11.029

Jenner, L., Starosta, A. L., Terry, D. S., Mikolajka, A., Filonava, L., Yusupov, M., et al. (2013). Structural basis for potent inhibitory activity of the antibiotic tigecycline during protein synthesis. *Proc. Natl. Acad. Sci. U. S. A.* 110, 3812–3816. doi: 10.1073/pnas.1216691110

Jo, J., and Ko, K. S. (2021). Tigecycline Heteroresistance and resistance mechanism in clinical isolates of *Acinetobacter baumannii*. *Microbiol. Spectr.* 9:e0101021. doi: 10.1128/Spectrum.01010-21

Jovcic, B., Novovic, K., Dekic, S., and Hrenovic, J. (2021). Colistin resistance in environmental isolates of *Acinetobacter baumannii*. *Microb. Drug Resist.* 27, 328–336. doi: 10.1089/mdr.2020.0188

June, C. M., Muckenthaler, T. J., Schroder, E. C., Klamer, Z. L., Wawrzak, Z., Powers, R. A., et al. (2016). The structure of a doripenem-bound OXA-51 class D β-lactamase variant with enhanced carbapenemase activity. *Protein Sci.* 25, 2152–2163. doi: 10.1002/pro.3040

Kabic, J., Novovic, K., Kekic, D., Trudic, A., Opavski, N., Dimkic, I., et al. (2023). Comparative genomics and molecular epidemiology of colistin-resistant *Acinetobacter baumannii*. *Comput. Struct. Biotechnol. J.* 21, 574–585. doi: 10.1016/j.csbj.2022.12.045

Kamoshida, G., Akaji, T., Takemoto, N., Suzuki, Y., Sato, Y., Kai, D., et al. (2020). Lipopolysaccharide-deficient *Acinetobacter baumannii* due to Colistin resistance is killed by neutrophil-produced lysozyme. *Front. Microbiol.* 11:573. doi: 10.3389/fmicb.2020.00573

Kamoshida, G., Yamada, N., Nakamura, T., Yamaguchi, D., Kai, D., Yamashita, M., et al. (2022). Preferential selection of low-frequency, lipopolysaccharide-modified, Colistin-resistant mutants with a combination of antimicrobials in *Acinetobacter baumannii*. *Microbiol. Spectr.* 10:e0192822. doi: 10.1128/spectrum.01928-22

Lean, S. S., Suhaili, Z., Ismail, S., Rahman, N. I., Othman, N., Abdullah, F. H., et al. (2014). Prevalence and genetic characterization of Carbapenem- and Polymyxin-resistant *Acinetobacter baumannii* isolated from a tertiary Hospital in Terengganu, Malaysia. *ISRN Microbiol.* 2014:953417. doi: 10.1155/2014/953417

Lee, C. R., Lee, J. H., Park, M., Park, K. S., Bae, I. K., Kim, Y. B., et al. (2017). Biology of *Acinetobacter baumannii*: pathogenesis, antibiotic resistance mechanisms, and prospective treatment options. *Front. Cell. Infect. Microbiol.* 7:55. doi: 10.3389/fcimb.2017.00055

Lee, Y., Yum, J. H., Kim, C. K., Yong, D., Jeon, E. H., Jeong, S. H., et al. (2010). Role of OXA-23 and AdeABC efflux pump for acquiring carbapenem resistance in an *Acinetobacter baumannii* strain carrying the blaOXA-66 gene. *Ann. Clin. Lab. Sci.* 40, 43–48.

Lenhard, J. R., Bulman, Z. P., Tsuji, B. T., and Kaye, K. S. (2019). Shifting gears: the future of Polymyxin antibiotics. *Antibiotics (Basel)* 8:42. doi: 10.3390/antibiotics8020042

Li, X., Liu, L., Ji, J., Chen, Q., Hua, X., Jiang, Y., et al. (2015). Tigecycline resistance in *Acinetobacter baumannii* mediated by frameshift mutation in plsC, encoding 1-acyl-sn-glycerol-3-phosphate acyltransferase. *Eur. J. Clin. Microbiol. Infect. Dis.* 34, 625–631. doi: 10.1007/s10096-014-2272-y

Li, X., Quan, J., Yang, Y., Ji, J., Liu, L., Fu, Y., et al. (2016). Abrp, a new gene, confers reduced susceptibility to tetracycline, glycylcine, chloramphenicol and fosfomycin classes in *Acinetobacter baumannii*. *Eur. J. Clin. Microbiol. Infect. Dis.* 35, 1371–1375. doi: 10.1007/s10096-016-2674-0

Li, H., Wang, Q., Wang, R., Zhang, Y., Wang, X., and Wang, H. (2017). Global regulator SoxR is a negative regulator of efflux pump gene expression and affects antibiotic resistance and fitness in *Acinetobacter baumannii*. *Medicine (Baltimore)* 96:e7188. doi: 10.1097/md.0000000000007188

Liao, Y. T., Kuo, S. C., Chiang, M. H., Lee, Y. T., Sung, W. C., Chen, Y. H., et al. (2015). *Acinetobacter baumannii* extracellular OXA-58 is primarily and selectively released via outer membrane vesicles after sec-dependent periplasmic translocation. *Antimicrob. Agents Chemother.* 59, 7346–7354. doi: 10.1128/aac.01343-15

Liao, Y. T., Kuo, S. C., Lee, Y. T., Chen, C. P., Lin, S. W., Shen, L. J., et al. (2014). Sheltering effect and indirect pathogenesis of carbapenem-resistant *Acinetobacter baumannii* in polymicrobial infection. *Antimicrob. Agents Chemother.* 58, 3983–3990. doi: 10.1128/aac.02636-13

Lin, M. F., and Lan, C. Y. (2014). Antimicrobial resistance in *Acinetobacter baumannii*: from bench to bedside. *World J. Clin. Cases* 2, 787–814. doi: 10.12998/wjcc.v2.i12.787

Lin, M. F., Lin, Y. Y., and Lan, C. Y. (2017a). Contribution of EmrAB efflux pumps to colistin resistance in *Acinetobacter baumannii*. *J. Microbiol.* 55, 130–136. doi: 10.1007/s12275-017-6408-5

Lin, M. F., Lin, Y. Y., Tu, C. C., and Lan, C. Y. (2017b). Distribution of different efflux pump genes in clinical isolates of multidrug-resistant Acinetobacter baumannii and their correlation with antimicrobial resistance. *J. Microbiol. Immunol. Infect.* 50, 224–231. doi: 10.1016/j.jmii.2015.04.004

Lin, M. F., Lin, Y. Y., Yeh, H. W., and Lan, C. Y. (2014). Role of the BaeSR two-component system in the regulation of *Acinetobacter baumannii* adeAB genes and its correlation with tigecycline susceptibility. *BMC Microbiol.* 14:119. doi: 10.1186/1471-2180-14-119

Lin, T., Tang, C. G., Li, Q. H., Ji, J., Ge, H. Y., Zhang, X. Y., et al. (2015). Identification of aac(2′)-I type b aminoglycoside-modifying enzyme genes in resistant *Acinetobacter baumannii*. *Genet. Mol. Res.* 14, 1828–1835. doi: 10.4238/2015.March.13.11

Liu, Y., and Liu, X. (2015). Detection of AmpC β-lactamases in *Acinetobacter baumannii* in the Xuzhou region and analysis of drug resistance. *Exp. Ther. Med.* 10, 933–936. doi: 10.3892/etm.2015.2612

Liu, Y. Y., Wang, Y., Walsh, T. R., Yi, L. X., Zhang, R., Spencer, J., et al. (2016). Emergence of plasmid-mediated colistin resistance mechanism MCR-1 in animals and human beings in China: a microbiological and molecular biological study. *Lancet Infect. Dis.* 16, 161–168. doi: 10.1016/s1473-3099(15)00424-7

Liu, C., Wang, L., Wang, P., Xiao, D., and Zou, Q. (2023). The mechanism of Tigecycline resistance in *Acinetobacter baumannii* revealed by proteomic and genomic analysis. *Int. J. Mol. Sci.* 24:1379. doi: 10.3390/ijms24108652

Lomovskaya, O., Sun, D., Rubio-Aparicio, D., Nelson, K. J., Thamlikitkul, V., Dudley, M. N., et al. (2018). Absence of TetB identifies minocycline-susceptible isolates of *Acinetobacter baumannii*. *Int. J. Antimicrob. Agents* 52, 404–406. doi: 10.1016/j.ijantimicag.2018.04.006

López, C., Ayala, J. A., Bonomo, R. A., González, L. J., and Vila, A. J. (2019). Protein determinants of dissemination and host specificity of metallo-β-lactamases. *Nat. Commun.* 10:3617. doi: 10.1038/s41467-019-11615-w

Lytvynenko, I., Brill, S., Oswald, C., and Pos, K. M. (2016). Molecular basis of polyspecificity of the small multidrug resistance efflux pump AbeS from *Acinetobacter baumannii*. *J. Mol. Biol.* 428, 644–657. doi: 10.1016/j.jmb.2015.12.006

Ma, F., Shen, C., Zheng, X., Liu, Y., Chen, H., Zhong, L., et al. (2019). Identification of a novel plasmid carrying mcr-4.3 in an *Acinetobacter baumannii* strain in China. *Antimicrob. Agents Chemother.* 63:e00133-19. doi: 10.1128/aac.00133-19

Martins-Sorenson, N., Snesrud, E., Xavier, D. E., Cacci, L. C., Iavarone, A. T., McGann, P., et al. (2020). A novel plasmid-encoded mcr-4.3 gene in a colistin-resistant *Acinetobacter baumannii* clinical strain. *J. Antimicrob. Chemother.* 75, 60–64. doi: 10.1093/jac/dkz413

Meyer, C., Lucaβen, K., Gerson, S., Xanthopoulou, K., Wille, T., Seifert, H., et al. (2022). Contribution of RND-type efflux pumps in reduced susceptibility to biocides in *Acinetobacter baumannii*. *Antibiotics (Basel)* 11:1635. doi: 10.3390/antibiotics11111635

Modarresi, F., Azizi, O., Shakibaie, M. R., Motamedifar, M., Valibeigi, B., and Mansouri, S. (2015). Effect of iron on expression of efflux pump (adeABC) and quorum sensing (luxI, luxR) genes in clinical isolates of *Acinetobacter baumannii*. *APMIS* 123, 959–968. doi: 10.1111/apm.12455

Moffatt, J. H., Harper, M., Adler, B., Nation, R. L., Li, J., and Boyce, J. D. (2011). Insertion sequence ISAba11 is involved in colistin resistance and loss of lipopolysaccharide in *Acinetobacter baumannii*. *Antimicrob. Agents Chemother.* 55, 3022–3024. doi: 10.1128/aac.01732-10

Moffatt, J. H., Harper, M., Harrison, P., Hale, J. D., Vinogradov, E., Seemann, T., et al. (2010). Colistin resistance in *Acinetobacter baumannii* is mediated by complete loss of lipopolysaccharide production. *Antimicrob. Agents Chemother.* 54, 4971–4977. doi: 10.1128/aac.00834-10

Moffatt, J. H., Harper, M., Mansell, A., Crane, B., Fitzsimons, T. C., Nation, R. L., et al. (2013). Lipopolysaccharide-deficient *Acinetobacter baumannii* shows altered signaling through host toll-like receptors and increased susceptibility to the host antimicrobial peptide LL-37. *Infect. Immun.* 81, 684–689. doi: 10.1128/iai.01362-12

Munoz-Price, L. S., and Weinstein, R. A. (2008). Acinetobacter infection. *N. Engl. J. Med.* 358, 1271–1281. doi: 10.1056/NEJMra070741

Ni, W., Li, Y., Guan, J., Zhao, J., Cui, J., Wang, R., et al. (2016). Effects of efflux pump inhibitors on Colistin resistance in multidrug-resistant gram-negative Bacteria. *Antimicrob. Agents Chemother.* 60, 3215–3218. doi: 10.1128/aac.00248-16

Novović, K., and Jovčić, B. (2023). Colistin resistance in *Acinetobacter baumannii*: molecular mechanisms and epidemiology. *Antibiotics (Basel)* 12:516. doi: 10.3390/antibiotics12030516

Nowak, J., Seifert, H., and Higgins, P. G. (2015). Prevalence of eight resistance-nodulation-division efflux pump genes in epidemiologically characterized *Acinetobacter baumannii* of worldwide origin. *J. Med. Microbiol.* 64, 630–635. doi: 10.1099/jmm.0.000069

Nurtop, E., Bayındır Bilman, F., Menekse, S., Kurt Azap, O., Gönen, M., Ergonul, O., et al. (2019). Promoters of Colistin resistance in *Acinetobacter baumannii* infections. *Microb. Drug Resist.* 25, 997–1002. doi: 10.1089/mdr.2018.0396

Olaitan, A. O., Morand, S., and Rolain, J. M. (2014). Mechanisms of polymyxin resistance: acquired and intrinsic resistance in bacteria. *Front. Microbiol.* 5:643. doi: 10.3389/fmicb.2014.00643

Oliveira, E. A., Paula, G. R., Mondino, P. J. J., Chagas, T. P. G., Mondino, S. S. B., and Mendonça-Souza, C. R. V. (2019). High rate of detection of OXA-23-producing Acinetobacter from two general hospitals in Brazil. *Rev. Soc. Bras. Med. Trop.* 52:e20190243. doi: 10.1590/0037-8682-0243-2019

Opazo, A. C., Mella, S. M., Domínguez, M. Y., Bello, H. T., and González, G. R. (2009). Multi-drug efflux pumps and antibiotic resistance in *Acinetobacter baumannii*. *Rev. Chil. Infectol.* 26, 499–503.

Pagdepanichkit, S., Tribuddharat, C., and Chuanchuen, R. (2016). Distribution and expression of the Ade multidrug efflux systems in *Acinetobacter baumannii* clinical isolates. *Can. J. Microbiol.* 62, 794–801. doi: 10.1139/cjm-2015-0730

Pakharukova, N., Tuittila, M., Paavilainen, S., Malmi, H., Parilova, O., Teneberg, S., et al. (2018). Structural basis for *Acinetobacter baumannii* biofilm formation. *Proc. Natl. Acad. Sci. U. S. A.* 115, 5558–5563. doi: 10.1073/pnas.1800961115

Papp-Wallace, K. M., McLeod, S. M., and Miller, A. A. (2023). Durlobactam, a broad-Spectrum serine β-lactamase inhibitor, restores Sulbactam activity against Acinetobacter species. *Clin. Infect. Dis.* 76, S194–s201. doi: 10.1093/cid/ciad095

Paton, R., Miles, R. S., Hood, J., Amyes, S. G., Miles, R. S., and Amyes, S. G. (1993). ARI 1: beta-lactamase-mediated imipenem resistance in *Acinetobacter baumannii*. *Int. J. Antimicrob. Agents* 2, 81–87. doi: 10.1016/0924-8579(93)90045-7

Peleg, A. Y., Potoski, B. A., Rea, R., Adams, J., Sethi, J., Capitano, B., et al. (2007). *Acinetobacter baumannii* bloodstream infection while receiving tigecycline: a cautionary report. *J. Antimicrob. Chemother.* 59, 128–131. doi: 10.1093/jac/dkl441

Peng, D., Hong, W., Choudhury, B. P., Carlson, R. W., and Gu, X. X. (2005). *Moraxella catarrhalis* bacterium without endotoxin, a potential vaccine candidate. *Infect. Immun.* 73, 7569–7577. doi: 10.1128/iai.73.11.7569-7577.2005

Pormohammad, A., Mehdinejadiani, K., Gholizadeh, P., Nasiri, M. J., Mohtavinejad, N., Dadashi, M., et al. (2020). Global prevalence of colistin resistance in clinical isolates of *Acinetobacter baumannii*: a systematic review and meta-analysis. *Microb. Pathog.* 139:103887. doi: 10.1016/j.micpath.2019.103887

Potron, A., Vuillemenot, J. B., Puja, H., Triponney, P., Bour, M., Valot, B., et al. (2019). ISAba1-dependent overexpression of eptA in clinical strains of *Acinetobacter baumannii* resistant to colistin. *J. Antimicrob. Chemother.* 74, 2544–2550. doi: 10.1093/jac/dkz241

Qu, J., Yu, R., Wang, Q., Feng, C., and Lv, X. (2020). Synergistic antibacterial activity of combined antimicrobials and the clinical outcome of patients with Carbapenemase-producing *Acinetobacter baumannii* infection. *Front. Microbiol.* 11:541423. doi: 10.3389/fmicb.2020.541423

Rangel, K., Lechuga, G. C., Provance, D. W. Jr., Morel, C. M., and De Simone, S. G. (2023). An update on the therapeutic potential of antimicrobial peptides against *Acinetobacter baumannii* infections. *Pharmaceuticals (Basel)* 16:1281. doi: 10.3390/ph16091281

Robledo, I. E., Aquino, E. E., Santé, M. I., Santana, J. L., Otero, D. M., León, C. F., et al. (2010). Detection of KPC in Acinetobacter spp. in Puerto Rico. *Antimicrob. Agents Chemother.* 54, 1354–1357. doi: 10.1128/aac.00899-09

Romero, R., Schaudinn, C., Kusanovic, J. P., Gorur, A., Gotsch, F., Webster, P., et al. (2008). Detection of a microbial biofilm in intraamniotic infection. *Am. J. Obstet. Gynecol.* 198, 135.e1–135.e5. doi: 10.1016/j.ajog.2007.11.026

Rostami, T., Ranjbar, M., Ghourchian, S., Darzi, F., Douraghi, M., and Nateghi-Rostami, M. (2021). Upregulation of abeM, amvA, and qacEΔ1 efflux pump genes associated with resistance of *Acinetobacter baumannii* strains to disinfectants. *Health Sci. Rep.* 4:e395. doi: 10.1002/hsr2.395

Rumbo, C., Fernández-Moreira, E., Merino, M., Poza, M., Mendez, J. A., Soares, N. C., et al. (2011). Horizontal transfer of the OXA-24 carbapenemase gene via outer membrane vesicles: a new mechanism of dissemination of carbapenem resistance genes in *Acinetobacter baumannii*. *Antimicrob. Agents Chemother.* 55, 3084–3090. doi: 10.1128/aac.00929-10

Saipriya, K., Swathi, C. H., Ratnakar, K. S., and Sritharan, V. (2020). Quorum-sensing system in *Acinetobacter baumannii*: a potential target for new drug development. *J. Appl. Microbiol.* 128, 15–27. doi: 10.1111/jam.14330

Salehi, B., Ghalavand, Z., Yadegar, A., and Eslami, G. (2021). Characteristics and diversity of mutations in regulatory genes of resistance-nodulation-cell division efflux pumps in association with drug-resistant clinical isolates of *Acinetobacter baumannii*. *Antimicrob. Resist. Infect. Control* 10:53. doi: 10.1186/s13756-021-00924-9

Saral, A., Leonard, D. A., Duzgun, A. O., Cicek, A. C., June, C. M., and Sandalli, C. (2016). Kinetic characterization of GES-22 β-lactamase harboring the M169L clinical mutation. *J. Antibiot. (Tokyo)* 69, 858–862. doi: 10.1038/ja.2016.48

Scaife, W., Young, H. K., Paton, R. H., and Amyes, S. G. (1995). Transferable imipenem-resistance in Acinetobacter species from a clinical source. *J. Antimicrob. Chemother.* 36, 585–586. doi: 10.1093/jac/36.3.585

Sheikhalizadeh, V., Hasani, A., Ahangarzadeh Rezaee, M., Rahmati-Yamchi, M., Hasani, A., Ghotaslou, R., et al. (2017). Comprehensive study to investigate the role of various aminoglycoside resistance mechanisms in clinical isolates of *Acinetobacter baumannii*. *J. Infect. Chemother.* 23, 74–79. doi: 10.1016/j.jiac.2016.09.012

Smani, Y., Fàbrega, A., Roca, I., Sánchez-Encinales, V., Vila, J., and Pachón, J. (2014). Role of OmpA in the multidrug resistance phenotype of *Acinetobacter baumannii*. *Antimicrob. Agents Chemother.* 58, 1806–1808. doi: 10.1128/aac.02101-13

Snyman, Y., Reuter, S., Whitelaw, A. C., Stein, L., Maloba, M. R. B., and Newton-Foot, M. (2021). Characterisation of mcr-4.3 in a colistin-resistant *Acinetobacter nosocomialis* clinical isolate from Cape Town, South Africa. *J. Glob. Antimicrob. Resist.* 25, 102–106. doi: 10.1016/j.jgar.2021.03.002

Srinivasan, V. B., Venkataramaiah, M., Mondal, A., and Rajamohan, G. (2015). Functional characterization of AbeD, an RND-type membrane transporter in antimicrobial resistance in *Acinetobacter baumannii*. *PLoS One* 10:e0141314. doi: 10.1371/journal.pone.0141314

Steeghs, L., den Hartog, R., den Boer, A., Zomer, B., Roholl, P., and van der Ley, P. (1998). Meningitis bacterium is viable without endotoxin. *Nature* 392, 449–450. doi: 10.1038/33046

Sumyk, M., Himpich, S., Foong, W. E., Herrmann, A., Pos, K. M., and Tam, H. K. (2021). Binding of Tetracyclines to *Acinetobacter baumannii* TetR involves two Arginines as specificity determinants. *Front. Microbiol.* 12:711158. doi: 10.3389/fmicb.2021.711158

Sun, B., Liu, H., Jiang, Y., Shao, L., Yang, S., and Chen, D. (2020). New mutations involved in Colistin resistance in *Acinetobacter baumannii*. *mSphere* 5:e00895-19. doi: 10.1128/mSphere.00895-19

Tamma, P. D., Aitken, S. L., Bonomo, R. A., Mathers, A. J., van Duin, D., and Clancy, C. J. (2022). Infectious Diseases Society of America guidance on the treatment of AmpC β-lactamase-producing Enterobacterales, Carbapenem-resistant Acinetobacter baumannii, and *Stenotrophomonas maltophilia* infections. *Clin. Infect. Dis.* 74, 2089–2114. doi: 10.1093/cid/ciab1013

Tan, Y., Su, J., Fu, M., Zhang, H., and Zeng, H. (2022). Recent advances in phage-based therapeutics for multi-drug resistant *Acinetobacter baumannii*. *Bioengineering (Basel)* 10:35. doi: 10.3390/bioengineering10010035

Thi Khanh Nhu, N., Riordan, D. W., Nhu, T. D. H., Thanh, D. P., Thwaites, G., Lan, N. P. H., et al. (2016). The induction and identification of novel Colistin resistance mutations in Acinetobacter baumannii and their implications. *Sci. Rep.* 6:28291. doi: 10.1038/srep28291

Toth, M., Lee, M., Stewart, N. K., and Vakulenko, S. B. (2022). Effects of inactivation of d,d-Transpeptidases of *Acinetobacter baumannii* on bacterial growth and susceptibility to β-lactam antibiotics. *Antimicrob. Agents Chemother.* 66:e0172921. doi: 10.1128/aac.01729-21

Trebosc, V., Gartenmann, S., Tötzl, M., Lucchini, V., Schellhorn, B., Pieren, M., et al. (2019). Dissecting Colistin resistance mechanisms in extensively drug-resistant *Acinetobacter baumannii* clinical isolates. *MBio* 10:e01083-19. doi: 10.1128/mBio.01083-19

Wand, M. E., Bock, L. J., Bonney, L. C., and Sutton, J. M. (2015). Retention of virulence following adaptation to colistin in *Acinetobacter baumannii* reflects the mechanism of resistance. *J. Antimicrob. Chemother.* 70, 2209–2216. doi: 10.1093/jac/dkv097

Wang, Z., Li, H., Zhang, J., Wang, X., Zhang, Y., and Wang, H. (2021). Identification of a novel plasmid-mediated tigecycline resistance-related gene, tet(Y), in *Acinetobacter baumannii*. *J. Antimicrob. Chemother.* 77, 58–68. doi: 10.1093/jac/dkab375

Wiradiputra, M. R. D., Thirapanmethee, K., Khuntayaporn, P., Wanapaisan, P., and Chomnawang, M. T. (2023). Comparative genotypic characterization related to antibiotic resistance phenotypes of clinical carbapenem-resistant *Acinetobacter baumannii* MTC1106 (ST2) and MTC0619 (ST25). *BMC Genomics* 24:689. doi: 10.1186/s12864-023-09734-2

Wu, X., Chavez, J. D., Schweppe, D. K., Zheng, C., Weisbrod, C. R., Eng, J. K., et al. (2016). *In vivo* protein interaction network analysis reveals porin-localized antibiotic inactivation in *Acinetobacter baumannii* strain AB5075. *Nat. Commun.* 7:13414. doi: 10.1038/ncomms13414

Xu, Q., Chen, T., Yan, B., Zhang, L., Pi, B., Yang, Y., et al. (2019). Dual role of gnaA in antibiotic resistance and virulence in *Acinetobacter baumannii*. *Antimicrob. Agents Chemother.* 63:e00694-19. doi: 10.1128/aac.00694-19

Yang, N., Jin, X., Zhu, C., Gao, F., Weng, Z., Du, X., et al. (2022). Subunit vaccines for *Acinetobacter baumannii*. *Front. Immunol.* 13:1088130. doi: 10.3389/fimmu.2022.1088130

Yang, C. H., Su, P. W., Moi, S. H., and Chuang, L. Y. (2019). Biofilm formation in *Acinetobacter Baumannii*: genotype-phenotype correlation. *Molecules* 24:1849. doi: 10.3390/molecules24101849

Yang, W., Zhang, S. Q., Chen, F. H., and Li, S. J. (2023). Whole gene sequencing analysis for a polymyxin B resistant strain of *acinetobacter baumannii* with LpsB mutation. *Chinese J. Clin. Lab. Sci.* 42, 111–116. doi: 10.13602/j.cnki.jcls.2023.02.07

Yang, Y., Yan, Y. H., Schofield, C. J., McNally, A., Zong, Z., and Li, G. B. (2023). Metallo-β-lactamase-mediated antimicrobial resistance and progress in inhibitor discovery. *Trends Microbiol.* 31, 735–748. doi: 10.1016/j.tim.2023.01.013

Ye, X. F., Yu, R., and Zhou, Y. Q. (2023). Study on polymyxin resistance mediated by eptA overexpression in *Acinetobacter baumannii* clinical isolates. *Chin. J. Antibiot.* 48, 433–437. doi: 10.13461/j.cnki.cja.007498

Yoon, E. J., Courvalin, P., and Grillot-Courvalin, C. (2013). RND-type efflux pumps in multidrug-resistant clinical isolates of *Acinetobacter baumannii*: major role for AdeABC overexpression and AdeRS mutations. *Antimicrob. Agents Chemother.* 57, 2989–2995. doi: 10.1128/aac.02556-12

Yuhan, Y., Ziyun, Y., Yongbo, Z., Fuqiang, L., and Qinghua, Z. (2016). Over expression of AdeABC and AcrAB-TolC efflux systems confers tigecycline resistance in clinical isolates of Acinetobacter baumannii and *Klebsiella pneumoniae*. *Rev. Soc. Bras. Med. Trop.* 49, 165–171. doi: 10.1590/0037-8682-0411-2015

Zhang, G., Meredith, T. C., and Kahne, D. (2013). On the essentiality of lipopolysaccharide to gram-negative bacteria. *Curr. Opin. Microbiol.* 16, 779–785. doi: 10.1016/j.mib.2013.09.007

Zhao, Y., Hu, K., Zhang, J., Guo, Y., Fan, X., Wang, Y., et al. (2019). Outbreak of carbapenem-resistant *Acinetobacter baumannii* carrying the carbapenemase OXA-23 in ICU of the eastern Heilongjiang Province, China. *BMC Infect. Dis.* 19:452. doi: 10.1186/s12879-019-4073-5

Zheng, W., Huang, Y., Wu, W., Zhu, J., and Zhang, T. (2023). Analysis of efflux pump system and other drug resistance related gene mutations in Tigecycline-resistant *Acinetobacter baumannii*. *Comput. Math. Methods Med.* 2023, 8611542–8611512. doi: 10.1155/2023/8611542

frontiers | Frontiers in Microbiology

TYPE Original Research
PUBLISHED 01 February 2024
DOI 10.3389/fmicb.2024.1342839

OPEN ACCESS

EDITED BY
Vijay Soni,
NewYork-Presbyterian, United States

REVIEWED BY
Prabhat Ranjan Singh,
Weill Cornell Medicine, United States
Arka Banerjee,
NewYork-Presbyterian, United States
Jojy John,
Sathyabama Institute of Science and Technology, India

*CORRESPONDENCE
Yali Cui
✉ serain33@163.com
Yongmei Jiang
✉ jiangyongmeiwst@163.com
Yi Xie
✉ xie_yi_77@163.com

†These authors have contributed equally to this work and share first authorship

RECEIVED 22 November 2023
ACCEPTED 08 January 2024
PUBLISHED 01 February 2024

CITATION
Miao C, Yan Z, Chen C, Kuang L, Ao K, Li Y, Li J, Huang X, Zhu X, Zhao Y, Cui Y, Jiang Y and Xie Y (2024) Serotype, antibiotic susceptibility and whole-genome characterization of *Streptococcus pneumoniae* in all age groups living in Southwest China during 2018–2022. *Front. Microbiol.* 15:1342839. doi: 10.3389/fmicb.2024.1342839

Serotype, antibiotic susceptibility and whole-genome characterization of *Streptococcus pneumoniae* in all age groups living in Southwest China during 2018–2022

Chenglin Miao[1†], Ziyi Yan[1†], Chunmei Chen[2,3], Linghan Kuang[1], Keping Ao[4], Yingying Li[1,5], Jialu Li[6], Xiaocui Huang[7], Xinghua Zhu[8], Yijia Zhao[2,3], Yali Cui[1,2,3]*, Yongmei Jiang[1,9]* and Yi Xie[4]*

[1]Department of Laboratory Medicine, West China Second University Hospital, Sichuan University, Chengdu, Sichuan, China, [2]Department of Laboratory Medicine, Meishan Women and Children's Hospital, Alliance Hospital of West China Second University Hospital, Sichuan University, Meishan, Sichuan, China, [3]Department of Laboratory Medicine, West China Second University Hospital (Tianfu), Sichuan University/Sichuan Provincial Children's Hospital, Meishan, Sichuan, China, [4]Department of Laboratory Medicine, West China Hospital, Sichuan University, Chengdu, Sichuan, China, [5]Department of Laboratory Medicine, Tibet Autonomous Region Women's and Children's Hospital, Lhasa, China, [6]Department of Obstetrics, Key Laboratory of Birth Defects and Related Disease of Women and Children of MOE, West China Second Hospital, Sichuan University, Chengdu, Sichuan, China, [7]Department of Laboratory Medicine, Chengdu Jinjiang District Maternal and Child Healthcare Hospital, Chengdu, Sichuan, China, [8]Department of Laboratory Medicine, The First People's Hospital of Longquanyi District, Chengdu, Sichuan, China, [9]Key Laboratory of Birth Defects and Related Diseases of Women and Children (Sichuan University), Ministry of Education, Chengdu, Sichuan, China

Background: *Streptococcus pneumoniae* is a common pathogen that colonizes the human upper respiratory tract, causing high morbidity and mortality worldwide. This study aimed to investigate the prevalence status of *S. pneumoniae* isolated from patients of all ages in Southwest China, including serotype, antibiotic susceptibility and other molecular characteristics, to provide a basis for clinical antibiotic usage and vaccine development.

Methods: This study was conducted from January 2018 to March 2022 at West China Hospital, West China Second University Hospital, First People's Hospital of Longquanyi District (West China Longquan Hospital), Meishan Women and Children's Hospital (Alliance Hospital of West China Second University Hospital) and Chengdu Jinjiang Hospital for Women and Children Health. Demographic and clinical characteristics of 263 pneumococcal disease (PD) all-age patients were collected and analyzed. The serotypes, sequence types (STs), and antibiotic resistance of the strains were determined by next-generation sequencing, sequence analysis and the microdilution broth method.

Results: The most common pneumococcal serotypes were 19F (17.87%), 19A (11.41%), 3 (8.75%), 23F (6.46%) and 6A (5.70%). Coverage rates for PCV10, PCV13, PCV15, PCV20 and PCV24 were 36.12, 61.98, 61.98, 63.12 and 64.26%, respectively. Prevalent STs were ST271 (12.55%), ST320 (11.79%), ST90 (4.18%), ST876 (4.18%) and ST11972 (3.42%). Penicillin-resistant *S. pneumoniae* (PRSP) accounted for 82.35 and 1.22% of meningitis and nonmeningitis PD cases,

respectively. Resistance genes *msrD* (32.7%), *mefA* (32.7%), *ermB* (95.8%), *tetM* (97.3%) and *catTC* (7.6%) were found among 263 isolates. Most isolates showed high resistance to erythromycin (96.96%) and tetracycline (79.85%), with more than half being resistant to SXT (58.94%). A few isolates were resistant to AMX (9.89%), CTX (11.03%), MEN (9.13%), OFX (1.14%), LVX (1.14%) and MXF (0.38%). All isolates were susceptible to vancomycin and linezolid.

Conclusion: Our study provides reliable information, including the prevalence, molecular characterization and antimicrobial resistance of *S. pneumoniae* isolates causing pneumococcal diseases in Southwest China. The findings contribute to informed and clinical policy decisions for prevention and treatment.

KEYWORDS

***Streptococcus pneumoniae*, serotype, molecular characterization, antibiotic resistance, whole-genome sequencing, China**

1 Introduction

Streptococcus pneumoniae is a common gram-positive, opportunistic pathogen in humans that colonizes the nasopharynx. It can cause not only noninvasive pneumococcal diseases (NIPDs), such as pneumonia, otitis media, conjunctivitis, nasosinusitis and bronchitis, but also severe invasive pneumococcal diseases (IPDs), including pleurisy, meningitis and septicemia (Zeng et al., 2023), especially in children and elderly individuals. According to the World Health Organization (WHO), *S. pneumoniae* is the most common pathogen causing pneumonia. More than approximately 800,000 children die due to pneumococcal diseases annually, and the vast majority are in developing and underdeveloped countries (O'Brien et al., 2009; Johnson et al., 2010). Furthermore, IPDs are age influenced, with incidence increasing with age and mortality higher in those over 65 years of age (Marrie et al., 2018).

There are currently more than 100 known *S. pneumoniae* serotypes circulating worldwide (Ganaie et al., 2020). However, only some of these serotypes cause pneumococcal disease (Namkoong et al., 2016). Currently, several countries have already incorporated pneumococcal conjugate vaccines (PCVs) and polysaccharide-based vaccines (PPVs) into national immunization programs, and use of vaccines targeting specific serotypes has significantly reduced IPDs caused by the vaccine serotypes (VTs) (Richter et al., 2014; Chan et al., 2019). Vaccines such as PCV7 (covering serotypes 4, 6B, 9 V, 14, 18C, 19F and 23F), PCV13 (additionally covering 1, 3, 5, 6A, 7F and 19A), and PPV23 (covering serotypes 1–5, 6B, 7F, 8, 9 N, 9 V, 10A, 11A, 12F, 14, 15B, 17F, 18C, 19A, 19F, 20, 22F, 23F, and 33F) are currently available in China. However, none of the above vaccines is a part of China National Vaccination Programs, and the cost is high. These reasons result in low coverage rates (Men et al., 2020; Wang et al., 2021). In general, use of vaccines has led to changes in the distribution of *S. pneumoniae* serotypes. Although these vaccines have provided protection against VTs, they have also contributed to a rise in noncovered serotypes (NVTs; Lo et al., 2022). The increase in NVTs is concerning, especially as these serotypes display resistance to antibiotics commonly used in PD treatment (Zhao et al., 2020).

Antibiotic resistance varies by region, and a better understanding of resistance will ultimately help in clinical anti-infective treatment and preventing the spread of antibiotic-resistant strains (Li et al., 2023). Meanwhile, the distribution of *S. pneumoniae* serotypes in a specific region can provide valuable evidence for local health authorities to introduce appropriate vaccines. Analysis of whole-genome sequencing technology based on next-generation sequencing (NGS) can obtain information about molecular serotype, sequence type (ST), and antibiotic resistance, providing an important basis for pathogenic surveillance.

Furthermore, research shows that the coronavirus disease 2019 (COVID-19) pandemic and subsequent lockdowns to interrupt the spread of the virus had an impact on the pathogenicity of *S. pneumoniae* (Amin-Chowdhury et al., 2021). Despite PD cases have declined significantly during the COVID-19 pandemic. However, the mortality rate of IPD/COVID-19 co-infection is very high (Mitsi et al., 2022). Therefore, molecular characterization of prevalent *S. pneumoniae* strains during the COVID-19 outbreak will provide important support and reference for investigating the current status of PDs and potential changes in subsequent isolates.

The aim of this study based on whole-genome NGS technology was to investigate the prevalence and molecular characteristics of clinical *S. pneumoniae* isolates obtained from patients of all ages in Southwest China from 2018 to 2022 by analyzing the distribution of serotypes, STs, antimicrobial susceptibility and their respective relationships.

2 Materials and methods

2.1 Patients enrolled

This study was conducted from January 2018 to March 2022 at West China Hospital, West China Second University Hospital, First People's Hospital of Longquanyi District (West China Longquan Hospital), Meishan Women and Children's Hospital (Alliance Hospital of West China Second University Hospital) and Chengdu Jinjiang Hospital for Women and Children Health, including one of China's largest general hospitals, one of China's largest specialty hospitals for children and women, and typical secondary and tertiary general or specialty hospitals. The hospitals' clinical laboratories have been accredited by the College of American Pathologists (CAP) or the China National Accreditation Service for Conformity Assessment

(CNAS) under the ISO15189 accreditation standard or are under the supervision of the abovementioned external quality assessment laboratory.

The enrolled subjects were patients from Southwest China presenting with an *S. pneumoniae* infection who were admitted to these hospitals. The participant eligibility criteria included the following: (1) clinical specimens from which *S. pneumoniae* was isolated and positively cultured (including blood, cerebrospinal fluid, drainage fluid, alveolar lavage fluid, sputum, and secretions); and (2) respiratory, neural, circulatory or local infectious manifestations (including fever, headache, cough, and sputum).

2.2 Isolation and identification of strains

Strains of *S. pneumoniae* were collected, isolated and identified in line with requirements for clinical procedures as previously reported (Yan et al., 2019). In brief, specimens were collected by specialized sample collection personnel or physicians, following the Standard Operating Procedure (SOP) of ISO/TS 20658:2017-Medical Laboratories-Requirements[1] for collection, transport, receipt, and handling of samples (blood, sputum, cerebrospinal fluid, chest drainage and secretions). The alveolar lavage fluid was collected by flexible bronchoscopy via the protocol of Chinese expert consensus on pathogen detection in bronchoalveolar lavage for pulmonary infectious diseases (2017 edition) (Qu et al., 2017). Blood, cerebrospinal fluid and chest drainage were cultured in vials using the BD BACTECTM FX system and then subcultured onto Columbia Agar +5% sheep blood plates (Autobio, Zhengzhou, China). Other samples were isolated on Columbia agar +5% sheep blood plates (Autobio, Zhengzhou, China) incubated at 35°C for 24–48 h in a 5% carbon dioxide (CO_2) environment. All isolates were identified by matrix-assisted laser desorption ionization time-of-flight mass spectrometry (MALDI-TOF MS; Vitek MS system; BioMerieux, Rhône, France), and the results were confirmed by PubMLST whole-genome signature sequence alignment.[2] The pneumococcal isolates were stored in 25% sterile glycerol broth at −70°C for subsequent analysis.

2.3 Genome sequencing, assembly and annotation

Genomic DNA was extracted by using QIAamp DNA Minikit (Qiagen, Hilden, Germany), and sequencing libraries were generated using NEBNext® Ultra™ DNA Library Prep Kit for Illumina (New England Biolabs, NEB, USA) following the manufacturer's recommendations. The whole genomes of *S. pneumoniae* were sequenced using the Illumina NovaSeq PE150 platform (Illumina, San Diego, CA, USA) with approximately 200× coverage at Beijing Novogene Bioinformatics Technology Co., Ltd.

Genome data were assembled and annotated as previously reported (Cui et al., 2022) with SPAdes software (v3.14.1) (Prjibelski et al., 2020) and Prokka software (v1.14.5) (Seemann, 2014). All of the assembled genomes were submitted to GenBank and approved (PRJNA914101, PRJNA915833 and PRJNA915821).[3]

2.4 Molecular serotyping and multilocus sequence typing

MLSTs were identified by pneumococcal capsule typing (PneumoCaT v1.2.1) based on genome data (*.fastq files) as previously reported (Kapatai et al., 2016). STs were identified through the multilocus sequence typing (MLST) database[4] and mlst software (v2.19.0) (Seemann T, mlst, GitHub[5]) (Jolley and Maiden, 2010), and all novel alleles and profiles were submitted to the pneumococcal MLST database to assign new numbers. Minimum spanning tree-like structures were illustrated by PHYLOVIZ software (version 2.1)[6] via goeBURST Full MST (goeBURST distance) at level 1 (SLVs) and level 6 (Feil et al., 2004; Francisco et al., 2012).

2.5 Phylogenetic analysis

The annotated pneumococcal genome data were analyzed using Roary (v3.13.0)[7] to create a multiFASTA alignment of core genes (>99%) (Page et al., 2015), and Snp-sites (v2.3.3)[8] were used to delete duplicate sites. Maximum-likelihood trees were constructed from the alignment produced by RAxML (v8.2.10)[9] using the GTRGAMMA method (Stamatakis, 2014), and the RAxML trees were visualized and annotated in iTOL (v6).[10]

2.6 Antibiotic susceptibility tests and resistance gene screening

Antibiotic susceptibility tests (ASTs) were performed based on the broth turbidimetry method using AST dishes (TDR STR-AST, Mindray, China). The antimicrobial agents used included penicillin (PEN), amoxicillin (AMX), cefotaxime (CTX), meropenem (MEM), vancomycin (VAN), erythromycin (ERY), ofloxacin (OFX), levofloxacin (LVX), moxifloxacin (MXF), tetracycline (TET) and trimethoprim-sulfamethoxazole (SXT). Quality control analysis was performed using *S. pneumoniae* ATCC49619. The operational processes and interpretation of the results were performed according to the manufacturer's instructions and the Clinical and Laboratory Standards Institute (CLSI) 2021 standard (Humphries et al., 2021).

1 https://www.iso.org/standard/68763.html
2 https://pubmlst.org/
3 https://submit.ncbi.nlm.nih.gov/
4 https://pubmlst.org/organisms/streptococcus-pneumoniae
5 https://github.com/tseemann/mlst
6 http://www.phyloviz.net
7 https://github.com/sanger-pathogens/Roary
8 https://github.com/andrewjpage/snp-sites
9 https://github.com/stamatak/standard-RAxML
10 https://itol.embl.de

Antimicrobial resistance genes were screened with ABRicate software (v1.0.1; Seemann T, Abricate, GitHub)[11] via NCBI AMRFinderPlus (Feldgarden et al., 2019).

2.7 Statistical analysis

Statistical Package for Social Science (SPSS) software for Windows was used to assess the statistical significance of the data (version 22.0; Chicago, IL, USA), as previously reported (Yan et al., 2019). In brief, the chi-square test, Fisher's exact test and T-test were used. Based on the chi-square test, the Bonferroni method was employed to determine whether differences among multiple groups were statistically significant, and p values <0.05 were considered statistically significant.

2.8 Ethics statement

The clinical experimental plan was approved by the Clinical Trial Ethics Committee of West China Second University Hospital, Sichuan University (No. 2020041). The work was carried out in accordance with the Declaration of Helsinki.

3 Results

3.1 Demographic and clinical characteristics

A total of 263 patients were enrolled from January 2018 to March 2022, including 93 patients under 3 years old (35.36%) and 101 patients above 50 years old (38.40%), with ages ranging from 0.08 to 95 years and a median age (P25-P75) of 8.00 (2.34–63.00) years. These patients were diagnosed with meningitis, bacteremia, pleurisy, otitis media, pneumonia, bronchitis and upper respiratory tract infection, including 88 IPD patients and 175 NIPD patients. The detailed data are shown in Table 1.

TABLE 1 Demographic and clinical characteristics of 263 patients.

Characteristics	No. of patients	(%)
Sex		
Male	166	63.12
Female	97	36.88
Age (years)		
≤3	93	35.36
3–18	48	18.25
18–50	21	7.98
50–95	101	38.40
Median age (P25-P75)	*8.00 (2.34–63.00)*	
Isolation time of year		
Quarter 1	60	22.81
Quarter 2	34	12.93
Quarter 3	49	18.63
Quarter 4	120	45.63
Sample type		
Blood	48	18.25
Cerebrospinal fluid	17	6.47
Chest drainage	12	4.56
Alveolar lavage fluid	11	4.18
Sputum	155	58.94
Nasopharyngeal swab	5	1.90
Tracheal secretions	9	3.42
Ear canal secretions	3	1.14
Others	3	1.14
Diagnosis		
Invasive pneumococcal disease (IPD)	88	33.46
Noninvasive pneumococcal disease (NIPD)	175	66.54
Total	263	100.00

3.2 Molecular serotyping and vaccine coverage rates

Among 263 isolates, 35 serotypes were successfully identified. The prevalent serotypes were 19F (n = 47, 17.87%), 19A (n = 30, 11.41%), 3 (n = 23, 8.75%), 23F (n = 17, 6.46%), 6A (n = 15, 5.70%), 23A (n = 15, 5.70%), 14 (n = 14, 5.32%), 34 (n = 13, 4.94%), 15A (n = 13, 4.94%) and 6E (n = 13, 4.94%). Detailed information can be found in Supplementary Table 1. The coverage rates for PCV10, PCV13, PCV15, PCV20 and PCV24 were 36.12% (n = 95), 61.98% (n = 163), 61.98% (n = 163), 63.12% (n = 166) and 64.26% (n = 169), respectively (Figure 1). The differences of the prevalent serotypes in this study and our previous report (Yan et al., 2019) was shown in Supplementary Figure 1 and Supplementary Table 2.

As classified by disease, 24 serotypes were identified in 88 IPD cases, and the prevalent serotypes in IPD were 19F (n = 19, 21.59%), 19A (n = 8, 9.09%), 14 (n = 7, 7.95%), 23F (n = 7, 7.95%), 34 (n = 6, 6.82%) and 6E (n = 6, 6.82%) (Supplementary Table 3), with coverage rates for PCV10, PCV13, PCV15, PCV20 and PCV24 of 44.32% (n = 39), 61.36% (n = 54), 61.36% (n = 54), 63.64% (n = 56) and 63.64% (n = 56), respectively (Figure 2). Thirty serotypes were identified in 175 NIPD cases, and the prevalent serotypes in NIPD were 19F (n = 28, 16.00%), 19A (n = 22, 12.57%), 3 (n = 18, 10.29%), 6A (n = 13, 7.43%), 23F (n = 10, 5.71%) and 23A (n = 10, 5.71%) (Supplementary Table 4), with coverage rates for PCV10, PCV13, PCV15, PCV20 and PCV24 of 32.00% (n = 56), 62.92% (n = 109), 62.92% (n = 109), 62.86% (n = 110) and 64.57% (n = 113), respectively (Figure 2).

As classified by age, 23 serotypes were identified in 141 pediatric cases (age < 18 years); the prevalent serotypes were 19F (n = 30, 21.28%), 19A (n = 16, 11.35%), 6A (n = 10, 7.09%), 6E (n = 10, 7.09%), 14 (n = 10, 7.09%), 15A (n = 9, 6.38%), 23A (n = 9, 6.38%)

11 https://github.com/tseemann/abricate

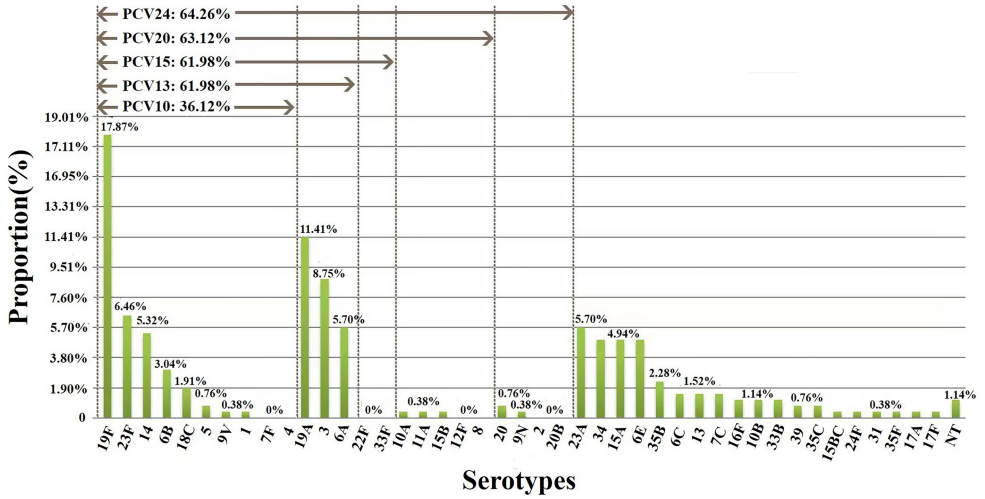

FIGURE 1
Serotype distribution and coverage of PCVs among 263 *S. pneumoniae* isolates. The prevalent serotypes were 19F ($n = 47$, 17.87%), 19A ($n = 30$, 11.41%), 3 ($n = 23$, 8.75%) and 23F ($n = 17$, 6.46%). NT, nontypable.

(Supplementary Table 5), with coverage rates for PCV10 and PCV13/PCV15/PCV20/PCV24 of 41.84% ($n = 59$) and 64.54% ($n = 91$), respectively (Figure 3). In addition, 28 serotypes were identified in 101 elderly patients (age > 50 years); the prevalent serotypes were 3 ($n = 16$, 15.84%), 19F ($n = 13$, 12.87%), 19A ($n = 12$, 11.88%), 34 ($n = 6$, 5.94%), 23F ($n = 6$, 5.94%), 6A ($n = 5$, 4.95%), 23A ($n = 5$, 4.95%), 35B ($n = 5$, 4.95%) (Supplementary Table 6), with coverage rates for PCV10, PCV13, PCV15, PCV20 and PCV24 of 24.75% ($n = 25$), 57.43% ($n = 58$), 57.43% ($n = 58$), 58.42% ($n = 59$) and 61.39% ($n = 62$), respectively (Figure 3). The prevalent serotypes in patients aged 18–50 years old were shown in Supplementary Table 7.

3.3 Multilocus sequence typing

Among the 263 isolates, 107 different STs were successfully identified by MLST analysis, including 38 novel STs ($n = 43/263$, 35.51%): ST17945-ST17947, ST17949-ST17952, ST17954, ST17956-ST17957, ST17959-ST17967, ST17969, ST17970, and ST18037-ST18053 (Figure 4A). Additionally, 19 novel alleles were identified by sequencing: *aroE* (617), *ddl* (1163–1,165), *gdh* (798–800), *gki* (825–830), *recP* (563–565), *spi* (777, 778) and *xpt* (1087). The numbers of novel STs and alleles were assigned by the MLST database after the sequences were identified (see text footnote 2). Prevalent STs included ST271 ($n = 33$, 12.55%), ST320 ($n = 31$, 11.79%), ST90 ($n = 11$, 4.18%), ST876 ($n = 11$, 4.18%), ST11972 ($n = 9$, 3.42%), ST902 ($n = 8$, 3.04%), ST81 ($n = 6$, 2.28%) and ST5242 ($n = 6$, 2.28%); detailed information can be found in Supplementary Table 8.

Nine global clones were found in this study by comparing strains with the pneumococcal molecular epidemiology network (PMEN), including Spain^{6B}-2 (ST90, $n = 11$, 4.2%), Spain^{23F}-1 (ST81, $n = 6$, 2.3%), Netherlands^{3}-31 (ST180, $n = 4$, 1.5%), Colombia^{23F}-26 (ST338, $n = 4$, 1.5%), Taiwan^{19F}-14 (ST236, $n = 2$, 0.8%), Taiwan^{23F}-15 (ST242, $n = 2$, 0.8%), Sweden^{15A}-25 (ST63, $n = 1$, 0.4%), USA^{1}-29 (ST615, $n = 1$, 0.4%), and Denmark^{14}-32 (ST230, $n = 1$, 0.4%).

Among the 263 isolates, 21 clonal complexes (CCs) and 48 singletons were obtained according to single-locus variants (SLVs) via goeBURST distance analysis (SLV, level 1, Figure 5). CC271 ($n = 75$, 28.5%), CC876 ($n = 14$, 5.3%), CC90 ($n = 12$, 4.6%), CC6011 ($n = 12$, 4.6%), CC2754 ($n = 11$, 4.2%) and CC338 ($n = 10$, 3.8%) were prevalent CCs.

By comparing STs with serotypes, a minimum spanning tree-like structure was illustrated via the goeBURST Full MST algorithm, and the serotype distribution showed ST/CC aggregation (Figure 4B and Supplementary Table 9). Serotype 19F was dominated by ST271, accounting for 70.21% ($n = 33/47$); serotype 19A was dominated by ST320, accounting for 96.67% ($n = 29/30$); serotype 23F was dominated by ST81, accounting for 35.29% ($n = 6/17$); serotype 14 was dominated by ST876, accounting for 71.43% ($n = 10/14$); serotype 34 was dominated by ST11945, accounting for 38.46% ($n = 5/13$); serotype 15A was dominated by ST11972, accounting for 69.23% ($n = 9/13$); serotype 6E was dominated by ST90, accounting for 92.31% ($n = 12/13$); and serotype 6B was dominated by ST902, accounting for 75.00% ($n = 6/8$) (Figure 6). The serotypes of isolates among novel STs were distributed in 3, 5, 13, 14, 20, 31, 34, 39, 10B, 11A, 15A, 15 BC, 16F, 17A, 19A, 19F, 23A, 23F, 33B, 35B, 35F, 6A, 6C and 9 N.

Regarding classification by disease, prevalent STs in IPD (88/263) were ST271 ($n = 11$, 12.50%), ST320 ($n = 9$, 10.23%), ST90 ($n = 6$, 6.82%), ST876 ($n = 5$, 5.68%), ST11972 ($n = 4$, 4.55%) and ST1937 ($n = 3$, 3.41%). Prevalent STs in NIPD (175/263) were ST271 ($n = 22$, 12.57%), ST320 ($n = 22$, 12.57%), ST902 ($n = 7$, 4.00%), ST876 ($n = 6$, 3.43%), ST90 ($n = 5$, 2.86%), ST5242 ($n = 5$, 2.86%), ST11972 ($n = 5$, 2.86%), ST81 ($n = 4$, 2.29%) and ST2754 ($n = 4$, 2.29%) (Figure 7A).

When classified by age, prevalent STs in pediatric cases (age < 18 years, $n = 141/263$) were ST271 ($n = 20$, 14.18%), ST320 ($n = 9$, 6.38%), ST90 ($n = 8$, 5.67%), ST876 ($n = 8$, 5.67%), ST902 ($n = 6$, 4.26%), ST1937 ($n = 5$, 3.55%), ST5242 ($n = 5$, 3.55%) and ST11972 ($n = 5$, 3.55%). Prevalent STs in elderly patients (age > 50 years) were ST271 ($n = 10$, 9.9%), ST320 ($n = 13$, 12.87%), ST11945 ($n = 4$, 3.96%),

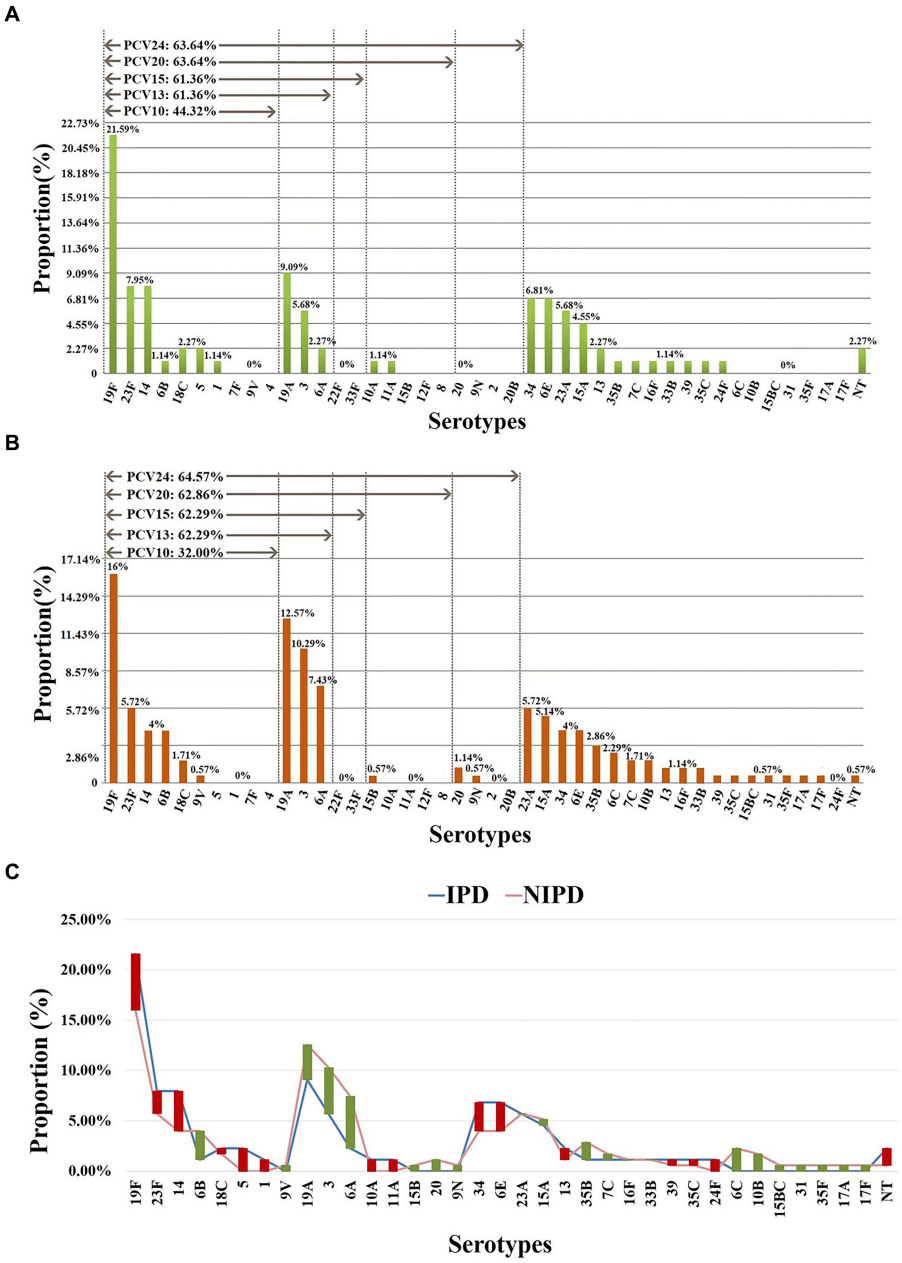

FIGURE 2
Serotype distribution in different diseases. **(A)** Proportions of each serotype in 88 IPD cases. **(B)** Proportions of each serotype in 175 NIPD cases. **(C)** The difference in the proportion of each serotype in IPD/NIPD cases. Red bar: the length indicates the value with a higher proportion of IPD than NIPD; green bar: the length indicates the value with a higher proportion of NIPD than IPD. NT, nontypable.

ST11972 ($n = 4$, 3.96%), ST81 ($n = 3$, 2.97%), ST180 ($n = 3$, 2.97%), ST338 ($n = 3$, 2.97%), ST505 ($n = 3$, 2.97%) and ST11967 ($n = 3$, 2.97%) (Figure 7B).

3.4 Phylogenetic analysis

The RAxML tree based on 263 isolate core gene sequences was visualized and annotated with strain, ST, serotype, age, specimen source and disease. Detailed information is shown in Figure 8.

3.5 Antibiotic susceptibility

The overall prevalence of PEN-nonsusceptible *S. pneumoniae* (PNSP) was 6.1% in nonmeningitis cases, including PEN-intermediate *S. pneumoniae* (PISP, 4.88%) and PEN-resistant *S. pneumoniae* (PRSP, 1.22%), and PRSP in meningitis cases was 82.35%. Most isolates showed high resistance to ERY (96.96%) and TET (79.85%), and more than half of the isolates were resistant to SXT (58.94%). A few isolates were resistant to AMX (9.89%), CTX (11.03%), MEN (9.13%), OFX (1.14%), LVX (1.14%) and MXF (0.38%). However, no isolate was found to have VAN- and LNZ-resistant phenotypes. The detailed

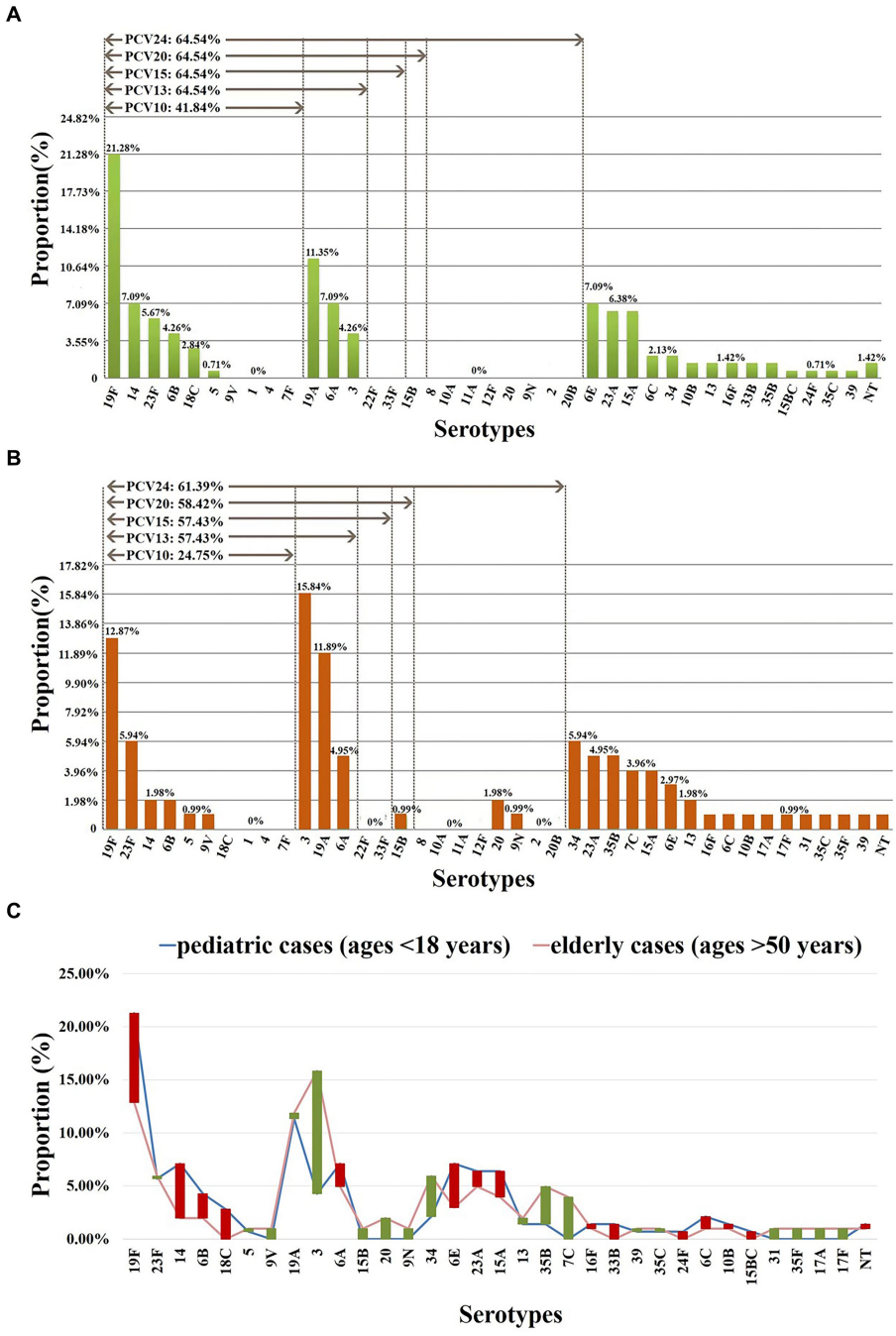

FIGURE 3
Serotype distribution in different ages. **(A)** Proportions of each serotype in 141 pediatric cases (ages <18 years). **(B)** Proportions of each serotype in 101 elderly cases (ages >50 years). **(C)** The difference in the proportion of each serotype in pediatric/elderly cases. Red bar: the length indicates the value with a higher proportion of pediatric cases than elderly cases; green bar: the length indicates the value with a higher proportion of elderly cases than pediatric cases. NT, nontypable. Proportions of each serotype in patients aged 18–50 years old were shown in Supplementary Table 7.

information is provided in Supplementary Figure 2 and Supplementary Table 10.

The relationship between antibiotic susceptibility and serotype is shown in Supplementary Figure 3A and Supplementary Table 11. In brief, serotypes 19A and 19F tended to be more resistant to AMX, CTX, MEM and SXT, whereas serotype 3 was more sensitive to these antibiotics. In addition, serotypes covered by PCV13 and PCV23 showed more resistance to PEN, AMX, CTX and SXT (Table 2). The differences of the antibiotic resistance in this study and our previous report (Yan et al., 2019) was shown in Supplementary Table 12.

The relationship between antibiotic susceptibility and STs is indicated in Supplementary Figure 3B and Supplementary Table 13. In brief, ST271 tended to be more resistant to AMX and CTX, whereas

10.3389/fmicb.2024.1342839

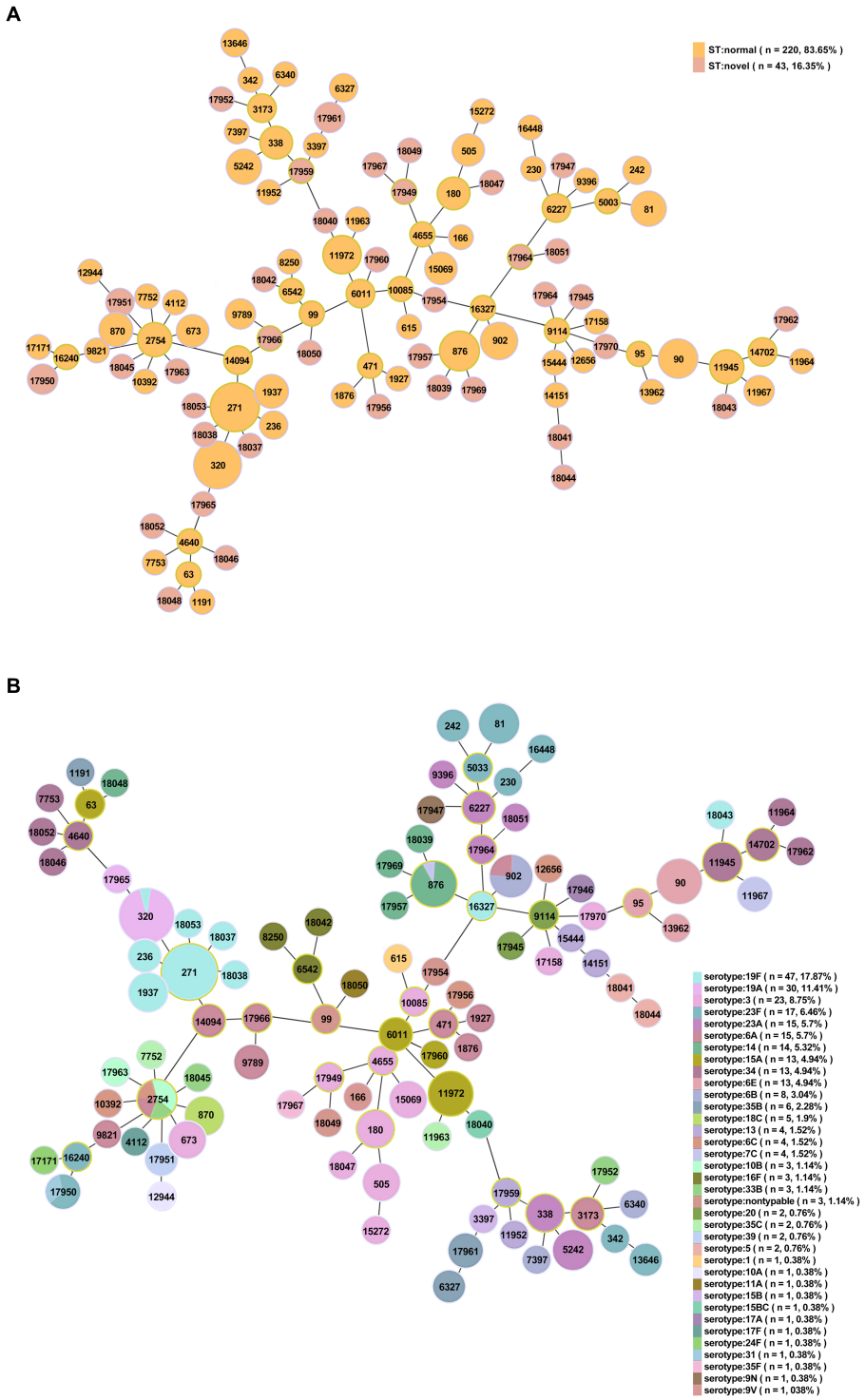

FIGURE 4
Minimum spanning tree-like structure via the goeBURST full MST algorithm (level 6). **(A)** Thirty-eight novel STs among 263 *S. pneumoniae* isolates ($n = 43$). Pink: novel STs. **(B)** The relationship between ST and serotype. Each disk represents an ST, and each color represents a serotype.

ST90 was more sensitive to AMX, CTX and MEN. ST876 and ST11972 were more sensitive to AMX and ST902 to AMX, CTX, MEN and SXT.

Among 263 isolates, 53.61% ($n = 141$) were defined as multidrug resistant (MDR), leading to serotypes 19F ($n = 36$, 25.35%), 19A ($n = 26$, 18.31%), ST271 ($n = 28$, 19.72%) and ST320 ($n = 27$, 19.01%). In addition, isolates with serotypes covered by PCV13 accounted for 70.21% ($n = 99$) of MDR isolates. Among MDR isolates, the most common phenotype was ERY/TET/SXT ($n = 78/142$, 54.9%),

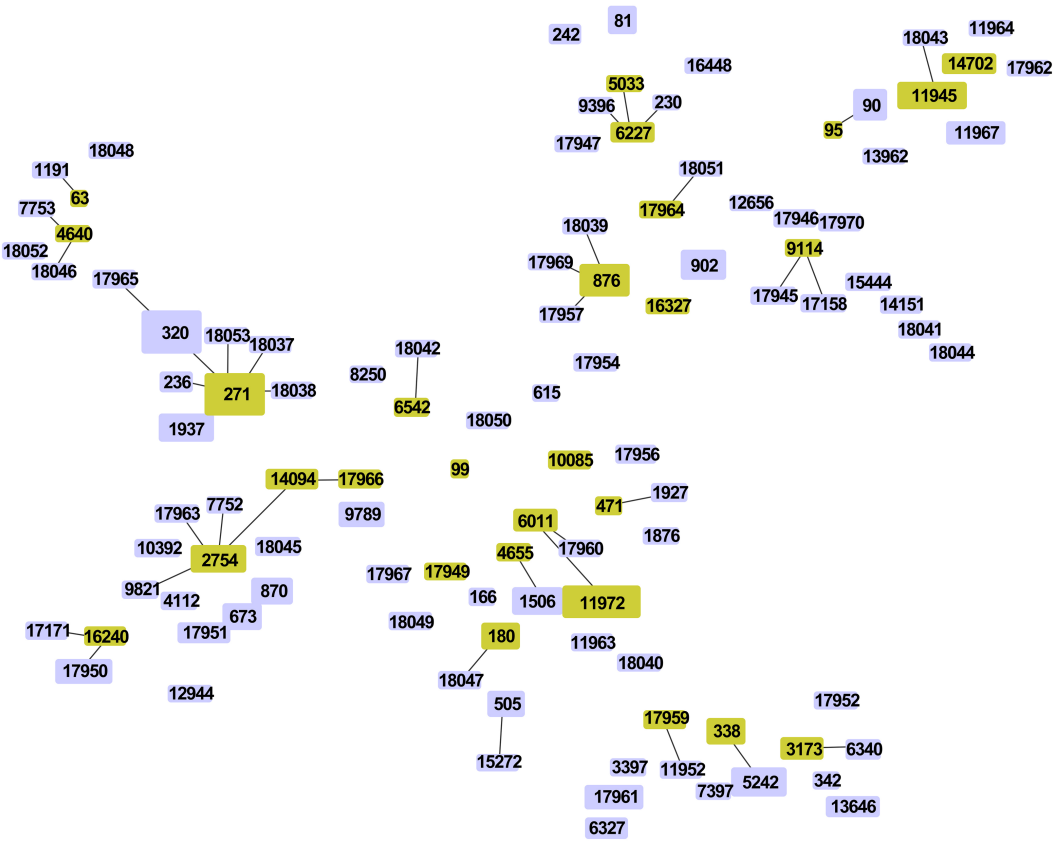

FIGURE 5
Minimum spanning tree-like structure via goeBURST distance analysis among 263 *S. pneumoniae* isolates (SLVs, level 1). SLV analysis showed that the 107 STs were divided into 21 CCs (linked) and 48 singletons.

including 22 IPD cases and 56 NIPD cases, with the leading serotypes of 19A ($n = 12$, 15.38%), 19F ($n = 9$, 11.54%), 23F ($n = 8$, 10.26%), and 6E ($n = 8$, 10.26%) and leading STs of ST320 ($n = 12$, 15.38%), ST90 ($n = 7$, 8.94%), ST271 ($n = 5$, 6.41%), and ST870 ($n = 4$, 5.13%). Other MDR phenotypes included CTX/ERY/TET/SXT ($n = 20/142$, 14.1%), with the leading serotype being 19F ($n = 16$, 80.00%) and leading ST being ST271 ($n = 13$, 65.00%), and MEM/ERY/TET/SXT ($n = 17/142$, 12.0%), with leading serotypes 19F ($n = 7$, 41.18%) and 19A ($n = 6$, 35.29%) and leading STs ST271 ($n = 6$, 35.29%) and ST320 ($n = 6$, 35.29%).

3.6 Resistance gene analysis

The resistance genes *msrD* ($n = 86$, 32.7%), *mefA* ($n = 86$, 32.7%), *ermB* ($n = 252$, 95.8%), *tetM* ($n = 256$, 97.3%) and *catTC* ($n = 20$, 7.6%) were found among the 263 isolates, which are associated with erythromycin, tetracycline and chloramphenicol. The erythromycin resistance genes *msrD*, *mefA* and *ermB* manifested as ST aggregation phenomena, and 28.9% ($n = 76$) of the isolates carried these three resistance genes, including ST271 ($n = 33/76$, 43.4%) and ST320 ($n = 29/76$, 38.2%) (Figures 9, 10). However, the ST aggregation of the tetracycline resistance gene *tetM* and chloramphenicol resistance gene *catTC* was not significant (Figure 10).

4 Discussion

In this study, we collected *S. pneumoniae* isolates from 263 PD patients in 5 hospitals and performed whole-genome sequencing. To our knowledge, this is the first all-age multicenter *S. pneumoniae* study conducted in Southwest China. Comprehensive identification of the molecular characteristics of pneumococcal isolates revealed prevalence characteristics, including serotype, ST, and the relationship among antibiotic susceptibility and the carrying antibiotic resistance genes in Southwest China from 2018 to 2022, covering the period before and during the COVID-19 outbreak. The results showed that 19F, 19A, 3, 23F, 6A, 23A, 14, 34, 15A and 6E were the top 10 prevalent serotypes. ST271, ST320, ST90, ST876, ST11972, ST902, ST81 and ST5242 were the most prevalent STs, and CC271, CC876, CC90, CC6011, CC2754 and CC338 were the most common CCs. Most isolates were resistant to ERY (96.96%) and TET (79.85%), and more than half of the isolates were resistant to SXT (58.94%).

The clinical isolates of *S. pneumoniae* were highly serotype heterogeneous. We identified 35 different serotypes, and 3 isolates were untypable. The top 5 serotypes in prevalence (19F, 19A, 3, 23F, and 6A) accounted for 50.19%, which was slightly different from the results reported previously in this region among pediatric patients (19F, 19A, 6B, 6A, and 14) (Yan et al., 2021), as well as those reported in Shanghai (19F, 6A, 19A, 23F and 14) (Zhao et al., 2019),

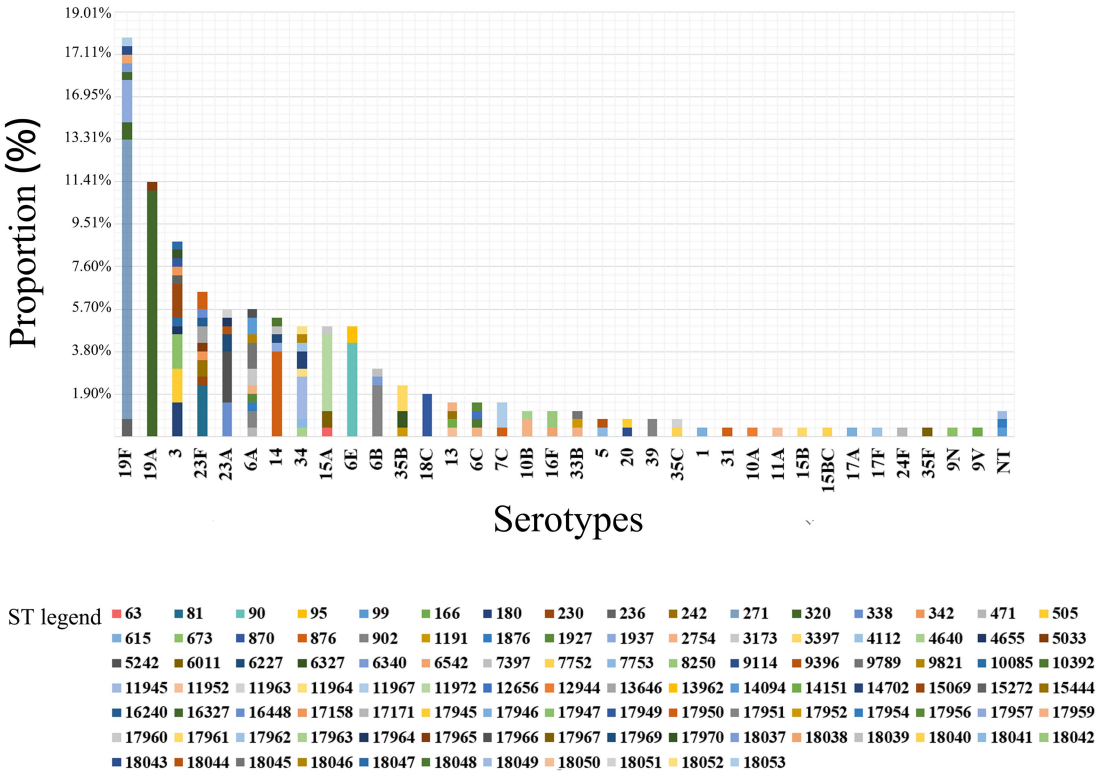

FIGURE 6
ST distribution in each serotype among 263 *S. pneumoniae* isolates. Serotype 19F was dominated by ST271, accounting for 70.21% (*n* = 33/47); serotype 19A was dominated by ST320, accounting for 96.67% (*n* = 29/30).

TABLE 2 Relationship between antibiotic resistance and vaccine coverage.

Antibiotic		R%			R%		
		PCV13 (*n* = 163)	Non-PCV13 (*n* = 100)	*p*	PPV23 (*n* = 155)	Non-PPV23 (*n* = 108)	*p*
PEN	(meningitis)	91.67	60.00	0.450	84.62	75.00	0.154
	(nonmeningitis)	0.61	2.00	0.034	0.65	1.85	0.031
AMX		14.11	3.00	0.007	14.84	2.78	0.000
CTX		14.72	5.00	0.015	16.13	3.70	0.002
MEM		12.27	4.00	0.051	12.90	3.70	0.016
VAN		0.00	0.00	NA	0.00	0.00	NA
ERY		96.93	97.00	1.000	96.77	97.22	1.000
OFX		0.00	3.00	0.000	0.00	2.78	0.001
LVX		0.00	3.00	0.053	0.00	2.78	0.062
MFX		0.00	1.00	0.617	0.00	0.93	0.636
TET		80.37	79.00	0.894	81.29	77.78	0.639
SXT		65.03	49.00	0.009	65.16	50.00	0.008
LNZ		0.00	0.00	NA	0.00	0.00	NA

Chongqing (19F, 6A/B, 19A) (Yu et al., 2019) and Beijing (19F, 19A, 23F, 14 and 6A) (Wang Q. et al., 2020). In this study, the most common serotypes among 88 IPD strains were 19F, 19A, 14, 23F, 34 and 6E. These findings are similar to the results of a multicenter study conducted in China (Zhao et al., 2013). Among 175 NIPD strains, the most common serotypes were 19F, 19A, 3, 6A, 23F and 23A. The prevalence of serotypes 3 and 23F in elderly patients was significantly higher than that in children. This finding, primarily the

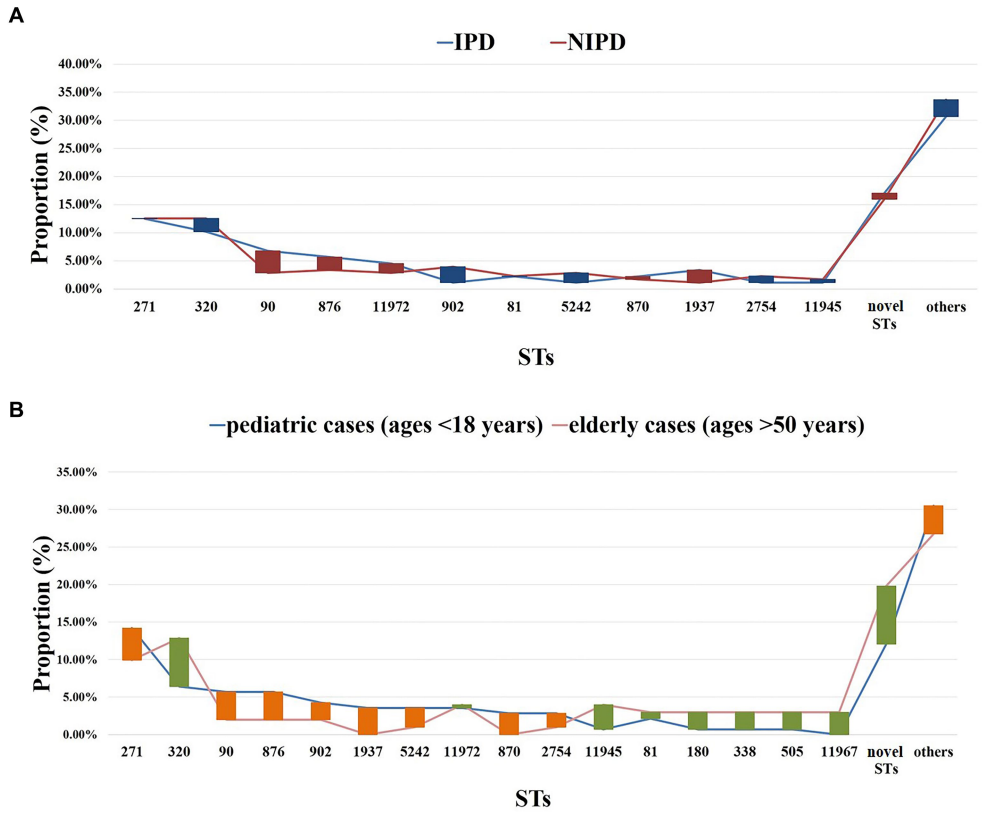

FIGURE 7
ST distribution in each group. **(A)** Proportions of each ST in different diseases. Blue line: IPD cases ($n = 88$); red line: NIPD cases ($n = 175$); red bar: the length indicates the value with a higher proportion of IPD than NIPD; blue bar: the length indicates the value with a higher proportion of NIPD than IPD. **(B)** Proportions of each ST in different ages. Blue line: pediatric cases ($n = 141$, ages <18 years); pink line: elderly cases ($n = 101$, ages >50 years); orange bar: the length indicates the value with a higher proportion of pediatric cases than elderly cases; green bar: the length indicates the value with a higher proportion of elderly cases than pediatric cases. Proportions of each ST in patients aged 18–50 years old were shown in Supplementary Table 7.

result of serotype 3, is significantly higher than our previous findings (8.75% vs. 3.13%) (Yan et al., 2021). The increase in the prevalence of serotype 3 is similar to the prevalence of *S. pneumoniae* in some developed countries (Goettler et al., 2020; Suaya et al., 2020; Hyams et al., 2023). Compared with our previous study (Yan et al., 2021), the PCV-covered serotypes decreased slightly (PCV10: 50.8% vs. 36.12%; PCV13: 77.3% vs. 61.98%). The difference in serotype distribution of *S. pneumoniae* may be due to serotype replacement after widespread use of PCVs (Hanquet et al., 2022; Lo et al., 2022).

We analyzed 263 isolates by MLST, and the results showed that ST271, ST320, ST90 and ST876 were the most prevalent STs in Southwest China, similar to other parts in China (Wang X. et al., 2020; Zhou et al., 2022) but different from those in other countries, such as northern Russia (Vorobieva S Jensen et al., 2020) and Latin America (Moreno et al., 2020). The present study further revealed 38 novel STs, which accounted for 35.51% of all isolates (43/263), strongly indicating the global diversity of *S. pneumoniae*. In addition, the study identified 19 novel alleles through sequencing. Phylogenetic tree analysis showed CC271, CC876, CC90, CC6011, and CC2754 to be common CCs, among which CC271 is prevalent globally and the most common CC in China (Zeng et al., 2023).

Penicillin has been the first-line treatment for *S. pneumoniae*, especially before the 1980s (Swartz, 2002). The current work shows that the resistance rate of isolates to PEN was 1.22% in nonmeningitis patients, consistent with results reported from other parts of East Asia, such as China (0.7–2.2%), Korea (1.0%) and Japan (1.7–2.2%) (Wang et al., 2019; Kim et al., 2020; Tsuzuki et al., 2020). These results suggest that PEN can continue to be used in treatment against nonmeningitis *S. pneumoniae* at higher concentrations but not against meningitis strains.

Macrolides and fluoroquinolones are the main alternatives to beta-lactam antibiotics in cases of reduced susceptibility to *S. pneumoniae* infections (Berbel et al., 2022). However, with widespread clinical use of macrolide antibacterial agents, the number of ERY-resistant *S. pneumoniae* (ERSP) strains has increased. This phenomenon is a cause for concern, and macrolides have been included in the list of Critically Important Antimicrobials for Human Medicine by the WHO. According to data from the China Antimicrobial Resistance Surveillance System in 2021, the resistance rate of *S. pneumoniae* to ERY average as high as 96.4% nationwide. In this study, rates of macrolide resistance (MR) were significantly high, with a rate of resistance to ERY of 96.96%, indicating that these agents had little clinical utility for treatment of *S. pneumoniae* infections,

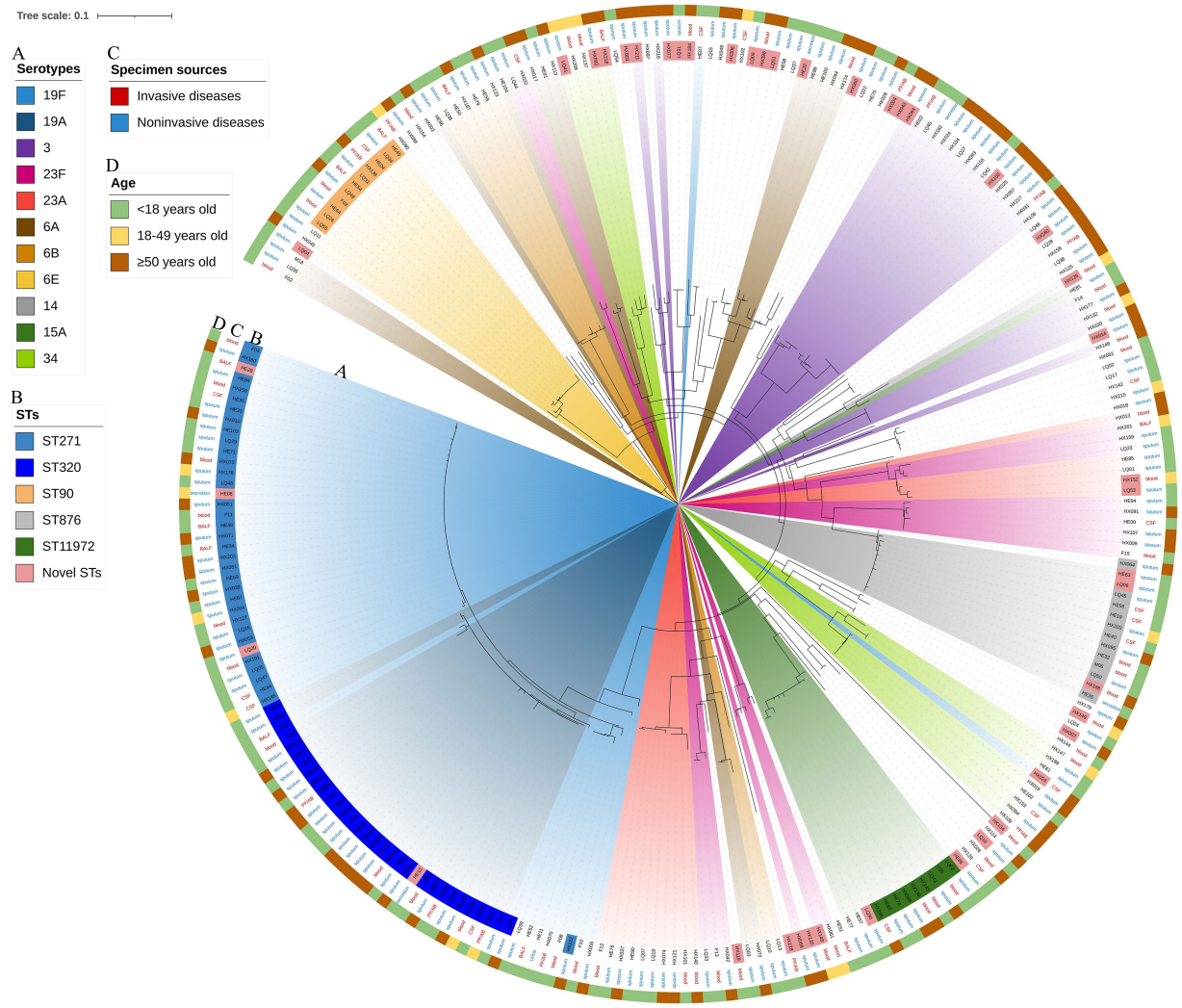

FIGURE 8
Maximum likelihood tree of 263 *S. pneumoniae* isolates. The RAxML tree was constructed from a multiFASTA alignment of core genes (>99%) using the GTRGAMMA method. **(A)** Serotypes with a proportion greater than 3%. **(B)** The top 5 proportion STs and novel STs. **(C)** Specimen sources (colored with IPD and NIPD). **(D)** Patients ages.

which is consistent with the results in Northeast China (98.57%) (Zhou et al., 2022) and Beijing (96.4%) (Zhou et al., 2012).

In China, MR increased from 15 to 95% over 16 years (2000–2016), mainly associated with the spread of *ermB* (Ip et al., 2002; Lu et al., 2017). Determinants of MR include modification by ribosomal methylases (*ermB*) and active antibiotic efflux pumps (*mefA*/*E*). *ermB* is the most common mechanism of ERY resistance in Asia, including mainland China, Taiwan, Sri Lanka, South Korea and Japan, whereas *mefA* is more common in Hong Kong, Singapore, Malaysia, India and the Philippines (Song et al., 2004; Kim et al., 2012). This is consistent with the results for *ermB* (252/263) and *mefA* (86/263) in this study, which may be responsible for the high degree of ERY resistance in this region. In Europe, *ermB* was found to be more common in Italy (55.8%), Poland (80.8%), Serbia (82.4%), Spain (88.3%), France (90%) and Belgium (91.5%) (Felmingham et al., 2007); furthermore, *mefA* is common in Germany (53.2%), Finland (55.4%), Australia (59.5%), Greece (66.2%) and the United Kingdom (70.8%) (Farrell et al., 2008).

Beta-lactam antibiotics and macrolides are commonly used to treat community-acquired infections in children because they are relatively safe and inexpensive. This chronic antibiotic pressure also contributes to resistance. In contrast, tetracyclines, quinolones and sulfonamides are prohibited or restricted in children of different ages due to their toxicity and adverse effects.

The resistance of *S. pneumoniae* to TET is also notably high in China, which may be related to misuse of TET in agriculture and livestock (Zhou et al., 2012). *tetM*, encoding ribosome protection proteins, is one of the causes of TET resistance (Widdowson et al., 1996; Widdowson and Klugman, 1998). In this study, the rate of TET resistance was 79.85%, whereas *tetM* was detected in almost all TET-resistant strains.

Development of resistance to any three or more antimicrobial agents of different classes is described as MDR. More than 30% of *S. pneumoniae* strains globally are reported to exhibit MDR (Jung et al., 2013). In a 2012–2017 study conducted in 6 Asian countries, 50.8% of *S. pneumoniae* strains exhibited MDR, with the highest rates

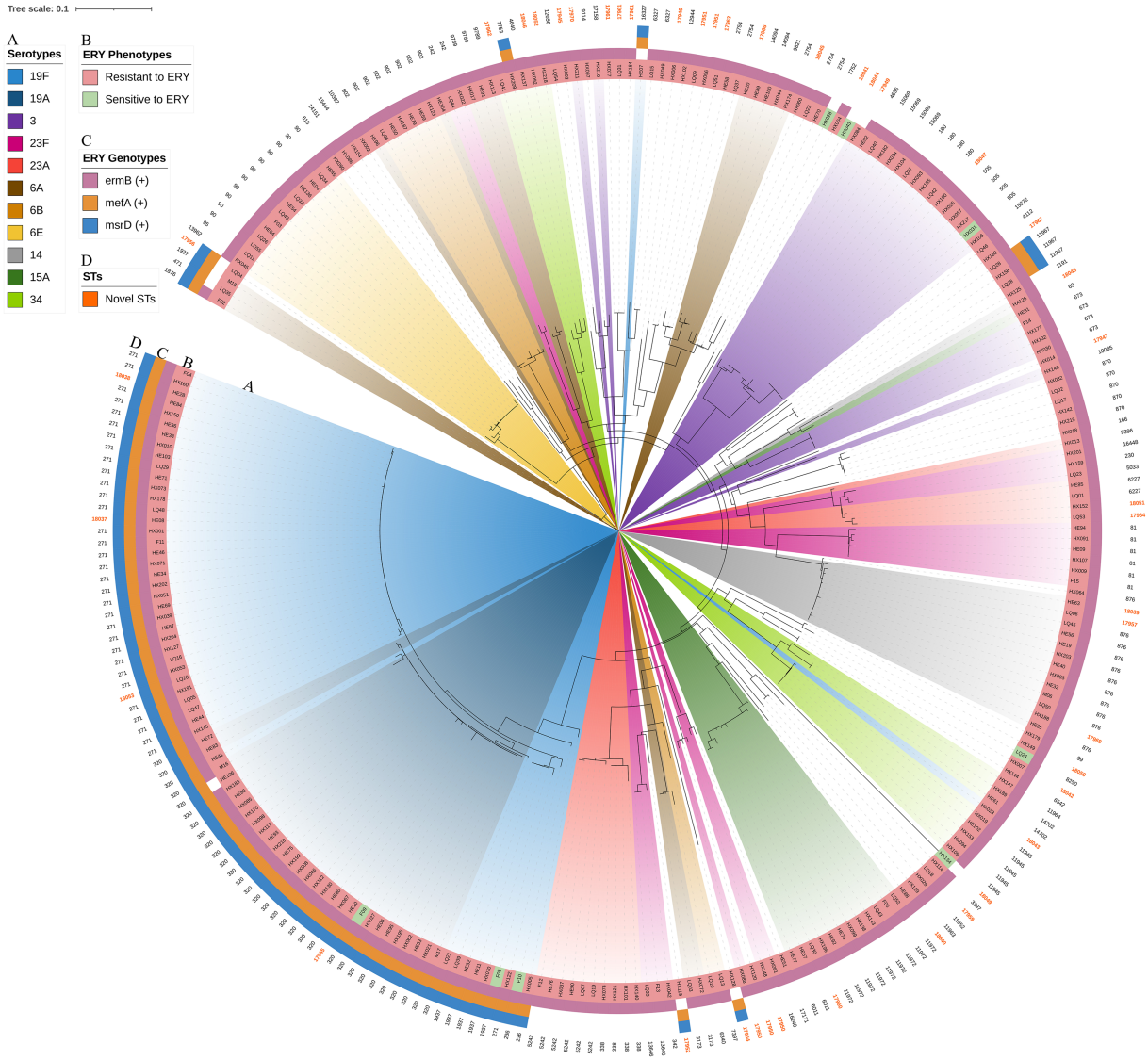

FIGURE 9
The relationship among erythromycin resistance phenotypes, erythromycin resistance genes, STs and serotypes. The RAxML tree was annotated with strain number, serotypes, erythromycin resistance phenotypes, erythromycin resistance genes (*msrD*, *MefA* and *ermB*) and STs. Erythromycin resistance genes manifested as an aggregation phenomenon. **(A)** Serotypes with a proportion greater than 3%. **(B)** Erythromycin resistance phenotypes. **(C)** Erythromycin resistance genes. **(D)** Novel STs were colored.

observed in China (76.0%) and Korea (64.0%) (Kim et al., 2020), much higher than that in other regions of the world, such as 40.8% in France and 42.9% in Greece (Niedzielski et al., 2013). Singapore (17.9%) and the Philippines (3.1%) have the lowest rates in 6 Asian countries (Kim et al., 2020). In this study, the rate of MDR was 53.99% (141/263). MDR *S. pneumoniae* is a growing concern because the infecting strains are resistant to standard treatments with beta-lactams and macrolides.

In this study, several associations were found between serotype, ST, and antibiotic susceptibility. The dominant STs of serotype 19F, 19A, 23F and 14 isolates were ST271, ST320, ST81, and ST876, respectively, which was similar to previously reported results (Li et al., 2018). Isolates 19F/ST271 and 19A/ST320, as the predominant prevalent strains in this region, were more resistant to AMX, CTX, MEM and SXT. In terms of the distribution of antibiotic resistance among serotypes, serotypes 19F, 19A and 14 exhibited higher resistance rates, while serotype 3 showed a relatively low rate. The high level of resistance among serotypes may be related to widespread international spread of their STs. In this study, serotype 3 had a high clonal diversity, as dominated by ST180 (17.39%), ST505 (17.39%), ST15069 (17.39%) and ST180 (17.39%). A study that performed whole-genome sequencing of 616 strains of serotype 3 from England and Wales found that the composition of their clade changed with antibiotic resistance (Groves et al., 2019). These findings confirm the importance and utility of routine whole-genome sequencing and its ability to identify novel variants, which provides a basis for surveillance and will influence future vaccine development.

Children and the elderly are most vulnerable to *S. pneumoniae* infection. A global study of disease burden showed that infectious syndromes caused by bacterial pathogens pose an enormous threat to

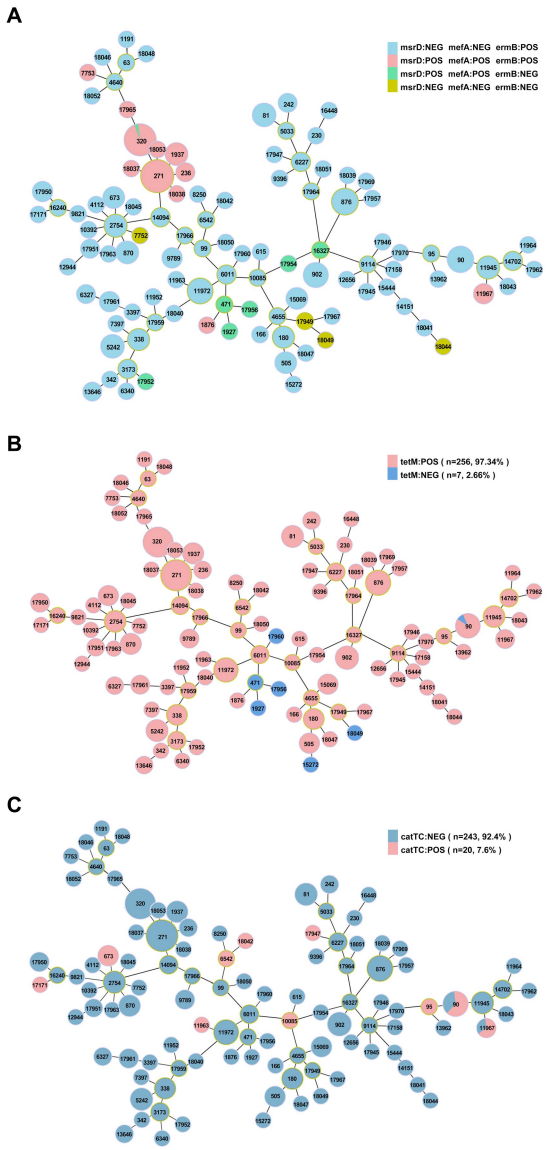

FIGURE 10
The relationship between antibiotic resistance genes and ST. **(A)** Minimum spanning tree-like structure showing the ST aggregation phenomenon of the erythromycin resistance genes *msrD*, *MefA* and *ermB*. **(B)** The relationship between the tetracycline resistance gene *tetM* and ST. **(C)** The relationship between the chloramphenicol resistance gene *catTC* and ST.

public health, with *S. pneumoniae* ranking among the top (Ikuta et al., 2022). Our study is the first to perform whole-genome sequencing of *S. pneumoniae* from PD patients of all ages in multiple centers in Southwest China. The total area of the southwestern region reaches 2.3406 million square kilometers, accounting for 24.5% of China's land area. Its population and area are approximately half of those of the European Union.[12] Thus, these research results are representative of the prevalence of *S. pneumoniae* in China. We discovered many novel ST types, and the whole-genome data can provide a basis for future research. In addition, the study incorporated data during the COVID-19 pandemic. As COVID-19 containment policies likely affected the spread of respiratory pathogens such as *S. pneumoniae* (Brueggemann et al., 2021), the molecular characterization in this study provides important support for the current status of PD and potential changes in subsequent isolates. However, it also has two limitations. First, this is a study in Southwest China and lacks research data from other regions. Second, our analysis of whole-genome data was not absolutely sufficient, prompting us to conduct more in-depth and correlation analyses in the future.

Overall, our study provides valuable insight into the prevalence and antibiotic susceptibility of PD-causing *S. pneumoniae* strains in Southwest China. The most prevalent strains in this study were 19F, 19A, 3, 23F, 6A and 23A; the prevalent STs were ST271, ST320, ST90, ST876 and ST11972. All strains were susceptible to VAN and LNZ but highly resistant to macrolides (96.96%), and the high prevalence of MR and MDR is alarming. These data highlight the importance of appropriate use of antimicrobial agents and underscore the need to monitor pneumococcal epidemiology in China. Considering the relatively high coverage rate of PCV13 and the worrisome rates of antibiotic nonsusceptibility, PCV13 vaccination may be beneficial in this region.

Data availability statement

The datasets presented in this study are deposited in the MLST repository (https://pubmlst.org/bigsdb?db=pubmlst_spneumoniae_seqdef&page=query) under accession numbers: ST17945-ST17947, ST17949-ST17952, ST17954, ST17956-ST17957, ST17959-ST17967, ST17969, ST17970, and ST18037-ST18053.

Ethics statement

The studies involving humans were approved by the Clinical Trial Ethics Committee of West China Second University Hospital, Sichuan University. The studies were conducted in accordance with the local legislation and institutional requirements. The human samples used in this study were acquired from primarily isolated as part of your previous study for which ethical approval was obtained. Written informed consent for participation was not required from the participants or the participants' legal guardians/next of kin in accordance with the national legislation and institutional requirements.

Author contributions

CM: Data curation, Investigation, Software, Writing – original draft. ZY: Software, Writing – original draft, Funding acquisition, Methodology. CC: Software, Writing – original draft, Visualization. LK: Writing – original draft, Validation. KA: Validation, Writing – original draft. YL: Writing – original draft, Data curation. JL: Writing – original draft, Validation. XH: Writing – original draft, Investigation. XZ: Investigation, Writing – original draft. YZ: Writing – original draft, Visualization. YC: Funding acquisition, Methodology, Resources, Writing – review & editing. YJ: Funding acquisition, Resources,

12 https://ec.europa.eu/eurostat/web/main/home

Writing – review & editing, Conceptualization, Supervision. YX: Conceptualization, Resources, Supervision, Writing – review & editing.

Funding

The author(s) declare financial support was received for the research, authorship, and/or publication of this article. This work was supported by the National Natural Science Foundation of China (No. 82300015), the Sichuan Science and Technology Program (Nos. 24NSFSC3511, 2023YFS0222, 2023YFS0223, and 2023NSFSC1699), the Cadres Healthcare Research Projects in Sichuan Province (No. 2021-1703), the Science and Technology Innovation Project of Maternal and Child Medicine in Sichuan Province (No. 21FX025) and the West China Second University Hospital (No. KL066). The funders had no role in the study design, data collection analysis, and interpretation of the data.

Acknowledgments

We thank Dong Deng and Xiang Wang from West China Second Hospital, Sichuan University for their technical suggestions.

Conflict of interest

The authors declare that the research was conducted in the absence of any commercial or financial relationships that could be construed as a potential conflict of interest.

Publisher's note

Supplementary material

The Supplementary material for this article can be found online at: https://www.frontiersin.org/articles/10.3389/fmicb.2024.1342839/full#supplementary-material

References

Amin-Chowdhury, Z., Aiano, F., Mensah, A., Sheppard, C. L., Litt, D., Fry, N. K., et al. (2021). Impact of the coronavirus disease 2019 (COVID-19) pandemic on invasive pneumococcal disease and risk of pneumococcal coinfection with severe acute respiratory syndrome coronavirus 2 (SARS-CoV-2): prospective National Cohort Study, England. *Clin. Infect. Dis.* 72, e65–e75. doi: 10.1093/cid/ciaa1728

Berbel, D., González-Díaz, A., López de Egea, G., Càmara, J., and Ardanuy, C. (2022). An overview of macrolide resistance in streptococci: prevalence, mobile elements and dynamics. *Microorganisms* 10:2316. doi: 10.3390/microorganisms10122316

Brueggemann, A. B., Jansen van Rensburg, M. J., Shaw, D., McCarthy, N. D., Jolley, K. A., Maiden, M. C. J., et al. (2021). Changes in the incidence of invasive disease due to *Streptococcus pneumoniae*, Haemophilus influenzae, and *Neisseria meningitidis* during the COVID-19 pandemic in 26 countries and territories in the invasive respiratory infection surveillance initiative: a prospective analysis of surveillance data. *Lancet Digit Health.* 3, e360–e370. doi: 10.1016/S2589-7500(21)00077-7

Chan, J., Nguyen, C. D., Dunne, E. M., Kim Mulholland, E., Mungun, T., Pomat, W. S., et al. (2019). Using pneumococcal carriage studies to monitor vaccine impact in low- and middle-income countries. *Vaccine* 37, 6299–6309. doi: 10.1016/j.vaccine.2019.08.073

Cui, Y., Miao, C., Chen, W., Shang, W., Qi, Q., Zhou, W., et al. (2022). Construction and protective efficacy of a novel *Streptococcus pneumoniae* fusion protein vaccine NanAT1-TufT1-PlyD4. *Front. Immunol.* 13:1043293. doi: 10.3389/fimmu.2022.1043293

Farrell, D. J., Couturier, C., and Hryniewicz, W. (2008). Distribution and antibacterial susceptibility of macrolide resistance genotypes in *Streptococcus pneumoniae*: PROTEKT year 5 (2003-2004). *Int. J. Antimicrob. Agents* 31, 245–249. doi: 10.1016/j.ijantimicag.2007.10.022

Feil, E. J., Li, B. C., Aanensen, D. M., Hanage, W. P., and Spratt, B. G. (2004). eBURST: inferring patterns of evolutionary descent among clusters of related bacterial genotypes from multilocus sequence typing data. *J. Bacteriol.* 186, 1518–1530. doi: 10.1128/JB.186.5.1518-1530.2004

Feldgarden, M., Brover, V., Haft, D. H., Prasad, A. B., Slotta, D. J., Tolstoy, I., et al. (2019). Validating the AMRFinder tool and resistance gene database by using antimicrobial resistance genotype-phenotype correlations in a collection of isolates. *Antimicrob. Agents Chemother.* 63, e00483–e00419. doi: 10.1128/AAC.00483-19

Felmingham, D., Cantón, R., and Jenkins, S. G. (2007). Regional trends in beta-lactam, macrolide, fluoroquinolone and telithromycin resistance among *Streptococcus pneumoniae* isolates 2001-2004. *J. Infect.* 55, 111–118. doi: 10.1016/j.jinf.2007.04.006

Francisco, A. P., Vaz, C., Monteiro, P. T., Melo-Cristino, J., Ramirez, M., and Carriço, J. A. (2012). PHYLOViZ: phylogenetic inference and data visualization for sequence based typing methods. *BMC Bioinformatics* 13:87. doi: 10.1186/1471-2105-13-87

Ganaie, F., Saad, J. S., McGee, L., van Tonder, A. J., Bentley, S. D., Lo, S. W., et al. (2020). A new pneumococcal capsule type, 10D, is the 100th serotype and has a large cps fragment from an oral streptococcus. *mBio* 11:e00937-20. doi: 10.1128/mBio.00937-20

Goettler, D., Streng, A., Kemmling, D., Schoen, C., von Kries, R., Rose, M. A., et al. (2020). Increase in *Streptococcus pneumoniae* serotype 3 associated parapneumonic pleural effusion/empyema after the introduction of PCV13 in Germany. *Vaccine* 38, 570–577. doi: 10.1016/j.vaccine.2019.10.056

Groves, N., Sheppard, C. L., Litt, D., Rose, S., Silva, A., Njoku, N., et al. (2019). Evolution of *Streptococcus pneumoniae* serotype 3 in England and Wales: a major vaccine evader. *Genes* 10:845. doi: 10.3390/genes10110845

Hanquet, G., Krizova, P., Dalby, T., Ladhani, S. N., Nuorti, J. P., Danis, K., et al. (2022). Serotype replacement after introduction of 10-valent and 13-valent pneumococcal conjugate vaccines in 10 countries, Europe. *Emerg. Infect. Dis.* 28, 137–138. doi: 10.3201/eid2801.210734

Humphries, R., Bobenchik, A. M., Hindler, J. A., and Schuetz, A. N. (2021). Overview of changes to the clinical and laboratory standards institute performance standards for antimicrobial susceptibility testing, M100, 31st edition. *J. Clin. Microbiol.* 59:e0021321. doi: 10.1128/JCM.00213-21

Hyams, C., Challen, R., Hettle, D., Amin-Chowdhury, Z., Grimes, C., Ruffino, G., et al. (2023). Serotype distribution and disease severity in adults hospitalized with *Streptococcus pneumoniae* infection, Bristol and Bath, UK, 2006–2022. *Emerg. Infect. Dis.* 29, 1953–1964. doi: 10.3201/eid2910.230519

Ikuta, K. S., Swetschinski, L. R., Aguilar, G. R., Sharara, F., Mestrovic, T., Gray, A. P., et al. (2022). Global mortality associated with 33 bacterial pathogens in 2019: a systematic analysis for the Global Burden of Disease Study 2019. *Lancet* 400, 2221–2248. doi: 10.1016/S0140-6736(22)02185-7

Ip, M., Lyon, D. J., Leung, T., and Cheng, A. F. (2002). Macrolide resistance and distribution of ERM and MEF genes among beta-haemolytic streptococci in Hong Kong. *Eur. J. Clin. Microbiol. Infect. Dis.* 21, 238–240. doi: 10.1007/s10096-001-0686-9

Johnson, H. L., Deloria-Knoll, M., Levine, O. S., Stoszek, S. K., Freimanis Hance, L., Reithinger, R., et al. (2010). Systematic evaluation of serotypes causing invasive pneumococcal disease among children under five: the pneumococcal global serotype project. *PLoS Med.* 7:e1000348. doi: 10.1371/journal.pmed.1000348

Jolley, K. A., and Maiden, M. C. (2010). BIGSdb: scalable analysis of bacterial genome variation at the population level. *BMC Bioinformatics* 11:595. doi: 10.1186/1471-2105-11-595

Jung, B., Park, S. Y., Lee, Y. W., and Lee, J. (2013). Biological efficacy of *Streptomyces* sp. strain BN1 against the cereal head blight pathogen fusarium graminearum. *Plant Pathol. J.* 29, 52–58. doi: 10.5423/PPJ.OA.07.2012.0113

Kapatai, G., Sheppard, C. L., Al-Shahib, A., Litt, D. J., Underwood, A. P., Harrison, T. G., et al. (2016). Whole genome sequencing of *Streptococcus pneumoniae*: development, evaluation and verification of targets for serogroup and serotype prediction using an automated pipeline. *PeerJ* 4:e2477. doi: 10.7717/peerj.2477

Kim, S. H., Chung, D. R., Song, J. H., Baek, J. Y., Thamlikitkul, V., Wang, H., et al. (2020). Changes in serotype distribution and antimicrobial resistance of *Streptococcus pneumoniae* isolates from adult patients in Asia: emergence of drug-resistant non-vaccine serotypes. *Vaccine* 38, 6065–6073. doi: 10.1016/j.vaccine.2019.09.065

Kim, S. H., Song, J. H., Chung, D. R., Thamlikitkul, V., Yang, Y., Wang, H., et al. (2012). Changing trends in antimicrobial resistance and serotypes of *Streptococcus pneumoniae* isolates in Asian countries: an Asian network for surveillance of resistant pathogens (ANSORP) study. *Antimicrob. Agents Chemother.* 56, 1418–1426. doi: 10.1128/AAC.05658-11

Li, L., Fu, J., Li, S., Guo, D., Chen, Z., Chen, S., et al. (2018). Phenotypic and molecular characterization of *Streptococcus pneumoniae* in pre-conjugate vaccine era: a Chinese hospital-based retrospective study. *Vaccine* 36, 599–605. doi: 10.1016/j.vaccine.2017.12.063

Li, L., Ma, J., Yu, Z., Li, M., Zhang, W., and Sun, H. (2023). Epidemiological characteristics and antibiotic resistance mechanisms of *Streptococcus pneumoniae*: an updated review. *Microbiol. Res.* 266:127221. doi: 10.1016/j.micres.2022.127221

Lo, S. W., Mellor, K., Cohen, R., Alonso, A. R., Belman, S., Kumar, N., et al. (2022). Emergence of a multidrug-resistant and virulent *Streptococcus pneumoniae* lineage mediates serotype replacement after PCV13: an international whole-genome sequencing study. *Lancet Microbe* 3, e735–e743. doi: 10.1016/S2666-5247(22)00158-6

Lu, B., Fang, Y., Fan, Y., Chen, X., Wang, J., Zeng, J., et al. (2017). High prevalence of macrolide-resistance and molecular characterization of *Streptococcus pyogenes* isolates circulating in China from 2009 to 2016. *Front. Microbiol.* 8:1052. doi: 10.3389/fmicb.2017.01052

Marrie, T. J., Tyrrell, G. J., Majumdar, S. R., and Eurich, D. T. (2018). Effect of age on the manifestations and outcomes of invasive pneumococcal disease in adults. *Am. J. Med.* 131, 100.e1–100.e7. doi: 10.1016/j.amjmed.2017.06.039

Men, W., Dong, Q., Shi, W., and Yao, K. (2020). Serotype distribution and antimicrobial resistance patterns of invasive pneumococcal disease isolates from children in mainland China-a systematic review. *Braz. J. Microbiol.* 51, 665–672. doi: 10.1007/s42770-019-00198-9

Mitsi, E., Reine, J., Urban, B. C., Solorzano, C., Nikolaou, E., Hyder-Wright, A. D., et al. (2022). *Streptococcus pneumoniae* colonization associates with impaired adaptive immune responses against SARS-CoV-2. *J. Clin. Invest.* 132:e157124. doi: 10.1172/JCI157124

Moreno, J., Duarte, C., Cassiolato, A. P., Chacón, G. C., Alarcon, P., Sánchez, J., et al. (2020). Molecular characterization of Latin American invasive *Streptococcus pneumoniae* serotype 19A isolates. *Vaccine* 38, 3524–3530. doi: 10.1016/j.vaccine.2020.03.030

Namkoong, H., Ishii, M., Funatsu, Y., Kimizuka, Y., Yagi, K., Asami, T., et al. (2016). Theory and strategy for pneumococcal vaccines in the elderly. *Hum. Vaccin. Immunother.* 12, 336–343. doi: 10.1080/21645515.2015.1075678

Niedzielski, A., Korona-Glowniak, I., and Malm, A. (2013). High prevalence of *Streptococcus pneumoniae* in adenoids and nasopharynx in preschool children with recurrent upper respiratory tract infections in Poland--distribution of serotypes and drug resistance patterns. *Med. Sci. Monit.* 19, 54–60. doi: 10.12659/msm.883742

O'Brien, K. L., Wolfson, L. J., Watt, J. P., Henkle, E., Deloria-Knoll, M., McCall, N., et al. (2009). Burden of disease caused by *Streptococcus pneumoniae* in children younger than 5 years: global estimates. *Lancet* 374, 893–902. doi: 10.1016/S0140-6736(09)61204-6

Page, A. J., Cummins, C. A., Hunt, M., Wong, V. K., Reuter, S., Holden, M. T., et al. (2015). Roary: rapid large-scale prokaryote pan genome analysis. *Bioinformatics* 31, 3691–3693. doi: 10.1093/bioinformatics/btv421

Prjibelski, A., Antipov, D., Meleshko, D., Lapidus, A., and Korobeynikov, A. (2020). Using SPAdes De novo assembler. *Curr. Protoc. Bioinformatics* 70:e102. doi: 10.1002/cpbi.102

Qu, J., Zhou, J., and Yu, Y. (2017). Chinese expert consensus on pathogen detection in bronchoalveolar lavage for pulmonary infectious diseases (2017 edition). *Chinese J. Tuberc. Respirat. Dis.* 40, 578–583. doi: 10.3760/cma.j.issn.1001-0939.2017.08.007

Richter, S. S., Diekema, D. J., Heilmann, K. P., Dohrn, C. L., Riahi, F., and Doern, G. V. (2014). Changes in pneumococcal serotypes and antimicrobial resistance after introduction of the 13-valent conjugate vaccine in the United States. *Antimicrob. Agents Chemother.* 58, 6484–6489. doi: 10.1128/AAC.03344-14

Seemann, T. (2014). Prokka: rapid prokaryotic genome annotation. *Bioinformatics* 30, 2068–2069. doi: 10.1093/bioinformatics/btu153

Song, J. H., Jung, S. I., Ko, K. S., Kim, N. Y., Son, J. S., Chang, H. H., et al. (2004). High prevalence of antimicrobial resistance among clinical *Streptococcus pneumoniae* isolates in Asia (an ANSORP study). *Antimicrob. Agents Chemother.* 48, 2101–2107. doi: 10.1128/AAC.48.6.2101-2107.2004

Stamatakis, A. (2014). RAxML version 8: a tool for phylogenetic analysis and post-analysis of large phylogenies. *Bioinformatics* 30, 1312–1313. doi: 10.1093/bioinformatics/btu033

Suaya, J. A., Mendes, R. E., Sings, H. L., Arguedas, A., Reinert, R. R., Jodar, L., et al. (2020). *Streptococcus pneumoniae* serotype distribution and antimicrobial nonsusceptibility trends among adults with pneumonia in the United States, 2009–2017. *J. Infect.* 81, 557–566. doi: 10.1016/j.jinf.2020.07.035

Swartz, M. N. (2002). Attacking the pneumococcus -- a hundred years' war. *N. Engl. J. Med.* 346:722. doi: 10.1056/NEJM200203073461002

Tsuzuki, S., Akiyama, T., Matsunaga, N., Yahara, K., Shibayama, K., Sugai, M., et al. (2020). Improved penicillin susceptibility of *Streptococcus pneumoniae* and increased penicillin consumption in Japan, 2013-18. *PLoS One* 15:e0240655. doi: 10.1371/journal.pone.0240655

Vorobieva S Jensen, V., Furberg, A.-S., Slotved, H.-C., Bazhukova, T., Haldorsen, B., Caugant, D. A., et al. (2020). Epidemiological and molecular characterization of *Streptococcus pneumoniae* carriage strains in pre-school children in Arkhangelsk, northern European Russia, prior to the introduction of conjugate pneumococcal vaccines. *BMC Infect. Dis.* 20:279. doi: 10.1186/s12879-020-04998-5

Wang, C. Y., Chen, Y. H., Fang, C., Zhou, M. M., Xu, H. M., Jing, C. M., et al. (2019). Antibiotic resistance profiles and multidrug resistance patterns of *Streptococcus pneumoniae* in pediatrics: a multicenter retrospective study in mainland China. *Medicine (Baltimore)* 98:e15942. doi: 10.1097/MD.0000000000015942

Wang, X., Cong, Z., Huang, W., and Li, C. (2020). Molecular characterization of *Streptococcus pneumoniae* isolated from pediatric patients in Shanghai, China. *Pediatr. Pulmonol.* 55, 2135–2141. doi: 10.1002/ppul.24877

Wang, Q., Shi, W., Li, Y., Gao, W., Yuan, L., Dong, F., et al. (2020). Serotype distribution of *Streptococcus pneumoniae* isolated from children hospitalized in Beijing children's hospital (2013-2019). *Vaccine* 38, 7858–7864. doi: 10.1016/j.vaccine.2020.10.005

Wang, J., Wu, Q. S., Lu, J., Ni, Y. H., and Zhou, F. (2021). Low vaccination coverage of pneumococcal conjugate vaccines (PCVs) in Shanghai, China: a database analysis based on birth cohorts from 2012 to 2020. *Vaccine* 39, 6189–6194. doi: 10.1016/j.vaccine.2021.09.011

Widdowson, C. A., and Klugman, K. P. (1998). The molecular mechanisms of tetracycline resistance in the pneumococcus. *Microb. Drug Resist.* 4, 79–84. doi: 10.1089/mdr.1998.4.79

Widdowson, C. A., Klugman, K. P., and Hanslo, D. (1996). Identification of the tetracycline resistance gene, tet(O), in *Streptococcus pneumoniae*. *Antimicrob. Agents Chemother.* 40, 2891–2893. doi: 10.1128/AAC.40.12.2891

Yan, Z., Cui, Y., Huang, X., Lei, S., Zhou, W., Tong, W., et al. (2021). Molecular characterization based on whole-genome sequencing of *Streptococcus pneumoniae* in children living in Southwest China during 2017-2019. *Front. Cell. Infect. Microbiol.* 11:726740. doi: 10.3389/fcimb.2021.726740

Yan, Z., Cui, Y., Zhou, W., Li, W., Tan, X., Chen, W., et al. (2019). Molecular characterization of *Streptococcus pneumoniae* in children living in Southwest China and assessment of a potential protein vaccine, rPfbA. *Vaccine* 37, 721–731. doi: 10.1016/j.vaccine.2018.12.021

Yu, Y. Y., Xie, X. H., Ren, L., Deng, Y., Gao, Y., Zhang, Y., et al. (2019). Epidemiological characteristics of nasopharyngeal *Streptococcus pneumoniae* strains among children with pneumonia in Chongqing, China. *Sci. Rep.* 9:3324. doi: 10.1038/s41598-019-40088-6

Zeng, Y., Song, Y., Cui, L., Wu, Q., Wang, C., Coelho, A. C., et al. (2023). Phylogenomic insights into evolutionary trajectories of multidrug resistant *S. pneumoniae* CC271 over a period of 14 years in China. *Genome Med.* 15:46. doi: 10.1186/s13073-023-01200-8

Zhao, W., Pan, F., Wang, B., Wang, C., Sun, Y., Zhang, T., et al. (2019). Epidemiology characteristics of *Streptococcus pneumoniae* from children with pneumonia in Shanghai: a retrospective study. *Front. Cell. Infect. Microbiol.* 9:258. doi: 10.3389/fcimb.2019.00258

Zhao, C., Xie, Y., Zhang, F., Wang, Z., Yang, S., Wang, Q., et al. (2020). Investigation of antibiotic resistance, serotype distribution, and genetic characteristics of 164 invasive *Streptococcus pneumoniae* from North China between April 2016 and October 2017. *Infect. Drug Resist.* 13, 2117–2128. doi: 10.2147/IDR.S256663

Zhao, C., Zhang, F., Chu, Y., Liu, Y., Cao, B., Chen, M., et al. (2013). Phenotypic and genotypic characteristic of invasive pneumococcal isolates from both children and adult patients from a multicenter surveillance in China 2005-2011. *PLoS One* 8:e82361. doi: 10.1371/journal.pone.0082361

Zhou, X., Liu, J., Zhang, Z., Cui, B., Wang, Y., Zhang, Y., et al. (2022). Characterization of *Streptococcus pneumoniae* macrolide resistance and its mechanism in Northeast China over a 20-year period. *Microbiol. Spectr.* 10:e0054622. doi: 10.1128/spectrum.00546-22

Zhou, L., Ma, X., Gao, W., Yao, K. H., Shen, A. D., Yu, S. J., et al. (2012). Molecular characteristics of erythromycin-resistant *Streptococcus pneumoniae* from pediatric patients younger than five years in Beijing, 2010. *BMC Microbiol.* 12:228. doi: 10.1186/1471-2180-12-228

frontiers | Frontiers in Microbiology

TYPE Original Research
PUBLISHED 17 April 2024
DOI 10.3389/fmicb.2024.1383989

OPEN ACCESS

EDITED BY
Vijay Soni,
NewYork-Presbyterian, United States

REVIEWED BY
Tripti Nair,
University of Southern California, United States
Biplab Singha,
University of Massachusetts Medical School, United States

*CORRESPONDENCE
B. R. M. Vyas
✉ brmvyas@hotmail.com

RECEIVED 08 February 2024
ACCEPTED 18 March 2024
PUBLISHED 17 April 2024

CITATION
Handa VL, Patel BN, Bhattacharya A, Kothari RK, Kavathia G and Vyas BRM (2024) A study of antibiotic resistance pattern of clinical bacterial pathogens isolated from patients in a tertiary care hospital. *Front. Microbiol.* 15:1383989. doi: 10.3389/fmicb.2024.1383989

A study of antibiotic resistance pattern of clinical bacterial pathogens isolated from patients in a tertiary care hospital

Vishal L. Handa[1], Bhoomi N. Patel[1], Dr. Arpita Bhattacharya[2], Ramesh K. Kothari[1], Dr. Ghanshyam Kavathia[2] and B. R. M. Vyas[1]*

[1]Department of Biosciences, Saurashtra University, Rajkot, Gujarat, India, [2]Department of Microbiology, Pandit Deendayal Upadhyay Medical College, Rajkot, Gujarat, India

We investigated antibiotic resistance pattern in clinical bacterial pathogens isolated from in-patients and out-patients, and compared it with non-clinical bacterial isolates. 475 bacterial strains isolated from patients were examined for antibiotic resistance. *Staphylococcus* spp. (148; 31.1%) were found to be the most prevalent, followed by *Klebsiella pneumoniae* (135; 28.4%), *Escherichia coli* (74; 15.5%), *Pseudomonas aeruginosa* (65; 13.6%), *Enterobacter* spp. (28; 5.8%), and *Acinetobacter* spp. (25; 5.2%). Drug-resistant bacteria isolated were extended spectrum-β-lactamase *K. pneumoniae* (8.8%), *E. coli* (20%), metallo-β-lactamase *P. aeruginosa* (14; 2.9%), erythromycin-inducing clindamycin resistant (7.4%), and methicillin-resistant *Staphylococcus* species (21.6%). Pathogens belonging to the Enterobacteriaceae family were observed to undergo directional selection developing resistance against antibiotics ciprofloxacin, piperacillin-tazobactam, cefepime, and cefuroxime. Pathogens in the surgical ward exhibited higher levels of antibiotic resistance, while non-clinical *P. aeruginosa* and *K. pneumoniae* strains were more antibiotic-susceptible. Our research assisted in identifying the drugs that can be used to control infections caused by antimicrobial resistant bacteria in the population and in monitoring the prevalence of drug-resistant bacterial pathogens.

KEYWORDS

antimicrobial resistance, extended spectrum-β-lactamase, methicillin-resistant *Staphylococcus aureus*, metallo-β-lactamase, erythromycin-induced clindamycin resistance

1 Introduction

Development and spread of antimicrobial resistance (AMR) in pathogenic bacteria is a global problem. According to GBD, 33 bacterial diseases were responsible for 7.7 million deaths worldwide (Ikuta et al., 2022). The proportion of animals infected with drug-resistant bacteria increased by 50% during 2000–2018, limiting the number of available treatments (Van Boeckel et al., 2019). Antibiotics used for treating lower respiratory tract infections in children grew by 46% globally during 2000–2018 (Browne et al., 2021). The top six antibiotic-resistant bacteria causing human deaths in the United States of America are *Escherichia coli*, *Streptococcus pneumoniae*, *Staphylococcus aureus*, *Acinetobacter baumannii*, *Klebsiella pneumoniae*, and *Pseudomonas aeruginosa* (CDC, 2019). According to the

United States Center for Disease Control and Prevention, there are 2.8 million cases of infections and 35,000 deaths caused by antibiotic resistant bacteria yearly, in the country. The extended spectrum-β-lactamase (ESBL) Enterobacteriaceae, methicillin-resistant *Staphylococcus aureus* (MRSA), vancomycin-resistant *Enterococcus*, and drug-resistant *Mycobacterium tuberculosis* are considered severe threats to human lives (CDC, 2019). MRSA-related death rate of 39.1% in middle-income and 32.1% in high-income countries, was reported by Bai et al. (2022). Natural selection facilitates the evolution of antibiotic resistance in bacteria especially in antibiotic-contaminated aquatic environments, which serve as routes for the spread of resistant bacteria to livestock, poultry, humans, and other animals (Baquero et al., 2021; Larsson and Flach, 2022). High antibiotic use, fixed-dose combinations, self-medication, access to antibiotics without a prescription from a doctor, poor management of industrial effluent treatment plants, lack of hygenic condition, and inefficient infection control procedures in healthcare, are some of the factors contributing to India's high AMR proportions (Gandra et al., 2017). Carbapenem and colistin-resistant *K. pneumoniae* was responsible for 69% death rate in India during 2011–2015 (Kaur et al., 2017). Bacteria isolated from soil and water samples near pharmaceutical industrial areas in Hyderabad revealed up to 70% resistance against cephalosporin antibiotics (Britto et al., 2019). In 2015, the cephalosporins were most frequently used in India, followed by penicillins and fluoroquinolones; majority of pathogenic bacteria isolated were resistant to cephalosporins, followed by fluoroquinolones and penicillins (Klein et al., 2019). *Escherichia coli* isolated from domestic (25%) and hospital wastes (95%) were observed to be resistant to third-generation cephalosporins (Akiba et al., 2015).

In this study, we aimed to provide descriptive data on infections and patterns of antibiotic resistance of the top six bacterial pathogens in Pandit Deendayal Upadhyay (PDU) Medical College and Hospital Rajkot, Gujarat. We looked for an answer to the crucial medical query "Does the pattern of antibiotic resistance of bacterial infections vary with isolation sources?" We also intended to compare the prevailing patterns of antibiotic resistance in clinical and non-clinical strains of *P. aeruginosa* and *K. pneumoniae*. We also focused on erythromycin-induced clindamycin resistance (EICR) and MRSA in *Staphylococcus* species and ESBL and metallo-β-lactamase (MBL) in Gram-negative bacteria.

2 Materials and methods

2.1 Location and context of the study

The PDU Medical College/Hospital is a tertiary care and teaching hospital that provides a full range of health care services, including medical, surgical, and superspecialty services, to patients in and around Rajkot district. In a 100-km radius of Rajkot, there is only one multispeciality government hospital. Every day, more than 400 patients load from Rajkot city as well as rural areas of Rajkot district. Also, people from Amreli, Jamnagar, Junagadh, Kachchh, Morbi, Porbandar, Surendranagar, and Veraval visit PDU Medical College/Hospital Rajkot for treatments. PDU Medical College/Hospital is located in the center of the Saurashtra region in Rajkot, Gujarat.

2.2 Sample collection and isolation of pathogens

Based on the data of the past 6 months, we selected the six most commonly reported pathogens from hospitalized and outpatient specimens, including *Pseudomonas aeruginosa*, *Escherichia coli*, *Enterobacter* spp., *Klebsiella pneumoniae*, *Staphylococcus* spp., and *Acinetobacter* spp. The top six most frequently observed bacterial strains were selected for the present study. Samples were collected during March to June 2022 from the in-patients and out-patients at PDU Medical College/Hospital in Rajkot, Gujarat. Samples were collected in sterile containers according to Cheesbrough (2005) in various wards by the assigned clinicians, and they were processed further at the bacteriology lab immediately. Preservation and storage of specimens varied from place to place and time to time; for example, blood, urine, and sputum were stored until the analysis and discussion with the assigned doctor. While for precious specimens like postoperative samples, body fluids were stored for 7–10 days, etc. Gender, age, ward, collection date, specimens, and other information were noted along with the sample collection. Ten samples were randomly selected daily for this survey, conducted for 3 months. PEEKSA (*Pseudomonas aeruginosa*, *Escherichia coli*, *Enterobacter* spp., *Klebsiella pneumoniae*, *Staphylococcus* spp. and *Acinetobacter* spp) were isolated from the collected samples (CLSI, 2018). Blood samples collected from adult patients (10–20 mL) and pediatric patients (5–10 mL) were mixed in brain heart infusion broth bottles and analyzed for bacterial growth up to 7 days using automated blood culture system BD-BACTEC FX40 (United States) (Procop et al., 2020). Absence of turbidity after 7 days was considered negative. Positive samples were subcultured on blood agar, nutrient agar, and MacConkey agar plates. Urine samples (20–30 mL) were collected in a sterile plastic container (50 mL capacity) and streaked on MacConkey agar, blood agar, cysteine lactose electrolyte deficient agar, and nutrient agar plates. Pus/swab samples were streaked on nutrient agar, blood agar, and MacConkey agar plates. Sputum samples (2–5 mL) were collected in a sterile plastic container (50 mL capacity) and streaked on chocolate agar, blood agar, nutrient agar, and MacConkey agar plates. The samples except blood were processed the same day; streaked plates were incubated at 35°C for 24–72 h and subcultured on nutrient agar plates. Bacterial identification was done based on colony morphology, biochemical tests, and the Gram reaction (Collee et al., 1996; Procop et al., 2020).

2.3 Antibiotic susceptibility test of bacterial isolates

Gram-positive and-negative bacterial isolates were evaluated for antibiotic susceptibility employing Kirby-Bauer disk-diffusion method (CLSI, 2018). A single colony was picked and suspended in sterile normal saline (0.85% NaCl) to generate the equivalent of 0.5 McFarland standard solution. 1 mL of bacterial suspension was mixed with 19 mL of sterile Muller-Hinton soft agar (45°C) and poured in Petri plates, incubated at 35°C for 24 h after the transfer of antibiotics disks by disk dispenser. PEEKSA isolates were classified as resistant, intermediate, and sensitive to antibiotics on the basis of the size of the zone of inhibition according to the Clinical Laboratory Standard Institute (CLSI) guidelines. Antibiotics used for antibiotic

susceptibility test of *Enterobacter* spp., *Klebsiella pneumoniae*, and *Escherichia coli* isolated from pus, swabs, sputum, and blood samples were ciprofloxacin (CIP), levofloxacin (LVX), gentamicin (GM), amikacin (AN), meropenem (MEM), cefuroxime (CXM), cefotaxime (CTX), ceftazidime (CAZ), ceftazidime-clavulanate (CAC), cefepime (FEP), piperacillin-tazobactam (TZP), trimethoprim-sulfamethoxazole (SXT), tetracycline (TE), and ampicillin-sulbactam (SAM). Strains isolated from urine samples were also evaluated for sensitivity against the antibiotics TR, NX, and NIT along with the above-mentioned antibiotics. Imipenem-EDTA (IE), imipenem (IPM), aztreonam (ATM), CIP, GM, LVX, AN, and FEP were employed for the evaluation of the antibiotic sensitivity of *Pseudomonas aeruginosa*. *Staphylococcus* spp. were against erythromycin (E), linezolid (LZD), CIP, rifamycin (RIF), clindamycin (CM), TE, vancomycin (VA), SXT, GM, chloramphenicol (C), meropenem (MEM), cefoxitin (FOX), and penicillin (P). Antibiotics class, abbreviation, and concentration in Supplementary Table S1.

2.4 Data processing and analysis

According to the CLSI recommendations, bacterial pathogens were classified as sensitive, intermediate, and resistant based on antibiotic susceptibility values (CLSI, 2022). Descriptive statistics such as relative abundance, percentage of categorical variation, and frequency were calculated. The chi-square test was used to compare the abundance of bacterial isolates with patient specimens. A Tukey *post-hoc* test was conducted for multiple comparisons between the mean values of the number of resistant antibiotics. *p* values less than 0.05 were considered statistically significant. Antibiotic resistance index (R_I) was derived by n/N where, "n" is number of resisrant isolates and "N" is the total number of isolates tested. Pearson's correlation analysis was studied between isolation source and its antibiotic resistance pattern (antibiotics that are tested more than 90% were used for the correlation study). Natural selection was determined by $(n/N) \times 100$, where "n" is the number of sensitive, intermediate, or resistant phenotypes expressed by each isolate and "N" is the total number of bacterial isolates.

3 Results

475 pathogenic bacterial strains isolated from 910 clinical samples were investigated for their antibiotic resistance patterns.

3.1 Prevalence of bacterial pathogens in clinical samples

475 clinical specimens in the present study exhibited bacterial growth; the majority (34%) of the 475 isolates originated from pus, followed by blood (24%), urine (20%), and sputum (13%), but other isolation sources were common for some pathogens (Figure 1A). The results of the chi-square test revealed that bacterial abundance in specimens was significantly different (p value <0.05 Pearson chi square test). The relative abundance of *Staphylococcus* spp. (148; 31%) were isolated most commonly from the collected specimen samples, i.e., 95 of the 148 isolates were observed to be prevalent in blood. *Klebsiella pneumoniae* (135; 28%) was the second most common isolate; that was most prevalent in pus and sputum specimens, 67 and 34, respectively. *Escherichia coli* (74; 15%) was prevalent in urine specimens 35. *Pseudomonas aeruginosa* (65; 14%) pus specimens 51 were most prevalent, followed by *Enterobacter* spp. (28; 6%), equally distributed in pus and sputum, and the majority of *Acinetobacter* spp. (25; 5%) from pus (Figure 1B). The most commonly tested (frequency > 0.9) antibiotics against all the studied bacterial pathogens were aminoglycosides, carbapenems, cephalosporins, and fluoroquinolones. Other classes of antibiotics were often tested for diverse infections; antifolates and tetracyclines were routinely tested against *Staphylococcus* spp., *K. pneumoniae*, *E. coli*, *Enterobacter* spp., *Acinetobacter* spp. except *P. aeruginosa*. Monobactam and lipopeptide-class antibiotics were tested only against *P. aeruginosa*, whereas macrolide, anisomycin, lincosamide, glycopeptide, etc. were tested against *Staphylococcus* spp. (Figure 1F). Patients were classified into three age groups, *viz*., 0–15 years (19%), 16–35 years (10%), >35 years (23%), and unknown age (49%) (Figure 1C; Table 1).

3.2 Antibiotic resistance index in bacterial pathogens

The penicillin resistance index (R_I) of *Staphylococcus* spp. was proportionately 1 (100%)and against ciprofloxacin, cefoxitin, and erythromycin was >0.8. Chloramphenicol was the most effective antibiotic against *Staphylococcus* spp. (Supplementary Figure S1A). *Pseudomonas aeruginosa* exhibited a 0.6 R_I to imipenem, ceftazidime, cefepime, and piperacillin-tazobactam. Imipenem-EDTA, and amikacin were most effective against *P. aeruginosa* (Supplementary Figure S1B). *Acinetobacter* spp. exhibited $R_I > 0.8$ against ciprofloxacin, gentamycin, ceftazidime, cefotaxime, piperacillin-tazobactam, ampicillin-sulbactam, and trimethoprim-sulfamethoxazole; however, meropenem resistance was <0.4 (Supplementary Figure S1C). *Klebsiella pneumoniae* exhibited high resistance against all antibiotics tested except tetracyclines (Supplementary Figure S1D). *Enterobacter* spp. exhibited a R_I of 0.5 to tetracyclines and amikacin but were more resistant (>0.6) to the other antibiotics (Supplementary Figure S1E). *Escherichia coli* was more sensitive to amikacin (<0.3), and highly resistant to other antibiotics (>0.7) (Supplementary Figure S1F). Similar report by Gupta et al. (2014) stated that uropathogenic *E. coli*, *Enterococcus faecalis*, *K. pneumoniae*, *Staphylococcus aureus*, *P. aeruginosa*, and *Proteus mirabilis* revealed ampicillin resistance up to 94–100%. Uropathogenic *E. coli* strains prevalent in Rajasthan, India, exhibited 95% resistance to nalidixic acid and 80% resistance to ampicillin and amoxiclav antibiotics (Sood and Gupta, 2012).

3.3 Does the antibiotic resistance pattern of bacterial pathogens vary with isolation sources?

Klebsiella pneumoniae spp. isolated from patients of medical and surgical wards exhibited a strong antibiotic-resistance correlation 0.85 (Table 2). Similarly, *K. pneumoniae* strains obtained from patients in medical ward and intensive care unit (ICU) exhibited antibiotic-resistance correlation 0.79. *Escherichia coli* isolates showed strong antibiotic-resistance correlation 0.96, 0.87, and 0.82 between the

10.3389/fmicb.2024.1383989

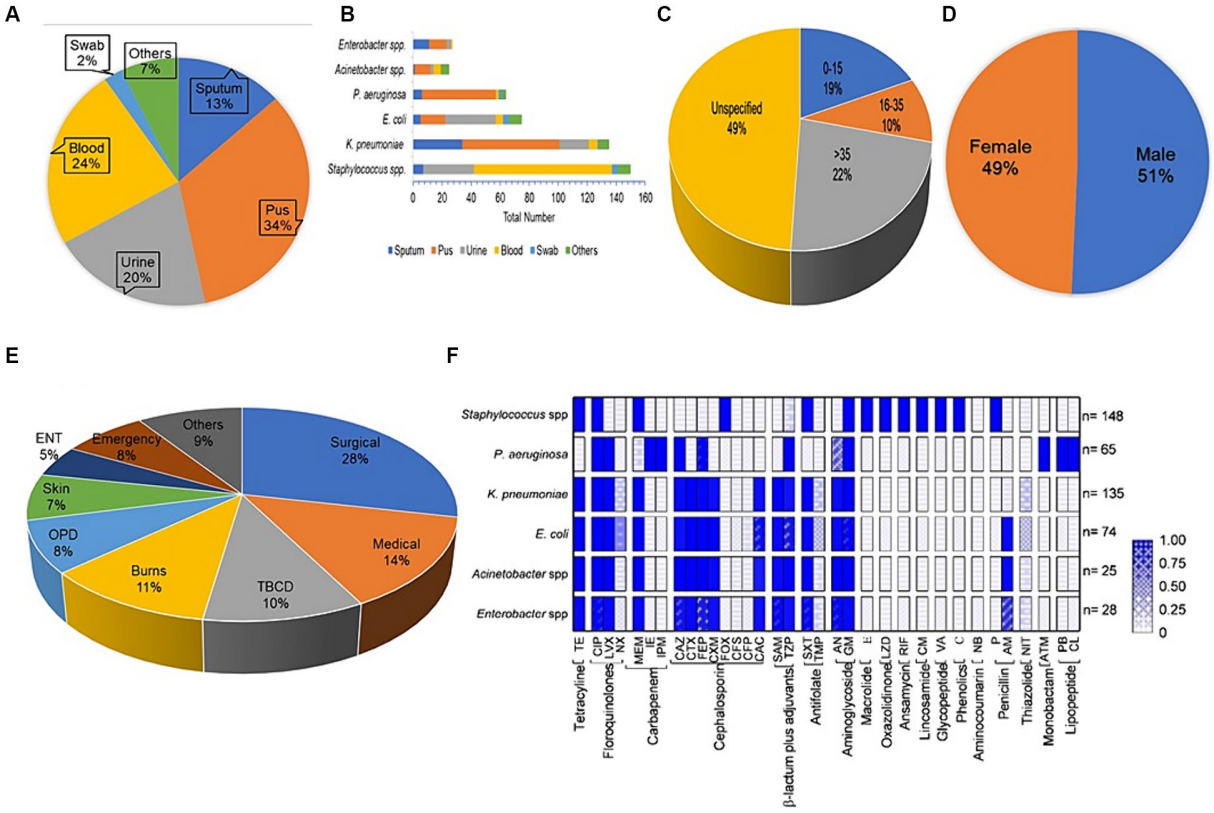

FIGURE 1
Datasets for antibiotic susceptibility tests. **(A)** Distribution of the specimens gathered for this investigation, **(B)** the source of the pathogenic bacterial strains, **(C)** Age-wise distribution of bacterial isolates, **(D)** Sample distributions by gender, **(E)** Prevalence of bacterial isolates in various wards of the hospital, **(F)** the frequency of testing for different antibiotics (grouped by antibiotic class) against bacterial strains.

TABLE 1 **Bacterial pathogens distribution with age group.**

Age group	*Enterobacter* spp.	*P. aeruginosa*	*Staphylococcus* spp.	*E. coli*	*K. pneumoniae*	*Acinetobacter* spp.
0–15	2	8	56	4	12	7
16–35	3	3	13	4	21	2
>35	8	17	24	28	25	5
Unspecified	15	37	55	38	77	11
Total	28	65	148	74	135	25

out-patient department (OPD) and medical ward, OPD and surgical ward, and surgical-medical wards, respectively. *Pseudomonas aeruginosa* isolated from skin-burns, skin-surgical, and burns-surgical wards, showed substantial antibiotic-resistance correlation of 0.97, 0.93, and 0.91, respectively. *Staphylococcus* spp. exhibited a strong antibiotic-resistance correlation 0.98 between medical and surgical wards, but a moderate antibiotic-resistance correlation 0.59 between Emergency and tuberculosis chest diseases (TBCD) wards. These findings strongly suggest that the antibiotic resistance patterns of the above-mentioned isolates were similar with respect to isolation sources. However, differences were also observed in the antibiotic resistance patterns of bacterial pathogens isolated from the patients of other wards; e.g., *K. pneumoniae* isolates revealed a weak antibiotic-resistance correlation 0.29 between burns and ICU wards. Similarly, *E. coli* exhibited an antibiotic-resistance correlation 0.30 between the ICU and medical ward and *P. aeruginosa* isolates showed antibiotic-resistance correlation 0.14 and 0.22 between the TBCD-ear nose throat (ENT) and burns-ENT wards, respectively (Kelch and Lee, 1978). There is ample published literature describing the antibiotic sensitivity phenotype of non-clinical *P. aeruginosa*, *E. coli*, *Enterobacter* spp., *K. pneumoniae*, and *Staphylococcus* spp. (Supplementary Table S2).

3.4 Changing antibiotic sensitivity phenotypes of pathogens

Klebsiella pneumoniae (102) and *Staphylococcus* (87) isolates were resistant to 6–10 tested antibiotics; *E. coli* (43) strains were resistant

TABLE 2 Antibiotic resistance correlation matrix for bacterial pathogens isolated from various wards of hospital.

K. pneumoniae	Medical	Surgical	ICU	TBCD	Burns				
Medical	1								
Surgical	0.85	1							
ICU	0.79	0.48	1						
TBCD	0.64	0.75	0.48	1					
Burns	0.65	0.73	0.29	0.70	1				
E. coli	Medical	Surgical	ICU	TBCD	OPD				
Medical	1								
Surgical	0.82	1							
ICU	0.30	0.46	1						
TBCD	0.77	0.57	0.14	1					
OPD	0.96	0.87	0.42	0.75	1				
P. aeruginosa	ENT	Surgical	TBCD	Burns	Emergency	Skin			
ENT	1								
Surgical	0.48	1							
TBCD	0.14	0.88	1						
Burns	0.22	0.91	0.87	1					
Emergency	0.76	0.86	0.65	0.75	1				
Skin	0.29	0.93	0.86	0.97	0.79	1			
Staphylococcus spp.	OPD	Children	Surgical	ICU	TBCD	Medical	Emergency	Skin	ENT
OPD	1								
Children	0.86	1							
Surgical	0.96	0.91	1						
ICU	0.89	0.91	0.91	1					
TBCD	0.86	0.77	0.79	0.78	1				
Medical	0.96	0.91	0.98	0.93	0.82	1			
Emergency	0.82	0.78	0.86	0.92	0.59	0.86	1		
Skin	0.95	0.87	0.94	0.84	0.82	0.95	0.74	1	
ENT	0.90	0.63	0.83	0.71	0.85	0.82	0.61	0.8434	1

ICU, Intensive care unit; TBCD, Tuberculosis chest disease; OPD, Out-patient department; ENT, Ear nose throat.

to >12 antibiotics; and *P. aeruginosa* (36) isolates were resistant to 4–6 antibiotics (Figure 2A). *Enterobacter* spp. and *E. coli* show 12 and 13 mean values for the number of resistant antibiotics, respectively. Whereas *P. aeruginosa* and *Staphylococcus* spp. only have four and six mean values for the number of antibiotic resistant. The mean values of number of resistant antibiotics (9) were not significant for *K. pneumoniae* and *Acinetobacter* spp. ($p = 0.80$). The comparison of *Enterobacter* spp. with other bacteria was significant ($p < 0.05$), except for *E. coli* and *Acinetobacter* spp. ($p = 0.167$) (Figure 2B). In the current study, we classified pathogens into three selection groups *viz.* directional selection, disruptive selection, and stabilizing selection. *Klebsiella pneumoniae* isolates were observed to undergo directional selection toward resistant phenotypes in gaining resistance to antibiotics CIP, LVX, FEP, TZP, and CXM; while it showed evolutionary disruptive selection toward antibiotics SXT, CAZ, CTX, GM, AN, TE, SAM, and CAC; and appeared to adopt stabilizing selection to antibiotic MEM in (Supplementary Figure S2A). *Escherichia coli* showed directional selection toward resistant phenotypes to antibiotics CIP, LVX, CAZ, FEP, TZP, CTX, and CXM, disruptive selection to antibiotics SXT, GM, TE, SAM, MEM, and CAC, and stabilizing selection to antibiotic AN (Supplementary Figure S2B). *Pseudomonas aeruginosa* isolates exhibited directional selection toward sensitive phenotypes to antibiotics ATM and IE, while toward resistant phenotype to antibiotic CIP, and disruptive selection to antibiotics GM, AN, CAZ, FEP, TZP, and IPM (Supplementary Figure S2C). *Staphylococcus* spp. were observed to adopt directional selection toward resistant phenotype to antibiotics CIP and E, and disruptive selection to antibiotics SXT, GM, TE, CM, C, and RIF (Supplementary Figure S2D). The selection patterns for *Enterobacter* and *Acinetobacter* spp. isolates are drawn in (Supplementary Figures S2E,F).

3.5 Comparison of antibiotic susceptibility between clinical and non-clinical isolates

Non-clinical *P. aeruginosa* isolated from caterpillar carcasses was more sensitive compared to clinical isolates against fluoroquinolones

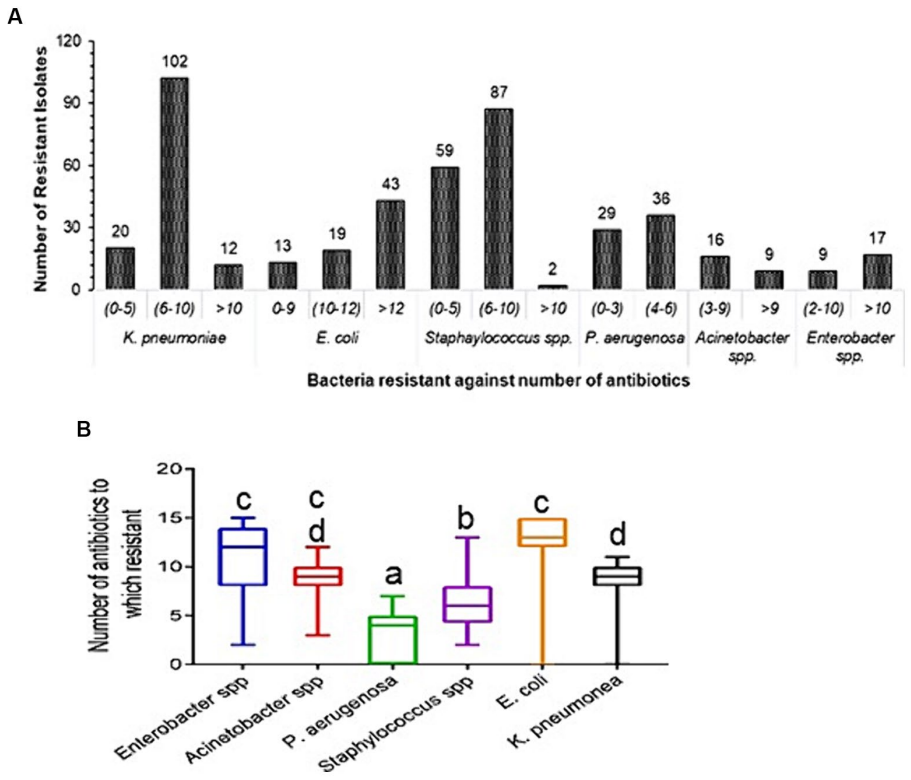

FIGURE 2
Prevalence of antibiotic resistance in clinical strains. **(A)** Diversity of antibiotic resistance in clinical isolates. Each bar represents the number of isolates that were resistant to antibiotics. **(B)** Total number of drugs for which resistance was found. It is plotted using box plots; the standard deviation is indicated by the error bar on both sides, and the middle line displays the mean value of the number of antibiotics resistant to each type of bacteria. Tukey *post-hoc* test was conducted for comparisons between the mean values of number of resistant antibiotics, $p < 0.05$ was considered statistically significant. Diference alphabets indicates statistical significant.

LVX, CIP, and NX, third generation cephalosporins cefpodoxime (CPD), ceftriaxone (CRO), and CTX, amikacin and gentamicin. The zone of inhibition of non-clinical *P. aeruginosa* was 1.1–1.5 times bigger than those of clinical *P. aeruginosa* against CIP and LVX, indicating higher resistance of clinical than non-clinical *P. aeruginosa* (Figures 3C,D). Similarly, clinical *K. pneumoniae* isolates tended to be resistant to LVX and CIP and second and third generation cephalosporins, while most being resistant also to fourth generation cephalosporins. Non-clinical *K. pneumoniae* strains were sensitive to CIP, LVX, and NX, third generation cephalosporins CPD, CTX, and CRO, with the exception of cefixime (CFM), and to AN and GM. More than 60% of clinical *K. pneumoniae* strains were resistant to the antibiotics AN and GM (Figures 3A,B).

4 Discussion

This study describes the prevalence of antibiotic resistance in bacterial pathogens isolated from clinical samples at PDU Hospital Rajkot, Gujarat. We observed that 52% patients were infected with pathogenic bacteria and the number of male and female patients carrying bacterial pathogens was nearly the same (Figure 1D). Our analysis of the antibiotic sensitivity of pathogenic bacterial strains revealed that around half of the bacterial strains (237; 49.89%) were from the patients of the surgical wards, medical wards and ICU of the hospital, and the remaining pathogenic bacterial strains (238; 50.1%) were isolated from more than 10 other wards of the hospital (Figure 1E). The development and spread of antibiotic resistance among bacterial pathogens has been a continuously growing global problem. Pathogens were categorized as methicillin-resistant, and EICR *Staphylococcus* spp., *K. pneumoniae*, *E. coli*, and *Enterobacter* spp. were categorized into ESBL, *P. aeruginosa* in MBL category based on the latest CLSI guidelines (CLSI, 2022).

Our data analysis on antibiotic resistance and susceptible antimicrobial patterns in some instances contradicts while in other instances supports the results of earlier national and international research. In this study, 8.8 and 20% ESBL strains of *K. pneumoniae* and *E. coli* were, respectively, isolated, which is similar to the figure reported (Sood and Gupta, 2012). While, Mohapatra et al., reported that 44.8% ESBL uropathogens infection were observed in the community in India (Mohapatra et al., 2022). In China, >50% bacterial pathogens isolated during 2000–2009, were MRSA, ESBL Enterobacteriaceae, and carbapenem-resistant *P. aeruginosa* (Xiao et al., 2011), which is considerably high than values we report. In the current study, *P. aeruginosa*, *K. pneumoniae*, *E. coli*, *Enterobacter* spp., *Acinetobacter* spp., and *Staphylococcus* spp. were observed to be highly resistant to the third and fourth generation cephalosporins (Table 3). These pathogens were found in the skin, surgical, emergency, and pediatric wards, as well as the surgical, medical, and ICU wards. 70–90% Enterobacterales were resistant to

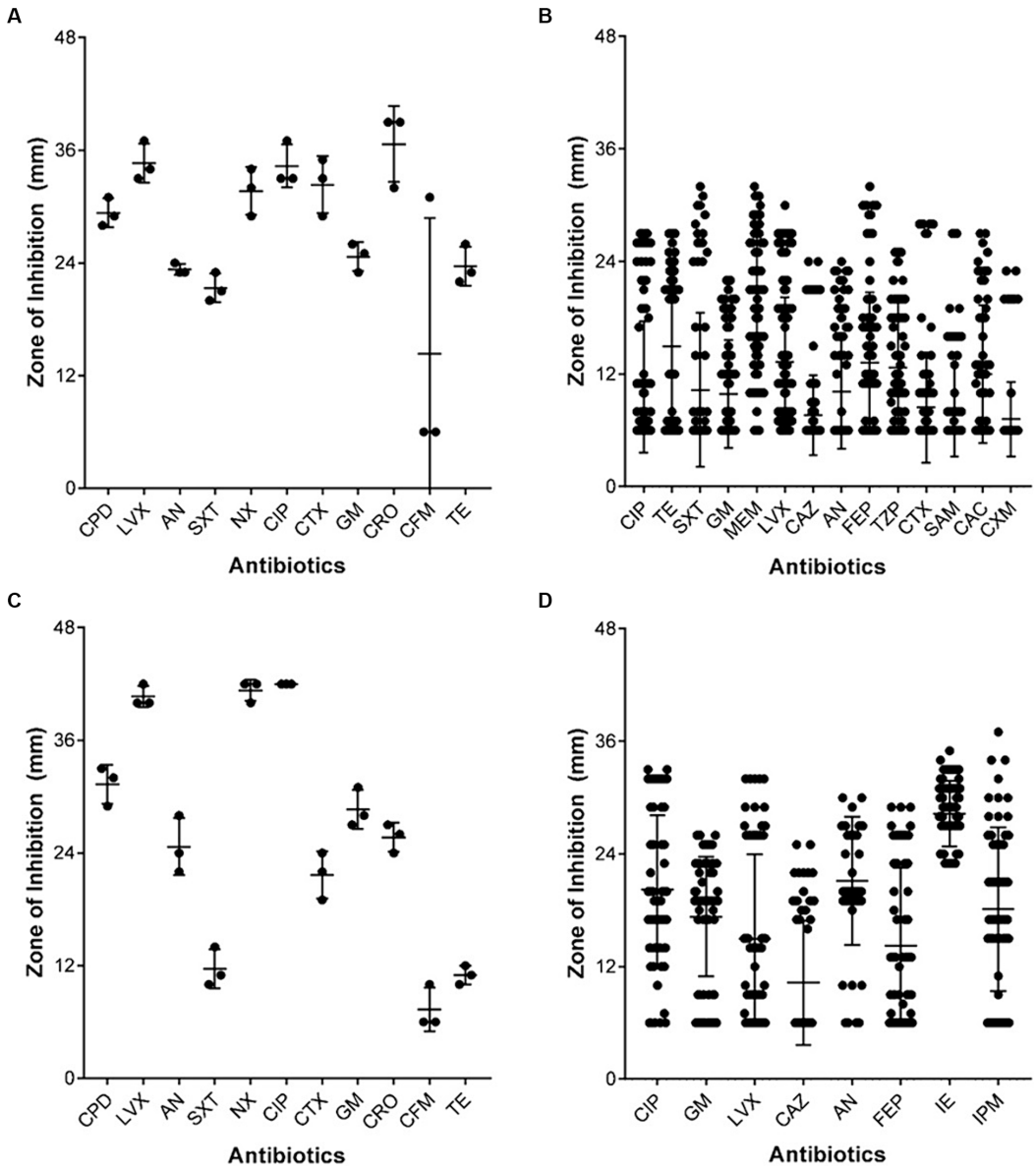

FIGURE 3
Comparison of the size of antibiotic susceptibility zone of Gram-negative bacteria. **(A)** *Klebsiella pneumoniae* isolated from *Spodoptera frugiperda* caterpillar carcasses, **(B)** *Klebsiella pneumoniae* isolated from clinical samples, **(C)** *Pseudomonas aeruginosa* isolated from *Spodoptera frugiperda* caterpillar carcasses, and **(D)** *Pseudomonas aeruginosa* isolated from clinical samples. Box plots were used for the comparison; each black dot represents an isolated bacterial strain, the central line shows the mean value of the zone of inhibition, and the error bar on both sides reflects the standard deviation.

fluoroquinolones, and the six bacterial pathogens studied (70–100%) were resistant to third generation cephalosporin, which is marginally higher than the recent reports (Diallo et al., 2020; Mannathoko et al., 2022; Murray et al., 2022). Meropenem, tetracycline, gentamycin, and amikacin effectively controlled enteric pathogens. Chloramphenicol, linezolid, vancomycin, tetracycline, clindamycin, and rifamycin were effective against *Staphylococcus* spp., but penicillin, ciprofloxacin, cefoxitin, and erythromycin were poor. 21.6% *Staphylococcus* spp. were methicillin-resistant and 7.4% were EICR. MRSA and EICR *Staphylococcus* strains have been reported to be isolated, albeit at a higher frequency (Gandra et al., 2016; Murray et al., 2022). In our study, Imipenem, amikacin, imipenem-EDTA, and gentamycin were most effective against *P. aeruginosa*. *P. aeruginosa* with MBL activity (14; 2.9%) showed similarity with earlier reports (Gandra et al., 2016; Lob et al., 2022). Levofloxacin and amikacin are effective against *Acinetobacter* spp. and (32%) resistant to MEM, which is comparatively lower than the previously reported 87.2% in India and 88% in South Korea (Gandra et al., 2016; Nordmann and Poirel, 2019; Murray et al., 2022; Lee et al., 2023). Multidrug resistant *E. coli*, *K. pneumoniae*, and *Acinetobacter baumannii*, methicillin-resistant *Staphylococcus* spp. reportedly increase mortality rates two to three times, in hospitalized patients in India (Gandra et al., 2019). In this study, *K. pneumoniae* and *E. coli* were resistant to more than 6–12 antibiotics, while *P. aeruginosa* was resistant to 6–10 antibiotics,

TABLE 3 Antibiotic resistance in clinical bacterial pathogens isolated from various wards of PDU Hospital, Rajkot.

Isolates	Hospital wards (*n* = Isolate)	Antibiotics resistance (%)														
		CIP	LVX	SXT	GM	AN	TE	CAZ	FEP	TZP	CTX	SAM	MEM	CAC	CXM	AMP
K. pneumoniae	Medical (21)	62	62	48	48	52	43	71	67	67	71	67	38	62	71	
	Surgical (37)	92	94	85	85	88	79	100	85	94	100	91	59	97	100	
	ICU (10)	90	50	30	50	70	10	100	100	100	100	100	70	100	100	
	TBCD (20)	85	25	90	80	55	35	100	57	80	100	90	5	80	100	
	Burns (30)	93	87	93	90	83	43	97	90	87	93	87	17	50	93	
E. coli	Medical (21)	100	95	86	86	76	95	100	95	95	100	95	67	95	100	
	Surgical (16)	100	100	94	100	69	81	100	100	100	100	100	69	100	100	
	ICU (5)	80	80	100	80	60	80	100	80	80	80	80	80	100	80	
	TBCD (4)	100	75	75	75	75	75	100	75	75	100	75	50	75	100	
	OPD (13)	100	77	77	54	31	69	100	92	92	100	92	8	92	100	
Enterobacter spp.	Surgical (11)	100	100	45	91	36	82	100	100	91	100	91		100	100	100
	TBCD (6)	50	50	33	33	33	33	83	50	33	100	33		50	100	100
	Burns (3)	100	33	100	100	100	67	100	100	100	100	100		100	100	100
		CIP	LVX	SXT	GM	AN	TE	CAZ	FEP	TZP	CTX	SAM	MEM			
Acinetobacter spp.	Surgical (9)	100	0	100	100	0	100	100	33	100	100	100	0			
	TBCD (3)	67	0	67	67	33	67	100	33	67	100	100	33			
	ICU (4)	100	100	100	100	100	50	100	75	100	100	100	75			
	Emergency (3)	100	0	100	100	100	0	100	100	100	100	100	100			
		CIP	GM	AN	CAZ	FEP	TZP	IE	IPM	ATM						
P. aeruginosa	ENT (13)	46	15	0	31	31	31	0	0	31						
	Surgical (17)	53	41	29	100	88	82	0	71	29						
	ICU (4)	0	0	0	0	0	0	0	0	0						
	TBCD (5)	0	0	0	20	20	20	0	20	0						
	Burns (10)	30	20	50	90	70	80	0	60	10						
	Emergency (8)	63	38	33	100	88	100	0	38	63						
	Skin (6)	50	33	67	100	100	100	0	100	0						
		CIP	E	SXT	GM	LZD	TE	P	FOX	CM	MEM	VA	C	RIF		

(Continued)

10.3389/fmicb.2024.1383989

TABLE 3 (Continued)

Isolates	Hospital wards (*n* = Isolate)	Antibiotics resistance (%)													
		CIP	LVX	SXT	GM	AN	TE	CAZ	FEP	TZP	CTX	SAM	MEM	CAC	CXM	AMP
Staphylococcus spp.	OPD (12)	92	92	18	36	18	0	100	73	27	45	9	0	9		
	Children (18)	94	67	50	83	0	11	100	100	50	72	11	0	22		
	Surgical (30)	100	87	13	57	13	10	100	93	33	70	23	3	20		
	ICU (39)	74	87	44	46	13	31	100	97	59	82	15	13	31		
	TBCD (4)	100	75	50	25	25	0	100	75	75	25	25	0	25		
	Medical (11)	91	91	18	64	18	18	100	91	55	64	27	9	27		
	Emergency (4)	50	100	25	50	25	25	100	100	50	100	25	25	25		
	Skin (20)	100	100	40	70	25	30	100	70	50	60	45	10	40		
	ENT (4)	100	75	0	0	25	0	100	50	25	25	25	0	25		

ICU, Intensive care unit; TBCD, Tuberculosis chest disease; OPD, Out-patient department; ENT, Ear nose throat.

somewhat lower than a recent report (Bassetti et al., 2019). *Staphylococcus* spp. resistant to 4–6 antibiotics (Figure 2B) comparable to earlier report (Kumar et al., 2017). Unscrupulous and haphazard administration of antibiotics is largely, if not entirely, responsible for the evolution of antibiotic resistance among various isolates (Beckley and Wright, 2021). Comparison of antibiotic susceptibility between clinical and non-clinical isolates can be important in the evaluation of the development and evolution of antibiotic resistance among clinical and non-clinical strains of human pathogens. Since clinical bacterial strains are regularly exposed to antibiotics and therefore exhibit directional selection toward resistance traits, they are more resistant than non-clinical strains. Non-clinical *P. aeruginosa* and *K. pneumoniae* were highly sensitive to tested antibiotics (Figures 3A,C). The antibiotic resistant rate in non-clinical *P. aeruginosa*, *K. pneumoniae*, *E. coli*, *Enterobacter* spp., and *Staphylococcus* spp. is comparatively lower than the clinical strains (Supplementary Table S2) and similar results was reported on antimicrobial resistance in animals (Van Boeckel et al., 2019). Environmental pressure is responsible for natural selection in every organism, which helps enhance the fitness of organisms. Three types of natural selection were observed (1) directional selection, (2) stabilizing selection, and (3) disruptive selection (Darwin, 1859). Presence of antibiotics in the surrounding environment is one of the factors responsible for natural selection pressure in bacteria (Baquero, 2001; Blazquez et al., 2002). Our analysis in the present study of enteric pathogens showed directional selection toward resistant phenotypes against TZP, FEP, and CXM, which are therefore less effective. All six bacterial pathogens in present study showed directional selection toward resistant phenotypes against CIP, and its effectiveness was very poor. Inappropriate use of antibiotics, and inappropriate timing of use (pre/post-operative antimicrobial prophylaxis) have been described as some of the factors responsible for the development of antibiotic resistance in bacteria (Goldmann, 1999; Thu et al., 2012; Lim et al., 2015). Such directional selection in *P. aeruginosa* (Barbosa et al., 2017) and an increased selection coefficient in response to a high concentration of cefotaxime in *E. coli* have been reported earlier for directional selection of antibiotic resistant phenotypes in bacteria (Negri et al., 2000). Such types of directional selection of antibiotic resistant phenotypes in bacteria make it more challenging to control these kinds of outbreaks. A comparison of the present research findings with results from earlier research can offer some validation of the findings of this present study and also offer methodological variations in their approaches. However, our findings contribute to regional and worldwide databases on the susceptibility and effectiveness of antibiotics against clinical isolates in this geographical area. This will help the clinicians of various hospitals in this region formulate empirical antimicrobial therapy and proper infection control measures. This study can be useful in studying the patterns of rising resistance among clinical bacterial isolates in this particular region of the country.

5 Conclusion

The study findings offer a valuable resource for cross-national and within-country comparisons of the antimicrobial resistance patterns among PEEKSA isolates in Gujarat, India. Cephalosporin and fluoroquinolone antibiotics show poor activity in controlling

bacterial pathogens. Tetracyclines and aminoglycosides effectively control *Escherichia coli*, *Enterobacter* spp., *Klebsiella pneumoniae*, and *Acinetobacter* spp. Chloramphenicol, linezolid, vancomycin, tetracycline, and rifamycin are the most effective antibiotics in descending order to control *Staphylococcus* spp. Imipenem-EDTA was the most effective treatment for *Pseudomonas aeruginosa*, followed by gentamycin, amikacin, and imipenem. Bacterial pathogens isolated from the surgical ward were comparatively more antibiotic resistant than those isolated from other wards. The widespread administration of antimicrobial agents and antibiotics in surgical wards appears to be the apparent reason. Non-clinical *P. aeruginosa* and *K. pneumoniae* were more sensitive to antibiotics than the clinical isolates. Unscrupulous and haphazard use of antibiotics to treat bacterial diseases increases the selection pressure toward resistance phenotypes in bacteria, narrowing the scope of reversing the directional shift from resistant to sensitive phenotypes. Comprehending the genetic makeup (resistance gene or plasmid) in bacteria exhibiting higher resistance rates could facilitate the understanding of mechanisms, and that will lead to the development of novel antibiotics with innovative mechanisms or more effective therapeutic approaches. Our findings serve as baseline datasets that can be used to link and implicate antibiotic stewardship programs in hospitals in this region of the country.

Data availability statement

The original contributions presented in the study are included in the article/Supplementary material, further inquiries can be directed to the corresponding author.

Ethics statement

Data collection and sample processing were done under the SOP guidelines and regulations of the PDU Medical College ethical panel. The Ethics Committee of PDU Medical College waived the requirement for informed consent.

Author contributions

VH: Conceptualization, Data curation, Formal Analysis, Investigation, Methodology, Software, Writing – original draft, Writing – review & editing. BP: Data curation, Formal Analysis, Software, Writing – review & editing. RK: Supervision, Writing – review & editing. AB: Data curation, Methodology, Validation, Writing – review & editing. GK: Conceptualization, Formal Analysis, Resources, Writing – review & editing. BV: Conceptualization, Methodology, Supervision, Validation, Visualization, Writing – review & editing.

Funding

The author(s) declare that no financial support was received for the research, authorship, and/or publication of this article.

Acknowledgments

The University Grant Commission, Ministry of Education, Government of India, fellowship program for Ph.D. study in India, [award number: No. F. 82-44/2020 (SA-III)] is gratefully acknowledged by VH. All authors thank M. J. Samani for granting permission for this work. Authors also, thank Riya and Nidhi for their support in experimental work. We thank the Medical Laboratory Technology students, Technical and Non-technical Staff of the Bacteriology Laboratory, Department of Microbiology, PDU Medical College, Rajkot.

Conflict of interest

The authors declare that the research was conducted in the absence of any commercial or financial relationships that could be construed as a potential conflict of interest.

Publisher's note

Supplementary material

The Supplementary material for this article can be found online at: https://www.frontiersin.org/articles/10.3389/fmicb.2024.1383989/full#supplementary-material

References

Akiba, M., Senba, H., Otagiri, H., Prabhasankar, V. P., Taniyasu, S., Yamashita, N., et al. (2015). Impact of wastewater from different sources on the prevalence of antimicrobial-resistant *Escherichia coli* in sewage treatment plants in South India. *Ecotoxicol. Environ. Saf.* 115, 203–208. doi: 10.1016/j.ecoenv.2015.02.018

Bai, A. D., Lo, C. K., Komorowski, A. S., Suresh, M., Guo, K., Garg, A., et al. (2022). *Staphylococcus aureus* bacteremia mortality across country income groups: a secondary analysis of a systematic review. *Int. J. Infect. Dis.* 122, 405–411. doi: 10.1016/j.ijid.2022.06.026

Baquero, F. (2001). Low-level antibacterial resistance: a gateway to clinical resistance. *Drug Resist. Updat.* 4, 93–105. doi: 10.1054/drup.2001.0196

Baquero, F., Martinez, J. L., Lanza, F. V., Rodríguez-Beltrán, J., Galán, J. C., San Millán, A., et al. (2021). Evolutionary pathways and trajectories in antibiotic resistance. *Clin. Microbiol. Rev.* 34:e0005019. doi: 10.1128/CMR.00050-19

Barbosa, C., Trebosc, V., Kemmer, C., Rosenstiel, P., Beardmore, R., Schulenburg, H., et al. (2017). Alternative evolutionary paths to bacterial antibiotic resistance cause distinct collateral effects. *Mol. Biol. Evol.* 34, 2229–2244. doi: 10.1093/molbev/msx158

Bassetti, M., Castaldo, N., Cattelan, A., Mussini, C., Righi, E., Tascini, C., et al. (2019). Ceftolozane/tazobactam for the treatment of serious *Pseudomonas aeruginosa* infections: a multicentre nationwide clinical experience. *Int. J. Antimicrob. Agents* 53, 408–415. doi: 10.1016/j.ijantimicag.2018.11.001

Beckley, A. M., and Wright, E. S. (2021). Identification of antibiotic pairs that evade concurrent resistance via a retrospective analysis of antimicrobial susceptibility test results. *Lancet Microb.* 2, e545–e554. doi: 10.1016/S2666-5247(21)00118-X

Blazquez, J., Oliver, A., and Gomez-Gomez, J. M. (2002). Mutation and evolution of antibiotic resistance: antibiotics as promoters of antibiotic resistance? *Curr. Drug Targets* 3, 345–349. doi: 10.2174/1389450023347579

Britto, C. D., John, J., Verghese, V. P., and Pollard, A. J. (2019). A systematic review of antimicrobial resistance of typhoidal *Salmonella* in India. *Indian J. Med. Res.* 149:151. doi: 10.4103/ijmr.IJMR_830_18

Browne, A. J., Chipeta, M. G., Haines-Woodhouse, G., Kumaran, E. P., Hamadani, B. H. K., Zaraa, S., et al. (2021). Global antibiotic consumption and usage in humans, 2000–18: a spatial modelling study. *Lancet Planet. Health* 5, e893–e904. doi: 10.1016/S2542-5196(21)00280-1

CDC (2019). *Antibiotic Resistance Threats in the United States*. Atlanta, GA: U.S. Department of Health and Human Services, CDC.

Cheesbrough, M. (2005). *District Laboratory Practice in Tropical Countries, Part 2*. New York: Cambridge University Press

CLSI (2018). Methods for dilution antimicrobial susceptibility tests for Bacteria that grow aerobically. CLSI standard M07, 11th Edn. Wayne, PA. Clinical and Laboratory Standard Institite.

CLSI (2022). Performance standards for antimicrobial susceptibility testing. 32nd ed. CLSI supplement M100.

Collee, J. G., Miles, R. S., and Watt, B. (1996). "Tests for the identification of Bacteria" in *Practical Medical Microbiology*. eds. J. G. Collee, B. P. Marmion, A. G. Fraser and S. A. Mackie. *McCartney Practical Medical Microbiology*, *14th* ed (New York: Churchill Livingstone), 131–150.

Darwin, C. (1859). *On the Origins of Species by Means of Natural Selection 247*. London: Murray, 1859

Diallo, O. O., Baron, S. A., Dubourg, G., Chaudet, H., Halfon, P., Camiade, S., et al. (2020). Major discrepancy between factual antibiotic resistance and consumption in south of France: analysis of 539,037 bacterial strains. *Sci. Rep.* 10:18262. doi: 10.1038/s41598-020-75158-7

Gandra, S., Joshi, J., Trett, A., Lamkang, A. S., and Laxminarayan, R. (2017). Scoping report on antimicrobial resistance in India. Center for Disease Dynamics, Economics & Policy: Washington, DC, USA, 2017, 1–146.

Gandra, S., Mojica, N., Klein, E. Y., Ashok, A., Nerurkar, V., Kumari, M., et al. (2016). Trends in antibiotic resistance among major bacterial pathogens isolated from blood cultures tested at a large private laboratory network in India, 2008–2014. *Int. J. Infect. Dis.* 50, 75–82. doi: 10.1016/j.ijid.2016.08.002

Gandra, S., Tseng, K. K., Arora, A., Bhowmik, B., Robinson, M. L., Panigrahi, B., et al. (2019). The mortality burden of multidrug-resistant pathogens in India: a retrospective, observational study. *Clin. Infect. Dis.* 69, 563–570. doi: 10.1093/cid/ciy955

Goldmann, D. A. (1999). The epidemiology of antimicrobial resistance. *Ecosyst. Health* 5, 158–163. doi: 10.1046/j.1526-0992.1999.09925.x

Gupta, S., Kapur, S., and Padmavathi, D. V. (2014). Comparative prevalence of antimicrobial resistance in community-acquired urinary tract infection cases from representative states of northern and southern India. *J. Clin. Diagn. Res.* 8:DC09. doi: 10.7860/JCDR/2014/9349.4889

Ikuta, K. S., Swetschinski, L. R., Aguilar, G. R., Sharara, F., Mestrovic, T., Gray, A. P., et al. (2022). Global mortality associated with 33 bacterial pathogens in 2019: a systematic analysis for the global burden of disease study 2019. *Lancet* 400, 2221–2248. doi: 10.1016/S0140-6736(22)02185-7

Kaur, A., Gandra, S., Gupta, P., Mehta, Y., Laxminarayan, R., and Sengupta, S. (2017). Clinical outcome of dual colistin-and carbapenem-resistant *Klebsiella pneumoniae* bloodstream infections: a single-center retrospective study of 75 cases in India. *Am. J. Infect. Control* 45, 1289–1291. doi: 10.1016/j.ajic.2017.06.028

Kelch, W. J., and Lee, J. S. (1978). Antibiotic resistance patterns of gram-negative bacteria isolated from environmental sources. *Appl. Environ. Microbiol.* 36, 450–456. doi: 10.1128/aem.36.3.450-456.1978

Klein, E. Y., Tseng, K. K., Pant, S., and Laxminarayan, R. (2019). Tracking global trends in the effectiveness of antibiotic therapy using the drug resistance index. *BMJ Glob. Health* 4:e001315. doi: 10.1136/bmjgh-2018-001315

Kumar, P., Bag, S., Ghosh, T. S., Dey, P., Dayal, M., Saha, B., et al. (2017). Molecular insights into antimicrobial resistance traits of multidrug resistant enteric pathogens isolated from India. *Sci. Rep.* 7:14468. doi: 10.1038/s41598-017-14791-1

Larsson, D. G., and Flach, C. F. (2022). Antibiotic resistance in the environment. *Nat. Rev. Microbiol.* 20, 257–269. doi: 10.1038/s41579-021-00649-x

Lee, Y. L., Ko, W. C., and Hsueh, P. R. (2023). Geographic patterns of *Acinetobacter baumannii* and carbapenem resistance in the Asia-Pacific region: results from the antimicrobial testing leadership and surveillance (ATLAS) program, 2012-2019. *Int. J. Infect. Dis.* 127, 48–55. doi: 10.1016/j.ijid.2022.12.010

Lim, M. K., Lai, P. S. M., Ponnampalavanar, S. S. L. S., Omar, S. F. S., Taib, N. A., Yusof, M. Y., et al. (2015). Antibiotics in surgical wards: use or misuse? A newly industrialized country's perspective. *J. Infect. Develop. Countries* 9, 1264–1271. doi: 10.3855/jidc.6731

Lob, S. H., Estabrook, M. A., DeRyke, C. A., Alekseeva, I., Siddiqui, F., Young, K., et al. (2022). Activity of ceftolozane/tazobactam against clinical isolates of *Pseudomonas aeruginosa* from patients in the Middle East and Africa–study for monitoring antimicrobial resistance trends (SMART) 2017-2020. *Int. J. Infect. Dis.* 125, 250–257. doi: 10.1016/j.ijid.2022.10.014

Mannathoko, N., Mosepele, M., Gross, R., Smith, R. M., Alby, K., Glaser, L., et al. (2022). Colonization with extended-spectrum cephalosporin-resistant Enterobacterales (ESCrE) and carbapenem-resistant Enterobacterales (CRE) in healthcare and community settings in Botswana: an antibiotic resistance in communities and hospitals (ARCH) study. *Int. J. Infect. Dis.* 122, 313–320. doi: 10.1016/j.ijid.2022.06.004

Mohapatra, S., Panigrahy, R., Tak, V., JV, S., KC, S., Chaudhuri, S., et al. (2022). Prevalence and resistance pattern of uropathogens from community settings of different regions: an experience from India. *Access Microbiology* 4:000321. doi: 10.1099/acmi.0.000321

Murray, C. J., Ikuta, K. S., Sharara, F., Swetschinski, L., Aguilar, G. R., Gray, A., et al. (2022). Global burden of bacterial antimicrobial resistance in 2019: a systematic analysis. *Lancet* 399, 629–655. doi: 10.1016/S0140-6736(21)02724-0

Negri, M. C., Lipsitch, M., Blázquez, J., Levin, B. R., and Baquero, F. (2000). Concentration-dependent selection of small phenotypic differences in TEM β-lactamase-mediated antibiotic resistance. *Antimicrob. Agents Chemother.* 44, 2485–2491. doi: 10.1128/aac.44.9.2485-2491.2000

Nordmann, P., and Poirel, L. (2019). Epidemiology and diagnostics of carbapenem resistance in gram-negative bacteria. *Clin. Infect. Dis.* 69, S521–S528. doi: 10.1093/cid/ciz824

Procop, G. W., Church, D. L., Hall, G. S., and Janda, W. M. (2020). *Koneman's Color Atlas and Textbook of Diagnostic Microbiology*. Philadelphia: Jones & Bartlett Learning, 253–320.

Sood, S., and Gupta, R. (2012). Antibiotic resistance pattern of community acquired uropathogens at a tertiary care hospital in Jaipur, Rajasthan. *Ind. J. Commun. Med.* 37, 39–44. doi: 10.4103/0970-0218.94023

Thu, T. A., Rahman, M., Coffin, S., Harun-Or-Rashid, M., Sakamoto, J., and Hung, N. V. (2012). Antibiotic use in Vietnamese hospitals: a multicenter point-prevalence study. *Am. J. Infect. Control* 40, 840–844. doi: 10.1016/j.ajic.2011.10.020

Van Boeckel, T. P., Pires, J., Silvester, R., Zhao, C., Song, J., Criscuolo, N. G., et al. (2019). Global trends in antimicrobial resistance in animals in low-and middle-income countries. *Science* 365:eaaw1944. doi: 10.1126/science.aaw1944

Xiao, Y. H., Giske, C. G., Wei, Z. Q., Shen, P., Heddini, A., and Li, L. J. (2011). Epidemiology and characteristics of antimicrobial resistance in China. *Drug Resist. Updat.* 14, 236–250. doi: 10.1016/j.drup.2011.07.001

frontiers | Frontiers in Microbiology

TYPE Review
PUBLISHED 29 April 2024
DOI 10.3389/fmicb.2024.1403168

OPEN ACCESS

EDITED BY
Vijay Soni,
NewYork-Presbyterian, United States

REVIEWED BY
Owais Rashid Hakiem,
University of California, Irvine, United States
Suyasha Roy,
National Institutes of Health (NIH),
United States

*CORRESPONDENCE
Vikas Yadav
✉ Vikasyadav40@gmail.com;
✉ vikas.yadav@med.lu.se

RECEIVED 18 March 2024
ACCEPTED 15 April 2024
PUBLISHED 29 April 2024

CITATION
Sharma S, Chauhan A, Ranjan A, Mathkor DM, Haque S, Ramniwas S, Tuli HS, Jindal T and Yadav V (2024) Emerging challenges in antimicrobial resistance: implications for pathogenic microorganisms, novel antibiotics, and their impact on sustainability. *Front. Microbiol.* 15:1403168. doi: 10.3389/fmicb.2024.1403168

Emerging challenges in antimicrobial resistance: implications for pathogenic microorganisms, novel antibiotics, and their impact on sustainability

Shikha Sharma[1], Abhishek Chauhan[2], Anuj Ranjan[3], Darin Mansor Mathkor[4], Shafiul Haque[4,5], Seema Ramniwas[6], Hardeep Singh Tuli[7], Tanu Jindal[2] and Vikas Yadav[8]*

[1]Amity Institute of Environmental Sciences, Amity University, Noida, Uttar Pradesh, India, [2]Amity Institute of Environmental Toxicology, Safety and Management, Amity University, Noida, Uttar Pradesh, India, [3]Academy of Biology and Biotechnology, Southern Federal University, Rostov-on-Don, Russia, [4]Research and Scientific Studies Unit, College of Nursing and Health Sciences, Jazan University, Jazan, Saudi Arabia, [5]Gilbert and Rose-Marie Chagoury School of Medicine, Lebanese American University, Beirut, Lebanon, [6]University Centre for Research & Development, University Institute of Pharmaceutical Sciences, Chandigarh University, Mohali, Punjab, India, [7]Department of Bio-Sciences and Technology, Maharishi Markandeshwar Engineering College, Maharishi Markandeshwar (Deemed to Be University), Ambala, India, [8]Department of Translational Medicine, Clinical Research Centre, Skåne University Hospital, Lund University, Malmö, Sweden

Overuse of antibiotics is accelerating the antimicrobial resistance among pathogenic microbes which is a growing public health challenge at the global level. Higher resistance causes severe infections, high complications, longer stays at hospitals and even increased mortality rates. Antimicrobial resistance (AMR) has a significant impact on national economies and their health systems, as it affects the productivity of patients or caregivers due to prolonged hospital stays with high economic costs. The main factor of AMR includes improper and excessive use of antimicrobials; lack of access to clean water, sanitation, and hygiene for humans and animals; poor infection prevention and control measures in hospitals; poor access to medicines and vaccines; lack of awareness and knowledge; and irregularities with legislation. AMR represents a global public health problem, for which epidemiological surveillance systems have been established, aiming to promote collaborations directed at the well-being of human and animal health and the balance of the ecosystem. MDR bacteria such as *E. coli*, *Staphylococcus aureus*, *Pseudomonas aeruginosa*, *Enterococcus* spp., *Acinetobacter* spp., and *Klebsiella pneumonia* can even cause death. These microorganisms use a variety of antibiotic resistance mechanisms, such as the development of drug-deactivating targets, alterations in antibiotic targets, or a decrease in intracellular antibiotic concentration, to render themselves resistant to numerous antibiotics. In context, the United Nations issued the Sustainable Development Goals (SDGs) in 2015 to serve as a worldwide blueprint for a better, more equal, and more sustainable existence on our planet. The SDGs place antimicrobial resistance (AMR) in the context of global public health and socioeconomic issues; also, the continued growth of AMR may hinder the achievement of numerous SDGs. In this review, we discuss the role of environmental pollution in the rise of AMR, different mechanisms underlying the antibiotic resistance, the threats posed by pathogenic microbes,

novel antibiotics, strategies such as One Health to combat AMR, and the impact of resistance on sustainability and sustainable development goals.

KEYWORDS

antibiotic resistance, mechanisms of resistance, gene transfer, novel antibiotic, sustainability, sustainable development goals

1 Introduction

The spread, persistence, and prevalence of antibiotic-resistant bacteria (ARB) and antibiotic-resistant genes (ARG) in the environment because of excessive and improper use of human and veterinary antibiotics is a global concern and issue. It is well acknowledged that antibiotic resistance poses a serious threat to human health on a global scale. In addition, multidrug-resistant (MDR) organisms have been frequently reported in community settings apart from hospitals, indicating that reservoirs of ARB exist elsewhere outside hospitals such as in water or aquatic environment (Munita and Arias, 2016), soil (Seyoum et al., 2021), foods (Shen et al., 2022) and air (Zhou et al., 2021). As bacteria continue to proliferate and evolve new forms of resistance to antimicrobial agents, some emerging community-associated illnesses may impede the progress of bacterial infections and diseases. The ARB and ARGs have been found in a variety of environmental compartments, including wastewater treatment plants, aquaculture farms, hospital wastewater, confined animal feeding operations, and surface and groundwater (Lamba et al., 2017; Chen et al., 2018; Manaia et al., 2018).

According to Lupo et al. (2012), one of the most dangerous health issues currently facing the world is bacterial antibiotic resistance evolution & its dissemination and appearance. Antibiotic resistance poses a severe concern to human health such as prolonged illness and increased death since it can spread from environmental compartments to drinking water sources as a main route of exposure. Freshwater in particular acts as a reactor in which novel resistances develop and become more prevalent. Numerous investigations found ARB and ARGs in untreated drinking water sources such as wells, groundwater, rivers, and lakes as well as in tap and bottled water (Sanganyado and Gwenzi, 2019; Kaiser et al., 2022; Li et al., 2023). Hydrological processes including runoff, infiltration, leachates, and groundwater recharge, as well as anthropogenic activity like wastewater discharge, etc. are what cause Antibiotic Resistance to spread from the various reservoirs into drinking water sources. The existence of resistance determinants in environmental and soil bacteria does not directly pose a threat to human health. However, when these determinants are mobilized to new hosts and expressed in different contexts, such as their transfer to plasmids and integrons in pathogenic bacteria, it can lead to a significant problem with widespread implications (Peterson and Kaur, 2018). The types and dosages of antibiotics administered to the animals are reflected in the antimicrobial resistance patterns seen in the animals (Reygaert, 2018). The direct oral route (which includes eating meat and ingesting faeces in contaminated water or food) is the most prevalent way for antibiotic resistance to spread from animals to humans. Direct human contact with the animals is another typical route (Wegener, 2012). Pharmaceutical industrial waste, human and animal faeces can release antibiotics and antibiotic resistance into the environment. Antibiotic-related water contamination is an environmental danger that must be addressed by the entire population. Antibiotics are found extensively in water and are eventually absorbed or digested by aquatic species. When antimicrobials are utilised in farmed fish production, AMR genes may reach the food chain and, eventually, the human body via seafood intake. High amounts of antibiotics in cattle manure can infiltrate the soil and water environment in a variety of ways, polluting the ecosystem. Residual antibiotics can enter the soil by animal dung and urine fertilisation and accumulate there, affecting soil fertility, crop chlorophyll production, enzyme release, and root development. Antibiotic residues also have an impact on the structure and activity of the soil microbial community, as well as the development and dissemination of antibiotic-resistant bacteria and resistance genes (Tian et al., 2021). Other sources of antibiotic contamination include hospitals, where antibiotics are commonly used to treat bacterial infections. Improper treatment of hospital wastewater discharges leads to the diffusion of antibiotics into the soil, and its reuse in crop irrigation of economically significant plants such as rice and wheat leads to antibiotic contamination (Zhu et al., 2019; Barathe et al., 2024).

Second-line antibiotics are more readily available in developing nations, which reduces the need for next-generation medicines and increases morbidity and death from illnesses that are resistant to antibiotics (Shiadeh et al., 2019). As per the World Health Organization (2014), one of the most serious three public health problems of the twenty-first century, is antibiotic resistance. Antibiotic-resistant illnesses kill at least 0.7 million people worldwide each year, and within 30 years, it is anticipated that the number would rise to 1.0 million which could significantly outnumber cancer-related fatalities (Lerminiaux and Cameron, 2019).

Modern medicine was also revolutionised by the discovery, widespread use, and commercialization of antimicrobial drugs for the treatment of infections, which also altered the therapeutic paradigm (Munita and Arias, 2016). Even though antimicrobials are crucial clinical tools for curing and preventing infectious diseases, resistance is still erupting, diversifying, and spreading quickly. The spread of resistant organisms, treatment failures, elevated mortality rates, the potential for undetected low levels of resistance, and the associated burden on healthcare expenses make the increase in microbial resistance a serious problem. Since antibiotic-resistant germs cannot be destroyed or inhibited in their growth, they appear to be more virulent. To find additional targets and develop the next generation of powerful antimicrobials, numerous efforts have been made to overcome the resistance (Murugaiyan et al., 2022).

Mutations are one of the causes of antibiotic resistance development (Urban-Chmiel et al., 2022). Mutations occurring in already-existing genes of the bacterial chromosome that are subsequently positively chosen by environmental pressures, drive the

evolution of all known antibiotic resistance mechanisms acquired by opportunistic and pathogenic bacteria. Two concurrent evolutionary factors are involved in the long-term preservation of antibiotic resistance genes in bacterial communities: selection favouring resistance phenotypes and selection reducing the fitness costs associated with carrying resistance genes (Bengtsson-Palme et al., 2018). Based on antimicrobial processes such as suppression of bacterial metabolic pathways, inhibition of protein synthesis, inhibition of nucleic acid synthesis, and inhibition of cell membrane depolarization, antibiotics can be categorised into several classes. Epigenetics may have a significant impact on how bacteria become resistant to antibiotics, according to many recent reports. The rapid emergence of drug resistance in bacteria can be explained by the inherent heterogeneity and temporary nature of epigenetic inheritance. Adenine and Cytosine Methylation can modulate mutation rates in bacterial genomes, modifying antibiotic susceptibility (Ghosh et al., 2020). The two types of antibiotic resistance mechanisms are acquired/genetic (chromosomal mutations and extra-chromosomal plasmid) and natural/intrinsic (Munita and Arias, 2016). Resistance mutations commonly arise in genes which encode important operations; as a result, these mutations are usually harmful in the absence of medications (Durão et al., 2018).

Horizontal Gene Transfer (HGT) gives infectious bacteria a path by which an antibiotic resistance gene (ARG) might cause an outbreak by spreading resistance across numerous unrelated bacteria (Lerminiaux and Cameron, 2019), such as sulfonamide resistance genes (*sul1*, *sul2* and *sul3*), encoding a dihydropteroate synthase (DHPS), play a crucial role in bacterial resistance to sulfonamides by causing the bacteria to develop a low affinity for sulfonamides. These genes are found on mobilised plasmids with transposons and a host range, which causes the bacteria to acquire numerous sulphonamide-co-selected antibiotic resistances (Adekanmbi et al., 2020). The horizontal acquisition of ARGs leads to the diversification of genomes and generates a potential for when bacteria are subjected to strong selective pressures such as the presence of antimicrobials. HGT can produce the genes needed for survival more quickly than spontaneous mutations (Lerminiaux and Cameron, 2019).

According to guidelines given by the WHO in the year 2021 and other members of the AMR Tripartite, AMR might have a substantial impact on a variety of the United Nations Sustainable Development Goals (SDGs) such as AMR raises treatment costs, many nations may be unable to afford the universal health care (Berkner et al., 2014). Addressing AMR is critical to accomplishing the SDGs. Many of the goals (e.g., greater access to clean water and sanitation, sustainable consumption, and production, such as more sustainable food production, and proper use of antimicrobials in people and animals) will contribute to addressing AMR. At the same time, growing AMR levels will make it more difficult to meet health, poverty reduction, food security, and economic growth goals.

The continued rise of AMR, for example, may hinder the achievement of Sustainable Development Goals 1 (No Poverty) and 2 (Zero Hunger). Food production is expected to increase by 50–70% between 2010 and 2030 due to increasing global population, economic growth, and changes in consumption habits; at the same time, the use of antimicrobials in food production (e.g., meat, milk, eggs) is expected to increase by a similar margin (Laxminarayan et al., 2016). Major reports have already demonstrated this: while global antibiotic consumption in human medicine increased by 10%, consumption of these drugs in animal husbandry increased by nearly 180% in the "BRICS" conglomerate countries (Brazil, Russia, India, China, and South Africa), with continued rising trends expected till 2030 (Van Boeckel et al., 2017), which will lead to the spread of AMR across the ecosystem (Figure 1).

In this review, we have explored the contemporary understanding and insights into the mechanisms driving antibiotic resistance among diversified bacteria, while also addressing the imminent threats posed by antibiotic resistance. Additionally, it aims to examine emerging novel antibiotics and evaluate the potential impacts of antibiotic resistance on achieving Sustainable Development Goals.

2 The mechanisms underlying antibiotic resistance

The organisms cannot be destroyed or stopped from growing, antibiotic-resistant strains seem to be more virulent. Both bacterial uptake of foreign DNA and changes in a bacterium's pre-existing genome can result in antibiotic resistance. In human or animals receiving antibiotic treatment, mutations happen easily and become fixed (Larsson and Flach, 2022). Even more frequent mutations result in genomic rearrangements (insertions, deletions, duplications, and inversions), which can hasten the development of antibiotic resistance. Physiology, genetics, antibiotic-bacterium interactions (e.g., an antibiotic itself can affect mutation rate, or different resistance mutations can be selected at different antibiotic doses) and the environment to which bacteria have been exposed in the past and present all have an impact on how quickly AR mutants emerge in bacteria (Harmand et al., 2017; Durão et al., 2018).

Selection pressure on resistance genes is created by the rise in antibiotic concentrations in the environment, especially in human waste streams where resistance genes are produced and mixed with antibiotics and other biocidal chemicals (Martínez et al., 2017). When environmental bacteria are exposed to this mixture, horizontal gene transfer (HGT) events are triggered (Michaelis and Grohmann, 2023), which spread genetic resistance components throughout various strains and species, increasing the microorganism's population and allowing it to colonise new niches and hosts. By using HGT processes, all of the genes from the extrinsic resistome can be transferred to pathogenic and non-pathogenic bacteria from a variety of habitats, including people and other animals as well as other ecosystems (Bello-López et al., 2019). When drugs are blocked from entering cells due to the absence of a target, such as a cell wall, intrinsic resistance develops (Figure 2). These bacteria include *Klebsiella*, *Pseudomonas aeruginosa*, and *E. coli*.

On the other hand, changes in bacterial genetic makeup result in decreased antibiotic sensitivity and higher acquired resistance (Uddin et al., 2021). Plasmid-mediated medication resistance is common in clinical settings. Genetic material found outside of chromosomes can multiply on its own in the cytoplasm. Gene resistance (r-genes) is present in these plasmids and is easily transfected from one plasmid to another. r-genes are easily transposable between R-plasmids and chromosomes. The three main agents that promote HGT through conjugation, transduction, and natural transformation are plasmids, bacteriophages, and extracellular DNA (Figure 3).

Antibiotics can induce conjugation, which is important in clinical settings where antibiotic usage is common. In the

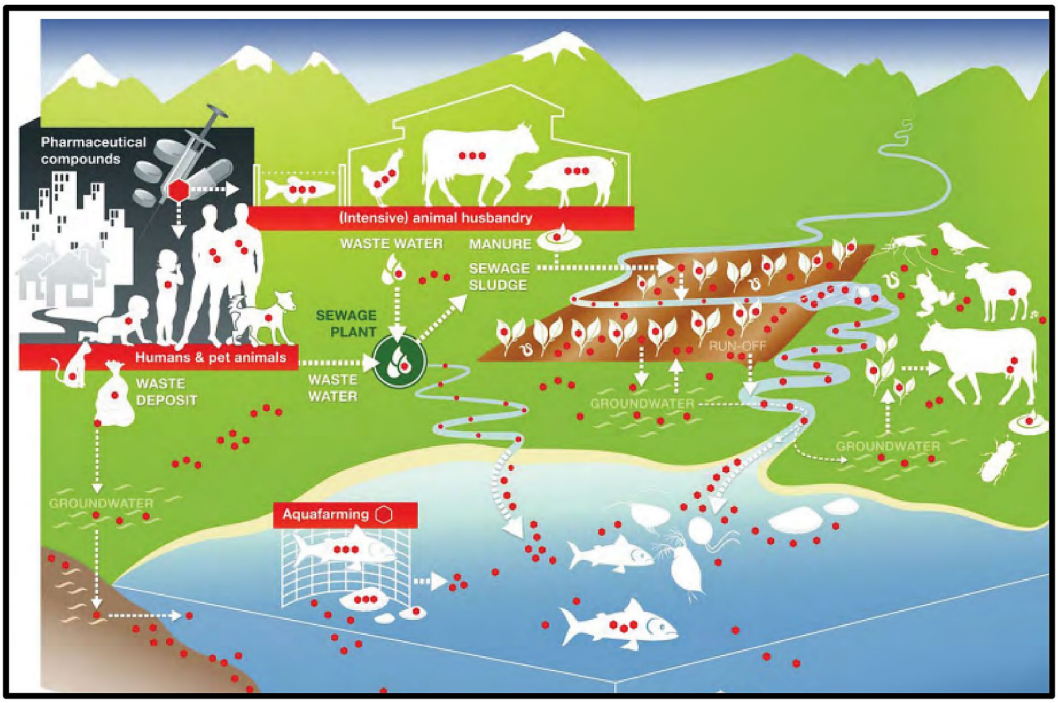

FIGURE 1
Spread of Antibiotic Resistance in the ecosystem [Adopted from Berkner et al. (2014)].

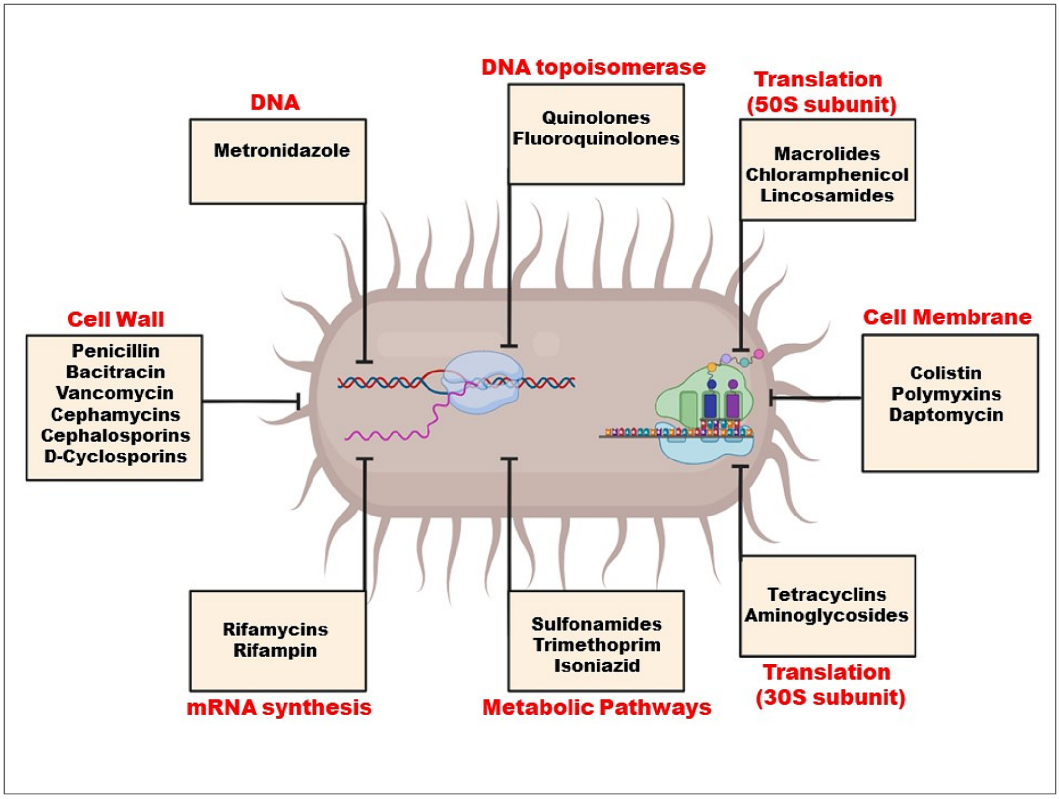

FIGURE 2
Mechanism of action of antibiotics.

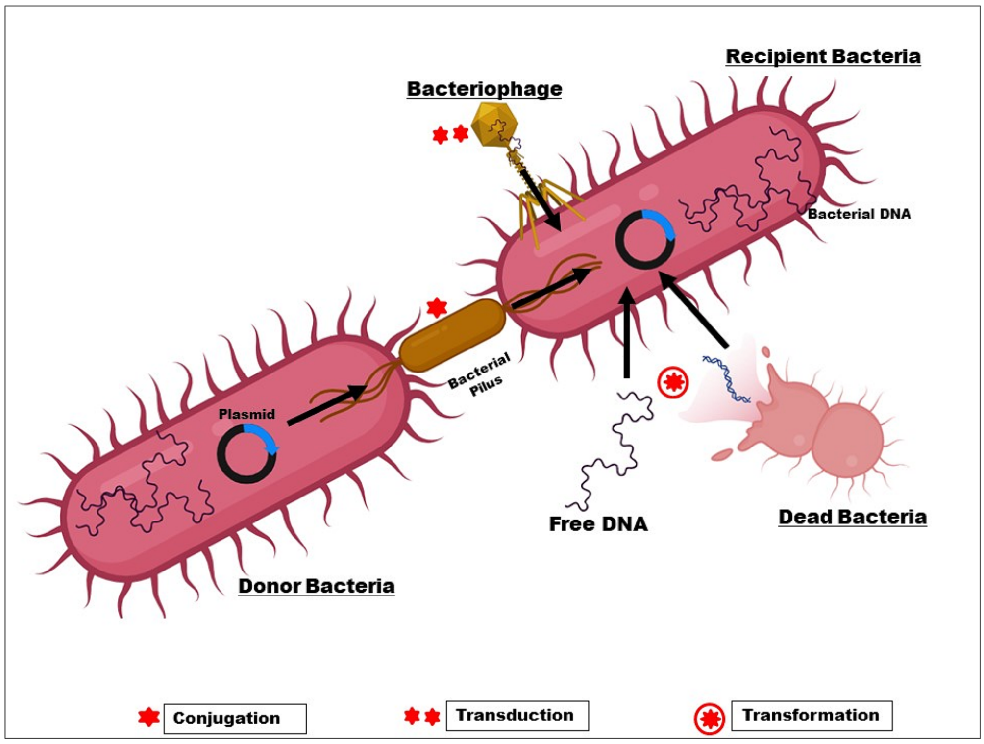

FIGURE 3
Transfer of r-gene from one bacterium to another.

Enterobacteriaceae, *Pseudomonas*, and *Acinetobacter*, B-lactam resistance genes are frequently found on plasmids and spread through inter-and intra-species conjugation (Martin et al., 2017; Phan et al., 2017; Gorrie et al., 2018). Globally, the plasmid pCT disseminated the blaCTX-M-14 to both animals and people on various continents. The widespread and quick spread of ESBLs suggests that these genes are instantly functional in newly formed host cells after HGT.

From the perspective of evolution, bacteria use two main genetic strategies to adapt to the antibiotic "attack": (i) mutations in gene(s) frequently linked to the compound's mechanism of action; and (ii) acquisition of foreign DNA through horizontal gene transfer (HGT) coding for resistance determinants (Munita and Arias, 2016).

Limiting a drug's absorption, altering a drug target, inactivating a drug, and active drug efflux are the basic mechanisms of resistance. Both endogenous to the bacteria and acquired from other microorganisms can be responsible for these mechanisms (Reygaert, 2018) (Table 1).

2.1 Limited drug uptake

Microbes may develop defence mechanisms that prevent an antimicrobial medicine from building up, which subsequently prevents the antibiotic from reaching its intended cellular target. Certain types of chemicals are blocked by the shape and functions of the lipopolysaccharide layer in gram-negative bacteria. Because of this, certain bacteria have an intrinsic resistance to classes of powerful antimicrobial medicines (Reygaert, 2018).

2.2 Drug target modification

Target site modifications frequently result from a bacterial gene's chromosomal spontaneous mutation. Minor changes to the target molecule can have a significant impact on antibiotic binding since antibiotic interactions with targets are typically extremely selective (Kapoor et al., 2017). Species that manufacture aminoglycosides, like *Streptomyces* spp., have this resistance mechanism, which gives them inherent resistance to the antibiotics they make. Enzymatic inactivation, however, is the most typical aminoglycoside resistance mechanism (Laws et al., 2019). Drugs that impact protein synthesis, such as macrolides, tetracycline, chloramphenicol, and aminoglycosides, become resistant when the 30S or 50S subunits of the ribosome are altered (Anandabaskar, 2021). While chloramphenicol, macrolides, lincosamides, and streptogramin B bind to the 50S ribosomal subunit to inhibit protein synthesis, AGs (aminoglycoside) bind to the 30S ribosomal subunit (Haider et al., 2022).

2.3 Drug inactivation

There are two basic ways that bacteria inactivate drugs: by degrading the medicine, or by adding a chemical group to the drug (Noor et al., 2021). The bacterial enzymes have been demonstrated to add chemical groups to antibiotic molecules' susceptible regions, preventing the antibiotic from attaching to its intended target (Ali et al., 2018). Hydroxyl and amide groups within an antibiotic's structure are easily altered by hydrolysis (Mehta et al., 2016). For instance, *Staphylococcus aureus* has demonstrated penicillin resistance, which is caused by the

TABLE 1 List of antibiotics used for different bacteria and their resistance mechanism.

S.No	Organism/strain	Resistance mechanism	Antibiotics used	References
1	*Enterococci* spp.	Acquiring B-lactamases or having PBP4/5 mutations	Penicillin	Hollenbeck and Rice (2012)
2	*Enterobacteriaceae, Klebsiella pneumoniae*, *Pseudomonas aeruginosa* and *Acinetobacter* baumannii	Porin mutations, efflux pumps, and enzyme production	Carbepenams	Suay-García and Pérez-Gracia (2021) and Codjoe and Donkor (2017)
3	*Enterococcus* spp.	Altering the process for the production of peptidoglycans, specifically by changing D-Alanine-D-Alanine (D-Ala-D-Ala) to either D-Alanine-D-Lactate (D-Ala-D-Lac) or D-Alanine-D-Serine (D-Ala-D-Ser).	Glycopeptides	Ahmed and Baptiste (2018)
4	*Pseudomonas aeruginosa*	driven by the aminoglycoside modifying enzymes (AME) like byaac(6′)-I, aac(6′)-II, ant(2″)-I, and aph(3′)-VI,	Aminoglycosides	Teixeira et al. (2016)
5	*Pseudomonas aeruginosa*	Limited permeability of the outer membrane, efflux systems that remove antibiotics from the cell, the development of B-lactamases and other antibiotic-inactivating enzymes, mutations, or horizontal gene transfer acquisition of resistance genes.	Sulfonamides	Pang et al. (2019) and Breidenstein et al. (2011)
		Antibiotic cleavage by β-lactamse enzymes, antibiotic expulsion by chromosomally encoded efflux mechanisms and reduced drug uptake owing to loss of outer membrane porin proteins.	Cephalosporins	Poole (2011)
		Antibiotic inactivation by Chloramphenicol acetyl transferase (CAT)	Chloramphenicol	Kapoor et al. (2017)
		Production of proteins that bind to the ribosome and alter the conformation of the active site	Tetracycline	Kapoor et al. (2017)
6	*Escherichia coli, Klebsiella pneumonia, Staphylococcus aureus*	Errors in the replication of the genes encoding the GyrA subunits of DNA gyrase and ParC of topoisomerase IV Overexpression of efflux pumps from the resistance-nodulation-cell division, Reduction of the membrane permeability by down regulation of extra-membrane proteins	Quinolones	Solano-Gálvez et al. (2020)
	Enterobacteriaceae species, Pseudomonas aeruginosa, Staphylococci, Streptococcus pneumoniae, Enterococcus faecalis and *Listeria monocytogenes*	Mutations in both target enzymes DNA gyrase in Gram-negative bacteria & topoisomerase IV in Gram-positive bacteria and increased expression of chromosomal gene leading to increased efflux of the fluoroquinolones.	Fluroquinolones	Yadav and Talwar (2019)
9	*Enterococci* spp., & *Staphylococcus aureus*	Mutations in the domain V region of 23S rRNA genes; acquisition of the ribosomal methyl-transferase gene *cfr*; and mutations in *rplD*, and *rplC* genes that encode 50S ribosomal proteins L4 and L3 respectively	Oxazolidinones	Stefani et al. (2010)
11	*Klebsiella pneumoniae*	Presence of the SHV-1 penicillinase in their chromosome, chromosomal mutations, and from acquisition of AMR genes via HGT, mainly via large conjugative plasmids.	Ampicillins	Wyres and Holt (2018)

blaZ gene, which produces the B-lactamase enzyme; by inhibiting the cross-links that make up the bacterial cell wall from forming, B-lactam antibiotics hinder the manufacture of the wall and weaken it, preventing bacterial growth (Monistero et al., 2020).

2.4 Active drug efflux

Reduced permeability and/or antibiotic efflux are two key mechanisms of antibiotic resistance in clinical strains. Gram-negative bacteria rely on the presence of their outer membrane, which acts as a permeability barrier, offering a pre-existing defence mechanism against hydrophilic antibiotics and other antimicrobial drugs like vancomycin. Thus, maintaining decreased permeability is vital for Gram-negative bacteria (Peterson and Kaur, 2018). Active efflux out of the cell frequently leads to resistance to B-lactams, tetracyclines, and fluoroquinolones, and it is rather typical for a single efflux pump to be able to transport a variety of antimicrobials. Except for polymyxin, all antibiotic classes are prone to activating efflux mechanisms. Efflux pumps can confer significant degrees of resistance

to formerly therapeutically effective antibiotics when they are overexpressed. Many efflux pumps, also referred to as multidrug resistance (MDR) efflux pumps, transport a large variety of structurally diverse substrates, in contrast to some efflux pumps that have a tight substrate specificity such as Tet pumps (Blair et al., 2015).

3 Alarming rise of antimicrobial resistance in pathogenic bacteria: a cause for concern

The formulation of thousands of tonnes of antibiotics has been spurred by population expansion, rising prosperity, and inappropriate use, and it is anticipated that production will continue to rise in the future years. A growing amount of evidence over the past few decades has demonstrated that antibiotics entering the environment can potentially have negative impacts on humans and non-target creatures (Christou et al., 2017). Antibiotics are released into the environment because of a variety of human actions, including the usage of veterinary drugs and the direct dumping of unused or expired prescriptions.

3.1 *Enterococci* spp.

Enterococci's clinical importance is mostly connected to their antibiotic resistance, which promotes colonisation and infection, particularly in hospitalised patients. Between 2001 and 2015, *Enterococcus faecalis* species had a lower rate of resistance than *Enterococcus faecium*. However, both species' rates of resistance significantly rose during this time. In comparison to general cases (hospitalised or outpatients without a specific underlying disorder), complicated cases (patients with underlying debilitating disorders) had higher mean resistance rates for vancomycin, gentamicin, ciprofloxacin, erythromycin, nitrofurantoin, chloramphenicol, trimethoprim-sulfametoxazol, imipenem, and teicoplanin. Except for penicillin and ampicillin, difficult cases had greater rates of antibiotic resistance than general patients (Asadollahi et al., 2018). *Enterococci species* (*E. faecalis*, *E. faecium*, and *E. casseliflavus*) found in 150 wild birds were tested for antimicrobial susceptibility. Antibiotics tetracycline, erythromycin, chloramphenicol, gentamicin, and streptomycin all showed high rates of resistance, while ampicillin and linezolid had low rates of resistance (Yahia et al., 2018). To characterize the virulence factors and antibiotic resistance profiles in enterococci taken from various clinical sources in the northwest of Iran, Jahansepas et al. (2018) conducted a study. From September 2014 to July 2015, 160 *enterococcal* clinical isolates were recovered from various wards of University Teaching Hospitals and identification was done by biochemical assay. 125 (78.12%) and 35 (21.88%) of the 160 *enterococcal* isolates were found to be *Enterococcus faecalis* and *Enterococcus faecium*, respectively. Resistance to rifampicin (76.25%) was the most prevalent pattern of antibiotic non-susceptibility, followed by erythromycin (73.12%). Vancomycin resistance was discovered in 30 isolates (11 *E. faecalis* and 19 *E. faecium*), with a minimum inhibitory concentration of >256 mg/mL (Jahansepas et al., 2018; Chauhan and Jindal, 2020).

The prevalence of vancomycin-resistant *E. faecium* in bloodstream infections is notably high, especially in Eastern Mediterranean nations, according to a 2019 meta-analysis study performed by Shiadeh et al. (2019), which is a major warning sign of resistance to this broad-spectrum antibiotic. According to the WHO's initial offices, American countries had the lowest rate of linezolid resistance in *Enterococcus faecalis* among all antibiotics. The Western Pacific, European, and American nations had the lowest prevalence of vancomycin resistance, while South-East Asia and the Eastern Mediterranean region had the highest prevalence. Additionally, it was discovered that Southeast Asia and America had the lowest and greatest levels of linezolid resistance for *Enterococcus faecium*, respectively. The highest rates of resistance were seen in Southeast Asian and Eastern Mediterranean nations, particularly for vancomycin and quinupristin/dalfopristin. Between 2000 and 2018, there were rising trends of antibiotic resistance in *Enterococcus* blood isolates, up to more than twice as much. Researchers concluded that these countries should be required to create acceptable rules for the use of antibiotics (Shiadeh et al., 2019) Asa1, hyl, cylA, efa, ebp, ace, esp., gelE, sprE, hemolysin, hydrogen peroxide, and biofilm production were among the virulence factors and antibiotic resistance that Gök et al. planned to examine in 2020 in *Enterococcus faecalis* and *E. faecalis* strains isolated from clinical specimens. The investigation contained a total of 110 *enterococcus* isolates that were recognised as infectious organisms. The isolates were identified, and virulence genes were found using the PCR technique. Of the 110 isolates of enterococci, 61 were determined to be *E. faecium* and 49 to be *E. faecalis*. Ciprofloxacin was shown to have the highest resistance rate (70.9%). Resistance to high level vancomycin and teicoplanin was 4.5%, high level gentamicin was 39.4%, high level streptomycin was 65.1%, and to ampicillin was 1.8% (Gök et al., 2020).

The level and distribution of resistance in commensal *E. faecalis* isolated from wild carnivorous mammals, as well as genetic linkages in terms of the source of these strains as well as resistance and virulence genes, were evaluated by Nowakiewicz et al. (2020). The findings revealed that over half (48%) of the examined animals carried one or more strains of *E. faecalis* that were resistant to multiple drugs. Moreover, two or three strains with distinct genotypes and resistance phenotypes were present in 44% of MDR-positive animals. High-level aminoglycoside resistance was present in a sizable proportion of bacteria (between 20% and as much as 57.5%) (Nowakiewicz et al., 2020). The percentage of antibiotic resistance profiles of *Enterococcus faecium*, *E. faecalis*, and *E. durans* isolated from traditional sheep and goat cheeses acquired from a chosen border region of Slovakia and Hungary (region Slanské vrchy) was calculated in Výrostková et al. (2021). *Enterococcus species*, including different strains of *E. faecalis*, *E. faecalis*, and *E. durans*, were found in cheese samples. *E. faecalis* strains were typically more resistant to antibiotics than *E. durans* and *E. faecium* strains. Their study showed high resistance to rifampicin (100%), vancomycin (85.7%), teicoplanin (71.4%), erythromycin (71.4%), minocycline (57.1%), nitrofurantoin (57.1%), ciprofloxacin (14.3%), and levofloxacin (14.3%) was seen in *E. faecalis*. Rifampicin (100%), teicoplanin (100%), vancomycin (66.7%), erythromycin (66.7%), nitrofurantoin (66.7%), and minocycline (33.3%) were all resistant to *E. durans*, while teicoplanin (100%), erythromycin (100%), and erythromycin (100%) were all resistant to *E. faecium* (Výrostková et al., 2021).

3.2 *Escherichia coli* and *Klebsiella pneumonia*

For the creation of medicines against MDR bacteria, the growth of extended-spectrum-lactamase (ESBL)-producing bacteria, especially *Escherichia coli* and *Klebsiella pneumoniae*, is of utmost importance (Chong et al., 2018). To evaluate the safety of bacterial isolates (*E. coli* strains) for human consumption as well as to give updated antibiotic data for effective patient treatment, Odonkor and Addo (2018) examined the microbiological quality and antibiograms of bacterial isolates from six different water sources in 2018. The results indicated that all the water sources tested had poor quality water. *E. coli*, *Enterobacter species*, *Klebsiella species*, *Salmonella typhi*, *Streptococcus species*, *Proteus vulgaris*, *Vibrio cholera*, *Shigella species*, *Pseudomonas aeruginosa*, and *Enterococcus faecalis* were among the bacteria that were isolated. MDR *E. coli* was present in 49.48% of cases. Isolates of *E. coli* exhibited high levels of antibiotic resistance. They were most resistant to tetracycline (21.45%), erythromycin (23.71%), cefuroxime (28.87%), and penicillin (31.9%). They were resistant to ciprofloxacin (74.2%), nalidixic acid (89.65%), nitrofurantoin (93.8%), cefotaxime and amikacin (91.75%), gentamicin (90.7%), chloramphenicol (69.07%), pipemidic acid (65.97%), and cefuroxime (52.58%) (Odonkor and Addo, 2018).

In a study published in Montso et al. (2019), isolated, identified, and characterised ESBL-producing *K. pneumoniae* and *E. coli* species from cattle faeces and samples of raw beef; Antimicrobial susceptibility testing showed that 66.7–100% of the isolates were multidrug-resistant and resistant to amoxicillin, aztreonam, ceftazidime, cefotaxime, and piperacillin. The ESBL gene determinants in the isolates that showed phenotypic resistance to ESBL antimicrobial susceptibility testing were checked and 53.1% of the isolates were found positive to have ESBL gene determinants (Montso et al., 2019).

After a thorough screening, Pormohammad et al. (2019) performed a meta-analysis on 39 studies, and the results showed that the overall MDR prevalence utilising the Disc Diffusion Method was 22, 31.3, and 5.7% in human, environmental, and animal *E. coli* isolates. MDR *E. coli* isolate rates were 12.6 and 22.2%, respectively, according to the results of the MIC. The incidence of MDR *E. coli* was higher in animal and environmental sources than in human sources, according to a comparison of isolates from various sources. Based on MIC, the prevalence of ESBL-producing *E. coli* was 42.4, 63.2, and 28.6%, respectively, in human, animal, and environmental or food isolates. Based on human, animal, and environmental/food isolates, the prevalence of ESBL-producing *E. coli* was 13, 26.3, and 25%, respectively. Animal isolates had a greater frequency of ESBL antibiotic resistance than observed in human isolates (Pormohammad et al., 2019).

For research on complex systems with multiple components, interactions and emergent processes are extremely important. Most of the research only considers pairwise interactions, ignoring higher-order interactions involving three or more components, Tekin et al. (2018) studied antibiotic combinations used to treat pathogenic *Escherichia coli* and gathered an unprecedented amount of detailed data (251 two-drug combinations, 1,512 three-drug combinations, 5,670 four-drug combinations, and 13,608 five-drug combinations). They discovered that the quantity of medications in the environment of the bacteria causes an increase in the frequency of higher-order interactions, which was directly contrary to earlier hypotheses and findings. More particularly, as more medications were introduced, rising incidences of emergent antagonistic effects (impact less than expected based on lower-order interaction effects), as well as increased occurrences of net synergy (effect more than expected based on independent individual effects), were observed. These results had significance for navigating issues related to the combinatorial complexity of multi-component systems and implications for the possible efficacy of medication combinations (Tekin et al., 2018). Nji et al. (2021) extracted study results obtained from 1989 to May 2020 in 2021. The search revealed a total of 9,363 publications, and 33 articles' prevalence statistics were retrieved and combined. This revealed a pooled prevalence of antibiotic resistance (top ten antibiotics frequently prescribed in LMICs) in commensal *E. coli* isolates from human sources in community settings in LMICs, including ampicillin, cefotaxime, chloramphenicol, ciprofloxacin, co-trimoxazole, nalidixic acid, oxytetracycline, streptomycin, tetracycline and trimethoprim at 72% of 13,531 isolates, 27% of 6,700 isolates, 45% of 7,012 isolates, 7% of 10,618 isolates, 63% of 10,561 isolates, 30% of 9,819 isolates, 78% of 1,451 isolates, 58% of 3,831 isolates, 67% of 11,847 isolates and 67% of 3,265 isolates, respectively. The study evaluated the evidence of commensal *E. coli*'s high incidence of antibiotic resistance in community settings in low-middle-income countries in the study (Nji et al., 2021).

The ability of clinical *Klebsiella pneumonia* isolates from Egypt to produce biofilms was examined by Mohamed et al. (2020), along with the bacteria's propensity for producing ESBLs, fimbrial genes, and antibiotic resistance. Ninety clinical *Klebsiella pneumonia* isolates were extracted from various sources in total. The determination of ESBL genotypic and phenotypic detection, biofilm assay, and antimicrobial susceptibility were done. The findings show a significant incidence of both biofilms forming capability (51%) and MDR (86.66%) among *Klebsiella pneumonia* isolates. In addition, *Klebsiella pneumonia* isolates that produced ESBLs were better able to form biofilms than those that did not. The prevalence of isolates with blaCTX-M was seen among ESBLS-biofilm makers, as were the occurrences of blaTEM and blaCTX-M. Fimbrial (mrkD and fimH) distribution among biofilm former isolates was 100 and 86.95%, respectively. ESBL-producing *Klebsiella pneumonia* isolates exhibited a higher potential to build a biofilm in contrast to non-ESBL-forming ones, according to the study, which also found that MDR was very prevalent among *Klebsiella pneumonia* in Egypt. Furthermore, our research provides compelling evidence that type 3 fimbriae greatly encourage biofilm development in *Klebsiella pneumonia* (Mohamed et al., 2020).

In Khaertynov et al. (2018) investigated the effects of antibiotic resistance and virulence variables in *K. pneumonia* strains on the clinical characteristics and outcomes of newborn infection. Testing of *K. pneumoniae* isolates for ESBL production in newborns with sepsis revealed positive results in 60% of cases, and in neonates with UTI—in 40% of cases. All *K. pneumoniae* isolates from blood and urine that produced ESBLs were resistant to third-generation cephalosporins and ampicillins. These isolates were additionally susceptible to meropenem, amikacin, and ciprofloxacin. Four blood isolates of *K. pneumoniae* and three urine isolates both contained the rmpA gene. In two cases, the rmpA gene was found in *K. pneumoniae* isolates that produce ESBL in neonates with sepsis. In two neonates with sepsis and three neonates with UTI, the genes for aerobactin and colibactin were found. Only rmpA-positive *K. pneumoniae* isolates were found in every case to have aerobactin and colibactin genes. We underestimate

how often virulent *K. pneumoniae* strains are in newborns with sepsis and other neonatal infections. In this investigation, virulent strains of *K. pneumoniae* caused the most severe cases of newborn sepsis with a poor prognosis (Khaertynov et al., 2018).

The goal of the study by Gandor et al. (2022) was to characterise the Carbapenem-Resistant *K. pneumoniae* (CRKP) isolates collected from patients hospitalised in the ICU of the Zagazig University Hospitals (ZUHs) in Egypt. As for blaNDM, blaOXA-48, and blaKPC, respectively, about 56.2, 41.0, and 32.4% of the isolates showed the presence. Many isolates included genes that encoded carbapenemase, with blaNDM was the most present gene. When CRKP isolates were tested for antimicrobial susceptibility, an MDR profile was discovered, with 100% of the isolates being resistant to piperacillin, piperacillin/tazobactam, cefepime, ceftazidime, azithromycin, and ticarcillin. Contrarily, 95.0% of the isolates exhibited high levels of resistance to tobramycin, gentamicin (83.2%), pefloxacin (95%) and ciprofloxacin (98.3%) (Gandor et al., 2022). Amikacin (40.8%), aztreonam (73.3%), ceftazidime (75.7%), ciprofloxacin (59.8%), colistin (2.9%), cefotaxime (79.2%), cefepime (72.6%), and imipenem (65.6%) were the drugs with the highest prevalence rates of drug resistance in *K. pneumonia* studied by Effah et al. (2020). Some of the resistance-mediated genes identified were TEM (39.5%), SHV-11 (41.8%), and KPC-2 (14.6%). The most virulent components used by *K. pneumoniae* include the hyper-mucoviscous phenotype, genes associated with mucoviscosity, genes that are involved in the synthesis of lipopolysaccharide, genes involved in iron uptake and transport, and adhesive genes (Effah et al., 2020).

A fluorocycline belonging to the tetracycline class, eravacycline, was recently authorized. It is effective against a wide range of pathogenic infections, including *K. pneumoniae*, *Acinetobacter* spp., and *E. coli* that produces ESBLs (Yusuf et al., 2021). In Xu et al. (2022) showed that the clinical isolate Kp43 of the carbapenem-resistant *K. pneumoniae* rapidly established eravacycline resistance. The lon gene was disrupted by mutations or had its expression level decreased by a Tn insertion upstream of the lon gene, as per the WGS analysis of the resistant mutants. Eravacycline resistance in bacteria was decreased by complementation with a wild-type lon gene. Eravacycline-resistant strains that originated from a clinical isolate of *K. pneumoniae* that included NDM-1 were also found to have mutations in the lon gene (Xu et al., 2022). Both ceftazidime-avibactam and eravacycline are also vulnerable to Kp43. The US Food and Drug Administration (FDA) and the European Medicines Agency (EMA) separately approved ceftazidime-avibactam for use in clinical trials in 2015 and 2016. However, *K. pneumoniae* clinical isolates that were ceftazidime-avibactam resistant were reported in 2016 and afterwards (Shields et al., 2016, 2017; Galani et al., 2021).

3.3 *Staphylococcus aureus*

A condition that has been widely established in *Staphylococcus aureus* infections with various cephalosporins is that an organism's *in vivo* susceptibility to a specific antibiotic may vary according to the size of the bacterial inoculum. There is evidence to show that some cephalosporins (such cefazolin) may not work in the case of high-inocula, deep-seated infections brought on by *S. aureus* that are susceptible to cephalosporins (Nannini et al., 2013).

With remarkable adaptive abilities, *Staphylococcus aureus* is a dangerous human pathogen. The primary mechanism through which antibiotic-resistant clones rapidly emerge is by acquiring antibiotic-resistance genes from other *S. aureus* strains or even from other genera (Haaber et al., 2017). Through a variety of processes, such as horizontal gene transfer and chromosomal mutation, resistance is rapidly evolving. *S. aureus* pathogenesis differs from common resistance mechanisms in that it can persist in the biofilm state on both surfaces that are biotic as well as abiotic. The World Health Organisation (WHO) identified MRSA as one of the top 12 infections that pose a hazard to human health (Craft et al., 2019). Many nosocomial infections are caused by *Staphylococcus aureus*. Nosocomial infections, also known as healthcare-associated infections (HAI), are infections or illnesses that develop while undergoing medical treatment but were absent at the time of admission. About 30% of people have *S. aureus*, a Gram-positive commensal, chronically colonising their skin and mucous membranes (Tong et al., 2015). Due to bacterial evolution and antibiotic misuse in recent years, *S. aureus* drug resistance has gradually grown, MRSA infection rates have climbed globally, and clinical anti-infective treatment for MRSA has gotten increasingly challenging (Guo et al., 2020).

Antibiotic resistance is also acquired by *S. aureus* from less closely related bacteria, including *enterococci* that exhibit vancomycin resistance (Haaber et al., 2017). The first MRSA strain with vanA and a minimum inhibitory concentration (MIC) to vancomycin greater than 1,000 mg/mL was discovered in 2002. A conjugative *Enterococcus faecalis* plasmid containing the vanA gene within the transposon element Tn1546 had been transmitted to an MRSA strain during coinfection, according to a genome study. The transposons then moved to a plasmid that was present in the original MRSA strain (Weigel et al., 2003). Since then, numerous instances of vancomycin-resistant *S. aureus* (VRSA) have been recorded; these cases frequently include the Tn1546 transposon element either being transferred by an enterococcalinc18-like plasmid or having transferred to a *S. aureus* plasmid (Haaber et al., 2017). According to Corvaglia et al. (2010) the transfer of genetic material from enterococci to *S. aureus* appears to be simpler in staphylococcal strains lacking a type-III endonuclease and the Hsd restriction modification systems. This transfer may also be facilitated by the presence of fp SK41 family plasmids in recipient *S. aureus* strains, possibly due to secreted plasmid factors (Zhu et al., 2013).

Antibiotic use in industrial hog operations (IHOs) can facilitate the growth of antibiotic-resistant (ABR) *Staphylococcus aureus*, was studied in 2017 by Hatcher et al. It's yet unknown how much exposure to ABR *S. aureus* IHO employees and the kids who live in their houses have experienced. They looked at the prevalence of ABR *S. aureus* nasal carriage in individuals who had occupational exposure to IHOs versus those who did not, as well as in kids who lived in their homes. Individuals in IHO had a greater prevalence of *S. aureus* nasal carriage (53%) compared to Community Residents (31%) (adjusted prevalence ratio (aPR): 1.40), although MRSA nasal carriage was infrequent (2–3%) in both IHO and CR individuals. IHO employees and CR people both had a similar incidence of MDRSA nasal carriage (12% vs. 8%; aPR: 1.14). Nasal carriage prevalence of *S. aureus*, MRSA and MDRSA was greater among IHO children than CR children. Additionally, they discovered hints that suggested that children residing with IHO employees who reported taking personal protective equipment (PPE) home from the IHO had a greater incidence of

S. aureus, MRSA, and MDRSA. Among IHO employees, *S. aureus* nasal carriage that was related to livestock predominated (Hatcher et al., 2017).

The peptidoglycan that forms when an MRSA strain is cultured with B-lactams is not well cross-linked. Exposure of the MRSA strain to β-lactams can lead to an increase in the pro-inflammatory effects of peptidoglycan, potentially contributing to pathology during infection (Müller et al., 2015). The global accessory gene regulator (Agr), which can be triggered in some MRSA strains, may not be able to do so due to the changed peptidoglycan structure (Rudkin et al., 2012). MRSA has become a barrier to clinical therapy due to its aspects of simple infection, high mortality, and antibiotic resistance (Khoshnood et al., 2019).

The prevalence of MRSA strains in *P. americana* and *B. germanica* cockroaches was 52.77 and 43.33%, respectively, according to a 2019 study by Abdolmaleki et al. MRSA strains were most prevalent (59.57%) in samples of *P. americana* cockroaches taken after external washing. The most common forms of resistance to penicillin (100%), ceftaroline (100%), tetracycline (100%), gentamicin (83.33%), and trimethoprim-sulfamethoxazole (80.55%) were found in MRSA isolates from external washing samples. The greatest rates of penicillin (100%), ceftaroline (100%), tetracycline (100%), trimethoprim-sulfamethoxazole (80%), and gentamicin (73.33%) resistance were seen in MRSA strains isolated from gut content samples (Abdolmaleki et al., 2019).

Gram-negative bacteria have a fundamentally different mechanism controlling entry into the persister stage than *S. aureus* (Conlon et al., 2016). *S. aureus* cells in stationary phase are resistant to bactericidal drugs, unlike Gram-negative bacteria. In any population of *S. aureus*, a tiny percentage of cells have already entered in the stationary phase, which is marked by ATP depletion (Foster, 2017). The entire population will enter stationary phase and turn into persisters if cells are purposefully deprived of ATP. A toxin-antitoxin system does not appear to be the mechanism(s) through which persister generation is accomplished. *S. aureus* cells in the persister state can be eliminated by the acylpepsipeptide antibiotic ADEP4 according to a study by Conlon et al. (2013). By releasing the enzyme from its ATP-dependent chaperone, it activates the ClpP protease, allowing it to uncontrollably break down intracellular proteins (Foster, 2017). Over 90% of *S. aureus* clinical isolates generate staphyloxanthin, which serves as a major virulence factor in the form of an antioxidant that protects against reactive oxygen species (ROS) produced by the host immune system (Liu et al., 2005, 2008). Therefore, preventing the manufacture of staphyloxanthin is a viable antivirulence tactic to stop *S. aureus* infection. The first beta-lactam antibiotic, penicillin, was shown to be a powerful tool against *S. aureus* infections in 1928. There were reports of *S. aureus* strains that were penicillin-resistant in the 1940s, just after it had been introduced into clinics (Rammelkamp and Maxon, 1942).

According to Gnanamani et al. (2017) the strains developed penicillinase, a plasmid-encoded beta-lactamase enzyme that enzymatically broke the beta-lactam ring of penicillin and rendered the antibiotic not active (Gnanamani et al., 2017). Penicillin resistance in the 1950s was only present in *S. aureus* hospital isolates. Due to plasmid transfer of the penicillinase gene (blaZ) and clonal spread of resistant strains, by the late 1960s, more than 80% of *S. aureus* isolates, regardless of their origin in the community or a hospital, were resistant to penicillin (Chambers, 2001; Lowy, 2003).

4 Novel antibiotics and AMR combating strategies

Most antibiotics currently in use come from the phylum *Actinobacteria*, with bacteria from the genus *Streptomyces* living in soil and producing over 80% of actinobacterial-derived antibiotics (Barka et al., 2016). The identification of new antibiotics designed to overcome resistance was used to address the growth of resistant strains of bacteria. This has gradually resulted in the selection of MDR bacteria, which have several resistance genes and are resistant to various types of antibiotics. A deeper understanding of the mechanisms and hotspots involved in the diffusion and development of novel resistances and MDR is urgently required considering their rapid emergence. Furthermore, resistance mechanisms aimed against newer antibiotics, such as-lactamases, frequently transmit resistance to earlier established antibiotics in the same class (Kakoullis et al., 2021). In terms of B-lactams, newly developed antibiotics comprise either novel cephalosporins or novel B-lactam inhibitors paired with existing B-lactams. Cephalosporins that have recently been developed include ceftobiprole, ceftaroline, cefiderocol, and ceftolozane, which is available in conjunction with tazobactam. Ceftobiprole is a fifth-generation cephalosporin and the first B-lactam to show antimicrobial efficacy against MRSA and VRSA *in vitro*. Ceftobiprole binds to PBP 2a, the altered PBP of MRSA, quickly and consistently. It is also effective against PBP 2x, a penicillin-resistant *Streptococcus pneumonia* PBP. Ceftobiprole, on the other hand, is sensitive to degradation by ESBLs, AmpC, and carbapenemases of Classes A, B, and D. Ceftobiprole is approved for the treatment of community and hospital-acquired pneumonia, as well as skin and soft-tissue infections such as diabetic foot infections (Lupia et al., 2021). Cefiderocol is a new siderophore cephalosporin with a structure identical to ceftazidime and cefepime but with a catechol moiety. Cefiderocol can bind to free iron because of catechol moiety, which mimics the naturally occurring siderophores of Gram-negative bacteria. Cefiderocol is actively carried into the periplasmic region after binding to iron, bypassing bacterial porins, where it dissociates from iron and binds to PBPs. Cefiderocol can thus accumulate in larger quantities in the periplasmic space than other cephalosporins. Cefiderocol is resistant to ESBLs, KPC (Class A), NDM, VIM, IMP (Class B), AmpC (Class C), and OXA-48 similar (Class D). It is permitted for the treatment of severe urinary tract infections, hospital-acquired pneumonia, and ventilator-associated pneumonia (Sato and Yamawaki, 2019; Abdul-Mutakabbir et al., 2020).

The World Health Organization's recommended tuberculosis (TB) control method is known as directly observed therapy, short-course (DOTS, commonly known as TB-DOTS). According to WHO, "the most cost-effective way to stop the spread of tuberculosis in high-incidence communities is to cure it." DOTS is the greatest cure for tuberculosis. DOTS includes five major components: (i) Establish a centralised and prioritised system for TB monitoring, documentation, and training. (ii) Detect cases by sputum smear microscopy. (iii) Standardised treatment regimen for six to 9 months, monitored by a healthcare provider or community health worker for the first 2 months. (iv) Drug supply. (v) Standardised recording and reporting system allowing treatment results assessment.

India established the Revised National Tuberculosis Control Programme (RNTCP) in 1997 to combat the growing TB epidemic, and it was expanded to encompass the whole country by 2006. This project investigated more than 650 TB suspects per 100,000 people, and over 1.5 million TB patients began the globally recommended Directly Observed Treatment Short-course (DOTS) per year. WHO created the DOTS approach for tuberculosis control in 1995, and it is presently being implemented in more than 180 countries worldwide. Under DOTS, TB mortality in India was lowered from 39 per 100,000 people in 1990 to 23 per 100,000 population in 2010, and the prevalence of TB was reduced to 256 per 100,000 population in 2010 from 456 per 100,000 population in 1997 (Chopra et al., 2018).

Ceftolozane is a new cephalosporin with a structure like ceftazidime that has been developed in conjunction with tazobactam. Ceftolozane-tazobactam's range of effectiveness includes Gram-negative bacteria such as *P. aeruginosa*, *E. coli, K. pneumoniae, Burkholderia cepacia, and M. catarrhalis*. Ceftolozane is particularly effective against *P. aeruginosa* because it can evade many of the bacterium's resistance mechanisms, such as the production of modified PBPs or the reduction of intracellular antibiotic concentrations via alterations in porins and the production of efflux pumps; it is even effective against *P. aeruginosa* strains resistant to ceftazidime or piperacillin-tazobactam. Ceftolozane-tazobactam has been authorised for the treatment of patients with complex intra-abdominal and urinary tract infections, and high-dosage ceftolozane-tazobactam is non-inferior to meropenem in the treatment of hospital acquired pneumonia (Sorbera et al., 2014; Zhanel et al., 2014; Kollef et al., 2019).

Omadacycline (aminomethylcycline subclass) and eravacycline (fluorocycline subclass) are two novel tetracyclines that are active against bacteria that contain efflux pumps or ribosome protection proteins, mechanisms that normally confer resistance to earlier tetracyclines (Koulenti et al., 2019; Shortridge et al., 2020; Eljaaly et al., 2021).

Dalbavancin, telavancin, and oritavancin are three new lipoglycopeptides used to treat MDR Gram-positive infections. Because of their various alterations, many antibiotics exhibit multiple modes of action in addition to inhibiting cell wall formation via transglycosylation and transpeptidation. The presence of lipid side chains in all three antibiotics allows them to attach to the cell membrane, significantly increasing their efficacy (Kakoullis et al., 2021).

Pharmacokinetics/pharmacodynamics-driven therapy has shown to be a viable strategy for optimising antimicrobial therapy based on the features of the specific patient being treated. It has become clear that human and veterinary pharmacologists share research goals of revising dosage regimens and developing drugs with improved pharmacokinetic/pharmacodynamic properties to maximise clinical efficacy, improve patient care, and reduce the adverse impacts of antimicrobial therapy on the naturally occurring microbiota (Guardabassi et al., 2020). In aquaculture, probiotics are used to fight both Gram-positive and Gram-negative bacteria. The application of Gram-positive bacteria as probiotics is common around the world. *Bacillus subtilis*, an endospore-forming bacillus genus, is widely used in aquaculture (Bhat and Altinok, 2023). To avoid such a dismal and oblique future, action must be taken now! Limiting the use of antimicrobials in farming and other phases of food production, as well as in medicine, can slow the spread of antibiotic resistance. Furthermore, further study is needed to discover and investigate other means of treating resistant diseases, such as the use of probiotics. Probiotics can be used to fight back on a bacterial level by replacing harmful germs with safer ones (Freeland et al., 2023). The World Bank's recently released One Health (OH) operational framework prioritises AMR. The phrase 'One Health' refers to a collaborative, multi-sectoral, and transdisciplinary strategy that works at the local, regional, national, and global levels to achieve optimal health outcomes while acknowledging the interconnectedness of humans, animals, plants, and their common environment (Guardabassi et al., 2020).

Current One Health initiatives to AMR are mostly focused on reducing antibiotic usage in food animals. Recent systematic reviews and meta-analyses found associations between reduced antibiotic use in food animals and a decrease in AMR in animals, with limited evidence of a reduction in humans, recognising that the system's complexity prevents the demonstration of a clear causal pathway and highlighting research gaps (White and Hughes, 2019).

Global changes are accelerating due to population growth, industrialization, and geopolitical issues, threatening biodiversity, ecosystems, and migratory patterns of both humans and other animals. Rapid climatic and environmental changes have resulted in the development and re-emergence of both infectious and non-infectious illnesses. Self-medication with antibiotics is an inappropriate approach to use antibiotics and a typical practice in resource-constrained nations that exposes people to the frightening danger of acquiring antimicrobial resistance and adverse effects (Torres et al., 2019). In India, the idea of One Health is still in its early stages, but it is gaining popularity. The Indian government has launched various measures to address emerging issues like as antibiotic resistance, zoonotic illnesses, and food safety with the OH approach, however there are numerous implementation hurdles (Aggarwal and Ramachandran, 2020) Antibiotic stewardship has evolved over the last 20 years and is now a worldwide initiative, with organisations striving to apply interventions to rationalise antibiotic usage in secondary care. Prescriber behaviours are influenced using frameworks from social science research. However, these frameworks frequently fail to integrate a contextual and cultural analysis (Charani and Holmes, 2019).

5 Influence of antibiotic resistance on sustainability

Antibiotics have saved millions of lives by lowering complications and death from infectious illnesses. However, increased antimicrobial medication usage is also linked to a rise in AMR. Pharmaceutical corporations, as manufacturers of these medications, can play a significant role in combating AMR. Without their efforts, the chances of successfully tackling the problem are slim. The rising use of antibiotics internationally, as well as the accompanying AMR, is increasing healthcare expenditures and adding to patient mortality.

A framework for analysis of AMR policies is a key step towards systematically consolidating information on previous and current policies, making sense of the diversity of national action against AMR, and relating this knowledge to nations' AMR situations. Formulating AMR strategies that are tailored to the particular

factors of AMR can help to provide an evidence-based and successful strategy for combating the worldwide problem of AMR (Ogyu et al., 2020). A Study was done by Huijbers et al. (2019) where they stated that Antibiotic resistance and environmental surveillance may help safeguard human, animal, and ecosystem health. However, the rationale for the selection of markers and sample locations that provide information about diverse risk situations is frequently missing. In the study, they described five fundamentally distinct goals for monitoring drugs and antibiotic resistance in the environment. The primary goal is to identify the risk of antibiotic-resistant microorganisms being transmitted to people through environmental channels. The second was which addresses the risk of speeding the evolution of antibiotic resistance in pathogens by contamination with agents and microbes of human or animal origin. The third goal was to address the risk that antibiotics represent for aquatic and terrestrial ecosystem health, particularly the effects on ecosystem functions and services. The other two objectives are similar to those of traditional clinical surveillance: to determine population-level resistance prevalence and population-level antibiotic usage. These two environmental monitoring aims are especially promising in areas where traditional clinical surveillance data and antibiotic usage statistics are few or unavailable. For each target, the levels of evidence offered by various phenotypic and genotypic microbial surveillance indicators, as well as antibiotic residues, were reviewed and evaluated conceptually. Furthermore, sites for which monitoring would be particularly useful are indicated. The suggested framework might be one of the beginning points for directing environmental monitoring and surveillance of antibiotics and antibiotic resistance at various spatiotemporal scales, as well as harmonising such operations with current human and animal surveillance (Huijbers et al., 2019).

India and China, the world's largest makers of generic pharmaceuticals, are also top in antibiotic usage among developing countries. According to studies, antibiotic usage in India and China climbed by 63 and 65%, respectively, between 2000 and 2015 (Klein et al., 2018).

The UN announced the SDGs in 2015 as part of the "2030 Agenda for Sustainable Development" programme to serve as a worldwide blueprint for a better, more equal, and more sustainable living on our planet. The UN Earth Summit in Rio de Janeiro in 1992 and the UN Millennium Summit in New York in 2000 generated the precursors of SDGs & Agenda 21 and the Millennium Development Goals (MDGs) respectively. The SDG initiatives contain 17 well-defined objectives from the disciplines of environment, climate change, societal concerns, economics, education, and healthcare, all of which are frequently interconnected, as well as well-defined actions, targets, and monitoring criteria to enable the evaluation of these goals' progress (Gajdács et al., 2021).

The growing levels of AMR pose a danger to the achievement of the SDGs since this phenomenon has a significant impact on changes in society and healthcare: the SDGs contextualise AMR as a global public health and social concern (World Health Organization, 2017). This may have been exacerbated by the onset of the global severe acute respiratory syndrome coronavirus 2 (SARS-CoV-2) pandemic, which has not only exacerbated societal inequalities and economic difficulties but has also resulted in a significant increase in antibiotic use worldwide for patient treatment; it is not yet known what the long-term consequences of this pandemic will be in the context of the SDGs (Hajek et al., 2020; Khor et al., 2020; Yadav, 2022; Yadav and Ravichandran, 2024).

The continued rise of AMR, for example, may hinder the achievement of Sustainable Development Goals 1 (No Poverty) and 2 (Zero Hunger). Food production is expected to increase by 50–70% between 2010 and 2030 due to increasing global population, economic growth, and changes in consumption habits; at the same time, the use of antimicrobials in food production (e.g., meat, milk, eggs) is expected to increase by a similar margin (Laxminarayan et al., 2016). Major reports have already demonstrated this: while global antibiotic consumption in human medicine increased by 10%, consumption of these drugs in animal husbandry increased by nearly 180% in the "BRICS" conglomerate countries (Brazil, Russia, India, China, and South Africa), with continued rising trends expected till 2030 which will lead to the spread of AMR across the ecosystem (Van Boeckel et al., 2017).

Several of the accepted objectives in the health-focused SDG 3 will be impossible to attain unless effective antibiotics are available. Antibiotics were included in a list of 13 life-saving commodities that contributed to the achievement of the Millennium Development Goals (MDGs) on maternal and child health in the Every Woman Every Child initiative. The advent of AMR is presently jeopardising the progress gained in lowering maternal mortality over the past 15 years, particularly in low-and middle-income countries (LMICs), where maternal death rates are up to 19 times higher than the rest of the world (Jasovský et al., 2016). Drug-resistant organisms have the potential to reverse the current good trend of reducing worldwide mortality rates from infectious illnesses, which have fallen from 23 to 17% of total fatalities in the preceding 15 years.

AMR impacts the poor, from the international development point of view. Resistance rates are high, and cheap treatment choices are frequently unavailable, especially since many patients pay for medications out of finances. Furthermore, poor sanitary systems facilitate disease transmission. Drug-resistant infections are more expensive, take longer to treat, and have a lower success rate than drug-susceptible illnesses. As a result of these considerations, AMR has a detrimental influence on national economic performance, potentially impeding progress towards SDG 1 (Laxminarayan et al., 2013).

Antibiotic residues and resistant bacteria are increasing in aquatic habitats as a result of waste products from hospitals, antibiotic production companies, and agriculture. Measurements at a wastewater treatment plant that received trash from around 90 pharma factories, for example, revealed that 45 kg of a popular antibiotic was dumped into a neighbouring river each day. The antibiotic concentration in the river was higher than it would be in a patient who had been treated with the medicine. As antibiotic residues are transported by water, sediments, and soil, gradients of differing antibiotic concentrations occur, and even very low antibiotic concentrations may be sufficient to select for highly resistant bacteria. Importantly, a lack of access to clean water and sanitation (SDG 6) promotes the spread of bacterial infections, resulting in increased morbidity and death, particularly among children (Jasovský et al., 2016).

Antimicrobial resistance to medicines currently causes an estimated 700,000 people each year and is expected to kill 10

million people and cost up to $100 trillion by 2050 if no effective action is taken. Loss of effective medicines for the treatment of infectious illnesses adds to state healthcare costs, lowers productivity, household income, and tax revenues, and leads to GDP losses. Such high expenses may jeopardise attempts to achieve long-term economic growth, as emphasised in SDG 8, making AMR a significant global development problem (Smith et al., 2005).

The recently introduced SDG indicator on antimicrobial resistance (AMR) intends to reduce the percentage of bloodstream infections caused by *Staphylococcus aureus* resistant to the drug methicillin (MRSA) and *Escherichia coli* resistant to 3rd-generation cephalosporin medicines. Controlling these two types of AMR pathogens effectively will eventually protect the ability to treat infections with current antimicrobials until new preventive and treatment strategies are developed. While providing data to monitor global trends, this new indicator will also be particularly useful for assessing progress in improving the country's ability to successfully execute AMR and health security national action plans.

AMR is one of the issues that governments must deal with. Many people are unaware that they or their cattle may have a resistant illness, and those who treat them are frequently clueless as well. This suggests that the issue is mainly unidentified and unrecorded. The absence of representative AMR data, particularly in LMICs, remains an issue. Because the true scope of the problem and its potential consequences are unknown, developing a compelling national AMR narrative to boost political participation, financial commitments, and public awareness is challenging. The phase-out of the use of antimicrobial drugs for animal growth promotion and the implementation of pollution-control methods may need modifications in agricultural practices, waste and wastewater management, and pharmaceutical production systems. Controlling ecosystem-based ways to reduce antibiotic usage in plant production is critical for human health and the environment. These safeguards are a critical investment in the protection of human, animal, plant, and planetary health. Countries will thus require a combination of incentives, education, training, and legislation to effect these reforms (World Health Organization, 2021).

The link between AMR and increasing climate change is subtle, but significant, according to Goal 13 (Climate Action). The parallels between climate change and AMR are highlighted in the WEF report as creeping, multidisciplinary, and critical concerns for mankind (World Economic Forum, 2019). Changes in global climate will undoubtedly alter the diversity and complexity of microbial populations around the world; while the emergence of novel bacterial diseases is unlikely, the number of people at risk for many of these infections, including vector-borne and zoonotic pathogens, and illnesses associated with food, will undoubtedly increase (Turner, 2018; Fouladkhah et al., 2020). A 1°C rise in ambient temperatures may result in a 5–10% increase in the incidence of foodborne salmonellosis cases, resulting in significant healthcare and economic expenses. It has also been suggested that rising temperatures may facilitate the selection of resistant isolates.

6 Conclusion and future prospects

One of the crucial actions against prevailing antibiotic resistance is the identification of novel compounds to safeguard lives now and in the future. A significant strategy must be made in conjunction with determined efforts in the direction of infection prevention, better antibiotic use, and stopping the spread of resistance when it does arise (Centers for Disease Control and Prevention, 2019). Antibiotic misuse and overuse have led to a rise in bacterial resistance and a decline in susceptibility. Drugs and antibiotics are now less effective at treating bacterial infections and other diseases as a result. Drug concentrations at the infection site must both stop the organism and stay below levels hazardous to human cells. To boost effectiveness, new medication combinations targeting various targets and methods of action must be created. Antibiotic exposure has resulted in the development of resistance to every single agent used. Despite the difficulty of identifying novel antibiotics, the continual discovery of new antibiotics remains the major technique for treating bacterial-associated illnesses. While new antibiotics may be capable of combating existing resistance mechanisms, improper administration of these drugs will ultimately result in the development of resistance mechanisms against them as well. Additionally, new drugs must be created that target resistance mechanisms (for example, to target bacteria) by preventing the capacity of previous drugs to attack. Bacteria that are resistant to antibiotics are the root of a growing therapeutic issue that has detrimental effects on human health. There are major repercussions from the current global increase in bacterial strains that are resistant to antibiotics mixed with the downward trend in the creation of new antibiotics. Antimicrobial efficacy must be viewed as a finite global public benefit on the edge of becoming rare, and the world must work together to protect it to save many future victims of drug-resistant illnesses. It is required to have an adaptable, multifaceted strategy that works across the SDGs and involves a wide range of stakeholders. As a result, we cannot rely solely on the biomedical or health industries for solutions. AMR is a system breakdown that necessitates a multi-sectoral solution. By including AMR on the SDG agenda, we hope to strengthen and broaden worldwide political commitment to finding a solution to this developing issue.

Author contributions

SS: Conceptualization, Data curation, Formal analysis, Investigation, Methodology, Writing – original draft, Writing – review & editing. AC: Conceptualization, Data curation, Formal analysis, Investigation, Methodology, Project administration, Supervision, Validation, Visualization, Writing – original draft, Writing – review & editing. AR: Conceptualization, Data curation, Formal analysis, Investigation, Methodology, Software, Supervision, Visualization, Writing – original draft, Writing – review & editing. DM: Conceptualization, Data curation, Formal analysis, Investigation, Visualization, Writing – original draft, Writing – review & editing. SH: Conceptualization, Data curation, Formal analysis, Investigation, Visualization, Writing – original draft, Writing – review & editing. SR: Data curation, Formal analysis, Investigation, Project administration, Visualization, Writing – original draft, Writing – review & editing. HT: Data curation, Formal analysis, Investigation, Methodology, Project administration, Supervision, Validation, Visualization, Writing – original draft, Writing – review & editing. TJ: Data curation, Formal

analysis, Supervision, Validation, Writing – original draft, Writing – review & editing. VY: Formal analysis, Funding acquisition, Methodology, Project administration, Resources, Supervision, Validation, Visualization, Writing – original draft, Writing – review & editing.

Funding

The author(s) declare financial support was received for the research, authorship, and/or publication of this article. The authors extend their appreciation to the Deputyship for Research & Innovation, Ministry of Education in Saudi Arabia for funding this research work through the project number ISP23-101.

Conflict of interest

The authors declare that the research was conducted in the absence of any commercial or financial relationships that could be construed as a potential conflict of interest.

Publisher's note

References

Abdolmaleki, Z., Mashak, Z., and Safarpoor Dehkordi, F. (2019). Phenotypic and genotypic characterization of antibiotic resistance in the methicillin-resistant *Staphylococcus aureus* strains isolated from hospital cockroaches. *Antimicrob. Resist. Infect. Control* 8, 1–14. doi: 10.1186/s13756-019-0505-7

Abdul-Mutakabbir, J. C., Alosaimy, S., Morrisette, T., Kebriaei, R., and Rybak, M. J. (2020). Cefiderocol: a novel Siderophore cephalosporin against multidrug-resistant gram-negative pathogens. *Pharmacotherapy* 40, 1228–1247. doi: 10.1002/phar.2476

Adekanmbi, A. O., Adejoba, A. T., Banjo, O. A., and Saki, M. (2020). Detection of sul 1 and sul2 genes in sulfonamide-resistant bacteria (SRB) from sewage, aquaculture sources, animal wastes and hospital wastewater in south-West Nigeria. *Gene Rep.* 20:100742. doi: 10.1016/j.genrep.2020.100742

Aggarwal, D., and Ramachandran, A. (2020). One health approach to address zoonotic diseases. *Indian J. Community Med.* 45, S6–S8. doi: 10.4103/ijcm.IJCM_398_19

Ahmed, M. O., and Baptiste, K. E. (2018). Vancomycin-resistant enterococci: a review of antimicrobial resistance mechanisms and perspectives of human and animal health. *Microb. Drug Resist.* 24, 590–606. doi: 10.1089/mdr.2017.0147

Ali, J., Rafiq, Q. A., and Ratcliffe, E. (2018). Antimicrobial resistance mechanisms and potential synthetic treatments. *Future Sci. OA* 4:FSO290. doi: 10.4155/fsoa-2017-0109

Anandabaskar, N. (2021). *Protein synthesis inhibitors. Introduction to basics of pharmacology and toxicology: Volume 2: Essentials of systemic pharmacology: From principles to practice*. Springer, 835–868.

Asadollahi, P., Razavi, S. H., Asadollahi, K. H., Pourshafie, M. R., and Talebi, M. (2018). Rise of antibiotic resistance in clinical enterococcal isolates during 2001–2016 in Iran: a review. *New Microbes New Infect.* 26, 92–99. doi: 10.1016/j.nmni.2018.08.018

Barathe, P., Kaur, K., Reddy, S., Shriram, V., and Kumar, V. (2024). Antibiotic pollution and associated antimicrobial resistance in the environment. *J. Hazard. Mater. Lett.* 5:100105. doi: 10.1016/j.hazl.2024.100105

Barka, E. A., Vatsa, P., Sanchez, L., Gaveau-Vaillant, N., Jacquard, C., Klenk, H. P., et al. (2016). Taxonomy, physiology, and natural products of Actinobacteria. *Microbiol. Mol. Biol. Rev.* 80, 1–43. doi: 10.1128/MMBR.00019-15

Bello-López, J. M., Cabrero-Martínez, O. A., Ibáñez-Cervantes, G., Hernández-Cortez, C., Pelcastre-Rodríguez, L. I., Gonzalez-Avila, L. U., et al. (2019). Horizontal gene transfer and its association with antibiotic resistance in the genus Aeromonas spp. *Microorganisms* 7:363. doi: 10.3390/microorganisms7090363

Bengtsson-Palme, J., Kristiansson, E., and Larsson, D. J. (2018). Environmental factors influencing the development and spread of antibiotic resistance. *FEMS Microbiol. Rev.* 42:fux053. doi: 10.1093/femsre/fux053

Berkner, S., Konradi, S., and Schönfeld, J. (2014). Antibiotic resistance and the environment—there and back again. *EMBO Rep.* 15, 740–744. doi: 10.15252/embr.201438978

Bhat, R. A. H., and Altinok, I. (2023). Antimicrobial resistance (AMR) and alternative strategies for combating AMR in aquaculture. *Turk. J. Fish. Aquat. Sci.* 23:68. doi: 10.4194/TRJFAS24068

Blair, J. M., Webber, M. A., Baylay, A. J., Ogbolu, D. O., and Piddock, L. J. (2015). Molecular mechanisms of antibiotic resistance. *Nat. Rev. Microbiol.* 13, 42–51. doi: 10.1038/nrmicro3380

Breidenstein, E. B., de la Fuente-Núñez, C., and Hancock, R. E. (2011). *Pseudomonas aeruginosa*: all roads lead to resistance. *Trends Microbiol.* 19, 419–426. doi: 10.1016/j.tim.2011.04.005

Centers for Disease Control and Prevention (2019). *Antibiotic resistance threats in the United States, 2019.* US Department of Health and Human Services, Centers for Disease Control and Prevention. https://www.cdc.gov/drugresistance/biggest-threats.html

Chambers, H. F. (2001). The changing epidemiology of *Staphylococcus aureus*? *Emerg. Infect. Dis.* 7, 178–182. doi: 10.3201/eid0702.010204

Charani, E., and Holmes, A. (2019). Antibiotic stewardship—twenty years in the making. *Antibiotics* 8:7. doi: 10.3390/antibiotics8010007

Chauhan, A., and Jindal, T. (2020). *Microbiological methods for environment, food and pharmaceutical analysis.* Springer Nature, 303–423.

Chen, B., Lin, L., Fang, L., Yang, Y., Chen, E., Yuan, K., et al. (2018). Complex pollution of antibiotic resistance genes due to beta-lactam and aminoglycoside use in aquaculture farming. *Water Res.* 134, 200–208. doi: 10.1016/j.watres.2018.02.003

Chong, Y., Shimoda, S., and Shimono, N. (2018). Current epidemiology, genetic evolution and clinical impact of extended-spectrum beta-lactamase-producing Escherichia coli and Klebsiella pneumoniae. *Infect Genet Evol.* 185–188. doi: 10.1016/j.meegid.2018.04.005

Chopra, R., Bhatt, R., Biswas, S. K., and Bhalla, R. (2018). Efficacy of alternate day directly observed treatment short-course (DOTS) in skeletal tuberculosis–a retrospective study. *Indian J. Tuberc.* 65, 70–75. doi: 10.1016/j.ijtb.2017.08.029

Christou, A., Agüera, A., Bayona, J. M., Cytryn, E., Fotopoulos, V., Lambropoulou, D., et al. (2017). The potential implications of reclaimed wastewater reuse for irrigation on the agricultural environment: the knowns and unknowns of the fate of antibiotics and antibiotic resistant bacteria and resistance genes–a review. *Water Res.* 123, 448–467. doi: 10.1016/j.watres.2017.07.004

Codjoe, F. S., and Donkor, E. S. (2017). Carbapenem resistance: a review. *Med. Sci.* 6:1. doi: 10.3390/medsci6010001

Conlon, B. P., Nakayasu, E. S., Fleck, L. E., LaFleur, M. D., Isabella, V. M., Coleman, K., et al. (2013). Activated ClpP kills persisters and eradicates a chronic biofilm infection. *Nature* 503, 365–370. doi: 10.1038/nature12790

Conlon, B. P., Rowe, S. E., Gandt, A. B., Nuxoll, A. S., Donegan, N. P., Zalis, E. A., et al. (2016). Persister formation in *Staphylococcus aureus* is associated with ATP depletion. *Nat. Microbiol.* 1, 1–7. doi: 10.1038/nmicrobiol.2016.51

Corvaglia, A. R., François, P., Hernandez, D., Perron, K., Linder, P., and Schrenzel, J. (2010). A type III-like restriction endonuclease functions as a major barrier to horizontal gene transfer in clinical *Staphylococcus aureus* strains. *Proc. Natl. Acad. Sci.* 107, 11954–11958. doi: 10.1073/pnas.1000489107

Craft, K. M., Nguyen, J. M., Berg, L. J., and Townsend, S. D. (2019). Methicillin-resistant *Staphylococcus aureus* (MRSA): antibiotic-resistance and the biofilm phenotype. *Medchemcomm* 10, 1231–1241. doi: 10.1039/C9MD00044E

Durão, P., Balbontín, R., and Gordo, I. (2018). Evolutionary mechanisms shaping the maintenance of antibiotic resistance. *Trends Microbiol.* 26, 677–691. doi: 10.1016/j.tim.2018.01.005

Effah, C. Y., Sun, T., Liu, S., and Wu, Y. (2020). *Klebsiella pneumoniae*: an increasing threat to public health. *Ann. Clin. Microbiol. Antimicrob.* 19, 1–9. doi: 10.1186/s12941-019-0343-8

Eljaaly, K., Ortwine, J. K., Shaikhomer, M., Almangour, T. A., and Bassetti, M. (2021). Efficacy and safety of eravacycline: a meta-analysis. *J. Glob. Antimicrob. Resist.* 24, 424–428. doi: 10.1016/j.jgar.2021.02.009

Foster, T. J. (2017). Antibiotic resistance in *Staphylococcus aureus*. Current status and future prospects. *FEMS Microbiol. Rev.* 41, 430–449. doi: 10.1093/femsre/fux007

Fouladkhah, A. C., Thompson, B., and Camp, J. S. (2020). The threat of antibiotic resistance in changing climate. *Microorganisms* 8:748. doi: 10.3390/microorganisms8050748

Freeland, G., Hettiarachchy, N., Atungulu, G. G., Apple, J., and Mukherjee, S. (2023). Strategies to combat antimicrobial resistance from farm to table. *Food Rev. Intl.* 39, 27–40. doi: 10.1080/87559129.2021.1893744

Gajdács, M., Urbán, E., Stájer, A., and Baráth, Z. (2021). Antimicrobial resistance in the context of the sustainable development goals: a brief review. *Eur. J. Investig. Health Psychol. Educ.* 11, 71–82. doi: 10.3390/ejihpe11010006

Galani, I., Karaiskos, I., and Giamarellou, H. (2021). Multidrug-resistant *Klebsiella pneumoniae*: mechanisms of resistance including updated data for novel β-lactam-β-lactamase inhibitor combinations. *Expert Rev. Anti-Infect. Ther.* 19, 1457–1468. doi: 10.1080/14787210.2021.1924674

Gandor, N. H. M., Amr, G. E. S., Eldin Algammal, S. M. S., and Ahmed, A. A. (2022). Characterization of Carbapenem-Resistant *K. pneumoniae* isolated from intensive care units of Zagazig University hospitals. *Antibiotics* 11:1108. doi: 10.3390/antibiotics11081108

Ghosh, D., Veeraraghavan, B., Elangovan, R., and Vivekanandan, P. (2020). Antibiotic resistance and epigenetics: more to it than meets the eye. *Antimicrob. Agents Chemother.* 64, e02225–e02219. doi: 10.1128/AAC.02225-19

Gnanamani, A., Hariharan, P., and Paul-Satyaseela, M. (2017). *Staphylococcus aureus*: overview of bacteriology, clinical diseases, epidemiology, antibiotic resistance and therapeutic approach. *Front. Staphylococcus aureus* 4, 10–5772. doi: 10.5772/67338

Gök, Ş. M., Kara, F., Arslan, U., and Fındık, D. (2020). Investigation of antibiotic resistance and virulence factors of Enterococcus faecium and *Enterococcus faecalis* strains isolated from clinical samples. *Mikrobiyol. Bul.* 54, 26–39. doi: 10.5578/mb.68810

Gorrie, C. L., Mirceta, M., Wick, R. R., Judd, L. M., Wyres, K. L., Thomson, N. R., et al. (2018). Antimicrobial-resistant *Klebsiella pneumoniae* carriage and infection in specialized geriatric care wards linked to acquisition in the referring hospital. *Clin. Infect. Dis.* 67, 161–170. doi: 10.1093/cid/ciy027

Guardabassi, L., Butaye, P., Dockrell, D. H., Fitzgerald, J. R., and Kuijper, E. J. (2020). One health: a multifaceted concept combining diverse approaches to prevent and control antimicrobial resistance. *Clin. Microbiol. Infect.* 26, 1604–1605. doi: 10.1016/j.cmi.2020.07.012

Guo, Y., Song, G., Sun, M., Wang, J., and Wang, Y. (2020). Prevalence and therapies of antibiotic-resistance in *Staphylococcus aureus*. *Front. Cell. Infect. Microbiol.* 10:107. doi: 10.3389/fcimb.2020.00107

Haaber, J., Penadés, J. R., and Ingmer, H. (2017). Transfer of antibiotic resistance in *Staphylococcus aureus*. *Trends Microbiol.* 25, 893–905. doi: 10.1016/j.tim.2017.05.011

Haider, A., Ikram, M., and Rafiq, A. (eds.) 2022). "Antimicrobials; drug resistance" in *Green nanomaterials as potential antimicrobials* (Cham: Springer International Publishing), 109–124.

Hajek, A., De Bock, F., Wieler, L. H., Sprengholz, P., Kretzler, B., and König, H. H. (2020). Perceptions of health care use in Germany during the COVID-19 pandemic. *Int. J. Environ. Res. Public Health* 17:9351. doi: 10.3390/ijerph17249351

Harmand, N., Gallet, R., Jabbour-Zahab, R., Martin, G., and Lenormand, T. (2017). Fisher's geometrical model and the mutational patterns of antibiotic resistance across dose gradients. *Evolution* 71, 23–37. doi: 10.1111/evo.13111

Hatcher, S. M., Rhodes, S. M., Stewart, J. R., Silbergeld, E., Pisanic, N., Larsen, J., et al. (2017). The prevalence of antibiotic-resistant *Staphylococcus aureus* nasal carriage among industrial hog operation workers, community residents, and children living in their households: North Carolina, USA. *Environ. Health Perspect.* 125, 560–569. doi: 10.1289/EHP35

Hollenbeck, B. L., and Rice, L. B. (2012). Intrinsic and acquired resistance mechanisms in enterococcus. *Virulence* 3, 421–569. doi: 10.4161/viru.21282

Huijbers, P. M., Flach, C. F., and Larsson, D. J. (2019). A conceptual framework for the environmental surveillance of antibiotics and antibiotic resistance. *Environ. Int.* 130:104880. doi: 10.1016/j.envint.2019.05.074

Jahansepas, A., Aghazadeh, M., Rezaee, M. A., Hasani, A., Sharifi, Y., Aghazadeh, T., et al. (2018). Occurrence of Enterococcus faecalis and *Enterococcus faecium* in various clinical infections: detection of their drug resistance and virulence determinants. *Microb. Drug Resist.* 24, 76–82. doi: 10.1089/mdr.2017.0049

Jasovský, D., Littmann, J., Zorzet, A., and Cars, O. (2016). Antimicrobial resistance—a threat to the world's sustainable development. *Ups. J. Med. Sci.* 121, 159–164. doi: 10.1080/03009734.2016.1195900

Kaiser, R. A., Polk, J. S., Datta, T., Parekh, R. R., and Agga, G. E. (2022). Occurrence of antibiotic resistant bacteria in urban karst groundwater systems. *Water* 14:960. doi: 10.3390/w14060960

Kakoullis, L., Papachristodoulou, E., Chra, P., and Panos, G. (2021). Mechanisms of antibiotic resistance in important gram-positive and gram-negative pathogens and novel antibiotic solutions. *Antibiotics* 10:415. doi: 10.3390/antibiotics10040415

Kapoor, G., Saigal, S., and Elongavan, A. (2017). Action and resistance mechanisms of antibiotics: a guide for clinicians. *J. Anaesthesiol. Clin. Pharmacol.* 33, 300–305. doi: 10.4103/joacp.JOACP_349_15

Khaertynov, K. S., Anokhin, V. A., Rizvanov, A. A., Davidyuk, Y. N., Semyenova, D. R., Lubin, S. A., et al. (2018). Virulence factors and antibiotic resistance of *Klebsiella pneumoniae* strains isolated from neonates with sepsis. *Front. Med.* 5:225. doi: 10.3389/fmed.2018.00225

Khor, W. P., Olaoye, O., D'Arcy, N., Krockow, E. M., Elshenawy, R. A., Rutter, V., et al. (2020). The need for ongoing antimicrobial stewardship during the COVID-19 pandemic and actionable recommendations. *Antibiotics* 9:904. doi: 10.3390/antibiotics9120904

Khoshnood, S., Heidary, M., Asadi, A., Soleimani, S., Motahar, M., Savari, M., et al. (2019). A review on mechanism of action, resistance, synergism, and clinical implications of mupirocin against *Staphylococcus aureus*. *Biomed. Pharmacother.* 109, 1809–1818. doi: 10.1016/j.biopha.2018.10.131

Klein, E. Y., Van Boeckel, T. P., Martinez, E. M., Pant, S., Gandra, S., Levin, S. A., et al. (2018). Global increase and geographic convergence in antibiotic consumption between 2000 and 2015. *Proc. Natl. Acad. Sci.* 115, E3463–E3470. doi: 10.1073/pnas.1717295115

Kollef, M. H., Nováček, M., Kivistik, Ü., Réa-Neto, Á., Shime, N., Martin-Loeches, I., et al. (2019). Ceftolozane–tazobactam versus meropenem for treatment of nosocomial pneumonia (ASPECT-NP): a randomised, controlled, double-blind, phase 3, non-inferiority trial. *Lancet Infect. Dis.* 19, 1299–1311. doi: 10.1016/S1473-3099(19)30403-7

Koulenti, D., Xu, E., Yin Sum Mok, I., Song, A., Karageorgopoulos, D. E., Armaganidis, A., et al. (2019). Novel antibiotics for multidrug-resistant gram-positive microorganisms. *Microorganisms* 7:270. doi: 10.3390/microorganisms7080270

Lamba, M., Graham, D. W., and Ahammad, S. Z. (2017). Hospital wastewater releases of carbapenem-resistance pathogens and genes in urban India. *Environ. Sci. Technol.* 51, 13906–13912. doi: 10.1021/acs.est.7b03380

Larsson, D. J., and Flach, C. F. (2022). Antibiotic resistance in the environment. *Nat. Rev. Microbiol.* 20, 257–269. doi: 10.1038/s41579-021-00649-x

Laws, M., Shaaban, A., and Rahman, K. M. (2019). Antibiotic resistance breakers: current approaches and future directions. *FEMS Microbiol. Rev.* 43, 490–516. doi: 10.1093/femsre/fuz014

Laxminarayan, R., Duse, A., Wattal, C., Zaidi, A. K., Wertheim, H. F., Sumpradit, N., et al. (2013). Antibiotic resistance—the need for global solutions. *Lancet Infect. Dis.* 13, 1057–1098. doi: 10.1016/S1473-3099(13)70318-9

Laxminarayan, R., Matsoso, P., Pant, S., Brower, C., Røttingen, J. A., Klugman, K., et al. (2016). Access to effective antimicrobials: a worldwide challenge. *Lancet* 387, 168–175. doi: 10.1016/S0140-6736(15)00474-2

Lerminiaux, N. A., and Cameron, A. D. (2019). Horizontal transfer of antibiotic resistance genes in clinical environments. *Can. J. Microbiol.* 65, 34–44. doi: 10.1139/cjm-2018-0275

Li, S., Ondon, B. S., Ho, S. H., Zhou, Q., and Li, F. (2023). Drinking water sources as hotspots of antibiotic-resistant bacteria (ARB) and antibiotic resistance genes (ARGs): occurrence, spread, and mitigation strategies. *J. Water Process Eng.* 53:103907. doi: 10.1016/j.jwpe.2023.103907

Liu, G. Y., Essex, A., Buchanan, J. T., Datta, V., Hoffman, H. M., Bastian, J. F., et al. (2005). *Staphylococcus aureus* golden pigment impairs neutrophil killing and promotes virulence through its antioxidant activity. *J. Exp. Med.* 202, 209–215. doi: 10.1084/jem.20050846

Liu, C. I., Liu, G. Y., Song, Y., Yin, F., Hensler, M. E., Jeng, W. Y., et al. (2008). A cholesterol biosynthesis inhibitor blocks *Staphylococcus aureus* virulence. *Science* 319, 1391–1394. doi: 10.1126/science.1153018

Lowy, F. D. (2003). Antimicrobial resistance: the example of *Staphylococcus aureus*. *J. Clin. Invest.*, 111, 1265–1273, doi: 10.1172/JCI18535

Lupia, T., Pallotto, C., Corcione, S., Boglione, L., and De Rosa, F. G. (2021). Ceftobiprole perspective: current and potential future indications. *Antibiotics* 10:170. doi: 10.3390/antibiotics10020170

Lupo, A., Coyne, S., and Berendonk, T. U. (2012). Origin and evolution of antibiotic resistance: the common mechanisms of emergence and spread in water bodies. *Front. Microbiol.* 3:18. doi: 10.3389/fmicb.2012.00018

Manaia, C. M., Rocha, J., Scaccia, N., Marano, R., Radu, E., Biancullo, F., et al. (2018). Antibiotic resistance in wastewater treatment plants: tackling the black box. *Environ. Int.* 115, 312–324. doi: 10.1016/j.envint.2018.03.044

Martin, J., Phan, H. T. T., Findlay, J., Stoesser, N., Pankhurst, L., Navickaite, I., et al. (2017). Covert dissemination of carbapenemase-producing *Klebsiella pneumoniae* (KPC) in a successfully controlled outbreak: long-and short-read whole-genome sequencing demonstrate multiple genetic modes of transmission. *J. Antimicrob. Chemother.* 72, 3025–3034. doi: 10.1093/jac/dkx264

Martínez, J. L., Coque, T. M., Lanza, V. F., de la Cruz, F., and Baquero, F. (2017). Genomic and metagenomic technologies to explore the antibiotic resistance mobilome. *Ann. N. Y. Acad. Sci.* 1388, 26–41. doi: 10.1111/nyas.13282

Mehta, S. C., Samanta, M., Chow, D. C., and Palzkill, T. (2016). Avoiding the Carbapenem trap: KPC-2 β-lactamase sequence requirements for Carbapenem hydrolysis. *FASEB J.* 30, 1083–1020. doi: 10.1096/fasebj.30.1_supplement.1083.20

Michaelis, C., and Grohmann, E. (2023). Horizontal gene transfer of antibiotic resistance genes in biofilms. *Antibiotics* 12:328. doi: 10.3390/antibiotics12020328

Mohamed, S. H., Khalil, M. S., Mabrouk, M. I., and Mohamed, M. S. (2020). Prevalence of antibiotic resistance and biofilm formation in *Klebsiella pneumoniae* carrying fimbrial genes in Egypt. *Res. J. Pharm. Technol.* 13, 3051–3058. doi: 10.5958/0974-360X.2020.00542.9

Monistero, V., Barberio, A., Biscarini, F., Cremonesi, P., Castiglioni, B., Graber, H. U., et al. (2020). Different distribution of antimicrobial resistance genes and virulence profiles of *Staphylococcus aureus* strains isolated from clinical mastitis in six countries. *J. Dairy Sci.* 103, 3431–3446. doi: 10.3168/jds.2019-17141

Montso, K. P., Dlamini, S. B., Kumar, A., and Ateba, C. N. (2019). Antimicrobial resistance factors of extended-spectrum beta-lactamases producing Escherichia coli and *Klebsiella pneumoniae* isolated from cattle farms and raw beef in North-West Province, South Africa. *Biomed Res. Int.* 2019, 1–13. doi: 10.1155/2019/4318306

Müller, S., Wolf, A. J., Iliev, I. D., Berg, B. L., Underhill, D. M., and Liu, G. Y. (2015). Poorly cross-linked peptidoglycan in MRSA due to mecA induction activates the inflammasome and exacerbates immunopathology. *Cell Host Microbe* 18, 604–612. doi: 10.1016/j.chom.2015.10.011

Munita, J. M., and Arias, C. A. (2016). Mechanisms of antibiotic resistance. *Microbiol. Spectr.* 4:10. doi: 10.1128/microbiolspec.VMBF-0016-2015

Murugaiyan, J., Kumar, P. A., Rao, G. S., Iskandar, K., Hawser, S., Hays, J. P., et al. (2022). Progress in alternative strategies to combat antimicrobial resistance: focus on antibiotics. *Antibiotics* 11:200. doi: 10.3390/antibiotics11020200

Nannini, E. C., Singh, K. V., Arias, C. A., and Murray, B. E. (2013). In vivo effects of cefazolin, daptomycin, and nafcillin in experimental endocarditis with a methicillin-susceptible *Staphylococcus aureus* strain showing an inoculum effect against cefazolin. *Antimicrob. Agents Chemother.* 57, 4276–4281. doi: 10.1128/AAC.00856-13

Nji, E., Kazibwe, J., Hambridge, T., Joko, C. A., Larbi, A. A., Damptey, L. A. O., et al. (2021). High prevalence of antibiotic resistance in commensal *Escherichia coli* from healthy human sources in community settings. *Sci. Rep.* 11:3372. doi: 10.1038/s41598-021-82693-4

Noor, Z. Z., Rabiu, Z., Sani, M. H. M., Samad, A. F. A., Kamaroddin, M. F. A., Perez, M. F., et al. (2021). A review of bacterial antibiotic resistance genes and their removal strategies from wastewater. *Curr. Pollut. Rep.* 7, 494–509. doi: 10.1007/s40726-021-00198-0

Nowakiewicz, A., Zięba, P., Gnat, S., Trościańczyk, A., Osińska, M., Łagowski, D., et al. (2020). A significant number of multi-drug resistant *Enterococcus faecalis* in wildlife animals; long-term consequences and new or known reservoirs of resistance? *Sci. Total Environ.* 705:135830. doi: 10.1016/j.scitotenv.2019.135830

Odonkor, S. T., and Addo, K. K. (2018). Prevalence of multidrug-resistant *Escherichia coli* isolated from drinking water sources. *Int. J. Microbiol.* 2018, 1–7. doi: 10.1155/2018/7204013

Ogyu, A., Chan, O., Littmann, J., Pang, H. H., Lining, X., Liu, P., et al. (2020). National action to combat AMR: a one-health approach to assess policy priorities in action plans. BMJ. *Glob. Health* 5:e002427. doi: 10.1136/bmjgh-2020-002427

Pang, Z., Raudonis, R., Glick, B. R., Lin, T. J., and Cheng, Z. (2019). Antibiotic resistance in *Pseudomonas aeruginosa*: mechanisms and alternative therapeutic strategies. *Biotechnol. Adv.* 37, 177–192. doi: 10.1016/j.biotechadv.2018.11.013

Peterson, E., and Kaur, P. (2018). Antibiotic resistance mechanisms in bacteria: relationships between resistance determinants of antibiotic producers, environmental bacteria, and clinical pathogens. *Front. Microbiol.* 9:2928. doi: 10.3389/fmicb.2018.02928

Phan, H. T. T., Stoesser, N., Maciuca, I. E., Toma, F., Szekely, E., Flonta, M., et al. (2017). Illumina short-read and minion long-read whole genome sequencing to characterise the molecular epidemiology of an ndm-1-*serratia marcescens* outbreak in Romania. *J. Antimicrob. Chemother.* 73, 672–679. doi: 10.1093/jac/dkx456

Poole, K. (2011). *Pseudomonas aeruginosa*: resistance to the max. *Front. Microbiol.* 2:65. doi: 10.3389/fmicb.2011.00065

Pormohammad, A., Pouriran, R., Azimi, H., and Goudarzi, M. (2019). Prevalence of integron classes in gram-negative clinical isolated bacteria in Iran: a systematic review and meta-analysis. *Iran. J. Basic Med. Sci.* 22, 118–127. doi: 10.22038/ijbms.2018.32052.7697

Rammelkamp, C. H., and Maxon, T. (1942). Resistance of *Staphylococcus aureus* to the action of penicillin. *Proc. Soc. Exp. Biol. Med.* 51, 386–389. doi: 10.3181/00379727-51-13986

Reygaert, W. C. (2018). An overview of the antimicrobial resistance mechanisms of bacteria. *AIMS Microbiol.* 4, 482–501. doi: 10.3934/microbiol.2018.3.482

Rudkin, J. K., Edwards, A. M., Bowden, M. G., Brown, E. L., Pozzi, C., Waters, E. M., et al. (2012). Methicillin resistance reduces the virulence of healthcare-associated methicillin-resistant *Staphylococcus aureus* by interfering with the agr quorum sensing system. *J. Infect. Dis.* 205, 798–806. doi: 10.1093/infdis/jir845

Sanganyado, E., and Gwenzi, W. (2019). Antibiotic resistance in drinking water systems: occurrence, removal, and human health risks. *Sci. Total Environ.* 669, 785–797. doi: 10.1016/j.scitotenv.2019.03.162

Sato, T., and Yamawaki, K. (2019). Cefiderocol: discovery, chemistry, and in vivo profiles of a novel siderophore cephalosporin. *Clin. Infect. Dis.* 69, S538–S543. doi: 10.1093/cid/ciz826

Seyoum, M. M., Obayomi, O., Bernstein, N., Williams, C. F., and Gillor, O. (2021). Occurrence and distribution of antibiotics and corresponding antibiotic resistance genes in different soil types irrigated with treated wastewater. *Sci. Total Environ.* 782:146835. doi: 10.1016/j.scitotenv.2021.146835

Shen, W., Chen, H., Geng, J., Wu, R. A., Wang, X., and Ding, T. (2022). Prevalence, serovar distribution, and antibiotic resistance of Salmonella spp. isolated from pork in China: a systematic review and meta-analysis. *Int. J. Food Microbiol.* 361:109473. doi: 10.1016/j.ijfoodmicro.2021.109473

Shiadeh, S. M. J., Pormohammad, A., Hashemi, A., and Lak, P. (2019). Global prevalence of antibiotic resistance in blood-isolated Enterococcus faecalis and *Enterococcus faecium*: a systematic review and meta-analysis. *Infect. Drug Resist.* 12, 2713–2725. doi: 10.2147/IDR.S206084

Shields, R. K., Nguyen, M. H., Press, E. G., Chen, L., Kreiswirth, B. N., and Clancy, C. J. (2017). "Emergence of ceftazidime-avibactam resistance and restoration of carbapenem susceptibility in *Klebsiella pneumoniae* carbapenemase-producing K pneumoniae: a case report and review of literature" *Open Forum Infect Dis.* 4. doi: 10.1093/ofid/ofx101

Shields, R. K., Potoski, B. A., Haidar, G., Hao, B., Doi, Y., Chen, L., et al. (2016). Clinical outcomes, drug toxicity, and emergence of ceftazidime-avibactam resistance among patients treated for carbapenem-resistant Enterobacteriaceae infections. *Clin. Infect. Dis.* 63, 1615–1618. doi: 10.1093/cid/ciw636

Shortridge, D., Pfaller, M. A., Streit, J. M., and Flamm, R. K. (2020). Update on the activity of delafloxacin against acute bacterial skin and skin-structure infection isolates from European hospitals (2014–2019). *J. Glob. Antimicrob. Resist.* 23, 278–283. doi: 10.1016/j.jgar.2020.09.027

Smith, R. D., Yago, M., Millar, M., and Coast, J. (2005). Assessing the macroeconomic impact of a healthcare problem: the application of computable general equilibrium analysis to antimicrobial resistance. *J. Health Econ.* 24, 1055–1075. doi: 10.1016/j.jhealeco.2005.02.003

Solano-Gálvez, S. G., Valencia-Segrove, M. F., Prado, M. J. O., Boucieguez, A. B. L., Álvarez-Hernández, D. A., and Vázquez-López, R. (2020). "Mechanisms of resistance to quinolones" in *Antimicrobial resistance-a one health perspective*. Intechopen.

Sorbera, M., Chung, E., Ho, C. W., and Marzella, N. (2014). Ceftolozane/Tazobactam: a new option in the treatment of complicated gram-negative infections. *Pharm. Therap.* 39, 825–832.

Stefani, S., Bongiorno, D., Mongelli, G., and Campanile, F. (2010). Linezolid resistance in staphylococci. *Pharmaceuticals* 3, 1988–2006. doi: 10.3390/ph3071988

Suay-García, B., and Pérez-Gracia, M. T. (2021). Present and future of carbapenem-resistant Enterobacteriaceae infections. *Adv. Clin. Immunol. Med. Microbiol. COVID-19 Big Data*, 435–456.

Teixeira, B., Rodulfo, H., Carreno, N., Guzman, M., Salazar, E., and Donato, M. D. (2016). Aminoglycoside resistance genes in *Pseudomonas aeruginosa* isolates from Cumana, Venezuela. *Revista do Instituto de Medicina Tropical de São Paulo* 58:58. doi: 10.1590/S1678-9946201658013

Tekin, E., White, C., Kang, T. M., Singh, N., Cruz-Loya, M., Damoiseaux, R., et al. (2018). Prevalence and patterns of higher-order drug interactions in *Escherichia coli*. *NPJ Syst. Biol. Appl.* 4:31. doi: 10.1038/s41540-018-0069-9

Tian, M., He, X., Feng, Y., Wang, W., Chen, H., Gong, M., et al. (2021). Pollution by antibiotics and antimicrobial resistance in livestock and poultry manure in China, and countermeasures. *Antibiotics* 10:539. doi: 10.3390/antibiotics10050539

Tong, S. Y., Davis, J. S., Eichenberger, E., Holland, T. L., and Fowler, V. G. (2015). *Staphylococcus aureus* infections: epidemiology, pathophysiology, clinical manifestations, and management. *Clin. Microbiol. Rev.* 28, 603–661. doi: 10.1128/CMR.00134-14

Torres, N. F., Chibi, B., Middleton, L. E., Solomon, V. P., and Mashamba-Thompson, T. P. (2019). Evidence of factors influencing self-medication with antibiotics in low and middle-income countries: a systematic scoping review. *Public Health* 168, 92–101. doi: 10.1016/j.puhe.2018.11.018

Turner, B. (2018). Tackling antimicrobial resistance and climate change. *Lancet* 392, 2435–2436. doi: 10.1016/S0140-6736(18)32413-9

Uddin, T. M., Chakraborty, A. J., Khusro, A., Zidan, B. R. M., Mitra, S., Emran, T. B., et al. (2021). Antibiotic resistance in microbes: history, mechanisms, therapeutic strategies and future prospects. *J. Infect. Public Health* 14, 1750–1766. doi: 10.1016/j.jiph.2021.10.020

Urban-Chmiel, R., Marek, A., Stępień-Pyśniak, D., Wieczorek, K., Dec, M., Nowaczek, A., et al. (2022). Antibiotic resistance in bacteria—a review. *Antibiotics* 11:1079. doi: 10.3390/antibiotics11081079

Van Boeckel, T. P., Glennon, E. E., Chen, D., Gilbert, M., Robinson, T. P., Grenfell, B. T., et al. (2017). Reducing antimicrobial use in food animals. *Science* 357, 1350–1352. doi: 10.1126/science.aao1495

Výrostková, J., Regecová, I., Dudriková, E., Marcinčák, S., Vargová, M., Kováčová, M., et al. (2021). Antimicrobial resistance of Enterococcus sp. isolated from sheep and goat cheeses. *Food Secur.* 10:1844. doi: 10.3390/foods10081844

Wegener, H. C. (2012). "Antibiotic resistance—linking human and animal health" in *Improving food safety through a one health approach: Workshop summary* (USA: National Academies Press), 331.

Weigel, L. M., Clewell, D. B., Gill, S. R., Clark, N. C., McDougal, L. K., Flannagan, S. E., et al. (2003). Genetic analysis of a high-level vancomycin-resistant isolate of *Staphylococcus aureus*. *Science* 302, 1569–1571. doi: 10.1126/science.1090956

White, A., and Hughes, J. M. (2019). Critical importance of a one health approach to antimicrobial resistance. *EcoHealth* 16, 404–409. doi: 10.1007/s10393-019-01415-5

World Economic Forum. (2019). *The global risks report*. Geneva, Switzerland: World Economic Forum.

World Health Organization (2014). *Antimicrobial resistance: global report on surveillance*. World Health Organization.

World Health Organization. (2017). *Six lines of action to promote health in the 2030 agenda for sustainable development*. Available at: https://www.who.int/gho/publications/world_health_statistics/2017/EN_WHS2017_Part1.pdf

World Health Organization. (2021). *Antimicrobial resistance and the United Nations sustainable development cooperation framework*. Available at: https://www.who.int/publications/i/item/9789240036024

Wyres, K. L., and Holt, K. E. (2018). *Klebsiella pneumoniae* as a key trafficker of drug resistance genes from environmental to clinically important bacteria. *Curr. Opin. Microbiol.* 45, 131–139. doi: 10.1016/j.mib.2018.04.004

Xu, C., Wei, X., Jin, Y., Bai, F., Cheng, Z., Chen, S., et al. (2022). Development of resistance to Eravacycline by Klebsiella pneumoniae and collateral sensitivity-guided Design of Combination Therapies. *Microbiol. Spectr.* 10, e01390–e01322. doi: 10.1128/spectrum.01390-22

Yadav, V. (2022). Computational evidence based perspective on the plausible repositioning of fluoroquinolones for COVID-19 treatment. *Curr. Comput. Aided Drug Des.* 18, 407–413. doi: 10.2174/1573409918666220909094645

Yadav, V., and Ravichandran, S. (2024). Significance of understanding the genomics of host-pathogen interaction in limiting antibiotic resistance development: lessons from COVID-19 pandemic. *Brief. Funct. Genomics* 23, 69–74. doi: 10.1093/bfgp/elad001

Yadav, V., and Talwar, P. (2019). Repositioning of fluoroquinolones from antibiotic to anti-cancer agents: an underestimated truth. *Biomed. Pharmacother.* 111, 934–946. doi: 10.1016/j.biopha.2018.12.119

Yahia, H. B., Chairat, S., Hamdi, N., Gharsa, H., Sallem, R. B., Ceballos, S., et al. (2018). Antimicrobial resistance and genetic lineages of faecal enterococci of wild birds: emergence of vanA and vanB2 harbouring *Enterococcus faecalis*. *Int. J. Antimicrob. Agents* 52, 936–941. doi: 10.1016/j.ijantimicag.2018.05.005

Yusuf, E., Bax, H. I., Verkaik, N. J., and van Westreenen, M. (2021). An update on eight "new" antibiotics against multidrug-resistant gram-negative bacteria. *J. Clin. Med.* 10:1068. doi: 10.3390/jcm10051068

Zhanel, G. G., Chung, P., Adam, H., Zelenitsky, S., Denisuik, A., Schweizer, F., et al. (2014). Ceftolozane/tazobactam: a novel cephalosporin/β-lactamase inhibitor combination with activity against multidrug-resistant gram-negative bacilli. *Drugs* 74, 31–51. doi: 10.1007/s40265-013-0168-2

Zhou, Z. C., Liu, Y., Lin, Z. J., Shuai, X. Y., Zhu, L., Xu, L., et al. (2021). Spread of antibiotic resistance genes and microbiota in airborne particulate matter, dust, and human airways in the urban hospital. *Environ. Int.* 153:106501. doi: 10.1016/j.envint.2021.106501

Zhu, W., Clark, N., and Patel, J. B. (2013). pSK41-like plasmid is necessary for Inc18-like vanA plasmid transfer from *Enterococcus faecalis* to *Staphylococcus aureus* in vitro. *Antimicrob. Agents Chemother.* 57, 212–219. doi: 10.1128/AAC.01587-12

Zhu, D., Giles, M., Yang, X. R., Daniell, T., Neilson, R., and Zhu, Y. G. (2019). Phyllosphere of staple crops under pig manure fertilization, a reservoir of antibiotic resistance genes. *Environ. Pollut.* 252, 227–235. doi: 10.1016/j.envpol.2019.05.098

frontiers | Frontiers in Microbiology

TYPE Original Research
PUBLISHED 14 May 2024
DOI 10.3389/fmicb.2024.1402319

OPEN ACCESS

EDITED BY
Vijay Soni,
NewYork-Presbyterian, United States

REVIEWED BY
Yaxin Li,
Cornell University, United States
Smriti Parashar,
University of California, San Diego, United States
Tripti Nair,
University of Southern California, United States

*CORRESPONDENCE
Wen-Liang Xiang
✉ biounicom@mail.xhu.edu.cn

†These authors share first authorship

RECEIVED 17 March 2024
ACCEPTED 15 April 2024
PUBLISHED 14 May 2024

CITATION
Zhu H-Y, Xiang W-L, Cai T, Zhang M and Wang H-Y (2024) PemK's Arg24 is a crucial residue for PemIK toxin–antitoxin system to induce the persistence of *Weissella cibaria* against ciprofloxacin stress. *Front. Microbiol.* 15:1402319. doi: 10.3389/fmicb.2024.1402319

PemK's Arg24 is a crucial residue for PemIK toxin–antitoxin system to induce the persistence of *Weissella cibaria* against ciprofloxacin stress

Hao-Yu Zhu[1†], Wen-Liang Xiang[1,2*†], Ting Cai[1,2], Min Zhang[1] and Han-Yang Wang[1]

[1]School of Food and Bioengineering, Xihua University, Chengdu, China, [2]Key Laboratory of Food Microbiology of Sichuan, Xihua University, Chengdu, China

The toxin-antitoxin (TA) system plays a key role in bacteria escaping antibiotic stress with persistence, however, the mechanisms by which persistence is controlled remain poorly understood. *Weissella cibaria*, a novel probiotic, can enters a persistent state upon encountering ciprofloxacin stress. Conversely, it resumes from the persistence when ciprofloxacin stress is relieved or removed. Here, it was found that PemIK TA system played a role in transitioning between these two states. And the PemIK was consisted of PemK, an endonuclease toxic to mRNA, and antitoxin PemI which neutralized its toxicity. The PemK specifically cleaved the U↓AUU in mRNA encoding enzymes involved in glycolysis, TCA cycle and respiratory chain pathways. This cleavage event subsequently disrupted the crucial cellular processes such as hydrogen transfer, electron transfer, NADH and $FADH_2$ synthesis, ultimately leading to a decrease in ATP levels and an increase in membrane depolarization and persister frequency. Notably, Arg_{24} was a critical active residue for PemK, its mutation significantly reduced the mRNA cleavage activity and the adverse effects on metabolism. These insights provided a clue to comprehensively understand the mechanism by which PemIK induced the persistence of *W. cibaria* to escape ciprofloxacin stress, thereby highlighting another novel aspect PemIK respond for antibiotic stress.

KEYWORDS

***Weissella cibaria*, toxin-antitoxin system, PemIK module, ciprofloxacin stress, persister cell, metabolic processes**

1 Introduction

The discovery of antibiotics in the late 1920s marked a significant milestone in the history of combating bacterial infection. However, it is now widely acknowledged that antibiotics are not the panacea they were once thought to be. Rather, antibiotics can and do fail, often with severe consequences (Page and Peti, 2016). This occurs because

bacteria acquire resistance mutations to render the antibiotics ineffective or activate their endogenous mechanisms to evade antibiotic stress (Page and Peti, 2016). The former is a major culprit, but it would be overly simplistic to attribute all failures solely to this factor (Maisonneuve and Gerdes, 2014). In fact, when bacteria are treated with antibiotic, it is nearly impossible to kill them completely. Even if they are sensitive to antibiotic, there will always be a small percentage of cells known as persister cells that can withstand the lethal effect of antibiotic (Wilmaerts et al., 2019). Bacterial persistence is a state of dormancy induced by an endogenous mechanism, and unlike drug-resistant mutant, it does not proliferate in the presence of antibiotic, but, randomly in time, switches from a dormant state back to a growing state when antibiotic stress is relieved or removed. Therefore, it is generally accepted that persistence is an important reason for failure of antibiotic prevention or treatment of bacteria (Wilmaerts et al., 2019).

Persister process of bacteria is a survival strategy that allows populations to survive in sudden adverse environments without going extinct completely (Gerdes and Maisonneuve, 2012; Page and Peti, 2016; Wilmaerts et al., 2019). To date, persistence has been observed in nearly all bacterial species, even eukaryotic microorganisms (Wilmaerts et al., 2019). Although persister process is governed by phenotypic switching in isogenic populations, it occurs stochastically and independently of environment, albeit at a higher frequency in adverse conditions (Maisonneuve and Gerdes, 2014; Page and Peti, 2016; Wilmaerts et al., 2019). Numerous researchers have suggested that persister formation depends on the expression level of toxin-antitoxin systems (TAs) in bacteria. These systems encode two components, a stable toxin protein that inhibits cell growth and a labile antitoxin (either RNA or protein) that regulates toxin activity. When toxin protein exceeds a certain threshold in bacterial cell, persistence is induced (Wilmaerts et al., 2019).

PemIK is a novel type II TA system, originally discovered in plasmid pCH91 of *Staphylococcus aureus* (Bukowski et al., 2013). The toxin PemK dimer, an RNase, specifically cleaves the mRNA in a ribosome-independent manner. The antitoxin PemI neutralizes the toxicity of PemK, thereby facilitating bacterial recovery from persistence (Bukowski et al., 2013; Wilmaerts et al., 2019). In pathogenic bacteria such as *S. aureus*, *Klebsiella pneumonia*, *Bacillus anthracis* and *Mycobacterium tuberculosis*, free PemK dimers lead to a rapid formation and higher proportion of persister cells (Kim et al., 2022). Although PemK can induce persister cells, it possesses distinct pattern in regulating physiological activities across different organisms. In *S. aureus*, it comprehensively regulates virulence by cleaving target mRNA encoding proteins involved in virulence synthesis (Bukowski et al., 2013; Kim et al., 2022). However, in *Caenorhabditis elegans*, it affects fundamental physiological processes including ATP production, lipid synthesis, cytoskeleton organization, stress response, and others (Kim et al., 2022). However, the mechanism by which PemK orchestrates the specific regulation of bacterial transcription, thereby manipulating the transition from growth to persistence, remains elusive.

Weissella cibaria, a novel probiotic and hetero-lactic bacterium, is usually present in various spontaneous fermentation foods. Interestingly, it can survive in various stresses through persistence, including antibiotic residue in raw materials, high acidity and nutrient hunger, and even growth inhibitor. In its persister cells, PemIK responds strongly to the persister formation under ciprofloxacin stress. Although the structure and function of PemIK in pathogenic bacteria, particularly *S. aureus*, are somewhat known, it remains unknown in *W. cibaria* due to its species-specific mode of regulation. Therefore, the present study analyzed the structure and function of PemIK in *W. cibaria*, and investigated the PemK's adverse effects on basic metabolic processes. Meanwhile, the detoxification effect of PemI on PemK was also determined. The results provided a structural basis for understanding the molecular mechanism by which PemIK induced persistence of *W. cibaria* to survive in ciprofloxacin stress, and also offered insights into strategies for discovering new agents that could activate or inhibit *W. cibaria*.

2 Materials and methods

2.1 Bacterial strains and culture conditions

Weissella cibaria CGMCC 1.19376 was cultured in De Man, Rogosa, and Sharpe (MRS) broth at 30°C (Cai et al., 2022). *Escherichia coli* BL21 was cultivated in Luria-Bertani (LB) liquid me-dium at 37°C.

2.2 Transcription analysis of PemIK

Total RNA was extracted using TRIzol Reagent (ThermoFisher Scientific Inc., Massachusetts, USA). Subsequently, cDNA synthesis was performed using the prime-script reverse transcriptase and random primers according to manufacturer's instructions (TaKaRa, Beijing, China). Polymerase chain reaction (PCR) was conducted with PemK-F, PemK-R, PemI-F, and PemI-R primers (**Supplementary Table 1**) for amplifying the PemI and PemK genes. Templates included cDNA, mRNA, and gDNA (genomic DNA of *W. cibaria*). The promoter and terminator analysis of PemKI were performed by BPROM program (Shahmuradov, 2003).

2.3 Structural analysis of PemK

The primary and secondary structures of PemK were analyzed by Clustal Omega and Jalview,[1] respectively. The results were visualized by ESPript 3.0 (Robert and Gouet, 2014). Three-dimensional models of PemK protein were generated using SWISS-MODEL (Waterhouse et al., 2018). The dimeric structure of PemK was submitted along with mRNA containing 5′ UAUU 3′ to the HADDOCK 2.2 webserver (Van Zundert et al., 2016). Subsequently, a model of PemK bound to RNA was generated and visualized by PyMOL (PyMOL Molecular Graphics System, version 2.3.0) (Schiffrin et al., 2020).

1 http://www.jalview.org

2.4 Identification of active residues in PemK

The SNAP2[2] predicted the mutation of active amino acid in PemK (Bromberg and Rost, 2007). The thermal stability, solvent-accessible surface area and electrostatic potential energy of PemK were analyzed by MUpro,[3] CCP4[4] and APBS plug in PyMOL, respectively.

2.5 Cytotoxicity analysis of PemIK

PemK and its mutant were ligated to pET28a plasmid, while PemI was ligated to pBAD43 plasmid. Subsequently, the recombinant pET28a and pBAD43 were co-transformed into *E. coli* BL21. Following cultivation to an optical density (OD) 600 nm of 0.2–0.3, PemK and PemI were induced by 1 mM IPTG and 0.2% L-arabinose, respectively. Cytotoxicity of PemK and neutralization of PemK by PemI were assessed through growth curves of *E. coli* BL21 at OD_{600nm}.

2.6 Regulation of cell membrane potential, endogenous reactive oxygen species (ROS) and intracellular ATP by PemK

Weissella cibaria at 1×10^7 CFU/ml in logarithmic stage was treated with 1/2 MIC ciprofloxacin (16 μg/ml) at 30°C for 1–8 h. Recombinant *E. coli* BL21 was cultured to logarithmic stage and adjusted to 1×10^7 CFU/ml, followed by induction of PemK using 1 mM IPTG at 37°C for 1–8 h. The cell membrane potential was assessed using the rhodamine 123 fluorescence method (Yu et al., 2022). The endogenous ROS level was analyzed following the method described by Xiong et al. (2023). Intracellular ATP was determined as described by Shan et al. (2017). PBS (pH 7.4) treatment served as control.

2.7 Effect of PemK on expression of metabolic enzymes

The splicing mRNA of PemK were analyzed based on the genome sequence of *W. cibaria*, focusing on metabolic enzymes in oxidative phosphorylation (OP), glycolysis, and citric acid cycle (TCA). To further validate these impacts, transcriptome analysis was conducted in recombinant *E. coli* BL21. The total RNA with high-quality from recombinant *E. coli* BL21 using TRIzol Reagent (ThermoFisher Scientific Inc., MA, USA) was used to construct the RNA-Seq library for sequencing on Illumina Hiseq platform (Hiseq 4000, 150PE) with NEBNext® Ultra™ RNA Library Prep Kit for Illumina® (NEB, USA) by Majorbio Technology Co. Ltd (Shanghai, China). The RNA-seq data analysis was conducted as methods described by Wang et al. (2015). The differential expression was calculated by DESeq R package (1.18.0). The transcription with $\log_2$ fold change > 1 was defined as the metabolic enzymes affected by PemK.

2.8 Regulation of cell persistence and morphology by PemK

The persister cells were detected using method of biphasic bactericidal curve (Sun et al., 2017). Briefly, *W. cibaria* was incubated in MRS broth at 30°C to 10^7 CFU/ml, then ciprofloxacin was added to 1/2 MIC and incubated again for 0, 1, 3, 5, 7 and 9 h. Subsequently, 0.5 ml cultures were transferred into 20 ml MRS broth containing MBC (2,048 μg/ml) ciprofloxacin and incubated at 30°C for 24 h. The 1 ml cultures were harvested by centrifugation at 4,000 rpm for 1 min and washed twice with PBS (pH 7.4). After cell pellets were resuspended and serially diluted 10-fold with PBS (pH 7.4), the dilution cells were inoculated on MRS agar plate to count after 24 h incubation at 30°C. The persister frequency was expressed as the ratio of viable bacteria in treated and untreated group with 1/2 MIC ciprofloxacin. After PemK was induced by IPTG in recombinant *E. coli* BL21, no-persister cells were killed with MBC ciprofloxacin in LB broth medium. The persister frequency of recombinant *E. coli* BL21 was carried out following similar procedures described above. The cell morphology was observed in FEI inspect F50 scanning electron microscope (Inspect F50, FEI, Hillsboro, USA).

2.9 Statistical analysis

All experiments were conducted in triplicate for each sample, and the data was presented as the mean values ± standard deviation, with variations less than 10%. Statistical significance analysis was carried out using analysis of variance (ANOVA) with Tukey's *post-hoc* test in SPSS 20.0, and a *p*-value less than 0.05 was considered statistically significant.

3 Results

3.1 PemIK is a typical II TA stress regulator

Co-localization and co-transcription in an operon are common characteristics of type II-TAs (Zhou et al., 2021). In *W. cibaria*, the PemI and PemK genes were situated at locus 8,267–8,949 on plasmid PA010 (**Supplementary Figure 1**), sharing a promoter and terminator in transcription but possessing independent start and stop codons in translation (**Figure 1A**). Both open reading frames (ORFs) consisted of a frame with 342 bp encoding 114 amino acids followed by a TAA termination codon. Interestingly, a genetic overlap of seven base pairs between them (**Figure 1A**), which distinguished it from other PemIK structures.

When *W. cibaria* was exposed to 1/2 MIC ciprofloxacin, the co-transcription of PemIK was activated (**Figure 1B**), while PemI

2 https://rostlab.org/services/snap/
3 https://www.ics.uci.edu/$\sim$baldig/mutation.html
4 http://www.ccp4.ac.uk/

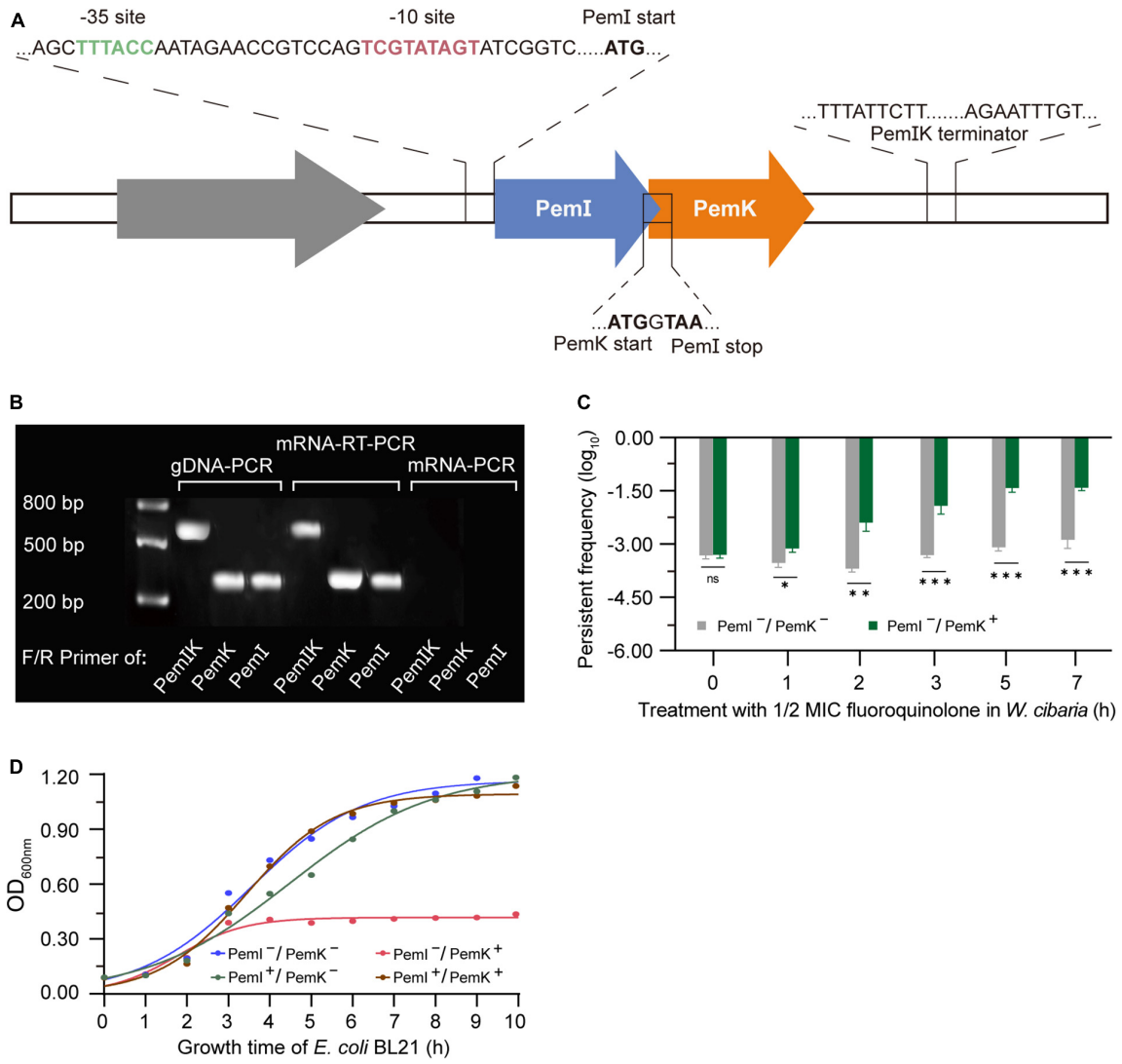

FIGURE 1
The structural characteristics and pressure response mechanism of PemIK. **(A)** Operon structure of PemIK of *W. cibaria*. **(B)** Validation of co-transcription. **(C)** Persister frequency of *W. cibaria* after treatment with 1/2 MIC ciprofloxacin. **(D)** Growth curve of recombinant *E. coli* BL21, demonstrating that PemI counteracted the cytotoxic effects of PemK through physical binding. Data were assessed by ANOVA with Tukey's *post-hoc* test. The asterisk (*) indicated significant level: $*P < 0.05$, $**P < 0.01$, $***P < 0.001$, not significant (ns), $P > 0.05$.

underwent degradation by Lon enzyme. Consequently, free PemK exhibited cytotoxicity to *W. cibaria*, leading to a severe growth inhibition and a significant increase in proportion of persister cells (Figure 1C). It has been demonstrated that PemI could counteract the cytotoxicity of PemK in recombinant *E. coli* BL21 (Figure 1D). Moreover, it also functioned as a transcription factor by inhibiting their co-transcription. Therefore, once the adverse conditions were alleviated or eliminated, the persistence of *W. cibaria* resumed its growth.

3.2 PemK is a novel specific endonuclease of mRNA

The toxins of II-type TAs are generally enzymes, particularly RNases (Díaz-Orejas et al., 2017). PemK from *W. cibaria* shared conserved residues and exhibited similar folds with its homologs, a barrel-shaped pattern of 7 β-sheets and 2 α-helices (Figure 2A). However, there were some differences in their secondary structures (Figure 2B), suggesting that they have similar functions but different mechanisms in controlling mRNA binding. The binding of mRNA typically occurred at the like-gate interfaces, which corresponded to the crevices between β1–β2 and β3–β4 sheets of one monomer and α1 helices of the other monomer in PemK dimers from *W. cibaria* (Figure 2C). The gate of PemK dimer from *W. cibaria* differed from that observed in its homologs from *S. aureus*, *E. coli*, *B. subtilis*, and *B. anthracis* (Figure 2B). Simultaneously, its electrostatic potential surface also displayed variations compared to its homologs (Figures 2D–H), it featured a weak positive charge plaque on its surface. These unique structural differences suggested that its mechanism for binding and cleaving mRNA differed from its homologs.

10.3389/fmicb.2024.1402319

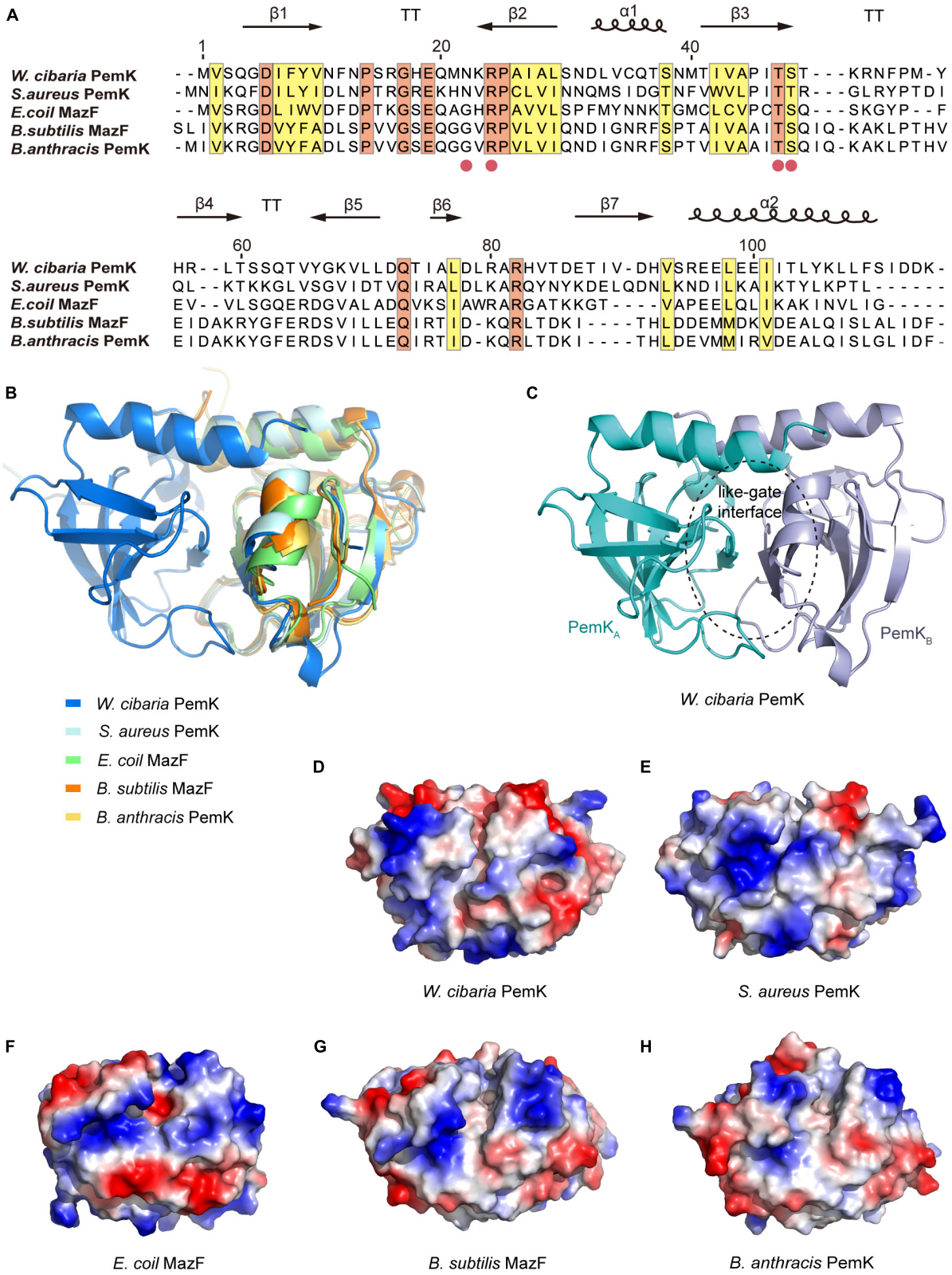

FIGURE 2
The structural comparison of PemK with its homologs. **(A)** Sequence alignment of PemK with its homologs. Secondary structures were denoted in the upper region. Potential active site residues are marked as red circles. Conserved and similar residues were shown in orange and yellow boxes, respectively. α: α-helix, β: β-sheet, T: turn. **(B)** Overlay structure of PemK with other homologs. **(C)** Overall structure of the PemK dimer. **(D–H)** Electrostatic surface potential represented the different charge distributions at the gate-like interface regions in PemK and its homologs.

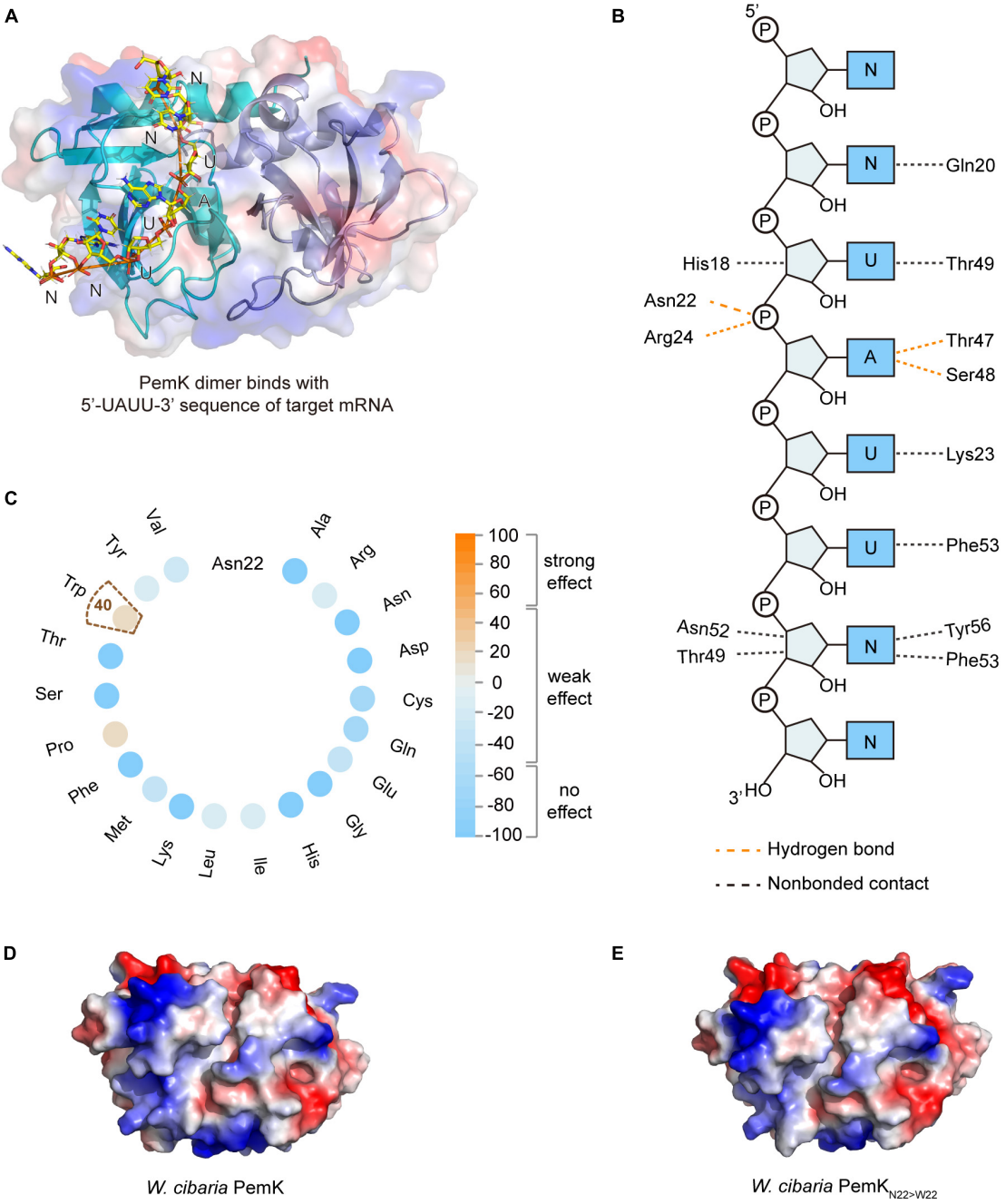

FIGURE 3
The mRNA binding and cleavage of PemK. **(A)** Model of PemK-mRNA complex depicted the stick model of PemK dimer and target mRNA. **(B)** NUCPLOT diagram of contacts between mRNA and PemK. Orange and black dotted lines represented hydrogen bonds and non-bonded contacts, respectively. **(C)** SNAP2 predicted the impact scores on the function of PemK after Asn_{22} (N_{22}) was mutated to 20 amino acids, respectively. **(D)** Electrostatic surface potential of PemK. **(E)** Electrostatic surface potential of $PemK_{N22>W22}$ that Asn_{22} was mutated to Trp_{22} (W_{22}).

PemK specifically recognizes and cleaves the tetrad U↓AHU (where H is C, A, or U) sequence in target mRNAs (Zhang et al., 2004; Zorzini et al., 2016; Cho et al., 2017). In *S. aureus*, Arg_{25} and Thr_{48} had been confirmed as key active residues for PemK (Kim et al., 2022). In *W. cibaria*, the mRNA's U↓AHU (where H is U) sequence bound to the like-gate interfaces of PemK dimer through four hydrogen bonds and four van der Waals contacts (**Figures 3A, B**). Specifically, Asn_{22} and Arg_{24} formed hydrogen bonds with the phosphate group between U↓A, while Thr_{47} and Ser_{48} bound to the adenine base of U↓A through hydrogen bonds (**Figure 3B**). However, among these residues, Asn_{22} was not highly conserved in homologs based on sequence alignment (**Figure 2A**), and its substitution with any amino acid had little impact on PemK's function (**Figure 3C**). Even when Asn_{22} was mutated to Trp *in situ*, there were no changes observed in the electrostatic potential surface of its gate interface (**Figures 3D, E**). Therefore, Arg_{24}, Thr_{47} and Ser_{48} might be important residues influencing mRNA-binding and catalytic activity.

10.3389/fmicb.2024.1402319

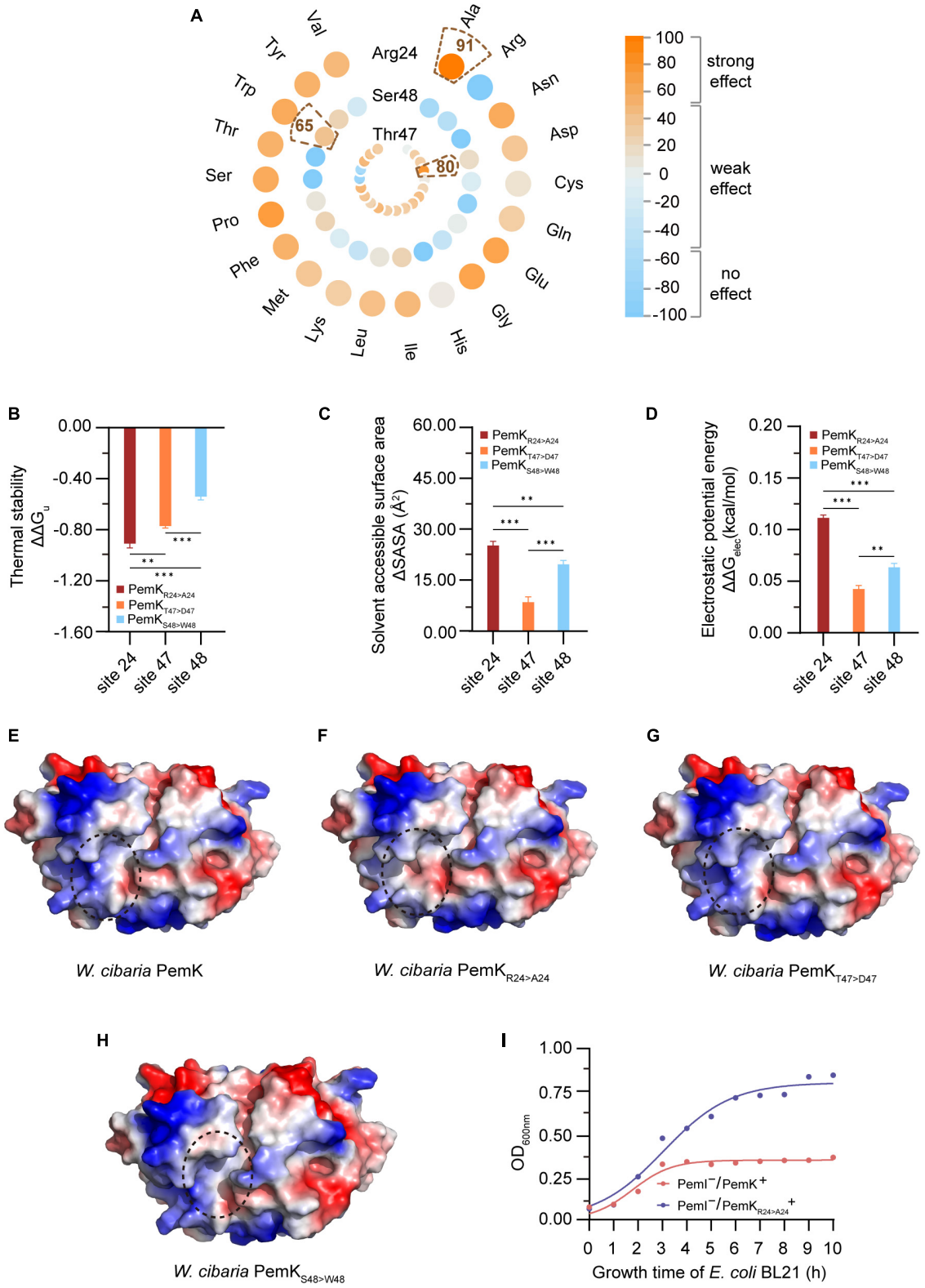

FIGURE 4
The properties of PemK after mutation of Arg_{24}, Thr_{47} and Ser_{48}. **(A)** SNAP2 predicted the impact scores on the function of PemK after Arg_{24}, Thr_{47} and Ser_{48} were mutated to 20 amino acids, respectively. **(B–D)** Differences of thermal stability, solvent accessible surface area, electrostatic potential energy of $PemK_{R24>A24}$ (Arg_{24} was mutated to Ala_{24}), $PemK_{T47>D47}$ (Thr_{47} was mutated to Asp_{47}) and $PemK_{S48>W48}$ (Ser_{48} was mutated to Trp_{48}), compared with the wild-type PemK. **(E–H)** Electrostatic surface potential of PemK, $PemK_{R24>A24}$, $PemK_{T47>D47}$, and $PemK_{S48>W48}$. The change in electrical potential energy at the point mutation locations were highlighted in dotted circles. **(I)** Growth curve of recombinant *E. coli* BL21 after induction of PemK and $PemK_{R24>A24}$ expression. Data were assessed by ANOVA with Tukey's *post-hoc* test. The asterisk (*) indicated significant level: $*P < 0.05$, $**P < 0.01$, $***P < 0.001$, not significant (ns), $P > 0.05$.

10.3389/fmicb.2024.1402319

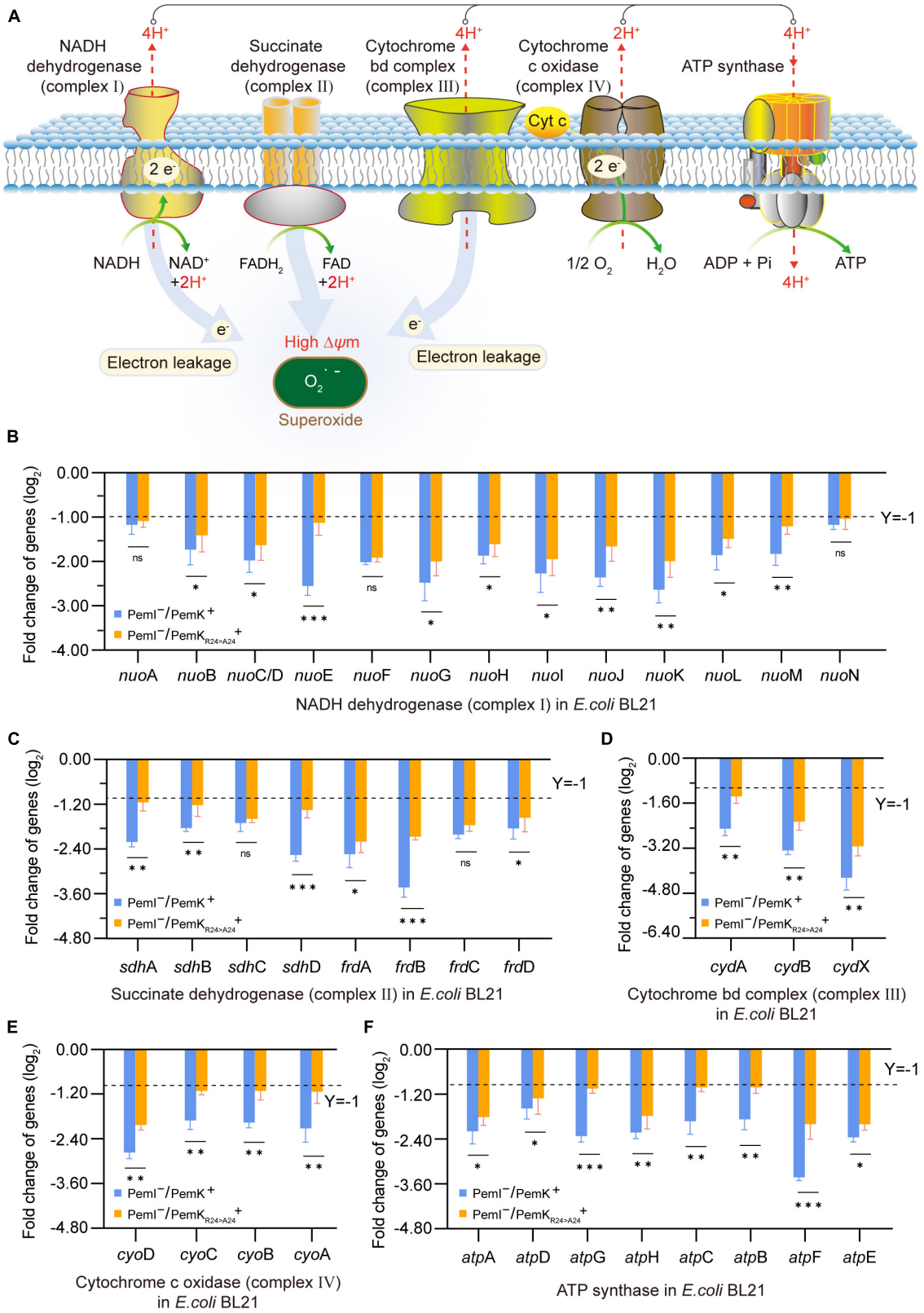

FIGURE 5
The effects on the respiratory chain before and after PemK mutation. **(A)** Schematic of respiratory chain. **(B–F)** Effects of PemK and PemK$_{R24>A24}$ on gene transcription of complexes I–IV and ATP-synthase in recombinant *E. coli* BL21. Data were assessed by ANOVA with Tukey's *post-hoc* test. The asterisk (*) indicated significant level: $*P < 0.05$, $**P < 0.01$, $***P < 0.001$, not significant (ns), $P > 0.05$.

TABLE 1 PemK cleaving the target mRNAs of enzymes in respiratory chain of *W. cibaria*.

Metabolic enzymes	Gene	Number of cleavage sites	Metabolic enzymes	Gene	Number of cleavage sites
NADH dehydrogenase	*nuo*A	2	Succinate dehydrogenase	*frd*B	1
	*nuo*B	2		*frd*C	2
	*nuo*C/D	3		*frd*D	3
	*nuo*E	3	Cytochrome C reductase	*cyd*A	4
	*nuo*F	2		*cyd*B	4
	*nuo*G	8		*cyd*X	1
	*nuo*H	2	Cytochrome C oxidase	*cyo*D	1
	*nuo*I	1		*cyo*C	1
	*nuo*J	1		*cyo*B	6
	*nuo*K	1		*cyo*A	5
	*nuo*L	6	ATP-synthase	*atp*A	3
	*nuo*M	6		*atp*D	1
	*nuo*N	3		*atp*G	1
Succinate dehydrogenase	*sdh*C	2		*atp*H	2
	*sdh*D	1		*atp*C	1
	*sdh*A	3		*atp*B	4
	*sdh*B	3		*atp*A	1
	*frd*A	2		*atp*E	1

3.3 Arg_{24} is crucial for the RNase activity of PemK

The function of protein is often closely related to its structure and charge distribution (Gorham et al., 2011). To gain more detailed insights into the active site of PemK, mutations were predicted *in situ* at Arg_{24}, Thr_{47}, and Ser_{48} residues (**Figure 4A**). Interestingly, substitution of Arg_{24} by most amino acid strongly affected PemK function, resulting in a score ranging from 52 to 91 (**Figure 4A** and **Supplementary Table 2**). While substitution of Ser_{48} had weak or no effects with a score below 65 (**Figure 4A**). The impact of Thr_{47} substitution was generally less pronounced than that of Arg_{24}, a score below 80 (**Figure 4A**). In PemK-mRNA complex, Arg_{24} bound to the phosphate group in U↓A through a hydrogen bond (**Figure 3B**). In *S. aureus* PemK and *B. subtilis* MazF, the amino acid residues, which bound to the phosphate group between U↓A via hydrogen bonding, were considered active sites involved in cleaving the tetrad U↓AUU sequence (Bukowski et al., 2013). Notably, Arg_{24} of PemK from *W. cibaria* corresponded well to Arg_{25} and Arg_{26} (**Figure 2A**), an important active residue in *S. aureus* PemK and *B. subtilis* MazF. So it might be a crucial active site for PemK to cleave the 3′,5′-phosphodiester bond of target mRNA.

The unfolding free energy (ΔGu) is an important indicator of protein thermostability, and the ΔΔGu ($\Delta\Delta G_u = \Delta G_{mut-u} - \Delta G_{wt-u}$) can characterize the change in the thermostability caused by site-directed mutations (Verstraeten et al., 2015). The substituting *in situ* of Arg_{24}, Thr_{47} and Ser_{48} decreased the thermostability of PemK, with substituting of Arg_{24} with Ala being more pronounced than the others, ΔΔGu = −0.91 (**Figure 4B**). In addition, the solvent accessible surface area (SASA) also characterized the instability caused by mutations (**Figure 4C**). A larger SASA value indicates a higher solvent-accessible surface area of protein, which is associated with lower stability. Three site-directed mutations *in situ* resulted in an increase in SASA of PemK, in which the $\Delta SASA_{Arg24>Ala24}$ (25.18) > $\Delta SASA_{Ser48>Trp48}$ (19.64) > $\Delta SASA_{Thr47>Asp47}$ (8.47) (**Figure 4C**).

The mutations may alter the charge distribution of protein's active site or ligand-binding site, thereby impacting its affinity and specificity for the target molecules (Gorham et al., 2011). In *W. cibaria*, substituting Arg_{24} with Ala significantly altered the charge distribution on electrostatic potential surface of PemK dimers (**Figures 4E, F**), particularly at the like-gate interfaces where a transition occurred from positive charge to weak negative charge. Moreover, substituting Arg_{24} with Ala led to a more pronounced destabilization of PemK compared to Thr_{47} and Ser_{48} mutations, as indicated by $\Delta\Delta G_{elec}$ ($\Delta\Delta G_{elec} = \Delta G_{mut-elec} - \Delta G_{wt-elec}$): $\Delta\Delta G_{elec-Arg24>Ala24}$ (0.11) > $\Delta\Delta G_{elec-Ser48>Trp48}$ (0.06) > $\Delta\Delta G_{elec-Thr47>Asp47}$ (0.04) (**Figures 4D, G, H**). Additionally, it was observed that $PemK_{Arg24>Ala24}$ significantly reduced its cellar toxicity, without a significant inhibition on the recombinant *E. coli* BL21 (**Figure 4I**). These findings suggested that Arg_{24} was more likely to affect PemK's ability to cleave U↓AUU sequence, thereby influencing cell regulation in response to adverse external environments.

3.4 $PemK_{Arg24>Ala24}$ mitigates the impairment of respiratory chain

Persistence has been associated with reduced levels of cellular ATP (Verstraeten et al., 2015; Wilmaerts et al., 2019). The respiratory chain is the main process to generate cellular ATP, which is composed of a series of hydrogen transfer and electron

10.3389/fmicb.2024.1402319

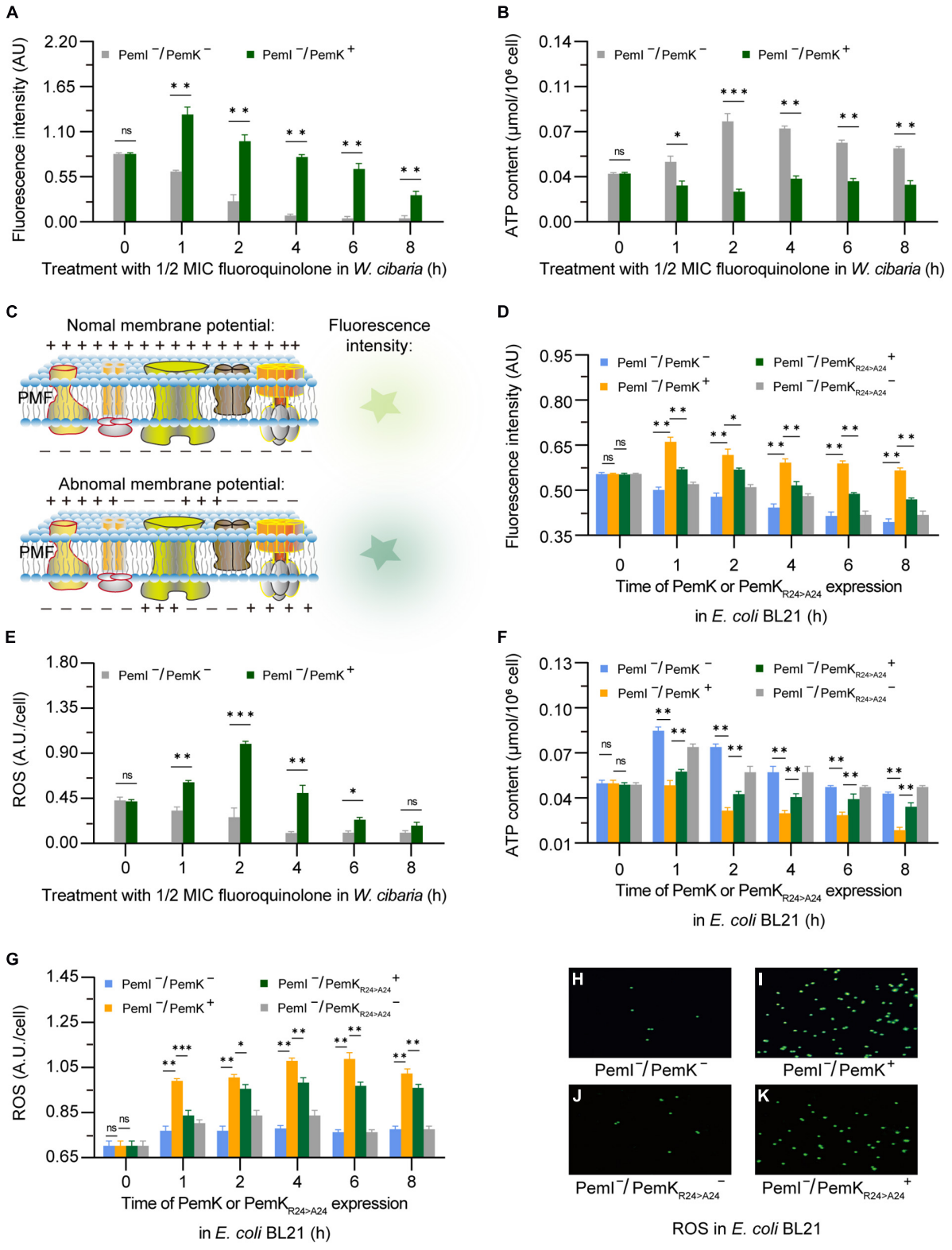

FIGURE 6
The alterations in membrane potential, ATP, and ROS caused by PemK and PemK$_{R24>A24}$ in *W. cibaria* and recombinant *E. coli* BL21, respectively. **(A,B,E)** Membrane potential, ATP, and ROS of *W. cibaria* after treatment with 1/2 MIC ciprofloxacin. **(C)** Schematic of membrane potential. **(D,F,G)** Membrane potential, ATP, and ROS of recombinant *E. coli* BL21 after induction of PemK and PemK$_{R24>A24}$ protein expression. **(H–K)** Fluorescence of intracellular ROS in recombinant *E. coli* BL21. Data were assessed by ANOVA with Tukey's *post-hoc* test. The asterisk (*) indicated significant level: $*P < 0.05$, $**P < 0.01$, $***P < 0.001$, not significant (ns), $P > 0.05$.

10.3389/fmicb.2024.1402319

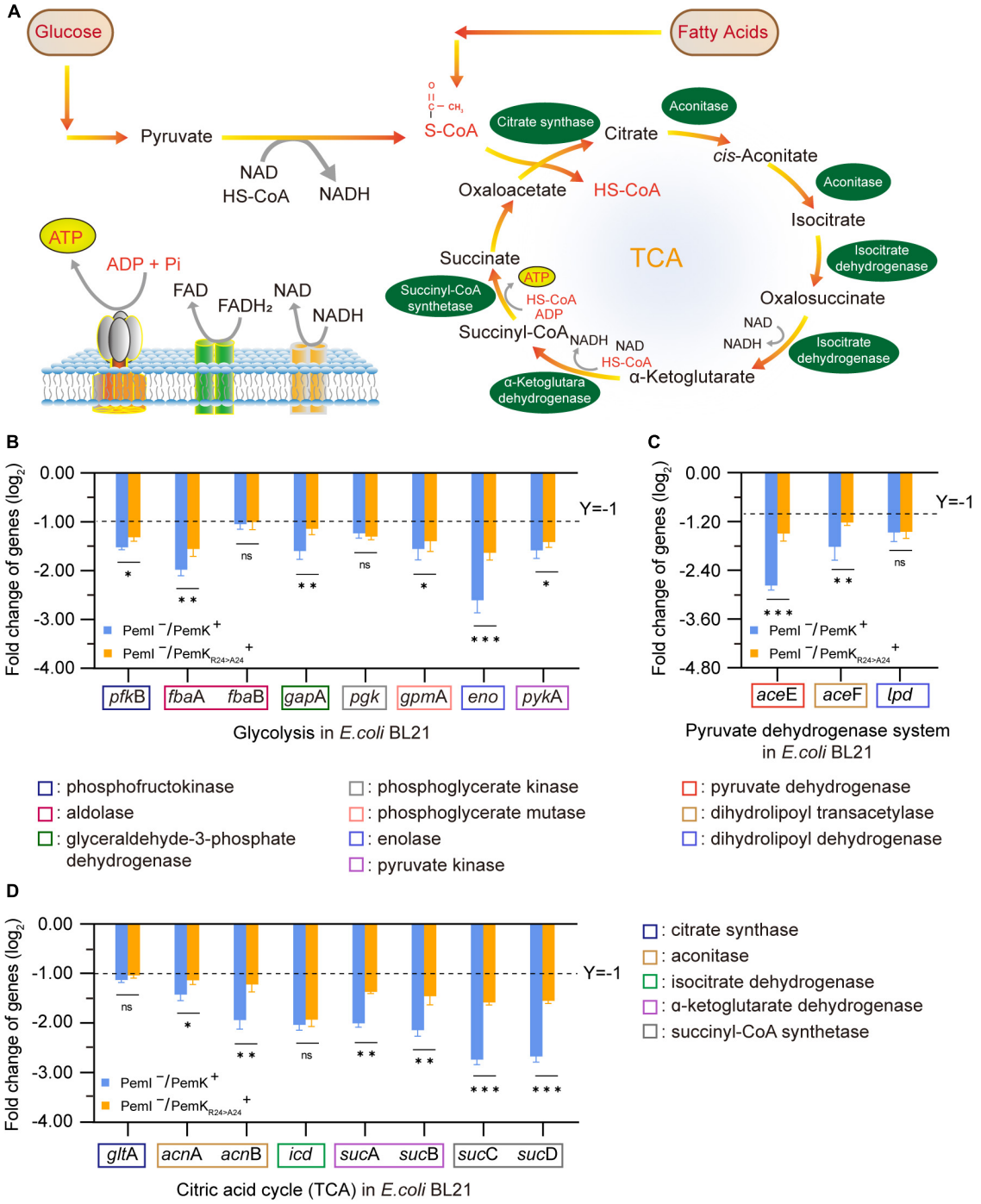

FIGURE 7
The effects on NADH and $FADH_2$ synthesis before and after PemK mutation in recombinant *E. coli* BL21. **(A)** Schematic of glycolysis and TCA cycle. **(B)** Effects of PemK and $PemK_{R24>A24}$ on the gene transcription of glycolysis. **(C)** Effects of PemK and $PemK_{R24>A24}$ on the gene transcription of pyruvate dehydrogenase system. **(D)** Effects of PemK and $PemK_{R24>A24}$ on the gene transcription of TCA cycle. Data were assessed by ANOVA with Tukey's *post-hoc* test. The asterisk (*) indicated significant level: $*P < 0.05$, $**P < 0.01$, $***P < 0.001$, not significant (ns), $P > 0.05$.

transfer reactions mediated by complexes I to IV and ATP-synthase on cell plasma membrane (Figure 5A). In *W. cibaria*, PemK cleaved the target mRNAs of complexes I–IV and ATP-synthase, including 13 genes in complex I, 8 genes of complex II, 3 genes of complex III, 4 genes of complex IV, and 8 genes of ATP-synthase (Table 1 and Supplementary Table 3). In recombinant *E. coli* BL21, Ala substitution for Arg_{24} impaired PemK's ability to cleave these target mRNAs, especially *nuo*E in complex I, *sdh*D and *frd*A in comolex II, *atp*G and *atp*F in ATP-synthase (Figures 5B–F), thus reducing the adverse effects of PemK on respiratory chain.

Cleavage of mRNA caused the mRNA to break before translation, thus it blocked the synthesis of complexes I–IV and ATPase, resulting in the failure of H^+ and e^- transfer reactions in respiratory chain, which reduced the membrane potential and

TABLE 2 PemK cleaving the target mRNAs of enzymes in glycolysis of *W. cibaria*.

Metabolic enzymes	Gene	Number of cleavage sites
Phosphofructokinase	*pfk*B	2
Aldolase	*fba*A	1
	*fba*B	5
Glyceraldehyde-3-phosphate dehydrogenase	*gap*A	1
Phosphoglycerate kinase	*pgk*	1
Phosphoglycerate mutase	*gpm*A	2
Enolase	*eno*	1
Pyruvate kinase	*pyk*A	1

ATP production of *W. cibaria* (Figures 6A, B). Alterations in membrane potential caused membrane depolarization (Figure 6C), so the heightened fluorescence intensity corresponded to a more lower membrane potential (Figure 6A). In recombinant *E. coli* BL21, PemK significantly reduced the membrane potential and increased the membrane depolarization, while Ala substitution for Arg_{24} significantly alleviated the degree of membrane potential reduction and membrane depolarization, with an alleviation of 7.8–19.6% (Figure 6D). The membrane potential generated a proton motive force (PMF), which promotes the movement of H^+ across cell membrane and ultimately produces ATP via ATP synthase. Therefore, the changes in membrane potential directly affected the production of ATP in *W. cibaria*, generally reducing the amount of ATP by 20–40% (Figure 6B). Additionally, blocked electron transport obstructed the reduction of O_2, leading to the accumulation of excess ROS in *W. cibaria* to 1.50–2.30 times of normal levels (Figure 6E). Similarly, Ala substitution for Arg_{24} had also moderated the adverse effects on the ATP production and reduced ROS accumulation in recombinant *E. coli* BL21, with ATP content increased by 20.8–276.60% and ROS accumulation reduced by 7.8–15.6%, respectively (Figures 6F–K). These insights implied that Arg_{24} played an important role in regulation of respiratory chain by PemK.

3.5 $PemK_{Arg24>Ala24}$ alleviates the adverse effects on NADH and $FADH_2$ synthesis

NADH and $FADH_2$ are the important reducing agents to supply H^+ for cells via the respiratory chain pathway, while glycolysis and TCA cycle serve as their primary sources. Glycolysis catalyzes a glucose into two pyruvates, accompanied by production of 2 NADH. This process involves ten enzyme-catalyzed reactions (Chandel, 2021), and any dysfunction of them can lead to disorders in NADH synthesis (Figure 7A). In glycolysis of *W. cibaria*, PemK only targeted the mRNA of one or two subunits of phosphofructokinase, aldolase, glyceraldehyde-3-phosphate dehydrogenase, phosphoglycerate kinase, phosphoglycerate mutase, enolase and pyruvate kinase (Table 2 and Supplementary Table 4).

TABLE 3 PemK cleaving the target mRNAs of pyruvate dehydrogenase system in *W. cibaria*.

Metabolic enzymes	Gene	Number of cleavage sites
Pyruvate dehydrogenase	*ace*E	6
Dihydrolipoamide transacetylase	*ace*F	2
Dihydrolipoamide dehydrogenase	*Ipd*	1

TABLE 4 PemK cleaving the target mRNAs of enzymes in TCA cycle of *W. cibaria*.

Metabolic enzymes	Gene	Number of cleavage sites
Citrate synthase	*glt*A	8
Aconitase	*acn*A	10
	*acn*B	5
Isocitrate dehydrogenase	*icd*	3
α-ketoglutarate dehydrogenase	*suc*A	2
	*suc*B	2
Succinyl-CoA synthetase	*suc*C	1
	*suc*D	1

Acetyl-CoA serves as the bridge between glycolysis and TCA cycle, generated by the pyruvate dehydrogenase system consisting of pyruvate dehydrogenase, dihydrolipoamide transacetylase, and dihydrolipoamide dehydrogenase. In *W. cibaria*, PemK also cleaved their mRNA (Table 3 and Supplementary Table 5). Acetyl-CoA enters TCA to undergo a series of enzymatic reactions into CO_2 and H_2O while producing 3 NADH and 1 $FADH_2$. However, PemK only targeted the mRNA of one or two subunit of citrate synthase, aconitase, isocitrate dehydrogenase, α-ketoglutarate dehydrogenase and succinyl-CoA synthetase in *W. cibaria* (Table 4 and Supplementary Table 6). In recombinant *E. coli* BL21, PemK significantly impaired the mRNA of these target enzymes involved in glycolysis, pyruvate oxidative decarboxylation and TCA cycle by −1.05–2.98 $\log_2$ folds (Figures 7B–D). However, Ala substitution for Arg_{24} effectively alleviated these adverse impacts except for phosphoglycerate kinase, dihydrolipoamide dehydrogenase, citrate synthase and isocitrate dehydrogenase. Therefore, Arg_{24} was a crucial site for PemK to disrupt the NADH and $FADH_2$ synthesis in *W. cibaria*.

3.6 $PemK_{Arg24>Ala24}$ attenuates growth inhibition and persister frequency

Induction of persistence appears to be the primary physiological function of TAs in bacteria, and stimulating the expression of type II toxins can significantly enhance the persister frequency (Maisonneuve and Gerdes, 2014; Merfa et al., 2016). In recombinant *E. coli* BL21, induction of PemK resulted in significant growth inhibition, with $OD_{600\,nm}$ maintained at 0.29–0.31 (Figure 8A). Although the persister frequency also increased from −3.5 $\log_{10}$ to −2.58 $\log_{10}$ during growth of *E. coli* BL21

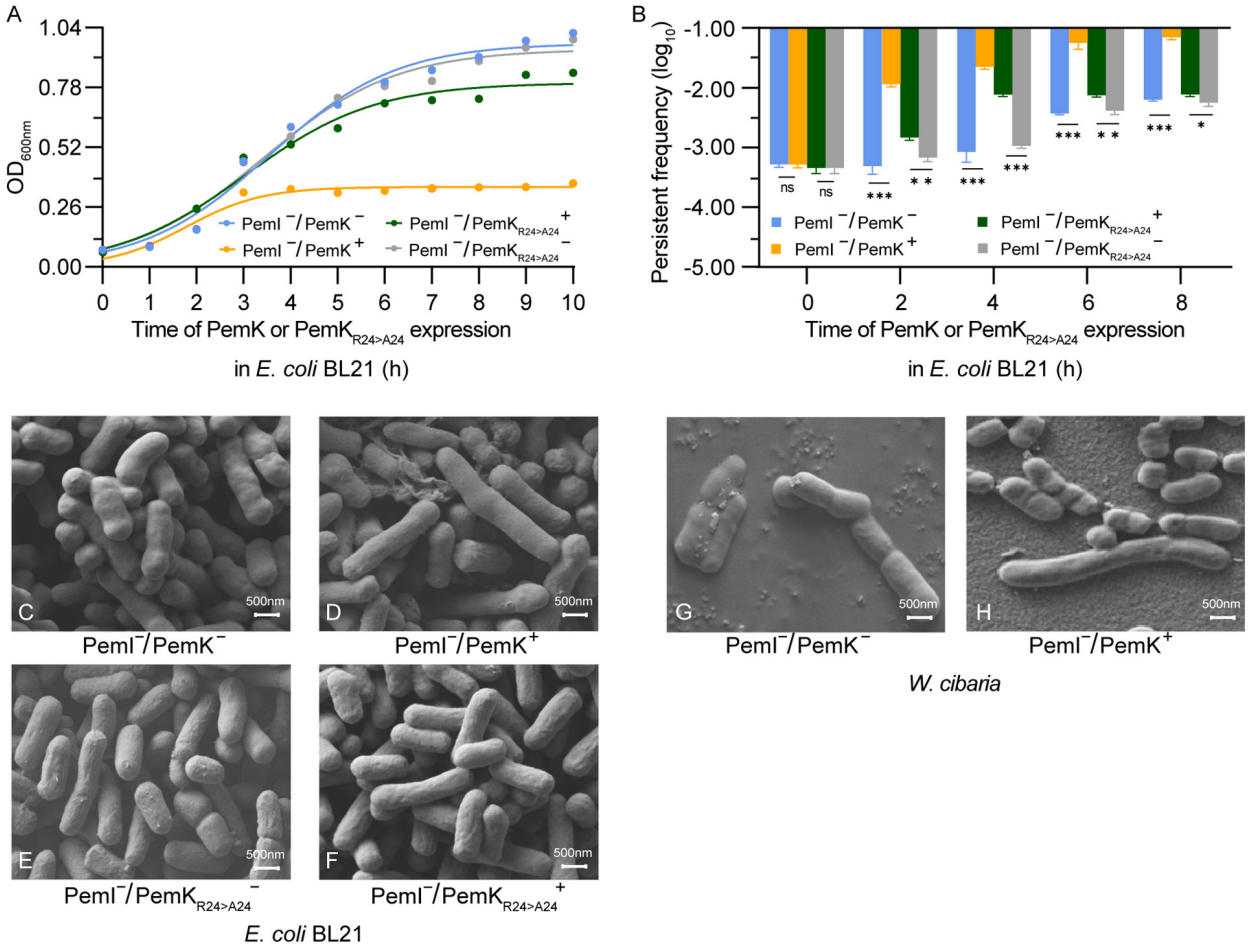

FIGURE 8
Persister frequency and cell morphology after induction of PemK and PemK$_{R24>A24}$ expression. **(A)** Growth curve of recombinant *E. coli* BL21. **(B)** Persister frequency of recombinant *E. coli* BL21. **(C–F)** Cell morphology of *E. coli* BL21. **(G,H)** Cell morphology before and after induction of PemK expression in *W. cibaria*. Data were assessed by ANOVA with Tukey's *post-hoc* test. The asterisk (*) indicated significant level: $*P < 0.05$, $**P < 0.01$, $***P < 0.001$, not significant (ns), $P > 0.05$.

with PemK$^-$/PemI$^-$, PemK expression dramatically elevated the persister frequency of *E. coli* BL21 with PemI$^-$/PemK$^+$ up to -1.82 log$_{10}$ to -0.24 log$_{10}$ (**Figure 8B**). Substitution of Arg$_{24}$ with Ala$_{24}$ significantly weakened the growth inhibition and induced persister frequency of *E. coli* BL21 with PemI$^-$/PemK$_{Arg24>Ala24}^+$, decreasing it to -2.82 to -2.24 log$_{10}$ (**Figure 8B**).

II-type toxin expression does not necessarily lead to changes in morphology of persister cells, but when it does, it usually involves abnormal elongation, filamentation, and even a transition from spiral to round coccoid (Cho et al., 2017; El Mortaji et al., 2020; Yu et al., 2023). In recombinant *E. coli* BL21, PemK expression significantly prolonged the morphology of some cells, increasing from 0.75–1.5 μm to 1.5–2.5 μm. This change was also observed in *W. cibaria*, but with more pronounced effects from 0.75–1.25 to 0.75–3.5 μm. However, the mutation PemK$_{Arg24>Ala24}$ did not induce significant alterations of *E. coli* BL21 (**Figures 8C–H**). It was generally believed that ectopic expression of a single toxin gene resulted in a phenotype similar to naturally occurring persister bacteria (Merfa et al., 2016; Page and Peti, 2016). Therefore, PemK have prolonged the persister cell of *W. cibaria* through the same mechanism as *E. coli* BL21.

4 Discussion

The mechanism underlying TA-mediated persistence remains incompletely understood, although it is generally believed that the direct cause is the shutdown or disruption of major cellular processes induced by TA toxins (Verstraeten et al., 2015; Wilmaerts et al., 2019). However, experimental confirmation of this understanding has been scarce. Our presented results revealed the molecular mechanism through which PemK induced persistence of *W. cibaria* by disrupting crucial cellular processes such as hydrogen transfer, electron transfer, NADH and FADH$_2$ synthesis (**Figures 3**, **5**, **7**). This disruption occurred via mRNA fragmentation of targeting metabolic enzymes involved in glycolysis, TCA cycle and respiratory chain pathways, ultimately leading to reduced ATP levels and membrane depolarization (**Figures 6A–C**). These findings provided valuable insights into how *W. cibaria* evaded ciprofloxacin stress, that was, when faced with ciprofloxacin stress, it entered the persistence, conversely, once the stress was alleviated, the persistence was awakened.

Bacterial persistence is a programmed phenotypic transformation with a genetic basis (Gerdes and Maisonneuve,

2012; Wilmaerts et al., 2019). Currently, it is widely accepted that TAs play a crucial role in bacterial persistence (Page and Peti, 2016). Our findings further supported this consensus, as PemKI's mRNA was one of the most up-regulated transcripts during the persistence of *W. cibaria* under ciprofloxacin stress (**Figure 1C**). Additionally, ectopic expression of PemK significantly increased the persistence frequency of recombinant *E. coli* BL21 (**Figure 8B**). In *W. cibaria*, the PemKI module consisted of PemK and its cognate antitoxin PemI (**Figures 1A, B**). Although PemK shared conserved residues and similar structure with homologs, its gate crevice and charge distribution differed from those homologs due to amino acid variations. Notably, the gate crevice of PemK closely resembled that of *S. aureus*, but differed significantly from *E. coli*, *B. subtilis* and *B. anthracis* (**Figure 2**). These unique characteristics determined its binding specificity for mRNA and physiological functions.

The significant function of PemK and its homologues is to catalyze the cleavage of bacterial mRNA with specific sequences (Bukowski et al., 2013; Kim et al., 2022), and their catalytic activities are closely related to the type and location of amino acid residues involved in mRNA binding and cleavage. In *E. coli*, MazF specifically cleaves the P-O5′ phosphoester bond between G↓ACA or G/UA↓CA of mRNA through transphosphorylation, with Arg_{29} and Thr_{52} likely serving as catalytic residues (Zorzini et al., 2016). MazF from *B. subtilis* cleaves mRNAs with U↓ACAU, where Arg_{25} and Thr_{48} are crucial for its activity, while Gln_{50} and Arg_{71} have minimal effect on activity (Simanshu et al., 2013). For *S. aureus*, Glu_{20}, Arg_{25}, Th_{r48}, and Arg_{84} are key residues involved in binding and cleavage of mRNA with U↓AUU. Among them, Arg_{25} and Thr_{48} may be responsible for mRNA cleavage, while Arg_{84} maintains the "closed form" conformation of PemK dimer despite not directly interacting with mRNA. Conserved Arg and Thr residues located in β2 and β3 sheet, respectively, are generally considered as the active residues for catalysis in PemK homologues, where Arg acts as both a general acid/base catalyst, while Thr stabilizes transition states during reactions. In *W. cibaria*, Arg_{24} bound the phosphate group between U↓A, its mutation significantly affected the conformation and charge distribution of its gate crevice, as well as the thermostability, SASA and instability of PemK, thus significantly reducing the catalytic activity of PemK (**Figures 3B**, **4–8**). Interestingly, substitution at Thr_{48} with any amino acid did not obviously affect any properties described above for PemK (**Figure 4A**), most likely due to fact that it bound the adenine between U↓A rather than phosphate group in target mRNA sequence (**Figure 3B**). Therefore, the active residues of PemK from *W. cibaria* differed significantly from those found in its homologs, where only Arg_{24} was the crucial active residue.

A decrease in intracellular ATP and/or low PMF across the membrane are characteristic indicators of persister formation resulting from TA-toxin attacking on conservative metabolic processes (Yu et al., 2023). Various small toxins, such as those in the Hok family, abrogate the PMF and inhibit ATP synthesis by depolarizing bacterial membranes (Harms et al., 2018). However, there is currently limited knowledge regarding the detailed mechanism through which TA-toxins target ATP and PMF. In *W. cibaria*, ATP synthesis primarily occurs through substrate level phosphorylation in glycolysis and TCA cycle, as well as oxidative phosphorylation in the respiratory chain. The former serves as an auxiliary pathway for energy acquisition, with only 3 ATP production. However, PemK inhibited their ATP synthesis, more importantly, it reduced the supply of NADH + H^+ and $FADH_2$ for oxidative phosphorylation by cleaving mRNA of enzymes in metabolic framework (**Figures 5–7**). The oxidative phosphorylation is the primary pathway for ATP production, generating 10 ATP molecules along with the efflux of 10 H^+ through complexes I, III, and IV, and the influx of 4 H^+ through ATP-synthase. Consequently, in *W. cibaria*, PemK cleaved target mRNAs encoding complexes I, III and IV to result in impaired H^+ efflux from inner-membrane, subsequently reduced the membrane potential and abolished PMF (**Figures 5**, **6A, C**). Simultaneously, PemK targeted complexes I–IV and ATP synthase to block the electron transfer and H^+ influx which ultimately disrupts ATP synthesis (**Figures 6B, F**). In bacteria, disruption of ATP synthesis appears to be a promising mechanism for TA-toxins as most antibiotics corrode active targets by energy-dependent processes. Therefore, the disruption of ATP synthesis leading to cell depolarization was likely to be the primary physiological function of PemK inducing *W. cibaria* persistence to evade ciprofloxacin stress.

Recently, it has been documented that ATP content was the decisive factor in whether exponentially growing cells transition into persister cells. However, this correlation was not observed in *S. aureus* (Kamphuis et al., 2006; Somerville and Proctor, 2009). Under ciprofloxacin stress, PemK significantly augmented the persister frequency of *W. cibaria*, from 0.03% up to 0.6% (**Figure 1C**), achieved through disruption of ATP synthesis pathway and depolarization of cell membrane, which has been further validated in recombinant *E. coli* BL21 (**Figures 6A–D, F**). Moreover, when Ala replaced Arg_{24}, $PemK_{Arg24>Ala24}$ considerably weakened its cytotoxicity to ATP synthesis pathway and membrane potential of recombinant *E. coli* BL21, resulting in a decrease in persister frequency from −1.82 to −1.24 $\log_{10}$ to −2.82 to −2.24 $\log_{10}$ (**Figures 6D**, **8A**). These ectopic results further corroborated the physiological mechanism underlying PemK's involvement in the persister formation of *W. cibaria*, while also highlighted the significance of Arg_{24} for maintaining PemK's activity.

The significance of TA system in bacterial persistence renders it a natural target for the discovery of innovative strategies that can either trigger the persistence or awaken the persister cell. Our study provided some crucial structural and functional insights into PemK of *W. cibaria*, serving as a fundamental basis for uncovering this novel approach. However, the pivotal question remains whether interference with mRNA and physiological function by ciprofloxacin-induced PemK characterizes universal regulatory on *W. cibaria* under diverse stresses, which currently lacks clarity and necessitates further investigation.

Data availability statement

The datasets presented in this study can be found in online repositories. The names of the repository/repositories and accession number(s) can be found in this article/**Supplementary material**.

Author contributions

H-YZ: Data curation, Formal analysis, Investigation, Methodology, Software, Validation, Visualization, Writing – original draft. W-LX: Conceptualization, Funding acquisition, Resources, Supervision, Writing – review & editing. TC: Data curation, Formal analysis, Writing – original draft. MZ: Data curation, Investigation, Methodology, Writing – original draft. H-YW: Formal analysis, Validation, Writing – original draft.

Funding

The authors declare that financial support was received for the research, authorship, and/or publication of this article. This research was funded by the Natural Science Foundations of Sichuan, China, grant number 2018JY0045, National Natural Science Foundations of China, grant number 31571935, and Open Foundation of State Key Laboratory of Environmental Criteria and Risk Assessment, China, grant number SKLECRA 20240618.

Acknowledgments

We are grateful to Keo Lee for advice on transcription experiments, statistical analysis, and stimulating discussions.

Conflict of interest

The authors declare that the research was conducted in the absence of any commercial or financial relationships that could be construed as a potential conflict of interest.

Publisher's note

All claims expressed in this article are solely those of the authors and do not necessarily represent those of their affiliated organizations, or those of the publisher, the editors and the reviewers. Any product that may be evaluated in this article, or claim that may be made by its manufacturer, is not guaranteed or endorsed by the publisher.

Supplementary material

The Supplementary Material for this article can be found online at: https://www.frontiersin.org/articles/10.3389/fmicb.2024.1402319/full#supplementary-material

References

Bromberg, Y., and Rost, B. (2007). SNAP: Predict effect of non-synonymous polymorphisms on function. *Nucleic Acids Res.* 35, 3823–3835. doi: 10.1093/nar/gkm238

Bukowski, M., Lyzen, R., Helbin, W. M., Bonar, E., Szalewska-Palasz, A., Wegrzyn, G., et al. (2013). A regulatory role for *Staphylococcus aureus* toxin–antitoxin system $PemIK_{Sa}$. *Nat. Commun.* 4:2012. doi: 10.1038/ncomms3012

Cai, T., Zhao, Q., Xiang, W., Zhu, L., Rao, Y., and Tang, J. (2022). HigBA toxin–antitoxin system of *Weissella cibaria* is involved in response to the bile salt stress. *J. Sci. Food Agric.* 102, 6749–6756. doi: 10.1002/jsfa.12042

Chandel, N. S. (2021). Glycolysis. *Cold Spring Harb. Perspect. Biol.* 13:a040535. doi: 10.1101/cshperspect.a040535

Cho, J., Carr, A. N., Whitworth, L., Johnson, B., and Wilson, K. S. (2017). MazEF toxin-antitoxin proteins alter *Escherichia coli* cell morphology and infrastructure during persister formation and regrowth. *Microbiology* 163, 308–321. doi: 10.1099/mic.0.000436

Díaz-Orejas, R., Espinosa, M., and Yeo, C. C. (2017). The importance of the expendable: Toxin–antitoxin genes in plasmids and chromosomes. *Front. Microbiol.* 8:1479. doi: 10.3389/fmicb.2017.01479

El Mortaji, L., Tejada-Arranz, A., Rifflet, A., Boneca, I. G., Pehau-Arnaudet, G., Radicella, J. P., et al. (2020). A peptide of a type I toxin-antitoxin system induces *Helicobacter pylori* morphological transformation from spiral shape to coccoids. *Proc. Natl. Acad. Sci. U. S. A.*117, 31398–31409. doi: 10.1073/pnas.2016195117

Gerdes, K., and Maisonneuve, E. (2012). Bacterial persistence and toxin-antitoxin loci. *Annu. Rev. Microbiol.* 66, 103–123. doi: 10.1146/annurev-micro-092611-150159

Gorham, R. D., Kieslich, C. A., and Morikis, D. (2011). Electrostatic clustering and free energy calculations provide a foundation for protein design and optimization. *Ann. Biomed. Eng.* 39, 1252–1263. doi: 10.1007/s10439-010-0226-9

Harms, A., Brodersen, D. E., Mitarai, N., and Gerdes, K. (2018). Toxins, targets, and triggers: An overview of toxin-antitoxin biology. *Mol. Cell* 70, 768–784. doi: 10.1016/j.molcel.2018.01.003

Kamphuis, M. B., Bonvin, A. M. J. J., Monti, M. C., Lemonnier, M., Muñoz-Gómez, A., Van Den Heuvel, R. H. H., et al. (2006). Model for RNA binding and the catalytic site of the RNase kid of the bacterial *par*D toxin–antitoxin system. *J. Mol. Biol.* 357, 115–126. doi: 10.1016/j.jmb.2005.12.033

Kim, D. H., Kang, S. M., Baek, S. M., Yoon, H. J., Jang, D. M., Kim, H. S., et al. (2022). Role of PemI in the *Staphylococcus aureus* PemIK toxin–antitoxin complex: PemI controls PemK by acting as a PemK loop mimic. *Nucleic Acids Res.* 50, 2319–2333. doi: 10.1093/nar/gkab1288

Maisonneuve, E., and Gerdes, K. (2014). Molecular mechanisms underlying bacterial persisters. *Cell* 157, 539–548. doi: 10.1016/j.cell.2014.02.050

Merfa, M. V., Niza, B., Takita, M. A., and De Souza, A. A. (2016). The MqsRA toxin-antitoxin system from *Xylella fastidiosa* plays a key role in bacterial fitness, pathogenicity, and persister cell formation. *Front. Microbiol.* 7:904. doi: 10.3389/fmicb.2016.00904

Page, R., and Peti, W. (2016). Toxin-antitoxin systems in bacterial growth arrest and persistence. *Nat. Chem. Biol.* 12, 208–214. doi: 10.1038/nchembio.2044

Robert, X., and Gouet, P. (2014). Deciphering key features in protein structures with the new ENDscript server. *Nucleic Acids Res.* 42, W320–W336. doi: 10.1093/nar/gku316

Schiffrin, B., Radford, S. E., Brockwell, D. J., and Calabrese, A. N. (2020). PYXLINKVIEWER: A flexible tool for visualization of protein chemical crosslinking data within the PYMOL molecular graphics system. *Protein Sci.* 29, 1851–1857. doi: 10.1002/pro.3902

Shahmuradov, I. A. (2003). PlantProm: A database of plant promoter sequences. *Nucleic Acids Res.* 31, 114–117. doi: 10.1093/nar/gkg041

Shan, Y., Brown Gandt, A., Rowe, S. E., Deisinger, J. P., Conlon, B. P., and Lewis, K. (2017). ATP-dependent persister formation in *Escherichia coli*. *mBio* 8:e02267-16. doi: 10.1128/mbio.02267-16

Simanshu, D. K., Yamaguchi, Y., Park, J. H., Inouye, M., and Patel, D. J. (2013). Structural basis of mRNA recognition and cleavage by toxin MazF and its regulation by antitoxin MazE in *Bacillus subtilis*. *Mol. Cell* 52, 447–458. doi: 10.1016/j.molcel.2013.09.006

Somerville, G. A., and Proctor, R. A. (2009). At the crossroads of bacterial metabolism and virulence factor synthesis in *Staphylococci*. *Microbiol. Mol. Biol. Rev.* 73, 233–248. doi: 10.1128/mmbr.00005-09

Sun, C., Guo, Y., Tang, K., Wen, Z., Li, B., Zeng, Z., et al. (2017). MqsR/MqsA toxin/antitoxin system regulates persistence and biofilm formation in *Pseudomonas putida* KT2440. *Front. Microbiol.* 8:840. doi: 10.3389/fmicb.2017.00840

Van Zundert, G. C. P., Rodrigues, J. P. G. L. M., Trellet, M., Schmitz, C., Kastritis, P. L., Karaca, E., et al. (2016). The HADDOCK2.2 Web Server: User-fiendly integrative modeling of biomolecular complexes. *J. Mol. Biol.* 428, 720–725. doi: 10.1016/j.jmb.2015.09.014

Verstraeten, N., Knapen, W. J., Kint, C. I., Liebens, V., Van den Bergh, B., Dewachter, L., et al. (2015). Obg and membrane depolarization are part of a microbial bet-hedging strategy that leads to antibiotic tolerance. *Mol. Cell* 59, 9–21. doi: 10.1016/j.molcel.2015.05.011

Wang, L., Zhang, J., Cao, Z., Wang, Y., Gao, Q., Zhang, J., et al. (2015). Inhibition of oxidative phosphorylation for enhancing citric acid production by *Aspergillus niger*. *Microb. Cell Fact.* 14:7. doi: 10.1186/s12934-015-0190-z

Waterhouse, A., Bertoni, M., Bienert, S., Studer, G., Tauriello, G., Gumienny, R., et al. (2018). SWISS-MODEL: Homology modelling of protein structures and complexes. *Nucleic Acids Res.* 46, W296–W303. doi: 10.1093/nar/gky427

Wilmaerts, D., Windels, E. M., Verstraeten, N., and Michiels, J. (2019). General mechanisms leading to persister formation and awakening. *Trends Genet.* 35, 401–411. doi: 10.1016/j.tig.2019.03.007

Xiong, H. B., Zhou, X. H., Xiang, W. L., Huang, M., Lin, Z. X., Tang, J., et al. (2023). Integrated transcriptome reveals that d-limonene inhibits *Candida tropicalis* by disrupting metabolism. *LWT Food Sci. Technol.* 176:114535. doi: 10.1016/j.lwt.2023.114535

Yu, H., Lin, Z. X., Xiang, W. L., Huang, M., Tang, J., Lu, Y., et al. (2022). Antifungal activity and mechanism of d-limonene against foodborne opportunistic pathogen *Candida tropicalis*. *LWT Food Sci. Technol.* 159:113144. doi: 10.1016/j.lwt.2022.113144

Yu, Z., Goodall, E. C. A., Henderson, I. R., and Guo, J. (2023). Plasmids can shift bacterial morphological response against antibiotic stress. *Adv. Sci.* 10:2203260. doi: 10.1002/advs.202203260

Zhang, J., Zhang, Y., Zhu, L., Suzuki, M., and Inouye, M. (2004). Interference of mRNA function by sequence-specific endoribonuclease PemK. *J. Biol. Chem.* 279, 20678–20684. doi: 10.1074/jbc.M314284200

Zhou, J., Li, S., Li, H., Jin, Y., Bai, F., Cheng, Z., et al. (2021). Identification of a toxin–antitoxin system that contributes to persister formation by reducing NAD in *Pseudomonas aeruginosa*. *Microorganisms* 9:753. doi: 10.3390/microorganisms9040753

Zorzini, V., Mernik, A., Lah, J., Sterckx, Y. G. J., De Jonge, N., Garcia-Pino, A., et al. (2016). Substrate recognition and activity regulation of the *Escherichia coli* mRNA endonuclease MazF. *J. Biol. Chem.* 291, 10950–10960. doi: 10.1074/jbc.M116.715912

frontiers | Frontiers in Microbiology

TYPE Original Research
PUBLISHED 14 June 2024
DOI 10.3389/fmicb.2024.1394775

OPEN ACCESS

EDITED BY
Vijay Soni,
NewYork-Presbyterian, United States

REVIEWED BY
Chuan Wang,
University of South China, China
Biplab Singha,
University of Massachusetts Medical School, United States

*CORRESPONDENCE
Jian Peng
✉ jianpeng@gmc.edu.cn
Guo Guo
✉ guoguo@gmc.edu.cn
Fei Mo
✉ mofei0312@gmc.edu.cn

†These authors have contributed equally to this work

RECEIVED 02 March 2024
ACCEPTED 23 May 2024
PUBLISHED 14 June 2024

CITATION
Qiu Z, Yuan K, Cao H, Chen S, Chen F, Mo F, Guo G and Peng J (2024) Cross-talk of MLST and transcriptome unveiling antibiotic resistance mechanism of carbapenem resistance *Acinetobacter baumannii* clinical strains isolated in Guiyang, China. *Front. Microbiol.* 15:1394775. doi: 10.3389/fmicb.2024.1394775

Cross-talk of MLST and transcriptome unveiling antibiotic resistance mechanism of carbapenem resistance *Acinetobacter baumannii* clinical strains isolated in Guiyang, China

Zhilang Qiu[1,2,3†], Kexin Yuan[1,3†], Huijun Cao[1†], Sufang Chen[2,3], Feifei Chen[2], Fei Mo[1*], Guo Guo[3,4*] and Jian Peng[1,2,3,4*]

[1]Center for Clinical Laboratories, The Affiliated Hospital of Guizhou Medical University, Guiyang, China, [2]Key Laboratory of Infectious Immune and Antibody Engineering of Guizhou Province, Cellular Immunotherapy Engineering Research Center of Guizhou Province, School of Biology and Engineering/School of Basic Medical Sciences, Guizhou Medical University, Guiyang, China, [3]The Key and Characteristic Laboratory of Modern Pathogen Biology, Basic Medical College, Guizhou Medical University, Guiyang, China, [4]Translational Medicine Research Center, Guizhou Medical University, Guiyang, China

Introduction: *Acinetobacter baumannii* (*A. baumannii*) is an important opportunistic pathogen causing nosocomial infection in the clinic. The occurrence rate of antibiotic resistance is increasing year by year, resulting in a highly serious situation of bacterial resistance.

Methods: To better understand the local epidemiology of multidrug-resistant *A. baumannii*, an investigation was conducted on the antibiotic resistance of different types of *A. baumannii* and its relationship with the genes of *A. baumannii*. Furthermore, the molecular mechanism underlying antibiotic resistance in *A. baumannii* was investigated through transcriptome analysis.

Results: These results showed that a total of 9 STs were detected. It was found that 99% of the strains isolated in the hospital belonged to the same STs, and the clone complex CC208 was widely distributed in various departments and all kinds of samples. Furthermore, these *A. baumannii* strains showed high resistance to ertapenem, biapenem, meropenem, and imipenem, among which the resistance to ertapenem was the strongest. The detection rate of $bla_{OXA\text{-}51}$ gene in these carbapenem resistance *A. baumannii* (CRAB) reached 100%; Additionally, the transcriptome results showed that the resistance genes were up-regulated in resistance strains, and these genes involved in biofilm formation, efflux pumps, peptidoglycan biosynthesis, and chaperonin synthesis.

Discussion: These results suggest that the CC208 STs were the main clonal complex, and showed high carbapenem antibiotic resistance. All these resistant strains were distributed in various departments, but most of them were distributed in intensive care units (ICU). The $bla_{OXA\text{-}23}$ was the main antibiotic resistance genotype; In summary, the epidemic trend of clinical *A. baumannii* in Guiyang, China was analyzed from the molecular level, and the

resistance mechanism of *A. baumannii* to carbapenem antibiotics was analyzed with transcriptome, which provided a theoretical basis for better control of *A. baumannii*.

KEYWORDS

carbapenem resistance *A. baumannii*, MLST typing, antibiotic resistance, antibiotic resistance mechanism, transcriptome

1 Introduction

The Gram-negative bacterium *Acinetobacter baumannii* (*A. baumannii*) is known as one of the most important nosocomial pathogens in healthcare-associated infections, especially with ventilator-associated pneumonia and catheter-associated infections (Liu et al., 2022; Kang et al., 2023). Additionally, *A. baumannii* has been reported to be associated with high mortality in intensive care units (ICUs), particularly among critically ill patients (Inchai et al., 2015). In 2017, The World Health Organization (WHO) also recently listed ESKAPE pathogens in the list of 12 bacteria against which new antibiotics are urgently needed (Mulani et al., 2019; Wang et al., 2022). Overuse of antibiotics has prompted the emergence of carbapenem resistance *A. baumannii* (CRAB), in consequence, either horizontal gene transfer or other opportunities, such as altered targets, decreased membrane permeability (Chusri et al., 2014), increased production of degrading enzymes (Lee et al., 2017), overexpression of efflux pumps (Roy et al., 2021), metabolic changes, biofilm formation (Yan and Bassler, 2019; Colquhoun and Rather, 2020; Gedefie et al., 2021), or increased nutrient sequestration mechanisms (Tiwari et al., 2019).

Antimicrobial resistance is a prominent feature that helps *A. baumannii* survive in an antimicrobial stress environment, causing the microorganism to pose a threat to humans and complicating treatments (Han et al., 2022). Multidrug-resistant *A. baumannii*, extensively drug-resistant *A. baumannii*, and pan-drug-resistant *A. baumannii* nosocomial isolates are now commonly found in hospitals (Ramirez et al., 2020). Additionally, *A. baumannii* is also an emerging pathogen among the elderly and immunocompromised patients in nursing homes and community hospitals (Mody et al., 2015).

The rise of resistant *A. baumannii* strains prompted the design and execution of epidemiological investigations of *A. baumannii* epidemics using various molecular typing methods, including multi-locus enzyme electrophoresis (MLEE), pulsed-field gel electrophoresis (PFGE), and subsequently confirmed by multi-locus sequence typing (MLST) (Montanaro et al., 2016). Among these methods, the MLST has become the gold standard for epidemiological (Ravaioli et al., 2022). Furthermore, a prominent advantage of MLST is the derived nomenclature, and sequence type (ST), which has been rapidly and extensively adopted by the community, thus widening the global collective knowledge of the distribution, dissemination, and biological characteristics of crucial clonal populations (Gaiarsa et al., 2019).

A large number of studies have shown that genes play a vital role in the antibiotic resistance of any bacteria (Roy et al., 2022). It reported that a variety of OXA-type β-lactamase genes were found in CRAB strains (Abouelfetouh et al., 2022). Among these genes, the OXA-23 and OXA-51 were key determinants of carbapenem resistance (Chan et al., 2022). In addition, genes associated with efflux pumps also play an important role in carbapenem antibiotic resistance. It is reported that the Δ*aceI* mutant strain showed lower resistance to chlorhexidine than the parental strain. This result suggests that *aceI* plays a key role in antibiotic resistance (Liu et al., 2018). Besides, the gene *purF*, which regulates the biofilm formation, also plays a fatal role in antibiotic resistance (Dai et al., 2021). In addition, the Chaperonin GroEL/GroES also plays an important role in *Escherichia coli* antibiotic resistance (Goltermann et al., 2015). However, the mechanism of antibiotic resistance of *A. baumannii* needs to be further explored.

In the present study, the MLST, antibiotic resistance genes and transcriptome of *A. baumannii* were analyzed. This study found that a total of 9 ST sequence types were detected, and the CC208 was the main clonal complex in this hospital and showed high antibiotic resistance to carbapenems; The $bla_{OXA\text{-}23}$ gene was the main antibiotic resistance genotypes; The transcriptome result suggests that carbapenem antibiotic resistance of *A. baumannii* involved biofilm formation, efflux pumps, peptidoglycan biosynthesis, and chaperonin synthesis.

2 Materials and methods

2.1 Bacterial strains

The 199 strains CRAB were isolated from patients in various departments of Affiliated Hospital of Guizhou Medical University, Guizhou, China from 2017 to 2019. Standard *A. baumannii* ATCC19606, pan-resistant *A. baumannii* strains are preserved in the Key Laboratory of Modern Pathogenic Biology, School of Basic Medicine, Guizhou Medical University.

The genomic DNA of *A. baumannii* was extracted using the kit (BIOTEKE, Beijing, China). Seven housekeeping genes were amplified by PCR. The primers used are listed in **Table 1**. The PCR reactions were performed using PrimeSTAR® Max DNA Polymerase (Takara, Japan) with the following amplification parameters: 95°C for 5 min; 94°C for 30 s, 50°C for 30 s, and 72°C for 40 s, 30 cycles; 72°C for 10 min.

2.2 Multilocus sequence typing (MLST)

The amplified products of MLST typing of *A. baumannii* were sequenced, and the sequence results were compared on the MLST

10.3389/fmicb.2024.1394775

TABLE 1 Primers for PCR amplification of *A. baumannii* housekeeping genes.

Locus	Primer	Sequences	Amplicon size (bp)	Usage
gltA	CitratoF1	AATTTACAGTGGCACATTAGGTCCC	722	amp/seq
	CitratoR12	GCAGAGATACCAGCAGAGATACACG		amp/seq
gyrB	APRU F	TGTAAAACGACGGCCAGTGCNGGRTCYTTYTCYTGRCA	909	amp
	M13[-21]	TGTAAAACGACGGCCAGT		seq
	UP1E-R	CAGGAAACAGCTATGACCAYGSNGGNGGNAARTTYRA		amp
	M13-F	CAGGAAACAGCTATGACC		seq
gdhB	GDHB1F	GCTACTTTTATGCAACAGAGCC	775	amp
	GDHSECF	ACCACATGCTTTGTTATG		seq
	GDHB775R	GTTGAGTTGGCGTATGTTGTGC		amp
	GDHSECR	GTTGGCGTATGTTGTGC		seq
recA	RA1	CCTGAATCTTCYGGTAAAAC	425	amp/seq
	RA2	GTTTCTGGGCTGCCAAACATTAC		amp/seq
cpn60	CPN-3F2	ACTGTACTTGCTCAAGC	479	amp/seq
	CPN-R2	TTCAGCGATGATAAGAAGTGG		amp/seq
gpi	gpi_F	AATACCGTGGTGCTACGGG	508	amp/seq
	gpi_R	AACTTGATTTTCAGGAGC		amp/seq
rpoD	70F-RPOD	ACGACTGACCCGGTACGCATGTAYATGMGNGARATCGCNACNCT	492	amp
	70FS	ACGACTGACCCGGTACGCATGTA		seq
	70R RPOD	ATAGAAATAACCAGACGTAAGTTNGCYTCNACCATYTGYTTYTT		amp
	70RS	ATAGAAATAACCAGACGTAAGTT		seq

comparison website of *A. baumannii*. The sequencing results were submitted to the website for comparison to obtain allele number and ST type. The Bio Numerics 7.1 software is used for typing data processing, and generating minimum spanning tree (MST).

2.3 Detection of antibiotic susceptibility and resistance genes

The minimal inhibitory concentration (MIC) values of *A. baumannii* isolated from clinical isolates were measured by the micro-dilution broth method. The antibiotics determined were imipenem, meropenem, ertapenem, and biapenem. There were three repeats for each strain and antibiotic. Except for 5 gradients of biapenem, 6 gradients were done. The concentration of the mother liquid before dilution is shown in Table 2. The results were judged by the Institute of Clinical and Laboratory Standards (CLSI2012).

TABLE 2 The preparation of antibiotics.

Antibiotic	Solvent/diluent	Concentration of mother liquor before dilution (μg/mL)
Imipenem	1 × Phosphate buffer pH 7.2	2,048
Ertapenem	1 × Phosphate buffer pH 7.2	4,096
Meropenem	ddH_2O	2,048
Biapenem	ddH_2O	512

In this study, the $bla_{OA\text{-}23}$ and $bla_{OXA\text{-}51}$ were selected as molecular markers for rapid identification of *A. baumannii*. The primers are listed in Table 3, and the PCR reaction system is 15 μL, including the premixTaq enzyme 7.5 μL, the primers 1 μL with 10 μM, DNA template 1 μL, and the ddH2O 4.5 μL. Meanwhile, the PCRs were performed at 94°C for 5 min, followed by 35 cycles of 30 s at 94°C, 30 s at 55°C, 30 s at 72°C, and a final extension of 10 min at 72°C. The 5 μL PCR products were sampled in 1% agarose gel and 30 min was electrophoretic at a constant voltage of 100V. The photos were taken by WD-9413B gel imaging analyzer.

2.4 RNA isolation, library construction and sequencing

The AB77 (weak imipenem resistance) and AB98 (strong imipenem resistance) were selected for transcriptome sequencing with three biological repeats per sample. After resuscitation of CRAB77 and CRAB98, respectively, 1 mL solution was absorbed and cultured in 100 mL LB liquid medium. After overnight incubation at 37°C 220 rpm until logarithmic growth, the organisms were collected by centrifugation, and three biological replicates were performed in each group, totaling six samples. The collected bacterial precipitates were immediately liquid nitrogen snap-frozen and stored in the refrigerator at −80°C. The total RNA of these samples was extracted using Trizol reagent (Sigma-Aldrich, United States) according to the specification described method. The RNA concentration and quality were measured using a Nanodrop 2000 micro-spectrophotometer (Thermo Fisher Scientific, Waltham, MA, USA), and agarose

gel electrophoresis. RNA-seq library construction and RNA sequencing were performed by the Meiji Biomedical Technology Co., Ltd. (Shanghai, China).

2.5 Identification of differentially expressed genes and annotation

The raw data was filtered to remove contaminated and low-quality sequences from connectors and to obtain clean reads. Bowtie2-2.5.0 was used to map the genome of the filtered sequence (Langmead and Salzberg, 2012). The reference genome of *A. baumannii* (ATCC 19606) was downloaded from GenBank (NZ_CP045110.1). The gene expression levels were calculated based on TPM (transcript per million) (Zhao et al., 2021). Differential expression analysis between CRAB77 and CRAB98 was performed using the DEGSeq2 R package. The significance of the DEGs was determined with a P-value < 0.05 found by DEseq2. Transcripts with log 2 (Fold Change) > 1 and P-value < 0.05 were considered significant differential expressions. KOBAS software was used to test the statistical enrichment of differentially expressed genes in KEGG pathways. Significantly enriched KEGG pathways was identified by a P-value < 0.05.

2.6 qRT-PCR

qRT-PCR was performed to confirm the DEGs identified using RNA-seq. The primer sequences of candidate genes and a housekeeping gene (16S rRNA) were designed using Primer Premier 5 (Table 4). The first strand of cDNA was synthesized by PrimeScript TMRT reagent Kit with gDNA Eraser (TaKaRa, Beijing, China) according to the manufacturer's instructions. The qRT-PCR was carried out with a PikoReal 96 real-time PCR system (Thermofisher Scientific) using PowerUp^{TM} SYBR^{TM} Green Master Mix (Thermo Fisher Scientific, Waltham, MA, USA). The sense and anti-sense primers were designed by Primer Premier 5 and they were synthesized by Sangon Biotech Co., Ltd. (Shanghai, China). Sequences of the primers used in this study were shown in detail in Table 4. The reactions were performed with three biological and technical replicates per sample. The data were analyzed using the $2^{-\Delta Ct}$ method (Schmittgen and Livak, 2008).

2.7 Statistical analysis

Statistical analysis was performed using SPSS21.0. All experiments were performed in triplicate. Statistical differences between groups were assessed by the two-tailed Student's t-test and one-way analysis of variance (ANOVA) followed by Tukey's multiple-comparison test or by the nonparametric Mann–Whitney U test and Kruskal-Wallis test, followed by Duncan's multiple-comparison test. A P-value < 0.05 was considered statistically significant.

3 Results

3.1 Molecular typing of the strains

The sequences of these 7 housekeeping genes in 199 *A. baumannii* strains were submitted to the MLST database

TABLE 3 Primers information for amplifying carbapenemase genes in *A. baumannii* strains.

Target gene	Primer	Primer sequence (5′ → 3′)	Product Size/bp	Temperature/°C
blaOXA-23	OXA-23-F	GATCGGATTGGAGAACCAGA	501	55
	OXA-23-R	ATTTCTGACCGCATTTCCAT		
blaOXA-51	OXA-51-F	ATGAACATTAAAGCACTCTTACTT	825	55
	OXA-51-R	CTATAAAATACCTAATTGTTCTAA		

TABLE 4 The Primers information for qRT-PCR.

Target gene	Primer name	Primer sequence (5′ → 3′)	Product Size/bp	Tm/°C
mltG	mltG-F	CCACCATTACCAGTCGCTACAAAA	180 bp	60
	mltG-R	TGCAAACTATAAGGGGAACATTACTCG		
dnaK	dnaK-F	ATTTTTAGGGTTTGTTACTGCCTGA	162 bp	60
	dnaK-R	GGTACTACCAACTCATGTGTTGCTGT		
groL	GroL-F	CAGCTGGTTTGTCTTCAGGAATGTC	151	60
	GroL-R	GCAACTGGCGAATATGGTGATATGT		
FQU82_RS13360	3360-F	GTTGGATAAGGAACAACACTCACACC	175	60
	3360-R	GTAGCAAAATCTACAACACGCCAAC		
aceI	AceI-F	AGTGAAGTGATGCTGCTTTAGCATT	194	60
	AceI-R	TGGTTTTGAGGGTGGTTTGC		
16S rRNA	16S rRNA-F	TACACACCGCCCGTCACACC	119	60
	16S rRNA-R	CGGCTACCTTGTTACGACTTCACC		

10.3389/fmicb.2024.1394775

TABLE 5 Alleles and sequence types in CRAB isolates.

ST	gltA	gyrB	gdhB	recA	cpn60	gpi	rpoD	Percent (%)
136	1	3	3	2	2	16	3	19.6
191	1	3	3	2	2	94	3	18.6
195	1	3	3	2	2	96	3	15.1
208	1	3	3	2	2	97	3	18.6
2,206	1	63	67	60	29	153	5	0.5
368	1	3	3	2	2	140	3	6
369	1	3	3	2	2	106	3	14.6
457	1	15	3	2	2	153	3	0.5
540	1	3	3	2	2	160	3	6.5

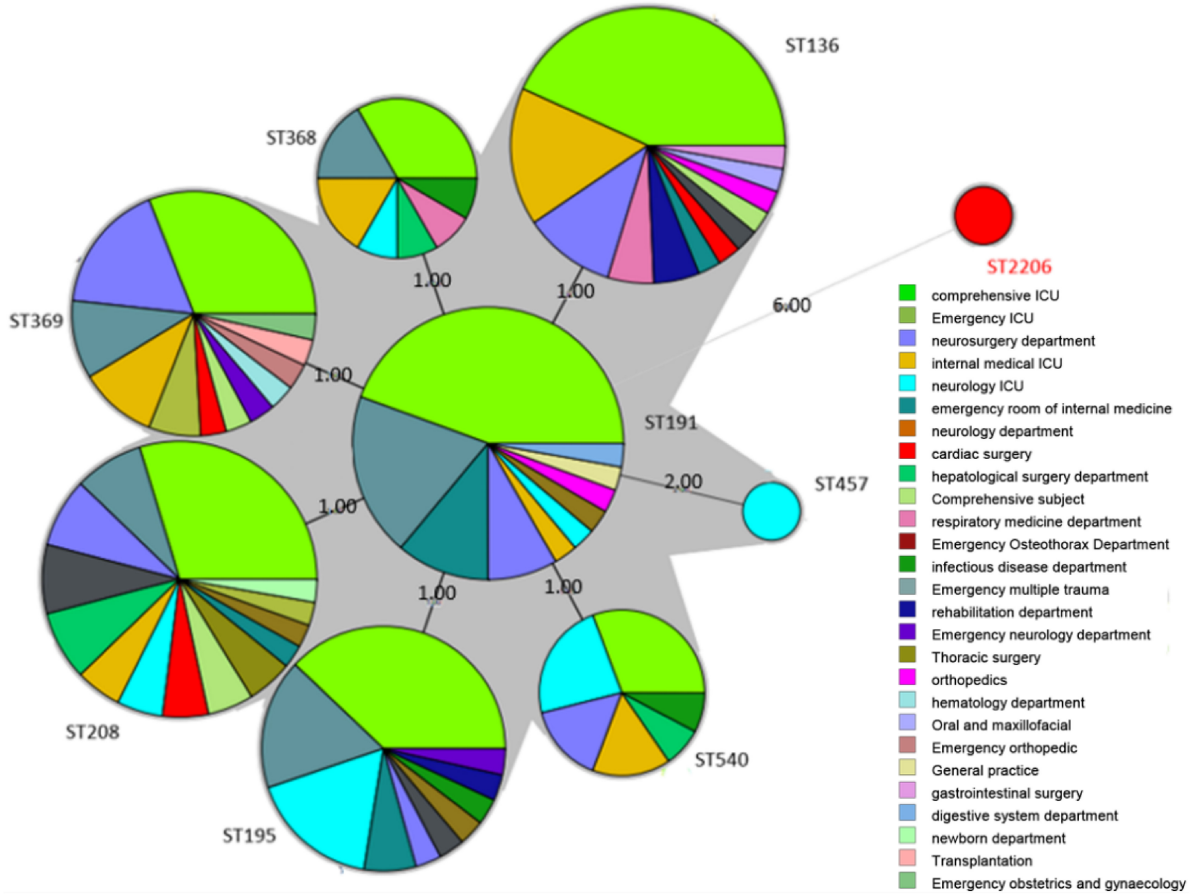

FIGURE 1
Minimum spanning tree (MST) of 199 *A. baumannii* strains. The size of the circle in MST represents the number of the same ST genotypes, and the black solid line indicates that there are 3 or fewer differences in housekeeping genes between the two ST genotypes. The thicker the black solid line, the smaller the difference in housekeeping genes between the two ST genotypes. The dotted line indicates that there are 4 or more differences in housekeeping genes between the two ST genotypes. The denser the dotted line, the greater the difference in housekeeping genes between ST genotypes.

of the Pasteur Institute[1] to investigate whether there were base substitutions or deletions. The sequences obtained from housekeeping gene sequencing of each strain were submitted to the database, and the corresponding alleles of each sequence were queried, to obtain the ST model of each strain. The results showed that there were 9 different sequence types (Table 5), among which ST136, ST191, and ST208 had high frequency in the hospital.

The minimum spanning tree showed that the ST types of the 199 strains are relatively concentrated, and all of them originated from ST191 (Figure 1). In addition, there is only *gpi* difference between ST136/ST195/ST368/ST369/ST208/ST540 and

1 https://pubmlst.org/abaumannii/

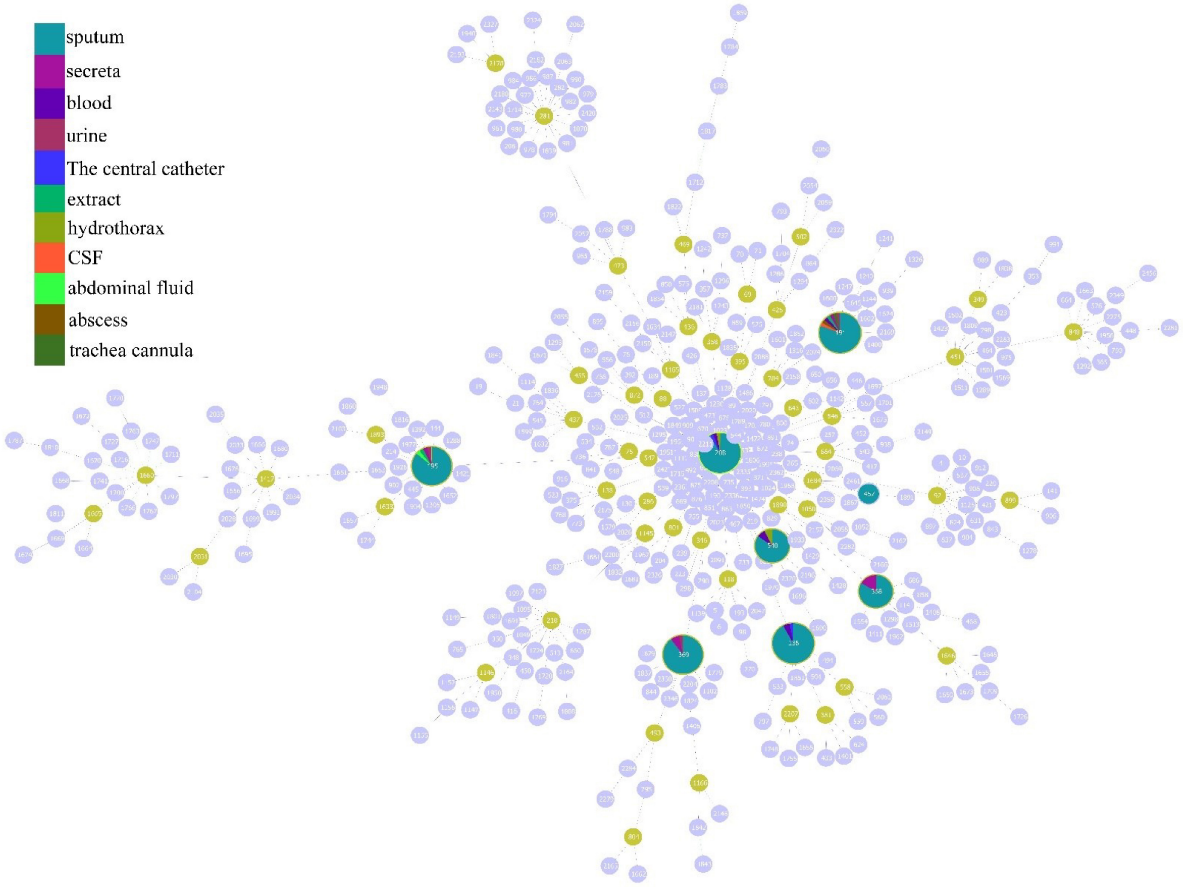

FIGURE 2
Minimum spanning tree analysis of CRAB isolates based on multilocus sequence typing (MLST) data. Each circle represents an independent sequence type (ST). The size of each circle corresponds to a different number of isolates, with larger sizes representing higher isolate quantity. The lines connecting the circles indicate the relationship between different STs. Different types of lines represent a difference in one allele (solid lines), two alleles (dashed lines), and three or more alleles (dotted lines).

ST191. While there are two alleles difference between ST457 and ST191, the genetic relationship is close. It is reported that the mutation rate and recombination rate of *gpi* in the MLST typing scheme of *A. baumannii* are higher than those of other housekeeping genes, and it is easy to mutate in the process of evolution. It is found that a similar situation in the study of *A. baumannii* typing, suggests that *A. baumannii* MLST scheme has a better resolution on the housekeeping gene *gpi*. Among the 199 strains of CRAB, there is only one ST, which is widely distributed in various departments. Among these departments, the ICU region is the most distributed. However, the ST2206 does not belong to these ST, and there are six allele differences between ST2206 and ST191, and the ST2206 is isolated in the comprehensive ICU region.

To understand the classification position of these identified strains in the entire *A. baumannii* database, the ST of all strains were placed in the *A. baumannii* ST database. The results showed that the ST136 / ST195 / ST368 / ST369 / ST208 / ST540 / ST191 belongs to CC208, and the ST2206 distant relatives (Figure 2).

According to the analysis of the source distribution of 199 CRAB strains, the results showed that most of these clinical strains came from sputum, and a total of 171 strains of each ST type were detected in these sputum samples, while the distribution was less in other samples (Figure 3A). Based on the analysis of sputum samples in various departments, these CRAB were found in all clinical sputum samples in many departments, while there were few types of CRAB samples in the remaining departments (Figure 3B). This result implies that the ST is widely prevalent in all departments in the hospital, and it is necessary to focus on detecting the presence of CRAB in sputum samples to timely control the spread of CRAB.

3.2 Antimicrobial susceptibility testing

The result of MIC values for the 199 *A. baumannii* strains showed that the MIC values for biapenem were concentrated at 128 μg/mL, accounting for 44.5%; the MIC value of meropenem was concentrated at 128 μg/mL, accounting for 39%; the MIC value for ertapenem was concentrated at 512 μg/mL, accounting for 39.5%; as well as the MIC values for imipenem were concentrated at 64 μg/mL, accounting for 51% (Figure 4 and Supplementary Table 1). These results indicate that all experimental strains were highly resistant to the four carbapenems antibiotics, among

10.3389/fmicb.2024.1394775

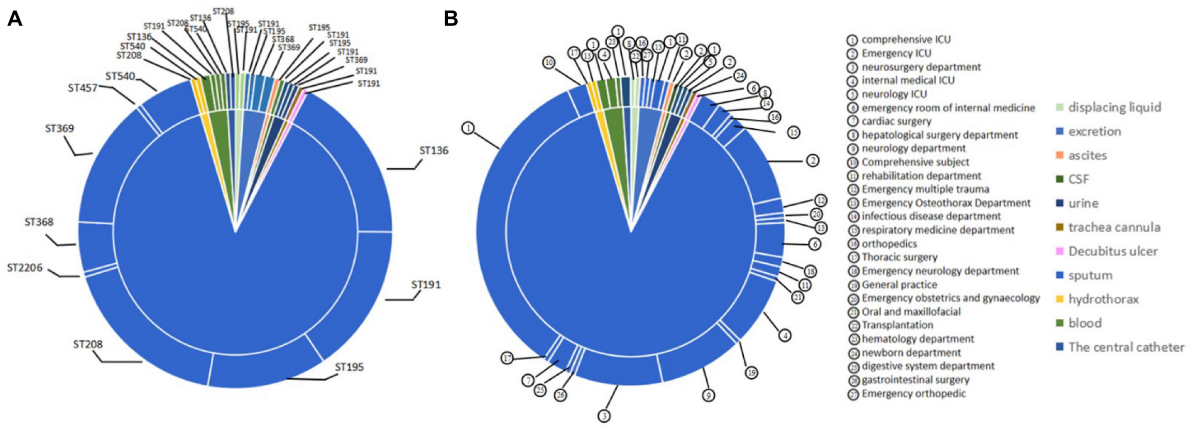

FIGURE 3
Molecular epidemiological characteristics of strains from different tissue and clinical departments. **(A)** The source of different typing strains. **(B)** The distribution of CRAB strains in sputum in each department.

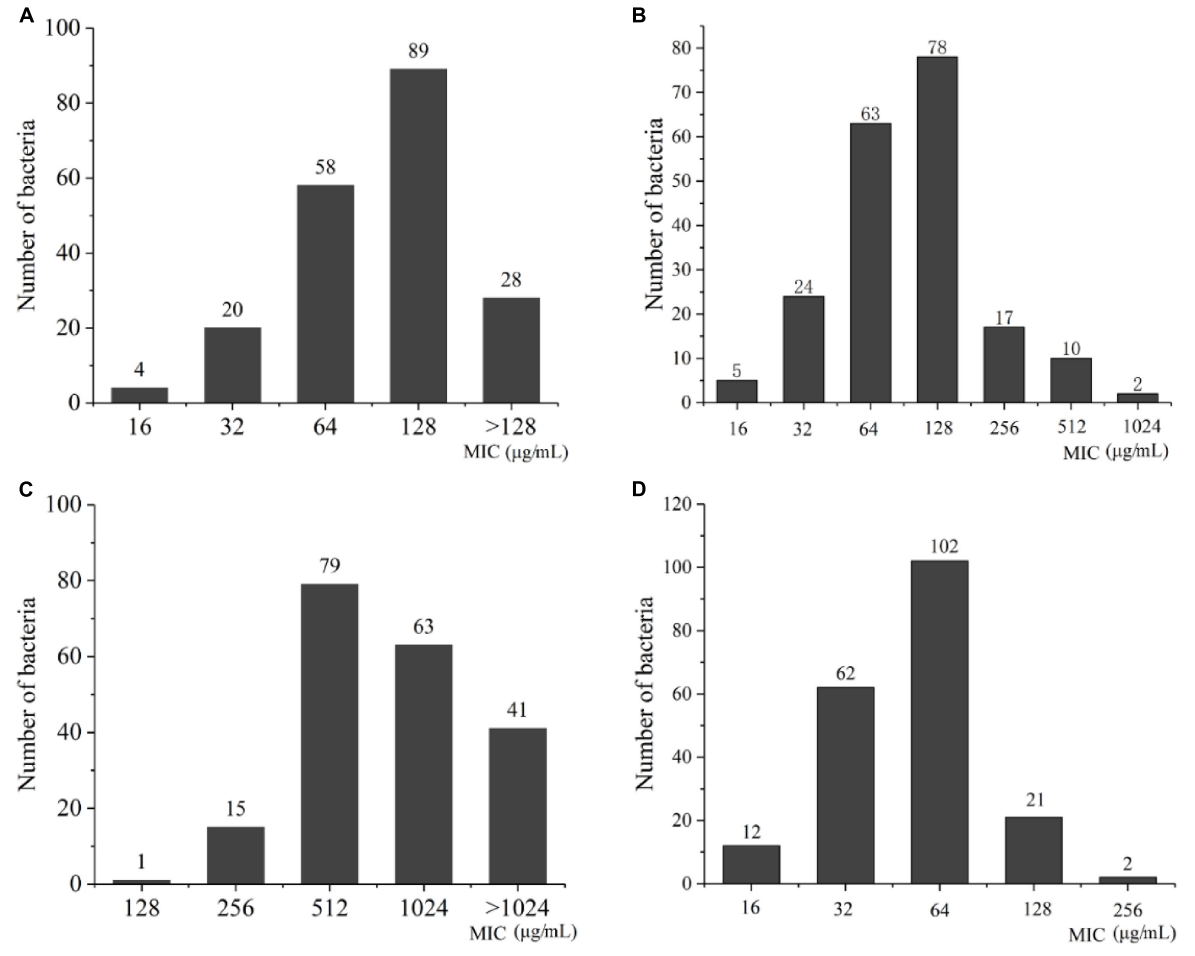

FIGURE 4
The distribution of MIC value in *A. baumannii*. **(A)** Biapenem; **(B)** meropenem; **(C)** ertapenem; **(D)** imipenem.

which the experimental strains had the strongest resistance to ertapenem.

According to the ST type classification of 199 CRAB strains, MIC values of these 199 CRAB strains against ertapenem were calculated. The results showed that ST136, ST191, ST195, and ST208 were more resistant to ertapenem than ST368, ST369, ST457, and ST540. However, the ST2206, which is distantly related to STs strain, also had a MIC value of 1,024 μg/mL.

10.3389/fmicb.2024.1394775

TABLE 6 Resistance of ST types to ertapenem in 199 CRAB strains.

ST	Ertapenem MIC (μg/mL)					
	<32	128	256	512	1,024	>1,024
ST136	0	0	2	9	14	14
ST191	0	0	0	14	13	10
ST195	0	0	3	9	13	5
ST208	0	1	1	19	10	6
ST2206	0	0	0	0	1	0
ST368	0	0	4	4	4	0
ST369	0	0	4	15	4	6
ST457	0	0	0	0	1	0
ST540	0	0	1	9	3	0

TABLE 7 Resistance of ST types to biapenem in 199 CRAB strains.

ST	Biapenem MIC (μg/mL)				
	16	32	64	128	>128
ST136	1	3	8	17	10
ST191	0	1	10	24	2
ST195	0	3	9	12	6
ST208	2	2	15	14	4
ST2206	0	1	0	0	0
ST368	1	3	2	5	1
ST369	0	4	9	11	5
ST457	0	0	0	1	0
ST540	0	3	5	5	0

TABLE 8 Resistance of ST types to meropenem in 199 CRAB strains.

ST	Meropenem MIC (μg/mL)						
	16	32	64	128	256	512	>512
ST136	0	5	4	24	3	2	1
ST191	0	2	6	21	8	0	0
ST195	0	4	8	13	3	1	1
ST208	1	7	18	9	1	1	0
ST2206	0	0	1	0	0	0	0
ST368	3	3	2	4	0	0	0
ST369	0	3	16	5	2	3	0
ST457	0	0	0	1	0	0	0
ST540	1	0	8	1	0	3	0

TABLE 9 Resistance of ST types to imipenem in 199 CRAB strains.

ST	Imipenem MIC (μg/mL)					
	<16	16	32	64	128	256
ST136	0	0	7	25	6	1
ST191	0	0	4	21	11	1
ST195	1	1	11	17	0	0
ST208	5	0	14	17	1	0
ST2206	0	0	1	0	0	0
ST368	3	0	4	5	0	0
ST369	0	0	12	14	3	0
ST457	0	0	0	1	0	0
ST540	2	0	9	2	0	0

This result indicates that ST2206 with strong antibiotic resistance (Table 6).

In addition, according to the antibiotic resistance detection of these 199 strains to biapenem, the results showed that the MIC values of ST types concentrated at 128 μg/mL. The result showed that these ST types have the same resistance to biapenem. However, the ST2206 showed lower resistance to biapenem than other ST types (Table 7).

According to the detection of the resistance for these 199 CRAB strains to meropenem, it was found that the MIC values of STs to meropenem in these 199 CRAB strains were higher, while the ST2206 showed low resistance to meropenem (Table 8).

Based on the detection of the resistance STs to imipenem in 199 CRAB strains, the results showed that MIC values were concentrated in 32 μg/mL-128 μg/mL, indicating strong resistance. Moreover, the ST2206 also showed resistance to imipenem, but the resistance was low, with a MIC value of 32 μg/mL (Table 9). According to this data, it was be defined weakly resistant strain with MIC values $\leq$ 32 to imipenem, while strains with MIC value $>$ 32 was defined as strongly resistant strain. By this definition, ST136 and ST208, have quite different resistance to imipenem; In this study, weakly resistant strains accounted for 18% in ST136, and 47.22% were weakly resistant strains in ST208. This result indicates that different STs may have different resistance mechanisms to imipenem.

3.3 Antimicrobial resistance genes testing

To understand the distribution of antibiotic resistance genes, the $bla_{OXA\text{-}23}$, *and* $bla_{OXA\text{-}51}$ were detected in 199 CRAB, standard *A. baumannii* (ATCC19606), pan-resistant *A. baumannii* (PRAB) and SJZ24 by using PCR amplification. The results showed that the target sequence of $bla_{OXA\text{-}23}$ (Figure 5A) and $bla_{OXA\text{-}51}$ (Figure 5B) genes were found in these strains. The BLAST analysis was conducted after sequencing these target bands, and it was found that these target bands were all target antibiotic resistance genes. Statistical data showed that the detection rate of the $bla_{OXA\text{-}23}$ gene and $bla_{OXA\text{-}51}$ gene in CRAB was 92.5 and 100%, respectively (Figure 5C). These results suggest that the class D carbapenemases genes are widely distributed in these 199 CRAB strains, which may be one of the reasons for its high antibiotic resistance to carbapenems antibiotics.

10.3389/fmicb.2024.1394775

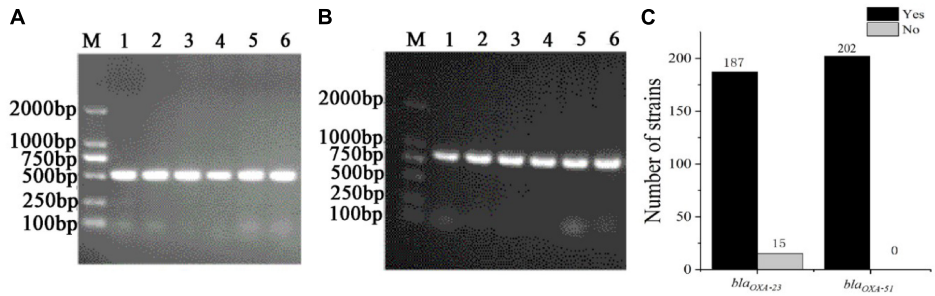

FIGURE 5
The PCR amplification of CRAB (part of the sample) resistance genes and the statistics of positive tests of antibiotic resistance genes. **(A)** *bla*$_{OXA\text{-}23}$; **(B)** *bla*$_{OXA\text{-}51}$; **(C)** Statistics of positive tests of antibiotic resistance genes; M, DNA maker; Yes, the number of positive strains; no, the number of negative strains.

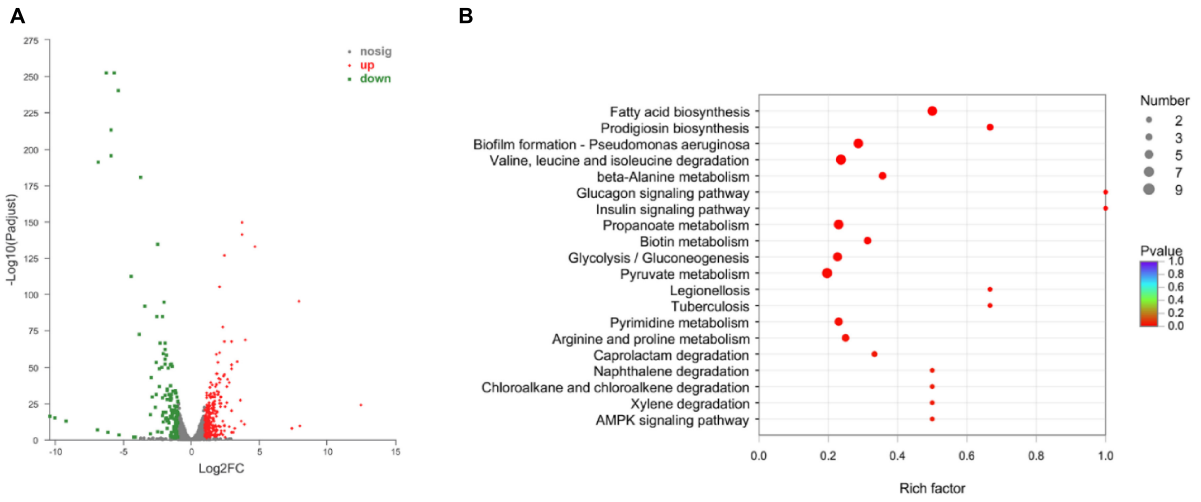

FIGURE 6
The Volcano diagram of differentially expressed genes between resistance strain and sensitive strain **(A)** and DEGs involved in KEGG pathway enrichment analysis in comparison with resistance strain and sensitive strain **(B)**. In **(A)**, The *x*-axis represents the multiple differential expressions; the *y*-axis represents significance. In **(B)**, The *x*-axis represents the Rich factor, GeneRatio = Term Candidate Gene Number/Term Gene Number. The *y*-axis represents KEGG Pathway. The size of the bubble is proportional to the number of genes in the KEGG Pathway. And the color represents the *P*-value of enrichment. The deeper the color, the smaller the *P*-value.

3.4 Transcriptome profiling and identifying differentially expressed genes (DEGs)

To understand the resistance mechanisms of different STs to imipenem, the transcriptome sequencing analysis between ST208 (AB77) and ST136 (AB98) was performed in this study. The results showed that a sum of 159.60 million reads was generated and each sample provided an average production of 26.60 million. A mean of 26.60 million clean reads was obtained from each library with an adequate read ratio of 94.63% after removing adaptor sequences, N-containing reads, and low-quality. A mean of 20.44 million CDS-mapped reads was obtained from each library with an adequate read ratio of 80.11% (Supplementary Table 2). A total of 3,829 genes were mapped from all the samples. The resistance strain and sensitive strain gene expression levels were analyzed, and 390 differentially expressed genes (DEGs) were recognized (Supplementary Table 3). Among such DEGs, the resistance strain had 256 DEGs up-regulated and 134 DEGs down-regulated (Figure 6A). It is worth pointing out that some genes related to antibiotic resistance, efflux pump, and biofilm formation were up-regulated in the resistance strain (Figure 6B). The increased expression level of these genes may increase the antibiotic resistance of *A. baumannii*.

3.5 Resistance genes regulated antibiotic resistance

Among these DEGs, 19 genes may be involved the carbapenem resistance, including biofilm formation, efflux pump, peptidoglycan biosynthesis, chaperonin synthesis, and drug transporter. In the biofilm formation process, there were pilus assembly protein (*Pap*, *FQU82_RS03605*), urease accessory protein (*UreD*, *FQU82_RS05390*), OmpA family protein (*FQU82_RS07900*), NADP-specific glutamate dehydrogenase

10.3389/fmicb.2024.1394775

TABLE 10 *A. baumannii* genes involved in antibiotic resistance identified by mRNA-seq.

Gene id	Gene name	Gene function	Log2FC	q value
FQU82_RS03605	*FQU82_RS03605*	Pilus assembly protein	1.121204	0.0441
FQU82_RS05390	*FQU82_RS05390*	Urease accessory protein UreD	1.87116	0.0000
FQU82_RS05470	*gdhA*	NADP-specific glutamate dehydrogenase	1.067204	0.0000
FQU82_RS07900	*FQU82_RS07900*	OmpA family protein	−2.33007	0.0000
FQU82_RS02520	*ptsP*	Phosphoenolpyruvate–protein phosphotransferase	−1.01688	0.0000
FQU82_RS13115	*purF*	amidophosphoribosyltransferase	1.175621	0.0000
FQU82_RS14285	*dacC*	D-alanyl-D-alanine carboxypeptidase PBP5/6	1.375552	0.0000
FQU82_RS14770	*mltG*	Endocytic transglycosylase MltG	1.084947	0.0000
FQU82_RS00890	*galE*	UDP-glucose 4-epimerase GalE	−1.13269	0.0000
FQU82_RS00325	*dnaK*	Molecular chaperone DnaK	1.044462	0.0000
FQU82_RS15275	*groL*	Chaperonin GroEL	1.287527	0.0000
FQU82_RS15280	*FQU82_RS15280*	Co-chaperone GroES	3.371287	0.0000
FQU82_RS03755	*FQU82_RS03755*	MFS transporter	1.581374	0.0000
FQU82_RS13360	*FQU82_RS13360*	ABC transporter substrate-binding protein	1.286576	0.0000
FQU82_RS08650	*FQU82_RS08650*	LysR family transcriptional regulator	−1.09716	0.0000
FQU82_RS09170	*FQU82_RS09170*	PACE efflux transporter	1.446246	0.0000
FQU82_RS12055	*aceI*	Chlorhexidine efflux PACE transporter AceI	1.787986	0.0000
FQU82_RS03105	*FQU82_RS03105*	MacB family efflux pump subunit	−2.07775	0.0000
FQU82_RS03110	*FQU82_RS03110*	MacA family efflux pump subunit	−2.5575	0.0000

(*gdhA*), phosphoenolpyruvate–protein phosphotransferase (*pstP*), and amido phosphoribosyl transferase (*purF*, *FQU82_RS13115*). In addition, there were 5 genes involved in efflux pump, including LysR family transcriptional regulator (*FQU82_RS08650*), PACE efflux transporter (*FQU82_RS09170*), chlorhexidine efflux PACE transporter (*aceI*, *FQU82_RS12055*), MacB family efflux pump subunit (*FQU82_RS03105*), MacA family efflux pump subunit (*FQU82_RS03110*). Meanwhile, there were 3 genes may contribute to peptidoglycan biosynthesis, including D-alanyl-D-alanine carboxypeptidase PBP5/6 (*dacC*, *FQU82_RS14285*), endocytic transglycosylase (MltG, *FQU82_RS14770*), and UDP-glucose 4-epimerase (*GalE*, *FQU82_RS00890*). Additionally, there were 3 chaperonins, including *DnaK*, *GroEL*, and *GroES* may be involved in antibiotic resistance. It is worth mentioning that the MFS transporter and ABC transporter substrate-binding protein may participate in drug transport (**Table 10**).

3.6 Verification of differential expression gene by quantitative real-time PCR

To confirm findings of gene expression obtained from transcriptome data, 6 DEGs concerned with antibiotic resistance were chosen for qRT-PCR. These DEGs are mainly involved in biofilm formation, efflux pump, peptidoglycan biosynthesis, and chaperonin synthesis. As shown in, the 6 DEGs had a very similar expression pattern based on the transcriptome data and qRT-PCR, which indicates the trustworthiness of the transcriptomic analysis (**Figure 7**).

4 Discussion

A. baumannii is mainly related to nosocomial infections globally and is an oxybiotic Gram-negative pathogen that results in infections of the skin, urinary tract, bloodstream, and other soft tissues (Lee et al., 2017). In recent years, *A. baumannii* have become a significant cause of critical healthcare-associated diseases and infections (Lima et al., 2019). Among these β-lactam antibiotics, the carbapenems are considered the most effective class with the most extensive spectrum of antimicrobial activity (O'Donnell et al., 2021). Hence, carbapenem antibiotics are also often used in the treatment of *A. baumannii* infection (Nguyen and Joshi, 2021). However, with the use of carbapenem antibiotics, some carbapenem-resistant bacteria, including *A. baumannii*, *Pseudomonas aeruginosa*, and *Stenotrophomonas maltophilia* were appeared (Nordmann and Poirel, 2019). It is reported that *A. baumannii* infections occur in critically ill patients in the ICU setting and account for up to 20% of infections in ICUs worldwide (Lee et al., 2017). To better understand the carbapenem resistance *A. baumannii* to be able to develop a good treatment plan. In this study, 199 CRAB strains were used as materials to study their typing. Among the 199 CRAB strains, two strains were used to explore the mechanism of antibiotic resistance.

According to the MLST analysis of the 199 CRAB strains, it was found that the ST136 and ST208 were the most STs of CRAB, which have strong resistance to the four kinds of carbapenem antibiotics. As in previous studies, the ST136 and ST208 belong to CC92, which is the most widely and largest disseminated complex worldwide (Alcantar-Curiel et al., 2019; Lima et al., 2019). Additionally, ST208 has become the main sequence type of

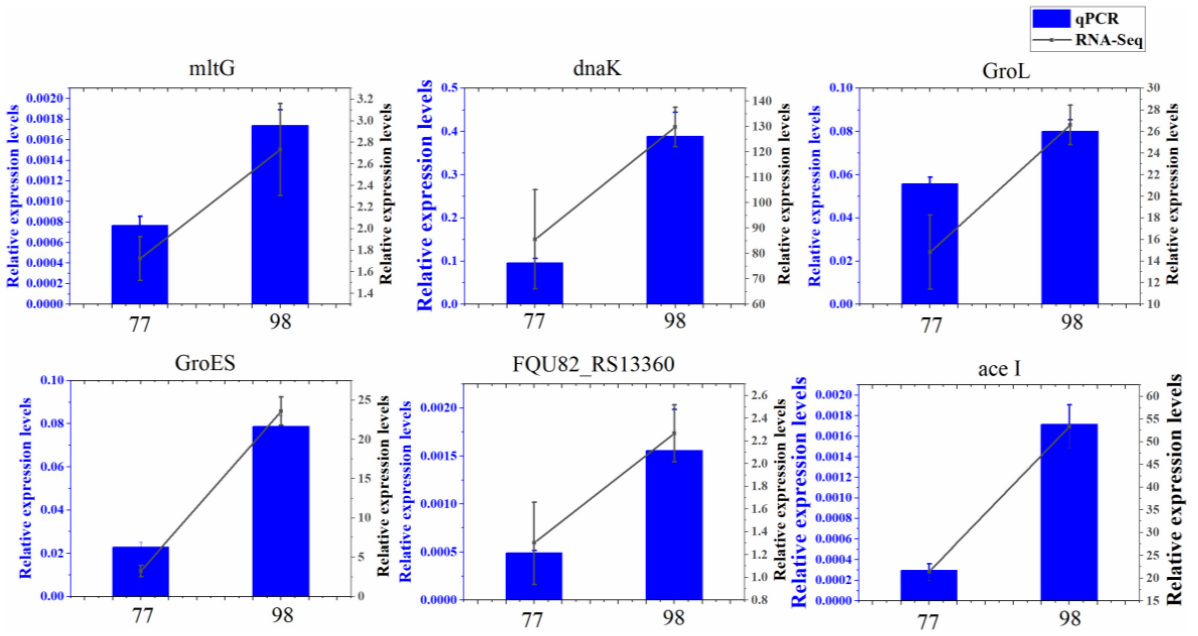

FIGURE 7
Relative expression levels of 6 DEGs in 77 and 98. *MltG*, endolytic transglycosylase MltG; *dnaK*, molecular chaperone DnaK; *GroL*, chaperonin GroEL; *GroES*, co-chaperone GroES; *FQU82_RS13360*, ABC transporter substrate-binding protein; *ace I*, chlorhexidine efflux PACE transporter AceI.

A. baumannii infection outbreak in western China (Qu et al., 2016; Gao et al., 2022). Furthermore, along with the global phenomenon, CC92 has become the dominant circulating strain in children (Kang et al., 2023). In addition, the present study showed that the ST195, ST191, and ST369 were divided into the same group, while the time of emergence of these two STs was different. It is worth noting that the virulence of ST369 is higher than that of ST191 (Jiang et al., 2021). Moreover, the resistance of ST191 to carbapenem is also very serious (**Tables 6–9**). Therefore, it is extremely important to control the spread of ST136, ST191, ST208, ST195, ST369.

Imipenem is a carbapenem antibiotic commonly used in clinical treatment and plays an important role in preventing *A. baumannii* infection (Khaled et al., 2021). A large number of studies have shown that *A. baumannii* ST136 is highly resistant to imipenem (Firoozeh et al., 2023; You et al., 2023). In the present study, ST136 also showed strong resistance to imipenem, while ST208 showed weak resistance to imipenem (**Table 9**). This phenomenon may be caused by differences in gene expression at different STs. Transcriptome results showed that these two STs *A. baumannii* were significantly differentially expressed in biofilm formation, efflux pump, peptidoglycan biosynthesis, and chaperone biosynthesis. These results suggest that the resistance ability of ST136 to imipenem is caused by the differential gene expression of these pathways.

As we all know, bacterial resistance to antibiotics involves many factors, such as the formation of biofilm, which can increase antibiotic resistance thousands of times (Guo et al., 2022). Additionally, the efflux pump, the chaperonins, and peptidoglycan biosynthesis also play important roles in antibiotic resistance (Grishin et al., 2020; Stevens et al., 2020; Barnabas et al., 2022). During the biofilm formation, the pilus assembly protein plays an important role in the formation of fimbriae (Sanchez et al., 2017; Shanmugasundarasamy et al., 2022). In this study, the pilus assembly protein was up-regulated in the antibiotic resistance strains (**Table 6**). In addition, the *ureD* (Maisuria et al., 2015), *ptsP* (Abisado et al., 2021), and *purF* (Li et al., 2021) also contribute to biofilm formation, which may play an important in the process of antibiotic resistance. In the meanwhile, a *ureD*, and *ptsP* were also up-regulated in this study (**Table 10**). These results suggest that biofilm formation plays an important role in carbapenem antibiotic resistance.

To date, different categories of efflux pumps have been identified in *A. baumannii*, including RND-family (resistance-nodulation-division), MFS (major facilitator superfamily), MATE (multidrug and toxic compound extrusion), SMR (small multi antibiotic resistance), PACE family and ABC (ATP-binding cassette) superfamilies are the main components of the efflux pump (Blair et al., 2014; Li et al., 2015; Hassan et al., 2018).

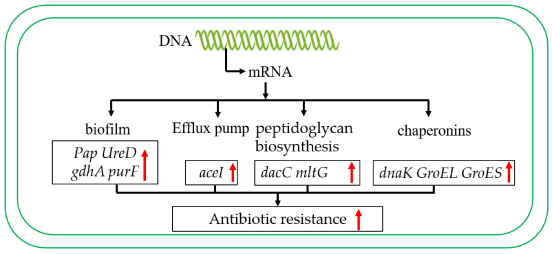

FIGURE 8
Carbapenem-resistant *A. baumannii* antibiotic resistance regulation model. The red arrow indicates that the expression level was up-regulated.

These efflux pumps play a key role in antibiotic resistance (Roy et al., 2022). In this study, the MFS transporter, and PACE efflux transporter were up-regulated (**Table 10**), which may improve the ability of carbapenem antibiotic resistance. Most importantly, LysR, a transcriptional regulator, also indirectly regulates the efflux pump (Fu et al., 2020; Lu et al., 2021), which is also significantly up-regulated in this study.

Besides, the peptidoglycan also contributes to antibiotic resistance (Kvesić et al., 2022). It is reported that the deposition of *Pseudomonas aeruginosa* with the interference of peptidoglycan circulation in the lungs of mice was significantly reduced, and the mortality caused by systemic infection was significantly reduced (Torrens et al., 2019). Moreover, the peptidoglycan synthesis related gene *dacC* was more frequently found in populations with lower relative fitness across the measured growth parameters (Barbosa et al., 2017). In the meanwhile, the *dacC* in the antibiotic resistance strain was upregulated (**Table 10**), indicating that *dacC* may also be involved in antibiotic resistance.

As in previous studies, chaperone proteins also play an important role in antibiotic resistance (Chiang et al., 2022). For instance, in *Escherichia coli*, the Chaperonin *GroEL/GroES* over-expression can promote aminoglycoside resistance and reduce drug susceptibilities (Goltermann et al., 2015). Moreover, the *GroEL* can increase the antibiotic resistance of *Klebsiella pneumoniae* by promoting the refolding of misfolded proteins (Ye et al., 2021). It is worth mentioning that the chaperone GroEL/GroES of *A. baumannii* has also been reported to play an important role in antimicrobial resistance (Abirami et al., 2023). In addition, the DnaK system supports rifampicin resistance (Fay et al., 2021). In this study, the chaperone proteins *GroEL*, *GroES* and *DnaK* are up-regulated in the antibiotic-resistance strain. These results suggest that chaperones may also play a crucial role in the process of carbapenem antibiotic resistance (**Figure 8**).

In summary, these results showed that the main STs of CRAB were ST136, ST191, ST208, ST195, ST369, and it was mainly distributed in ICU. The analysis of the antibiotic resistance mechanism suggested that the antibiotic resistance mechanism of *A. baumannii* was mainly due to the expression of biofilm formation and efflux pump-related genes. In addition, to peptidoglycan biosynthesis, chaperonin synthesis also plays an important role. This study provides a theoretical basis for better control of CRAB.

5 Conclusion

In this study, there were 9 ST sequence types were detected, and the CC208 was the main clonal complex in this hospital and showed high carbapenems resistance; as well as the $bla_{OXA\text{-}23}$ gene was the main carbapenems resistance genotypes; the results of transcriptome data showed that the mechanism of enhanced carbapenems resistance of *A. baumannii* may be due to the enhanced biofilm-forming ability, efflux pump expression, peptidoglycan biosynthesis, and molecular chaperone protein expression. Therefore, we need to strengthen the research and development of new antibiotics to provide an effective way to control carbapenem-resistant *A. baumannii*. This study lays the foundation for the detection and control of carbapenem *A. baumannii*. In summary, the epidemic trend of clinical *A. baumannii* in Guiyang, China was analyzed from the molecular level, and the antibiotic resistance mechanism of *A. baumannii* to carbapenem antibiotics was analyzed with transcriptome, which provided a theoretical basis for better control of *A. baumannii*.

Data availability statement

The original contributions presented in this study are included in this article/**Supplementary material**, further inquiries can be directed to the corresponding authors.

Author contributions

ZQ: Funding acquisition, Methodology, Resources, Writing – original draft. KY: Methodology, Software, Writing – original draft. HC: Methodology, Software, Writing – original draft. SC: Methodology, Software, Writing – review & editing. FC: Writing – review & editing. FM: Funding acquisition, Writing – review & editing: GG: Funding acquisition, Writing – review & editing. JP: Funding acquisition, Resources, Writing – review & editing.

Funding

The authors declare that financial support was received for the research, authorship, and/or publication of this article. This research was funded by the National Natural Science Foundation of China (82002180, 81660347), Characteristic Key Laboratory of Guizhou Province [2021] 313, Guizhou Provincial Natural Science Foundation (ZK [2022] Key Program 039), the Science and Technology Fund Project of Guizhou Provincial Health Commission (gzwkj2023-567), and the High-Level Talent Initiation Project of Guizhou Medical University (J[2022]023).

Conflict of interest

The authors declare that the research was conducted in the absence of any commercial or financial relationships that could be construed as a potential conflict of interest.

Publisher's note

Supplementary material

The Supplementary Material for this article can be found online at: https://www.frontiersin.org/articles/10.3389/fmicb.2024.1394775/full#supplementary-material

References

Abirami, G., Alexpandi, R., Sudhin, S., Durgadevi, R., Roshni, P. S., Kumar, P., et al. (2023). Pyrogallol downregulates the expression of virulence-associated proteins in *Acinetobacter baumannii* and showing anti-infection activity by improving non-specific immune response in zebrafish model. *Int. J. Biol. Macromol.* 226, 853–869. doi: 10.1016/j.ijbiomac.2022.12.045

Abisado, R. G., Kimbrough, J. H., McKee, B. M., Craddock, V. D., Smalley, N. E., Dandekar, A. A., et al. (2021). Tobramycin adaptation enhances policing of social cheaters in *Pseudomonas aeruginosa*. *Appl. Environ. Microbiol.* 87:e0002921. doi: 10.1128/AEM.00029-21

Abouelfetouh, A., Mattock, J., Turner, D., Li, E., and Evans, B. A. (2022). Diversity of carbapenem-resistant *Acinetobacter baumannii* and bacteriophage-mediated spread of the Oxa23 carbapenemase. *Microb. Genom.* 8:752. doi: 10.1099/mgen.0.000752

Alcantar-Curiel, M. D., Rosales-Reyes, R., Jarillo-Quijada, M. D., et al. (2019). Carbapenem-resistant *Acinetobacter baumannii* in three tertiary care hospitals in Mexico: Virulence profiles, innate immune response and clonal dissemination. *Front. Microbiol.* 10:2116. doi: 10.3389/fmicb.2019.02116

Barbosa, C., Trebosc, V., Kemmer, C., Gayosso-Vázquez, C., Fernández-Vázquez, J. L., Toledano-Tableros, J. E., et al. (2017). Alternative evolutionary paths to bacterial antibiotic resistance cause distinct collateral effects. *Mol. Biol. Evol.* 34, 2229–2244. doi: 10.1093/molbev/msx158

Barnabas, V., Kashyap, A., Raja, R., Newar, K., Rai, D., Dixit, N. M., et al. (2022). the extent of antimicrobial resistance due to efflux pump regulation. *ACS Infect. Dis.* 8, 2374–2388. doi: 10.1021/acsinfecdis.2c00460

Blair, J. M., Richmond, G. E., and Piddock, L. J. (2014). Multidrug efflux pumps in gram-negative bacteria and their role in antibiotic resistance. *Future Microbiol.* 9, 1165–1177.

Chan, K. W., Liu, C. Y., Wong, H. Y., Chan, W. C., Wong, K. Y., and Chen, S. (2022). Specific amino acid substitutions in OXA-51-type β-lactamase enhance catalytic activity to a level comparable to carbapenemase OXA-23 and OXA-24/40. *Int. J. Mol. Sci.* 23:4496.

Chiang, M.-H., Chang, F.-J., Kesavan, D. K., Vasudevan, A., Xu, H., Lan, K. L., et al. (2022). Proteomic network of antibiotic-induced outer membrane vesicles released by extensively drug-resistant *Elizabethkingia anophelis*. *Microbiol. Spectr.* 10:e0026222. doi: 10.1128/spectrum.00262-22

Chusri, S., Na-Phatthalung, P., Siriyong, T., Paosen, S., and Voravuthikunchai, S. P. (2014). *Holarrhena antidysenterica* as a resistance modifying agent against *Acinetobacter baumannii*: Its effects on bacterial outer membrane permeability and efflux pumps. *Microbiol. Res.* 169, 417–424. doi: 10.1016/j.micres.2013.09.004

Colquhoun, J. M., and Rather, P. N. (2020). insights into mechanisms of biofilm formation in *Acinetobacter baumannii* and Implications for uropathogenesis. *Front. Cell Infect. Microbiol.* 10:253. doi: 10.3389/fcimb.2020.00253

Dai, W., Zhang, Y., Zhang, J., Xue, C., Yan, J., Li, X., et al. (2021). Analysis of antibiotic-induced drug resistance of *Salmonella enteritidis* and its biofilm formation mechanism. *Bioengineered* 12, 10254–10263. doi: 10.1080/21655979.2021.1988251

Fay, A., Philip, J., Saha, P., Hendrickson, R. C., Glickman, M. S., and Burns-Huang, K. (2021). The DnaK chaperone system buffers the fitness cost of antibiotic resistance mutations in mycobacteria. *mBio* 12:21. doi: 10.1128/mBio.00123-21

Firoozeh, F., Nikibakhsh, M., Badmasti, F., Zibaei, M., and Nikbin, V. S. (2023). Clonal relatedness of carbapenem-resistant *Acinetobacter baumannii*: High prevalence of ST136pas in a burn center. *Ann. Clin. Microbiol. Antimicrob.* 22:9. doi: 10.1186/s12941-023-00589-9

Fu, Y., Zhang, L., Wang, G., Lin, Y., Ramanathan, S., Yang, G., et al. (2020). The LysR-type transcriptional regulator YeeY plays important roles in the regulatory of furazolidone resistance in *Aeromonas hydrophila*. *Front. Microbiol.* 11:577376. doi: 10.3389/fmicb.2020.577376

Gaiarsa, S., Batisti Biffignandi, G., Esposito, E. P., Castelli, M., Jolley, K. A., Brisse, S., et al. (2019). Comparative analysis of the two *Acinetobacter baumannii* multilocus sequence typing (MLST) schemes. *Front. Microbiol.* 10:930. doi: 10.3389/fmicb.2019.00930

Gao, Y., Li, H., Chen, H., Zhang, J., Wang, R., Wang, Z., et al. (2022). Origin, phylogeny, and transmission of the epidemic clone ST208 of carbapenem-resistant *Acinetobacter baumannii* on a global scale. *Microbiol. Spectr.* 10:e0260421. doi: 10.1128/spectrum.02604-21

Gedefie, A., Demsis, W., Ashagrie, M., Kassa, Y., Tesfaye, M., Tilahun, M., et al. (2021). *Acinetobacter baumannii* biofilm formation and its role in disease pathogenesis: A review. *Infect. Drug Resist.* 14, 3711–3719. doi: 10.2147/IDR.S332051

Goltermann, L., Sarusie, M. V., and Bentin, T. (2015). Chaperonin GroEL/GroES over-expression promotes aminoglycoside resistance and reduces drug susceptibilities in *Escherichia coli* Following exposure to Sublethal aminoglycoside doses. *Front. Microbiol.* 6:1572. doi: 10.3389/fmicb.2015.01572

Grishin, A. V., Karyagina, A. S., Vasina, D. V., Vasina, I. V., Gushchin, V. A., and Lunin, V. G. (2020). Resistance to peptidoglycan-degrading enzymes. *Crit. Rev. Microbiol.* 46, 703–726. doi: 10.1080/1040841x.2020.1825333

Guo, H., Tong, Y., Cheng, J., Abbas, Z., Li, Z., Wang, J., et al. (2022). Biofilm and small colony variants–an update on *Staphylococcus aureus* strategies toward drug resistance. *Int. J. Mol. Sci.* 23:1241. doi: 10.3390/ijms23031241

Han, L., Gao, Y., Liu, Y., Yao, S., Zhong, S., Zhang, S., et al. (2022). An outer membrane protein YiaD contributes to adaptive resistance of Meropenem in *Acinetobacter baumannii*. *Microbiol. Spectr.* 10:e0017322. doi: 10.1128/spectrum.00173-22

Hassan, K. A., Liu, Q., Elbourne, L. D. H., Ahmad, I., Sharples, D., Naidu, V., et al. (2018). Pacing across the membrane: The novel PACE family of efflux pumps is widespread in Gram-negative pathogens. *Res. Microbiol.* 169, 450–454. doi: 10.1016/j.resmic.2018.01.001

Inchai, J., Pothirat, C., Bumroongkit, C., Limsukon, A., Khositsakulchai, W., and Liwsrisakun, C. (2015). Prognostic factors associated with mortality of drug-resistant *Acinetobacter baumannii* ventilator-associated pneumonia. *J. Intensive Care* 3:9. doi: 10.1186/s40560-015-0077-4

Jiang, M., Chen, X., Liu, S., Zhang, Z., Li, N., Dong, C., et al. (2021). Epidemiological analysis of multidrug-resistant *Acinetobacter baumannii* isolates in a tertiary hospital over a 12-year period in China. *Front. Public Health* 9:707435. doi: 10.3389/fpubh.2021.707435

Kang, H. M., Yun, K. W., and Choi, E. H. (2023). Molecular epidemiology of *Acinetobacter baumannii* complex causing invasive infections in Korean children during 2001-2020. *Ann. Clin. Microbiol. Antimicrob.* 22:32. doi: 10.1186/s12941-023-00581-3

Khaled, J. M., Alharbi, N. S., Siddiqi, M. Z., Alobaidi, A. S., Nauman, K., Alahmedi, S., et al. (2021). A synergic action of colistin, imipenem, and silver nanoparticles against pandrug-resistant *Acinetobacter baumannii* isolated from patients. *J. Infect. Public Health* 14, 1679–1685. doi: 10.1016/j.jiph.2021.09.015

Kvesić, M., Kalinić, H., Dželalija, M., Šamanić, I., Andričević, R., and Maravić, A. (2022). Microbiome and antibiotic resistance profiling in submarine effluent-receiving coastal waters in Croatia. *Environ. Pollut.* 292:118282. doi: 10.1016/j.envpol.2021.118282

Langmead, B., and Salzberg, S. L. (2012) Fast gapped-read alignment with bowtie 2. *Nat. Methods* 9, 357–359.

Lee, C. R., Lee, J. H., Park, M., Park, K. S., Bae, I. K., Kim, Y. B., et al. (2017). Biology of *Acinetobacter baumannii*: Pathogenesis, antibiotic resistance mechanisms, and prospective treatment options. *Front. Cell Infect. Microbiol.* 7:55. doi: 10.3389/fcimb.2017.00055

Li, L., Li, Y., Zhu, F., Li, Y., Zhu, F., Cheung, A. L., et al. (2021). new mechanistic insights into purine biosynthesis with second messenger c-di-AMP in relation to biofilm-related persistent methicillin-resistant *Staphylococcus aureus* infections. *mBio* 12:e0208121. doi: 10.1128/mBio.02081-21

Li, X. Z., Plesiat, P., and Nikaido, H. (2015). The challenge of efflux-mediated antibiotic resistance in Gram-negative bacteria. *Clin. Microbiol. Rev.* 28, 337–418. doi: 10.1128/CMR.00117-14

Lima, W. G., Silva Alves, G. C., Sanches, C., Antunes Fernandes, S. O., and de Paiva, M. C. (2019). Carbapenem-resistant *Acinetobacter baumannii* in patients with burn injury: A systematic review and meta-analysis. *Burns* 45, 1495–1508. doi: 10.1016/j.burns.2019.07.006

Liu, M., Hernandez-Morales, A., Clark, J., Le, T., Biswas, B., Bishop-Lilly, K. A., et al. (2022). Comparative genomics of *Acinetobacter baumannii* and therapeutic bacteriophages from a patient undergoing phage therapy. *Nat. Commun.* 13:3776. doi: 10.1038/s41467-022-31455-5

Liu, Q., Hassan, K. A., Ashwood, H. E., Gamage, H. K. A. H., Li, L., Mabbutt, B. C., et al. (2018). Regulation of the aceI multidrug efflux pump gene in *Acinetobacter baumannii*. *J. Antimicrob. Chemother.* 73, 1492–1500. doi: 10.1093/jac/dky034

Lu, H. F., Tsai, Y. C., Li, L. H., Lin, Y. T., and Yang, T. C. (2021). Role of AzoR, a LysR-type transcriptional regulator, in SmeVWX pump-mediated antibiotic resistance in *Stenotrophomonas maltophilia*. *J. Antimicrob. Chemother.* 76, 2285–2293. doi: 10.1093/jac/dkab203

Maisuria, V. B., Hosseinidoust, Z., and Tufenkji, N. (2015). Polyphenolic extract from maple syrup potentiates antibiotic susceptibility and reduces biofilm formation of pathogenic bacteria. *Appl. Environ. Microbiol.* 81, 3782–3792. doi: 10.1128/AEM.00239-15

Mody, L., Gibson, K. E., Horcher, A., Prenovost, K., McNamara, S. E., Foxman, B., et al. (2015). Prevalence of and risk factors for multidrug-resistant *Acinetobacter baumannii* colonization among high-risk nursing home residents. *Infect. Control Hosp. Epidemiol.* 36, 1155–1162. doi: 10.1017/ice.2015.143

Montanaro, L., Ravaioli, S., and Ruppitsch, W. (2016). Molecular characterization of a prevalent ribocluster of methicillin-sensitive *Staphylococcus aureus* from orthopedic implant infections. correspondence with MLST CC30. *Front. Cell Infect. Microbiol.* 6:8. doi: 10.3389/fcimb.2016.00008

Mulani, M. S., Kamble, E. E., Kumkar, S. N., Tawre, M. S., and Pardesi, K. R. (2019). Emerging strategies to combat ESKAPE pathogens in the era of

antimicrobial resistance: A review. *Front. Microbiol.* 10:539. doi: 10.3389/fmicb.2019.00539

Nguyen, M., and Joshi, S. G. (2021). Carbapenem resistance in *Acinetobacter baumannii*, and their importance in hospital-acquired infections: A scientific review. *J. Appl. Microbiol.* 131, 2715–2738. doi: 10.1111/jam.15130

Nordmann, P., and Poirel, L. (2019). Epidemiology and diagnostics of carbapenem resistance in gram-negative bacteria. *Clin. Infect. Dis.* 69, S521–S528. doi: 10.1093/cid/ciz824

O'Donnell, J. N., Putra, V., and Lodise, T. P. (2021). Treatment of patients with serious infections due to carbapenem-resistant *Acinetobacter baumannii*: How viable are the current options? *Pharmacotherapy* 41, 762–780. doi: 10.1002/phar.2607

Qu, J., Du, Y., Yu, R., and Lu, X. (2016). The first outbreak caused by *Acinetobacter baumannii* ST208 and ST195 in China. *Biomed. Res. Int.* 2016:9254907. doi: 10.1155/2016/9254907

Ramirez, M. S., Bonomo, R. A., and Tolmasky, M. E. (2020). Carbapenemases: Transforming *Acinetobacter baumannii* into a yet more dangerous menace. *Biomolecules* 10:720. doi: 10.3390/biom10050720

Ravaioli, S., Campoccia, D., Ruppitsch, W., Allerberger, F., Poggi, A., Chisari, E., et al. (2022). Comparison of automated ribotyping, spa typing, and MLST in 108 clinical isolates of *Staphylococcus aureus* from orthopedic infections. *Int. J. Mol. Sci.* 23:1660. doi: 10.3390/ijms23031660

Roy, S., Chatterjee, S., Bhattacharjee, A., Chattopadhyay, P., Saha, B., Dutta, S., et al. (2021). Overexpression of efflux pumps, mutations in the pumps' regulators, chromosomal mutations, and AAC(6')-Ib-cr are associated with fluoroquinolone resistance in diverse sequence types of neonatal septicaemic *Acinetobacter baumannii*: A 7-year single center study. *Front. Microbiol.* 12:602724. doi: 10.3389/fmicb.2021.602724

Roy, S., Chowdhury, G., Mukhopadhyay, A. K., Dutta, S., and Basu, S. (2022). Convergence of biofilm formation and antibiotic resistance in *Acinetobacter baumannii* infection. *Front. Med.* 9:793615. doi: 10.3389/fmed.2022.793615

Sanchez, B. C., Chang, C., Wu, C., Tran, B., and Ton-That, H. (2017). Electron transport chain is biochemically linked to pilus assembly required for polymicrobial interactions and biofilm formation in the gram-positive *Actinobacterium Actinomyces oris*. *mBio* 8, e399–e317. doi: 10.1128/mBio.00399-17

Schmittgen, T. D., and Livak, K. J. (2008). Analyzing real-time PCR data by the comparative C(T) method. *Nat. Protoc.* 73, 1101–1108. doi: 10.1038/nprot.2008.73

Shanmugasundarasamy, T., Karaiyagowder Govindarajan, D., and Kandaswamy, K. (2022). A review on pilus assembly mechanisms in gram-positive and Gram-negative bacteria. *Cell Surf.* 8:100077. doi: 10.1016/j.tcsw.2022.100077

Stevens, M., Howe, C., Ray, A. M., Washburn, A., Chitre, S., Sivinski, J., et al. (2020). Analogs of nitrofuran antibiotics are potent GroEL/ES inhibitor pro-drugs. *Bioorg. Med. Chem.* 28:115710. doi: 10.1016/j.bmc.2020.115710

Tiwari, V., Rajeswari, M. R., and Tiwari, M. (2019). Proteomic analysis of iron-regulated membrane proteins identify FhuE receptor as a target to inhibit siderophore-mediated iron acquisition in *Acinetobacter baumannii*. *Int. J. Biol. Macromol.* 125, 1156–1167. doi: 10.1016/j.ijbiomac.2018.12.173

Torrens, G., Sanchez-Diener, I., Jordana-Lluch, E., Barceló, I. M., Zamorano, L., Juan, C., et al. (2019). In vivo validation of peptidoglycan recycling as a target to disable AmpC-mediated resistance and reduce virulence enhancing the cell-wall-targeting immunity. *J. Infect. Dis.* 220, 1729–1737. doi: 10.1093/infdis/jiz377

Wang, Y., Yang, J., Sun, X., Li, M., Zhang, P., Zhu, Z., et al. (2022). CRISPR-Cas in *Acinetobacter baumannii* contributes to antibiotic susceptibility by targeting endogenous AbaI. *Microbiol. Spectr.* 10, e0082922. doi: 10.1128/spectrum.00829-22

Yan, J., and Bassler, B. L. (2019). Surviving as a community: Antibiotic tolerance and persistence in bacterial biofilms. *Cell Host Microbe* 26, 15–21. doi: 10.1016/j.chom.2019.06.002

Ye, C., Li, W., Yang, Y., Liu, Q., Li, S., Zheng, P., et al. (2021). Inappropriate use of antibiotics exacerbates inflammation through OMV-induced pyroptosis in MDR *Klebsiella pneumoniae* infection. *Cell Rep.* 36:109750. doi: 10.1016/j.celrep.2021.109750

You, Q., Du, X., Hu, N., Zhang, Y., Zhang, N., Wang, F., et al. (2023). Local characteristics of molecular epidemiolgy of *Acinetobacter baumannii* in Jilin province (northeast China). *BMC Microbiol.* 23:19. doi: 10.1186/s12866-023-02761-9

Zhao, Y., Li, M. C., and Konate, M. M. (2021). TPM, FPKM, or Normalized counts? A comparative study of quantification measures for the analysis of RNA-seq data from the nci patient-derived models repository. *J. Transl. Med.* 19:269. doi: 10.1186/s12967-021-02936-w

frontiers | Frontiers in Microbiology

TYPE Original Research
PUBLISHED 16 July 2024
DOI 10.3389/fmicb.2024.1429027

OPEN ACCESS

EDITED BY
Vijay Soni,
NewYork-Presbyterian, United States

REVIEWED BY
Murugesh Narayanappa,
Stanford University, United States
Tripti Nair,
University of Southern California,
United States

*CORRESPONDENCE
Savita Lochab
✉ savita.lochab@patanjali.res.in
Anurag Varshney
✉ anurag@patanjali.res.in

RECEIVED 07 May 2024
ACCEPTED 07 June 2024
PUBLISHED 16 July 2024

CITATION
Balkrishna A, Joshi M, Kabdwal M, Tomer M, Lochab S and Varshney A (2024) Robust anti-tubercular profile of *Solanum virginianum* extract in enhancing isoniazid bioavailability and curtailing stress tolerance in *Mycobacterium smegmatis*. *Front. Microbiol.* 15:1429027. doi: 10.3389/fmicb.2024.1429027

Robust anti-tubercular profile of *Solanum virginianum* extract in enhancing isoniazid bioavailability and curtailing stress tolerance in *Mycobacterium smegmatis*

Acharya Balkrishna[1,2,3,4], Monali Joshi[1], Manisha Kabdwal[1], Meenu Tomer[1], Savita Lochab[1]* and Anurag Varshney[1,2,5]*

[1]Drug Discovery and Development Division, Patanjali Research Foundation, Haridwar, Uttarakhand, India, [2]Department of Allied and Applied Sciences, University of Patanjali, Haridwar, Uttarakhand, India, [3]Patanjali Yog Peeth (UK) Trust, Glasgow, United Kingdom, [4]Vedic Acharya Samaj Foundation, Inc., Groveland, FL, United States, [5]Special Centre for Systems Medicine, Jawaharlal Nehru University, New Delhi, India

Introduction: The formidable survival mechanisms employed by *Mycobacterium tuberculosis* (*Mtb*), combined with the low bioavailability of anti-tubercular drugs and their associated hepatotoxicity, worsen tuberculosis management. Traditional medicinal plants offer potential solutions to these challenges. This study focuses on exploring the anti-tubercular potential of *Solanum virginianum* against *Mycobacterium smegmatis*, *mc²155*.

Methods and results: HPTLC and UHPLC phytochemically characterized the hydro-methanolic extract of *Solanum virginianum* (SVE). SVE curtails the growth and viability of *mc²155* under normal and *in vitro* stress conditions. The compromised cell wall integrity of *mc²155* with SVE is depicted through scanning electron microscopy (SEM) while EtBr permeability assays and TLC-based comparative changes in lipids extraction addressed the integrity of the cell wall. Furthermore, SVE augmented the susceptibility of *mc²155* towards Isoniazid (INH) through enhanced bioavailability. Adjunct treatment of SVE with INH demonstrated a markedly reduced survival of the intracellular bacilli. The study also uncovered the hepatoprotective potential of SVE in HepG2 cells.

Conclusion: This research paves the way for deeper exploration into the potential of *Solanum virginianum* against virulent *Mtb* strains, emphasizing over the significance of traditional medicinal plants in tuberculosis treatment. Collectively, the findings suggest SVE as a potent candidate for independent or adjunct anti-tubercular therapy.

KEYWORDS

***mc²155*, isoniazid, adjunct therapy, tuberculosis, stress tolerance, targeted metabolomics**

Introduction

Tuberculosis over the centuries has emerged as a persistent threat to human health. The 2022 Global Tuberculosis Report reflected the repercussions of the COVID-19 pandemic highlighting a notable 4.5% increase in tuberculosis incidences and death rates

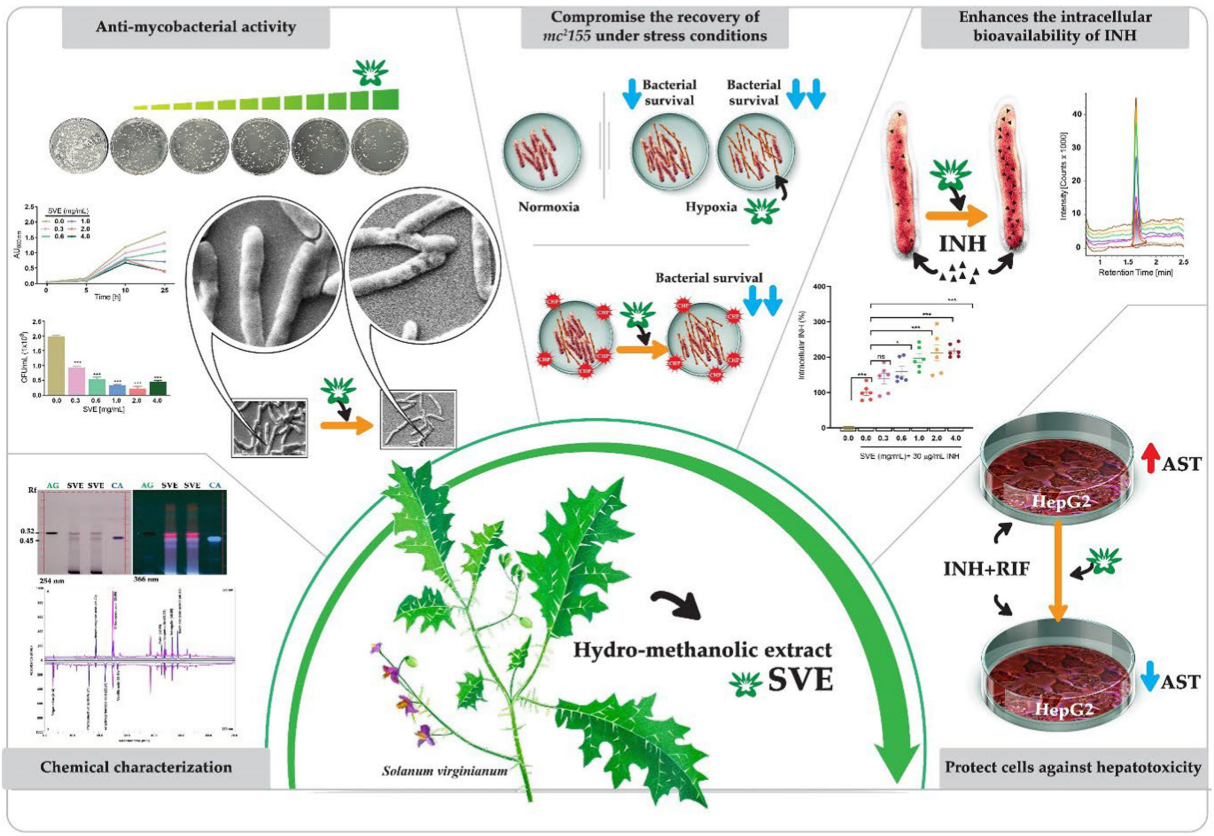

GRAPHICAL ABSTRACT
A schematic showing the canvas painting of the aerial part *Solanum virginianum* (SVE) that was utilized for the preparation of hydro-methanolic extract. SVE was subjected to chemical characterization to determine the enriched phytochemicals present in the extract. SVE exhibits the anti-mycobacterial property by retarding the *mc²155* growth and viability. The SEM images depicted the damaged *mc²155* structure of bacilli with SVE treatment. SVE was tested for its ability to compromise the survival of *mc²155* under stress conditions generated with CHP (cumene hydroperoxide) and hypoxia. The UPLC-LCMS/QToF approach determined that the SVE treatment enhanced the bioavailability of INH inside the *mc²155*. SVE also exacerbated the susceptibility of *mc²155* to INH. SVE treatment in INH + RIF-treated HepG2 cells showed reduced AST levels in the supernatant indicating the hepatoprotective potential of SVE.

climbing from 1.5 million in 2020 to 1.6 million in 2021 (Bagcchi, 2023). Furthermore, the objectives that were aiming for a 35% reduction in death rate and a 20% reduction in incidences in the End TB Strategy 2020 were nowhere achieved (The Lancet Public Health, 2023). The plethora of survival strategies employed by the causative bacteria, *Mycobacterium tuberculosis (Mtb)*, contribute significantly to the challenges in treating tuberculosis (Pieters, 2008). The primary treatment for tuberculosis relies on a fixed-dose combination of rifampicin (RIF), isoniazid (INH), and pyrazinamide (PZ). However, insufficient therapeutic plasma levels of these drugs, stemming from their low bioavailability, frequently contribute to the failure of anti-tubercular therapy and the concomitant development of antimicrobial drug resistance (AMR). Indeed, a higher minimum inhibitory concentration (MIC) of isoniazid has earlier been associated with the possibility of tuberculosis relapse (Bagcchi, 2023). Additionally, drug-induced hepatotoxicity, often referred to as drug-induced liver injury (AT-DILI), is potentially an adverse effect that accounts for another key factor in the failure of anti-tubercular therapy (Kashyap et al., 2018; Tella et al., 2022; Ezhilarasan, 2023).

Medicinal plants are considered an enduring gift of nature, having been utilized for treating various human diseases since ancient times. According to the World Health Organization (WHO), 80% of the population in developing countries relies on traditional medicines for preventing and curing primary health issues. Hepatotoxicity, a major reason for withdrawal of the anti-tubercular therapy, calls for adjunct therapies for tuberculosis. These adjunct therapies should function synergistically with first-line drugs in combating *Mtb* infection (Liu et al., 2008). The adjunct therapies could either compromise the mycobacterial survival or enhance the efficacy of primary drugs. Several plants have been listed in the Indian traditional medicinal system, Ayurveda, for the treatment of tuberculosis (Mangwani et al., 2020). Previous studies have

Abbreviations: SVE, hydro-methanolic extract of *Solanum virginianum*; *Mtb*, *Mycobacterium tuberculosis*; INH, isoniazid; RIF, rifampicin; HPTLC, high-performance thin liquid chromatography; UHPLC, ultra-high-performance liquid chromatography; UPLC/QToF-MS, ultra-performance liquid chromatography/quadrupole time-of-flight mass spectrometry; SEM, scanning electron microscopy; TLC, thin layer chromatography; CFU, colony-forming unit; OD, optical density; DMEM, Dulbecco's Modified Eagle Medium; RPMI 1640, Roswell Park Memorial Institute-1640; FBS, fetal bovine serum; EDTA, ethylenediaminetetraacetic acid; AST, aspartate aminotransferase.

demonstrated that piperine, an alkaloid present in *Piper nigrum* and *Piper longum*, enables the attainment of therapeutic serum levels of rifampicin when administered at significantly lower doses. This improved bioavailability of rifampicin at a reduced dose not only curtailed the likelihood of hepatotoxicity but also enhanced patient compliance by reducing the emergence of drug resistance (Nageswari et al., 2018). *Carum carvi* extract has been shown to increase plasma levels of rifampicin, isoniazid, and pyrazinamide by favorably modifying the pharmacokinetics of anti-tubercular treatment (Choudhary et al., 2014). Additionally, a flavonoid glycoside isolated from *Cuminum cyminum*, known as 3′,5-dihydroxyflavone 7-O-beta-D-galacturonide 4'-O-beta-D-glucopyranoside (CC-I), enhanced rifampicin levels in rat plasma by 35% in C_{max} and 53% in AUC, potentially through a permeation enhancing effect, thereby highlighting the potential of herb–drug synergism in modulating drug bioavailability (Sachin et al., 2007).

Along similar lines, we have explored the therapeutic potential of *Solanum virginianum* L., a plant belonging to the Solanaceae family. The plant is well documented in the ancient manuscripts of Ayurveda for its beneficial effects against bronchial asthma and cough (Raja et al., 2014). The current study, therefore, tested the biological activity of the plant extract against tuberculosis. *Mycobacterium smegmatis mc²155* serves as a commonly employed model system for the investigation of *Mtb*. This non-pathogenic, rapidly replicating mycobacterium shares substantial genomic similarities with *Mtb* (Sparks et al., 2023). The primary objective of this research was to conduct initial phytochemical screening and assess the anti-mycobacterial activity against *mc²155*. This serves as an initial step for our future investigations aiming to elucidate the anti-mycobacterial potency in pathogenic strains of *Mtb*. This study is part of a broader research endeavor focused on developing herbal medicines that could serve as independent or adjunct-anti-tubercular therapy with clearly deciphered mechanisms of action and herb–drug synergism.

The study presents a phytochemical characterization of the hydro-methanolic extract prepared from *Solanum virginianum* (hereafter, SVE) employing HPTLC and UHPLC. The mycobacterial strain *mc²155* when treated with SVE demonstrated compromised growth and viability. Mycobacteria possess numerous survival strategies to combat the stressful environment inside the host. The SVE treatment exacerbated the tolerance ability of *mc²155* toward different hostile environments. Various *in vitro* stress experiments were conducted generating oxidative, hypoxia, and nutrient stress for the bacilli. High-resolution scanning electron microscopy (SEM) depicted the distorted and aberrant ultra-structures in *mc²155* when treated with SVE. EtBr permeabilization assay corroborated the findings with a mechanism highlighting SVE-induced cell wall damage in *mc²155*. The chloroform-mediated lipid extraction process visualized on the TLC plate is a classical metabolomic method that depicted a dose-dependent reduction in total lipids extracted from SVE-treated *mc²155*. However, the key focus is to seek the potential of SVE as an adjuvant for tubercular drugs. The study utilized the UPLC/QToF-MS-based targeted metabolomic approach to quantify and assess the intracellular bioavailability of INH inside the complex biological matrix of *mc²155*. Furthermore, the combinatorial treatment demonstrated that *mc²155* becomes more susceptible and sensitive to INH in the presence of SVE. The study also addressed the efficacy of INH coupled with SVE in THP-1 cells infected with *mc²155*. Finally, the hepatoprotective role of SVE toward INH and RIF-mediated hepatotoxicity was also uncovered. Collectively, our research establishes the foundation for subsequent investigations of anti-mycobacterial attributes of SVE against pathogenic *Mtb* strains (Graphical Abstract). The collective findings suggest that SVE could emerge as a potent candidate for adjunct-anti-tubercular therapy, offering a well-defined mechanism of action. It demonstrates the ability to improve the bioavailability of INH, enhance mycobacterial clearance when combined with INH, and provide hepatoprotection.

Materials and methods

Chemicals

Cell culture media, including Dulbecco's Modified Eagle Medium (DMEM) and RPMI 1640 (Roswell Park Memorial Institute-1640), Antibiotic-Antimycotic (100X), Dulbecco's Phosphate Buffered Saline, Fetal Bovine Serum (FBS), and 0.5% Trypsin–EDTA were purchased from HiMedia Laboratories Pvt. Ltd., India. Rifampicin (557303), isoniazid (I3377), and 2 mM L-glutamine (G7513) were purchased from Sigma Aldrich, USA. The AR grade solvents, toluene, ethyl acetate, formic acid, acetic acid, and methanol (HPLC grade) were procured from Merck India Pvt. Ltd. Acetonitrile from Honeywell (34,967, Germany) and deionized water obtained from a Milli-Q system (Millipore, USA) were utilized for the experiments.

Plant procurement and hydro-methanolic extract preparation

The aerial part of *Solanum virginianum* L. (Syn. *Solanum xanthocarpum* Schrad.) (Family: Solanaceae) was collected from Morni Hills, Panchkula, Haryana, India. It was subsequently compared and authenticated with the taxonomists at Patanjali Research Foundation Herbarium (collection no. 222, accession no. 1604) located at Haridwar, Uttarakhand, India, and Central Scientific and Industrial Research–National Institute of Science Communication and Information Resources (CSIR–NISCAIR), New Delhi, Government of India.

The plant material weighing 200 g was cleaned, pulverized, and extracted in 1.4 L of water: methanol (1:1) solvent at 60–65°C for 2 h under reflux conditions. The extract was filtered through a 10-µm filter cloth, and the extract that remained in the cloth was again subjected to two more rounds of extraction repeats maintaining all the processes described above. Finally, the filtrate was pooled and concentrated in a rotary evaporator under reduced pressure. The process yielded 8.82% (w/w) light brown colored hydro-methanolic extract powder. We prepared 100 mg/mL of extract in autoclaved 0.2 µm filter-sterilized water. For treatments, the extract was further diluted in either mammalian cell culture media or 7H9 media as per requirement.

High-performance thin liquid chromatography (HPTLC) analysis

The HPTLC system (Camag, Switzerland) appendaged with an automated TLC sampler (ATS_4) and scanner 4 was deployed for the identification of phytochemicals in SVE. Analysis was carried out using integrated software, Win-CATS. In total, 300 mg of SVE was dissolved in 6 mL of water: methanol (1:1) followed by sonication and centrifugation to obtain a clear solution. Separation of this solution was performed on aluminum-backed TLC plates with precoated silica gel $60F_{254}$. Sample and standards were applied on the TLC plate using the spray-on technique. The phytoconstituents in SVE were identified and quantified by equating the Rf values of observed bands with the Rf values of respective standards. A mobile phase comprising of toluene: ethyl acetate: formic acid (5: 5: 0.5 v/v/v) was used to separate apigenin (AG) and cinnamic acid (CA). The TLC plates were air-dried and scanned at wavelengths of 254 and 366 nm for visualizing bands and generating 3D overlay desitograms. Standards AG (purity: 97.90) and CA (purity: 97.20) were procured from Natural Remedies and Sigma Aldrich, respectively.

Ultra-high-performance liquid chromatography (UHPLC) analysis

Standards of trigonelline (potency: 99.0%, Natural Remedies), protocatechuic acid (potency: 99.5%, Natural Remedies), 4-hydroxy benzoic acid (potency: 99.96%, Sigma Aldrich, USA), vanillic acid (potency: 98.2%, Sigma Aldrich, USA), rutin (potency: 94.2%, Sigma Aldrich, USA), isoquercetin (potency: 98.0%, ChemFaces), astragalin (potency: 98.0%, ChemFaces), neochlorogenic acid (potency: 98.0%, ChemFaces), chlorogenic acid (potency: 98.4%, SRL), and isochlorogenic acid (potency: 98.0%, SRL) were dissolved in methanol to prepare 1,000 ppm primary stock solution, independently. The SVE test solution for HPLC analysis was prepared by dissolving 500 mg of extract in 10 mL of methanol: water (80:20). The test solution was then sonicated, centrifuged, and passed through 0.45-µm filters. The quantification of standards and respective peaks in the SVE test solution was performed using UHPLC (Shimadzu Prominence XR, Japan) or HPLC (Prominence-i LC-2030c 3D Plus, Shimadzu, Japan). The system was equipped with a quaternary pump (Nexera XR LC-20AD XR) comprising of degassing unit (DGU-20A 5R), a DAD detector (SPD-M20 A), and an auto-sampler (Nexera XR SIL-20AC XR). Separation was achieved using a Shodex C18-4E (5 µm, 4.6*250 mm) column subjected to binary gradient elution. The two solvents used for the analysis consisted of 0.1% orthophosphoric acid in water (solvent A, pH 2.5) and acetonitrile (solvent B). Gradient programming of the solvent system was as follows: 0–2% B from 0 to 5 min, 2–8% B from 5 to 10 min, 8–10% B from 10 to 20 min, 10–12% B from 20 to 30 min, 12–25% B from 30 to 45 min, 25–40% B from 45 to 55 min, 40–60% B from 55 to 60 min, 60–70% B from 60 to 65 min, 70–0% B from 65 to 66 min, and 0–0% B from 67 to 70 with a flow rate of 1.0 mL/min. A total of 10 µL of the standard and test solution was injected, and the column temperature was maintained at 35°C. The wavelength was set at 278 nm and 325 nm to depict the phytochemicals and their respective standard peaks.

Bacterial growth conditions and treatments

Mycobacterium smegmatis strain *mc²155* was procured from ATCC and routinely propagated at 37°C, 200 rpm in Middlebrook 7H9 broth base (M0178, Sigma Aldrich, USA), supplemented with 0.5%(v/v) glycerol, 0.05% (w/v) Tween 80, and 10% albumin-glucose-catalase enrichment (ADC; Sigma Aldrich, USA). The survival and viability of *mc²155* in all experiments were evaluated by either spotting or spreading the serially diluted cultures on Middlebrook 7H11 agar base (M0428, Sigma Aldrich, USA) plates, which were incubated at 37°C for 3 days.

SVE was resuspended at 200 mg/mL in growth media and sonicated in a water bath sonication for 30 min and passed through 0.2-µm filters to prepare a homogenous solution. For the treatment in mammalian cell lines, a stock concentration of 100 mg/mL SVE was prepared by resuspending the extract in 30% DMSO-containing sterile deionized water. Subsequent dilutions were prepared in respective media. Isoniazid was prepared in sterile water at 10 mg/mL concentration as a stock solution, which was subsequently diluted in the respective media.

In vitro stress experiments

For nutrient limitation experiments, *mc²155* was passaged once in Sauton's Fluid Medium Base (Himedia) before initiating the experiment with SVE. Oxidative stress was generated in *mc²155* by inoculating the mid-log phase cultures (0.6–0.8 OD at 600 nm) at 0.05 OD in 7H9 media supplemented with 50 µM CHP in the presence and absence of SVE at indicated concentrations for 4 h and 8 h. Viability of the bacilli was evaluated through CFU enumeration. The mid-log phase culture of *mc²155* was freshly inoculated at 0.05 OD 600 nm in 7H9 growth media containing 1.5 µg/mL methylene blue served as a visual indicator of hypoxia (Tizzano et al., 2021). Loss of blue color occurs after 7 days. The culture was inoculated in screw caps, tightly closed, and secured with parafilm, maintaining a headspace of 15% with indicated doses of SVE. After 7 days when the blue media became colorless, the growth of the culture was evaluated by OD at 600 nm and viability by serially diluting and plating the culture on 7H11 plates. CFU enumeration was conducted after 3–4 days of incubation.

Scanning electron microscope

The effect of SVE on the microarchitecture of *mc²155* was monitored through a scanning electron microscope (Flex SEM 1000, Hitachi, Japan). The samples were prepared as described before (Miao and Xiang, 2020). Post-treatment with SVE, *mc2155* cultures were fixed with 4% formaldehyde, washed with deionized water, and air-dried on coverslips.

Ethidium bromide (EtBr) permeability assay

Mid-log phase *mc²155* cultures treated with SVE (0.6–4.0 mg/mL) for 24 h were centrifuged, washed, and resuspended in PBS at 0.4 OD containing 2 µg/mL EtBr. Fluorescence of the cells was recorded in an Envision multi-plate reader (PerkinElmer, Waltham, MA, USA) at excitation and emission wavelengths of 530 nm and 585 nm, respectively, every 10 min until 60 min (Mohamadi et al., 2018).

Determination of minimum inhibitory concentration (MIC)

The anti-mycobacterial activity of SVE was tested using the resazurin microtiter assay (REMA) as described previously (Taneja and Tyagi, 2007). In brief, the susceptibility was performed in a 96-well plate using resazurin as an indicator of cell viability or growth inhibition. A working concentration of SVE was prepared in 7H9 growth media to obtain a final concentration ranging from 0.19 mg/mL to 100 mg/mL using the 2-fold serial dilution method. For INH, the treatment varied from 0.19 µg/mL to 100 µg/mL. The plates were incubated on slow shaking for 24 h at 37°C. In total, 25 µL of resazurin 0.02% w/v was added to each well and incubated at 37°C until color development (from blue to pink).

Detection of intracellular INH utilizing UPLC/QToF-MS

The bacilli *mc²155* were treated with INH at 30 µg/mL in the presence or absence of SVE. Post 2 h of treatment, the cultures were centrifuged, washed twice in sterile water before lysis in sterile water with a probe sonicator, and centrifuged to collect supernatant (test solution) for the analysis of INH through ultra-performance liquid chromatography/quadrupole time-of-flight mass spectrometry (UPLC/QToF-MS). INH standard solutions of 25 ppb, 50 ppb, 100 ppb, 200 ppb, and 400 ppb were injected to generate linearity and facilitate quantification of INH in the test samples. A total of 5 µL of INH standard and test solutions was injected. The analysis was performed on the Xevo G2-XS QToF coupled with Acquity UPLC-I Class (Waters Corporation, Milford, MA, USA). The isocratic elution of 0.1% formic acid in water at a flow rate of 0.25 mL/min with a Waters Acquity UPLC HSS T3 (2.1 × 100 mm, 1.7 µm) column was used for the analysis. The column temperature was maintained at 35°C, and the sample temperature was maintained at 10°C during the analysis.

Mammalian cell line maintenance

The human hepatocarcinoma cell lines, HepG2, and the human monocytic cell line, THP-1, were obtained from an ATCC licensed cell repository at the National Centre for Cell Sciences (NCCS, Pune, India). The HepG2 cells were propagated in Dulbecco's Modified Eagle Medium (DMEM) supplemented with 10% fetal bovine serum (FBS) and 1% Anti-Anti (Antibiotic-Antimycotic, GIBCO). The THP-1 was propagated in RPMI 1640 supplemented with 10% fetal bovine serum (FBS), 2 mM L-glutamine, and 1% Anti-Anti (Antibiotic-Antimycotic, GIBCO). The growing conditions were maintained at 37°C and 5% CO_2 in a humified incubator. Cryopreserved cells were passaged at least twice before being used for the experiments in this study.

Alamar blue cell viability assay

The THP-1 cells were seeded at 0.8–1 × 10^4/ml per well density in 96-well tissue culture plates. Monocytic cells were allowed to differentiate into macrophages with the induction of 10 ng/mL of phorbol myristate acetate (PMA) for 12 h. PMA-containing media were replaced with fresh RPMI every day for 3 days. The cells were then treated with different concentrations of SVE (0.1, 0.3, 1, 3, 10, and 30) for 72 h. Three hours before the indicated time period, Alamar Blue at a working concentration of 15 µg/mL was added to the cells. The fluorescence was recorded in an Envision multi-plate reader (PerkinElmer, Waltham, MA, USA) at excitation and emission wavelengths of 560 nm and 590 nm, respectively. Percent cell viability was calculated using the following formula:

$$\%\text{Cell Viability} = \left[\left(AU_{\text{Treated}} - \text{Blank}\right) / \left(AU_{\text{Untreated}} - \text{Blank}\right)\right] X\,100$$

Infection experiment

The PMA-differentiated THP-1 cells, as described above, were then infected with *mc²155* at 1:10 MOI for 4 h. The cells were washed with sterile PBS thrice and replenished with complete RPMI media containing indicated concentrations of INH alone or in combination with SVE. Post 24 h, cell lysate prepared in 0.05% SDS was 10-fold serially diluted before plating on 7H11 plates for enumerating intracellular infection.

Assessment of AST levels

The HepG2 cells were seeded at a density of 5×10^5 cells/mL in a 12-well tissue culture plate. The cells were treated with SVE (1–30 µg/mL) or stimulated with rifampicin (300 µM) + isoniazid (150 µM) and co-treated with SVE (0–30 µg/mL) for 24 h (Darvin et al., 2018). Post-incubation, the supernatant was analyzed for AST levels using an Erba 200 biochemical analyzer (Erba Mannheim, Germany) as per the manufacturer's instructions. The data were represented as mean ± SEM ($n = 3$).

Data analysis

Software GraphPad Prism 8.0 and MS Office Excel 2010 were used to execute statistical calculations. To determine the *p*-values, analysis of the mean values was performed through one-way or two-way analysis of variance (ANOVA) using Dunnett's multiple comparison test.

Results

Quantification of phytochemicals in SVE

SVE was subjected to HPTLC and UHPLC methodology for the phytochemical characterization. SVE along with the reference standard was resolved on TLC plates, which were exposed at 254 nm and 366 nm to visualize the phytochemicals. The TLC plate predicted the presence of apigenin (AG) and caffeic acid (CA) in SVE at Rf values of 0.52 and 0.4, respectively (Figure 1A). A 3D chromatogram shows the peaks of SVE matching at the Rf of AG and *CA*. To identify more phytochemicals, SVE was separated through UHPLC methodology (Figure 1B). The chromatogram generated at 270 nm and 325 nm for SVE was overlayed with the chromatogram of the standard mix. The chromatograms indicated the presence of trigonelline (2.52 µg/mg), protocatechuic acid

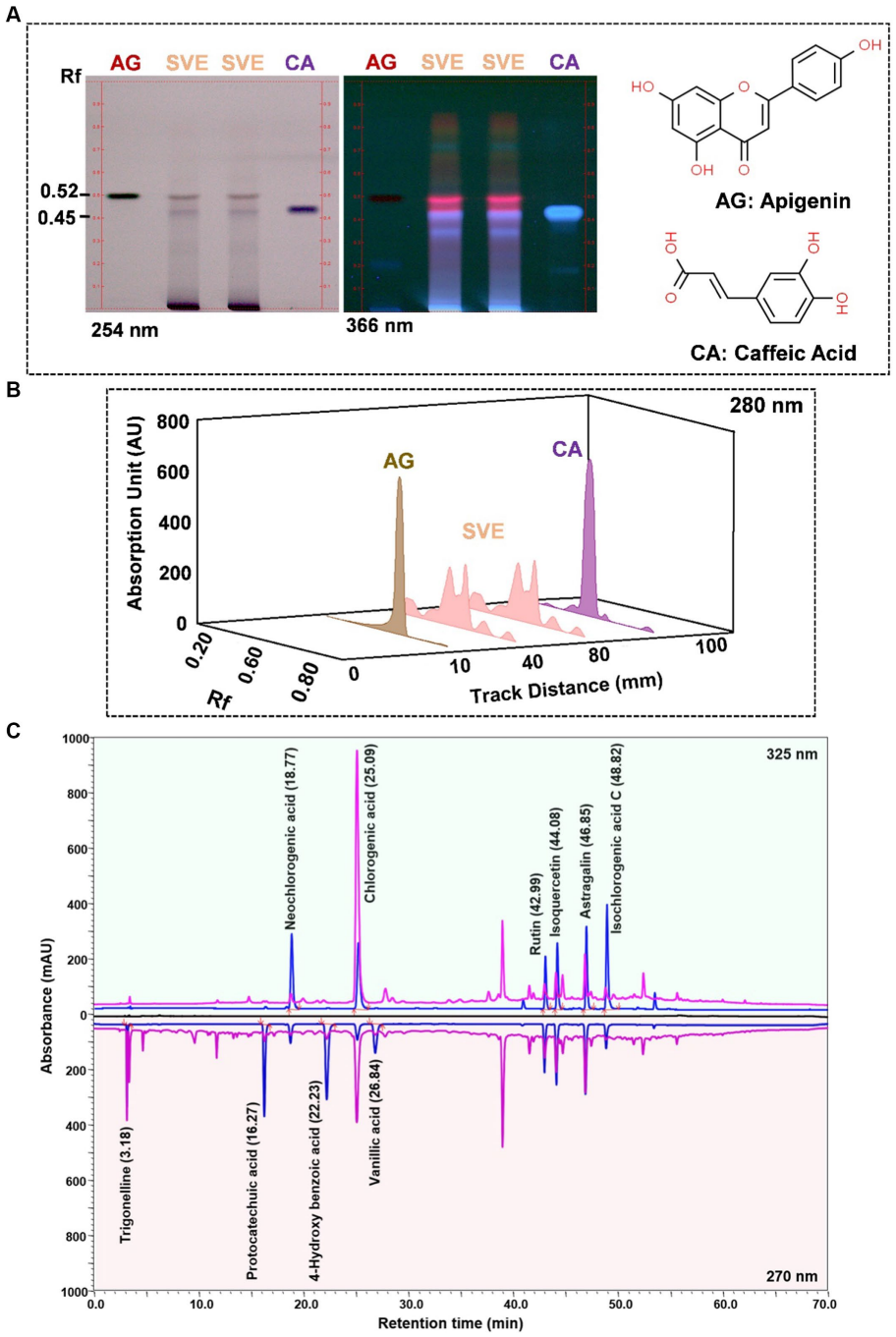

FIGURE 1
Quantification of phytochemicals in SVE. **(A)** (Left) The digital fingerprinting of the TLC plate captured at 254 nm (left panel) and 366 nm (right panel) depicts the band resolved in SVE. Bands in the same TLC indicating at apigenin (AG) and caffeic acid (CA) in the subsequent lanes. The chemical structures for AG and CA are viewed toward the right of the TLC plates. **(B)** 3-D overlay densitogram recorded at 280 nm shows the absorption units depicting the intensity of peaks for AG, SVE, and CA. **(C)** The mirror plot of the chromatogram generated at 270 nm (lower side) and 325 nm (upper side) shows the overlay of the SVE sample (pink) with the standards (blue). Peaks in SVE that align with the standard have been labeled with their respective names with retention time given in parenthesis.

(0.1 μg/mg), 4-hydroxy benzoic acid (0.22 μg/mg), and vanillic acid (0.19 μg/mg) at 270 nm, whereas neochlorogenic acid (0.48 μg/mg), chlorogenic acid (9.72 μg/mg), isochlorogenic acid (0.32 μg/mg), rutin (0.87 μg/mg), isoquercetin (1.22 μg/mg), and astragalin (1.61 μg/mg) were visualized in the chromatogram at 325 nm (Figure 1C and Table 1).

SVE exhibits anti-mycobacterial activity

To determine the anti-mycobacterial effect of SVE on the growth and viability of *mc²155*, as well as its efficacy, an initial screening was conducted using the spread-plate method followed by CFU enumeration. The results on the 7H11 plates indicated that SVE dose-dependently

10.3389/fmicb.2024.1429027

TABLE 1 Identification and quantification of phytochemicals present in SVE using UHPLC.

S. No.	RT (nm)[#]	Phytochemical identified	Molecular formula	Molecular weight (g/mol)	Chemical structure **	Content (µg/mg)
1	3.22 (270)	Trigonelline	$C_7H_7NO_2$	137.14	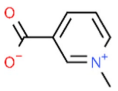	2.52
2	16.63 (270)	Protocatechuic acid	$C_7H_6O_4$	154.12	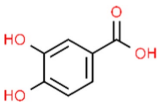	0.18
3	22.60 (270)	4-Hydroxy benzoic acid	$C_7H_6O_3$	138.12	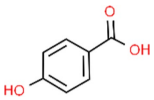	0.22
4	27.55 (270)	Vanillic acid	$C_8H_8O_4$	168.14	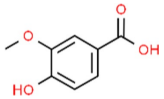	0.48
5	19.03 (325)	Neochlorogenic acid	$C_{16}H_{18}$	354.30	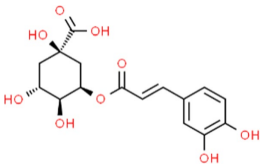	0.11
6	25.96 (325)	Chlorogenic acid	$C_{16}H_{18}$	354.30	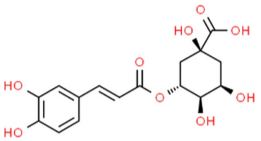	9.72
7	49.78 (325)	Isochlorogenic acid	$C_{16}H_{18}$	354.30	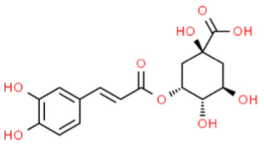	0.32
8	42.99 (325)	Rutin	$C_{27}H_{30}O_{16}$	610.52	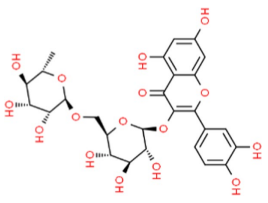	0.87
9	44.08 (325)	Isoquercetin	$C_{21}H_{20}O_{12}$	464.37	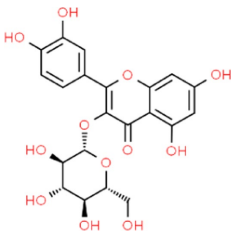	1.22
10	46.85 (325)	Astragalin	$C_{21}H_{20}O_{11}$	448.37	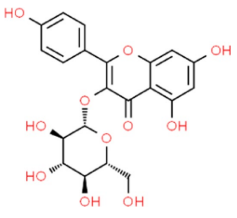	1.61

[#]RT (nm) is the retention time in min (minutes) at wavelength (in nm); **chemical structures adapted from www.chemspider.com.

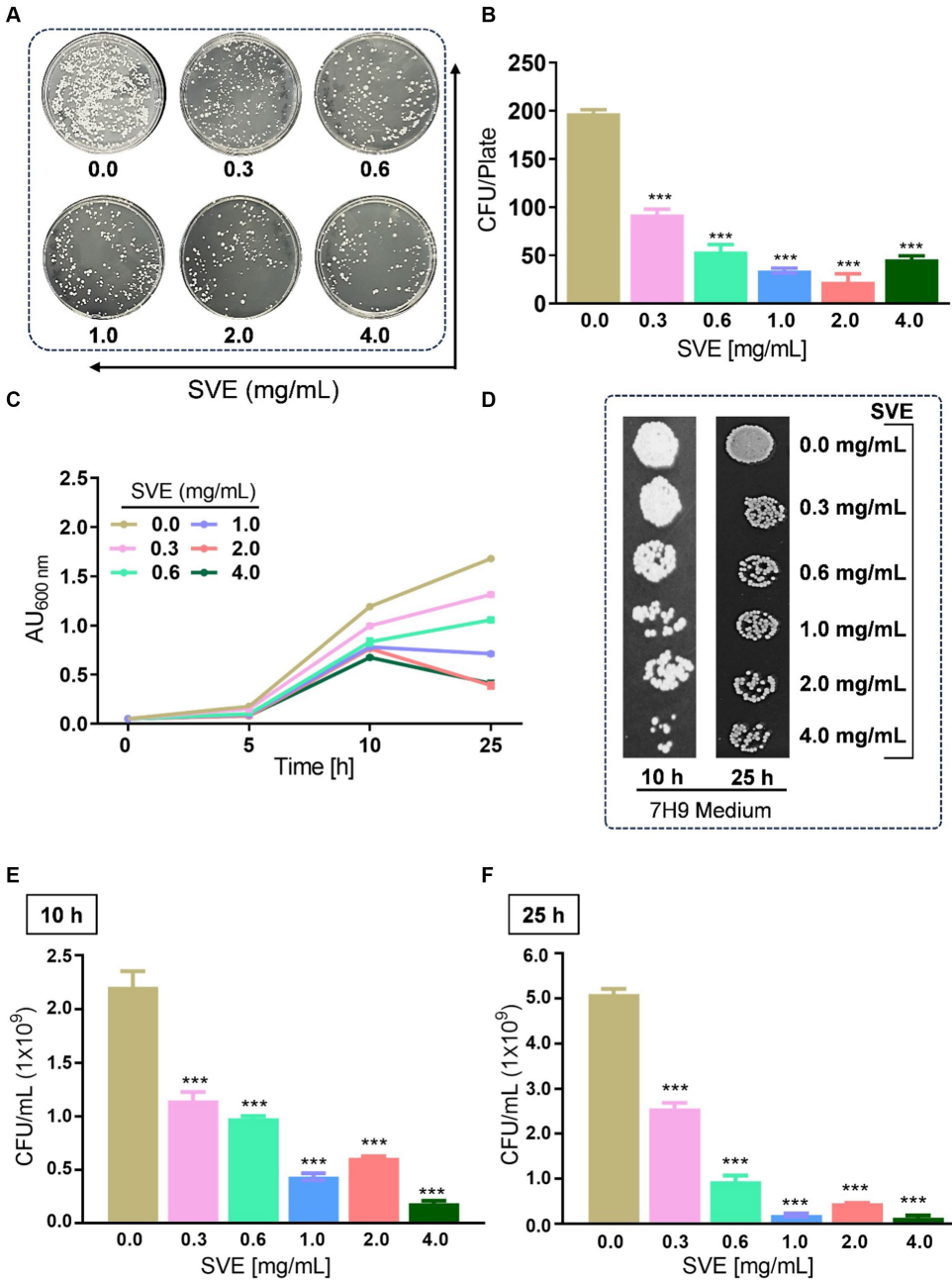

FIGURE 2
SVE exhibits anti-mycobacterial activity. **(A)** Representative digital images of 7H11 agar plates with CFUs from *mc²155* bacilli. The viability of *mc²155* was tested by spreading an equal volume of serially diluted actively growing culture on 7H11 agar plates containing SVE at indicated doses (0.3–4.0 mg/mL). **(B)** The bar graph representing CFU/plate from three independent experiments. **(C)** The line graph representing the growth profile of *mc²155* treated with indicated doses of SVE in 7H9 growth media until 25 h. The growth profile was assessed by monitoring absorbance (optical density, OD) at 600 nm. The absorbance units on the *y*-axis were blank-corrected by subtracting the absorbance of the respective blank at 600 nm. **(D)**. The cultures from **(C)** were serially diluted and spotted on 7H11 agar plates to visualize the viability of *mc²155*. **(E)** The cultures from **(C)** were serially diluted and plated on 7H11 agar plates to enumerate CFU/mL at 10 h and **(F)** 25 h. The error bars represent mean ± SEM; the significance of data is represented as ***$p < 0.0005$.

inhibited the growth of *mc²155* (Figure 2A). Subsequent CFU enumeration determined that SVE at 0.3 mg/mL reduced the CFUs by 2-fold, which escalated to approximately 10-fold at 0.6, 1.0, 2.0, and 4.0 mg/mL of SVE (Figure 2B). Furthermore, SVE retarded the growth progression of *mc²155* treated with 0.3, 0.6, 1.0, 2.0, and 4.0 mg/mL concentrations of SVE. The absorbance of the cultures at 10 and 25 h indicates a dose-dependent inhibition of the bacilli growth by SVE (Figure 2C). The viability of the bacilli was tested at 10 h and 25 h by spotting and plating the 10-fold serial dilution of the cultures on 7H11 agar plates (Figure 2D). At 10 h, CFU/mL showed a significant half-fold reduction at doses below 1.0 mg/mL and a 10-fold reduction at doses higher than 1.0 mg/mL (Figure 2E). By 25 h, the reduction in CFU/mL escalated to 2-fold at the lowest dose of 0.3 mg/mL and further reduced to more than 10-fold at doses of 0.6 mg/mL and above (Figure 2F).

SVE subverts the stress tolerance ability of *mc²155*

Mycobacteria possess numerous survival strategies to combat the stressful environment inside the host. To address the effect of SVE on the tolerance ability of *mc²155* toward different hostile environments, *in vitro* stress experiments were performed. The growth profile of *mc²155* in Sauton's minimal media indicates that SVE drastically inhibits the growth of *mc²155* under nutritional stress conditions (Figure 3A). The CFU/mL and spot dilutions at 10 h (upper panel) and 25 h (lower panel) of the growth profile suggest a more than 10-fold reduction in *mc²155* viability with SVE. The spot plating of the cultures highlights the difference more apparently (Figure 3B). The bacilli propagated under oxidative stress generated with cumene hydroperoxide (CHP) showed a significant reduction in growth profile in the presence of 0.6 mg/mL and above (Figure 3C). CFU/mL enumeration at 8h post-CHP treatment showed ~10-fold dose-dependent reduction in the viability of *mc²155* (Figure 3D). The comparative change in the percentage survival of *mc²155* under the oxidative stress of CHP demonstrated that SVE at 0.3 and 0.6 mg/mL significantly reduced the survival by ~20% (Figure 3E). Mycobacteria remarkably counteract the hypoxic stress, evident with growth profile. However, SVE treatment inhibited the growth of *mc²155*, post 7 days of hypoxia induction (Figure 3F). The viability of bacilli on day 7 of hypoxia induction demonstrated that SVE led to ~ two-log fold reduction in the CFU/mL (Figure 3G).

SVE compromises the cell wall integrity of *mc²155*

The effect of SVE on the cell wall permeability of *mc²1555* was evaluated. EtBr intracellular accumulation was determined through fluorescence. SVE treatment caused a dose-dependent increase in fluorescence, with the maximal effect observed at 4.0 mg/mL of SVE, indicating enhanced permeability in the bacilli due to the SVE treatment (Figure 4A). To closely monitor morphological changes in *mc²155* with SVE, SEM was performed. SVE treatment induced serious morphological aberrations in the bacilli. The yellow arrows indicate the altered integrity and morphology of *mc²155* (Figure 4B). The cell wall integrity of the *mc²155* cell was subsequently evaluated through TLC of organic solvent-extracted lipids. An equal mass of SVE-treated *mc²155* was subjected to a chloroform-mediated lipid extraction process (Brennan et al., 1982). TLC plate visualized under white light (upper panel) and at 254 nm (lower panel) depicted a dose-dependent reduction in lipids extracted from SVE-treated *mc²155* (Figure 4C). The 3D chromatogram depicting the intensity of the bands also showed dose-dependent reduction (Figure 4D). The area under the curve of the peaks in the 3D chromatogram also reduced dose-dependently (Figure 4E).

SVE potentiates the INH susceptibility in *mc²155* by enhancing its bioavailability

The MIC of INH against *mc²155* was determined to be 7.8 µg/mL (Figure 5A), while the MIC of SVE was evaluated as 7.15 mg/mL (Figure 5B). To address the effect of SVE on the MIC of INH, *mc²155* was treated with INH at doses less than the evaluated MIC. However, each INH treatment was accompanied by SVE treatment. The concentrations selected for SVE were also less than the MIC evaluated. The percent inhibition of INH at the indicated doses of 0.25, 0.5, 1.0, 2.0, and 4.0 µg/mL significantly increased when combined with SVE treatment (Figure 5C). The concentration of 4.0 mg/mL showed effective inhibition of *mc²155* when combined with INH at all doses. INH at 0.25 µg/mL was inhibiting *mc²155* by ~5%. Interestingly, this inhibition increased up to ~35% with SVE treatment (Figure 5C). We speculated that SVE probably enhances the bioavailability of INH inside *mc²155*. To address this, the UPLC-LCMS/QToF was utilized to assess the intracellular INH levels inside *mc²155* co-treated with INH and SVE. Intensity counts of INH in the *mc²155* with respective treatments indicate the presence of the highest amount of INH in SVE treatment at 4.0 mg/mL (Figure 5D). The results were evaluated with different SVE treatments in percentage change of intracellular INH level. SVE treatment at and above 0.6 mg/mL significantly increases the intracellular INH levels by up to 200% (Figure 5E).

SVE reduces the intracellular survival of *mc²155* inside the host and subsequently curtails the anti-tubercular drug-induced hepatotoxicity

To further investigate the role of compromising *mc²155* under stress conditions, *mc²155* was infected in THP-1 cells to create a host-mediated stress environment. To address SVE as a host-mediated adjuvant therapy, the cell viability of SVE was assessed through an Alamar Blue Assay. Doses approximately a hundred to ten thousand times lower than those used in *mc²155* were tested for cytotoxicity at a half-log fold difference in the THP-1 cells. THP-1 showed no cytotoxicity even with 30 µg/mL of SVE (Figure 6A). THP-1cells treated with SVE at 1.0, 3.0, 10, and 30 µg/mL showed a significant reduction in the intracellular survival of *mc²155*. INH treatment at 1 µg/mL significantly reduced the *mc²155* survival; however, when combined with SVE, a better reduction in the intracellular survival of *mc²155* was observed. Upon comparison with SVE alone, SVE+ INH showed a better and more significant reduction (Figure 6B). Anti-tubercular drug combination (INH + RIF)-mediated hepatotoxicity was observed through AST levels in HepG2 cells. SVE at 3.0, 10, and 30 µg/mL showed a significant reduction in the release of AST levels of HepG2 cells (Figure 6C).

Discussion

With constant global interventions from the WHO, tuberculosis remains a health concern, necessitating the exploration of alternative or adjunct therapeutic approaches (Bagcchi, 2023). Plants are recognized to have unique bioactive metabolites that could be explored for potential adjuvant therapy in tuberculosis. Indigenous knowledge throughout the world provides valuable insights into the single or polyherbal formulations that could alleviate the symptoms of tuberculosis. Numerous studies have been conducted demonstrating the antimicrobial potential in different phytochemical groups,

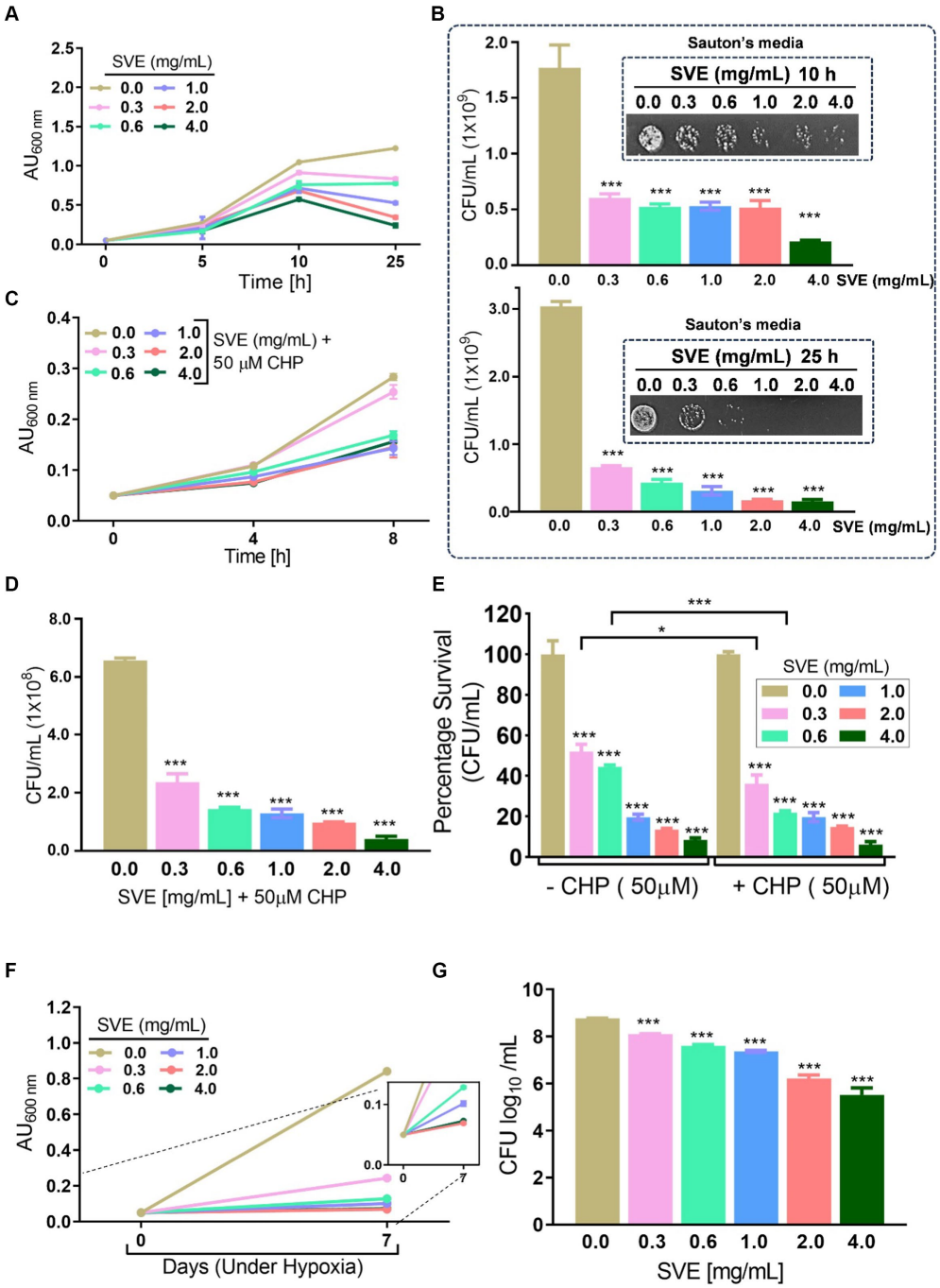

FIGURE 3
SVE compromises the ability of *mc²155* to subvert stress conditions. **(A)** Line graph representing growth profile of *mc²155* treated with indicated doses of SVE in Sauton's nutrient limiting media until 25 h. The growth profile was assessed by monitoring absorbance (optical density, OD) at 600 nm. The absorbance units on the *y*-axis were blank-corrected by subtracting the absorbance of the respective blank at 600 nm **(B)**. The serially diluted cultures from **(A)** were spotted and plated on 7H11 agar plates to visualize the viability of *mc²155* at 10 h (upper panel) and 25 h (lower panel). **(C)** The *mc²155* grown in 7H9 media treated with indicated doses of SVE in the presence or absence of 50 µM cumene hydroperoxide (CHP) for 8 h. Bar graph representing CFU/mL in cultures treated with SVE+ CHP. **(E)** The bar graph representing percent survival calculated from CFU/mL obtained in **(D)** *mc²155* treated with SVE alone or in the presence of CHP with respect to the untreated (0.0 mg/mL SVE). **(F)** Hypoxia was established in *mc²155* cultures for 7 days. The line graph representing the absorbance (optical density, OD at 600 nm) of cultures on day 0 before setting up hypoxia and on day 7 after hypoxia establishment. A zoomed line graph in the inset to show better resolution of the graph. **(G)** Subsequently, the cultures from **(F)** were serially diluted and plated on 7H11 agar plates for CFU enumeration. The bar graph representing the percent survival calculated from the CFU $\log_{10}$/mL (shown in the inset). The error bars represent mean ± SEM; the significance of data is represented as ***$p < 0.0005$.

10.3389/fmicb.2024.1429027

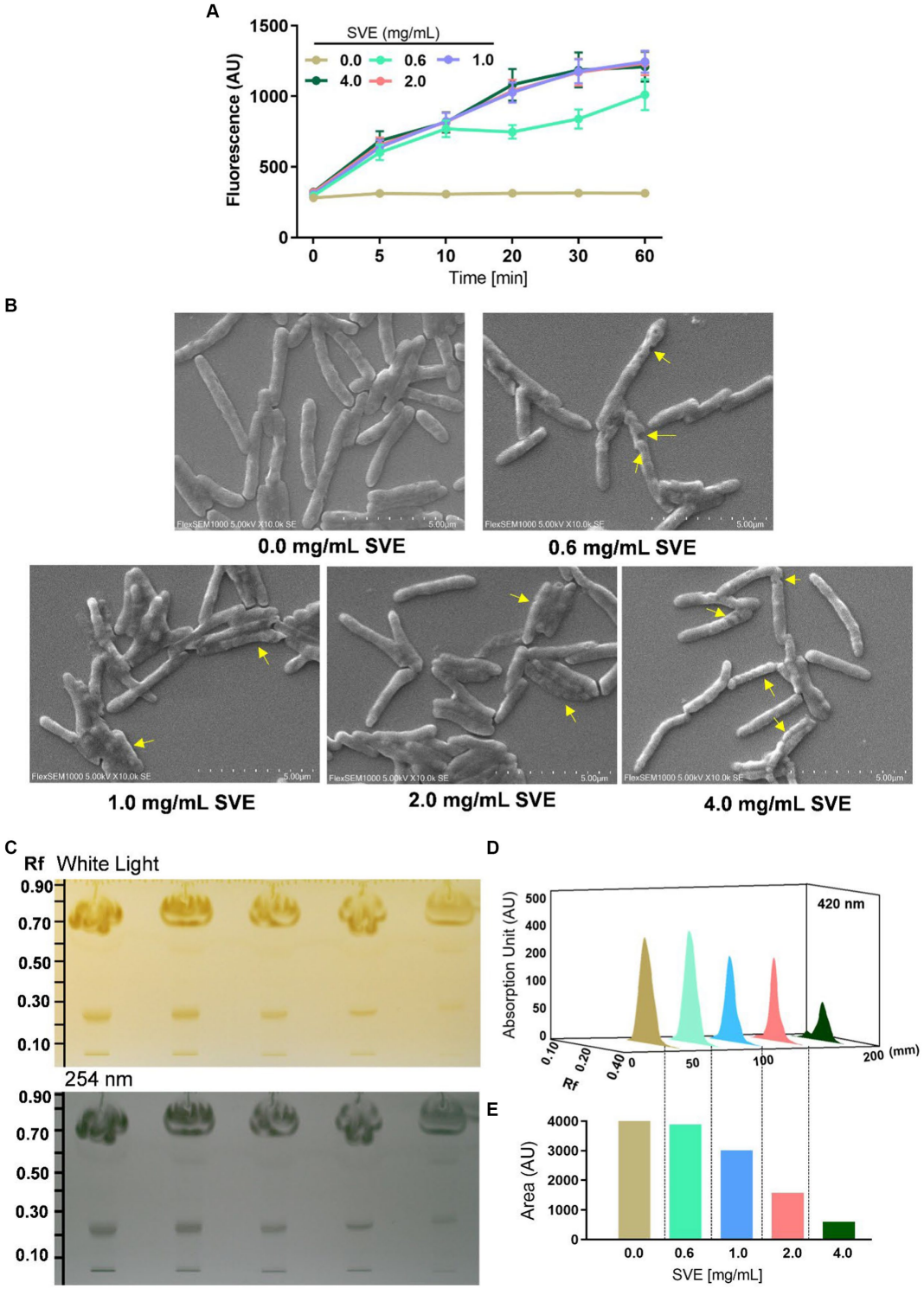

FIGURE 4
SVE compromises the cell wall integrity of *mc²155*. **(A)** *mc²155* treated with indicated doses of SVE for 24 h. Bacilli from all treatments were pelleted and resuspended equally in PBS. The cultures were incubated with 2 μg/mL of EtBr, following which fluorescence was monitored every 10 min until 60 min. The line graph was plotted with the arbitrary units generated by the plate reader. **(B)** Digital images generated through SEM analysis depicting the microarchitectures of *mc²155* treated with SVE for 24 h. The yellow arrows indicate the damaged and deteriorated bacterium. **(C)** Lipids extracted using chloroform: methanol method were resolved on a TLC plate and visualized under white light (upper panel) and 254 nm (lower panel). **(D)** The bands at Rf of 0.24 were quantified and represented as absorption units indicating the intensity of the bands. **(E)** The percent change in the lipid content calculated from the area under the peaks in **(D)** was plotted as bar graphs (lower panel). The error bars represent mean ± SEM; the significance of data is represented as $*p < 0.05$, $**p < 0.005$ and non-significant (ns) if $p < 0.05$.

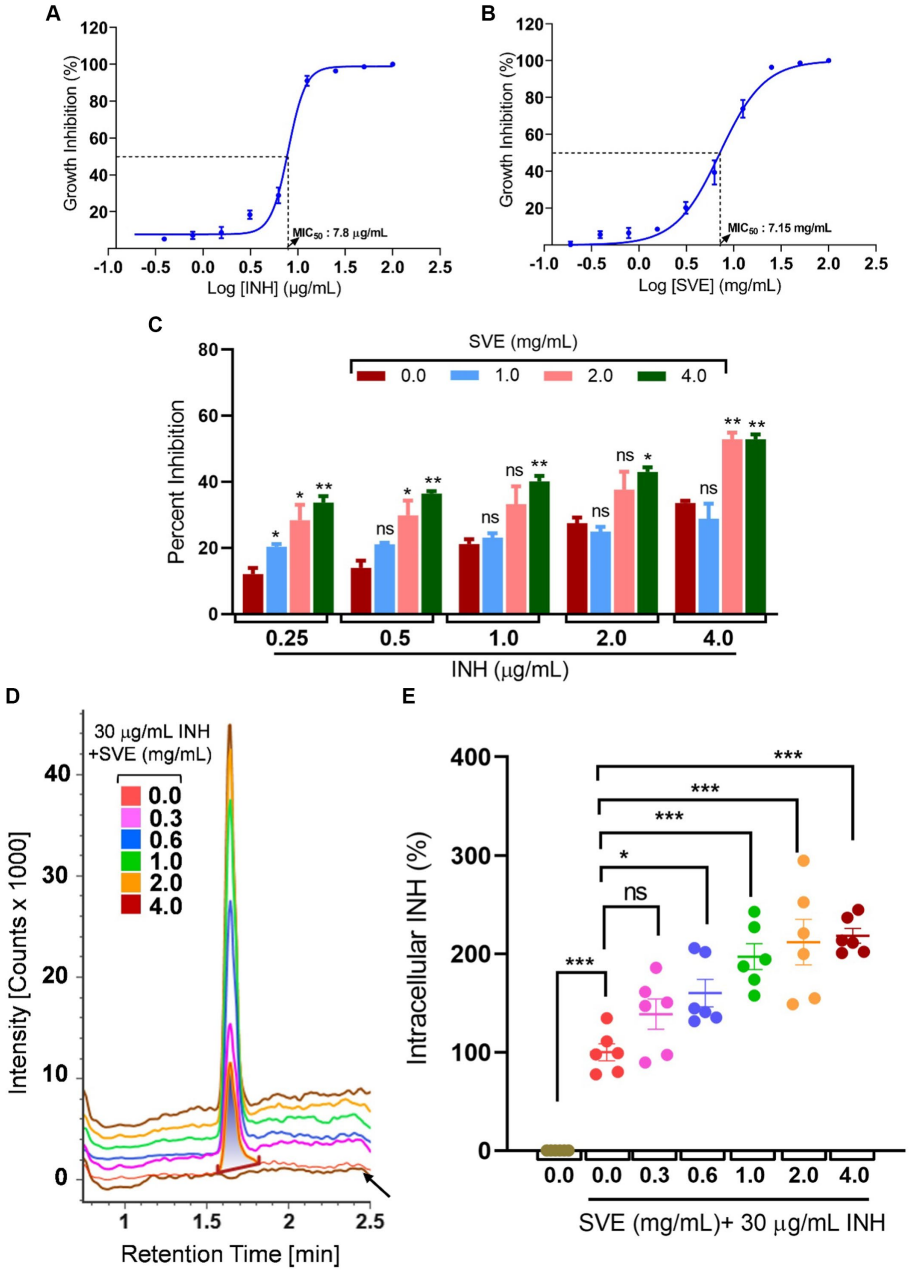

FIGURE 5
SVE enhances the intracellular bioavailability of INH inside the *mc²155*. **(A)** A dose–response curve showing a normalized dose-dependent inhibitory effect of INH on the growth of *mc²155*. **(B)** A dose–response curve showing a normalized dose-dependent inhibitory effect of SVE on the growth of *mc²155*. MIC_{50} of INH and SVE representing 50% growth inhibition determined through non-linear regression analysis. **(C)** Percentage growth inhibition plotted for *mc²155* treated with indicated combinatorial doses of INH and SVE. **(D)** UPLC-LCMS/QToF-based analysis of INH in the lysates of *mc²155* treated with indicated combinations of INH and SVE for 1 h. Representative plot showing the intensity counts of INH detected versus retention time generated through UPLC-LCMS/QToF. A flat brown line labeled with an arrow is the lysate of *mc²155* bacilli without INH or SVE treatment. **(E)** Intracellular INH calculated in **(D)** represented as percent change with respect to the untreated (0.0 µg/mL INH and 0.0 mg/mL SVE) from six independent experiments. The error bars represent mean ± SEM; the significance of data is represented as $*p < 0.05$, $**p < 0.005$, and $***p < 0.0005$ and not significant (ns) if $p > 0.05$.

including phenolic compounds, alkaloids, terpenoids, glucosinolates, saponins, iridoids, secoiridoids, limonoids, polyacetylenes, sulfides, sulfonamides, and anthranoids (Patra, 2012; Borges et al., 2015). We identified some of the notable phytochemicals in SVE that could be propelling the pharmacological activities (Figure 1). Phenolic compounds, p-hydroxybenzoic acid, protocatechuic, vanillic acid, and caffeic acid, identified in SVE possess robust antimicrobial properties due to the presence of hydroxyl groups on the phenol groups (Merkl et al., 2010). Trigonelline, chlorogenic acid and its isoforms, astragalin, and apigenin have been shown to exhibit anti-oxidant, anti-inflammatory, anti-bacterial, anti-viral,

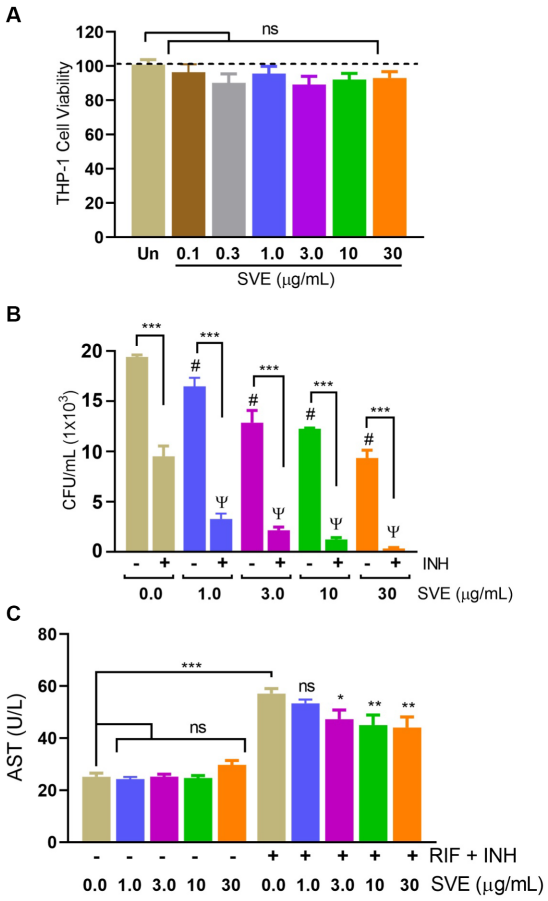

FIGURE 6
SVE reduces the intracellular survival of *mc²155* inside the host and subsequently curtails the anti-tubercular drug-induced hepatotoxicity. **(A)** Percent cell viability with Alamar blue assay was evaluated in THP-1 cells treated with indicated doses of SVE (0.1-30 mg/mL) for 24 h. **(B)** THP-1 cells were infected with mc2155 at 1:10 MOI and thereafter treated with either INH alone, SVE alone or in combination of INH and SVE at indicated doses for 24 h. Error bars represent mean ± SEM; the significance of data is represented as, ***$p < 0.0005$; #$p < 0.05$ with respect to the infected condition without any treatment; ψ$p < 0.05$ with respect to the infected and treated with INH alone condition. not significant (ns) if $p < 0.05$. **(C)** Hepatotoxicity in HepG2 cells treated with INH+RIF in the presence or absence of SVE evaluated through AST levels in media of HepG2 cells. Error bars represent mean ± SEM; the significance of data is represented as, *$p < 0.05$, **$p < 0.005$, ***$p < 0.0005$ and not significant (ns) if $p < 0.05$.

hypoglycemic, lipid-lowering, anti-cardiovascular, anti-mutagenic, anti-cancer, immunomodulatory properties (Liu et al., 2008; Qin et al., 2017; Mohamadi et al., 2018; Riaz et al., 2018; Salehi et al., 2019; Miao and Xiang, 2020). Quercetin and its glycosides, such as isoquercitrin or rutin, are among the most ubiquitous flavonoids present in plants. A previous study has demonstrated that rutin could inhibit *Mtb* growth *in vitro* and *ex vivo* while remaining non-toxic to mice peritoneal macrophages (Sharma et al., 2023). This study demonstrates that SVE enriched with phytometabolites exhibits an anti-mycobacterial effect (Figure 2). *Mtb* upon infection, inside the host cell, encounters a hostile environment, such as oxidative burst, nitrosative stress, acidic pH, osmotic pressure, low oxygen, and nutrient challenges. However, *Mtb* has been evolving for centuries and can survive these challenges. The study assessed whether SVE could lower the tolerance of *mc²155* toward such stress under *in vitro* settings. We determined that SVE treatment drastically reduced the survival of *mc²155* under nutrient, oxidative, and hypoxia conditions (Figure 3). We were keen on observing the SVE-mediated morphological changes on *mc²155*. SEM technique is commonly employed to study the bacterium's microarchitectures. SEM analysis revealed that SVE damaged the bacilli, causing them to lose their integrity, shape, and usual width compared to untreated bacilli. The after-effects of SVE-mediated damages in *mc²155* could be observed through enhanced permeability and reduced cell wall extractions on the TLC plate, all indicating the SVE-induced disruption in the cell membrane. Mycobacteria contain intricate lipid structures, constituting approximately 60% of their dry cell mass as cell wall lipids. The lipidomic profile of Mycobacteria remains distinctive, showcasing its ability to adapt to various stressors. In our study, we conducted a non-targeted lipid analysis focusing on qualitative and relative quantitative alterations following treatment with SVE. Utilizing a conventional TLC-based approach, we examined the comparative changes in lipid patterns extracted from *mc²155* upon SVE treatment. The observed diminishing lipid patterns on the TLC plate suggest compromised bacilli health upon SVE treatment (Figure 4). Weakened structural integrity of the cell wall led us to speculate whether SVE treatment is enhancing the permeability of mycobacteria toward anti-tubercular drugs. SVE enhanced the bioavailability of INH inside the bacilli and thereby made the bacilli more susceptible to INH. The MIC_{50} of SVE and INH against *mc²155* was 7.8 mg/mL and 7.15 µg/mL, respectively. To assess the susceptibility of *mc²155* to INH treatment, we chose the INH doses less than MIC_{50} where we observed minimal inhibition. These doses of INH were then combined with SVE at 0.5, 0.25, and 0.125 times less than the calculated MIC_{50} of SVE. Interestingly, even at 0.25 µg/mL of INH (which is 0.03 times the MIC_{50} of INH), when combined with SVE, it showed ~40% inhibition in *mc²155* growth. This indicated that SVE potentiates the susceptibility of *mc²155* to INH. We speculated whether SVE has increased the levels of INH inside bacilli. We utilized the UPLC-LCMS/QToF technology and treated *mc²155* with INH. The selection of 30 µg/mL of INH was based on the sensitivity of UPLC-LCMS/QToF. The technical challenges could not allow us to use lower doses. Notably, the treatment was only for 1 h since our objective was to assess the intracellular INH levels inside *mc²155*. SVE treatment dose-dependently increased the bioavailability of INH in *mc²155* (Figure 5). SVE acts like a bioenhancer that not only increases the bioavailability of INH but also enhances the susceptibility of mycobacteria at a lower dose. This would largely contribute to a decrease in the development of frequent INH resistance. We showed that SVE is anti-mycobacterial. To explore further, we investigated the host-mediated response modulated by SVE toward *mc²155* infection. For this, we treated cells with SVE at doses 100 to 10,000 times less than what was used in *mc²155*. We subjected *mc²155* to the actual host response by infecting the bacilli in the THP-1 macrophages. INH was used at 1.0 µg/mL, again a sub-optimal

dose to clear the intracellular bacteria. We subsequently combined INH with SVE at 1, 3, 10, and 30 µg/mL. Interestingly, SVE alone significantly reduced the intracellular *mc²155* survival inside the host. INH alone showed a better clearance compared to SVE. However, INH and SVE cotreatment showed significantly better clearance of intracellular survival, suggesting SVE as a potential adjunct therapy. Medicinal plants are known for healing properties and ameliorating drug toxicities. The hepatotoxicity induced by anti-tubercular drugs is a significant factor leading to the withdrawal of treatment by patients and the emergence of multi-drug resistance (MDR) in tuberculosis. Anti-tubercular medications are known to cause increased levels of crucial enzymes, including alkaline phosphatase (ALP), serum glutamic oxaloacetic transaminase (SGOT or AST), and serum glutamic pyruvic transaminase (SGPT or ALT), which serve as indicative markers for hepatotoxicity (González et al., 2017). Nonetheless, traditional medicinal plants, such as *Apium graveolens*, *Apium paniculata*, *Ficus religiosa*, *Fumaria indica*, *Glycyrrhiza glabra*, *Syzygium aromaticum*, *Withania somnifera*, and *Tinospora cordifolia,* have been historically employed for tuberculosis treatment, concurrently exhibiting hepatoprotective attributes (Liu et al., 2008; Samal, 2016; Anwer et al., 2023). These plants represent abundant reservoirs of alkaloids, flavonoids, diterpenoids, tannins, lipids, sterols, etc., showcasing antimicrobial properties and protective effects on the liver (Ansari et al., 2023). Investigating the hepatoprotective capabilities of SVE, a combination treatment involving a high dosage of INH and RIF was administered to HepG2 cells to induce hepatotoxicity. The extent of hepatotoxicity was assessed by determining the elevated AST levels. Intriguingly, the administration of SVE substantially decreased AST levels in HepG2 cells, pointing toward the hepatoprotective effects of SVE.

The resilience and anti-tubercular drug limitations in *Mtb* drive multi-drug resistance and hepatotoxicity. We propose potential herb–drug synergy in SVE and INH, wherein the SVE enhances the potency and intracellular efficacy of INH. SVE attenuates cell viability, compromises the bacterial cell wall, and exhibits hepatoprotective effects. These findings underscore SVE as a potent adjunct therapy against tuberculosis.

Data availability statement

The raw data supporting the conclusions of this article will be made available by the authors, without undue reservation.

Ethics statement

Ethical approval was not required for the studies on humans in accordance with the local legislation and institutional requirements because only commercially available established cell lines and bacterial strains were used. Ethical approval was not required for the studies on animals in accordance with the local legislation and institutional requirements because only commercially available established cell lines were used.

Author contributions

AB: Conceptualization, Resources, Supervision, Writing – review & editing. MJ: Formal analysis, Investigation, Methodology, Writing – original draft. MK: Formal analysis, Investigation, Methodology, Writing – original draft. MT: Formal analysis, Investigation, Methodology, Writing – original draft. SL: Data curation, Formal analysis, Investigation, Methodology, Visualization, Writing – original draft, Writing – review & editing. AV: Conceptualization, Project administration, Visualization, Supervision, Writing – review & editing.

Funding

The author(s) declare financial support was received for the research, authorship, and/or publication of this article. This study has been conducted using internal research funds from a non-profit Patanjali Research Foundation Trust, Haridwar, India.

Acknowledgments

We extend our gratitude to Mr. Vallabh Prakash Mulay for providing the sample extraction for research purposes. We appreciate the efforts of Mr. Sudeep Verma, Dr. Seema Gujral, and Dr. Jyotish Srivastava for their support in analytical chemistry. We thank Dr. Vivek Gohel for his support in evaluating AST levels in HepG2 cells. We thank Dr. Swati Haldar for her support in SEM analysis and Dr. Rishabh Dev for his timely guidance. We thank Mr. Devendra Kumawat for his help in designing the graphics. It is our pleasure to thank Mr. Mir Chand for his assistance in maintaining the tissue culture facility. We extend our gratitude to Mr. Tarun Rajput and Mr. Gagan Kumar for their swift administrative support.

Conflict of interest

AB is an honorary trustee in Divya Yog Mandir Trust, which governs Divya Pharmacy, Haridwar. In addition, he holds an honorary managerial position in Patanjali Ayurved Ltd., Haridwar, India and is employed by Vedic Acharya Samaj Foundation, Inc. Divya Pharmacy and Patanjali Ayurved Ltd., commercially manufacture and sell several Ayurvedic products. MJ, MK, MT, SL, and AV have been employed at Patanjali Research Foundation which is governed by Patanjali Research Foundation Trust (PRFT), Haridwar, Uttarakhand, India. PRFT is an independent not-for-profit organization.

Publisher's note

References

Ansari, M. A., Shoaib, S., Alomary, M. N., Ather, H., Ansari, S. M. A., Hani, U., et al. (2023). Deciphering the emerging role of phytocompounds: implications in the management of drug-resistant tuberculosis and ATDs-induced hepatic damage. *J. Infect. Public Health* 16, 1443–1459. doi: 10.1016/j.jiph.2023.07.016

Anwer, T., Alruwaili, M. N., Alshahrani, S., Alqahtani, S. S., Jali, A., Ahmed, R. A., et al. (2023). Hepatoprotective potential of diosmin against hepatotoxic effect of isoniazid and rifampin in wistar rats. *Hum. Exp. Toxicol.* 42:960327122114 91. doi: 10.1177/09603271221149199

Bagcchi, S. (2023). WHO's global tuberculosis report 2022. *Lancet Microbe* 4:e20. doi: 10.1016/S2666-5247(22)00359-7

Balkrishna, A., Rastogi, S., Kharayat, B., Tomer, M., Varshney, Y., Singh, K., et al. (2022). Anu taila, an herbal nasal drop, suppresses mucormycosis by regulating host TNF-α response and fungal ergosterol biosynthesis. *J. Appl. Microbiol.* 132, 3355–3374. doi: 10.1111/jam.15451

Borges, A., Saavedra, M. J., and Simões, M. (2015). Insights on antimicrobial resistance, biofilms and the use of phytochemicals as new antimicrobial agents. *Curr. Med. Chem.* 22, 2590–2614. doi: 10.2174/0929867322666150530210522

Brennan, P. J., Heifets, M., and Ullom, B. P. (1982). Thin-layer chromatography of lipid antigens as a means of identifying nontuberculous mycobacteria. *J. Clin. Microbiol.* 15, 447–455. doi: 10.1128/jcm.15.3.447-455.1982

Choudhary, N., Khajuria, V., Gillani, Z., Tandon, V., and Arora, E. (2014). Effect of Carum carvi, a herbal bioenhancer on pharmacokinetics of antitubercular drugs: A study in healthy human volunteers. *Perspect Clin. Res.* 5:80.

Darvin, S. S., Esakkimuthu, S., Toppo, E., Balakrishna, K., Paulraj, M. G., Pandikumar, P., et al. (2018). Hepatoprotective effect of lawsone on rifampicin-isoniazid induced hepatotoxicity in in vitro and in vivo models. *Environ. Toxicol. Pharmacol.* 61, 87–94. doi: 10.1016/j.etap.2018.05.006

Ezhilarasan, D. (2023). Antitubercular drugs induced liver injury: an updated insight into molecular mechanisms. *Drug Metab. Rev.* 55, 239–253. doi: 10.1080/03602532.2023.2215478

Gautam, S., Qureshi, K. A., Jameel Pasha, S. B., Dhanasekaran, S., Aspatwar, A., Parkkila, S., et al. (2023). Medicinal plants as therapeutic alternatives to combat *Mycobacterium tuberculosis*: a comprehensive review. *Antibiotics* 12:541. doi: 10.3390/antibiotics12030541

González, L. T., Minsky, N. W., Espinosa, L. E. M., Aranda, R. S., Meseguer, J. P., and Pérez, P. C. (2017). In vitro assessment of hepatoprotective agents against damage induced by acetaminophen and CCl4. *BMC Complement. Altern. Med.* 17:39. doi: 10.1186/s12906-016-1506-1

Kashyap, A., Singh, P. K., and Silakari, O. (2018). Mechanistic investigation of resistance via drug-inactivating enzymes in *Mycobacterium tuberculosis*. *Drug Metab. Rev.* 50, 448–465. doi: 10.1080/03602532.2018.1533966

Liu, Q., Garner, P., Wang, Y., Huang, B., and Smith, H. (2008). Drugs and herbs given to prevent hepatotoxicity of tuberculosis therapy: systematic review of ingredients and evaluation studies. *BMC Public Health* 8:365. doi: 10.1186/1471-2458-8-365

Mangwani, N., Singh, P. K., and Kumar, V. (2020). Medicinal plants: adjunct treatment to tuberculosis chemotherapy to prevent hepatic damage. *J. Ayurveda Integr. Med.* 11, 522–528. doi: 10.1016/j.jaim.2019.02.004

Merkl, R., Hrádková, I., Filip, V., and Šmidrkal, J. (2010). Antimicrobial and antioxidant properties of phenolic acids alkyl esters. *Czech J. Food Sci.* 28, 275–279. doi: 10.17221/132/2010-CJFS

Miao, M., and Xiang, L. (2020). Pharmacological action and potential targets of chlorogenic acid. *Adv. Pharmacol.* 87, 71–88. doi: 10.1016/bs.apha.2019.12.002

Mohamadi, N., Sharififar, F., Pournamdari, M., and Ansari, M. (2018). A review on biosynthesis, analytical techniques, and pharmacological activities of Trigonelline as a plant alkaloid. *J. Diet Suppl.* 15, 207–222. doi: 10.1080/19390211.2017.1329244

Nageswari, A. D., Rajanandh, M. G., Uday, M. K., Nasreen, R. A., Pujitha, R. J., Prathiksha, R. R., et al. (2018). Effect of rifampin with bio-enhancer in the treatment of newly diagnosed sputum positive pulmonary tuberculosis patients: A double-center study. *J. Clin. Tubercul. Mycobact. Dis.* 12, 73–77.

Patra, A. K. (2012). "An overview of antimicrobial properties of different classes of phytochemicals" in Dietary phytochemicals and microbes. ed. A. K. Patra (Netherlands, Dordrecht: Springer), 1–32.

Pieters, J. (2008). Mycobacterium tuberculosis and the macrophage: maintaining a balance. *Cell Host Microbe* 3, 399–407. doi: 10.1016/j.chom.2008.05.006

Qin, W., Guan, D., Ma, R., Yang, R., Xing, G., Shi, H., et al. (2017). Effects of trigonelline inhibition of the Nrf2 transcription factor in vitro on Echinococcus granulosus. *Acta Biochim. Biophys. Sin. Shanghai* 49, 696–705. doi: 10.1093/abbs/gmx067

Raja, W., Nosalova, G., Ghosh, K., Sivova, V., Nosal, S., and Ray, B. (2014). In vivo antitussive activity of a pectic arabinogalactan isolated from *Solanum virginianum* L. in Guinea pigs. *J. Ethnopharmacol.* 156, 41–46. doi: 10.1016/j.jep.2014.08.012

Riaz, A., Rasul, A., Hussain, G., Zahoor, M. K., Jabeen, F., Subhani, Z., et al. (2018). Astragalin: a bioactive phytochemical with potential therapeutic activities. *Adv. Pharmacol. Sci.* 2018, 1–15. doi: 10.1155/2018/9794625

Rodrigues, L., Wagner, D., Viveiros, M., Sampaio, D., Couto, I., Vavra, M., et al. (2008). Thioridazine and chlorpromazine inhibition of ethidium bromide efflux in Mycobacterium avium and *Mycobacterium smegmatis*. *J. Antimicrob. Chemother.* 61, 1076–1082. doi: 10.1093/jac/dkn070

Sachin, B. S., Sharma, S. C., Sethi, S., Tasduq, S. A., Tikoo, M. K., Tikoo, A. K., et al. (2007). Herbal modulation of drug bioavailability: enhancement of rifampicin levels in plasma by herbal products and a flavonoid glycoside derived from Cuminum cyminum. *Phyther. Res.* 21, 157–163.

Salehi, B., Venditti, A., Sharifi-Rad, M., Kręgiel, D., Sharifi-Rad, J., Durazzo, A., et al. (2019). The therapeutic potential of Apigenin. *Int. J. Mol. Sci.* 20:1305. doi: 10.3390/ijms20061305

Samal, J. (2016). Ayurvedic management of pulmonary tuberculosis: a systematic review. *J. Intercult. Ethnopharmacol.* 5, 86–91. doi: 10.5455/jice.20151107020621

Sharma, R., Muthu, S. A., Agarwal, M., Mehto, N. K., Pahuja, I., Grover, A., et al. (2023). Atosiban and Rutin exhibit anti-mycobacterial activity - an integrated computational and biophysical insight toward drug repurposing strategy against *Mycobacterium tuberculosis* targeting its essential enzyme HemD. *Int. J. Biol. Macromol.* 253:127208. doi: 10.1016/j.ijbiomac.2023.127208

Sparks, I. L., Derbyshire, K. M., Jacobs, W. R., and Morita, Y. S. (2023). *Mycobacterium smegmatis*: the vanguard of mycobacterial research. *J. Bacteriol.* 205:e0033722. doi: 10.1128/jb.00337-22

Taneja, N. K., and Tyagi, J. S. (2007). Resazurin reduction assays for screening of anti-tubercular compounds against dormant and actively growing *Mycobacterium tuberculosis*, *Mycobacterium bovis* BCG and *Mycobacterium smegmatis*. *J. Antimicrob. Chemother.* 60, 288–293. doi: 10.1093/jac/dkm207

Tella, J. O., Adekoya, J. A., and Ajanaku, K. O. (2022). Mesoporous silica nanocarriers as drug delivery systems for anti-tubercular agents: a review. *R. Soc. Open Sci.* 9:220013. doi: 10.1098/rsos.220013

The Lancet Public Health (2023). Taking tuberculosis out of the shadows. *Lancet Public Health* 8:e247. doi: 10.1016/S2468-2667(23)00063-4

Tizzano, B., Dallenga, T. K., Utpatel, C., Behrends, J., Homolka, S., Kohl, T. A., et al. (2021). Survival of hypoxia-induced dormancy is not a common feature of all strains of the *Mycobacterium tuberculosis* complex. *Sci. Rep.* 11:2628. doi: 10.1038/s41598-021-81223-6

Yang, X., Lan, W., and Xie, J. (2022). Antimicrobial and anti-biofilm activities of chlorogenic acid grafted chitosan against *Staphylococcus aureus*. *Microb. Pathog.* 173:105748. doi: 10.1016/j.micpath.2022.105748

Frontiers in Microbiology

Explores the habitable world and the potential of microbial life

The largest and most cited microbiology journal which advances our understanding of the role microbes play in addressing global challenges such as healthcare, food security, and climate change.

Discover the latest Research Topics

See more →

Frontiers

Avenue du Tribunal-Fédéral 34
1005 Lausanne, Switzerland
frontiersin.org

Contact us

+41 (0)21 510 17 00
frontiersin.org/about/contact